

**Proceedings of the 7th
U.S. – Japan Workshop on
Earthquake Disaster Prevention
For Lifeline Systems**



PB99-142986

**Held at Cavanaugh's on Fifth Avenue
Seattle, Washington
November 4 – 7, 1997**

Edited by
Donald Ballantyne
EQE International, Inc.
Seattle, Washington USA

Sponsored by
National Institute in Standards and Technology, and
National Science Foundation
Grant No. CMS-9732398
United States

Public Works Research Institute
Japan

November 1998

**EQE International, Inc.
1411 4th Avenue, Suite 500
Seattle, Washington 98101
EQE Project Number: 150737.01**


REPORT DOCUMENTATION PAGE	1. Report No.	2.	3. Recipient's Accession No.
4. Title and Subtitle Proceedings of the 7th U.S.-Japan Workshop on Earthquake Disaster Prevention for Lifeline Systems		5. Report Date November 1998	
7. Authors  PB99-142986		6.	
9. Performing Organization Name and Address Donald Ballantyne EQE International, Inc. 1411 4th Avenue Building Suite 500 Seattle, Washington 98101		8. Performing Organization Report No. 10. Project/Task/Work Unit No. 150737.01	
12. Sponsoring Organization Name and Address National Institute in Standards and Technology and National Science Foundation United States Public Works Research Institute Japan		11. Contract (C) or Grant (G) No. (C) (G) CMS-9732398	
15. Supplementary Notes		13. Type of Report & Period Covered Technical report	
16. Abstract (limit 200 words) The workshop focused on the current research and implementation activities of both countries. Papers addressed case studies related to seismic vulnerability assessment and design and retrofit of various lifeline systems. Particular emphasis was given to studies that summarize the recent performance of lifeline systems in major U.S. and Japan earthquakes. The following lifeline systems were considered: water and sewage, electric power and communications, natural gas and oil, transportation, and ports and harbors. Six technical sessions were conducted with the following themes: seismic damage of lifeline systems, seismic behavior of lifeline facilities, socio-economic impacts of seismic damage to lifeline facilities, seismic damage estimation and prediction for lifeline facilities, research and development in earthquake disaster prevention technology after the Northridge and Hanshin earthquakes, lifeline facilities and urban earthquake disaster prevention.		14.	
17. Document Analysis a. Descriptors Earthquake engineering. b. Identifiers/Open-Ended Terms c. COSATI Field/Group			
18. Availability Statement Release unlimited.		19. Security Class (This Report) Unclassified	21. No. of Pages 512
		20. Security Class (This Page) Unclassified	22. Price

TABLE OF CONTENTS

	PAGE
FORWARD	
I. SEISMIC DAMAGE OF LIFELINE FACILITIES	
Loss of Regional Economy at Kushiro Port due to Kushiro-oki Earthquake in 1993 Nozu, T. Uwabe, T. Sano	3
Damage to Bridges from the Northridge Earthquake: Consequences On Highway System Performance N. Basoz	23
Earthquake Damage to Buried Water Supply Pipes and their Renovation By Hose Lining Technology T. Sato, I. Yagi, H. Sakuragi, T. Driver	39
Factors Affecting Water Supply Damage Caused by the Northridge Earthquake S. Toprak, T. Rourke, Y. Sano	57
Seismic Risk Reduction at Port Facilities (paper not submitted) S. Dickenson	
II. SEISMIC BEHAVIOR OF LIFELINE FACILITIES	
Liquefaction Hazard Mapping in the Puget Sound Region P. Grant	71
City of Seattle Bridge Seismic Retrofit Program R. Miller, J. Lem, R. Shulock	87
Floating Characteristics of a Sewer Due to Soil-Liquefaction M. Kaneko, K. Tamura, H. Kobayashi	95
Reliability of Buried Pipelines Subjected to Large Permanent Ground Displacements C. Scawthorn, D. Ballantyne	111
Effect of Spatial Variation of Ground Motion for Ordinary Bridges M. Shinozuka, G. Deodatis	127

SPECIAL PRESENTATIONS AND PAPERS

Design Methods of Bridge Foundations Against Soil Liquefaction and Liquefaction-Induced Ground Flow 143
K. Yokoyama, K. Tamura, O. Matsuo

Experimental Study of the Effects of Liquefaction-Induced Ground Flow on Bridge Foundation 167
K. Tamura, T. Azuma

III. SOCIO-ECONOMIC IMPACTS OF SEISMIC DAMAGE TO LIFELINE FACILITIES

Highway System Performance Measures and Economic Impact 183
S. Chang, N. Nojima

System to Assess Socio-Economic Effect of Earthquake Disaster 199
T. Nozaki, H. Sugita

Influence of the Restoration of Hanshin Expressway Kobe Route from The Earthquake upon the Surrounding Area 213
N. Hamada, T. Yonekura, K. Yamamura

Reliability and Restoration of Water Supply Systems for Fire Suppression And Drinking Following Earthquakes 231
D. Ballantyne

Integrated Evaluation of Risks and Vulnerabilities for the Water System at Portland, Oregon, Including Natural and Human Caused Hazards 243
W. Elliott

IV. SEISMIC DAMAGE ESTIMATION AND PREDICTION FOR LIFELINE FACILITIES

Earthquake Loss Estimation for Transportation and Utility Lifelines 259
M. O'Rourke

Development of Real-Time Damage Estimation System for Road Facilities 271
H. Sugita, T. Hamada

Seismic Hazard Mapping in Eugene-Springfield, Oregon 285
Y. Wang, D. Keefer, Z. Wang

	Seismic Risk Evaluation and Improvement Program for the Metropolitan Wastewater Department, City of San Diego D. Hu, P. Wong, R. Eguchi, K. Merz, D. Ballantyne	305
	Mapping Predictions of Liquefaction Induced Lateral Spread Displacements M. Mabey	315
	Integrated Real-Time Disaster Information Systems: The Application of New Technologies R. Eguchi, J. Goltz, H. Seligson	329
V.	RESEARCH AND DEVELOPMENT IN EARTHQUAKE DISASTER PREVENTION TECHNOLOGY AFTER THE NORTHRIDGE AND KOBE EARTHQUAKES	
	Development of Seismic Risk Analysis of Power Systems J. Tohma, S. Higashi, Y. Shumuta	339
	Current Developments in Seismic Design Criteria and Mitigation Efforts for Electric Power Transmission Systems L. Kempner	347
	The 1996 Seismic Design Specifications for Highway Bridges T. Terayama, K. Yokoyama, K. Tamura, S. Unjoh, J. Hoshikuma	363
	Aseismic Countermeasure Technologies for Outdoor Telecommunication Facilities Implemented Following the 1995 Hyogo-ken Nanbu Earthquake M. Okutsu, K. Honda, Y. Yamaguchi, A. Sawaguchi, K. Ikeda	385
	Comparison of Recovery and Reconstruction Strategies in Water Supply Systems Between the 1994 Northridge and the 1995 Kobe Earthquakes-Emphasizing on an Emergency Response J. Ueno, S. Takada, R. Ozaki	401
VI.	LIFELINE FACILITIES AND URBAN EARTHQUAKE DISASTER PREVENTION	
	Development of Seismic Isolation Systems for Underground Structures And the Mechanism of Seismic Isolation J. Hoshikuma, S. Unjoh, K. Nagaya, K. Murai	417
	Seismic Design of Liquid Storage Tanks D. Hu, B. Hendrickson	431

Research and Development on the Seismic Isolation System Applied to Urban Tunnels (Part-1: Development of Seismic Isolation Materials and Construction Methods)	447
T. Suzuki, T. Tanaka	
Research and Development on the Seismic Isolation System Applied to Urban Tunnels (Part -2: Effects of Seismic Isolation and Seismic Design)	461
T. Tanaka, T. Suzuki	
Translating Earthquake Damage Data into New Performance Requirements for Earthquake Actuated Automatic Gas Shutoff Devices in the United States	477
Douglas Honegger	
 RESOLUTIONS	 493
 APPENDICES	
Workshop Agenda	495
Participant List	499
Photos	505

FORWARD

This is the first workshop where adequate time has passed to have allowed research of the 1994 Northridge, and 1995 Hanshin earthquakes. The U.S. and Japan are both leaders in earthquake engineering, but do not always excel in the same areas. Both countries can benefit from the exchange of ideas developed across the Pacific in a different technological and academic environment. For the last 20 years, the U.S. and Japan have supported exchange of information through technical meetings focusing on lifeline earthquake engineering. One ongoing activity has meetings under the auspices of the U.S.-Japan Natural Resources (UJNR) program.

There have been six previous workshops organized by the Panel on Wind and Seismic Effects of the UJNR program with specific focus on the seismic performance of lifelines:

U.S.- Japan Workshop on Lifeline Systems, Washington DC, 1984

Second U.S.-Japan Workshop on Seismic Behavior of Buried Pipelines and Telecommunication Systems, Tsukuba, Japan, 1984

Third U.S.-Japan Workshop on Earthquake Disaster Prevention for Lifeline Systems, Tsukuba, Japan, 1989

Fourth U.S.-Japan Workshop on Earthquake Disaster Prevention for Lifeline Systems, Los Angeles, California, 1991

Fifth U.S.-Japan Workshop on Earthquake Disaster Prevention for Lifeline Systems, Tsukuba, Japan, 1992

Sixth U.S.-Japan Workshop on Earthquake Disaster Prevention for Lifeline Systems, Osaka, Japan, 1995

The following proceedings document the results of the Seventh U.S.-Japan Workshop on Earthquake Disaster Prevention for Lifeline Systems. This workshop was jointly sponsored by the National Institute of Standards and Technology (NIST) and the National Science Foundation (NSF) in the U.S. and the Public Works Research Institute (PWRI) of Japan. The workshop was held at Cavanaugh's on Fifth Avenue, in Seattle, Washington, between November 4 and 7, 1997. The workshop was organized by Task Committee F, "Disaster Prevention Methods for Lifeline Systems" UJNR Panel on Wind and Seismic Effects. Mr. Donald Ballantyne of EQE International, Dr. Riley Chung of NIST, and Dr. Koichi Yokoyama of PWRI led the organization of this workshop.

The workshop focused on the current research and implementation activities of both countries. Papers addressed case studies related to seismic vulnerability assessment and

design and retrofit of various lifeline systems. Particular emphasis was given to studies that summarize the recent performance of lifeline systems in major U.S. and Japanese earthquakes. The following lifeline systems were considered:

- Water and Sewage
- Electric Power and Communications
- Natural Gas and Oil
- Transportation
- Ports and Harbors

Six technical sessions were conducted with the following themes:

- 1) Seismic damage of lifeline systems
- 2) Seismic behavior of lifeline facilities
- 3) Socio-economic impacts of seismic damage to lifeline facilities
- 4) Seismic damage estimation and prediction for lifeline facilities
- 5) Research and development in earthquake disaster prevention technology after the Northridge and Hanshin earthquakes
- 6) Lifeline facilities and urban earthquake disaster prevention

There is a trend in the United States to consider all hazards when assessing system vulnerability. Flood, wind, and earthquake are considered the three most significant hazards. The workshop included one paper on an ongoing multi-hazard assessment case study of a lifeline system.

Two special presentations each, were made by U.S. and Japanese researchers. On the U.S. side, Dr. Brian Atwater, from the USGS, discussed *Past Liquefaction/Tsunamis Occurrences at the Metro West Point Wastewater Treatment Plant*, one of the study tour stops. Dr. Atwater made one of the initial discoveries showing Seattle has been subjected to large subduction earthquakes. Dr. Craig Weaver's presentation on *Seismicity of the Pacific Northwest* focused on current research on crustal earthquakes caused by north-south compression. On the Japanese side, Dr. Yokoyama presented his research results on *Design Methods of Bridge Foundations Against Soil Liquefaction and Liquefaction-Induced Ground Flow*, followed by Dr. Tamura's special presentation on the *Experimental Study of the Effects of Liquefaction-Induced Ground Flow on Bridge Foundation*.

Forty-nine lifeline experts participated in the workshop, 33 from the US, and 16 from Japan. The US workshop organizers paid special attention to inviting young lifeline researchers, giving them the opportunity to develop relationships with their Japanese counterparts. Over one-third of the US presenters were less than five years out of school.

A total of thirty-three papers were presented in the two days of plenary sessions; 16 papers from Japan, and 17 papers from the U.S. An active question/answer period was held after each session. Resolutions fully supported by the participants of both countries identified five areas of joint U.S.-Japanese activities:

- 1) Continued cooperative research programs,
- 2) Continued exchange of personnel and research data,
- 3) Interaction between UJNR Task Committees and Panels,
- 4) Future task committee activities to support real time seismic information, loss estimation models, and post-earthquake response and recovery.
- 5) Future workshop on seismic effects and earthquake disaster prevention methods for lifeline systems.

Following the two days of technical sessions, two days of study tours were conducted visiting the following lifeline facilities in the Seattle area with instructive presentations at each:

- 1) Seattle bridges seismic upgrade
- 2) King County Metro West Point Wastewater Treatment Plant
- 3) Seattle Public Utilities Magnolia tank and pump station seismic retrofit
- 4) South of downtown Seattle transportation issues
- 5) Washington State Department of Transportation Regional Traffic Control Center, and
- 6) Bonneville Power Administration 550 kv Monroe Substation damaged in a recent earthquake.

The material in this proceedings are presented as follows:

- 1) Technical papers and presenter information
- 2) Resolutions unanimously adopted by workshop participants
- 3) Appendices including the workshop agenda, list of workshop participants, and workshop photos.

ACKNOWLEDGEMENTS

The workshop organizers would like to thank the National Institute of Standards and Technology, the National Science Foundation, and the Public Works Research Institute for sponsoring the workshop and publication of these proceedings. At the National Science Foundation, we would like to thank Dr. S.C. Liu for their guidance in this effort.

We extend our sincere appreciation to the hosts of the six study tours:

Seattle Bridges - Richard Miller

King County Metro - Allen Alston

Seattle Public Utilities - Aziz Alfi

Seattle Department of Transportation - Ron Borowski

Washington State Department of Transportation - David McCormick

Bonneville Power Administration - Dr. Leon Kempner

We would also like to thank the EQE International staff that provided support in organizing the workshop and assemble the proceedings, including Leslie Rose, Steven Ting, and Leona Nguyen.

Donald Ballantyne
EQE International

Riley Chung
National Institute of Standards and
Technology

Koichi Yokoyama
Public Works Research Institute

Workshop Organizers

I. SEISMIC DAMAGE OF LIFELINE FACILITIES

“Loss of Regional Economy at Kushiro Port due to
Kushiro-oki Earthquake in 1993”

Nosu, T. Uwabe, T. Sano

“Damage to Bridges from the Northridge Earthquake:
Consequences on Highway System Performance”

N. Basoz

“Earthquake Damage to Buried Water Supply Pipes
and their Renovation by Hose Lining Technology”

T. Sato, I Yagi, H. Sakuragi, T. Driver

“Factors Affecting Water Supply Damage Caused
by the Northridge Earthquake”

S. Toprak, T. Rourke, Y. Sano

“Seismic Risk Reduction at Port Facilities”

S. Dickenson



LOSS OF REGIONAL ECONOMY AT KUSHIRO PORT DUE TO KUSHIRO-OKI EARTHQUAKE IN 1993

Atsushi NOZU*, Tatsuo UWABE** and Tohru SANO***

*Member of Earthquake Disaster Prevention Laboratory,
Port and Harbour Research Institute

**Chief of Earthquake Disaster Prevention Laboratory,
Port and Harbour Research Institute

***Chief of the 1st Construction Section, Hakodate Port Construction Office, Hakodate
Development Construction Department, Hokkaido Development Bureau

ABSTRACT

The 1993 Kushiro-oki Earthquake brought considerable damage to ports and harbours along the Pacific coast of Hokkaido, especially to Kushiro Port. In this research, the loss of economy at Kushiro Port due to the earthquake was investigated by means of interview and questionnaires. Based on the results, economic rationality of countermeasures against liquefaction are investigated using cost-benefit analysis. Results of this study is summarized as follows. The loss of economy at Kushiro Port due to the 1993 Kushiro-oki Earthquake was at least 250,902,000 Yen including 60,000,000 Yen for "port-dependent industries" and 190,902,000 Yen for "port-related industries". Even when the damage to the quaywall itself is slight, the damage to cargo-handling equipment tends to bring impacts to regional economy. Economic rationality of countermeasures against liquefaction was recognized for 5 among 7 facilities at Kushiro port.

INTRODUCTION

Damage to port facilities due to earthquake brings economic impacts to industries of which activity is dependent on the port functions. For example, port-dependent industries,

which utilize ports as a measure of transportation of resources and products, are temporally forced to change their transportation route and to pay more for transportation than usual. Port-related industries, which are engaged in cargo handling, etc., lose part of their incomes. Loss of economy due to earthquake can be very serious some times, as it was in Kobe Port during Hyogo-ken Nanbu earthquake of 1995. Earthquake resistant design of port facilities is quite important to prevent loss of regional economy as well as to prevent damage to human life. On the other hand, constructing earthquake-resistant structure is sometimes very costly especially when countermeasures against liquefaction is necessary. Thus we face the problem of determining the optimum initial construction cost which minimize the sum of initial construction cost and loss due to earthquake.

Purpose of this research is to show the economical rationality of countermeasures against liquefaction using cost-benefit analysis in terms of the damage to Kushiro port due to the 1993 Kushiro-oki Earthquake. In this analysis, two types of losses are taken into account; loss of economy and cost of repair. For this purpose, loss of economy due to damage to port function is quantitatively investigated. Investigation was conducted both for port-related industries and port-dependent industries by means of interview and questionnaires.

REVIEW OF DAMAGE TO KUSHIRO PORT

Kushiro Port is located in the eastern part of Hokkaido island as shown in Fig. 1. Kushiro port is one of the most important ports in Hokkaido island, which treated 20,992,000 ton in the year of 1991. Figure 1 also shows the source region of the 1993 Kushiro-oki earthquake(M7.8). Figure 2 shows the accelerogram obtained on the surface of reclaimed land in Kushiro port during the earthquake (Ueda et al., 1993). Peak horizontal ground acceleration was over 400 Gal. Figure 3 shows the outline of the damage (Ueda et al., 1993) both for East Port and West Port, which are the parts of Kushiro Port. Extent of damage to each facilities are classified into five ranks (0-IV), which is explained in Table 1. This category has been used to represent the extent of damage to port structures since the 1964 Niigata earthquake. According to Fig.3, 36% of facilities remained sound, 40% were classified into rank I, 22% were classified into rank II, 2% were classified into rank III, and only 3 facilities were classified into rank IV.

In this report, 7 quaywalls(①~⑦), shown in Table 2, are selected as targets of

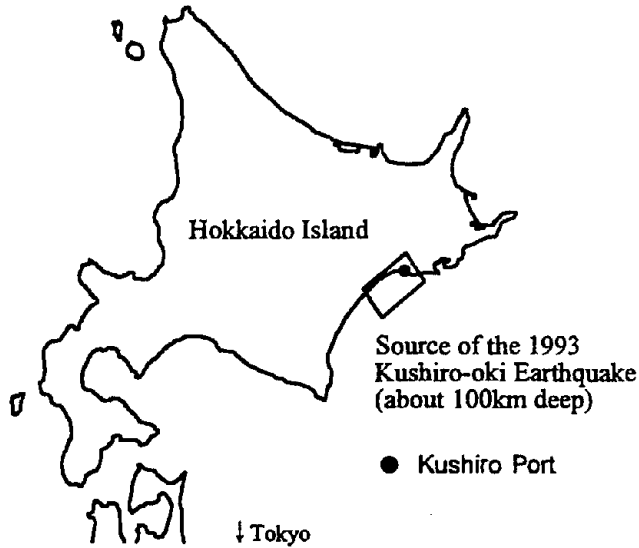


Fig.1 Location of Kushiro Port

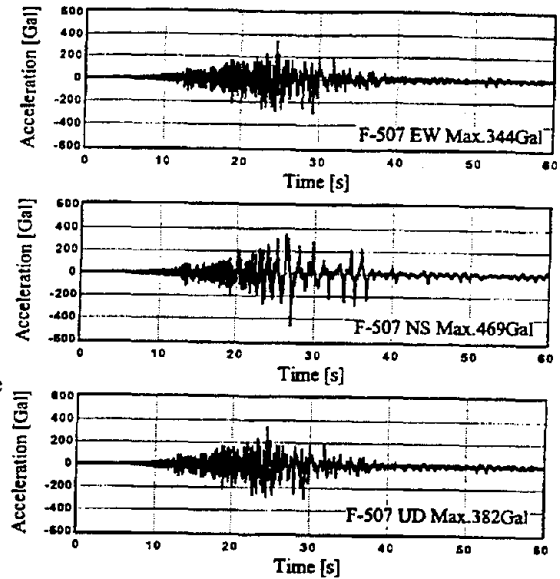


Fig.2 Accelerograms obtained in Kushiro Port

cost-benefit analysis. These quaywalls are selected because countermeasures against liquefaction were taken together with repair work after the earthquake for these facilities and therefore we know the practical cost of countermeasures against liquefaction for these quaywalls. Location of these quaywalls are shown in Fig. 3 with the symbols ①~⑦. Damage to these quaywalls are summarized in Table 2. It is estimated due to following two reasons that these quaywalls suffered damage because of the liquefaction in the backfill soil.

- 1) According to the investigation after the earthquake, sand spout due to liquefaction was found on the backfill soil.
- 2) According to stability analysis which was conducted for these quaywalls following present design method of port structures, seismic force which acted on these quaywalls were estimated to be larger than or at least close to empirical upper limit of seismic force without liquefaction as shown in Fig.4, indicating that without any liquefaction, these structures would have remained sound (Nozu, et al., 1997).

Among four main cargo-handling machines in Kushiro Port, three machines for grains had been installed on the south-side quaywall(-12.0m) of the 2nd terminal (⑤). Another machine for coals had been installed on the south-side quaywall(-12.0m) of the 3rd terminal (⑧) as shown in Fig. 3. All of these machines suffered damage due to the earthquake and became out of order.

Figure 5(a)-(h) shows the change in the numbers and total weight of ships and total weight of cargo for the quaywalls listed in Table 2 (except for the south-side quaywall of Fishery Terminal, East Port) and another quaywall worthy of notice, the south-side quaywall(-12.0m) of the 3rd terminal (⑧). According to Fig.5, decrease of the amount of cargo due to the damage is apparent for the west-side quaywall(-9.0m) of the 1st terminal (②), the

Table 1 Rank of Damage

Rank	Extent of Damage
0	No Damage
I	Main structure is not damaged. Failure and/or deformation is recognized in additional structure.
II	Certain amount of deformation is recognized in main structure.
III	Failure is recognized in main structure but it preserves it's original shape.
IV	Structure does not preserve it's original shape.

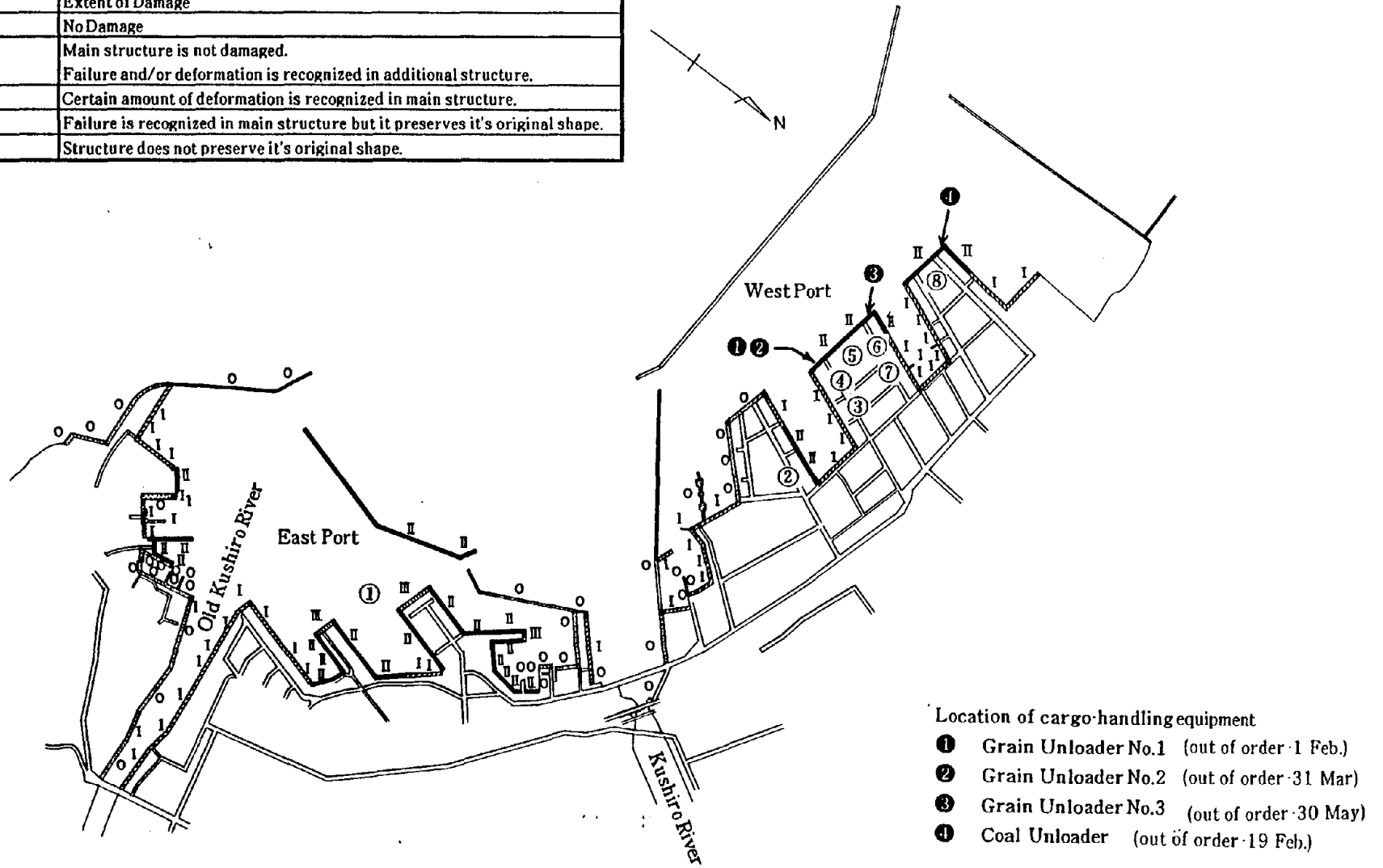


Fig.3 Outline of damage to Kushiro Port

Table 2 Quaywalls selected for cost-benefit analysis

No. of quaywall	Name	Location	Water depth	Rank of damage	Swelling of faceline	Settlement of faceline
①	the south-side quaywall of Fishery Terminal	East Port	-7.5m	III	50cm	30cm
②	the west-side quaywall of 1st Terminal	West Port	-9.0m	II	70cm	35cm
③	the east-side quaywall of 2nd Terminal	West Port	-7.5m	I	10cm	30cm
④	the east-side quaywall of 2nd Terminal	West Port	-10.0m	I	5cm	30cm
⑤	the south-side quaywall of 2nd Terminal	West Port	-12.0m	II	30cm	45cm
⑥	the west-side quaywall of 2nd Terminal	West Port	-9.0m	II	40cm	40cm
⑦	the west-side quaywall of 2nd Terminal	West Port	-7.5m	I	25cm	30cm

*Swelling and settlement of faceline are maximum values in the report (Ueda, et al., 1993).

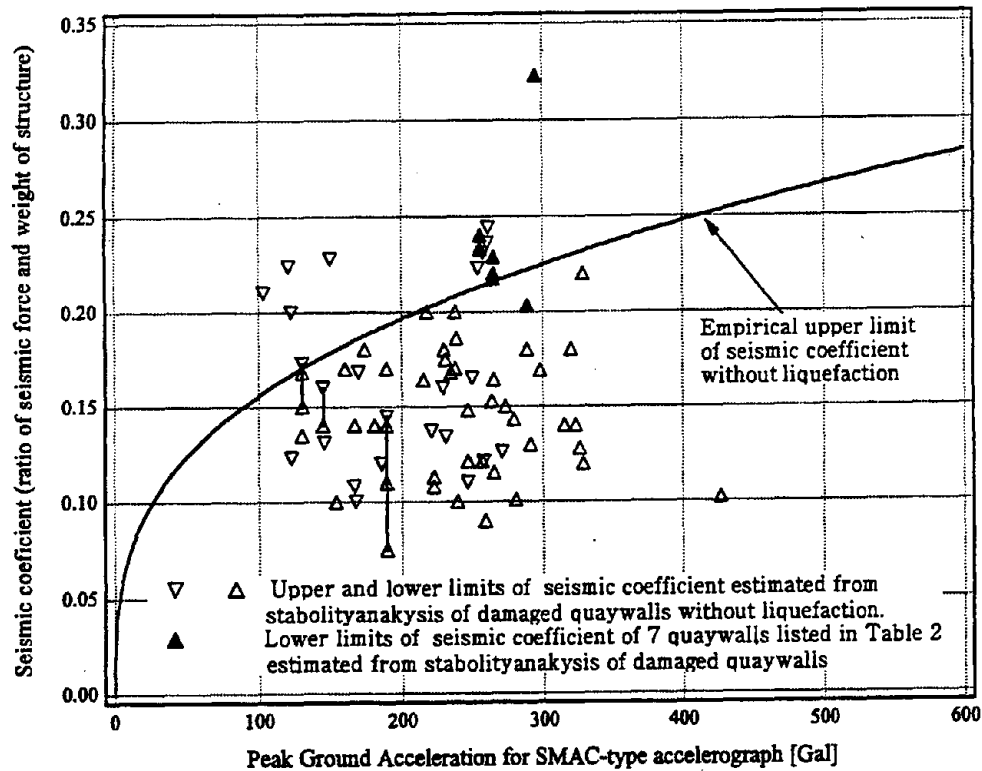


Fig.4 Results of stability analysis for 7 quaywalls listed in Table 2 and empirical upper limit of seismic force (Nozu, et al., 1997)

south-side quaywall(-12.0m) of the 2nd terminal (⑤), the west-side quaywall(-9.0m) of the 2nd terminal (⑥), and the south-side quaywall(-12.0m) of the 3rd terminal (⑧). Decrease of cargo is not apparent for the other quaywalls. Strong correlation is found between the availability of cargo-handling equipment(Fig.3) and amount of cargo for the quaywalls on which cargo-handling machines are installed(Fig.5).

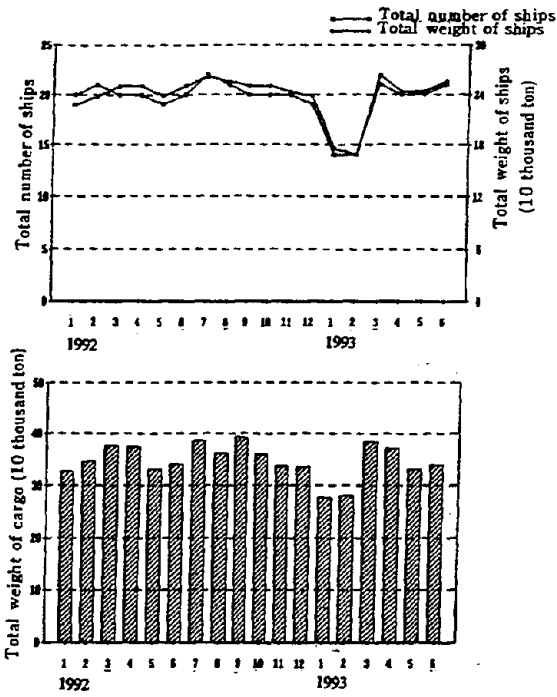


Fig.5(a) Change in the amount of cargo
 (2) west-side quaywall of 1st Terminal -9.0m

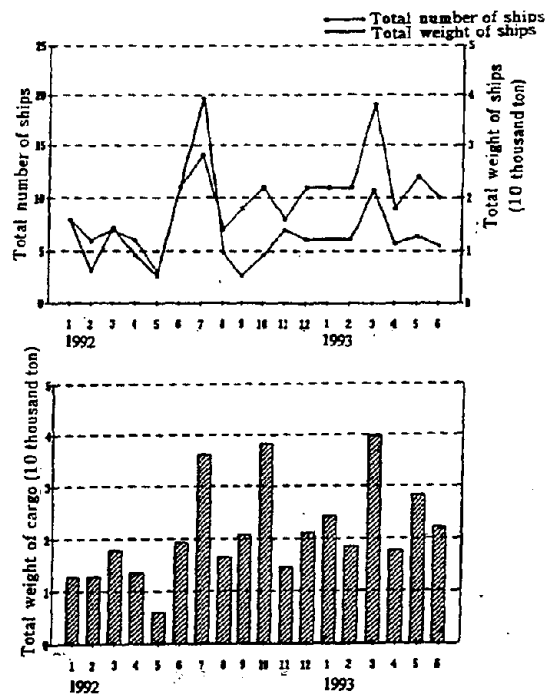


Fig.5(b) Change in the amount of cargo
 (3) east-side quaywall of 2nd Terminal -7.5m

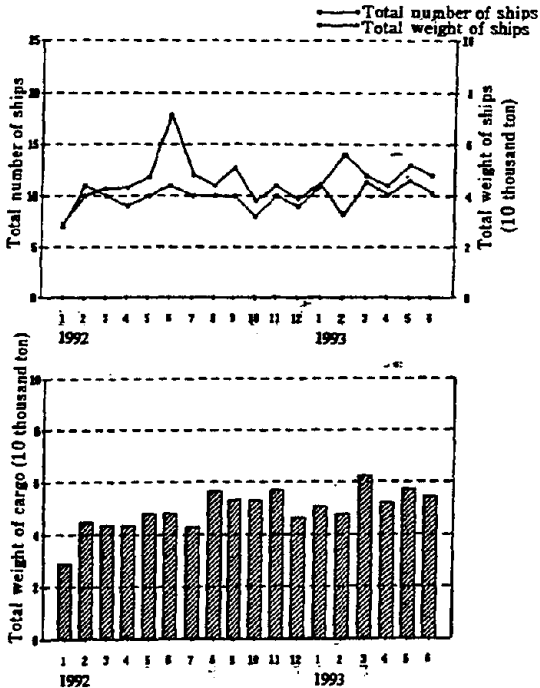


Fig.5(c) Change in the amount of cargo
 (4) east-side quaywall of 2nd Terminal -10.0m

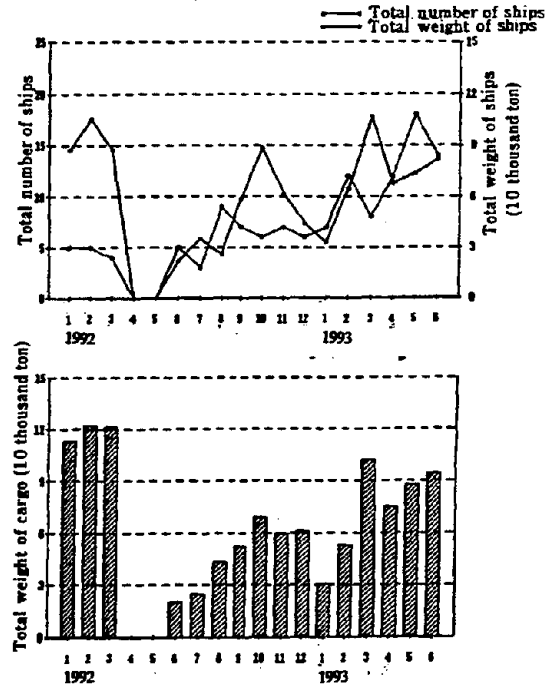


Fig.5(d) Change in the amount of cargo
 (5) south-side quaywall of 2nd Terminal -12.0m, east part

1992 1993 1992 1993

1992 1993 1992 1993

1992 1993 1992 1993

1992 1993 1992 1993

1992 1993 1992 1993

1992 1993 1992 1993

1992 1993 1992 1993

1992 1993 1992 1993

In this report, cost indicated by * is considered to be loss of economy.

•

•

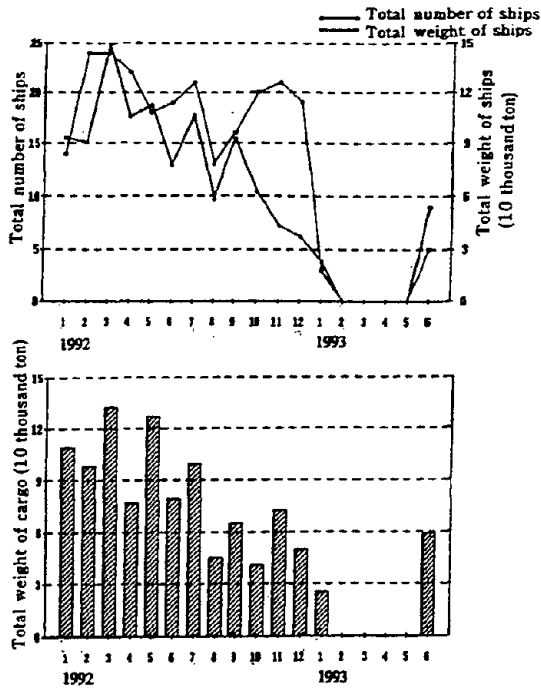


Fig.5(e) Change in the amount of cargo
 (⑤ south-side quaywall of 2nd Terminal -12.0m, west part)

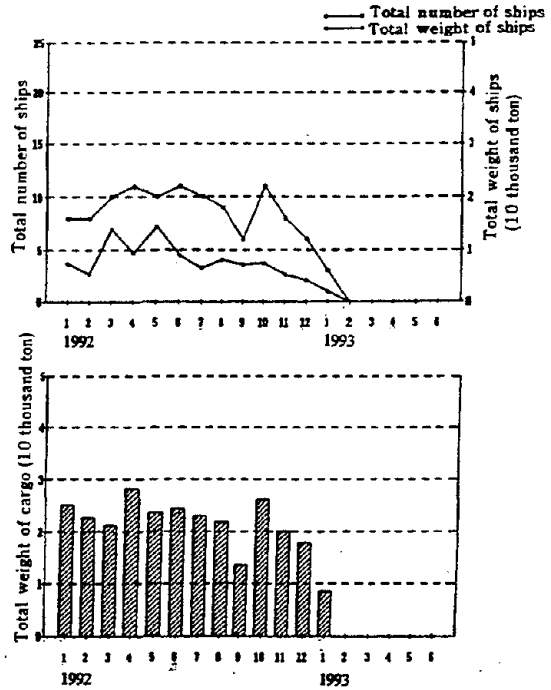


Fig.5(f) Change in the amount of cargo
 (⑥ west-side quaywall of 2nd Terminal -9.0m)

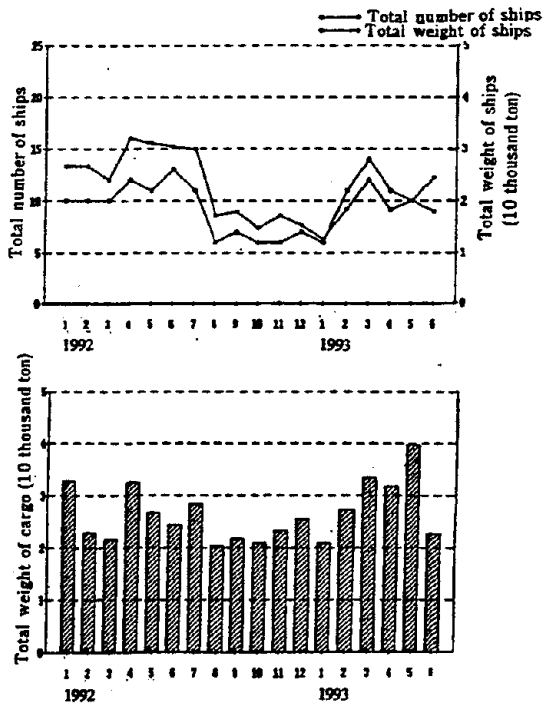


Fig.5(g) Change in the amount of cargo
 (⑦ west-side quaywall of 2nd Terminal -7.5m)

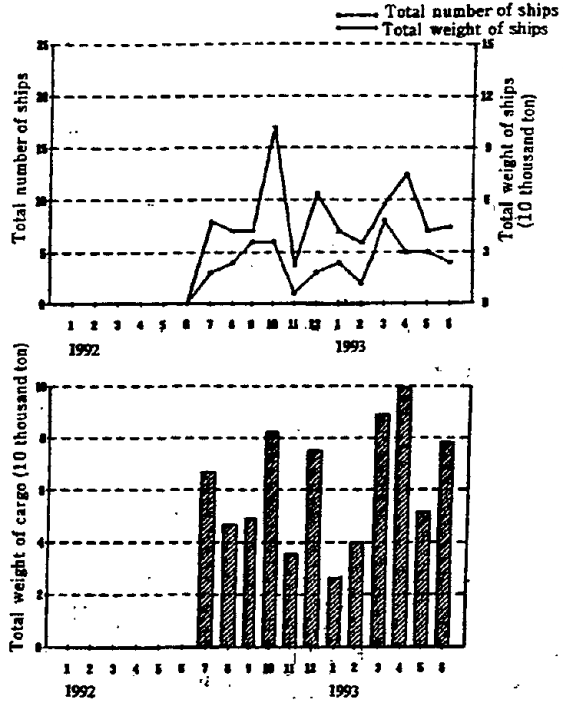
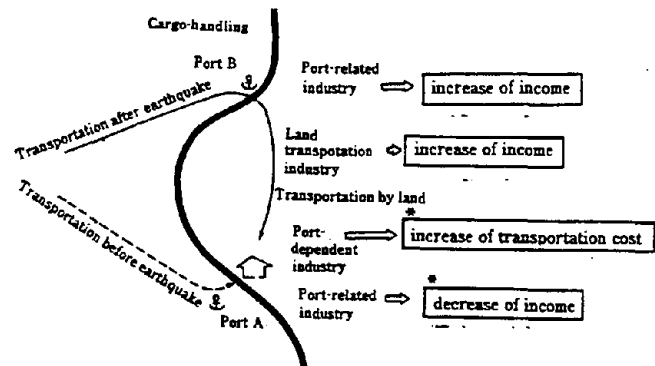


Fig.5(h) Change in the amount of cargo
 (⑧ south-side quaywall of 3rd Terminal -12.0m)

* * *

LOSS OF REGIONAL ECONOMY

First of all, definition of the "loss of regional economy" which is treated in this report is presented. Figure 6 shows the concept of "loss of economy". Assume that a big earthquake hit a port A and some of facilities become out of order. Then, port-dependent industries, which utilize port A as a measure of transportation of resources and products, will be temporarily forced to change their transportation route and to pay, for example, for the transportation on land between



In this report, cost indicated by * is considered to be loss of economy.

Fig.6 Concept of "loss of economy"

neighboring port B and port A. Port related industry, which are engaged in cargo-handling, etc. in the port A will lose part of it's income because of the decrease of cargo. On the other hand, the port-related industries in port B and the land transportation industry will gain more because of the earthquake. In this report, loss of both industries in port A is considered. Gain of land transportation industry and port-related industry in port B is neglected. In addition, higher-order impacts to other industries is neglected.

Investigation of loss of regional economy was carried out both for port-related industries and port-dependent industries by means of interview and questionnaires.

At first, loss of port-related industries during the period before restoration works are investigated. First questionnaires are sent to 23 port-related industries, asking just whether damage to Kushiro port affected their economic activity or not. Answers were obtained from 19 companies, and 10 companies among them stated that they suffered from loss of economy. Then interviews with 10 companies are conducted to know whether they were able to numerate their loss of economy or not. Five companies were positive, to which second questionnaires are sent, asking the amount of their loss. Answers were obtained from 3 companies. According to the answers, loss of port-related industries during the period before restoration works was at least 164,494,000 Yen. Figure 7 shows the breakdown of the loss in terms of the kind of cost, period, the kind of goods and the quaywall which was

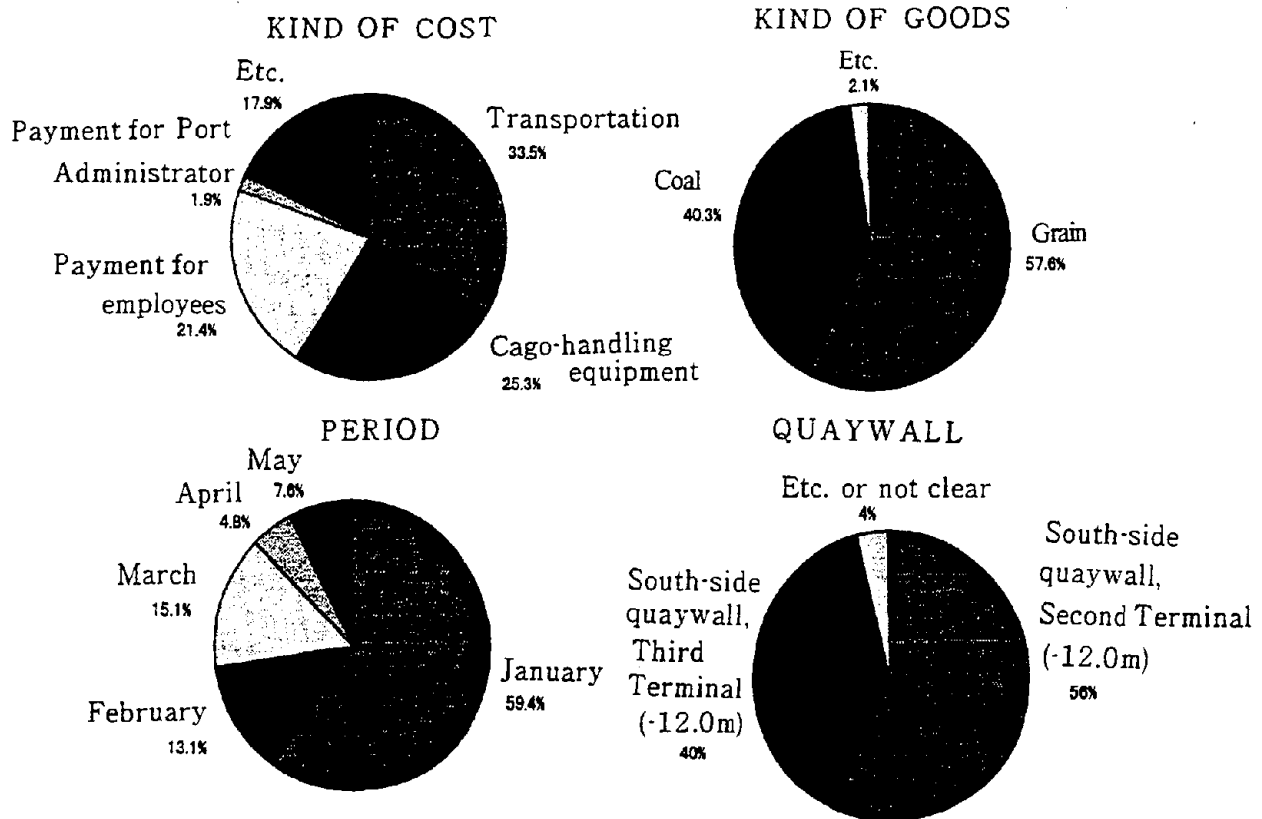


Fig.7 Breakdown of loss of economy for port-related industry during the period between earthquake and restoration work

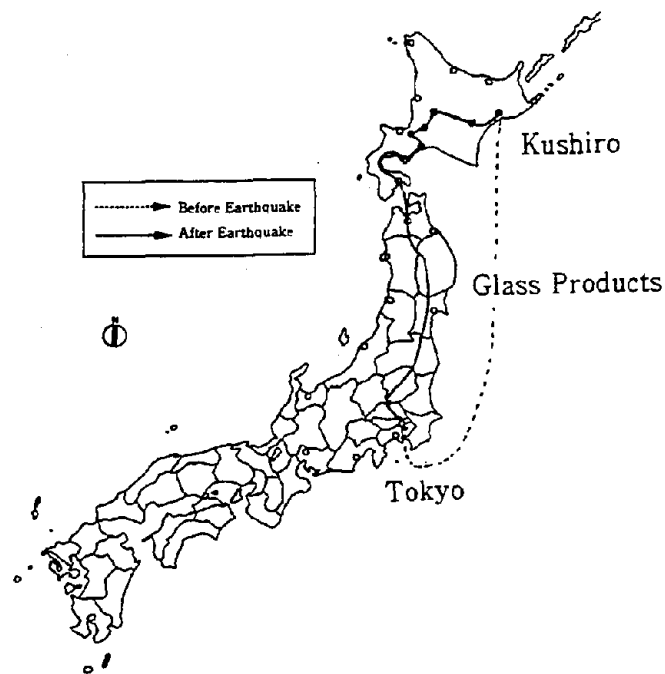


Fig.8 Example of the change of transportation route

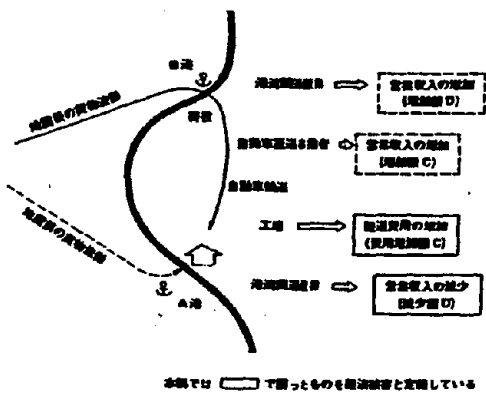


図-1 経済被害の定義²⁾

Fig. 7

responsible for the loss of economy. As shown in Fig.7, 56% of the loss was due to the south-side quaywall(-12.0m) of the 2nd terminal (⑤) and 40% was due to the south-side quaywall(-12.0m) of the 3rd terminal (⑧).

Secondary, loss of port-related industries during restoration work are investigated. This investigation was concentrated on two quaywalls, the east-side quaywall(-7.5m) of the 2nd terminal (③) and the west-side quaywall(-9.0m) of the 2nd terminal (⑥), because it was in these facilities that the restriction of use was most strict during restoration work. As a result, it was estimated that loss of economy due to the east-side quaywall(-7.5m) of the 2nd terminal (③) was approximately 2,739,000 Yen and that due to the west-side quaywall(-9.0m) of the 2nd terminal (⑥) was approximately 23,669,000 Yen. Total loss of port-related industries was at least 190,902,000 Yen.

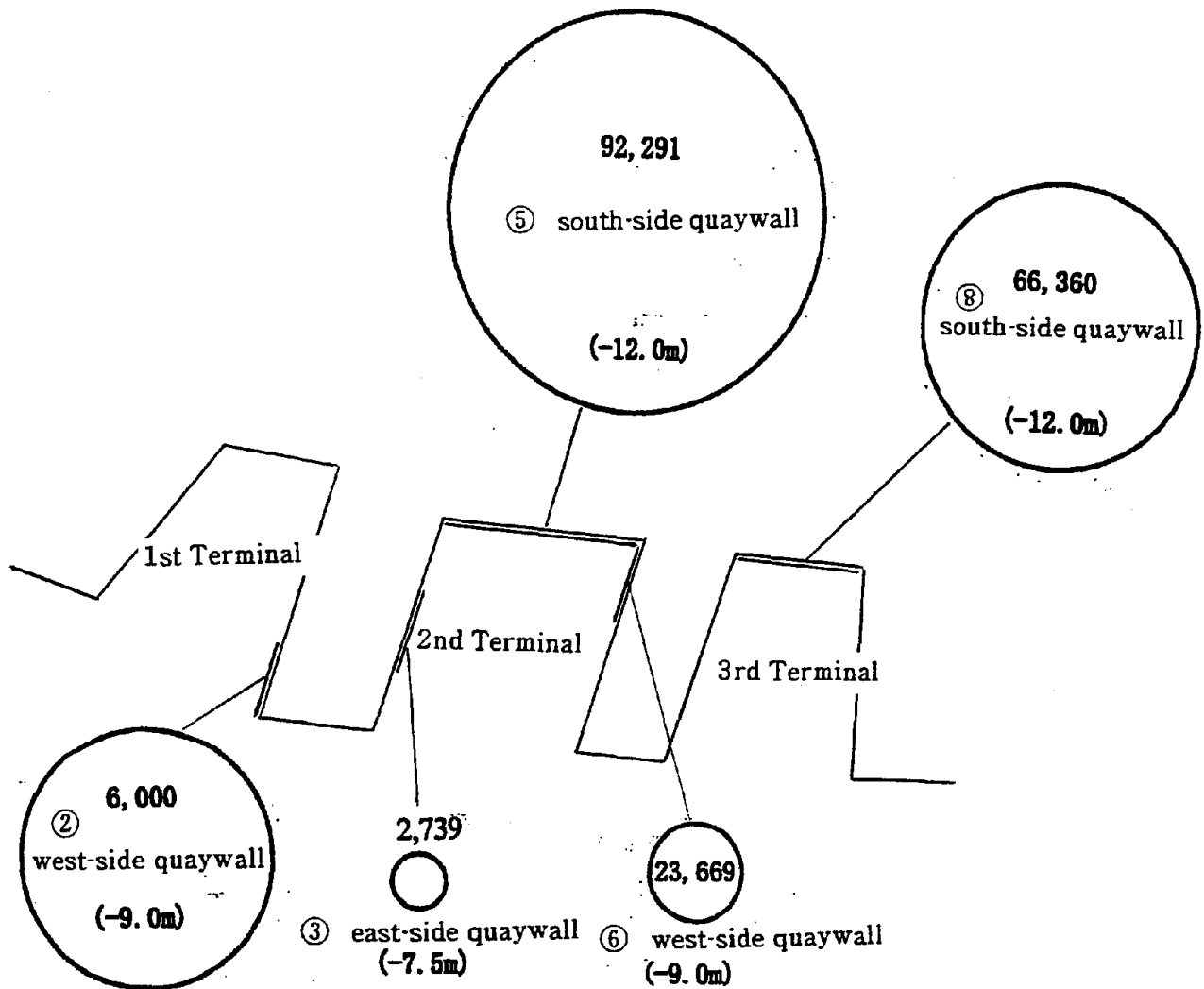


Fig.9 Breakdown of loss of economy in terms of the quaywall which is responsible for the loss

unit: 10 thousand yen

Thirdly, loss of port-dependent industries are investigated. First of all, port-dependent industries are listed up by means of interviews to Kushiro City Government. Then, questionnaires were sent to 29 port-dependent companies. Answers were obtained from 23 companies. According to the answer, loss of port-dependent industries was at least 60,000,000 Yen. These loss were due to the west-side quaywall(-9.0m) of the 1st terminal (②) and occurred during the period between the earthquake and the restoration work. Figure 8 shows the example of the change of transportation route which caused loss of economy.

Summarizing above investigations, it is concluded that the loss of economy at Kushiro Port due to the 1993 Kushiro-oki Earthquake was at least 250,902,000 Japanese Yen including 60,000,000 Yen for "port dependent industries" and 190,902,000 Yen for "port related industries". Figure 9 shows the breakdown of the loss in terms of the quaywall which was responsible for the loss of economy.

ECONOMICAL RATIONALITY OF COUNTERMEASURE AGAINST LIQUEFACTION

To show the economic rationality of countermeasures against liquefaction, cost-benefit analysis is conducted in terms of the damage to Kushiro port due to the Kushiro-oki Earthquake. In this report, following two scenario is considered for each of 7 quaywalls listed in table 2.

[Scenario A] Countermeasures against liquefaction is taken before the earthquake. Therefore, the facility remain sound during earthquake.

[Scenario B] Countermeasures against liquefaction is not taken before the earthquake. Therefore, the facility suffers damage. Cost of repair and loss of economy occurs.

[Scenario B] actually became reality during Kushiro-oki earthquake. [Scenario A] is imaginary, but it would have become reality if countermeasures had been taken for the 7 quaywalls before the earthquake, because damage to these quaywalls is due to liquefaction as mentioned earlier. For [Scenario A], the cost of countermeasures against liquefaction is evaluated. For [Scenario B], the sum of the cost of repair work and the loss of economy is evaluated. It is defined that the countermeasures against liquefaction is "economically rational" when the cost of countermeasures are smaller than the sum of the cost of repair work and the loss of economy.

Table 3 Details of cost of repair (unit: thousand yen)

No. of quaywall	Name	Water depth	Total cost of repair	Cost of countermeasures against liquefaction C1	Net cost of repair B1
①	the south-side quaywall of Fishery Terminal	-7.5m	1,280,267	35,345	1,244,922
②	the west-side quaywall of 1st Terminal	-9.0m	207,526	80,048	127,478
③	the east-side quaywall of 2nd Terminal	-7.5m	81,672	34,831	46,841
④	the east-side quaywall of 2nd Terminal	-10.0m	137,846	49,779	88,067
⑤	the south-side quaywall of 2nd Terminal	-12.0m	2,364,415	1,074,951	1,289,464
⑥	the west-side quaywall of 2nd Terminal	-9.0m	112,644	31,422	81,222
⑦	the west-side quaywall of 2nd Terminal	-7.5m	129,617	60,621	68,996
sum			4,313,987	1,366,997	2,946,990

*Cost of restoration of the south-side quaywall of 2nd Terminal includes cost of repair of cargo-handling equipments.

Table 4 Results of cost-benefit analysis (unit: thousand yen)

No. of quaywall	Name	Water depth	Net cost of repair B1	Loss of regional economy B2	Total loss B	Cost of countermeasures C1	Additional cost C2	Total cost C	Comparison
①	the south-side quaywall of Fishery Terminal	-7.5m	1,244,922	-	1,244,922	35,345	38,589	73,934	B>C
②	the west-side quaywall of 1st Terminal	-9.0m	127,478	60,000	187,478	80,048	45,676	125,724	B>C
③	the east-side quaywall of 2nd Terminal	-7.5m	46,841	2,739	49,580	34,831	20,615	55,446	C>B
④	the east-side quaywall of 2nd Terminal	-10.0m	88,067	-	88,067	49,779	32,034	81,813	B>C
⑤	the south-side quaywall of 2nd Terminal	-12.0m	1,289,464	92,291	1,381,755	1,074,951	156,370	1,231,321	B>C
⑥	the west-side quaywall of 2nd Terminal	-9.0m	81,222	23,669	104,891	31,422	22,154	53,576	B>C
⑦	the west-side quaywall of 2nd Terminal	-7.5m	68,996	-	68,996	60,621	38,323	98,944	C>B
sum			2,946,990	178,699	3,125,689	1,366,997	353,761	1,720,758	B>C

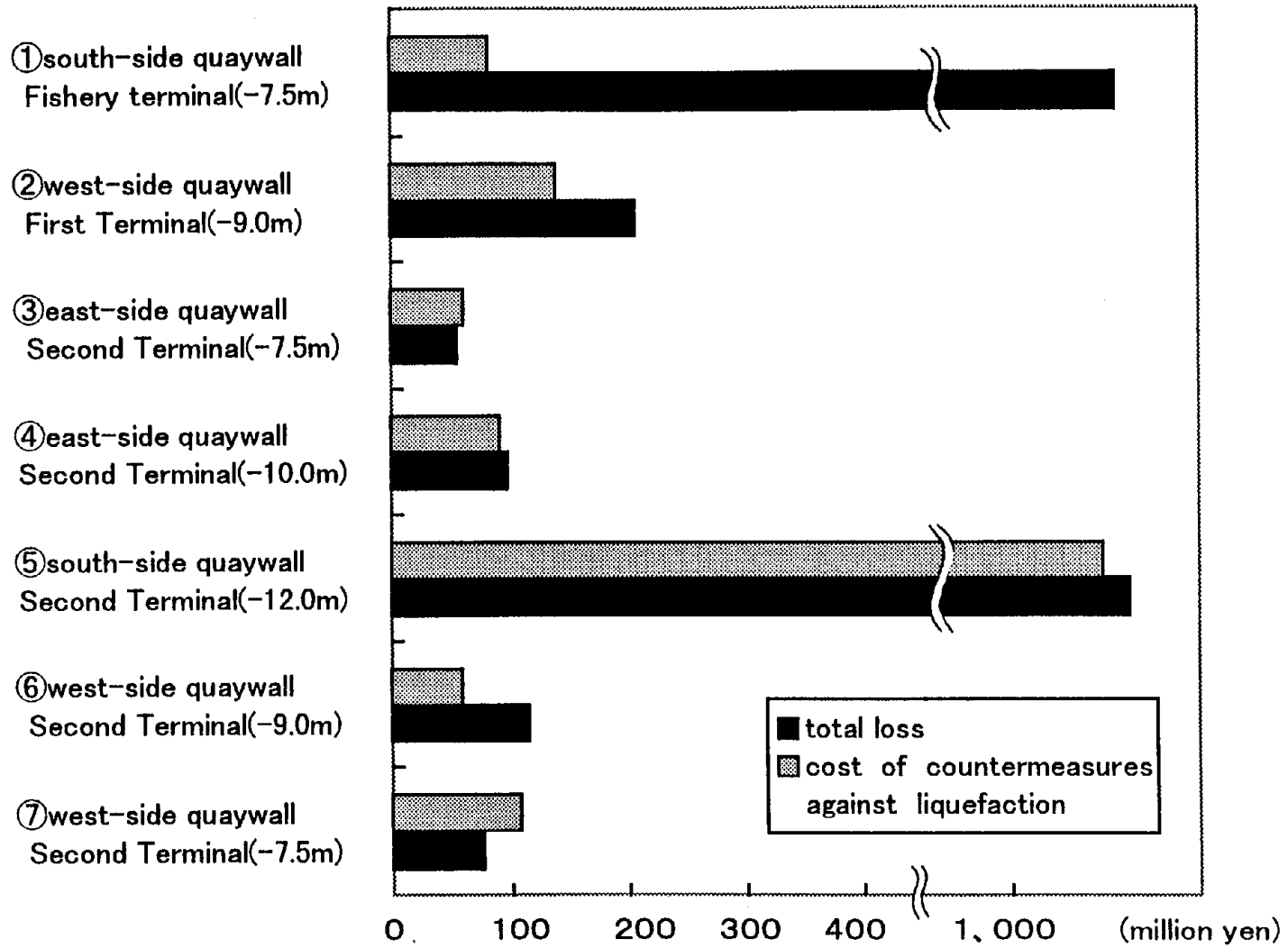


Fig.10 Results of cost-benefit analysis

At first, for [Scenario B], the sum of the cost of repair work and the loss of economy is evaluated. In the restoration work after the earthquake, countermeasures against liquefaction were taken. Table 3 shows the total cost of repair including cost of countermeasures, cost of countermeasures (C1) and net cost of repair work (B1) for each quaywall. Loss of regional economy due to each quaywall is already obtained in the above investigation. Table 4 shows the net cost of repair work (B1), loss of economy (B2) and the sum of them(B) for each quaywall.

Secondary, for [Scenario A], cost of countermeasures against liquefaction is evaluated. Here we take the advantage of the fact that countermeasures against liquefaction were actually taken for these 7 quaywalls after the earthquake to know the realistic cost of countermeasures. Table 4 shows net cost of countermeasures (C1), which coincides with C1 in Table 3, additional cost(C2) which is necessary to take countermeasures alone(not together with repair work) and total cost of countermeasures(C).

Finally, B and C are compared for each quaywalls in Table 4 and Fig.10. We can conclude that economic rationality of countermeasures against liquefaction was recognized for at least 5 quaywalls among 7 facilities at Kushiro port. For the rest two quaywalls, the cost C is larger than the loss B by only little margin.

CONCLUSIONS

In this research, the loss of economy at Kushiro Port due to the Kushiro-oki Earthquake in 1993 was investigated by means of interview and questionnaires. Based on the results, economic rationality of countermeasures against liquefaction are investigated using cost-benefit analysis. Results of this study is summarized as follows. The loss of economy at Kushiro Port due to the 1993 Kushiro-oki Earthquake was at least 250,902,000 Yen including 60,000,000 Yen for "port-dependent industries" and 190,902,000 Yen for "port-related industries". Even when the damage to the quaywall itself is slight, the damage to cargo-handling equipment tends to bring impacts to regional economy. Economic rationality of countermeasures against liquefaction was recognized for 5 among 7 facilities at Kushiro port.

ACKNOWLEDGEMENT

The authors are grateful for the people of port-related and port-dependent industries who took time and cooperated in the interviews and questionnaires. The authors wish to express their thanks to the people of Hokkaido Development Bureau and Kushiro City Government, who helped us a lot in the investigation of loss of economy. The authors also thank to late Mr. Hisashi Takada and Mr. Jyunpei Jindai of Kumashiro System Design Co., Ltd. and Mr. Kunihiro Amakuni and Kosuke Masunaga of Pacific Consultants Co., Ltd. who helped us in the investigation.

REFERENCES

- 1) Ueda, S., Inatomi, T., Uwabe, T., Iai, S., Kazama, M., Matsunaga, Y., Fujimoto, T., Kikuchi, Y., Miyai, S., Sekiguchi, S. and Fujimoto, Y. (1993) : "Damage to Port Structures by the 1993 Kushiro-oki Earthquake", Technical Note of the Port and harbour research Institute, Ministry of Transport, Japan, No.766, Dec. 1993 (in Japanese).
- 2) Nozu, A., Uwabe, T., Sato, Y. and Shinozawa, T. (1997) : "Relation between Seismic Coefficient and Peak Ground Acceleration Estimated from Attenuation Relation", Technical Note of the Port and harbour research Institute, Ministry of Transport, Japan (in print) (in Japanese).
- 3) Nozu, A., Uwabe, T. and Sano, T. (1997) : "Economic Damage at Kushiro Port due to the Kushiro-oki Earthquake and Cost-benefit Analysis on Economic Rationality of Countermeasures against Liquefaction", Technical Note of the Port and harbour research Institute, Ministry of Transport, Japan, No.879, Sep. 1997 (in Japanese).

PERSONAL CAREER

NAME: Atsushi Nozu

POSITION: Research Engineer,
Earthquake Disaster Prevention
Laboratory, Structural Division,
Port and Harbour Research Institute
Ministry of Transport

ADDRESS: 3-1-1 Nagase Yokosuka 239, Japan
Tel: +81-468-44-5030
Fax: +81-468-44-0839
e-mail: nozu@ipc.phri.go.jp



DATE OF BIRTH: January 6, 1968

EDUCATION: Bachelor(1991) and Master Degree(1993) of Engineering, Kyoto University

MAJOR SUBJECT: Attenuation relation for peak ground motions in Japan.
Seismic hazard in Japanese coastal area.
Shaking table tests and numerical analysis on the behavior of
floating structure during earthquake.

MAJOR AREA OF EXPERIENCE:

1993-present Research Engineer of Earthquake Disaster Prevention Laboratory,
Structural Division, Port and Harbour Research Institute

TRAVEL ABROAD: USA, MEXICO

MAJOR PUBLICATIONS:

Experimental Research on Behavior of Floating Structure with Tension
Leg, 1997 (in Japanese)
Deformation of Gravity-Type Quaywall and Frequency Contents of
Ground Motion, 1997 (in Japanese)

1992 1993 1992 1993

1992 1993 1992 1993

1992 1993 1992 1993

1992 1993 1992 1993

1992 1993 1992 1993

1992 1993 1992 1993

1992 1993 1992 1993

1992 1993 1992 1993

In this report, cost indicated by * is considered to be loss of economy.

•

•

DAMAGE TO BRIDGES FROM THE NORTHRIDGE EARTHQUAKE AND ITS CONSEQUENCES ON HIGHWAY SYSTEM PERFORMANCE

Nesrin Başöz¹ and Anne S. Kiremidjian²

¹Senior Staff Engineer, K2 Technologies Inc.

²Director and Professor, The John A. Blume Earthquake Engineering Center, Stanford University

ABSTRACT

Recent tornadoes, hurricanes and earthquakes that caused significant life and property losses have demonstrated the risks associated with natural hazards. These disasters have emphasized the vulnerability of lifeline systems and the need to mitigate the risk consequent to failure of these systems. In particular, the need to mitigate seismic risk to highway bridges has become evident after recent earthquakes. The 1994 Northridge, California earthquake damaged several bridges, in some instances resulting in severe disruptions to the highway system of the region. The Northridge earthquake provided valuable information for evaluating the seismic performance of bridges and the performance of the highway system, which was disrupted due to bridge failures.

This paper presents results from studies on earthquake damage to bridges from the Northridge earthquake and its consequences on the performance of the highway system. About two percent of the bridge inventory exposed to significant ground shaking experienced damage. Only six bridges in the area collapsed. The ground shaking levels and soil types at bridge sites were obtained within GIS. The analyses of data on bridge damage showed that concrete structures designed/built with older design standards were more prone to damage under seismic loading. The ground shaking level, skew angle, abutment type, pier type and span continuity were found to be the structural characteristics that showed the highest correlation with observed damage. The total estimated repair cost was about \$150 million. Repair and/or reconstruction of the collapsed structures formed about seventy five percent of the total repair cost. Network connectivity analyses were performed to identify critical structures and potential time delays and to determine all possible alternate routes in the highway system in the affected area. The results from the analyses were presented using GIS.

INTRODUCTION

Lifeline systems are vital for the daily activities of a society. Especially for fast recovery after a natural disaster, such as an earthquake, the availability and functionality of lifeline systems are crucial. Damage sustained by lifelines can cause significant economic losses mainly due to service disruption. Lifeline systems have functional interaction among themselves. After an earthquake the interaction between different lifelines becomes more evident. This interaction may exacerbate decreases in the capacities of lifelines throughout the disaster sequence. For example, malfunctioning of the transportation system is a hindrance to recovery since mobility essential to the restoration process.

Seismic risk to lifeline systems and its consequences can be reduced by means of mitigation, emergency response planning and management and effective recovery efforts. Assessment of damage to highway systems from an earthquake and the estimation of consequent losses provide valuable information for these activities. A risk assessment methodology for highway transportation systems was developed by Basöz and Kiremidjian [1996]. The methodology is intended to serve as a tool in the decision process for:

- retrofitting critical components of a lifeline system as a means of pre-disaster risk mitigation,
- pre-disaster emergency response planning,
- emergency response operations immediately after the disaster.

The methodology is based on the vulnerability and importance assessment of highway transportation systems.

The vulnerability assessment includes hazard analysis, classification of the critical components of interest, such as bridges or tunnels, and fragility analysis. It evaluates the seismic response of bridges in the system. With the large number of existing bridges, it is rather difficult, if not impossible, to evaluate the seismic response of each individual bridge in detail. In order to evaluate the seismic response of a large number of bridges, bridges can be grouped into different classes according to their structural characteristics. Then, generic ground motion-damage relationships can be employed to assess the vulnerability of bridges in the highway system.

The vulnerability assessment of a bridge can be expressed for different damage levels. Most of the time, damage states are expressed qualitatively, such as minor, moderate and major damage, without any consensus on their definitions. Vulnerability of bridges is expressed in terms of Damage Probability Matrices (DPMs) and fragility curves, for the ATC-13 [1985] and NIBS [RMS, 1995] bridge classes, respectively.

In order to link the vulnerability and importance assessment, the consequences of physical damage to bridges are quantified. The vulnerability assessment determines the likelihood of a bridge being in a certain damage state under given seismic loading. These physical damage states should be associated with bridge *functionality levels* in order to evaluate the consequences of failure of a bridge, such as life safety, effectiveness and efficiency of emergency response and socioeconomic

impacts. For assessment of the importance criterion, network analyses that evaluate the system performance are conducted. Decision analysis methods are used both to integrate engineering, economic and social factors to assess the importance criterion and to combine the vulnerability and importance criteria. The synthesis of engineering, economic and social factors that influence risk reduction decisions is based on multi-attribute utility theory. Connectivity and serviceability network analyses are conducted such that these decisions are based on the system performance as well as the component functionality.

Data on bridge damage from earthquakes are becoming increasingly more available. Such data, however, have not been systematically studied with the objective to evaluate damage characteristics and to correlate damage and repair cost to ground motion levels. The 1994 Northridge, California earthquake has provided valuable information. Data on bridge damage from the Northridge earthquake were studied as part of a project sponsored by NCEER with funding provided by the Federal Highway Administration. In another project sponsored by National Science Foundation, damage data from the Northridge earthquake were also used to model post-earthquake conditions and to evaluate the adequacy of the developed network models to represent a real highway system. In this paper, some of the results from these studies are presented.

EVALUATION OF BRIDGE DAMAGE DATA FROM THE NORTHRIDGE EARTHQUAKE

Data on bridge damage from the Northridge earthquake were studied to correlate observed bridge damage to: (i) structural characteristics of a bridge, (ii) local ground motions, and (iii) repair cost. In order to achieve these objectives, first an inventory of bridges in the Greater Los Angeles area and bridge damage and repair cost data from the Northridge earthquake were compiled. Statistical analyses on structural characteristics of bridges, ground shaking levels at bridge sites, damage characteristics and repair cost were performed. Then, bridges were grouped based on their structural characteristics. Empirical damage probability matrices and fragility curves were developed from data on bridge damage for different classes of bridges. In addition, correlation between structural characteristics and observed damage was determined.

Analysis Method for Bridge Damage Data

Characteristics of the Database

The database compiled for the Northridge earthquake consisted of five types of data: (i) structural characteristics, (ii) bridge damage, (iii) repair cost, (iv) ground motion levels at bridge sites, and (v) soil types at bridge sites. A commercial relational database management system (RDBMS), dBase™, was used to compile and perform queries for data on damage and structural characteristics of bridges. In addition, a geographic information system (GIS), Arc/Info™, was used to obtain the ground motion levels and soil types at each bridge site.

Structural Characteristics: Several structural characteristics of bridges were compiled in a database for the groups of bridges that were exposed to ground shaking in the Northridge earthquake. These structural characteristics include abutment type, number of spans, type of superstructure and

substructure, length and width of the bridge, skew, number of hinges at joints and bents, abutment and column foundation types, and design year to represent design standards, such as column reinforcement and seat width. These structural attributes were obtained from the Structural Maintenance System (SMS) database compiled and managed by Caltrans. In addition, more detailed information on structural characteristics was obtained from Caltrans for some of the damaged bridges. Caltrans is currently in the process of compiling a database that includes information on abutment, column/pier and footing details, such as seat width and type of bearings, footing type and column/footing connection. However, only about 15 percent of all the California bridges are currently in this database and hence, the detailed information in this database could not be used in the statistical analyses.

Bridge Damage: Detailed damage descriptions and the corresponding damage states were compiled for damaged bridges. The damage descriptions were obtained mainly from bridge damage reports compiled by Caltrans [1994] and were cross-referenced with those provided by Buckle [1994], Earthquake Engineering Research Institute [1995], and Yashinsky [1995]. Judgment was used to treat inconsistencies in these sources.

Damage State Definitions: Currently, no guidelines for evaluating physical bridge damage exist. Four damage states (*minor, moderate, major* and *collapse*) were used in reporting bridge damage from the Northridge earthquake. The terms *minor, moderate* and *major* damage are subjective. Definitions of damage states for columns, abutments, and joints and connections for concrete bridges were proposed which were based on the observed bridge damage in the Northridge earthquake [Basöz and Kiremidjian, 1996].

Repair Cost: The estimated repair cost values for bridges damaged in the Northridge earthquake were compiled in a database. These estimated repair costs were obtained from supplementary bridge reports compiled by Caltrans following the earthquake. The database includes total estimated repair cost and a more detailed information on repair work and cost for each bridge that has been repaired. The repair cost ratio, defined as the ratio of repair cost to replacement cost of a bridge, was calculated for all the damaged bridges.

Ground Motion Levels and Soil Type: In addition to structural characteristics, soil type at each bridge site and peak ground acceleration (PGA) levels observed in the Northridge earthquake were compiled. In order to obtain empirical ground motion-damage relationships for the bridges damaged in the Northridge earthquake, two sets of peak ground acceleration (PGA) values were used as the ground motion levels: (i) PGA values reported by USGS [1994], and (ii) PGA values reported by WCFS [1995]. Figure 1 shows the recorded PGA values [USGS, 1994] and the state bridges in the four counties. The PGA value at a given bridge site is obtained within GIS by overlaying the ground shaking map and the bridge location map. Subsequently, the highest PGA values obtained at a bridge site were 1.55g and 0.66g for the USGS and WCFS maps, respectively. Since the PGA levels from the two data sets varied considerably the correlation studies are performed for both data sets. The soil types were obtained from USGS surface geology maps.

Classification of Bridges

The compiled inventory of bridges was reviewed to: (i) select bridges to be used in correlation studies, (ii) select structural characteristics (attributes) that best describe the seismic response of

bridges, and (iii) verify the correctness of the attribute values included in the bridge inventory database.

Data Sets: Several data sets were used for statistical analyses. All the analyses were performed for the state bridges since most of the reported damage pertained to state bridges while only a few local bridges sustained damage. First, all highway state bridges were selected and were gathered in the *highway bridge data set*. Statistics on design year and ground shaking levels were obtained for this data set. Most of the bridge damage pertained to concrete structures. Therefore, concrete bridges were selected from the *highway bridge data set*.

One of the objectives of the study was to identify the effect of various structural characteristics on bridge damage susceptibility. Two structural characteristics were considered: Abutment type and number of columns per bent. In order to determine the effect of each characteristic, only bridges with homogeneous structural characteristics were selected from the *concrete highway bridge data set* and the new data set was referred to as the *homogeneous data set*. For the purpose of this study, bridges with single abutment type and one column bent type were defined as homogeneous. For example, a bridge with both multiple and single columns bent was defined as a *heterogeneous* bridge, and was excluded from the *homogeneous data set*. Bridges with incomplete information were also excluded from this data set.

The available ground shaking maps for Northridge earthquakes are limited to certain geographic areas and do not cover the locations of all bridges that were exposed to lower ground shaking levels. A complete data set for correlation analyses requires that all the bridges exposed to a given ground shaking level be included in the data set. In order to satisfy this requirement, PGA of 0.15g was selected as a threshold value. This PGA level was determined based on the available ground motion maps. Bridges that were exposed to PGA of 0.15g or higher were extracted from the *homogeneous data set* and the new data set was referred to as the *correlation data set*.

The bridges in the *correlation data set* were grouped first by the superstructure type and substructure material. Then, these bridges were further classified into sub-categories based on other structural characteristics, such as number of spans, abutment type, column bent type and span continuity. The damaged bridges were classified into these sub-categories in order to group bridges that are expected to experience similar damage levels under a given seismic loading. Bridges were also grouped using the bridge classifications defined by the National Institute of Building Sciences (NIBS) Technical Manual [RMS, 1996] and ATC-13 [1985]. The NIBS classification was used to compare the empirical fragility curves obtained in this study to those provided in NIBS. The ATC classification was used to compare the repair cost ratios to damage probability matrices (DPMs) provided in ATC-13 [1985].

Correlation Studies

Correlation analyses were performed using the data on bridge damage and repair cost to accomplish the following objectives:

- (i) To determine the structural characteristics that best represent damage such that bridges can be grouped using these characteristics
- (ii) To obtain ground motion-damage relationships for bridges with similar structural characteristics

- (iii) To obtain ground motion-repair cost ratio relationships to estimate direct economic losses due to damage to bridges
- (iv) To correlate damage and repair cost ratio.

The data on bridge damage were compiled in the form of damage matrices. Then, the damage probability matrices (DPMs), i.e., the probability of being in a damage state given the ground motion level were obtained for each group of bridges. The damage matrices were used as input data to logistic regression analysis to obtain empirical fragility curves both unconditional and conditional on damage. Similar procedures were used to obtain ground motion-repair cost ratio relationships. The goal of logistic regression analysis is to find the best fitting and model to describe the relationship between a discrete outcome values and a set of independent variables. The fit of the model is then appraised, and the coefficients are evaluated to indicate the impact of the individual variables. In this study, the statistical software package SAS is used to perform the logistic regression analysis.

Example Statistics and Results

The bridges in the Greater Los Angeles area, including Los Angeles, Ventura, Riverside, and Orange Counties, were exposed to ground shaking during the 1994 Northridge earthquake. Table 1 lists the number of state and local bridges and the number of damaged state bridges in each of the four counties. Of the 3,533 state bridges, a total of 233 bridges were reported as damaged. The bridge damage from the Northridge earthquake pertained mostly to state bridges in Los Angeles and Ventura Counties. Bridges in these two counties also experienced much higher accelerations in the Northridge earthquake than bridges in Riverside and Orange Counties. Figure 2 shows the distribution of state highway bridges in four counties by design year. Seventy six percent of the state highway bridges were designed by pre-1971 design standards. Figure 3 shows the distribution of damaged bridges by design year and damage state. Seventy seven percent of the damaged bridges were designed with pre-1971 design standards.

Majority of the bridge inventory in the four counties is concrete structures and about 90 percent of the bridges damaged in the Northridge earthquake were concrete structures. Figure 4 shows empirical fragility curves developed for multiple span concrete bridges. Comparison of the data points to the empirical fragility curves is also shown in this figure. Empirical ground motion damage relationships were obtained for concrete bridges grouped by three structural characteristics: abutment type (*monolithic, non-monolithic* and *bin or cellular closure type*), column bent type (single columns per bent, multiple columns per bent and pier walls) and span continuity. Using these structural characteristics, twenty-one bridge sub-categories (3 for single span bridges and 18 for multiple span bridges) were defined and empirical fragility curves were developed for these sub-categories [Basöz and Kiremidjian, 1997]. For example, the empirical fragility curves showed that the probability of exceeding a given damage state at any given PGA was higher for a single span bridge with non-monolithic type abutments than it was for single span bridges for monolithic type abutments. Similarly, the probability of exceeding a given damage state was found to be higher for multiple span bridges with monolithic type abutments, continuous spans and multiple column bents than those with non-monolithic type abutments, continuous spans and multiple column bents.

The correlation studies were also carried out using the bridge classification defined by the National Institute of Building Sciences (NIBS) Manual [RMS, 1995], and ATC-13, [1985]. The observed damage data do not appear to agree well with the available ground motion-damage relationships in the majority of the cases investigated in this study. The NIBS fragility curves, in general, overestimated the exceedance probabilities for any given damage state [Basöz et al., 1997].

In addition, unconditional and conditional (i.e., given a bridge is damaged) empirical fragility curves were developed for bridges grouped by design year, number of spans, type of abutment, type of column bent and retrofit history. As an example, Figure 5 shows the comparison of probabilities of exceeding different damage states for bridges with multiple column bents, single column bents and pier walls. Bridges with single column bent had the worst performance among the three column bent types.

An extensive database on *repair cost* was compiled from the supplementary bridge reports obtained from Caltrans [1994]. The database includes total estimated repair cost and a more detailed information on repair work and cost for 130 bridges in Los Angeles and Ventura Counties. A total of about \$150 million was reported as repair cost in these reports. The total repair cost for the six collapsed bridges constitute seventy five percent of the repair cost of all damaged bridges. Table 4 shows the estimated repair cost of damaged bridges by damage states. Data on component repair costs were not reported for all bridges. Figure 6 shows the distribution of repair cost by bridge components for different damage states. The collapsed bridges were not included in this figure since a detailed description of repair by component type was not available for those bridges. According to Figure 6, most of the bridges with *minor* damage experienced approach settlement. Bridges with *minor* damage did not suffer damage to the columns or joints. While approach settlement was not reported for bridges that suffered *moderate* damage, the damage to abutments was the most significant type of damage for these bridges. Although abutment damage contributed significantly to repair cost for bridges with *major* damage, the highest repair cost for bridges with *major* damage was due to column damage. Damage to joints was observed mostly in bridges with *major* damage. The total repair cost for bridges that suffered *major* damage was more than 15 times than for those with moderate damage. Under *miscellaneous* repairs, repair to railings, curbs, sidewalks and electrical conduits were included.

Similar to ground motion-damage relationships, fragility curves were developed to represent ground motion-repair cost ratio relationships. The repair cost ratio, also known as the damage factor, was defined as the ratio of repair cost to replacement cost. Figure 7 shows an example of the ground motion-repair cost ratio curves for multiple span bridges. When the ATC-13 DPMs were compared with the observed repair cost ratios from the Northridge earthquake, it was found that the ATC-13 DPMs agree quite well with the observed damage and the repair cost ratios for low MMI values. In most cases for MMI values VII and higher ATC-13 DPMs overestimated the observed values from the Northridge earthquake.

PERFORMANCE OF HIGHWAY SYSTEMS IN THE NORTHRIDGE AREA

The application of the methods developed for emergency response planning and management activities were illustrated for the Northridge area to: (i) determine all available fastest paths and

associated time delays for given origin-destination points, (ii) determine the fastest path to disaster areas in the damaged system immediately after the earthquake, (iii) investigate the benefits of multiple resource locations, (iv) estimate the functionality of the network during the emergency response period. Results for the first two applications are presented in this paper. For emergency response period activities, the bridges that experienced total collapse or severe damage were grouped as *inaccessible* (or nonfunctional). Bridges with *moderate* or *minor* damage are assumed to be functional during this period.

Connectivity network analyses were conducted to identify alternate routes for various origin-destination (*OD*) sets. For both of the *OD* sets listed in Table 3, fastest paths and critical bridge sets were identified. All the city streets in the area were considered in the network analyses. For the second *OD* set, the connectivity of the system is retained by the arterial system even after several bridges become inaccessible. For the first *OD* set, however, the connectivity of the system is disrupted when several pairs of bridges failed simultaneously. Figure 8 shows the ten bridges that were determined to be part of at least one critical bridge set for *OD* set 1. No single bridges was determined to be critical for any of the origin-destination sets. The pre- and post-earthquake routes for *OD* set 1 are also shown in Figure 8.

Emergency Response Planning: Figure 9 shows some of the possible alternate routes and the associated time delays for *OD* set 2. In case of failure of any set of bridges, the system connectivity was maintained via one of these routes. Part of an emergency response plan might be to allocate resources at different locations before the earthquake in order to insure accessibility of the disaster areas. To illustrate this, an example for an *OD* set in the vicinity of the I-5/SR14 interchange was studied for single and multiple origin points [Basöz and Kiremidjian, 1996]. Multiple origin points provided more redundancy for the highway system.

Emergency Response Management: In order to simulate the conditions immediately after the earthquake, a routing from the Office of Emergency Services in Pasadena to the 1994 Northridge Earthquake epicenter area is performed. Bridges that experienced major damage or collapsed in the 1994 Northridge Earthquake [Caltrans, 1994] are considered to be inaccessible. Then, the fastest path to the destination point is determined. The pre-and post-earthquake routes determined by the network analysis are depicted in Figure 10.

CONCLUSIONS

The Northridge earthquake provided valuable information to evaluate bridge damage and its impact on the performance of the highway system. Only about two percent of the bridges that were subjected to significant ground shaking experienced damage and only 6 of these bridges collapsed. Most of the damaged bridges were designed by pre-1971 design standards. Bridges with non-monolithic abutment types, in-span hinges and single column bents performed poorly as also observed in previous earthquakes.

Data from the Northridge earthquake were analyzed to identify structural characteristics that best represent seismic performance of bridges. The analyses show that structural characteristics used in defining bridge classes were highly correlated with observed damage. Particularly, structural material and type, skew, span continuity, abutment type, PGA levels and number of spans were

found to correlate well with the observed damage. These include the characteristics used in the classification by Basöz and Kiremidjian [1996] and suggest that data show good agreement with the structural characteristics used in that bridge classification.

Empirical fragility curves were obtained for concrete bridges grouped by these structural characteristics. The fragility curves developed in this study should be modified, as more data become available. The empirical fragility curves developed in this study can be used as the prior information in a Bayesian updating. Currently available bridge classes and the corresponding ground motion-damage relationships were also compared with the observed damage, however, little agreement was found for most cases.

In addition to bridge classes, damage states for components of concrete bridges were defined. The damage state definitions proposed in this research can be used to: (i) develop analytical fragility curves, (ii) to assess the vulnerability of bridges, and (iii) to develop a post-earthquake investigation form that will assist to compile data on bridge damage more consistently than the current practice.

Repair cost estimates for different components were obtained for different damage states. Repair cost ratio-ground motion relationships were developed for bridges grouped by various structural characteristics. The observed repair cost ratio for single span bridges was not more than 10 percent while for multiple span bridges repair cost ratios as high as 50 percent were observed.

The performance of highway system in Los Angeles County was also evaluated using ground motion and bridge damage data from the Northridge earthquake. The methods developed for emergency response planning and management activities proved to be very efficient for applications to large areas. These methods integrate vulnerability assessment of the components in the system with the analyses for system performance. Examples of different conditions that involve disruption in the system during post-earthquake period were modeled using these methods. The results can be used to prepare a response plan, which includes strategic planning options for immediate consideration and action. The information on the observed damage in the system, however, is crucial for the utilization of the method. When this information is available, the method can be used to re-route the emergency response crews efficiently to the disaster areas immediately after the earthquake.

A comprehensive database was compiled for the Northridge earthquake. This database includes information on bridge damage and the structural characteristics that are important for vulnerability assessment of bridges. This type of a database provides an essential base to improve our understanding of bridge damage from past earthquakes. The risk assessment methodology used in this study can be applied prior to major future events to develop policies for disaster mitigation and strategies for emergency response.

ACKNOWLEDGMENTS

The authors would like to thank bridge engineers from the Structure Maintenance and Investigation Division for their help in providing the bridge damage and inventory data. The discussions with Dr. Ian G. Buckle are highly appreciated. This research was partially supported by NCEER Grants 91-3521A and 92-4401, NSF Grant EID 9021032 and CMS-9416420; and NCEER Federal Highway Project.

REFERENCES

- ATC-13, [1985]. *Earthquake Damage Evaluation Data for California*, Report ATC-13, Applied Technology Council, Redwood City, CA.
- Basöz, N. [1996]. *Risk Assessment for Highway Transportation Systems*. Ph.D. Dissertation, Department of Civil Engineering, Stanford University. (July).
- Basöz, N., and A. S. Kiremidjian. [1997]. *Evaluation of Bridge Damage Data from Recent California Earthquakes*, to be submitted to NCEER.
- Basöz, N., A. S. Kiremidjian, S. A. King, and K. H. Law. [1997]. "Characteristics of Bridge Damage in the 1994 Northridge, CA Earthquake.", submitted to *Earthquake Spectra*.
- Buckle, I. G. [1994]. *The Northridge, California Earthquake of January 17, 1994: Performance of Highway Bridges*, Technical Report NCEER-94-0008.
- California Department of Transportation, (Caltrans). [1994]. *The Northridge Earthquake*, Caltrans PEQIT Report, Division of Structures, Sacramento, CA.
- EERI. [1995]. *Northridge Earthquake of January 17, 1994 Reconnaissance Report*, Earthquake Spectra, Earthquake Engineering Research Institute, Oakland, CA.
- RMS. [1995]. *Development of a Standardized Earthquake Loss Estimation Methodology*. Prepared for National Institute of Building Sciences by Risk Management Solutions, Inc., Menlo Park, CA.
- USGS. [1994]. US Geological Survey, *Open-File Report 94-197*. Menlo Park, CA.
- Yashinsky, M., P. Hipley, and Q. Nguyen. [1995]. *The Performance of Bridge Seismic Retrofits During the Northridge Earthquake*. Caltrans Office of Earthquake Engineering, Sacramento, CA.
- WCFS. [1995]. *Contoured Ground Motion Parameters for the 1994 Northridge Event*. ASCII files.

TABLE 1. Distribution of State and Local Bridges and the Number of Damaged State Bridges in the Greater Los Angeles Area

County	Number of State Bridges	Number of Local Bridges	Total Number of Bridges	Number of Damaged Bridges
Los Angeles	2097	1553	3650	228
Riverside	644	338	982	-
Orange	463	505	968	-
Ventura	329	175	504	5

TABLE 2. Distribution of Estimated Repair Cost by Damage State

Damage state	Estimated repair cost
collapse	\$121,765,750
major	\$18,398,057
moderate	\$6,895,731
minor	\$446,950

TABLE 3. Origin-Destination Sets for Emergency Response Analysis

<i>OD Set No</i>	Origin(s)	Destination
1	Sherman Oaks Hospital	Northridge Meadows Apartments
2	Kaiser Permanente Hospital	Holy Cross Hospital

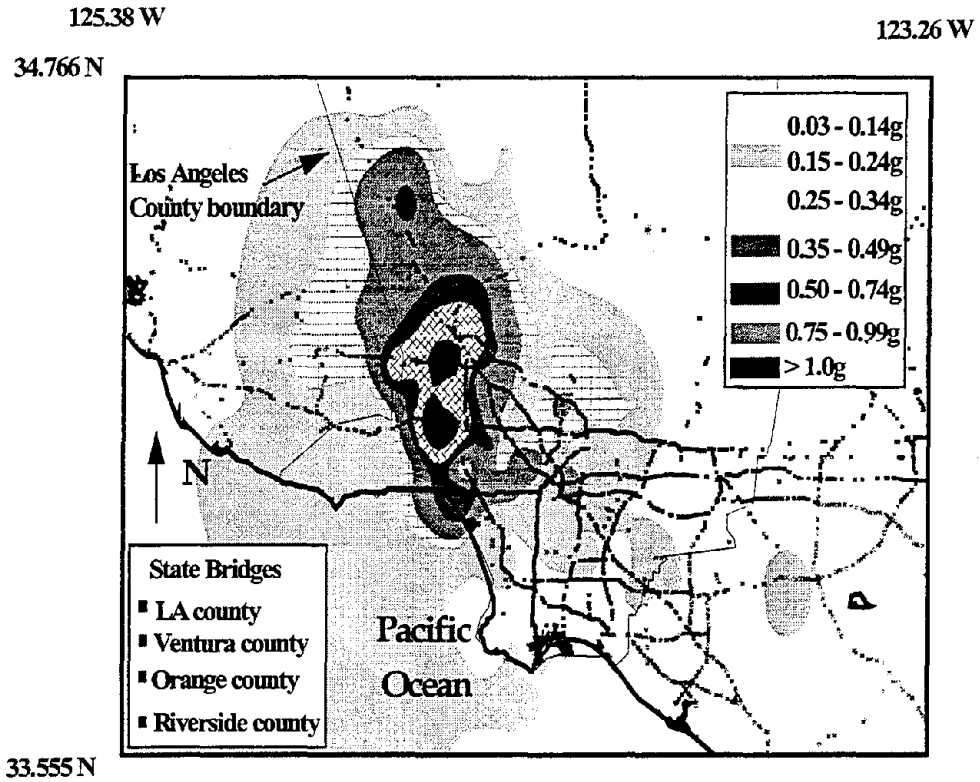


FIGURE 1. PGA levels observed in the Greater Los Angeles area from the Northridge earthquake [USGS, 1994]

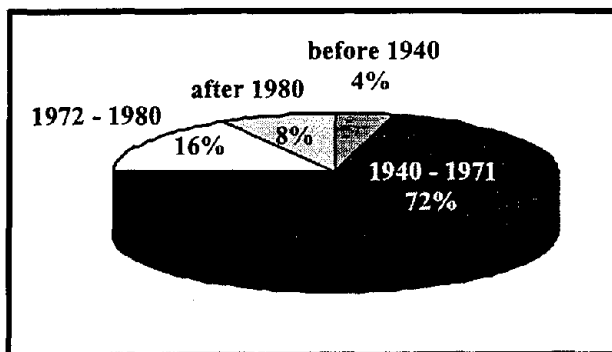


FIGURE 2. Distribution of State Highway Bridges in Los Angeles, Ventura, Orange and Riverside Counties by Design Year

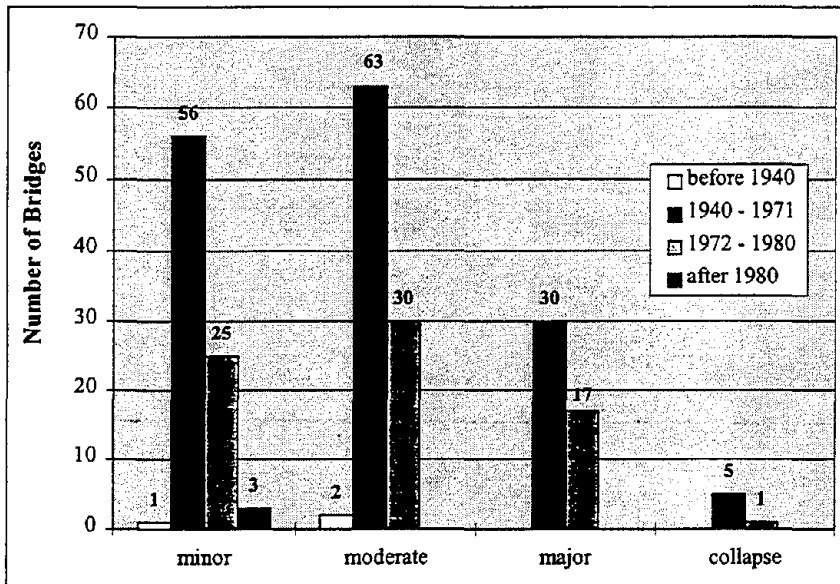


FIGURE 3. Distribution of All Damaged Bridges by Design Year and Damage State

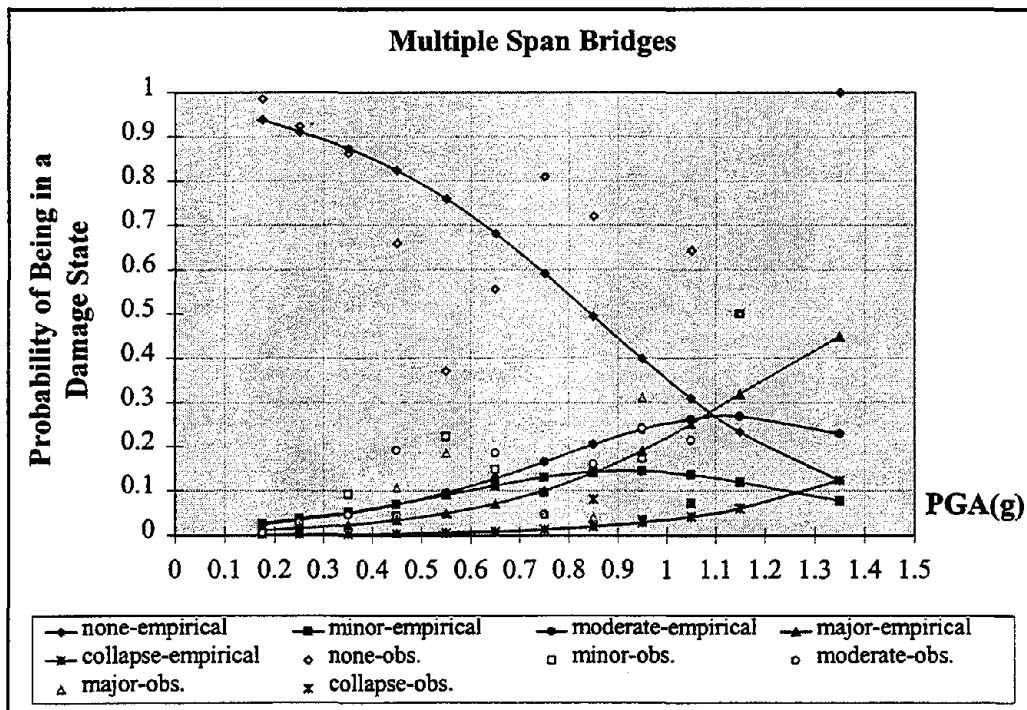


FIGURE 4. Empirical Fragility Curves and Observed Data for Multiple Span Bridges for Different Damage States

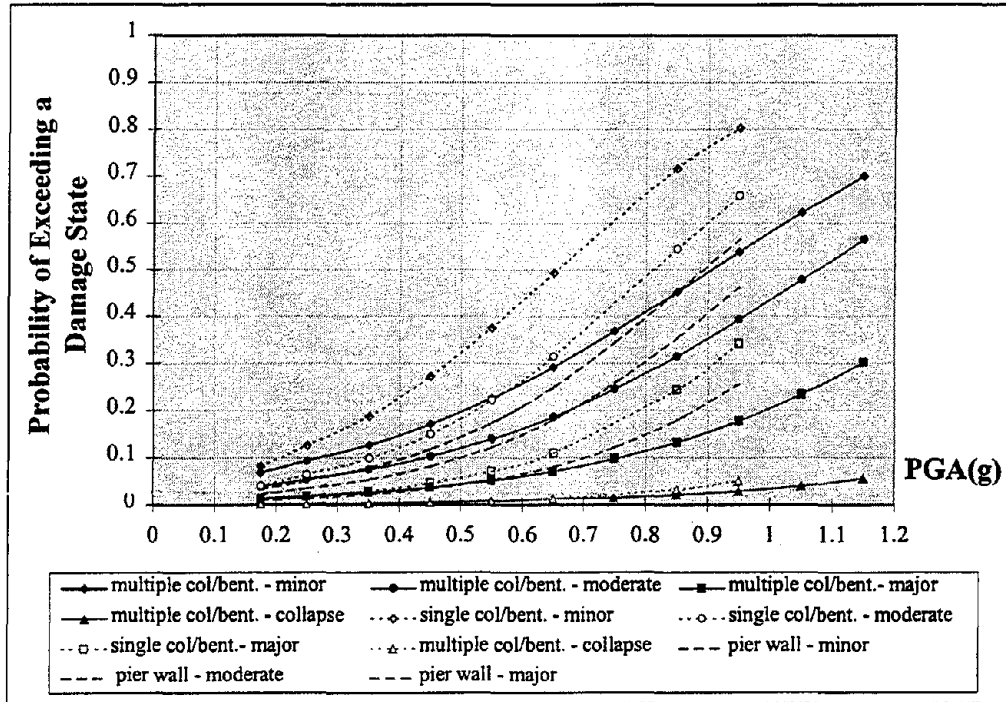


FIGURE 5. Performance Comparison of Different Types of Column Bents

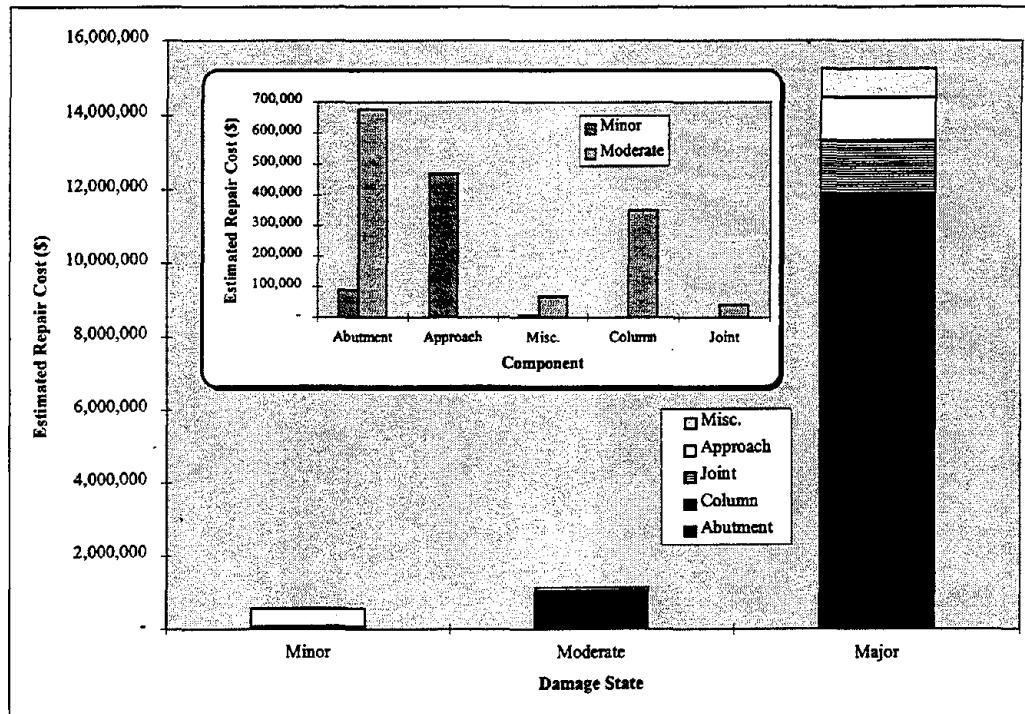


FIGURE 6. Distribution of Estimated Repair Cost by Bridge Components for Different Damage States

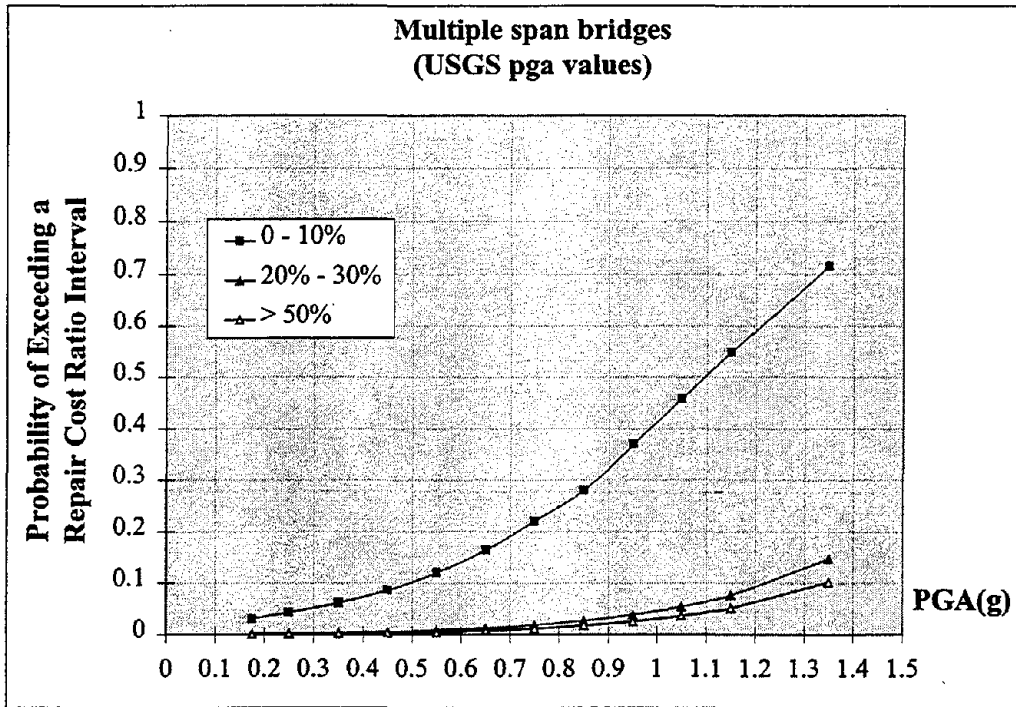


FIGURE 7. Empirical Fragility Curves for Multiple Span Bridges, Unconditional on Repair Cost Ratio

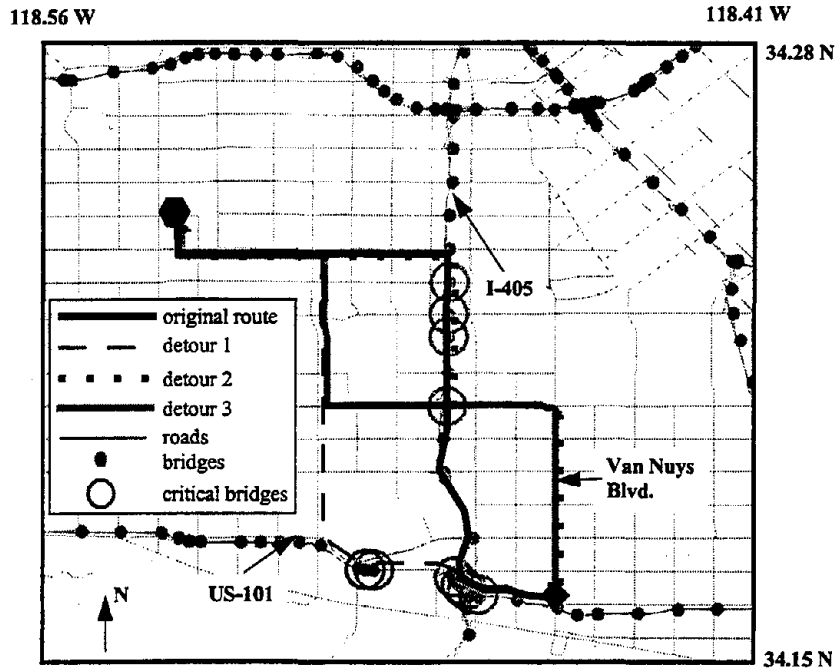


FIGURE 8. Critical Bridges and Fastest Paths for OD Set 1

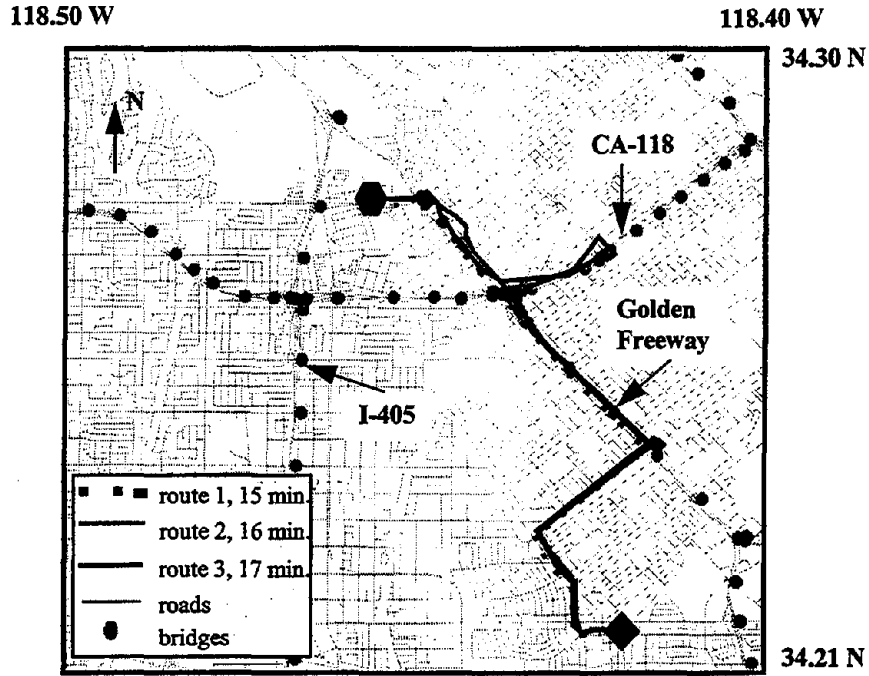


FIGURE 9. Fastest Paths and Travel Times in Minutes for OD Set 21

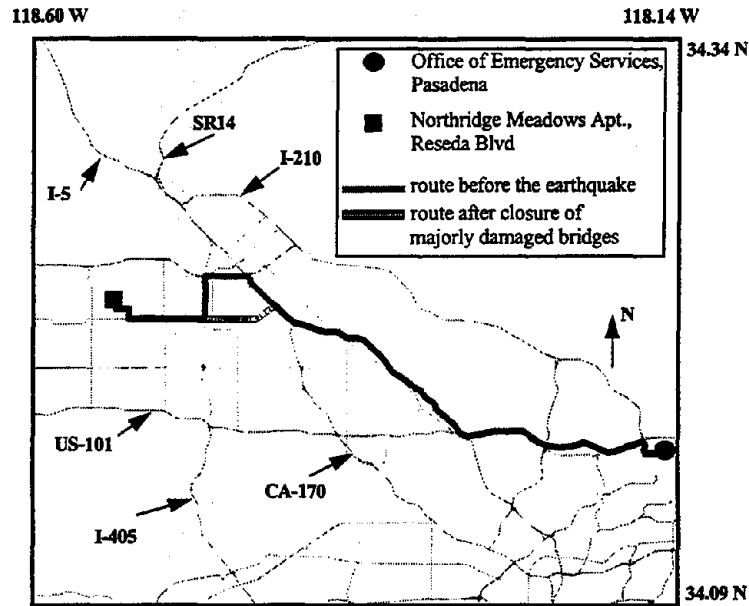


FIGURE 10. Pre- and Post-earthquake Fastest Routes from OES to 1994 Northridge Earthquake Epicenter Area

¹ The diamond and the hexagon signs depict the origin and destination points, respectively.

NESRIN I. BASOZ

Date of Birth: 12/05/1968

Birthplace: Ankara, Turkey

Education: Degrees

Middle East Technical University, B.S.,
Civil Engineering, 1990

Middle East Technical University, M.S.,
Civil (*Structural*) Engineering, 1992

Stanford University, Ph.D.,
Civil (*Structures and Geomechanics*) Engineering, 1996



Position:

Senior Staff Engineer
K2 Technologies, Inc
4000 Moorpark Ave. Ste. 215
San Jose, CA 95117

Dr. Basöz is currently working within a team of engineers on catastrophic loss modeling and insurance loss estimation for natural hazards.

Previously, Dr. Basöz worked as a post-doctoral researcher at Stanford University (7/96 – 1/97). During this period, she conducted research on bridge damage in Loma Prieta and Northridge earthquakes sponsored by NCEER with funding from FHWA and consulted on geographic information system (GIS) applications for a research project on Reliability and Restoration of Water Supplies Following Earthquakes sponsored by NIST. For her doctoral work (9/92 – 7/96) she developed a methodology for risk assessment of transportation highway systems specifically for emergency response management and bridge prioritization applications. She worked on risk assessment using geographic information systems (GIS) and illustrated the applicability of the risk methodology to real highway networks using GIS and land use transportation systems (LUTS). She developed a new classification method for bridges based on their structural characteristics, implemented an expert system for that classification, and generated damage state definitions for components of concrete bridges to be used in post-earthquake damage assessment. Dr. Basöz also developed network analysis algorithms for emergency response, post-earthquake recovery and bridge prioritization applications and constructed a decision analysis model to integrate technical and social factors in risk mitigation and emergency response decisions. She concurrently worked on projects related to highway system performance following the Northridge earthquake and participated in development of methodologies for evaluating the socioeconomic consequences of large earthquakes, sponsored by the California Universities for Research in Earthquake Engineering and Kajima Corporation.

Dr. Basöz is a member of ASCE, EERI, SEAONC and TCLEE/ASCE.

EARTHQUAKE DAMAGE TO BURIED WATER SUPPLY PIPES AND THEIR RENOVATION BY HOSE LINING TECHNOLOGY

Tadanobu SATO

Disaster Prevention Research Institute, Kyoto University, Uji, Kyoto 611, JAPAN

Izabro YAGI, Hiroyuki SAKURAGI

Ashimori Industry Company, Ltd., Osaka, Japan

and Tom DRIVER

Insituform Technologies, Inc., St Louis, Louisiana, USA

ABSTRACT

A new technology for renovating old pipes, Hose-Lining-Method, is introduced and seismic durability of hose lined pipes with joints has been examined through static and dynamic cyclic loading tests. The damage to water distribution pipes during the 1995 Hyogoken-Nanbu Earthquake, especially values of opening at breaks were surveyed to grasp necessary deformability of pipe joints under strong ground shaking condition.

INTRODUCTION

The water and gas supply systems have been deeply connected with human life and key factors for minimizing the urban earthquake disaster. Components of these systems are usually buried and have suffered severe earthquake damage. Recommended methods to mitigate the earthquake damage to pipes can be classified into two procedures; upgrading pipe materials and use of earthquake proof joints. Implementation of these procedures for newly constructing pipelines is not so difficult but for existing pipelines this is not efficient because the cost of upgrading the old pipes is almost the same as that of newly constructing ones, and the upgrading has not been performed except very important main lines. However a new very efficient method, Hose-Lining-Method¹⁾, to renovate and rehabilitate existing pipes without excavating them have been developed. A revised seal hose with tensile strength of 687-784 kPa (7-8 kgf/cm²) is inserted in pipe and turned inside out. Lining of the seal hose to the pipe wall is performed by a thermo-setting type adhesive. After lining is finished, the lined seal hose behaves like a thin strong pipe and follows well to the deformation of pipe.

In this paper we examine the earthquake resistibility of pipe strengthened by hose lining, especially of joint parts. Since data about actual joint deformation during strong earthquake have not been gathered, deformation of joints and breaks of pipes were surveyed at Kobe City after the 1995

OUTLINE OF HOSE LINING METHOD

There are many methods to rehabilitate damaged pipes from inside such as the epoxy lining, the bitumen lining, the cement mortar lining and the slip lining. The method introduced here is a lining method using reversed seal hose which have been developed by Tokyo Gas Company and Ashimori Industry in corporation. The reversal of seal hose is performed like turning socks inside out as shown in Fig.1. The tip of seal hose is fixed at the open end of reversal apparatus. The seal hose is turned inside out by adding air pressure to the reversal apparatus. Pulling the guide belt which is implemented inside of the hose and controlling a speed of the caterpillar to carry out the seal hose, the reversal of seal hose is processed continuously. Adding heat by steam to a thermo-setting type adhesive applied to the inside of the seal hose, the reversed seal hose is stuck to the pipe wall as shown in Fig.2.

The seal hose set inside of the pipes with joints composes a long thin pipe without joints and can sustain a pressure of 980 kPa (10 kg/cm^2) at maximum, therefore water leaks from ruptured portions of the pipe are completely prevented after insertion of the seal hose. The seal hose possesses a remarkable ductility along the pipe axis and follows well to the deformation of the pipe caused by ground movement due to earthquakes, land slides or fault dislocation. For the case that a joint deformation exceeds an allowable limit, or a part of the pipe breaks as the result of the plastic deformation, the seal hose peels off from the pipe wall and can extend until fibers of seal hose exceed a certain strain limit, usually more than ten percent. This prevents a sudden decrease of supply capacity of pipe networks just after these events.

The diameter of seal hose before setting in the pipe is a bit smaller than that of the pipe and is expanded by adding inner pressure to fit the pipe wall. Therefore the smooth surface is renovated except some small wrinkles around bent and flow efficiency is restored to the same level of new pipes because the friction loss is remarkably reduced. Moreover the pipelines renovated by this method are rust proof and the seal hose usually possesses high water and chemical resistibility. The life time of renovated pipes is expected to be more than 30 years base on the accelerated tests of fibers used for weaving seal hose.

EXPANSION OF JOINTS AND BREAKS OF PIPES DURING THE 1995 HYOGOKEN-NANBU EARTHQUAKE

The 1995 Hyogoken-Nanbu Earthquake struck the densely populated corridor between the cities of Osaka and Kobe at 5:46 am (local time) on January 17, 1995. The damage due to this earthquake was severe, especially 6,308 mortality was Japan's worst disaster² since the Great Kanto

Earthquake of 1923 (M=7, 140,000 mortality). As the direct damage due to ground shaking of this earthquake, not only many buildings including wooden houses but other facilities and structures such as bridges, port facilities, lifeline facilities including subways and rail ways were severely damaged. The soil liquefaction induced large ground displacements in the horizontal direction, which resulted in serious damage to buried lifeline facilities and foundation of bridges as well as buildings. The buried water and gas supply network systems of this region were firstly experienced this kind of strong ground motions and displacements. The most severely damaged areas were Kobe, Ashiya, Nishinomiya and Takarazuka cities³⁾.

After the earthquake, joint expansions (including opening of pipe breaks) of water supply system in Kobe City were measured using photographs which were taken just after the excavation to renovate damaged pipes. The total number of data collected is 626 and the summaries of obtained data are shown in Tables 1, 2 and 3 for cast iron pipes, ductile cast iron pipes and polyvinyl chloride pipes, respectively. The measured values of opening at breaks of ductile cast iron pipes with diameter of 150 mm are plotted in Fig.3. The values of opening have a characteristic of log normal distribution. For data range below excess probabilities of 5%, 10% and 15%, mean values and confidential ranges of data are shown in Figs.4, 5 and 6 for three kinds of pipe data. For the case of cast iron pipes, pipe diameters are 75, 100, 150, 200 and 300mm. The number of data for each pipe diameter is 5, 19, 28, 18 and 24. The number of data for the case of pipe diameter of 75mm is not enough to calculate the average value and standard deviation of opening at breaks, but for the data from another pipe diameters the number of data is sufficient to calculate stochastic characteristics. Because the data for pipe diameter of 200mm includes the case of thrusting and the scattering is very large the measured result for this pipe diameter is omitted in Fig.4. The average value of opening at break becomes larger as the pipe diameter increases and the maximum value of opening is about 10 cm. For the case of cast iron pipes the data obtained are for pipe diameters of 75,100,150, 200, 300 and 400mm. The number of data is sufficient except for pipe diameters of 75 and 400mm to get the statistics. The average value of opening also becomes larger as the pipe diameter increases as shown in Fig.5 and this value is about 200mm for the pipe with diameter 400mm but within 100mm for the case of pipe diameter being less than 200mm as can be seen in Table 2. The number of data for polyvinyl chloride pipes is not enough to extract statistical values but the average value of opening is less than 10cm.

In the Recommended Practice for Earthquake Resistant Design of Gas Pipelines⁴⁾ (1983 Japan Gas Association), the standard design ground displacement for medium-pressure transmission pipes is 5 cm. The joint, therefore, must be designed to be able to absorb completely this amount of the ground displacement at the worst case. The data obtained by the survey of damaged water supply pipes in Kobe City show the value of maximum opening at break is far beyond 5cm and reaches to 40cm for the case of large diameter pipe. This means that the design ground displacement should be selected larger than 5 cm. It is, however, not practical to design pipe systems being

survived for the extremely large deformation caused by ground failure due to liquefaction. We propose this value to be changed to 10cm because the deformability of joint is most important parts for upgrading earthquake resistibility of pipe systems.

DURABILITY OF HOSE LINING PIPES AT JOINT FOR LARGE DEFORMATION

The joint capacity for absorbing the ground displacement must sustain at least the axial joint expansion of 10 cm depend on the damage survey of water supply pipes in Kobe City as mentioned above. In the following, we check the durability of hose lined pipes for such displacement. Two steel pipes with the length of 200cm are butted and lined with a seal hose as described in the second section. The butted part is considered as a joint without possessing any resistibility for extensional deformation. There are twenty eight small holes in each side to observe the length of seal hose peeling off from the pipe. The specification of lining materials is given in Table 4. The set up of test specimen and configuration of test apparatus is shown in Fig.7.

The internal pressure 5.0kgf/cm² was applied by air. The inner diameter of test pipes is 155mm. In the static extension test, axial deformation was applied until the joint opening reaches 100mm. The combinations of test conditions are given in Table 5. There are no breaks of lining hose up to 100mm of static extensional displacement at the joint. An example of test results for static extension test is shown in Fig.8 in which the relation between axial extensional force and opening of the joint is plotted. To explain the mechanism of load-displacement behavior at the joint we develop the following theoretical discussion about the peeling off length of seal hose and its elongation.

The peeling off of the seal hose starts when the maximum shear stress τ exceeds the maximum unit bonding strength of adhesive τ_{cf} . However τ_{cf} can not measure directly because the uniform stress distribution along the bonding face could no be expected. To overcome this difficulty, shearing several specimens possessing different bonding area, the average bonding strength of each specimen was obtained. The results are plotted in Fig.9. The maximum unit bonding strength is obtained by extrapolating the observed average bonding strength to that of a specimen with null bonding area:

$$\tau_{cf} = 13720 \text{ kPa} (140 \text{ kg/cm}^2) \text{ for WHT, } 10976 \text{ kPa} (112 \text{ kg/cm}^2) \text{ for WR} \quad (1)$$

The triangular shear stress distribution along the bonding face is assumed as shown in Fig.10(a) for the case that the seal hose stuck to the pipe wall is pulled by axial force. The extensional force P_{cf} when the peeling off starts is given by

$$P_{cf} = \int_0^l \tau dx = l \times \tau_{cf} \times d\pi / 2 \quad (2)$$

Substituting the value of τ_{cf} and P_{cf} of 39.9kn (4.07 tonf) for WHT and 32.0kn (3.27 tonf) for

WR obtained from static experiments into Eq.2, the effective length of shear stress distribution along bonding face l is calculated,

$$l = 11.9mm \text{ for WHT, } 12.0mm \text{ for WR}$$

Since the frictional stress acts on the peeled off part after peeling of seal hose starts, the shear stress distribution along bonding face and the interface between the pipe and seal hose can be assumed as shown in Fig.10(b). The magnitude of extensional force P is expressed by considering equilibrium of forces acting on the pipe and seal hose

$$P = P_{cf} + \sigma\mu\chi \quad (3)$$

in which σ is the internal pressure, μ is the coefficient of friction between the pipe and seal hose along the peeled off part and χ is its length.

Placing the x-axis as shown in Fig.10(b) and considering the elongation, du , of peeled off part of seal hose with an original length of dx , the following differential equation is obtained

$$EA \frac{d^2u}{dx^2} = \sigma\mu \quad (4)$$

in which E is Young's modulus of the seal hose and A is the cross sectional seal of seal hose. The boundary condition to solve Eq.(4) is given by

$$\begin{aligned} \text{At } x=0 \quad u &= 0 \\ \text{At } x=\chi \quad p &= EA \frac{du}{dx} \end{aligned} \quad (5)$$

From Eqs.(4) and (5), the elongation of peeled off part of seal hose, u , at $x=\chi$ is expressed as follows:

$$U = \frac{P}{EA} \chi - \frac{\sigma\mu}{EA} \frac{\chi^2}{2} \quad (6)$$

Neglecting the pipe extension and that of seal hose bonded to the pipe wall, the amount of opening at the joint, V , is equal to twice of U . Therefore the relationship between P and V is obtained by eliminating χ from Eqs.(3) and (6):

$$P = \sqrt{EA\sigma\mu V + P_{cf}^2} \quad (7)$$

Eliminating P from Eqs.(3) and (6), the length of peeling off χ is given by

$$\chi = \frac{-P_{cf} + \sqrt{P_{cf}^2 + \sigma\mu VEA}}{\sigma\mu} \quad (8)$$

To evaluate Eq.(7), the value of E and μ must be given. The Several experiments have been conducted as given in Table 6 and we used $E = 612.9MPa(0.06129tonf/mm^2)$ for calculation. The coefficient of friction μ is chosen as 0.41 which is the average of values given in Table 7. The thickness of peeled off seal hose is assumed to be 2.0 mm. The relation between P and V for a lined pipe with diameter of 155 mm and internal pressure of 490 kpa (5.0 kgf/cm²) was shown in Fig.11 for both cases of WHT and WR. Depend on Eq.(7) the length of seal hose being peeled off

from the pipe wall is 327.4mm when the opening of joint is 100mm. Therefore the slip out of seal hose from the pipe was not occurred.

Dynamic cyclic loading tests were also performed by applying sinusoidal displacement to the specimens of which static extension test was finished. The initial static displacements and neutral point of actuator as well as the amplitudes and frequencies for dynamic tests are listed in Table 5. For all cases the dynamic test is conducted 30 seconds. The number of repeated loading is 30 and 90 for the sinusoidal frequency of 1 and 3 Hz, respectively. The breaks of lining hose are not seen for 1Hz dynamic loading through static and dynamic loadings. However for the case of 3Hz loading the breaks occur when the number of repetitions exceeds 30 times. An example of load-displacement relation for the case No.4 defined in Table 5 is shown in Fig.12.

CONCLUDING REMARKS

The survey of pipe damage during the 1995 Hyogoken-Nanbu Earthquake the average values of opening at breaks were about 10 cm in axial direction of pipe. Since a hose lined pipe joint could absorb completely this amount of displacement, the high seismic durability is expected for pipes renovated by the Hose-Lining-Method. However we could not expect the seismic durability of joint for a large ground displacement such as the pipe slip out from the joint and the seal hose is exposed to soil. This kind of large displacement of the ground usually caused by liquefaction. In this case the joint-pipe system ceases its function. There were several water supply pipes renovated by this method in Kobe area before the 1995 Hyogoken-Nanbu Earthquake. The damage survey of these pipes reveals that there were no leakage of water and gas reported as shown in Tables 8 and 9.

REFERENCES

- [1] Sato T, T. Shibata and M. Hyodo, "Earthquake Damage to Buried Pipes and Their Renovation by Hose Lining, Proceedings of the 1985 pressure Vessels and Piping Conference, Seismic Performance of Pipelines and Storage Tanks, pp.125-131, PVP-Vol.98-4, 1985.
- [2] Committee of Earthquake Engineering, JSCE, "The 1995 Hyogoken-Nanbu Earthquake, -Investigation into Damage to Civil Engineering Structures-", June, 1996.
- [3] Japan Water Works Association, "The Damage to Water Supply Pipes During the 1995 Hyogoken-Nanbu Earthquake and Its Analyses", July, 1996 (in Japanese).
- [4] Japan Gas Association, "Specification for Earthquake Resistant Design of Gas Pipelines", March, 1982.

Table1 Displacement at opennig for Cast Iron Pipes

Apertuer (mm)	Average	Standard Deviation	n	Confidence Interval			Lower Limit			Upper Llimit			Average in the interval		
				0.05	0.1	0.15	0.05	0.1	0.15	0.05	0.1	0.15	0.05	0.1	0.15
75	25.00	10.00	5	8.77	7.36	6.44	16.23	17.64	18.56	33.77	32.36	31.44	26.7	26.7	26.7
100	36.04	24.03	19	10.80	9.07	7.93	25.24	26.98	28.11	46.84	45.11	43.98	33.2	33.2	33.2
150	76.09	116.05	28	42.98	36.07	31.57	33.11	40.02	44.52	119.07	112.16	107.66	59.0	56.6	61.0
200	138.33	440.45	18	203.47	170.76	149.45	-65.14	-32.43	-11.12	341.80	309.09	287.78			
250															
300	73.52	38.84	24	15.54	13.04	11.41	57.98	60.48	62.11	89.06	86.56	84.93	63.4	69.0	69.0

Table2 Displacement at opennig for Ductil Cast Iron Pipes

Apertuer (mm)	Average	Standard Deviation	n	Confidence Interval			Lower Limit			Upper Llimit			Average in the Interval		
				0.05	0.1	0.15	0.05	0.1	0.15	0.05	0.1	0.15	0.05	0.1	0.15
75	63.86	24.67	5	21.63	18.15	15.89	42.23	45.71	47.97	85.48	82.01	79.74	64.5	74.5	74.5
100	71.87	56.03	39	17.59	14.76	12.92	54.29	57.11	58.96	89.46	86.63	84.79	76.1	76.1	73.8
150	108.11	100.92	131	17.28	14.50	12.69	90.82	93.60	95.41	125.39	122.61	120.80	101.4	102.5	104.9
200	104.14	105.51	63	26.05	21.87	19.14	78.08	82.27	85.00	130.19	126.00	123.27	100.3	100.7	100.2
250							0.00	0.00	0.00	0.00	0.00	0.00			
300	139.03	259.83	61	65.20	54.72	47.89	73.82	84.31	91.14	204.23	193.75	186.92	118.2	119.5	121.0
400	193.18	347.09	6	277.72	233.07	203.98	-84.55	-39.90	-10.80	470.90	426.25	397.15			

Table3 Displacement at opennig for Hard Vinyl Pipes

Apertuer (mm)	Average	Standard Deviation	n	Confidence Interval			Lower Limit			Upper Llimit			Average in the interval		
				0.05	0.1	0.15	0.05	0.1	0.15	0.05	0.1	0.15	0.05	0.1	0.15
50	55.941	41.626	4	40.792	34.234	29.961	15.149	21.707	25.981	96.734	90.176	85.902	54.4	54.4	54.4
75	50.958	25.809	4	25.293	21.226	18.577	25.665	29.731	32.381	76.250	72.184	69.534	38.3	38.3	38.3

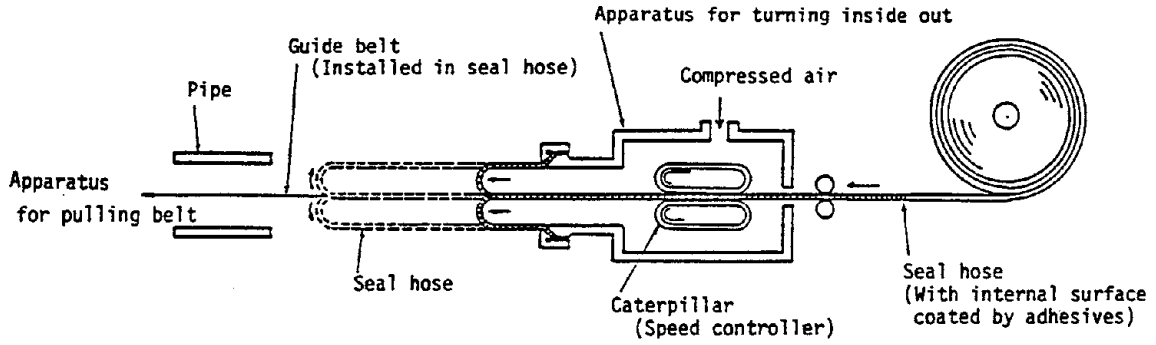


Fig.1 Schematic Illustration of Hose-Lining Apparatus

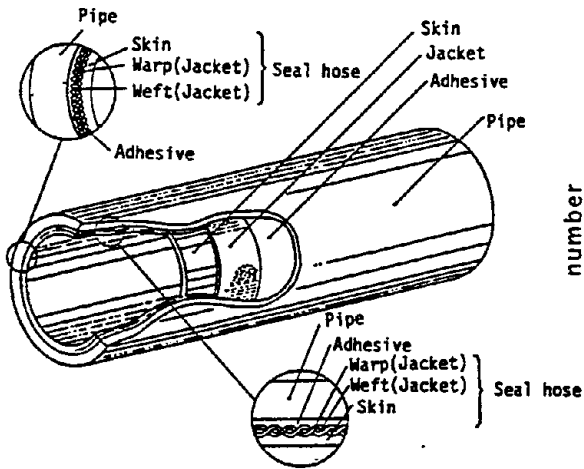


Fig.2 Cross Section of Pipe Lined by Hose

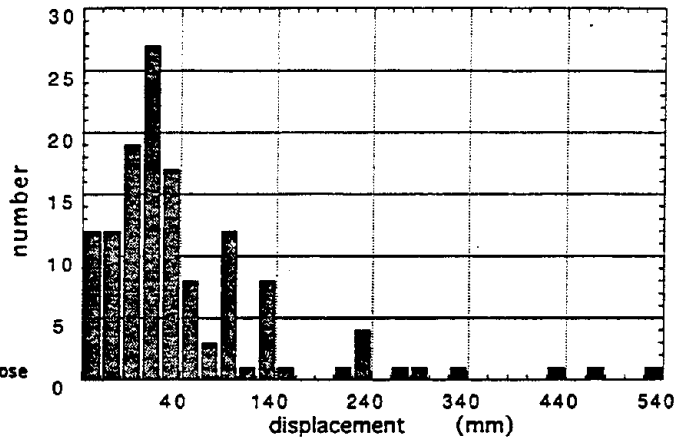


Fig.3 Frequency Distribution Value of Openings for FCD (φ 150mm)

Table4 Specification of Seal Hose

Sample Sign	Jacket Material			Skin Material	Thickness of hose (mm)	Weight (g / m)	Tensile Strength (kg / cm ²)	Burst Pressure (kg / cm ²)
	Warp	Wool	Reinforce-ment					
WHT	Polyester Fiber	Polyester Fiber	Polyester Fiber	Polyester Resin	2.4	710	over 210	over 7.5
WR	Polyester Fiber	Polyester Fiber	—	Polyester Resin	1.8	600	over 210	over 5

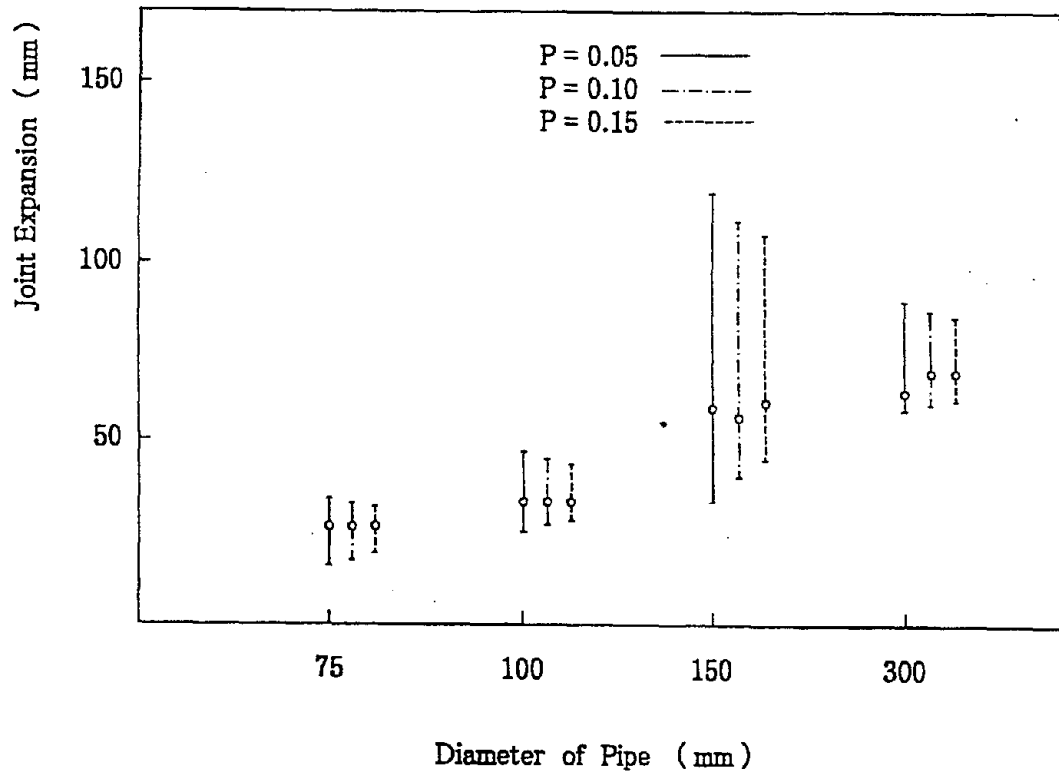


Fig.4 Displacement at opening (FC Pipe)

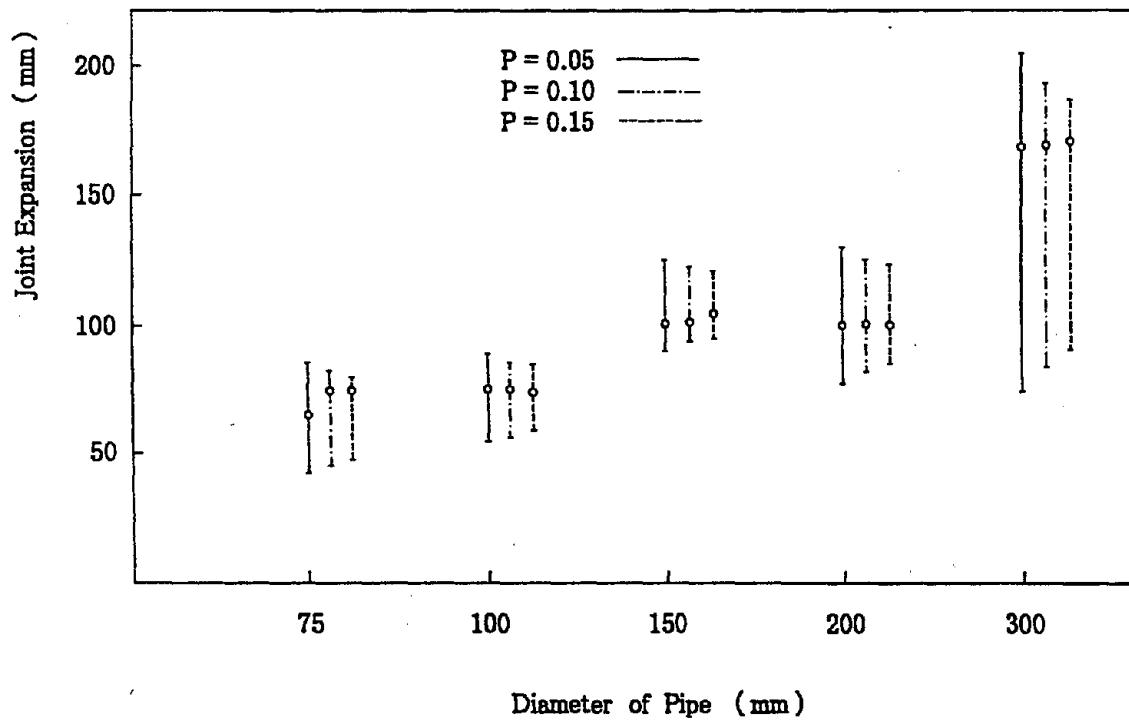


Fig.5 Displacement at opening (DFC Pipe)

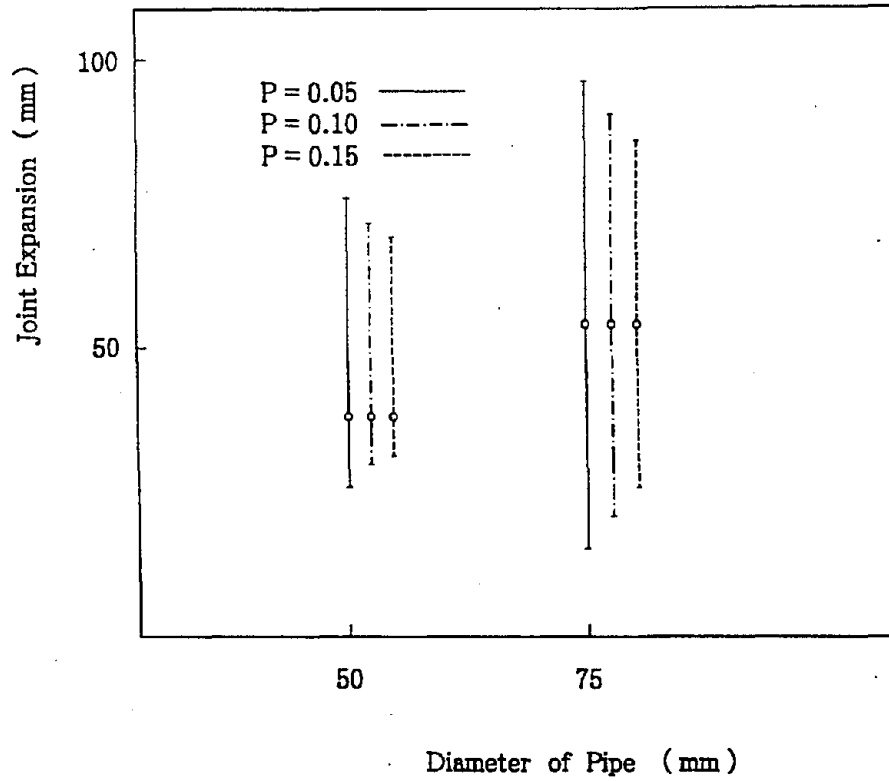


Fig.6 Displacement at opening (HIVP)

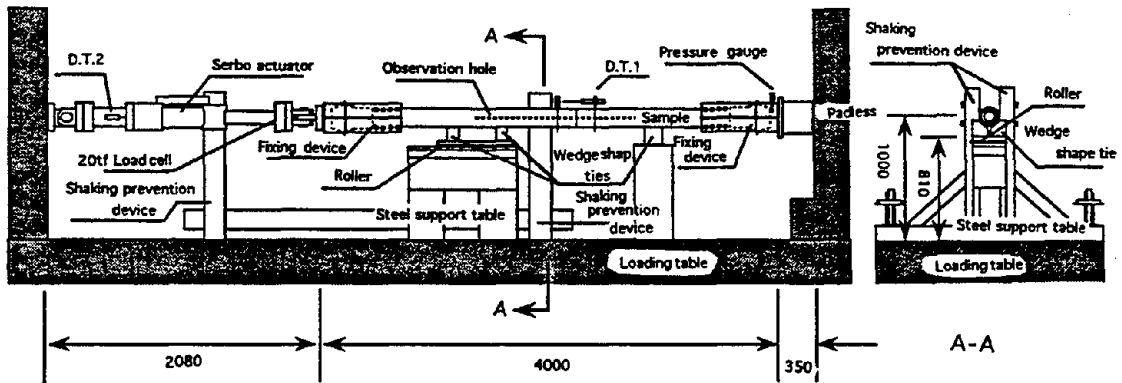



Fig.7 Tension Test System (unit:mm)

Table5 Specification of Static and Dynamic Loading Test

No.	Type of Seal Hose	Frequency (Hz)	Amplitude (mm)	First tension (mm)	Center point (mm)	Note																																	
01	WR	1.0	100	100	100	The connection moves when a inner pre-ssure decreases to 1.0 kgf/cm ² . disp.100mm (messurement 105mm) → load 5tf 83mm (messurement 90mm) → load 0tf																																	
02	WR	1.0	100	100	100	Seal hose is peelfd off up to the pipe edge. →Leak (discontinuance)																																	
03	WHT	1.0	100	100	100	Disp.100mm (messurement 105mm) OK (messurement 90mm)																																	
04	WHT	3.0	60	100	100	Static →OK, Airtightness →OK Dynamic 30 times →OK, Then burst.																																	
05	WHT	3.0	60	100	100	Static →OK, Airtightness →OK Dynamic about 60times →OK																																	
06	WHT	First time : Static tension (Length of exfoliation)																																					
		<table border="1"> <thead> <tr> <th>Displacement(mm)</th> <th>10</th> <th>20</th> <th>30</th> <th>40</th> <th>50</th> <th>60</th> <th>70</th> <th>80</th> <th>90</th> <th>100</th> </tr> </thead> <tbody> <tr> <td>Actuator side</td> <td></td> <td>15</td> <td>20</td> <td>20</td> <td>20~25</td> <td>35</td> <td>55</td> <td>—</td> <td>65</td> <td></td> </tr> <tr> <td>Fixed side</td> <td></td> <td>10</td> <td>15</td> <td>20</td> <td>20</td> <td>20</td> <td>25</td> <td>—</td> <td>25</td> <td></td> </tr> </tbody> </table>					Displacement(mm)	10	20	30	40	50	60	70	80	90	100	Actuator side		15	20	20	20~25	35	55	—	65		Fixed side		10	15	20	20	20	25	—	25	
		Displacement(mm)	10	20	30	40	50	60	70	80	90	100																											
Actuator side		15	20	20	20~25	35	55	—	65																														
Fixed side		10	15	20	20	20	25	—	25																														
 <p>Actuator side Fixed side Static → OK Load → 6.2tf</p>																																							
Second time : Deynamic tension																																							
<table border="1"> <thead> <tr> <th>Frequency(Hz)</th> <th>Amplitude(mm)</th> <th>First tension (mm)</th> <th>Center(mm)</th> <th>Result</th> </tr> </thead> <tbody> <tr> <td>3.0</td> <td>20</td> <td>100</td> <td>100</td> <td>Dynamic →OK Airtightness →OK</td> </tr> </tbody> </table>					Frequency(Hz)	Amplitude(mm)	First tension (mm)	Center(mm)	Result	3.0	20	100	100	Dynamic →OK Airtightness →OK																									
Frequency(Hz)	Amplitude(mm)	First tension (mm)	Center(mm)	Result																																			
3.0	20	100	100	Dynamic →OK Airtightness →OK																																			
07	WHT	First time : Static tension (Length of exfoliation)																																					
		<table border="1"> <thead> <tr> <th>Displacement(mm)</th> <th>10</th> <th>20</th> <th>30</th> <th>40</th> <th>50</th> <th>60</th> <th>70</th> <th>80</th> <th>90</th> <th>100</th> </tr> </thead> <tbody> <tr> <td>Actuator side</td> <td>10</td> <td>10</td> <td>15</td> <td>25</td> <td>30</td> <td>35</td> <td>35</td> <td>40</td> <td>50</td> <td>65</td> </tr> <tr> <td>Fixed side</td> <td>10</td> <td>10</td> <td>15</td> <td>15</td> <td>20</td> <td>25</td> <td>25</td> <td>25</td> <td>30</td> <td>35</td> </tr> </tbody> </table>					Displacement(mm)	10	20	30	40	50	60	70	80	90	100	Actuator side	10	10	15	25	30	35	35	40	50	65	Fixed side	10	10	15	15	20	25	25	25	30	35
		Displacement(mm)	10	20	30	40	50	60	70	80	90	100																											
Actuator side	10	10	15	25	30	35	35	40	50	65																													
Fixed side	10	10	15	15	20	25	25	25	30	35																													
Second time : Deynamic tension																																							
<table border="1"> <thead> <tr> <th>Frequency(Hz)</th> <th>Amplitude(mm)</th> <th>First tension (mm)</th> <th>Center(mm)</th> <th>Result</th> </tr> </thead> <tbody> <tr> <td>3.0</td> <td>40</td> <td>100</td> <td>100</td> <td>Broken</td> </tr> </tbody> </table>					Frequency(Hz)	Amplitude(mm)	First tension (mm)	Center(mm)	Result	3.0	40	100	100	Broken																									
Frequency(Hz)	Amplitude(mm)	First tension (mm)	Center(mm)	Result																																			
3.0	40	100	100	Broken																																			
08	WHT	3.0	40	100	100	Static OK Dynamic Broken in 30 times																																	
09	WR	3.0	20	100	100	Static OK Dynamic OK Airtightness OK																																	
10	WR	3.0	40	100	100	Static OK Dynamic OK																																	

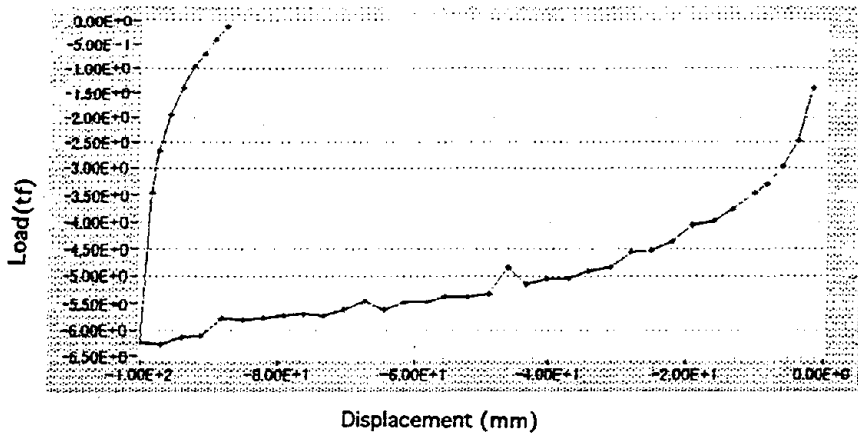


Fig.8 Static Loading Test Result for Case No.8 (WHT)

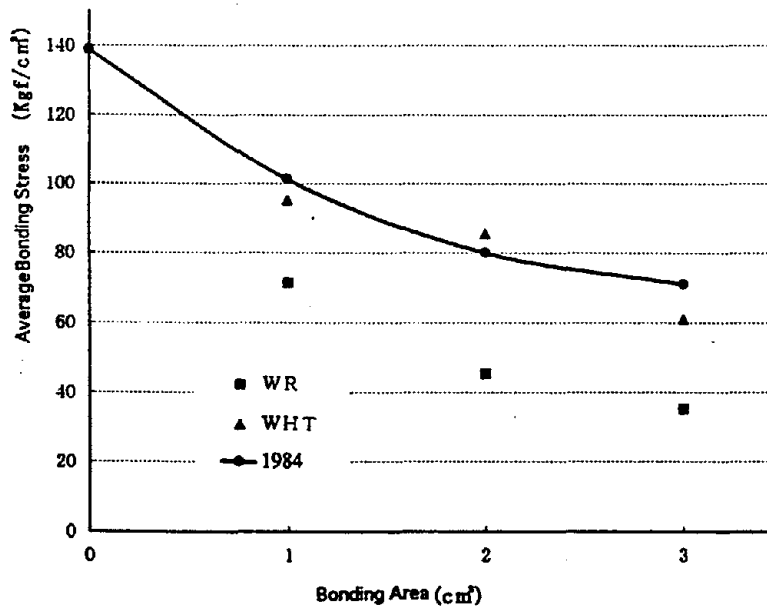


Fig.9 A comparison between Bonding Area and Average Bonding Stress

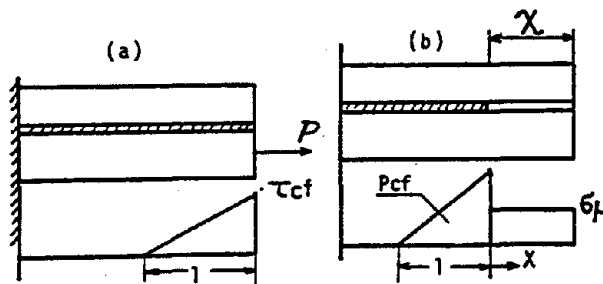


Fig.10 Stress Distribution between Seal Hose and Pipe Wall

Table6 Young's module of Seal Hose
(Extension Test)

TS velocity	Item	Maximam Stress (kgf / mm^2)	Strain when stress is maximam (%)	Young's module
1m / sec	1	16.41	19.2	0.08547
	2	15.69	19.7	0.07964
	3	16.62	20.4	0.08147
	4	16.21	19.6	0.08270
	5	14.44	18.9	0.07640
	Average			0.08114
0.6m / sec	1	14.80	20.0	0.07400
	2	14.75	19.8	0.07449
	3	16.52	21.0	0.07867
	4	14.96	19.2	0.07792
	5	15.58	19.3	0.08073
	Average			0.07716
0.3m / sec	1	15.90	21.6	0.07361
	2	15.90	19.8	0.07571
	3	15.58	21.0	0.07675
	4	16.00	21.3	0.07512
	5	14.75	19.7	0.07487
	Average			0.075212
0.1m / sec	1	16.36	27.0	0.06059
	2	16.46	28.5	0.05775
	3	16.28	27.0	0.06030
	4	15.79	25.5	0.06192
	5	16.17	27.0	0.05989
	Average			0.06129

Table.7 Coefficient of friction

Vertical load(Kg)	15.59	31.17	62.34	93.51
Horizontal load(Kg)	5.0	17.0	22.0	40.0
μ	0.32	0.55	0.35	0.43

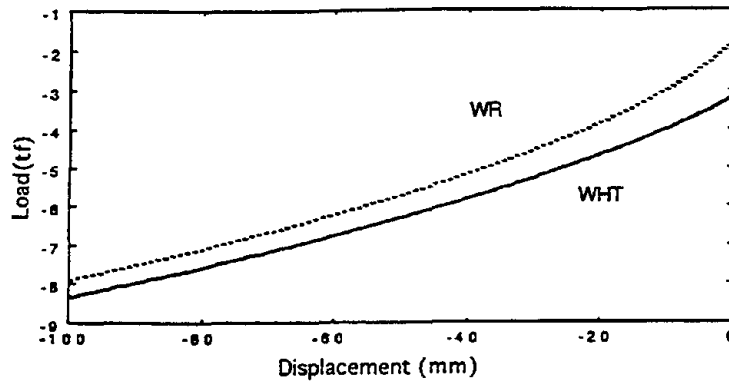


Fig.11 Relation between Tension Load and Displacement at butt joint (Theoretical Value)

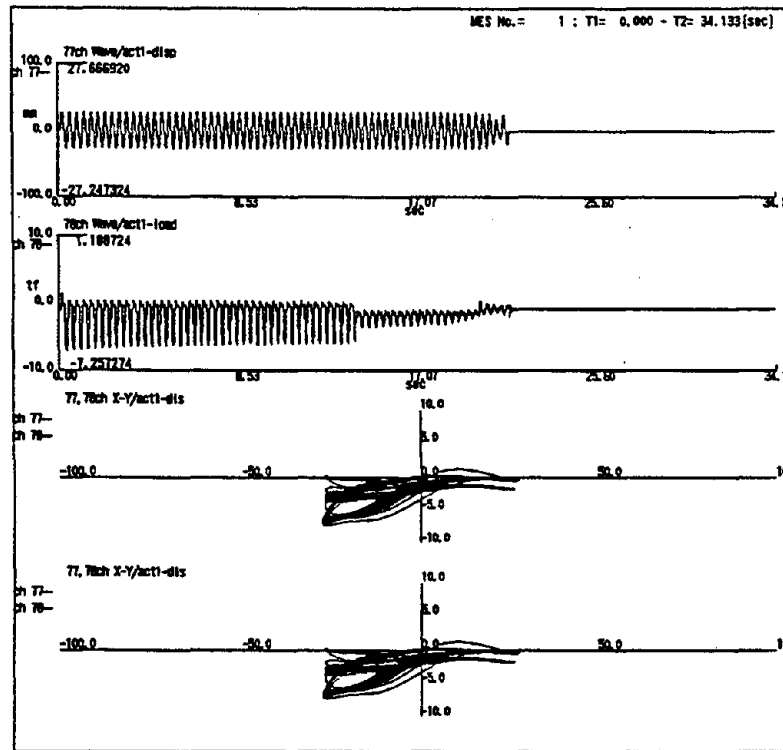


Fig.12 Dynamic Loading Test Result for Case No.4 (WHT) [3Hz, Amplitude:60mm]

Table8 Damage during 1995 Hyogoken-Nanbu Earthquake
for Hose-Lined Water Supply Pipes in Kobe City

No.	Aperture (mm)	Type of pipe	Length (mm)	Location	Damage by Hyogoken Nanbu Earthquake	Seismic intensity near the location
1	500	FC	600	Nagata area Kobe city	No leakage of water	JMA6
2	300	FC	46	Nada area Kobe city	No leakage of water	JMA7
3	300	FC	38	Nada area Kobe city	No leakage of water	JMA6
4	75	FC	138	Nada area Kobe city	No leakage of water	JMA6
5	75	FC	200	Nada area Kobe city	No leakage of water	JMA6
6	400	FC	33	Nada area Kobe city	No leakage of water	JMA6
7	300	Steel	45	Suma area Kobe city	No leakage of water	JMA7
8	200	Steel	43	higasinada area Kobe city	No leakage of water	JMA7

Table9 Damage during 1995 Hyogoken-Nanbu Earthquake
for Hose-Lined Gas Supply Pipes in Kobe City

No.	Aperture (mm)	Type of pipe	Length (mm)	Location	Damage by Hyogoken Nanbu Earthquake	Seismic intensity near the location
1	300	FC	455	area nininomiya city	No leakage of gas	JMA6
2	300	FC	593	Chuoku area Kobe city	No leakage of gas	JMA7
3	300	FC	247	Hyogo area Kobe city	No leakage of gas	JMA7
4	500	FC	778	Nagata area Kobe city	No leakage of gas	JMA7

PERSONAL CAREER

NAME: Tadanobu Sato

POSITION: Professor

Section of Dynamics of foundation Structures
Division of Earthquake Disaster Prevention
Disaster Prevention research Institute
Kyoto University

ADDRESS: Gokasho, Uji, Kyoto 611, JAPAN

Tel. +81-774-38-4065

Fax. +81-774-38-4070

E-mail: sato@catfish.dpri.kyoto-u.ac.jp



DATE OF BIRTH: February 27, 1942

EDUCATION: Bachelor of Engineering (1969, Civil Engineering, Kyoto University)

Master of Engineering (1971, Civil Engineering, Kyoto University)

Doctor of Engineering (1975, Civil Engineering, Kyoto University)

ACADEMIC EXPERIENCE:

1974-77 Research Associate, Kyoto University, Kyoto

1977-94 Associate Professor of Kyoto University, Disaster
Prevention Research Institute (DPRI), Kyoto University

1994- Professor of Kyoto University, DPRI, Kyoto University

AWARDS:

1991 Thesis Prize of Japan Society of Civil Engineers on Structural Control Theories

TEACHING EXPERIENCE:

Graduate course; Application of partial differential equations to civil engineering problems (1978-1995),
Soil-structure interaction (1978-1983), Special problems in soil related
disaster (1983-1986), Advanced Geotechnical Engineering (1996-), Lifeline Engineering
(1996-)

Undergraduate course; Soil Mechanics (1988-1992), Structural Mechanics (1989-1994),
Geotechnical Engineering (1995-)

MAJOR RESEARCH FIELDS: Researches on dynamic constitutive relation of soil (1978-1986), non-linear
soil-structure interaction problem (1971-), non-linear seismic response of surface ground (1975-),
seismic response analysis of surface ground with irregular soil profile (1977-), identification and
simulation of earthquake motion (1979-), damage estimation of lifeline systems (1980-), optimal
control of seismic response of structural systems (1988-), earthquake damage to structure systems (1986-)

TRAVEL ABROAD: More than 30 countries including U.S.A., U.K. and Canada, France, Germany, Spain,
Swiss, Austria, Australia, Turkey, Greece, Mexico, China, Indonesia, Singapore, India, Nepal,
Philippine, Taiwan, Korea, Netherlands, Slovenia, Hong Kong

PERSONAL CAREER

NAME : Isaburo Yagi

POSITION : General Manager
R & D Department
Ashimori Engineering Co., Ltd.

ADDRESS : 11-7, 7-Chome, Senrioka, Settsu- City,
Osaka, 566 Japan
Tel. 06-337-6271
Fax. 06-388-7511



DATE OF BIRTH : September 23, 1951

EDUCATION : Bachelor (1974) of Industrial Chemistry, Shizuoka University

MAJOR SUBJECT : High Polymer Chemistry

MAJOR AREA OF EXPERIENCE :

- 1974-1978 Hose Production Division, Ashimori Industry Co., Ltd.
- 1978-1989 Research & Development Staff, PALTEM Division, Ashimori Industry Co., Ltd.
- 1989-1992 Managing Director, Ashimori Europe Limited
- 1993-1995 Manager, Osaka PALTEM Sales Department, Ashimori Industry Co., Ltd.
- 1995-1996 Assistant General Manager, R&D Department, Ashimori Engineering Co., Ltd.
- 1996- General Manager, R&D Department, Ashimori Engineering Co., Ltd.

TRAVEL ABROAD : U.S.A., Canada, UK, France, Germany etc.

MAJOR PUBRICATIONS :

- “Case Study of Hose Lining Method” Civil Engineering, Dobokugijutsusha
- “Report for Damages of Lined Pipe by Rehabilitation Method due to 1995 Hyogoken-Nanbu Earthquake” Trenchless Technology, Japan Society for Trenchless Technology

FACTORS AFFECTING WATER SUPPLY DAMAGE CAUSED BY THE NORTHRIDGE EARTHQUAKE

T.D. O'Rourke¹

S. Toprak²
and

Y. Sano³

1, 2 - Professor and Graduate Research Assistant, respectively
School of Civil and Environmental Engineering,
Cornell University, Ithaca, NY

and

3 - Engineer, Konoike Construction Co., Osaka, Japan

ABSTRACT

This paper describes how a geographic information system (GIS) was used to evaluate Northridge earthquake damage patterns for the Los Angeles water supply pipeline system. The key sources of pipeline failure and the most vulnerable system components are identified. Pipeline damage, expressed as repairs per km, is evaluated in terms of seismic parameters, such as Modified Mercalli Intensity (MMI) peak acceleration, peak velocity, and spectrum intensity. Substantial water supply pipeline damage was sustained in an area of relatively high water table and liquefiable soils near the intersection of Balboa Blvd. and Rinaldi St. Photogrammetric analyses of air photos taken before and after the earthquake were used to show a good correlation between pipeline repair rates and permanent ground strains. On the basis of the records associated with the Northridge and other recent earthquakes, recommendations are made for improving loss estimation procedures.

INTRODUCTION

The 1994 Northridge earthquake led to significant disruption of the water supply system of Los Angeles, causing damage at 15 locations in the three transmission systems providing water from Northern California, 74 locations in water trunk lines (nominal pipe diameter ≥ 600 mm), and 1013 locations in the Los Angeles Department of Water and Power (LADWP) distribution pipeline network. The damage was distributed over approximately 1200 km². Damage of such a widespread nature invites questions about its spatial variability and its relationship with parameters such as earthquake intensity, peak acceleration, peak velocity, groundwater levels, and areas of permanent ground deformation (PGD). Large water supply systems are composed of pipelines constructed with different materials, diameters, and joint characteristics. Hence, there also are questions about how the damage patterns are influenced by different material and mechanical characteristics.

This paper provides a description of how a geographic information system (GIS) database was assembled for water supply damage caused by the Northridge earthquake. ARC/INFO software was used in the GIS analyses (ESRI, 1994). Graphical information is provided regarding the overall statistics and spatial patterns of pipeline damage. Spatial relationships between earthquake damage and various seismic parameters are explored. Correlations between pipeline repair rates and seismic parameters used are developed. Photogrammetric analyses of air photos before and after the earthquake are used to evaluate PGD patterns and their relationship with water supply damage.

NORTHRIDGE EARTHQUAKE DAMAGE

Figure 1 shows that the portion of the Los Angeles water supply system most seriously affected by the Northridge earthquake superimposed on the topography of Los Angeles. The water supply system includes transmission lines, trunk lines and distribution lines. All large diameter pipelines upstream of the treatment plants are considered to be transmission facilities.

The aqueduct systems that supply water from northern California are the Foothill Feeder, operated by the Metropolitan Water District (MWD), and Los Angeles Aqueducts No. 1 and 2, operated by LADWP. In total, there were 11 repair locations in LADWP Aqueducts No. 1 and 2, of which 4 involved either circumferential cracks or compressive buckling at welded slip joints. Excessive axial pullout occurred at two Dresser couplings. Damage to the MWD transmission system occurred near the Jensen Filtration Plant at a welded slip joint of a 2160-mm steel pipeline and as cracks and leakage in a reinforced concrete conduit. Damage was sustained by another steel pipeline at a sleeve-type coupling and in an area of differential settlement and horizontal movement adjacent to the Jensen Plant. Sixty-seven of the 74 trunk line repairs were located in the San Fernando Valley, with the highest concentrations of damage in the Van Norman Complex, near the intersection of Balboa Blvd. and Rinaldi St., and along Roscoe Blvd.

Figure 2 presents a map of distribution pipeline repair locations and repair rate contours for cast iron (CI) pipeline damage. The CI mains were shown to have the broadest geographic

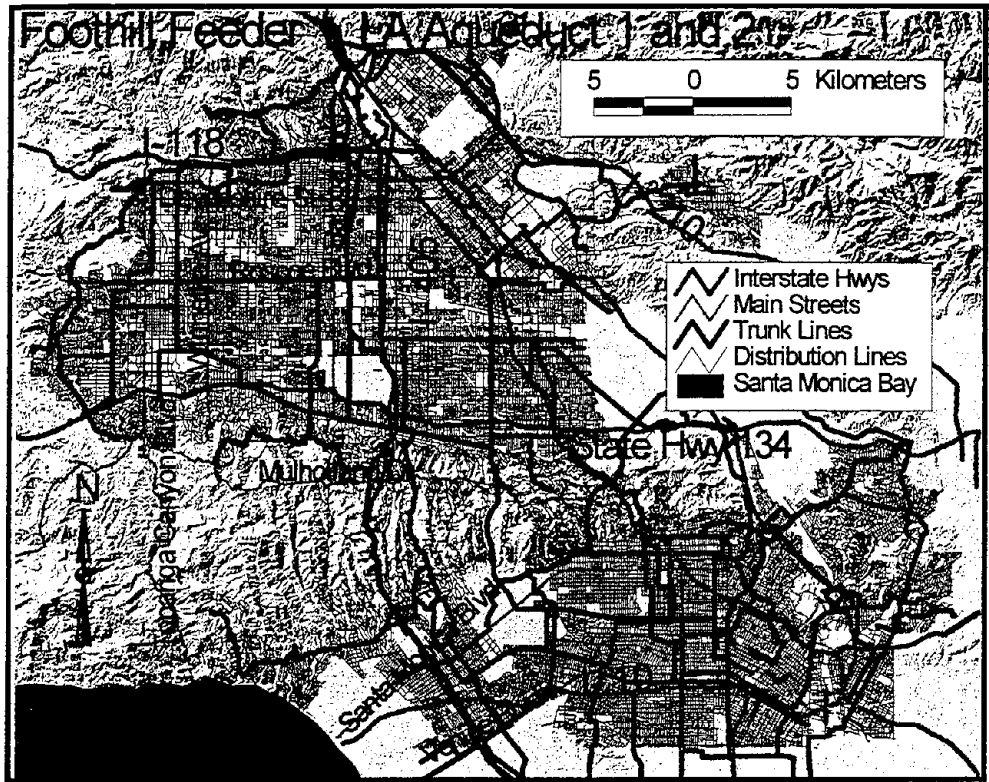


Figure 1. Map of Los Angeles water supply system affected by the Northridge earthquake.

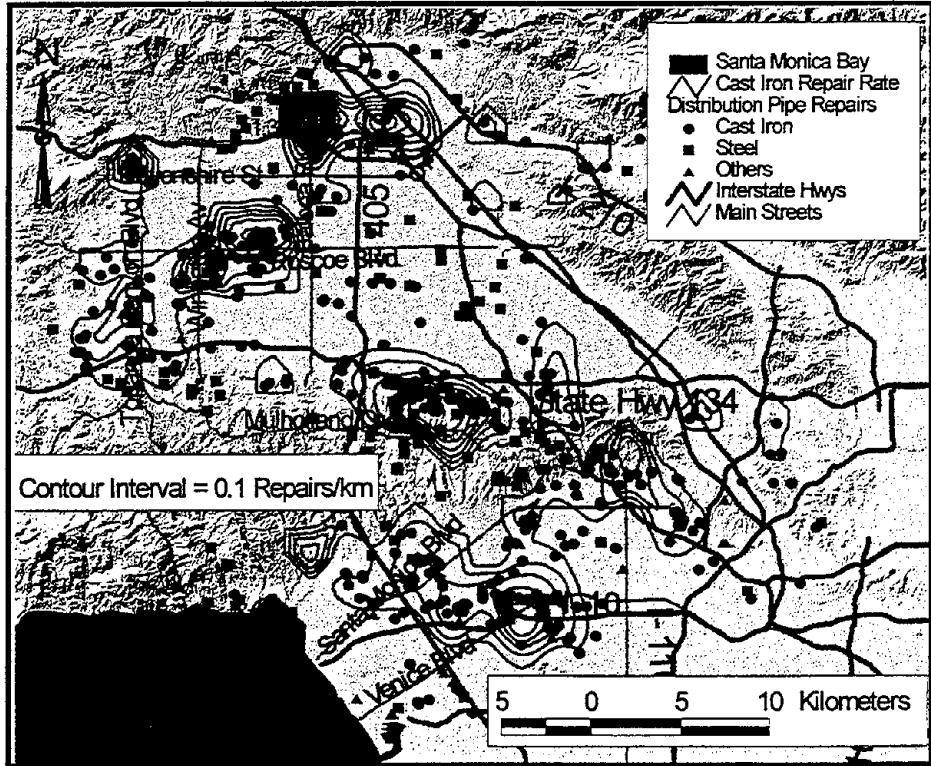


Figure 2. Cast iron pipeline repair rate contours.

coverage, and therefore to provide the most consistent basis for evaluating seismic response throughout the entire system (O'Rourke and Toprak, 1997). The repair rate contours were developed by dividing the map into 2 km x 2 km areas, determining the number of CI pipeline repairs in each area, and dividing the repairs by the distance of CI main in that area. Contours then were drawn from the spatial distribution of repair rates, each of which was centered on its tributary area. The 2 km x 2 km grid was found to provide a good representation of damage patterns for the map scale of the figure.

The overall statistics of pipeline damage are summarized in Figure 3 in the form of pie and bar charts. Please note that the bar chart scale is logarithmic. Most repairs to trunk lines occurred in steel pipelines, with 80% of all repairs in riveted and continuous wall steel piping. Sixty-six percent of repairs were in continuous wall steel pipe, whereas only 56% of all trunk lines were composed of this type of pipe. The steel trunk lines were damaged heavily by compressive wrinkling of welded slip joints, with this type of damage recorded at 20 locations. There also were 10 reported locations of pullout at compression couplings.

Seventy-one percent of the distribution line repairs were in CI pipelines, which constitute 76% of the system. Twenty-two percent of the repairs were in steel pipelines, which constitute only 11% of the system. The relatively high concentration of steel pipeline repairs is associated with various types of steel, such as Mannesman and Matheson steel, which are prone to corrosion, as well as damage at certain types of elastomeric joints that are vulnerable to creep and leakage.

EARTHQUAKE DAMAGE VS. SEISMIC INTENSITY

Figure 4 shows the repair rate contours for CI pipelines superimposed on zones of Modified Mercalli Intensity (MMI) mapped by USGS (Dewey, et al., 1995). The locations of highest repair rate coincide with areas of MM IX and MM VIII.

Figures 5 and 6 show the repair rate contours for CI pipelines superimposed on zones of peak acceleration and velocity measured by free-field strong motion instruments. The free-field records used to plot peak acceleration and velocity zones are identical to those described by Chang, et al. (1996) in their evaluation of the engineering implications of the earthquake motion. The records from approximately 240 rock and soil stations were used. The maximum horizontal acceleration of 1.78 g measured at the Tarzana-Cedar Hill Nursery was removed from the database prior to GIS evaluation to avoid distortions from possible topographic influences. In addition, records from stations at dam abutments were screened when a station downstream of the dam was available, again to minimize distortion from topographic effects.

The zones of highest peak acceleration coincide reasonably well with the locations of highest repair rate, especially near the northern edge of the San Fernando Valley, the Santa Monica Mountains, and the Los Angeles Basin. The zones of highest peak velocity show similar spatial correlation with repair rate concentrations. The velocities do not coincide as well with repair concentrations in the Los Angeles Basin, but correlate better with CI pipeline repairs in the western and central portions of San Fernando Valley.

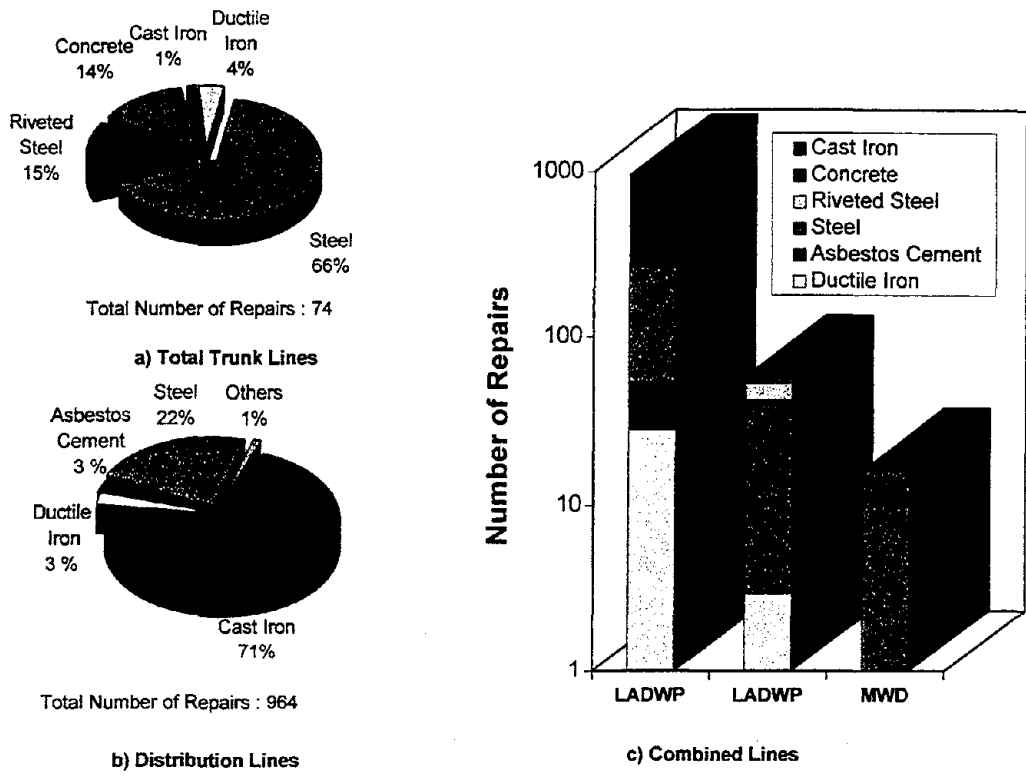


Figure 3. Repair statistics of water trunk and distribution lines.

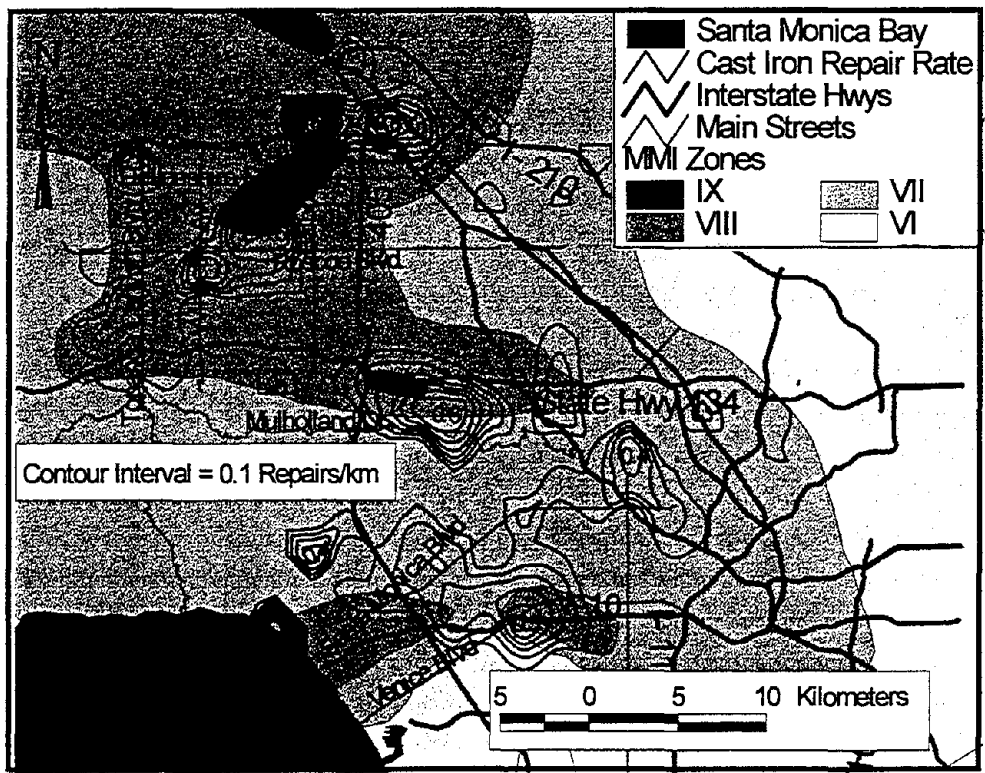


Figure 4. Pipeline repair rate contours plotted relative to MMI.

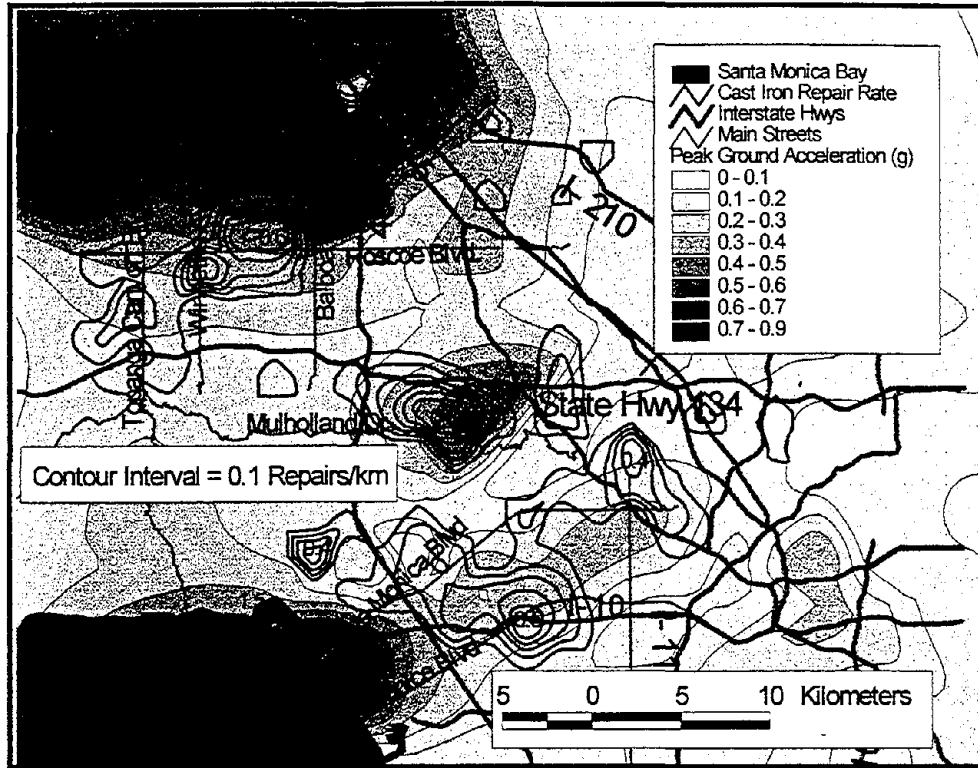


Figure 5. Pipeline repair rate contours plotted relative to peak ground acceleration.

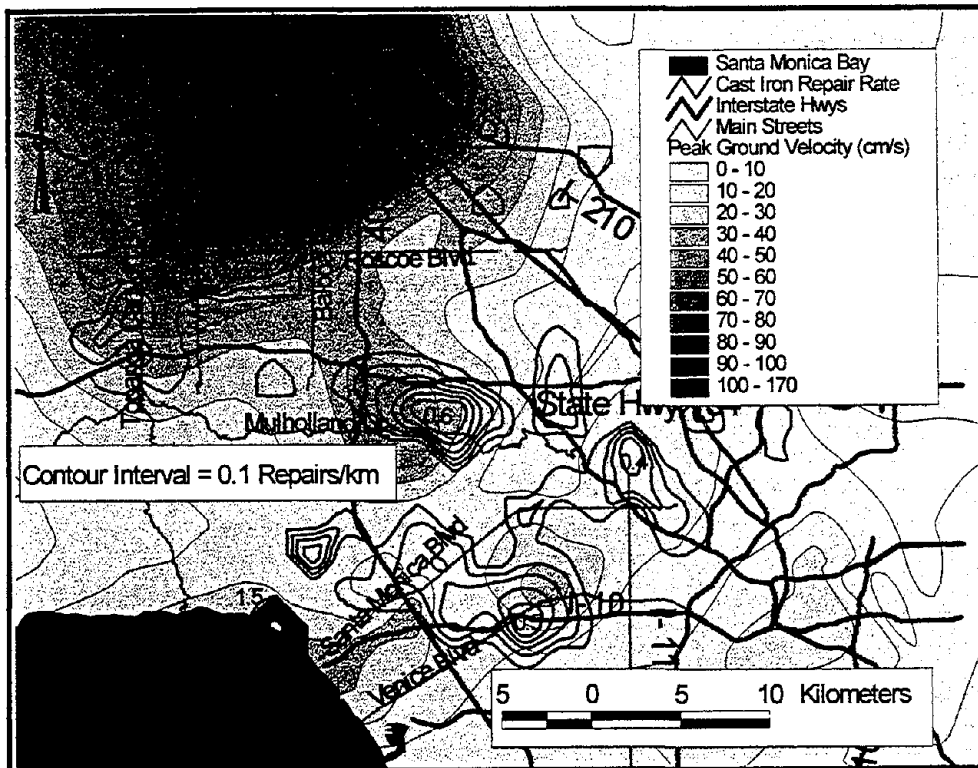


Figure 6. Pipeline repair rate contours relative to peak ground velocity.

It is notable that high concentrations of repair rate occur in the northern portion of the Santa Monica Mountains in the Sherman Oaks area. This location coincides with a zone of extensive slope movements, ground fissures, and cracking of artificial fill. Ground failure of this type is likely affected by acceleration levels, which were very high in the Sherman Oaks area, as illustrated in Figure 5. Zones of high acceleration, therefore, would be expected to correlate with locations of ground failure and thus PGD effects on pipelines. In contrast, zones of high velocity would be expected to correlate well with locations of high transient ground strain and be correlated less directly with PGD.

DAMAGE CORRELATIONS WITH SEISMIC PARAMETERS

Figure 7a shows the regressions between repair rate and MMI for CI pipelines. The isoseismal contours presented in Figure 4 were used to obtain the repair rate values. In addition to the linear fit for all four points, a bilinear fit, as suggested by Eguchi (1991), is plotted.

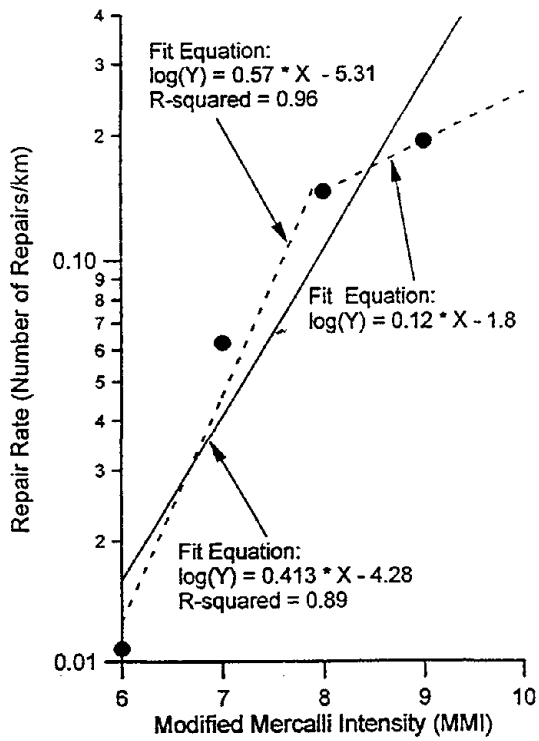
Figure 7b shows the linear regression between repair rate and maximum horizontal ground acceleration for CI pipelines. Peak ground acceleration contours presented in Figure 5 were used to obtain the repair rate values. A single repair rate was calculated for all areas of the map corresponding to a particular range of acceleration, and the acceleration midway between the upper and lower values was used in the correlation. Only those areas bounded by the contours that contain pipe lengths greater than 150 km were used in the correlations. This pipe length corresponds to approximately 2% of the overall CI pipelines, and was chosen to yield a sample sufficiently large to represent faithfully the population statistics. Similar procedures and length criteria were applied for peak ground velocity and spectrum intensity correlations.

Figure 7c shows the linear regression between repair rate and peak horizontal ground velocity for CI pipelines. Peak ground velocity contours presented in Figure 6 were used to obtain repair rate values. Figure 7d shows the regression between repair rate and spectrum intensity for CI pipelines. The definition of spectrum intensity adopted here was taken from Katayama, et al. (1988) as the average amplitude of the 20% damped velocity response spectrum between $T = 0.1$ and 2.5 seconds, where T is the natural period of a single degree of freedom oscillator. Correlations for spectral velocity and spectrum intensity are very similar.

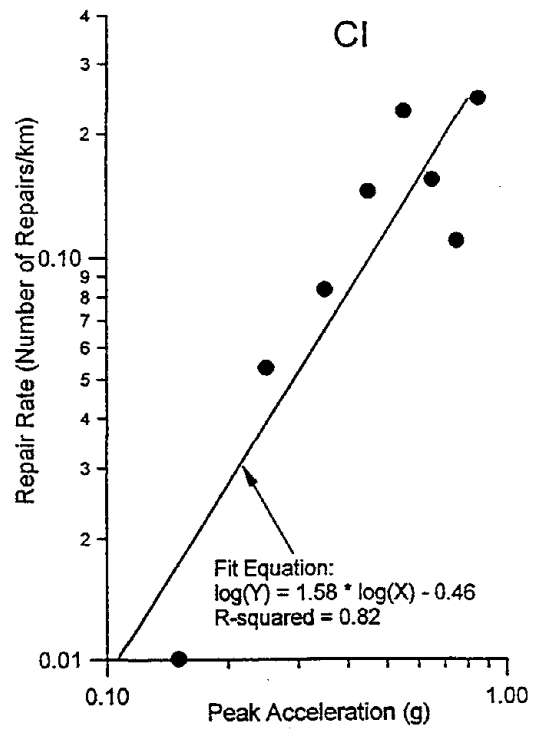
PIPELINE DAMAGE AND GROUND STRAINS

Air photo measurements were conducted by using aerial photographs around the Van Norman Complex taken before and after the Northridge earthquake. Aero-triangulation with simultaneous bundle adjustment was conducted in this measurement, as described by Sano (1998). The number of points measured was 1,010, from which estimates of PGD horizontal displacement and settlement were made. The relative accuracy of horizontal displacement measurements was ± 19.7 cm. Corrections for tectonic displacement were performed, so the displacements in this area represent actual PGD associated with liquefaction and other causes.

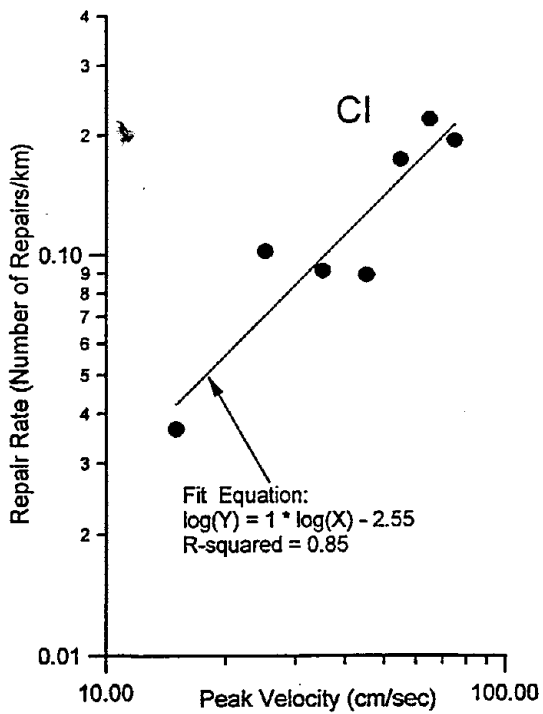
The area near the intersection of Balboa Blvd. and Rinaldi St. was influenced by liquefaction-induced lateral spread (Holzer, et al., 1996) that resulted in the failures of a gas



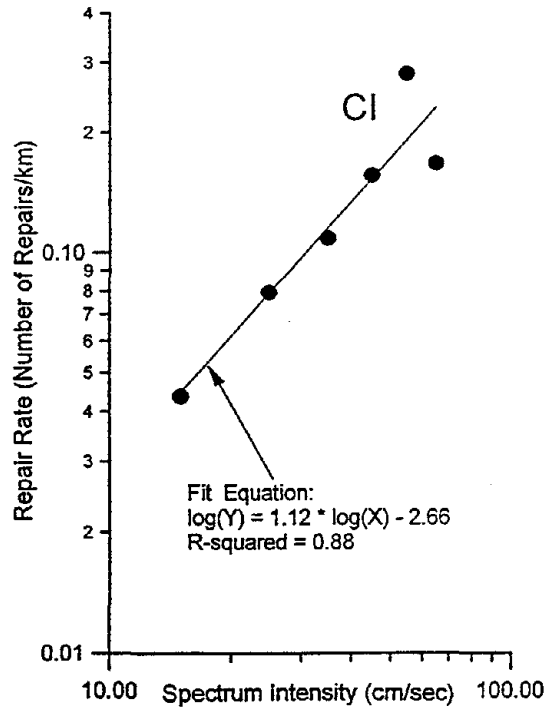
a) MMI



b) Acceleration



c) Velocity



d) Spectrum Intensity

Figure 7. Pipeline repair rate correlation with MMI, peak acceleration, peak velocity, and spectrum intensity.

transmission and two water trunk lines. Ground strains were calculated in this area from the air photo measurements of horizontal displacement by superimposing regularly spaced grids with GIS software onto the maps of horizontal displacement and calculating the mean displacement for each grid. Grid dimensions of 100 x 100 m were found to provide the best results (Sano, 1998).

Knowing the coordinates of the center of each grid cell and corresponding displacement, the compressive and tensile strains in the EW and NS directions and shear strains were obtained by computing the spatial derivatives by means of linear interpolation. The eigenvalues and eigenvectors of these strain tensors were then computed, which yielded the principal strains and directions. Contour lines of principal compressive and tensile ground strains were generated and superimposed on the map of the area surrounding the Balboa Blvd. and Rinaldo St. intersection.

Similar analysis of ground strains was performed with survey measurements in this area conducted by the Los Angeles Bureau of Engineering (LABE). Strain contours developed from air photo measurements were checked with those developed from LABE surveys, and found to compare favorably.

Repair rates for CI mains were calculated and compared with ground strains. Figure 8 illustrates the procedure for obtaining repair rates for each strain range. Using GIS software, ground strain contours, pipeline network, and repair locations were combined, after which repair rates corresponding to the areas delineated by a particular contour interval were calculated.

Figure 9 shows the repair rate contours for CI mains superimposed on the areal distribution of ground strains, identified by various shades and tones. In the study area, there were 34 repairs to CI mains and two for steel pipelines. There were 5 trunk line repairs in the area. The repair rate contours were developed by dividing the map into 100 m x 100 m cells, determining the number of CI pipeline repairs in each cell, and dividing the repairs by the length of the distribution mains in that cell. The intervals of strain and repair rate contours are 0.001 (0.1%) and 5 repairs/km, respectively. The zones of high tensile and compressive strains coincide well with the locations of high repair rate.

In Figure 10, the relationship between ground strains and repair rates is presented graphically using linear regressions. The repair rate in each ground strain range, 0-0.1, 0.1-0.3, and 0.3-0.5%, was calculated as explained previously. Ground strain contours obtained both from the air photo measurements and LABE survey were used. As shown in this figure, repair rates increase linearly with ground strain. It should be noted that the strain range of 0.1-0.3% from the LABE survey represents a locally high and unrepresentative concentration of repairs within the area between ground strain contour lines. When performing this type of GIS analyses, repair rates may occasionally be exaggerated because contour intervals coincide with a local concentration of damage over a small length of pipeline. These conditions should be identified by careful examination of the data. Although the locally high repair rate is plotted in Figure 10, it was not used in the regression analyses. High r^2 values show that a large percentage of the data variability can be explained by the regression lines.

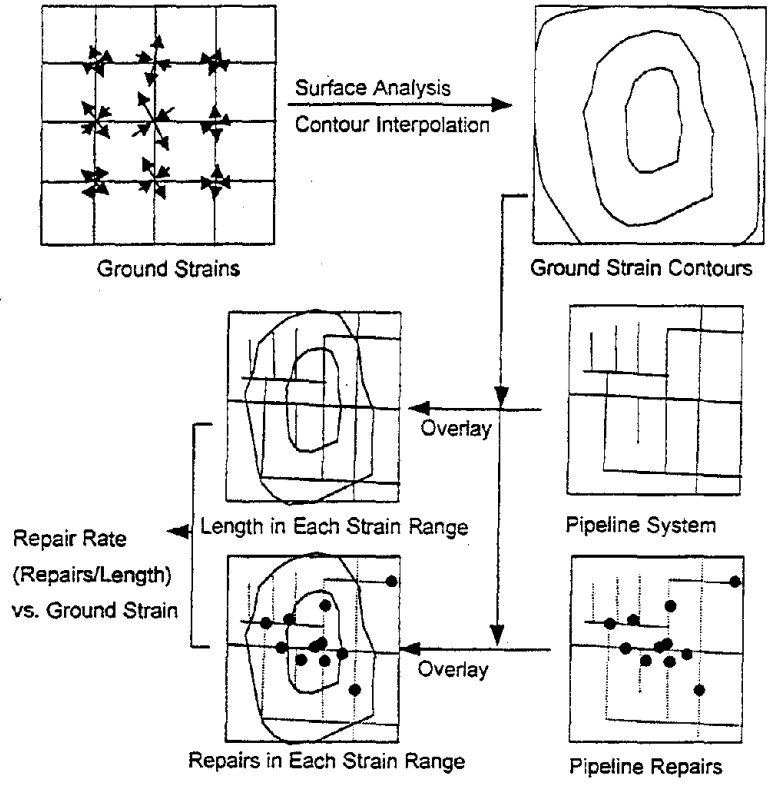


Figure 8. Procedure for calculating repair rate in each strain range.

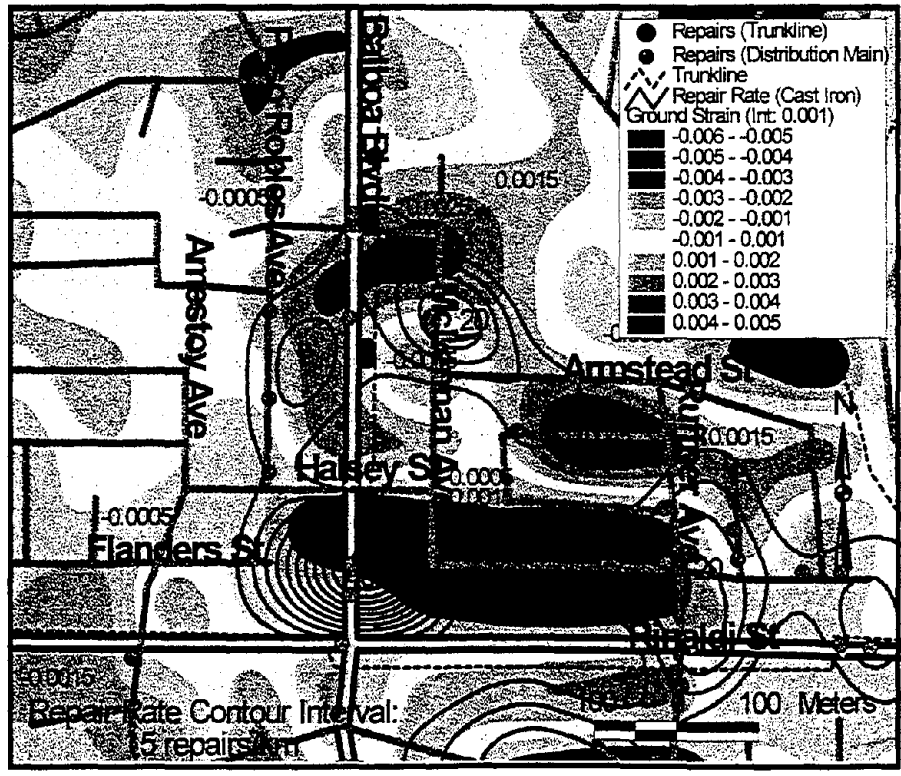


Figure 9. Distribution of CI repair rate and ground strain.

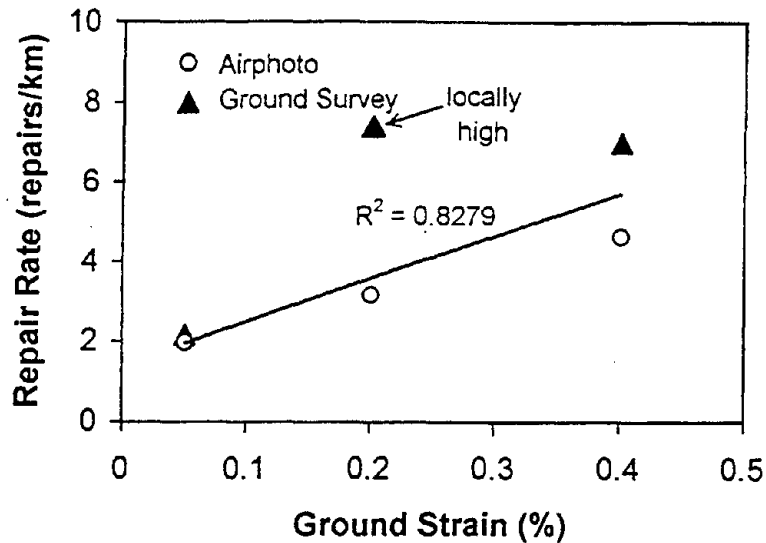


Figure 10. Correlation between ground strain and CI repair rate.

CONCLUSIONS

The research described in this paper represents the first time that comprehensive GIS analyses were performed for a large US water supply with extensive earthquake damage and strong motion data. It was found that the spatial distribution of pipeline damage can be used to delineate areas vulnerable to site amplification and ground failure. In the San Fernando Valley, three areas of intense pipeline damage: 1) near the intersection of Balboa Blvd. and Rinaldi St., 2) in the west central part of the valley, and 3) at Sherman Oaks coincide with locally high groundwater tables. At the first two locations, subsurface investigations have disclosed either liquefiable sands, soft saturated clays, or some combination of both (Holzer, et al., 1996).

Good spatial correlations between pipeline repair rates and both peak acceleration and velocity were found, although neither parameter provides consistently strong correlations at all locations. Linear regressions with relatively high r^2 were developed between CI pipeline repair rates and both peak acceleration and velocity. These correlations were derived from sampling areas containing a minimum of 150 km of pipeline. Screening data to evaluate areas containing more than 100 to 150 km of pipeline provides a sampling size sufficient to represent average population performance. Such transient motion correlations, however, represent average, not site-specific, response. Locally high concentrations of damage are related to local geotechnical conditions, such as the presence of saturated loose sands and soft clay that either can result in liquefaction or site amplification.

Locations of locally high repair rates, such as those influenced by liquefaction-induced lateral spread, cannot be predicated with acceleration and velocity correlations developed for average system performance. Site specific characteristics are needed to evaluate the potential for ground failure or strong motion amplification. Studies of pipeline system performance during

earthquakes, however, can help to delineate geotechnical hazards so that locally vulnerable areas can be identified for future seismic mitigation.

Detailed air photo and GIS analyses of an area of large PGD near the Balboa Blvd. and Rinaldi St. intersection were performed. Good spatial correlations between pipeline repair rate and permanent ground strain were shown, and a linear regression between repair rate and permanent ground strain was developed. Regressions of this type provide opportunities for predicting local damage from estimates of PGD. Improved capabilities in predicting both average system performance from transient motion estimates and local damage concentrations from PGD estimates will enhance loss estimation procedures and emergency planning for future earthquakes.

ACKNOWLEDGMENTS

Research reported in this paper was supported by the National Center for Earthquake Engineering Research, Buffalo, NY, under Contract Nos. R91598 and R91605. The authors express their deep gratitude to Mr. H. Dekermenjian and C. Davis of LADWP for their assistance in obtaining valuable information. The authors also thank Prof. M. Hamada of Waseda University and Mr. Yasuda of Hasshu Co., Ltd. for their assistance in the air photo measurements. The manuscript was prepared by L. McCall, and A. Avcisoy helped prepare the figures.

REFERENCES

- Chang, S.W., Bray, J.D., and Seed, R.B., "Engineering Implications of Ground Motions from the Northridge Earthquake," *Bulletin of the Seismological Society of America*, Vol. 86, No. 1B, Feb., 1996, pp. 5270-5288.
- Dewey, J.W., Reagor, B.G., Dengler, L., and Moley, K., "Intensity Distribution and Isoseismal Maps for the Northridge, California, Earthquake of January 17, 1994," *U.S. Geological Survey Open-File Report 95-92*, U.S. Department of the Interior, Washington, DC, 1995.
- Eguchi, R.T., "Seismic Hazard Input for Lifeline Systems," *Structural Safety*, E.H. Vanmarcke, Ed., Elsevier Science Publishers, Vol. 10, May 1991, pp. 193-198.
- ESRI, *The ARC/INFO User's Guide*, Environmental Systems Research Institute, Inc., Redlands, CA, 1994.
- Holzer, T.L., Bennett, M.J., Tinsley, J.C. III, Ponti, D.J., and Sharp, R.V., "Causes of Ground Failure in Alluvium During the Northridge, California Earthquake of January 17, 1994," *Technical Report NCEER-96-0012*, National Center for Earthquake Engineering Research, Buffalo, NY, 1996, pp. 345-360.
- Katayama, T., Sato, N., Kimimasa, S., "SI-Sensor for the Identification of Destructive Earthquake Ground Motion," *Proceedings*, 9th World Conference on Earthquake Engineering, Tokyo-Kyoto, Japan, August 1988, pp. 667-672.

O'Rourke, T.D. and Toprak, S., "GIS Assessment of Water Supply Damage from the Northridge Earthquake," Geotechnical Special Publication No. 67, J.D. Frost, Ed., ASCE, New York, NY, 1997, pp. 117-131.

Sano, Y., "GIS Evaluation of Northridge Earthquake Ground Deformation and Water Supply Damage," MS Thesis, Cornell University, Ithaca, NY, 1998.

SELCUK TOPRAK

Graduate Research Assistant
The School of Civil and Environmental Engineering
Cornell University
Ithaca, NY 14853

Phone: (607) 255-4292 (Office)
(607) 277-4072 (Home)
FAX: (607) 255-9004
E-mail: st31@cornell.edu



Education

Ph.D. in Civil Engineering, Cornell University, NY, December, 1997.
MS in Civil Engineering, Bogazici University, Istanbul, Turkey, May 1992.
BS in Civil Engineering, Bogazici University, Istanbul, Turkey, May 1991.

Professional Memberships

American Society of Civil Engineers (ASCE) .
Earthquake Engineering Research Institute (EERI).
Seismological Society of America (SSA).

Recent Publications

- O'Rourke, T.D. and **Toprak, S.**, " Case History of Pipeline Response to Ground Deformation at Balboa Blvd., 1994 Northridge Earthquake, " Proceedings, Sixth U.S. - Japan Workshop on Earthquake Disaster Prevention for Lifeline Systems, Osaka, Japan, July 1995, pp. 3-20.
- O'Rourke, T. D., **Toprak, S.**, and Sano, Y., "Los Angeles Water Pipeline System Response to the 1994 Northridge Earthquake, " Technical Report NCEER-96-0012, National Center for Earthquake Engineering Research, Buffalo, NY, 1996, pp. 1-16.
- O'Rourke, T. D. and **Toprak, S.**, "GIS Assessment of Water Supply Damage from the Northridge Earthquake , " Geotechnical Special Publication No. 67, J. D. Frost, Ed., ASCE, NY, 1997, pp.117-131.

II. SEISMIC BEHAVIOR OF LIFELINE FACILITIES

“Liquefaction Hazard Mapping in the Puget Sound Region”

P. Grant

“City of Seattle Bridge Seismic Retrofit Program”

R. Miller, J. Lem, R. Shulock

“Floating Characteristics of a Sewer Due to Soil-Liquefaction”

M. Kaneko, K. Tamura, H. Kobayashi

“Reliability of Buried Pipelines Subjected to Large
Permanent Ground Displacements”

C. Scawthorn, D. Ballantyne

“Effect of Spatial Variation of Ground Motion for
Ordinary Bridges”

M. Shinozuka, G. Deodatis

LIQUEFACTION HAZARD MAPPING IN THE PUGET SOUND REGION

W. Paul Grant¹

ABSTRACT

Research efforts by sponsored by the US Geological Survey (USGS) have led to the development of liquefaction hazard maps for 12 quadrangles in the greater Puget Sound Region. This mapping has been conducted by the Washington State Department of Natural Resources (DNR) and also consultants in private industry (Grant, 1990 and 1993). The methodologies of these studies was generally similar. First subsurface boring data was collected throughout the study area for the differing geologic units. The liquefaction potential of the geologic units was evaluated using Seed's empirical procedure which is based upon Standard Penetration Test (SPT) N-values. The liquefaction potential was generally evaluated for a scenario earthquake which would result in a peak ground surface acceleration of 0.30g. This acceleration is consistent with a 10 percent chance of occurrence in a 50 year interval. All studies used a thickness criteria which related the relative liquefaction susceptibility of the geologic strata to the percent of borings within in the unit that would show at least 3m (10 feet) of liquefaction. Using this criteria, liquefaction hazard maps were developed for the different quadrangles delineating areas of high, moderate, and low potential for liquefaction. Typically, uncontrolled fill and holocene alluvium was found to have the highest relative liquefaction potential whereas glacially consolidated Pleistocene sediments had the lowest relative liquefaction potential.

¹ Principal Geotechnical Engineer, Kleinfelder Inc., 2405-140th Ave NE, Suite A101, Bellevue, Washington, 98005.

Introduction

Liquefaction is the phenomena in which loose sands existing below the water table develop excess hydrostatic pore pressures during strong earthquake ground shaking to the point where the material essentially loses its shear strength. Liquefaction has been well documented in past earthquakes and in the results of laboratory testing of soils. The direct consequences of liquefaction are settlements and potential lateral movements to structures that are founded on or above the liquefiable soils. Indirect damage resulting from liquefaction may include rupture of utility lines and potential secondary damage resulting from fires or the inability to extinguish fires because of lack of water from severed water mains.

The Puget Sound region has experienced losses related to liquefaction during both the 1949 and 1965 Puget Sound earthquakes (Chleborad and Schuster, 1990). Future liquefaction related losses may be greatly reduced by mapping potentially hazardous areas and requiring special foundation treatment for structures built in these zones. Similarly, knowledge of areas which may be highly damaged as a result of earthquake induced liquefaction may be used in disaster response planning efforts. Thus, liquefaction identification is a key element in reducing future earthquake losses.

Recognizing the opportunity to reduce future earthquake losses, the USGS has sponsored several efforts in developing earthquake hazard maps for various geographic locations within the Puget Sound Region. Through these efforts, liquefaction hazard maps have been developed for the greater Seattle and Tacoma areas (Grant, 1990 and 1993) as well as adjoining areas between these two metropolitan regions (Palmer and others, 1994 and 1995; Dragovich and Pringle 1995). Additionally, work is in progress for liquefaction hazard mapping of the highly populated areas east of Seattle (see figure 1). The following briefly describes the geology and tectonic conditions in the Puget Sound area, the methodologies of these various studies, and the general findings of these efforts.

Geology

The greater Puget Sound area, as shown on figure 1, is located in what is termed the Puget Lowland, a structural and topographic trough that is bounded on the east by the Cascade Mountains and on the west by the Olympic Mountains. The Puget Lowland is a northerly-trending feature which extends through Western Washington to southern British Columbia. It is underlain chiefly by thick Quaternary sediments overlying Tertiary volcanic and sedimentary bedrock. The depth of bedrock is quite variable, typically ranging from approximately 425m (1,400 feet) to 610m (2,000 feet) in the Seattle/Tacoma area (Hall and Othberg, 1974).

The Quaternary sediments overlying the bedrock include Pleistocene glacial deposits, which are pervasive throughout the study area, as well as Holocene alluvial deposits. Excluding the most recent glacial recessional outwash sands and gravels, all Pleistocene and older sediments have been extremely overconsolidated by the weight of massive ice

sheets. These sediments, including glacial recessional deposits and till, are typically present in the upland areas. The low-lying river valleys have been filled by Holocene alluvial sediments. Alluvium within the Puyallup River Valley and the Green River Valley (see Figure 1) consists of mixtures of sand and silt. The alluvium-filled valleys typically have a high water table (generally within 10 to 15 feet of the ground surface) while discontinuous, perched groundwater conditions exist in the upland areas.

Major land modifications conducted within the Puget sound region include the filling of Commencement Bay in Tacoma and Elliot Bay in Seattle at the turn of the century to accommodate an expanding population and industrial base. This filling was also accompanied by a straightening of the channels of the Puyallup River in Tacoma and the Green and Duwamish Rivers in Seattle. These old channels are typically composed of loose sands and silts that were placed under hydraulic conditions.

Tectonics and Seismicity

Historical seismic activity within the Puget Sound region has consisted of numerous earthquakes of low to moderate magnitude and occasional strong shocks. The majority of earthquakes experienced within the region are shallow events with magnitudes less than 5. However, the strongest historic earthquakes in the region, the 1949 and the 1965 Puget Sound earthquakes, were both deep events with focal depths in excess of 40 kilometers. Both of these earthquakes are believed to be associated with stress relief within the subducting Juan de Fuca plate beneath the Puget Lowland. The Olympia earthquake of April 13, 1949, had a magnitude of 7.1 and a maximum epicentral intensity of VIII. The April 29, 1965, Seattle-Tacoma earthquake had a magnitude of approximately 6.5 and a maximum intensity of VII-VIII. The only earthquake instrumentally recorded in Tacoma was the event of April 29, 1965. This event was recorded at the Tacoma County City Building, which is located in the uplands area, and underlain by Pleistocene deposits of glacially consolidated sands and gravels. The recorded a peak ground acceleration at this site from the 1965 event was approximately 0.06g. It is estimated that accelerations in Tacoma during the 1949 event may have been on the order 0.10g. Both the 1949 and 1965 earthquakes were recorded in Seattle. Both events had recorded peak ground accelerations of 0.10g or less.

Research into Paleoseismic events within Western Washington suggests that the region has experienced subduction zone earthquakes of magnitude 8 or greater several times during the past 2,000 years (Atwater, 1987). Additional research has suggested a magnitude 7.0 to 7.5 earthquake may have occurred on the Seattle Fault as recently as 1,100 years ago (Bucknam and others, 1992). The Seattle Fault is a westerly-trending structure, which passes below Seattle and parallels Interstate 90 (see figure 1). A lineament with a structure similar to the Seattle Fault is mapped through Commencement Bay at Tacoma with a southeasterly-trending strike, virtually along the axis of the Puyallup River Valley. Instrumentally recorded seismicity, however, does not occur preferentially along these or any other block boundaries. The majority of instrumentally recorded events occurs in a diffuse pattern throughout the Puget Lowland.

Regional Hazard Mapping

Research Efforts

The earthquake liquefaction hazard maps that have been developed to date are schematically shown on figure 1. The mapped areas include the Seattle North and Seattle South quadrangles (Grant, 1990), portions of the Gig Harbor, Steilacoom, Tacoma North, Tacoma South, Poverty Bay, and Puyallup quadrangles near Tacoma (Grant, 1993); the DesMoines and Renton quadrangles (Palmer, Schasse, and Norman, 1994); the Auburn and Poverty Bay quadrangles (Palmer and others, 1995); and the Sumner quadrangle (Dragovich and Pringle, 1995). In all, these quadrangles account for liquefaction hazard mapping over an area of approximately 1300 km². Additionally, work is currently ongoing to map liquefaction hazard potential in the greater Bellevue area which includes the Redmond, Kirkland, Issaquah, and Mercer Island quadrangles. All of these study efforts have been funded through external research grants of the USGS.

Historical Liquefaction

Liquefaction has reportedly occurred at numerous locations in the greater Puget Sound area during both the 1949 and 1965 earthquakes (Chleborad and Schuster, 1990). Sites in the Tacoma area where liquefaction has occurred during both the 1949 and 1965 earthquakes are shown in figure 2. Reports of liquefaction were more extensive in the region during the larger 1949 earthquake than the 1965 event. Within this area, approximately 20 percent of the reported cases of liquefaction occurred along the Tacoma tide flats fill at the mouth of Commencement Bay. Liquefaction of the hydraulic fills that were placed in this area is consistent with the observed liquefaction from the 1989 Loma Prieta earthquake (USGS, 1989), which indicated that areas of severe liquefaction also correlated with locations of uncontrolled, random fills.

However, within the Tacoma region, the vast majority of reported instances of liquefaction occurred in the Puyallup River Valley approximately 8 km (5 miles) southeast of the tide flats area. The areas of reported liquefaction occurred within alluvial deposits that quite likely includes a hyperconcentrated flow deposit (Lahar runoff) from Mount Rainier. This deposit has been termed "Puyallup Sand" by Palmer and others (1991). This material is the water dominated runoff of a mud flow from Mt. Rainier and contains angular to subangular sand size volcanic fragments from a volcanic eruptions from about 2200 years ago.

Study Methodology

All of the liquefaction efforts conducted to date generally follow a similar work sequence. Specifically, the first steps in each of these investigations was to gather subsurface boring information from available sources to characterize the engineering properties of the various geologic units in the area. These efforts typically included reviewing data from 100 to 400 borings.

The second element in the liquefaction studies was the selection of an appropriate peak ground acceleration for use in evaluating the liquefaction potential of the various geologic units. Essentially all studies conducted in the region used a singular value of acceleration of 0.30g. Regional seismic hazard mapping would suggest that this peak ground acceleration would have a 10 percent probability of occurrence during a 50 year interval (475 year return interval) (Algermissen, 1988). The various liquefaction mapping studies selected this return interval and peak ground acceleration to be consistent earthquake design provisions of the 1991 and later editions of the Uniform Building Code (ICBO, 1991) which is used for the design of new buildings in the western United States. For simplicity, the liquefaction evaluations assumed that this 0.30g ground acceleration would occur as a result of a magnitude 7.5 scenario earthquake.

The liquefaction potential of the underlying soils was estimated using the empirical procedures of Seed (Seed and others, 1984). The liquefaction hazard ratings for locations within the Seattle and Tacoma areas were derived based upon two criteria. First, a threshold criteria (Grant, 1990) was used to relate the liquefaction hazard ranking of a geologic unit based upon the percent of the SPT N-values that fall below a threshold N-value needed to resist liquefaction from a 0.30g ground acceleration. Secondly, a thickness criteria was used to establish the liquefaction hazard rating based upon the percentage of the borings in which at least 3m (10 feet) of liquefaction would be computed for a 0.30g peak ground acceleration. The following summarizes both rating criterias:

Table 1. Liquefaction hazard rating criteria

<u>Hazard Ranking</u>	<u>Threshold Criteria (percent of N-value below the 0.30g threshold criteria)</u>	<u>Thickness Criteria (percent of borings with 3m of computed liquefaction for 0.30g acceleration)</u>
High	>50	>50
Moderate	25-50	25-50
Low	10-25	<25
Very low	<10	---

The work conducted by the DNR in the populated areas between Seattle and Tacoma used a thickness criteria similar to that used in the studies of Seattle and Tacoma. This thickness criteria rating was a common element among all studies in the area.

Figures 3 and 4 present an example of the use of the above criteria to classify the liquefaction potential of the fill and alluvial soils at the mouth of the Puyallup River in Tacoma. First, the data presented in figure 3 correspond to the threshold evaluation criteria in which the standard penetration N-values have been differentiated for both clean

sand and silty sand with further differentiation based upon drilling technique (auger borings and rotary borings). As shown on this figure, the mean SPT N-values for the tide flats alluvium typically falls below the liquefaction threshold indicating that liquefaction would occur in over 50 percent of the data between the depths of about 10 and 30 feet below the ground surface. Thus, according to the threshold criteria, this unit would have a high liquefaction hazard rating.

A similar characterization of the liquefaction potential of the fill soils in the Tacoma tide flat is presented in figure 4 corresponding to the thickness criteria. This figure indicates that approximately 65 percent of the borings would have 3m (10 feet) cumulative thickness of potentially liquefied sediments. This finding corresponds to a high liquefaction hazard rating using the thickness criteria. This rating is also in agreement with the conclusions derived using the threshold criteria.

Liquefaction Hazard Maps

Using the criteria and methodology discussed above, studies were completed for evaluating the liquefaction potential of the different geologic units in the Puget Sound region. An example of the results of these studies is shown on figure 5 which illustrates the liquefaction hazard potential of the soils in the Tacoma area. The results of this study indicate that the fills and Holocene alluvium at the mouth of the Puyallup river and along the Puyallup River Valley would have a high liquefaction hazard potential. The results of the liquefaction studies for other mapped quadrangles in the region similarly indicated that Holocene alluvium and fill soils along the Puyallup River and Green River/ Duwamish Rivers had a high liquefaction susceptibility rating. This rating is also consistent with the historic reports of liquefaction occurring within these areas. This high susceptibility ranking is also consistent with a ranking scheme developed by Youd and Perkins (1978).

The results of the liquefaction studies in the Puget Sound region also indicated that the Holocene alluvium encountered in the upland areas would have a moderate liquefaction rating. This rating is also consistent with historical observations which denoted no liquefaction in these relatively limited upland areas during either the 1949 or 1965 earthquakes. The geologic ranking of Youd and Perkins (1978) would also suggest a moderate liquefaction hazard potential for these materials.

Finally, Pleistocene glacially consolidated sediments would have either a low or very low liquefaction rating. This susceptibility is also consistent with criteria of Youd and Perkins (1978).

Map Applications

An excellent use of these earthquake liquefaction hazard maps has been by the City of Seattle which has incorporated the liquefaction hazard map into its sensitive areas folio. Seattle's sensitive area folio delineates areas that may be affected by earthquake induced instability as well as ground movements that may be initiated through excessive rainfall or other triggering mechanisms. Within these areas, special studies are needed to address potential hazards and to develop remediation schemes, if appropriate. Thus, any new buildings located in an area which has been designated as having a high liquefaction hazard potential would need to have specialized geotechnical studies to address this hazard and provide specific recommendations to mitigate its potential occurrence or its effect upon the performance of the structure.

The second use of the liquefaction hazard maps for Seattle has been by insurance companies that have used these maps to evaluate potential portfolio losses as well as to evaluate whether or not the company will underwrite earthquake insurance policies for specific locations. In instances where earthquake insurance may be denied, the application of these hazard maps has more of an influence on existing owners to take appropriate steps to mitigate earthquake losses at their facilities.

A final use of the earthquake hazard map for the City of Seattle has been with the Seattle Engineering Department (Seattle Public Utilities) which has used this information to evaluate which bridges within Seattle may be vulnerable to earthquake damage and may be inoperative following a future event. This information was used both by the engineering department and the planning department to develop appropriate emergency response plans.

Conclusions

In Conclusion, the Puget Sound region is located in an area which has experienced several historic earthquakes that have resulted in reported liquefaction. The areas of highest liquefaction potential are located in the low lying areas along the Puyallup River, the Green River, and the Duwamish River. These low lying areas typically support much of the industrial and commercial base for the greater Seattle Tacoma area. Through research efforts sponsored by the USGS, maps have been developed covering 12 quadrangles (over 1300 km²). These maps are currently being used by cities to evaluate potential emergency response scenarios to a future earthquake. These maps have also served as a basis for delineating areas in which specialized geotechnical studies are needed to confirm the occurrence of liquefaction and to develop appropriate mitigation strategies for new structures. By identifying these high hazard areas, the engineering community is better able to assess the potential effects of a future earthquake in the region and to take appropriate action to reduce future earthquake losses.

References

- Algermissen, S.T., 1988, Earthquake hazard and risk assessment -- some applications to problems of earthquake insurance in workshop on earthquake risk: Information Needs of the Insurance Industry, USCG Open File Report 88-669, p. 9-39.
- Atwater, B.F., 1987, Evidence for great Holocene earthquakes along the outer coast of Washington state: *Science*, v. 236, p. 942-944.
- Bucknam, R.C., Hemphill-Haley, E., and Leopold, E.B., 1992, Abrupt uplift within the past 1,700 years at southern Puget Sound, Washington: *Science*, v. 258, p. 1611-1613.
- Chleborad, A.F., and Schuster, R.L., 1990, Ground failure associated with the Puget Sound region earthquakes of April 13, 1949, and April 29, 1965: USGS Open File Report 90-687, 136 p.
- Dragovich, J.D. and Pringle P.T., 1995, Liquefaction susceptibility for the Sumner 7.5 minute Quadrangle, Washington: Washington Division of Geology and Earth Resources, Geologic Map GM-44, Olympia, Washington, scale 1:24,000.
- Grant, W.P., 1990, Evaluation of liquefaction potential, Seattle, Washington: USGS Report, Contract No. 14-08-0001-G-1385, 47 p.
- Grant, W.P., 1993, Evaluation of liquefaction potential, Tacoma, Washington: USGS Report, Contract No. 14-08-0001-G-1978, 43 p.
- Grant, W.P., Perkins, W.J., and Youd, T.L., 1992, Evaluation of liquefaction potential, Seattle, Washington: in Rogers, A.M., Walsh, T.J., Cockleman, W.J., and Priest, G.R., compilers, Earthquake Hazards in the Pacific Northwest of the United States: USGS Open File Report 91-441-T.
- Hall, J.B., and Othberg, A.L., 1974, Thickness of unconsolidated sediments, Puget Lowland, Washington: Washington Division of Geology and Earth Resources Geologic Map GM-12, 3 p.; 1 sheet, Scale 1:250,000.
- International Conference of Buildings Officials, 1991, Uniform Building Code: Whittier, Calif., 1,050 p.
- Palmer, S.P., Pringle, P.T., and Shulene, J.A., 1991, Analysis of liquefiable soils in Puyallup, Washington, in International Conference on Seismic Zonation, 4th Stanford University, California, 1991, Proceedings: Oakland, Calif., Earthquake Engineering Research Institute, v. 2, p. 621-628.

- Palmer, S.P., Schasse, H.W., and Norman, D.K., 1994, Liquefaction susceptibility for the Des Moines and Renton 7.5-minute Quadrangles, Washington: Washington Division of Geology and Earth Resources, Geologic Map GM-41, Olympia, Washington, scale 1:24,000.
- Palmer, S.P., Walsh T.J., Logan R.L., and Gerstel, W.J. 1995, Liquefaction susceptibility for the Auburn and Poverty Bay 7.5-minute Quadrangles, Washington: Washington Division of Geology and Earth Resources, Geologic Map GM-43, Olympia, Washington, scale 1:24,000
- Seed, H.B., Tokimatsu, K., Harder, L.F., and Chung, R.M., 1984, The influence of SPT procedures in soil liquefaction resistance evaluations: Berkeley, California, University of California UCB/EERC-84/15.
- U.S. Geological Survey (USGS), 1989, Lessons learned from the Loma Prieta, California, earthquake of October 17, 1989: USGS Circular 1045, 48 p.
- Youd, T.L., and Perkins, D.M., 1978, Mapping liquefaction-induced ground failure potential: Journal of the Geotechnical Engineering Division, American Society of Civil Engineers, v. 104, no. GT4. p. 433-446.

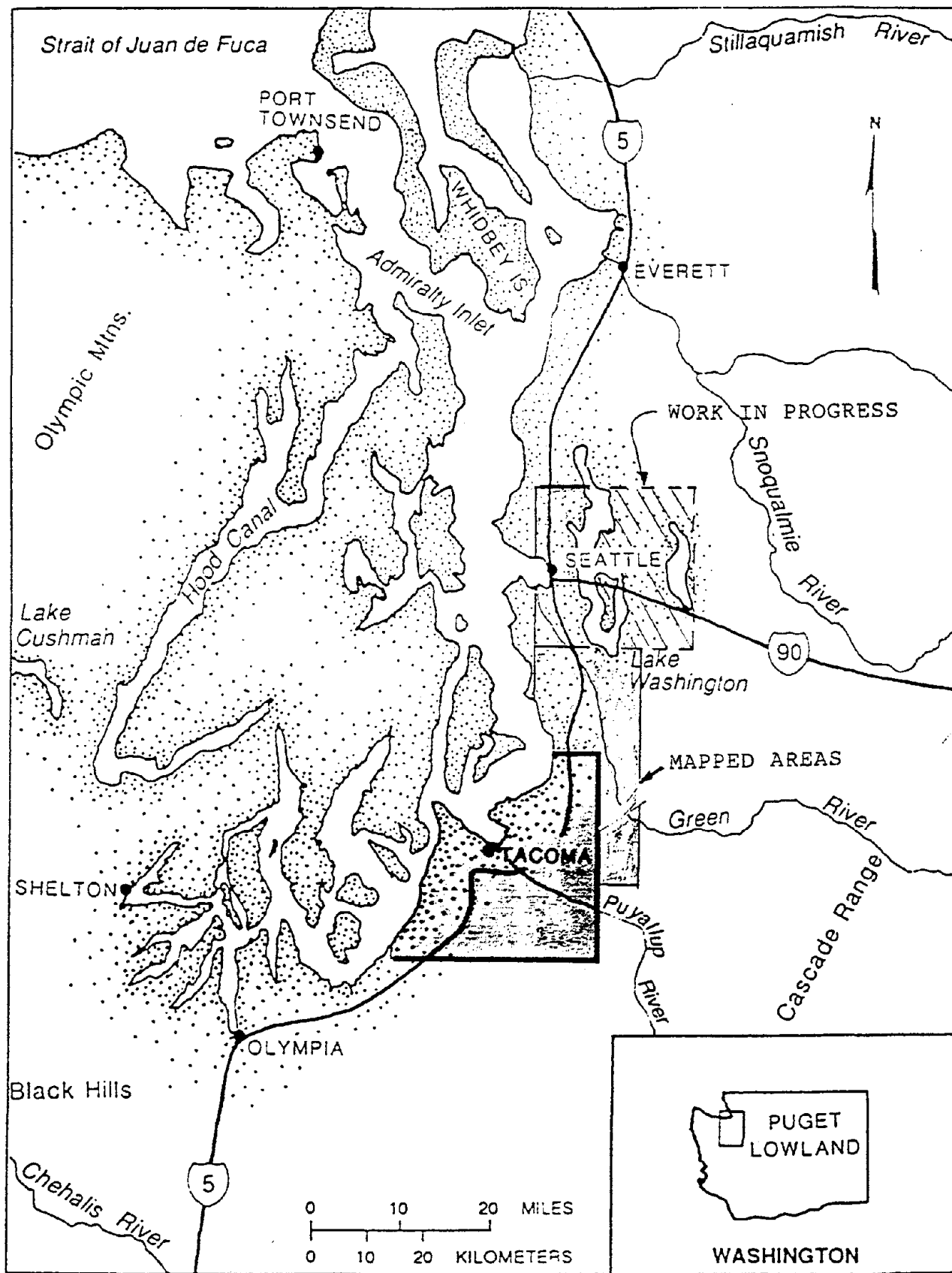


Figure 1. Location of study area.

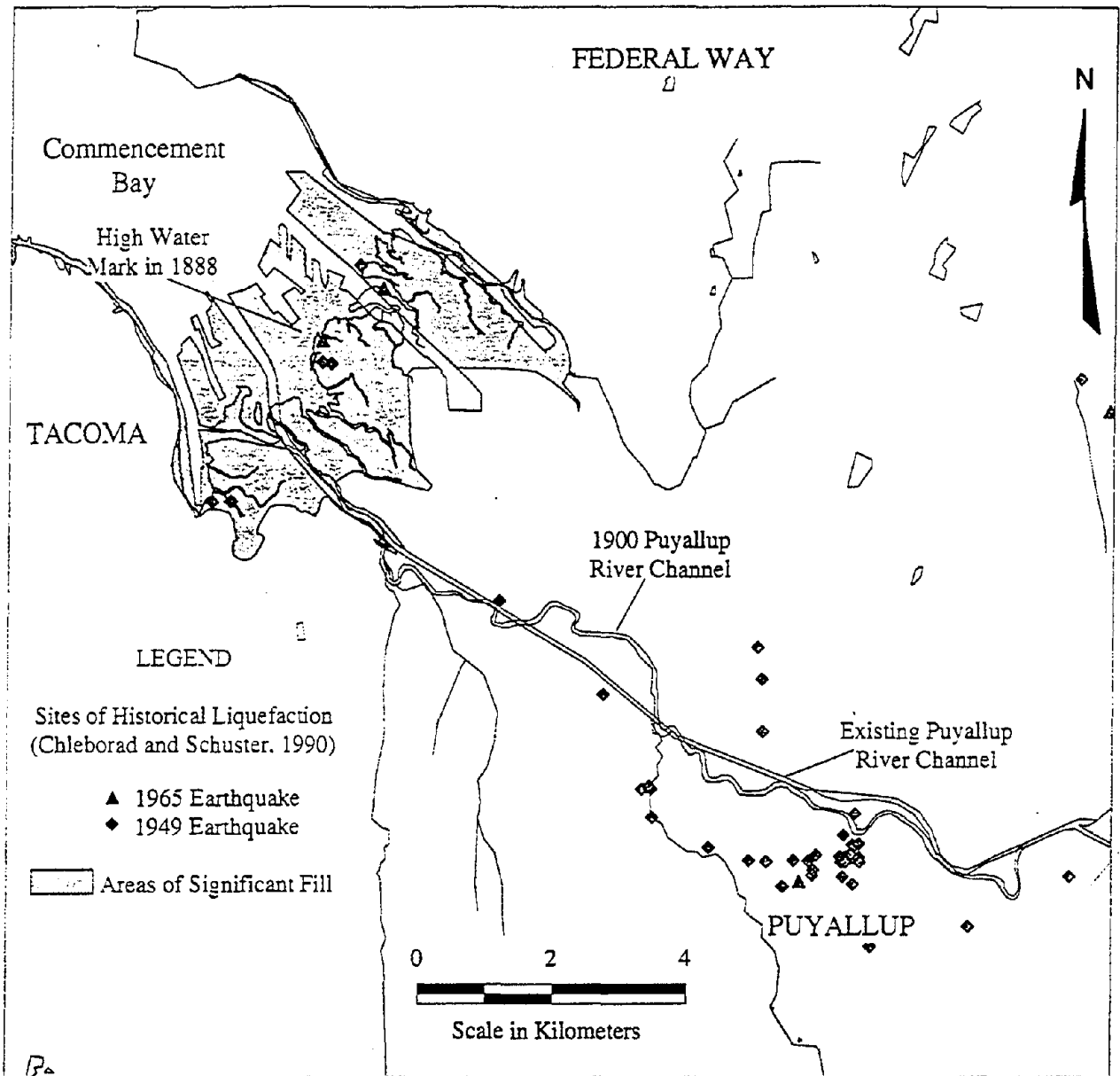


Figure 2. -Historical land modification and sites of liquefaction.

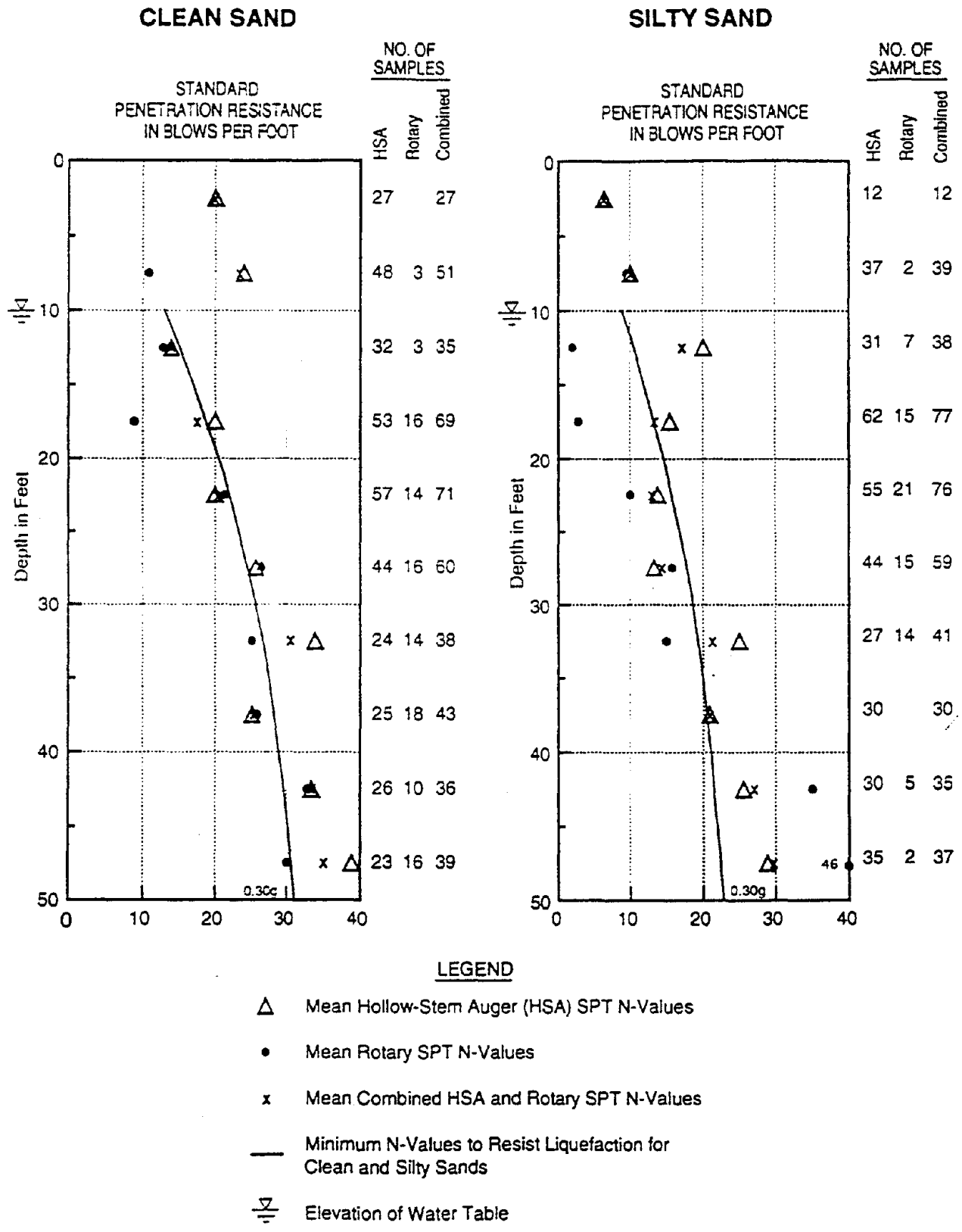
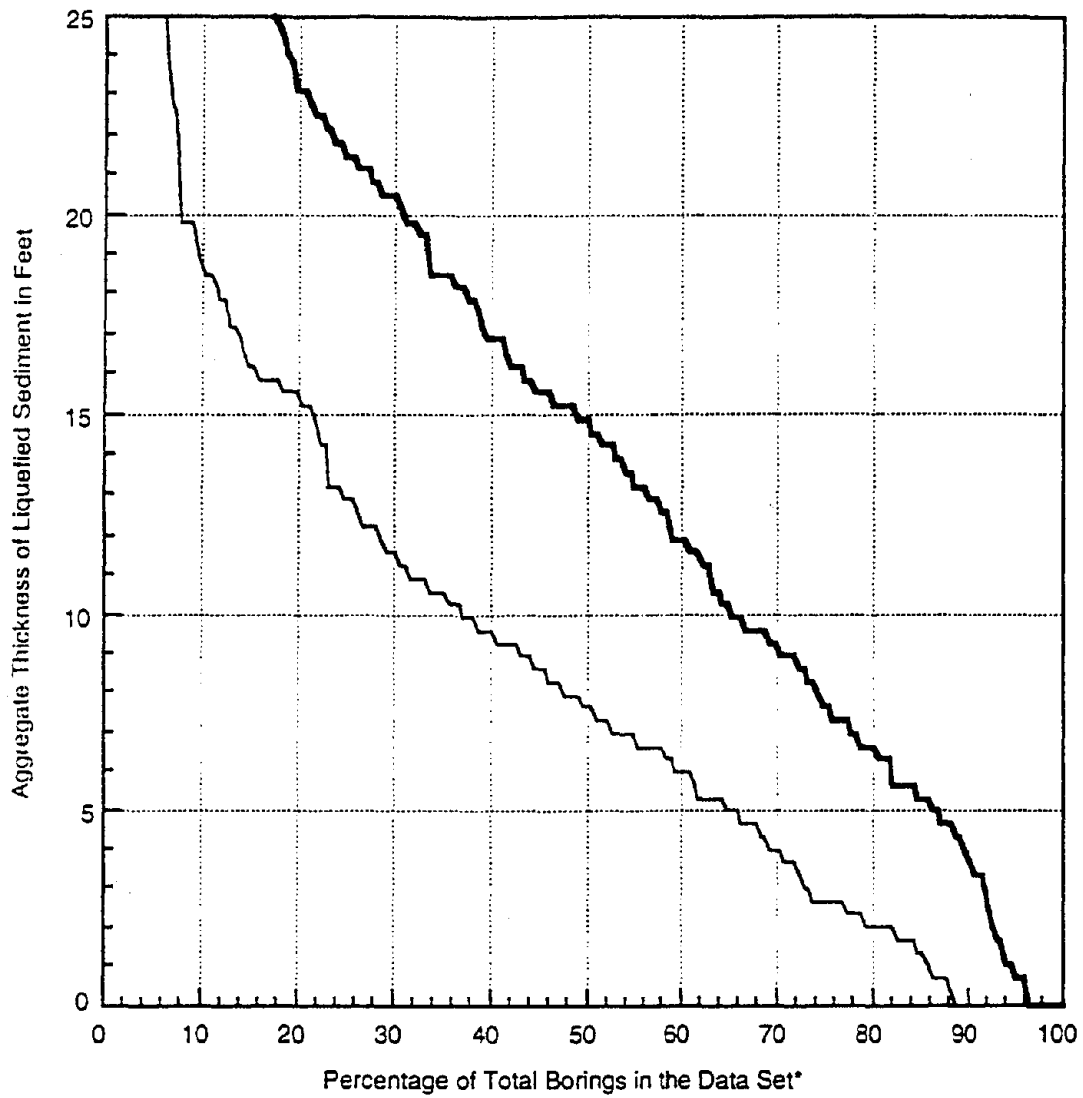


Figure 3. -Liquefaction evaluation, Tacoma tideflats alluvium, threshold criteria.

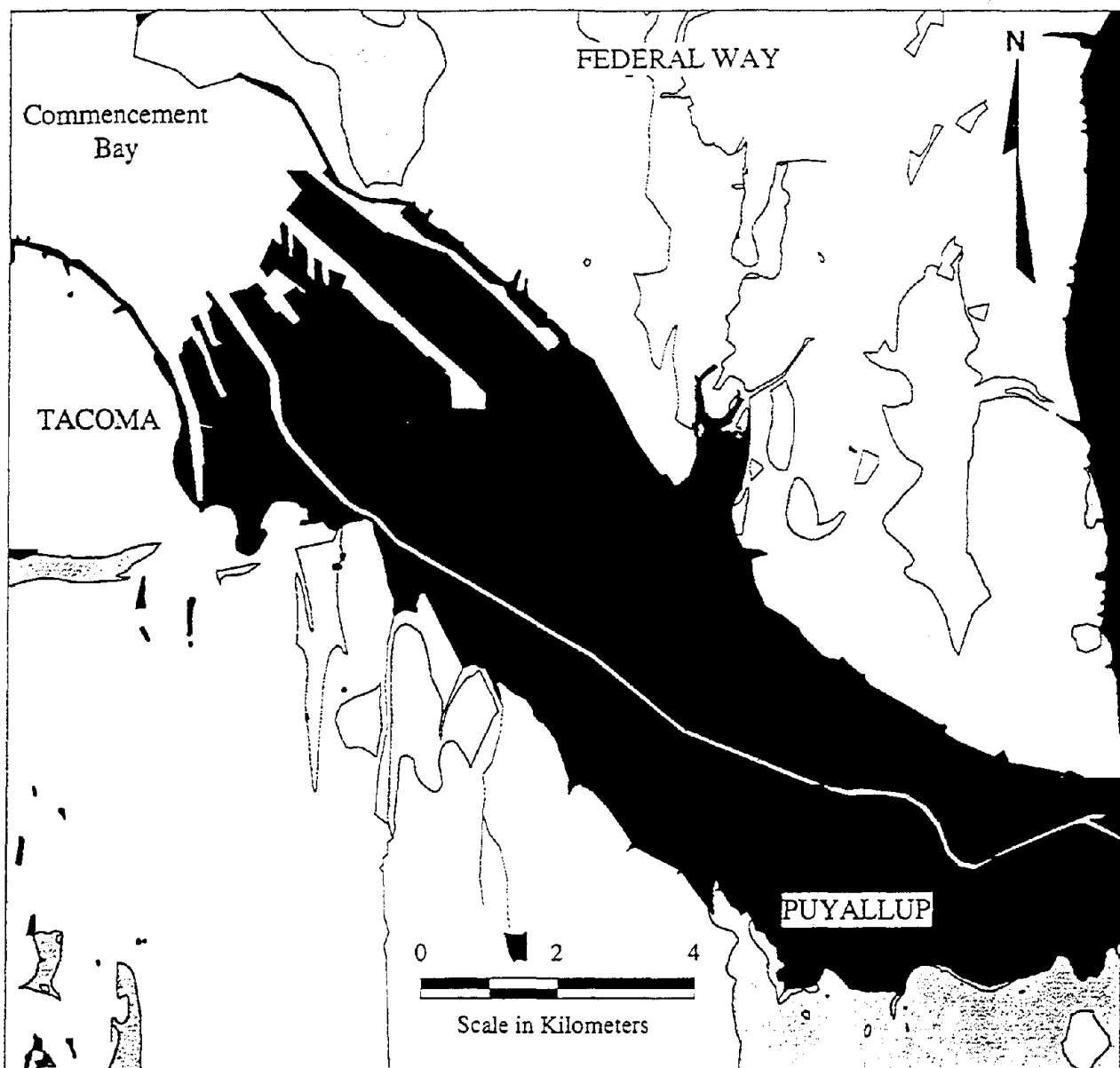


LEGEND

- Cumulative Thickness of Liquefaction for M7.3, 0.30g Event
- Cumulative Thickness of Liquefaction for M7.3, 0.15g Event

* The number of borings in the Data Set is 202.

Figure 4. -Liquefaction evaluation, Tacoma tideflats fill, thickness criteria.



EXPLANATION

Zone and Liquefaction Susceptibility	Geologic Units
High 	Fill, Puyallup River Valley Alluvium (Holocene)
Moderate 	Other Alluvium, Upland Closed Depression Deposits (Holocene)
Low 	Vashon Recessional Outwash (Pleistocene)
Very Low 	Steilacoom Gravel, Glacially Consolidated Sediment (Pleistocene)

Figure 5. -Liquefaction potential map, Tacoma, Washington.

W. PAUL GRANT

Principal Geotechnical Engineer

Summary of Experience

Mr. Grant has more than 25 years of engineering experience, the majority of which has focused upon earthquake engineering. He has developed earthquake criteria for either the design of new facilities or for the evaluation of existing structures; performed or directed seismicity studies which developed and characterized the design earthquake for major projects; performed or directed earthquake engineering studies which established peak ground motions and response spectra for various design earthquakes; performed soil structure interaction studies that evaluated the dynamic behavior of nuclear facilities; and conducted innumerable evaluations of the ground stability, including landslide and liquefaction potential, of various projects. Mr. Grant has received numerous research grants from the U.S. Geological Survey, the U.S. Nuclear Regulatory Commission, and the National Science Foundation for various earthquake engineering studies.

Education

MBA Business Administration, University of Washington, 1996
MS Civil Engineering, University of California, Berkeley, 1971
BS Civil Engineering, University of Vermont, 1970

Registrations

Professional Engineer (Civil), Washington, Alaska, California

Professional Affiliations

American Society of Civil Engineers
Consulting Engineers Council of Washington, 1992-94 Board of Directors
International Society for Soil Mechanics and Foundation Engineering
Earthquake Engineering Research Institute
Seismological Society of America
Structural Engineers Association of Washington
Tau Beta Pi
Chi Epsilon

Select Project Experience

A representative selection of Mr. Grant's projects is included below.

Seismic Design Technical Manual Development for FHWA. Project Manager and Principal in charge of efforts to assist the Federal Highway Administration (FHWA) in developing a manual to assist Highway bridge engineers in conducting seismic design studies of new bridges. Specific elements of this work included assisting the project team leader, Berger ABAM, in developing a course manual outlining the elements of seismic design of bridges and providing input to 7 examples illustrating the concepts provided in the course. Specific responsibilities included provision of geotechnical

from:
13th Annual International Bridge Conference
June 1996 - Proceedings

Seismic Retrofit Design for the University Bridge

JOYCE M. LEM, ROBERT J. SHULOCK, Anderson Bjornstad Kane Jacobs, Inc.,
Seattle, Washington

IBC-96-70

INTRODUCTION

As part of its bridge seismic retrofit program begun in 1990, the City of Seattle Engineering Department authorized the seismic retrofit design of the University Bridge. Because the bridge is a component of a City-designated "lifeline" route, the goal of the retrofit design was to ensure the bridge could remain open to emergency vehicles following a major earthquake. The 1467-ft long bridge consists of a series of structural units of different construction types, with the units separated by expansion joints. A number of seismic retrofit schemes were considered for each structural unit or group of units. This paper describes the bridge, seismic retrofit schemes selected for final design, and key retrofit elements.

BRIDGE DESCRIPTION

As shown in Figure 1, the University Bridge is delineated into the South Approach, a 200-ft long decked truss on piers; the 291-ft long double-leaf

Bascule Bridge; and the North Approach, which consists of 3 decked truss units and two multi-span reinforced concrete beam-and-slab structures totaling 975 ft in length. The Bascule Bridge was originally constructed in 1916. When the bascule bridge was modified in the early 1930's, the South and North Approaches as they exist today were constructed. The Bascule Bridge piers and some of the approach piers are located in the Lake Washington Ship Canal, which provides water access between Lake Washington and Puget Sound. The bridge carries four lanes of vehicular traffic and has sidewalks and bicycle lanes along both sides. Typical out-to-out width of the bridge is 75 ft.

For the seismic retrofit design, original bridge plans (as-builts) were available, but there was limited information regarding construction specifications other than the structural notes on the plans.

The bridge foundations typically consist of spread footings that are supported upon glacial till. However, three piers (2, 3, and 16) that are located adjacent to large diameter (9 ft to 16 ft) utilities are supported

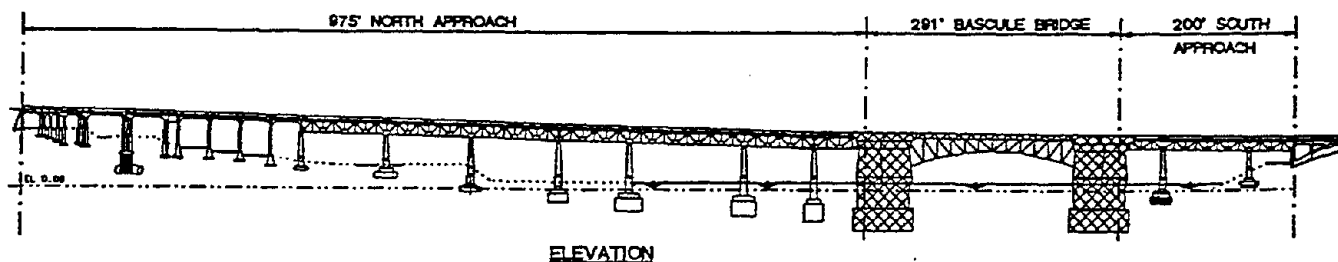


FIGURE 1: EXISTING CONDITION

upon timber piles which extend through the utility backfill and bear upon the underlying till soils. The South Bascule Pier is also supported upon timber pilings that were driven through outwash deposits and also extend to the till. These piles have lengths on the order of 30 ft or less and ultimate compressive capacities of about 90 tons.

DESIGN CRITERIA

Seismic design loading was based on current AASHTO Standard Specifications for Highway Bridges (15th Edition). The design parameters included using acceleration coefficient $A = 0.3$ and soil coefficient $S = 1.2$ (Type II soil profile). The acceleration coefficient corresponds to a seismic event with a recurrence interval of approximately 475 years, and takes into account the probability of seismic activity along the Seattle Fault and the Cascadia Subduction Zone off the west coast of Washington. Liquefaction potential was deemed very low due to the dense nature of the glacial till underlying the entire bridge.

In its existing condition, major damage to the University Bridge is anticipated under the design seismic loading. In the retrofitted condition, acceptable damage to the bridge in the retrofitted condition is limited to that which will not cause collapse nor prevent emergency vehicle access. This objective is beyond the AASHTO standard design goal of "preventing collapse."

Seismic analysis included response spectrum analyses of global and local models using the program GTSTRUDL, displacement capacity analyses using WFRAME and WSECTION, and limited time-history analysis.

SEISMIC DESIGN ISSUES

The retrofit design for the bridge was an evolutionary and iterative process. Schemes were proposed, analyzed, and discarded due to construction feasibility and/or problems in the assumed load path(s) or interaction of the individual bridge units. Some of the schemes and structural issues involved are described here:

In its existing condition, the South Approach trusses transmit both longitudinal and transverse loads to the South Bascule Pier at the deck level. The deck slab at the pier acts as a "bumper" for the South Approach slab. Loads are also transmitted in the transverse direction as the configuration of the deck slab expansion joint is like a shear key (see Figure 2, Plan). However, it was determined that additional lateral loads other than those imposed by the Bascule

leaf were undesirable. An isolation bearing scheme was proposed to limit the loads to the bascule pier, but the extensive joint details required at the deck level to permit isolation were costly and difficult to construct.

During the design process, connecting the bascule leaves at midspan was considered. The objective was to develop a simple span between the two bascule pier supports in place of the independently acting leaf spans of the existing condition. This proved impractical for a number of reasons, including unevenness in the existing midspan joint and that the result was large transfer loads in the lightest (weakest) portion of the bascule trusses.

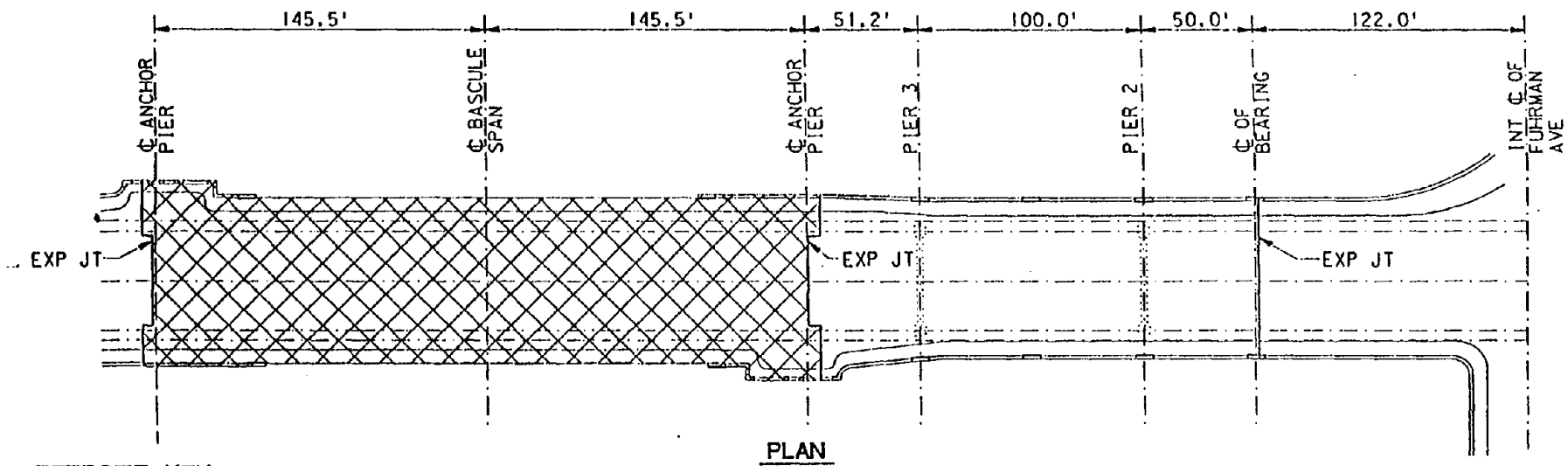
At the North Approach trusses, there initially was debate between "stiff" and "soft" solutions. The stiff scheme involved strengthening and stiffening of two of the pier bents by adding shear walls and drilled shaft foundations. This scheme also required a review and strengthening of the load path for transferring lateral shear from the deck level to the piers. To reduce the lateral seismic loads to the structural system, a soft solution involving isolation bearings at all the north truss bearings was also considered. The cost and difficulty of modifying the deck joint was determined to be unfeasible, so seismic isolation was limited to six of the seven North Approach truss spans.

At the transition between the north trusses and the concrete units, interaction between the structures needed to be evaluated. "Tension" and "compression" models involving these sets of structures were considered throughout the design process.

The analysis of the North Approach concrete units' focused on displacement capacity of the columns. One solution considered included using drilled shafts behind the North Abutment wall as anchors tied to the concrete deck slab by high strength rods in conjunction with shear walls at selected pier bents. Deflections were still problematic with this scheme. Shear walls alone at selected bents were also considered. However, the aesthetics of shear walls were viewed unfavorably in light of a newly installed at-grade public art sculpture which interlaced with several bent columns. The final design of a "superbent" provides a solution which satisfied both aesthetic and functional concerns.

SEISMIC RETROFIT DESIGN FEATURES

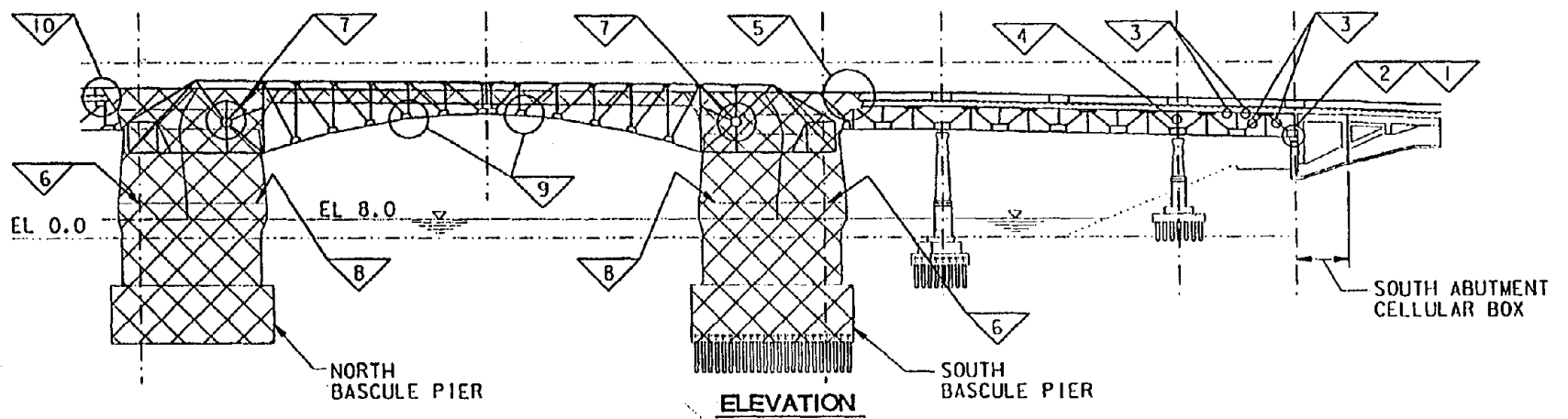
SOUTH APPROACH - Figure 2 includes an elevation of the three-span continuous truss (50'-100'-50'), South Abutment, and two concrete piers that comprise the South Approach. The truss and stringers at the north end of the South Approach truss are supported by the South Bascule Pier. Thermal



PLAN

RETROFIT KEY

- | | | | | | |
|---|---|---|--|----|--|
| 1 | INSTALL SOIL ANCHORS, TRANSFER BEAM, & AUXILIARY STRUTS AT BOTTOM CHORD | 5 | RELEASE LATERAL RESTRAINT AT TRUSS & STRINGER BEARINGS | 9 | MODIFY BOTTOM LATERALS, TYP |
| 2 | "PIN" FLOOR BEAM TO ABUTMENT WALL | 6 | ADD WALL BETWEEN ANCHOR PIERS | 10 | CONNECT NORTH APPROACH TRUSS TO BASCULE PIER |
| 3 | REINFORCE TRUSS TOP CHORD OR DIAGONAL | 7 | MODIFY TRUNNION BEARINGS | | |
| 4 | REINFORCE TRUSS VERTICAL | 8 | MODIFY CHANNEL PIER WALL | | |



ELEVATION

FIGURE 2: SO. APPROACH BASCULE & NO. APPROACH CONNECTION

expansion is accommodated by rocker nest bearings and roadway deck joints at the Abutment and Bascule Pier. A typical cross-section of the decked truss with its cast-in-place concrete deck and an elevation of the pier bent are shown in Figure 3. The trusses are spaced at 45 ft; floor beams that cantilever outboard of the trusses support the concrete deck. The height of the pier bents varies, increasing at piers closer to the bascule.

Figure 2 also indicates the seismic retrofit elements for the South Approach. At the South Bascule Pier, the anchor bolts at the stringer and truss bearing are cut to eliminate existing lateral restraint (and load transfer to the bascule pier) and the stringers are braced against buckling by simple diaphragms made of structural steel channels. The decked truss is pinned longitudinally at the South Abutment using tensioned soil anchors through the South Abutment, which is a 20 ft deep, filled cellular box structure, and into the backfill behind the abutment. Transverse transfer beams along the abutment face transfer soil anchor loads to the truss main members and to auxiliary struts at the truss bottom chord level. This system transmits axial loads developed along the truss. The connection of the soil anchors to the existing truss is completed after the anchors are tensioned to ensure that the pretensioning force is in the soil anchors and not taken up by the

truss. Where necessary, existing truss members are reinforced with plates and angles to sustain the axial loads transmitted to the soil anchors. To transmit transverse seismic loads, the floor beam adjacent to the abutment wall is connected to the wall by six 9-inch diameter steel pins. At Pier 2, the truss verticals are reinforced with bolted-on web plates to help transfer loads to the bearings and pier.

This retrofit scheme achieves several goals. A primary accomplishment is that no lateral seismic loads are imposed on the South Bascule Pier. Also, there is minimum retrofitting required at the South Bascule Pier and no modifications are required at deck expansion joints. The latter condition also eliminates the need for traffic closures on the bridge during construction of the South Approach retrofit elements. Finally, by "fixing" the truss at the South Abutment, a substantial reduction in longitudinal and transverse loads to the existing concrete piers is achieved, thereby eliminating the need for cost retrofit of the piers.

BASCULE BRIDGE AND FIRST NORTH APPROACH TRUSS SPAN - The double leaf Bascule Bridge consists of two nearly identical structures (Figure 2). In plan, each bascule leaf is 143 ft long from midspan to back of counterweight. The counterweight is housed inside the lightly-reinforced concrete bascule pier under a 45-ft long fixed span. The

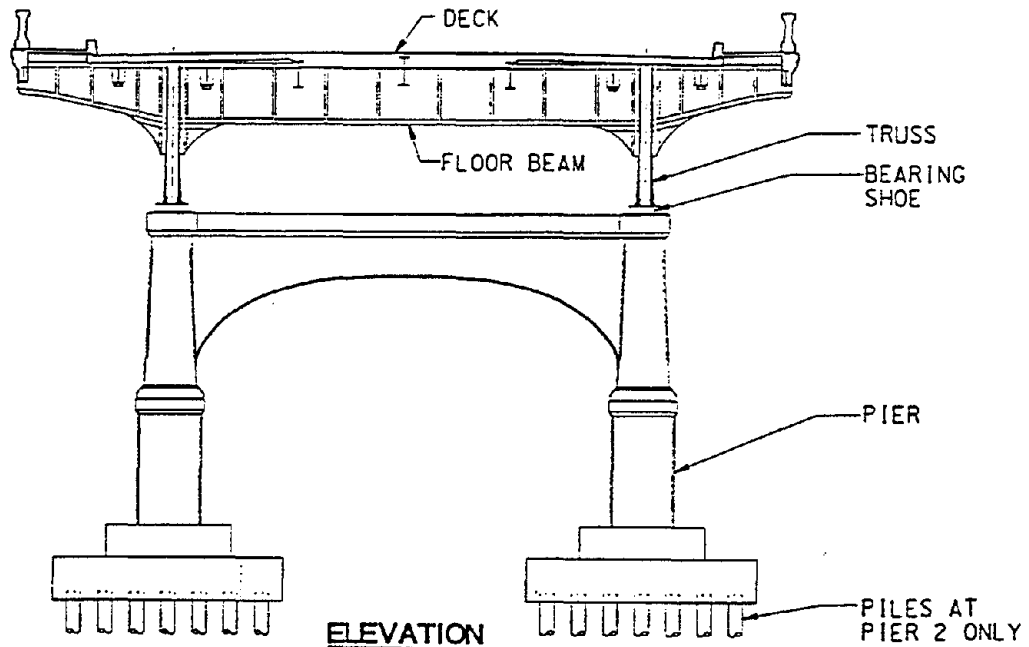


FIGURE 3: TYPICAL TRUSS SECTION AT PIER

bascule piers are 72-ft x 63-ft in plan and 96 ft tall, measured from bottom of footing to roadway deck. Each pier consists of four main corner columns connected by longitudinal and transverse walls. The primary difference between the two piers is that the South Pier footings are on untreated timber piles while the North Pier is on spread footings. The bascule spans operate independently. There is no span lock tying the leaves together at midspan. The bascule spans were analyzed and retrofitted for the closed position only.

Under lateral seismic loading, the bascule leaves and counterweights translate transversely, imposing shear and torsion on their respective piers. Hence, the retrofit scheme for the Bascule Bridge involves strengthening structural elements along this load path. Retrofit consists of reinforcing the leaves by providing an additional lateral bracing system. The brace elements are 1-inch diameter high strength rods (ASTM A722), lightly pretensioned, and designed as a stand-alone tension bracing system. Connection of the trunnion bearings to the supporting bascule pier is ensured by adding a system of high strength bolts and steel keeper plates and, where feasible, encasing the trunnion bearings in reinforced and post-tensioned concrete. Because the existing walls of the bascule piers are lightly reinforced, selected walls were strengthened by thickening and adding high-strength post-tensioning bars. These pier wall modifications create a stronger box wall system which can resist the lateral loads from the bascule leaves and counterweights.

As previously discussed, the isolation of the majority of the North Approach truss spans necessitated the attachment of the adjacent 56-ft long North Approach truss span to the North Bascule Pier. To do this, a system of 1-inch diameter high strength rods connected by brackets to the top chords and through a new concrete bolster cast inside the bascule pier is designed to resist tension loads. A steel bumper at the top chord transmits impact (compression) loads to the bascule pier.

NORTH APPROACH TRUSSES - Figure 4 depicts the three truss units at the North Approach: the 56-ft single span adjacent to the North Bascule Pier and two 3-span units (80.5'-132.5'-80.5' and 100'-100'-100'). The cross-section is similar to that of the South Approach (Figure 3). The lateral framing at the bottom chord is nominal and cannot support the seismic shear loads induced by the deck mass. The truss bearings are a mix of fixed shoes at Piers 5, 6, 8 and 9 and rocker nests at the ends of the truss units (expansion joints). The concrete is cracked at the tops of the some of the columns where the anchor

bolts for the bearings are embedded and the capacity of the anchor bolts is suspect. It was apparent that bearing anchorages would need to be addressed in any seismic retrofit design scheme.

A seismic isolation system was designed for the two 3-span truss units acting together as a system while the single-span truss was attached to the North Bascule Pier. Load reduction provided by seismic isolation addresses a number of issues: the limited shear capacity of the concrete piers, the condition of the existing bearings and their anchorage to the columns, and the weakness of the load path from the deck slab to the bearings.

Two proprietary bearing systems were selected as allowable systems: a lead rubber bearing system and a friction pendulum system. Modifications to the trusses were designed for jacking and support of the trusses during installation of the bearings. Repairs to the concrete column caps where there is crack damage is specified. In the cases of fixed bearings, the tops of the column caps need to be removed to provide space (height) for the isolation bearings. At Pier 7 where the ends of the trusses share a common pier support, the two truss units are connected at the floor beam and bearing levels to ensure they behave as a single superstructure unit.

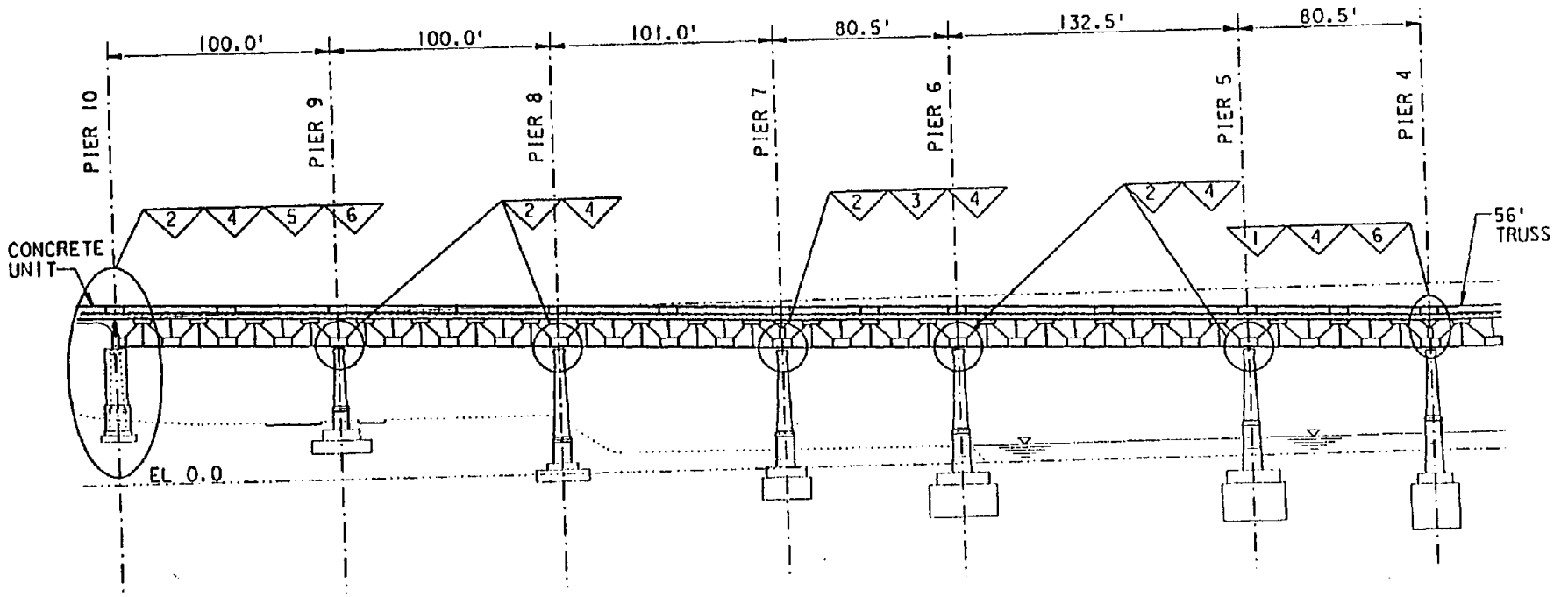
At the ends of the isolated truss units, the expansion joints at the deck needed to be modified to allow the large deflections required for successful behavior of the isolation bearings. A joint system combining a proprietary steel-reinforced rubber plate and steel plates was designed, providing a joint that can withstand everyday truck loading and thermal movements. However, under seismic movements of ± 7.5 inches, the joint is expected to "pull apart." A steel plate to bridge the opened joint may be needed if the joint pulls apart. At the end of the north truss (Pier 10), the truss stringers in the existing condition are supported directly by Pier 10. In order to isolate the truss superstructure from the concrete units, a new transverse truss which behaves like a floor beam carries the stringer loads to the truss bearings.

NORTH APPROACH CONCRETE UNITS - The north 321 ft of the North Approach, from Pier 10 to the North Abutment, consists of two multi-span concrete girder units (Figure 5). Typically, the concrete deck is supported by four reinforced concrete haunched girders. From Bent 11 to Bent 17, the girders are supported by four-column bents. The girders and columns are spaced transversely at 17 ft or 20 ft. Bent 18 has five columns; the fifth column added at the east side supports a fifth girder which spans to the abutment wall. The columns are aligned under the girders. The deck slab, girders and haunched

RETROFIT KEY

- 1 ISOLATION BEARING SYSTEM AT NORTH TRUSS BEARINGS. SLIDING BEARING AT BEARING OF 56' TRUSS
- 2 ISOLATION BEARING SYSTEM AT TRUSS BEARINGS
- 3 CONNECT FLOOR BEAMS ACROSS EXPANSION JOINT

- 4 MODIFY TRUSS FOR JACKING DURING BEARING REPLACEMENT
- 5 CONSTRUCT TRANSVERSE TRUSS BELOW STRINGERS. REMOVE EXISTING STRINGER BEARINGS
- 6 REPLACE DECK EXPANSION JOINT. REMOVE AND REPLACE ROADWAY ASPHALT OVERLAY

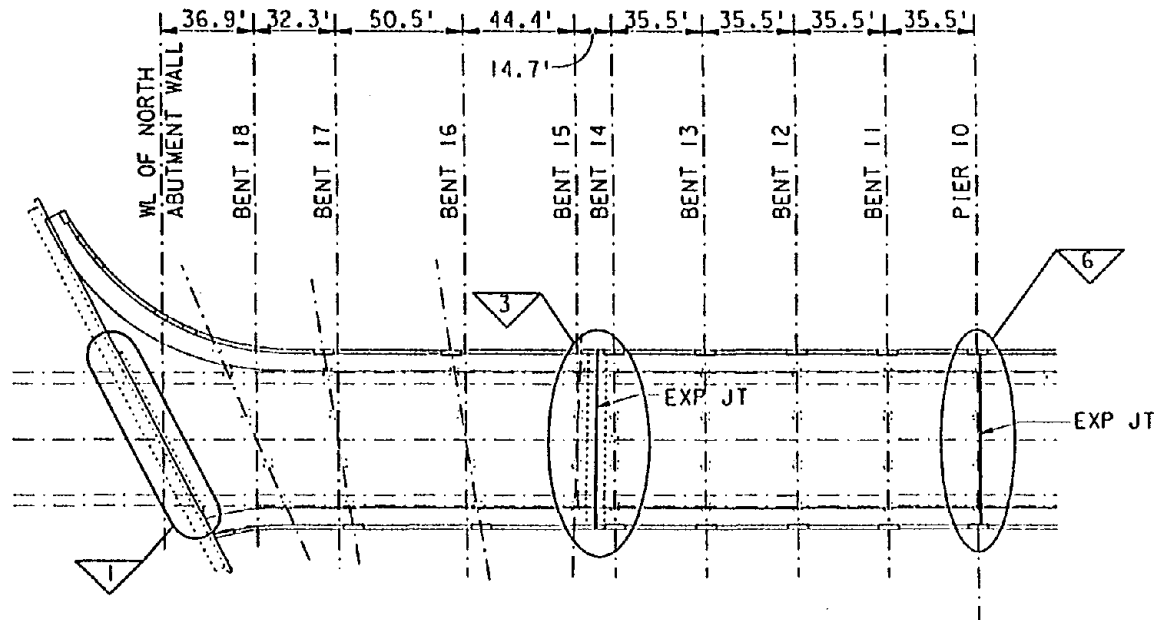


92

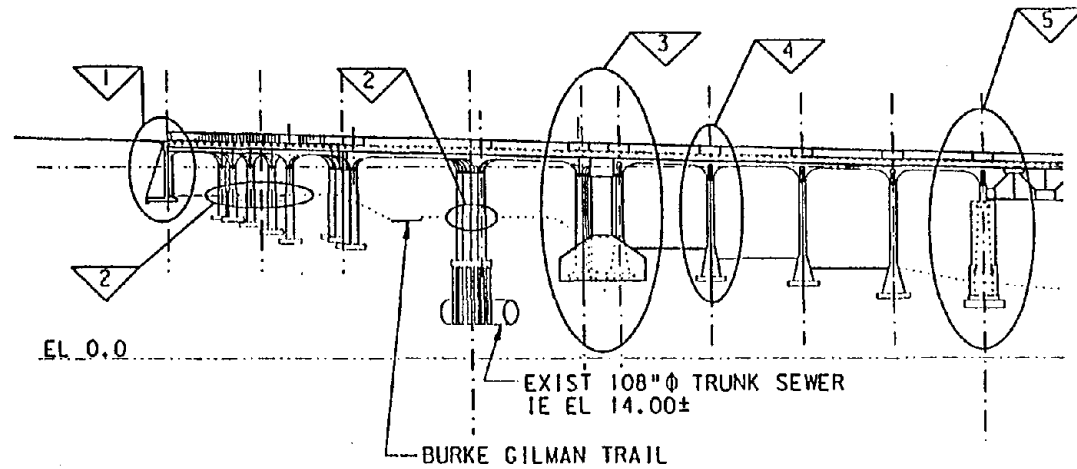
FIGURE 4: NORTH APPROACH TRUSSES

RETROFIT KEY

- 1 FASCIA WALL & GIRDER END BLOCKS AT NORTH ABUTMENT WALL
- 2 GRADE SLAB JOINTS
- 3 SUPERBENT, ELIMINATE EXPANSION JOINT
- 4 MODIFY EXISTING COLUMN REINFORCING
- 5 STEEL COLUMN JACKETS, POST-TENSION MODIFIED CROSSBEAM, WALL ABOVE CROSSBEAM
- 6 REPLACE DECK EXPANSION JOINT, REMOVE AND REPLACE ROADWAY ASPHALT OVERLAY



PLAN



ELEVATION

FIGURE 5: NORTH APPROACH CONCRETE UNITS

crossbeams at the column tops are monolithic. Columns are also monolithic with crossbeams except at Pier 10 and Bents 17 and 18 where steel rocker bearings are concealed in the tops of the columns. The rocker bearings are aligned to allow rotation along the longitudinal axis of the bridge. At the south end of the concrete units, Pier 10 is a combination of the typical two-column bent supporting the truss span to the south, with four columns extending above the crossbeam to support the concrete girders to the north.

At the south concrete unit, the bents are square to the bridge centerline, spaced at 35.5 ft. At the north unit, the spans range from 32 ft to 51 ft and the abutment and bents are skewed up to 27 degrees. There is a 1-inch open deck joint between the short cantilever spans of the two units.

For seismic design, the two concrete units are treated as a single structural system. In the transverse direction, the primary load carrying elements are Pier 10, which is strengthened, a new superbent between Bents 14 and 15, and a fascia-catcher wall at the North Abutment. In both the transverse and longitudinal directions, the superbent furnishes stiffness needed to limit deflections of the existing columns to sustainable levels.

The new superbent, constructed in the space where the cantilevered spans and expansion joint are located, connects the two concrete units. The superbent consists of a deep H-shaped spread footing, two 9-ft x 9.5-ft columns outboard of the original bent columns and a crossbeam cast below the existing deck slab. The crossbeam interlocks and connects the girders and crossbeams of the concrete units by filling the spaces between them. The crossbeam and foundations are designed to sustain the plastic moment capacity of the columns. In the longitudinal direction, the superbent limits the deflections at Pier 10 to about 3.5 inches.

At Pier 10, steel column jackets installed at the lower pier columns provide the ductility capacity needed to sustain transverse deflections. Because it provides direct vertical support for the concrete girders, the crossbeam is strengthened by post-tensioning. This increases the beam's flexural capacity to be greater than the plastic moment capacity of the jacketed columns below. The crossbeam post-tensioning is encased in reinforced concrete cast at the sides and below the beam. An infill wall above the crossbeam confines the stub columns and the rocker bearings concealed in the columns.

At the North Abutment, a 12-inch thick concrete fascia wall with corbels below the girders is

constructed against the existing wall. Concrete shoulders are added to the sides of the girders. These girder shoulders provide greater transverse capacity and will bear on the fascia wall below in a catcher condition. Hence, the abutment wall retrofit provides shear wall stiffness in the transverse direction and a catcher system in the longitudinal direction. The abutment backfill also acts as a "bumper" in the longitudinal direction.

Other retrofit items required to survive seismic deflections include cutting joints in the grade slab at Bents 16 and 18 to ensure that the columns there are not restrained laterally. Also, at Bent 14, the longitudinal reinforcing is reduced at the top and bottom of the columns to allow plastic hinges to form in the columns without risk of shear failure.

CONCLUDING REMARKS

Several analyses of the University Bridge structures were performed, in its existing and retrofitted conditions. In particular, load path and capacity of the existing structures were taken into account. The goals of functionality following the design seismic event, cost-effectiveness and constructability were evaluated throughout the design process. The resulting design includes a variety of seismic retrofit measures which depend on structure type and behavior.

ACKNOWLEDGEMENTS

The seismic retrofit design for the University Bridge has been a team effort. The retrofit of the Bascule Bridge and the South Approach was designed by Exeltech Engineering (Olympia, WA). Andersen Bjornstad Kane Jacobs, Inc. designed the North Approach retrofit with assistance from Civiltech Corporation (Bellevue, WA). The geotechnical engineer was Shannon & Wilson, Inc (Seattle, WA). Design was coordinated through Sverdrup Civil, Inc. (Bellevue, WA). Peer review was coordinated through Parsons Brinkerhoff Quade & Douglas, Inc. Thanks are extended to all the consultants and to the staff of the Seattle Engineering Department who participated in the design and review for this challenging project.

FLOATING CHARACTERISTICS OF A SEWER DUE TO SOIL-LIQUEFACTION

Keiichi Tamura ¹, Masahiro Kaneko ² and Hiroshi Kobayashi ³

- 1 Head, Ground Vibration Division, Public Works Research Institute
Ministry of Construction, 1 Asahi, Tsukuba-shi, Ibaraki-ken 305 Japan
2 Senior Research Engineer, ditto
3 Researcher Engineer, ditto

ABSTRACT

In Japan, sewers are often constructed in the liquefiable soil layers. Sewers in these soil layers have suffered damage by floating due to soil-liquefaction in past earthquakes. Presented are the floating characteristics of sewers in liquefiable layers and the effectiveness of backfilling (crushed stone, dense sand etc.) to reduce floating due to soil-liquefaction by shaking table tests.

INTRODUCTION

Japan's land area of about 378,000 km² (146,000 square miles) is one twenty-fifth that of the United States. Nearly 70% of Japan's land area is mountainous. Japan has a population of 123.61 million (1990), half that of the United States, and the population is greatest along the strip of coastal plain where the transportation and industrial facilities are most highly developed. Lifeline facilities (road, port, sewer, waterworks, electricity, telephone, gas etc.) also exist there.

Coastal plain generally has loose sand layer with high underground water level, where soil-liquefaction occurs frequently during earthquakes. Lifeline facilities have been frequently damaged due to soil-liquefaction in Japan. For example, photos 1 and 2 show the damage to sewers in Niigata earthquake (1964) and Kushiro-oki earthquake (1993). Sewers' damage due to soil-liquefaction have also occurred in many other earthquakes.

In this paper we study floating characteristics of sewers in liquefiable layers and the effectiveness of backfilling (crushed stone, dense sand etc.) to reduce floating due to soil-liquefaction by shaking table tests.



Photo 1 Damage to sewer in Niigata earthquake (1964)

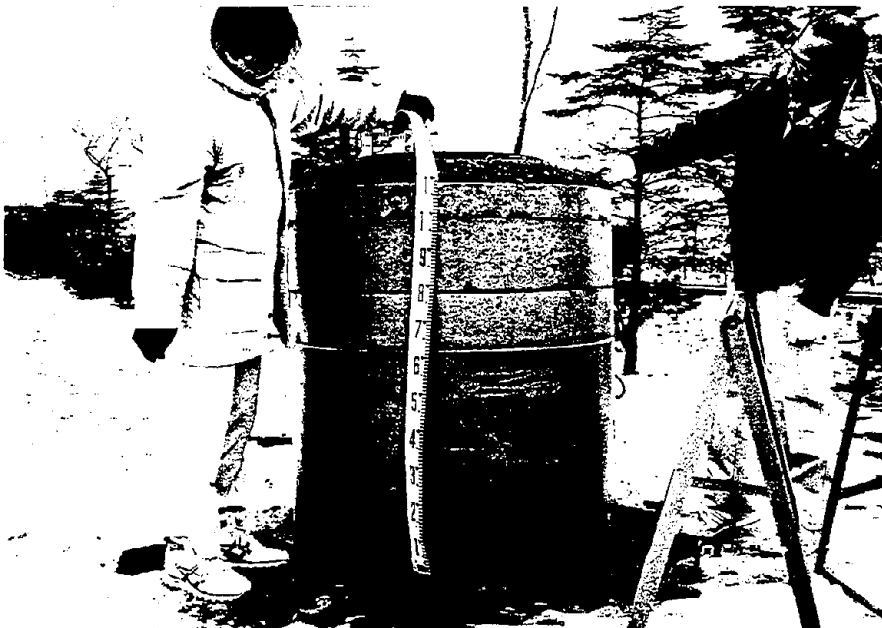


Photo 2 Damage to sewer in Kushiro-oki earthquake (1993)

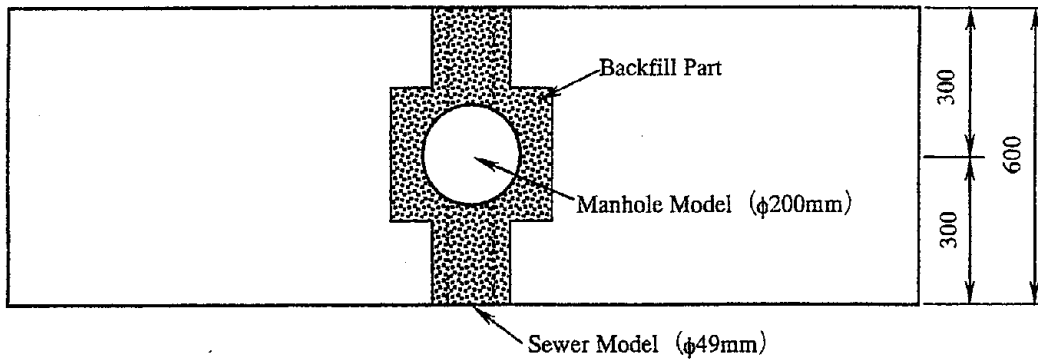
METHODS OF EXPERIMENTS

Experiment Models

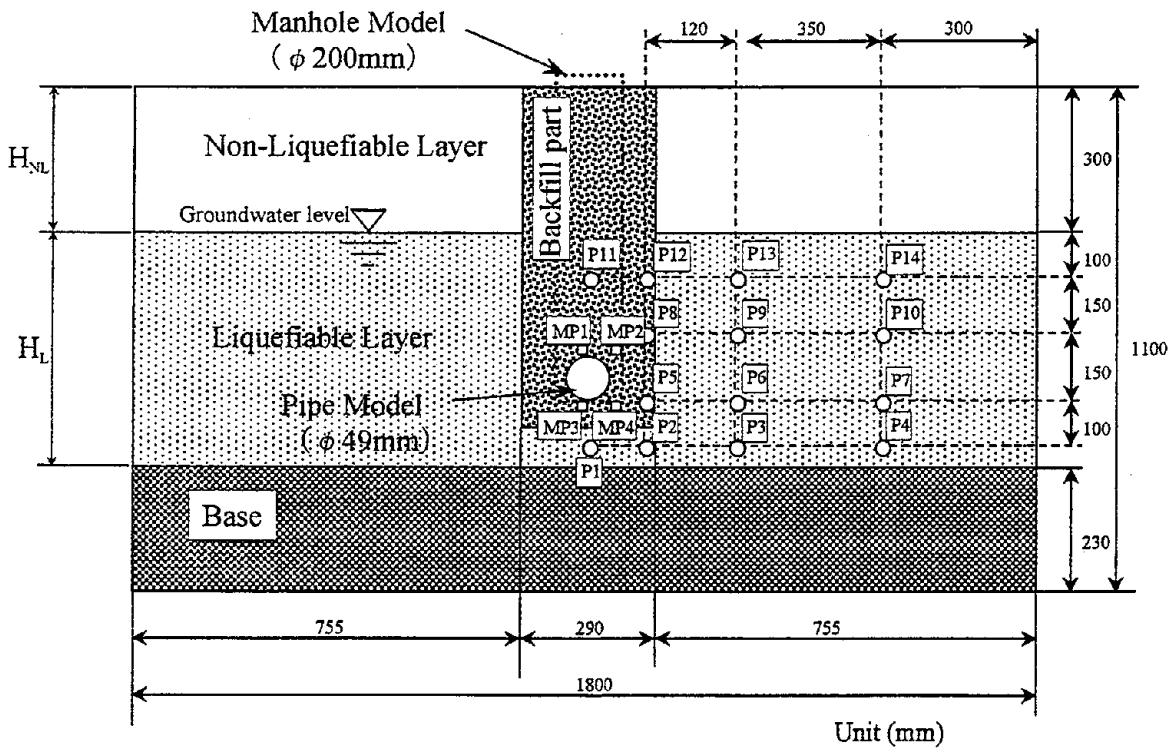
Experiments were conducted for nine different sewer and/or backfill. A sewer model consisted of a manhole model and a pipe model, and was buried in liquefiable layer. A sewer, backfill and the ground around them were modeled in a large container (1.8m long, 0.6m wide and 1.1m deep), which was placed on a shaking table. An overall view of experiment model is given in Figure 1. The backfill part is 60cm long, 29cm(Case 1-6) or 19cm(Case 7-9) wide and 77cm high. The ground model was composed of three layers, that is, base layer, liquefiable layer and non-liquefiable layer. The base layer was of dense sand. The upper two layers were of loose sand, and were made by putting clean sand into the water. The relative density of these layers was 22%, and the other physical properties of the sand are listed in Table 1. The liquefiable and non-liquefiable layers were distinguished by adjusting the water level. The thicknesses of liquefiable layer H_L and non-liquefiable layer H_{NL} were set as $H_L=57\text{cm}$, $H_{NL}=30\text{cm}$. The ground models had vertical lines on their sides so that ground deformation could be observed through the transparent glass of the container. These lines were made of colored sand. Photo 3 shows the side views of experiment model before and after excitation.

Table 1 Physical properties of sand

Specific Gravity of Soil Particle	2.633
Maximum Dry Density	1.350 gf/cm^3
Maximum Void Ratio	0.944
Minimum Void Ratio	0.593
60% Grain Size	0.195mm
10% Grain Size	0.130mm
Mean Grain Size	0.180mm
Coefficient of Uniformity	1.500



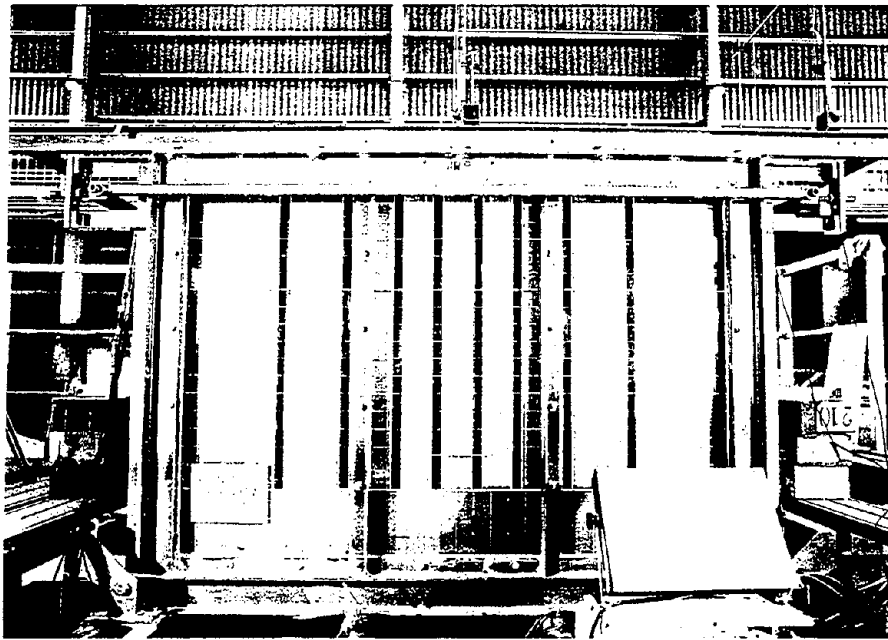
(a) Plan



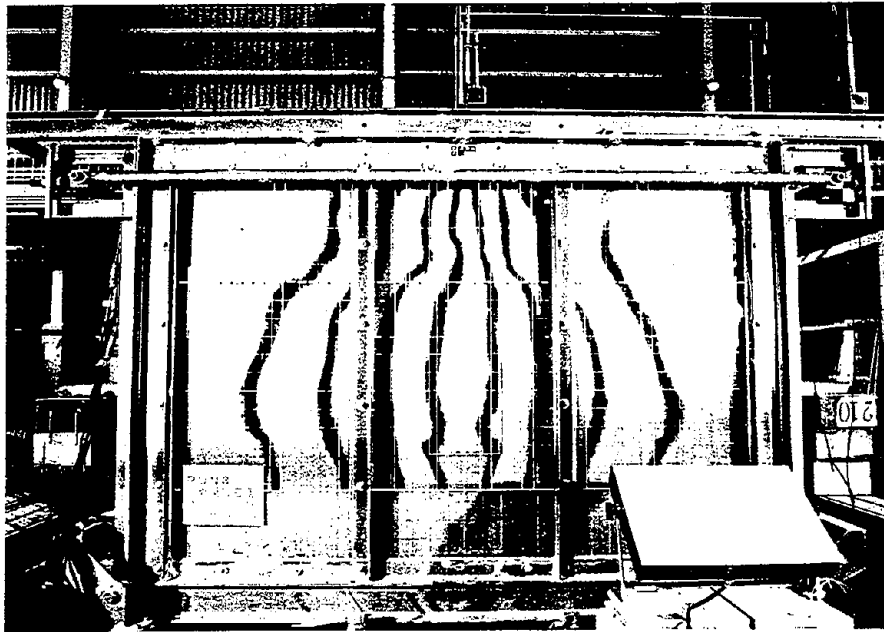
Unit (mm)
 ○ - Pore water pressure meter
 □ - Water pressure meter with model

(b) Elevation

Figure 1 Overall View of Experiment Model



(a) Original form



(b) After excitation with 0.15G

Photo 3 Failure mode of Case 9 test

Experiment Model Cases

Nine cases of experiments were conducted for different kind of sewer and backfill. Sewer types are manhole (manhole and pipe) and pipe. Backfill types are crushed stone and dense sand. Table 2 and Figure 2 show experiment model cases.

Table 2 Experiment model case

	Sewer Type	Backfill Type	Conditions of Backfill
Case 1	Manhole ¹⁾	Dense Sand	filled with sand (Dr = 22% ²⁾)
Case 2	Manhole ¹⁾	Crushed stone	filled with crushed stone
Case 3	Manhole ¹⁾	Crushed stone	filled upper part from pipe-center with crushed stone
Case 4	Manhole ¹⁾	Crushed stone	filled lower part from pipe-center with crushed stone
Case 5	Pipe	Crushed stone	filled lower part from pipe-center with crushed stone
Case 6	Manhole ¹⁾	Crushed stone	filled lower part from 7cm up pipe-center with crushed stone
Case 7	Pipe	Dense Sand	filled with sand (Dr = 22% ²⁾)
Case 8	Pipe	Dense Sand	filled with sand (Dr = 37% ²⁾)
Case 9	Pipe	Dense Sand	filled with sand (Dr = 55% ²⁾)

1)Manhole and Pipe

2)Dr : Relative Density

Test Procedures

In the experiments, liquefaction were generated by shaking the container on a shaking table. Sinusoidal waves with frequency of 3Hz were inputted in all Case 1-9 tests. For each case, the test was conducted with acceleration level of 0.15G on the shaking table and the duration of excitation was 30 seconds.

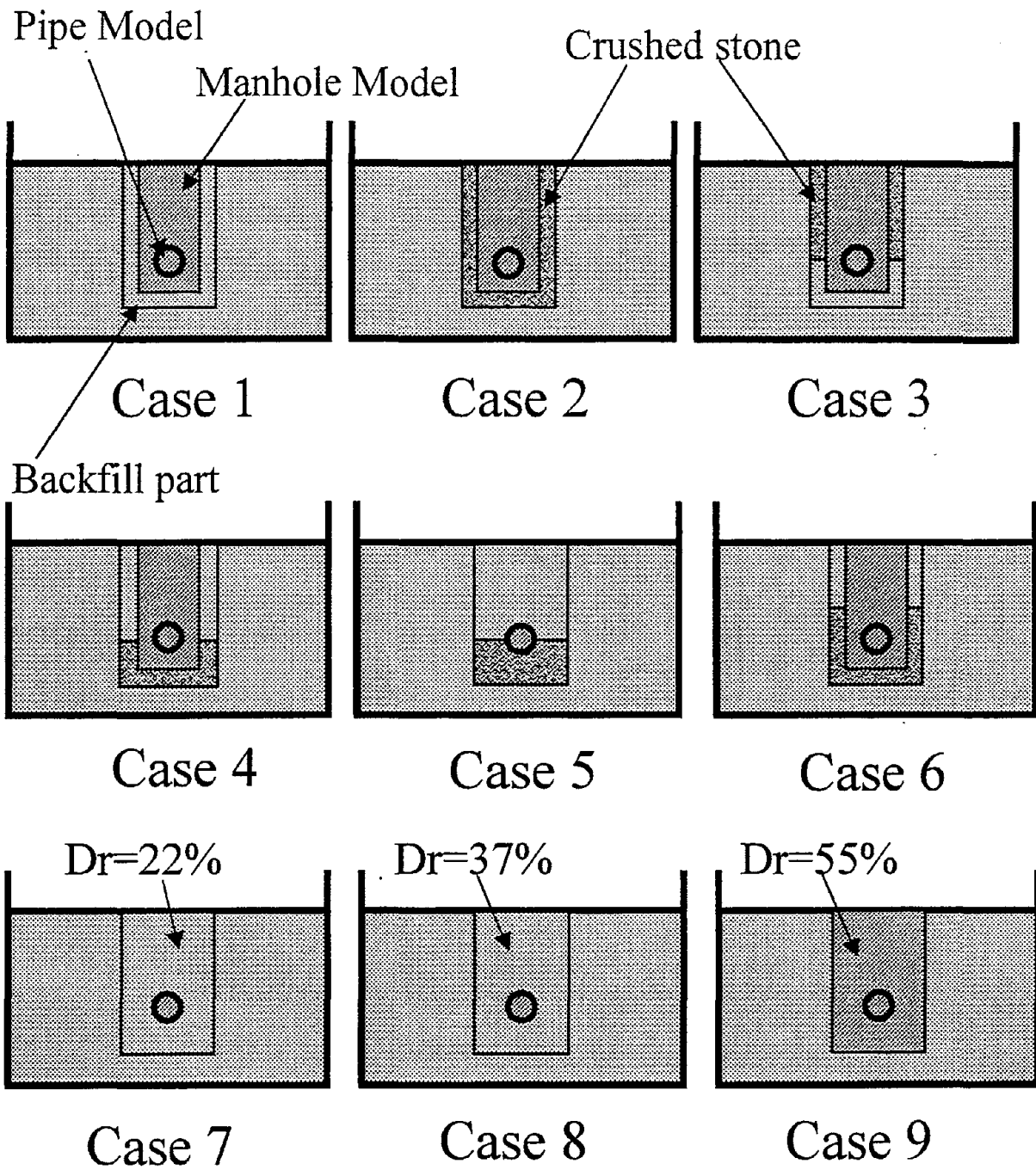


Figure 2. Experiment model case

Floating Safety Factor

Floating Safety Factor (F_s) is defined as safety standard of a sewer against soil-liquefaction by equation (1) ^{1) 2)}. F_s is calculated assuming the following conditions 1) to 5).

$$F_s = \frac{W_s + W_b + Q_s + Q_d}{U_s + U_d} \quad (1)$$

F_s : Floating safety factor

W_s : Weight of soil over a vertical projected plane of pipe model

W_b : Weight of a sewer model

Q_s : Shear resistance of soil over a sewer model

Q_b : Friction resistance on the side of a sewer model

U_s : Uplift force by hydrostatic at the bottom of a sewer model

U_d : Uplift force by excess porewater pressure

- 1) Hydraulic pressure was considered to act on a vertical projected plane of pipe model and on the base area of manhole model as for uplift calculation
- 2) Q_b is not considered in the sand of backfill, because liquefaction occurs in the sand of backfill judging from experiment data of excess porewater pressure
- 3) Q_b is considered in all upper part from pipe-center in Cases 2 and 3, in only 7 cm upper part from pipe-center in Case 6.
- 4) Q_s is not considered, because soil deformation happened over a sewer.
- 5) Value of water pressure at the bottom of a sewer, which is represented as MP-3 in Figure 1, is considered as value of excess porewater pressure at the bottom of a sewer.

RESULTS OF EXPERIMENTS

Recorded Time Histories

Time histories of floating displacement of a sewer, excess porewater pressure ratio in the backfill and in the ground around backfill, and floating safety factor from Case 1-9 tests are shown in Figures 3-6, respectively. Excess porewater pressure ratio is the ratio of excess porewater pressure to effective overburden pressure. The floating displacement is an average of values measured at four points around a sewer model. The excess porewater pressure ratios were measured at four depths, which were horizontally 45.5cm (10.5cm in Cases 2 and 3) from the edge of backfill.

As for floating displacement of a sewer, floating occurred in Cases 1, 4, 5, 6, 7 and 8. By contrast, sinking occurred in Cases 2, 3 and 9. Floating in Case 8 and all sinking are slight. Floating displacement begins to increase rapidly at 2 seconds and keeps to increase during excitation in Cases 1, 4, 5, 6 and 7. Floating displacement of a sewer increased gradually in Case 7. Comparing Case 1 with Case 7, it can be seen that uplift force of manhole is larger than that of pipe. These results show that pipe is harder to float as compared with manhole. It is also showed by the comparison between Case 4 and Case 5.

Excess porewater pressure ratio in the backfill finally exceed 1.0 in Cases 1, 4, 5, 6, 7 and 9, and did not exceed 1.0 in Cases 2 and 3 except at MP-3. As for excess porewater pressure ratio in the ground around backfill, excess porewater pressure ratio finally exceed 1.0 in all cases. These results indicate that soil-liquefaction occurred in the ground around backfill in all cases, and that it did not occur in the backfill in Cases 2 and 3.

Fs did not become less than 1.0 and floating did not occur in Cases 2 and 3. In Cases 5, Fs became less than 1.0 after 15 seconds and floating occurred slightly. In all cases except Cases 2 and 3, Fs is lower than 1.0 after about 1 second. In Cases 1, 4, 5, 6 and 7, floating displacement rapidly began to increase at 2 seconds when Fs became lower than 1.0.

Relationship between Floating Displacement and Floating Safety Factor

Figure 7 illustrates the relationship between the floating displacement of a sewer and Floating safety factor (Fs). In all cases except Cases 4 and 5, floating or sinking of a sewer occurred when Fs became lower than 1.0. Floating occurred when Fs becomes lower than 0.75 in Case 4, and floating occurred when Fs is not lower than 1.0 in Case 5. From these results, Fs may be used as safety standard of a sewer against soil-liquefaction.

CONCLUSIONS

The main conclusions of the present study may be summarized as follows;

- 1) Floating characteristics of a sewer depends on the method of backfilling and compaction of the backfill.
- 2) Floating safety factor may be used as safety standard of a sewer against soil-liquefaction.
- 3) Floating due to soil-liquefaction was reduced by the countermeasure that upper part from pipe-center of backfill is filled with crushed stone.

REFERENCES

- 1) Japan Road Association: Design Guidelines for Common Utility Duct, 1986 (in Japanese)
- 2) Koga, Y., Kozeki, J., Taniguti, E., Morisita, T. and Washida, S.: Technical Memorandum Public Works Research Institute vol.2550, Experimental Study on the Stability of Semi-buried Roads during Earthquake, February, 1988 (in Japanese)

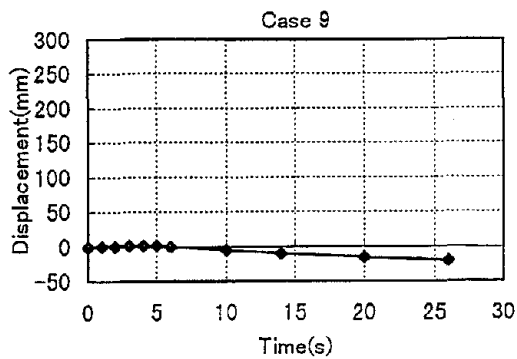
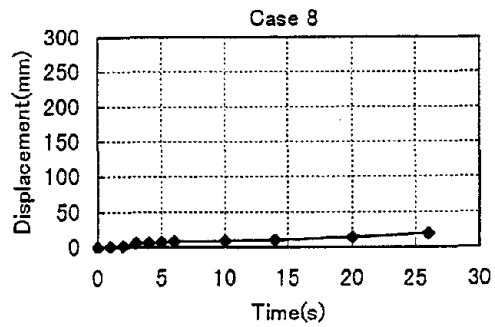
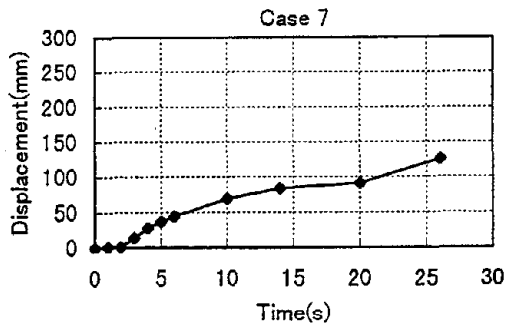
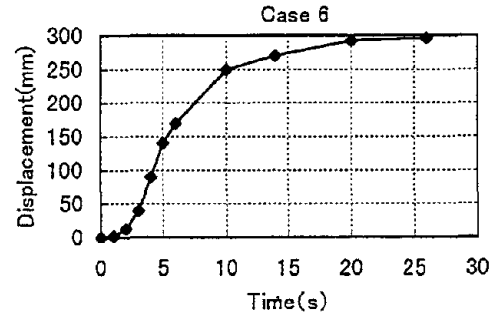
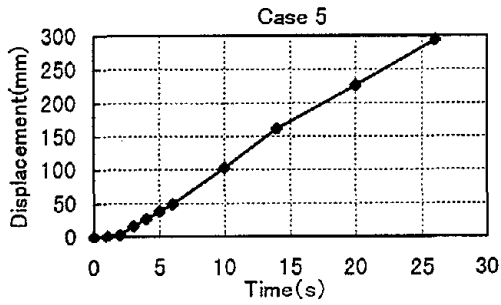
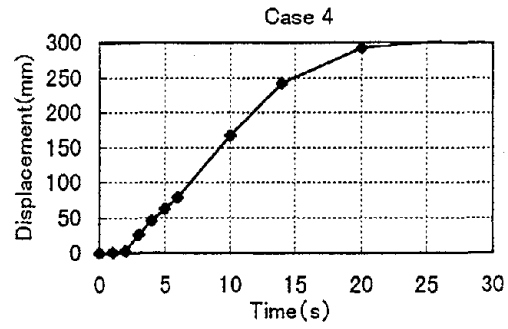
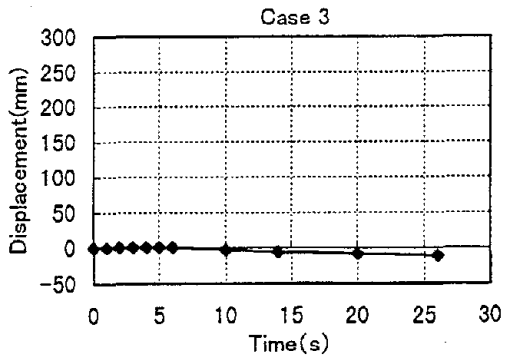
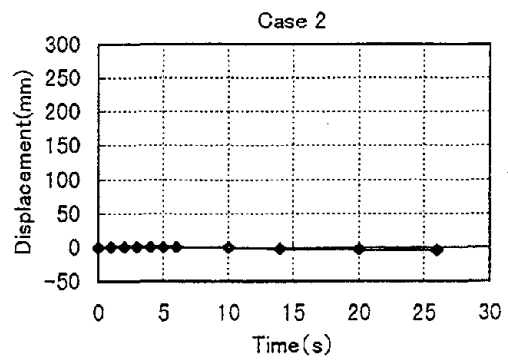
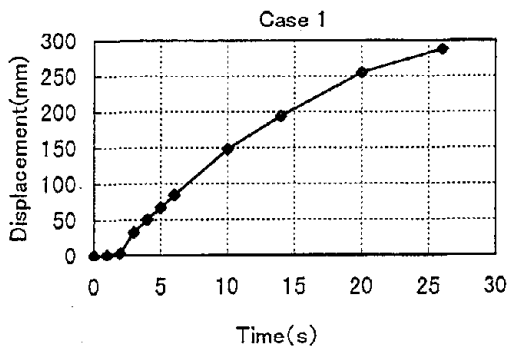


Figure 3. Time history of floating displacement of Sewer Model

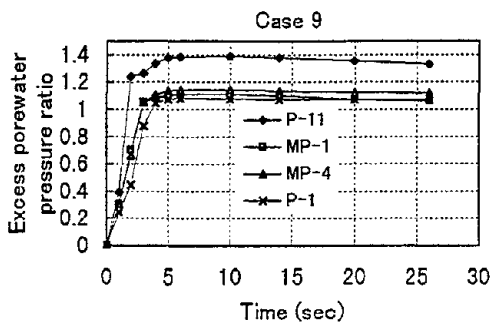
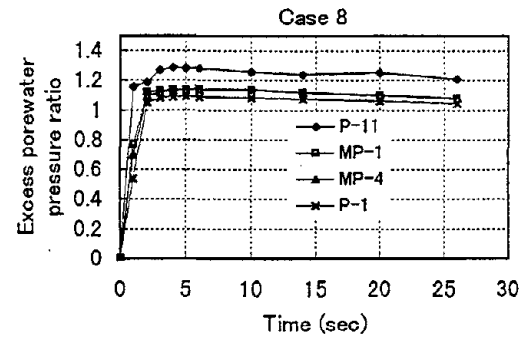
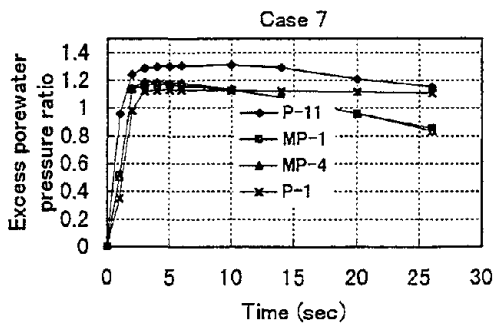
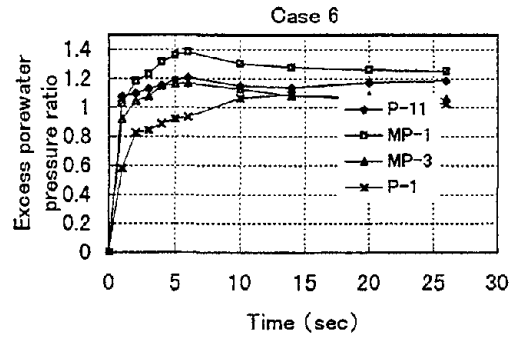
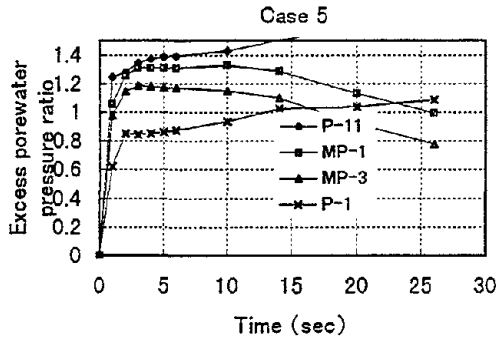
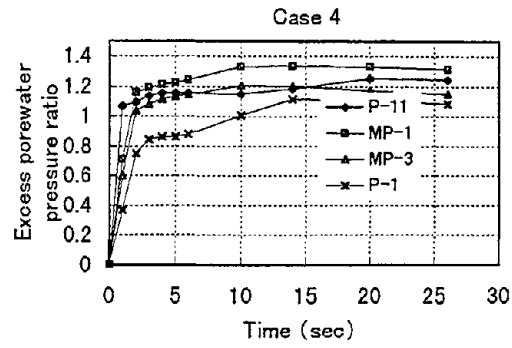
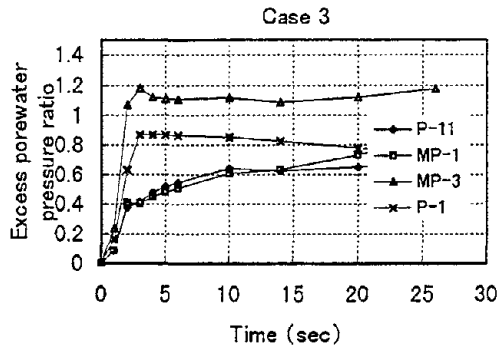
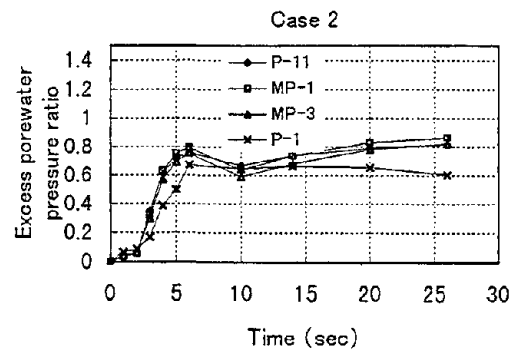
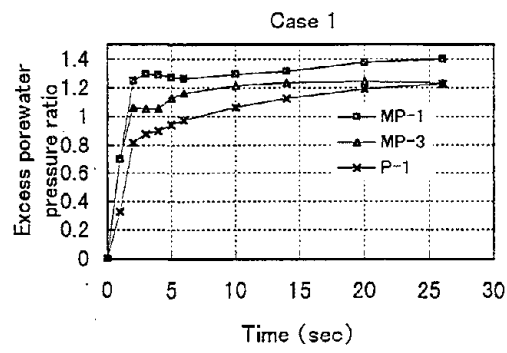


Figure 4. Time history of excess porewater pressure ratio in the backfill

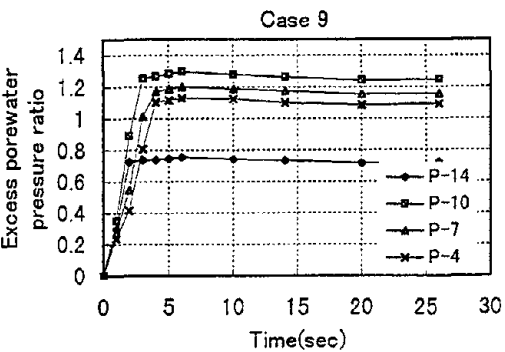
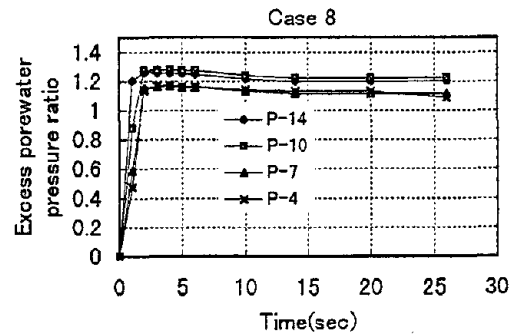
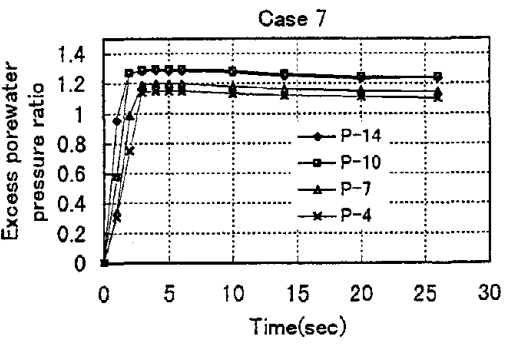
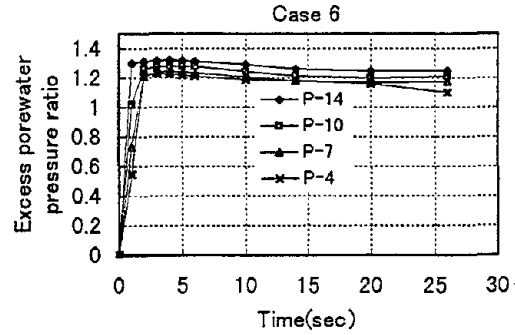
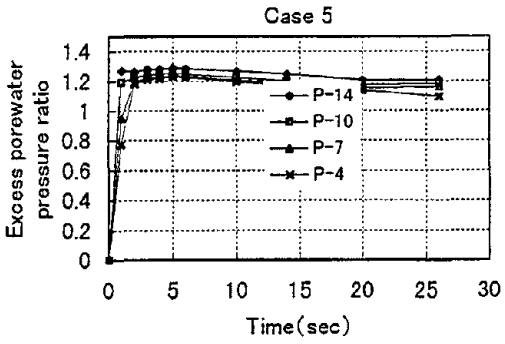
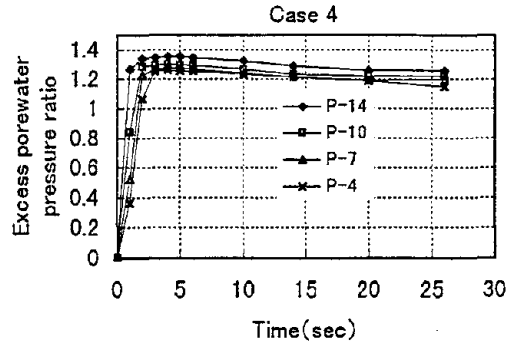
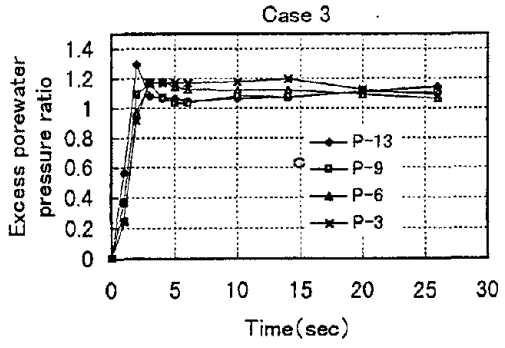
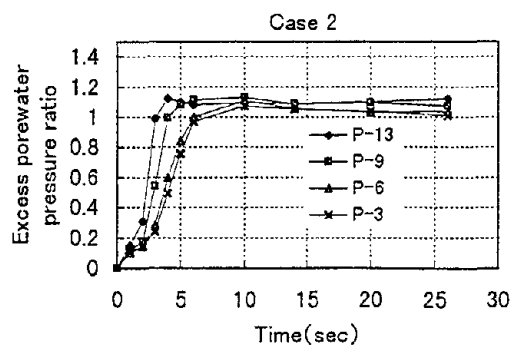
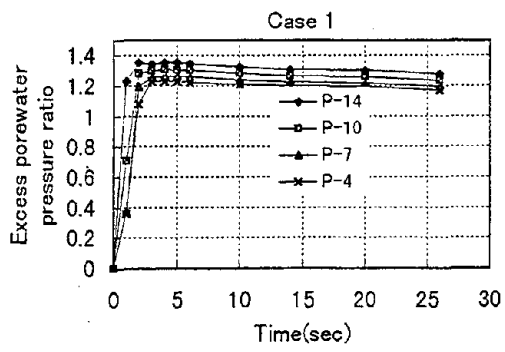


Figure 5. Time history of excess porewater pressure ratio in the ground around backfill

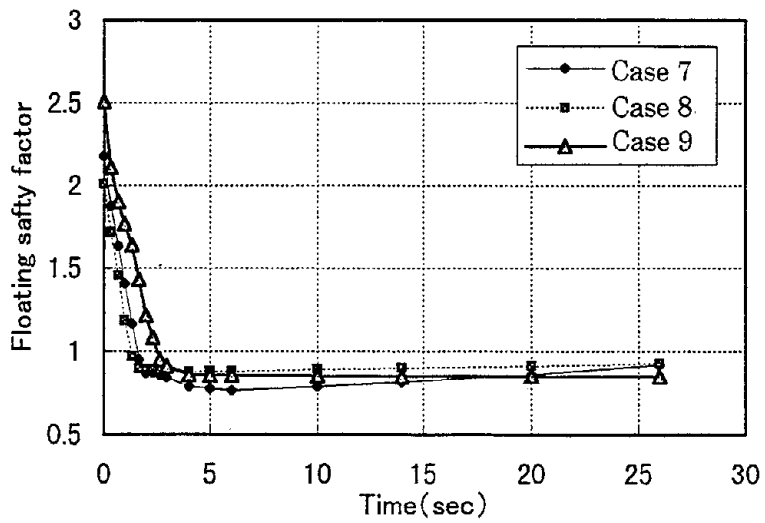
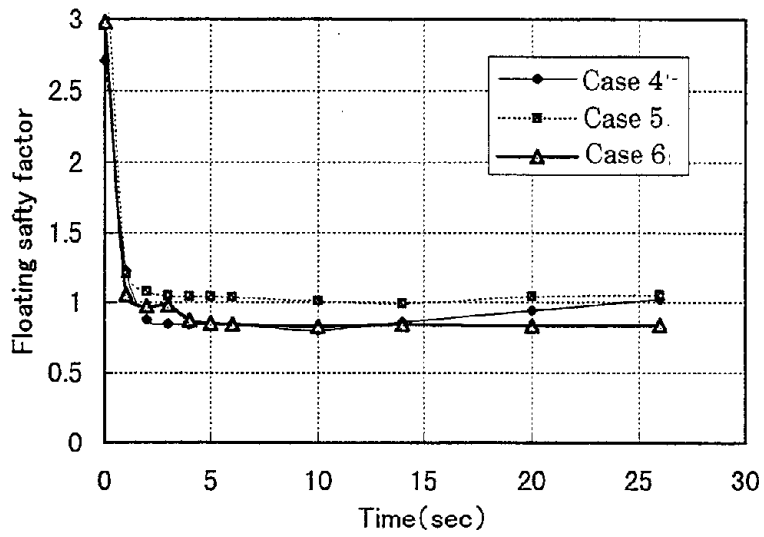
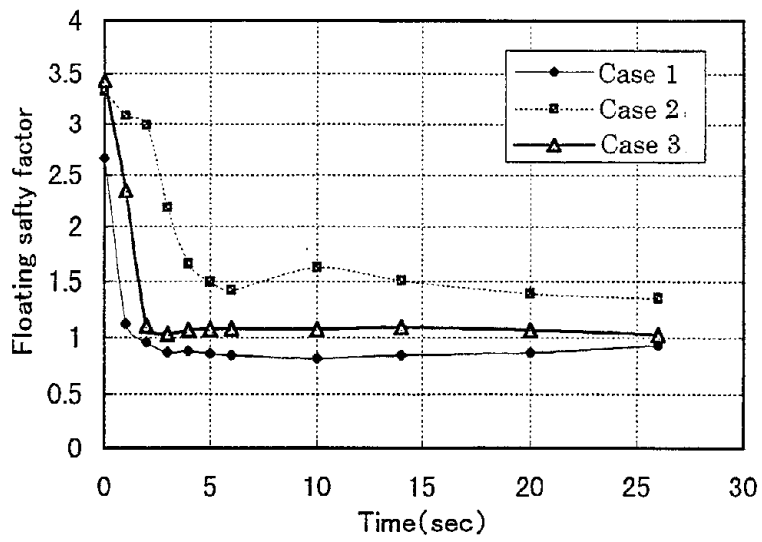


Fig 6. Time history of floating safety factor

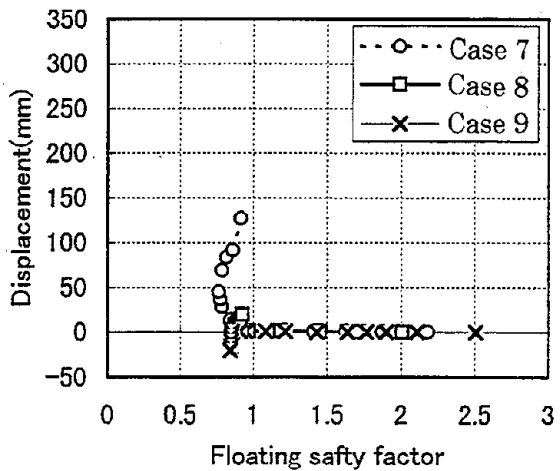
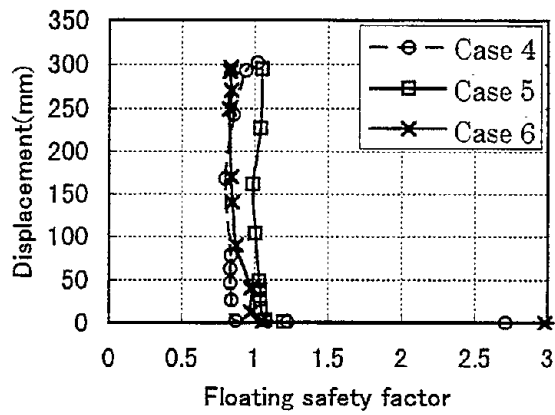
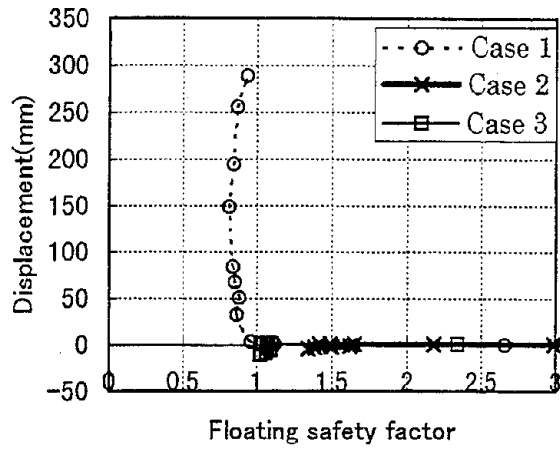


Figure 7. Relationship between floating displacement and safety factor

PERSONAL CAREER

NAME: Masahiro KANEKO

POSITION: Senior Research Engineer
Ground Vibration Division
Earthquake Disaster Prevention Research Center
Public Works Research Institute
Ministry of Construction



ADDRESS: 1, Asahi, Tsukuba-shi
Ibaraki-ken
305 Japan
Tel: 0298-64-4963
Fax: 0298-64-0598
E-mail:kaneko@pwri.go.jp

DATE OF BIRTH: May 23, 1962

EDUCATION: Bachelor (1985) and Master Degree (1987) of Engineering, Kyoto University

MAJOR SUBJECT: Earthquake Engineering

MAJOR AREA OF EXPERIENCE:

- 1987-1989 Public Works Department, Kumamoto prefecture
- 1989-1992 Research Engineer, Traffic Environment Division, PWRI
- 1992-1993 Chief of the Structure Standard Unit, Planning Division, Road Bureau
- 1993-1994 Research Engineer, Ground Vibration Division, PWRI
- 1994- Senior Research Engineer, Ground Vibration Division, PWRI

TRAVEL ABROAD: France

MAJOR PUBLICATIONS:

RELIABILITY OF BURIED PIPELINES SUBJECTED TO LARGE PERMANENT GROUND DISPLACEMENTS

Charles Scawthorn and Donald B. Ballantyne

EQE International
San Francisco CA and Seattle WA

ABSTRACT

Buried pipelines, carrying oil, gas or the main water supply for a city, are required to be highly reliable. A significant failure mode for buried pipelines are large permanent ground deformations such as in earthquakes. This paper outlines a procedure (with example) for assessing the reliability of such pipelines, using earthquake-induced liquefaction as an example. The procedure involves the estimation under uncertainty of liquefaction occurrence, the extent of lateral spread and the post-buckling capacity of the pressurized pipe to accommodate the displacement demands. The procedure is made more efficient by eliminating sections of pipeline in which the surrounding soil cannot mobilize the pipe capacity, based on work by O'Rourke et al (1995). A number of aspects of the process involve uncertainties, for which further research is required - while the geotechnical aspects are extremely difficult, an aspect particularly deserving of further work is the post-buckling capacity of internally pressurized pipe.

INTRODUCTON

An important problem in pipeline design is the reliability of buried pipelines under large permanent ground deformations (PGD). Large PGD may occur due to several causes, including lateral spreading due to earthquake-induced liquefaction, landsliding, or failure of earth retaining structures. Buried pipelines are often required to have high reliability. Examples include water transmission lines, and oil and gas transmission lines - the former in order to provide emergency and potable water supply for an urban region, and the latter to avoid fire and explosion as well as to provide needed fuels. In this context, we define reliability as the probability of maintaining the pressure boundary given large PGD. Water, oil, gas or other buried pipelines may be constructed using a variety of materials, including welded steel, jointed steel or ductile iron, high density polyethylene (HDPE) etc. Current codes and standards do not provide design methodologies for these pipelines when subjected to large PGD, and a variety of approaches are taken, including ignoring the problem, or attempting to mitigate the problem by re-routing or various soil remediation techniques, such as putting the pipelines on piles, or lowering liquefaction potential via relieving excess pore water pressure through the use of granular backfills, stone columns, wicks or other means. However, recent trends in technology and society are increasingly

requiring that low-probability high-consequence events be quantified - that is, that the reliability or risk of failure be determined. Because of the important nature of many water, oil or gas transmission lines, a methodology for assessing the reliability of buried pipelines subjected to large PGD is required. The objective of this paper is to discuss aspects of this problem and outline an approach for assessing the reliability of buried pipelines subjected to large PGD. The emphasis will be on butt welded steel pressurized pipe. In order to provide a perspective on the problem, in the next section we briefly review the performance of selected pipelines subjected to large PGD.

EARTHQUAKE PERFORMANCE OF BURIED PIPELINES

This section briefly reviews the performance of buried pipelines in several recent earthquakes, with emphasis on welded steel gas transmission lines. An excellent summary of the topic is provided in O'Rourke (1996).

1995 M_w 6.9 Hyogo-Ken Nanbu Earthquake: Although 106 failures occurred in the medium pressure gas system (approximately 0.1 MPa to 1 MPa) and over 26000 failures occurred in the low pressure (1 to 2.5 kPa), no failures occurred in the transmission mains. The outstanding performance of the transmission pipelines is attributed to the fact that these lines were usually located away from the areas that experienced the most earthquake damage and that the high pressure transmission lines were constructed of welded steel. It is interesting to note that of the 106 medium pressure failures, 96 occurred in steel pipe. However, none of the steel pipe failures occurred in the pipe body and the 14 failures that occurred in welded joints were all attributed to low quality welds. Of over 25000 low pressure steel pipeline failures, none occurred in the pipe body or at welded joints. Steel pipe low and medium pressure failures occurred primarily in screwed, SGM, mechanical or flanged joints. (Oka, 1996; Yamazaki, 1996)

1994 M_w 6.7 Northridge Earthquake: Approximately 250 non-corrosion failures were observed in metallic gas transmission and distribution mains. Thirty-five of the failures occurred in transmission mains. Of these 35 failures, 27 occurred in 1925 to 1930 vintage oxy-acetylene welded joints. The other six failures occurred in 1920 to 1945 electric arc welds. Only two of the 35 failures were attributed to effects from PGD. Although post-1945 electric arc weld joint transmission pipelines were prevalent in many areas that received severe ground shaking and/or experienced PGD from surface faulting or lateral spread, no failures occurred in these "modern" welded steel pipelines. For instance, two 750 mm 1950's natural gas transmission lines paralleled a 550 mm natural gas line constructed in 1941. Although the 1941 line broke and ignited due to permanent ground displacements, the two 750 mm lines were undamaged. (O'Rourke, 1994; O'Rourke, 1995)

1989 M_w 7.1 Loma Prieta Earthquake: There are almost 10,000 kilometers of natural gas transmission piping in Northern California. On the order of 10 to 20 percent of this transmission piping was within the area affected by the Loma Prieta Earthquake. However, only two failures occurred. Both of these failures occurred on a 300 mm line near the epicenter. Two leaks

occurred in 1930 oxy-acetylene welds. These leaks were repaired without affecting customer service. (Phillips, 1990)

Other Earthquakes: In the 1979 Imperial Valley earthquake, three SCG welded steel natural gas transmission lines constructed in 1948 and 1966 were subjected to between 315 mm to 600 mm of fault movement (cause by creep and fault rupture). None of the lines failed. Similarly, three Southern California Gas welded steel transmission lines constructed in 1966 were located in a utility corridor that experienced from two to three meters of lateral spread in the 1971 San Fernando earthquake. None of these lines were damaged. In the 1954 Kern County earthquake, a post-1945, 850 mm PG & E transmission main that crossed the White Wolf Fault remained undamaged in spite of over 1 meter of fault movement. However, numerous failures in Southern California Gas transmission pipelines built prior to 1945 were caused by the 1971 San Fernando earthquake. Failures occurred from both wave propagation effects and permanent ground displacement. Similar to the Northridge Earthquake, the failures occurred in poor quality oxy-acetylene and electric arc welds. A total of approximately 20 failures occurred in 1920's and 1930's vintage welded steel natural gas transmission lines during the 1933 Long Beach and 1952 and 1954 Kern County earthquakes. With the exception of a two pin hole failures located in corrosion-weakened Kern County pipe bodies, all of the failures occurred in the joint welds. (O'Rourke, 1995)

Summary: Welded steel natural gas transmission lines designed, constructed and maintained in accordance with current industry standards and governmental regulations have performed exceptionally well in past earthquakes. Although several of these lines have been exposed to severe ground shaking and/or permanent ground displacements that have exceeded 1 meter, no earthquake-caused failures have been documented in the United States in these lines. The excellent performance of these lines is particularly significant because until recently, most natural gas lines in the United States were not specifically designed for seismic hazards. The exceptional performance of natural gas transmission lines is generally attributed primarily to the ductility of these pipelines. Although overall excellent performance of these pipelines is expected in future earthquakes, failure is still possible. Large permanent ground displacements from fault rupture, liquefaction or landslide could overstress even highly ductile lines, particularly if the lines were anchored near these areas by bends, valve pits, etc. On the other hand, welded steel natural gas transmission pipelines constructed with poor quality welded joints and/or that have suffered structural deterioration have performed poorly in past earthquakes. In the United States, welded pipeline joints constructed with older welding techniques prior to 1945 have performed particularly poorly. These poor quality welds create discontinuities that result in stress concentrations at the joints. These stress concentrations, coupled with the weak welds have resulted in numerous failures. Deterioration from corrosion has also resulted in failure of welded steel natural gas transmission main pipe bodies. Even gradually occurring non-earthquake related permanent ground displacements have caused failures in natural gas transmission pipelines with construction defects or pipelines that have deteriorated from corrosion.

BURIED PIPELINES SUBJECT TO LARGE PGD

In the following, we shall focus on earthquake-related liquefaction-induced PGD to outline an approach for determining the reliability of buried pipelines subject to large PGD. Pipelines may be subject to one or more of several kinds of liquefaction-induced PGD, as shown in Figure 1, which will depend on whether the pipeline is in the liquefied layer, or in a non-liquefied soil layer above a liquefied layer. A non-liquefied soil layer above a liquefied layer is termed the *cap layer*. Pipes in the cap layer may be subject to subsidence and/or lateral spreading of the soil - the lateral spread may be parallel or transverse to the pipe, or a combination of both. Thus, the pipe may be subjected to bending (due to transverse lateral spreading and/or subsidence), and/or axial deformation (due to lateral spreading). A pipe in the liquefiable layer may be similarly subject to subsidence or loss of bearing, or conversely, flotation or buoyancy, depending on the relative densities. Similar to the pipe in the cap layer, the pipe may also be subject to transverse and/or axial deformations due to movements of the soil - however, since the soil is effectively a liquid, these forces are due to viscous drag on the pipe, rather than shear or bearing of the soil.

As noted above, we define reliability as the probability of maintaining the pressure boundary given large PGD. Assessment of the seismic reliability of a buried pipe potentially subject to PGD is equivalent to determining the probability of pipe Capacity exceeding pipe Demand. Determination of Capacity and Demand involves consideration of two aspects (likelihood or probability of occurrence, vs. severity or magnitude) of a number of factors:

Seismic Hazard - since PGD is a function of the duration and intensity of shaking, the epicentral location, magnitude and probability of earthquake occurrence are important random variables. Probabilistic seismic hazard assessment (PSHA) methods are employed integrating these variables to determine the probability of peak ground acceleration or other measures required for determining the likelihood of liquefaction, and the amount of permanent ground deformation. Methods for PSHA are well-known (Kawasumi, 1951; Cornell and Vanmarcke, 1969; Reiter, 1990), and will not be discussed further herein.

Liquefaction - in the context of this discussion, the relevant factors are the likelihood and extent of liquefaction, and the expected direction and magnitude of PGD given liquefaction. These factors are quite uncertain even when geotechnical data (soil profile, grain size distribution, depth of water table etc) are very well known - however, geotechnical data often have significant uncertainty in themselves, as discussed below. While the likelihood of liquefaction can be determined from laboratory tests on soil samples, a useful determination can be made using Seed's Simplified Procedure (Seed et al, 1982). This method consists of several steps:

- determine Cyclic Stress Ratio, CSR:

$$CSR = \frac{0.65r_d h \gamma a_{max}}{d_w \gamma + (h - d_w) \bar{\gamma}} MSF \quad (1)$$

where r_d , h , γ , a_{max} , d_w are defined below and $MSF = 10^{2.24} / M_w^{2.56} = (M_w / 7.5)^{-2.56}$, (Youd et al, 1997), where M_w is moment magnitude. Uncertainty in a_{max} is accounted for in the seismic

hazard. Uncertainty in r_d varies with depth, see Fig. 2, corresponding to a coefficient of variation (COV) of nil to a maximum 30%, although realistic COV's would be on the order of 5%. Uncertainty in h should be small, corresponding to a COV<5%; for γ , also small, with COV < 10%; for d_w , somewhat larger, but with COV< 20%. Uncertainty for MSF is in the range (10% < COV < 20%) with decreasing COV for larger M . Overall, uncertainty on CSR can be characterized by a COV of 10~20%.

- compare CSR against Standard Penetration Test (SPT) blow count, N , to determine whether liquefaction occurs. The criteria for comparison is shown in Figure 3, due to Seed et al (1985). Uncertainty in N has been shown to be significant, due to differences in operator control of hammers, conversion between different sampler sizes, etc. Overall, uncertainty on N can be characterized by a COV of 10~20%.
- Probability of Liquefaction - From Figure 3 (after Seed et al, 1985), the CSR- N boundary for liquefaction (for percent fines <5%) has been approximated by the authors as the 90th percentile of a lognormal distribution, where the standard deviation of $\ln(N)=0.5$, and the mean is $\ln(45*CSR)$.

The magnitude of PGD given liquefaction has been the subject of empirical, experimental and numerical investigations (see for example, Hamada, et al, 1986, and Iai et al., 1992). A useful estimator is the Multiple Linear Regression (MLR) results of Bartlett et al (1992) where, for example, for sloping ground conditions:

$$\begin{aligned} \text{Log}(\delta + 0.01) = & -15.87 + 1.178M - .0927\text{Log}R - 0.013R + 0.429\text{Log}S \\ & + 0.348\text{Log}T_{15} + 4.527\text{Log}(100 - F_{15}) - 0.922D50_{15} \end{aligned} \quad (3)$$

while, for free face conditions

$$\begin{aligned} \text{Log}(\delta + 0.01) = & -16.366 + 1.178M - .0927\text{Log}R - 0.013R + 0.657\text{Log}W \\ & + 0.348\text{Log}T_{15} + 4.527\text{Log}(100 - F_{15}) - 0.922D50_{15} \end{aligned} \quad (4)$$

Estimation of permanent ground displacement (PGD) given the occurrence in liquefaction still involves considerable uncertainty, as indicated by Bartlett et al¹, so that this aspect is quite uncertain.

¹ Bartlett et al, 1992 do not precisely quantify the uncertainty in MLR, but estimate that about 90% of observed displacements fall within a region bounded by a factor of 2 above and below the mean MLR estimates - that "doubling of the predicted displacement provides an estimate with a high probability of not being greatly exceeded" [Bartlett et al, 1992]. Statistical parameters are not provided by the authors - based on a 90% double-tails normal and/or lognormal distribution, the coefficient of variation for the distribution can be estimated to be, very approximately, 0.5.

Pipe Loading and Resulting Strains - large PGD induce loading on the pipe, so that pipeline position and resulting pipe strains are the key parameters defining Demand on the pipe. Simplified methods for determining pipe strains as a result of imposed soil displacements do not exist, so that the soil - pipeline system needs to be modeled using the finite element method (FEM) of analysis, or other numerical/computation methods. In this method, the soil-pipe interaction is modeled using soil spring-sliders in both the longitudinal and lateral direction as shown in Figure 4 for a straight pipeline. The force displacement relationship for these spring-slider elements have stiffness K_L or K_H , up to a limiting displacement, d_L , or d_H , after which the spring resistance is a constant F_L or F_H . The soil restraint values for the spring-sliders are calculated in accordance with relationships given in ASCE (1984). Uncertainty for this aspect requires additional research - for the example given below, we have assumed a COV=10%.

Pipe Acceptance Criteria - essentially, this is the pipe Capacity, based on material criteria- that is, reliably accommodating pipe strain limits under imposed deformations while maintaining pressure integrity. This is a challenging area, since traditionally civil engineers have regarded onset of buckling (also termed wrinkling, in the case of cylindrical shells and pipes) as the ultimate capacity. While this is true in most structural situations, where columns are *load-controlled*, buried pipes are not load-controlled but rather *displacement-controlled*. Two recent investigations have linked experimental results and detailed shell finite element method (FEM) modeling to examine post-buckling response of butt welded line pipe. Murray et al (1997) also performed experimental and FEM modeling, concluding that displacement-constrained loading results in *non-catastrophic behavior as wrinkling develops*. Zimmerman et al (1995) investigated pipe performance in three ways. They first reviewed existing data and analytical methods. Next, a large-scale experimental testing program was conducted, subjecting five full-size pressurized pipe specimens ($D=610\text{mm}$, $t=7$ and 15mm) to combinations of bending and tension. This testing program was extrapolated via a non-linear FEM model to develop semi-empirical equations of performance. The final result, based on limiting tensile hoop strain so as not to exceed ultimate tensile strains across pipe seam welds, were new design criteria and semi-empirical equations of performance. For X70 to X90 grade steel for example, Zimmerman et al (1995) indicates ultimate strains are:

$$\varepsilon_{\max} = 0.21 \left(\frac{t}{D} \right)^{0.55} - 110 \left(\frac{390 - \sigma_h}{E} \right)^{1.5} \quad (5)$$

where

$$\sigma_h = \frac{P(D - 2t)}{2t} \quad (6)$$

This equation is shown in Figure 4 for various internal pressures and D/t ratios, and compared against a relation developed by NASA (1968) on the basis of very thin wall cylinders. Based on these investigations, it may be inferred that (a) substantial post-buckling capacity exists for pressurized pipe, subject to certain reservations discussed below, and (b) the fundamental

limiting criteria for pressurized pipe is not compressive buckling or *wrinkling*, but rather maximum tensile strain, which are induced in the circumferential (hoop) direction even when the pipe is subjected to axial compression.

Much additional research on this aspect remains to be performed. For example, welded pipe in reality consists of three materials - the pipe base metal, the weld metal (particularly in the girth or full circumferential weld connecting pipe sections), and the heat affected zone (HAZ) around the weld itself. Pipe base metal is typically specified to be very tough and ductile, capable of sustaining large uniaxial tensile strains, prior to rupture, on the order to 10~20% or more. Maximum allowable tensile strains across the weld and HAZ may be significantly less however, and are very much a function of the specific welding procedures and non-destructive examination methods utilized. The significant hoop strain associated with pressurized pipe will tend to reduce the maximum allowable tensile strains, relative to data derived from uniaxial tests. When project-specific test data (factored to account for biaxial stresses) is lacking, a survey of expert opinion has found a consensus that tensile strains be limited to 5%. - again, uncertainty for this aspect requires additional research - for the example given below, we have assumed a COV=10%.

The foregoing aspects are sufficient to determine the seismic reliability of a buried pipe potentially subject to PGD. Two additional aspects are worthy of mention, however. These are:

Screening - Pipelines can be hundreds of kilometers in length, so that detailed determination of seismic reliability at all points along the pipeline is an extremely expensive task. While significant sections of a pipeline can be seen by inspection as not being potentially subject to PGD, many sections crossing rivers or poor soils will still remain. Therefore, *screening* criteria based on bounds established on the basis of pipewall shear stress development, maximum likely extent of PGD etc can be very valuable in eliminating significant sections of pipeline from detailed examination. O'Rourke et al (1995) have developed screening criteria based on wrinkling of the pipe wall in compression, finding that in most cases the onset of wrinkling is governed by the length of pipe in the PGD zone. This is an important finding - *if the length of pipeline in an area which is subject to large PGD is below a simply determined criteria, the soil will not be able to mobilize the pipe sufficient to cause wrinkling - therefore, the pipe will not fail.* From O'Rourke et al (1995), the specific length L_{cr} below which the pipe will not fail is determined by:

$$\epsilon_{mx} = \frac{\beta_{\rho} L_{cr}}{2E} \left[1 + \left(\frac{n}{1+r} \right) \left(\frac{\beta_{\rho} L_{cr}}{2\sigma_y} \right)^r \right] \quad (7)$$

where $\epsilon_{mx} = 0.1t/D - 6.0 \times 10^{-7} D d$, $\beta_{\rho} = \frac{f_m}{\pi D t}$, and other terms are defined below.

Mitigation - lastly, where pipe under ordinary as-built conditions has insufficient reliability, the spectrum of mitigation techniques needs to be reviewed to identify the most cost-effective mitigation technique for each situation. This spectrum includes (a) Realign the Pipe (relocate to avoid the liquefiable area; relocate to avoid populated areas to minimize failure consequences;

install below liquefiable layer, e.g. micro-tunneling), (b) Improve Soils (strengthen to resist lateral spread - e.g., soil/cement mixing, pin piles, cut-off walls, etc; modify to mitigate liquefaction - e.g., stone columns, grouting, densification; (c) Modify Soil/Pipe Design to Reduce Soil Lateral Force Resistance (use compressible backfill, reduce burial depth), (d) Modify Soil/Pipe Interface to Reduce Longitudinal or Lateral Load Transfer (coat pipe with hard, smooth coatings, and wrap with geotextile to minimize friction; (e) Accept Damage and Plan Emergency Response (monitor ground motion, liquefaction, and/or lateral spread to control isolation valves and to provide information for emergency response activities; install automated valves to isolate vulnerable pipelines; prepare, implement, and practice an emergency response plan).

In addition to cost, a number of other factors may be included in determining the optimum mitigation alternative. Factors to consider include:

- Life safety
- Experience with new/untried technologies
- Familiarity by contractor with construction methods
- Constructability
- Nuisance (noise, dust and other pollution)
- Reliability/consequences of failure
- Traffic disruption
- Environmental impact
- Local resident opposition
- Interactions with other lifelines
- Maintenance
- Schedule

EXAMPLE APPLICATION

This section presents an example pipeline analysis, using the approach discussed above. The layout, dimensions etc are shown in Figure 5 and Table 1 - the example consists of a 600 mm. diameter X60 butt welded steel pipeline, with wall thickness of 10mm and depth of burial of 1.5 m. The pipeline has two bends 294m apart, between which a 160m section of the pipeline is in soils which may be liquefiable. For the given material conditions, the first issue given this data is: *Is liquefaction likely?* This requires the following analysis: Given that $PGA=0.32$ g (with probability of occurrence of 10^{-3} per year) and that normalized SPT in liquefaction layer =10, we find that the Cyclic Stress Ratio, $CSR = 0.24$. Plotting CSR on Figure 3, we find a relatively high probability of liquefaction (i.e., 56%). Since the pipe is in the cap layer, and given the ground slope, the pipe is expected to be subjected to transverse displacements, due to the cap layer displacing laterally, due to liquefaction beneath the cap layer. Given the pipe exposure length, $L = 160$ m, and based on a de-aggregation of contributing magnitudes from seismic hazard analysis results, telling us that the mean earthquake magnitude is a $M=7$ event at 14 km, we find from equation (3) that the PGD $d = 2.81$ m. Modeling the soil-pipe system using a widely available nonlinear Finite Element Method program (e.g. ANSYS), with spring sliders etc per ASCE (1984), we find that the maximum pipe strain demands are 0.069% in compression, and 1.54% in tension. Per Zimmerman et al (1995), the compressive strains are well below limiting strains. However, the tensile strains are about one-third the consensus maximums of 5%. A Monte Carlo simulation was performed for this example using the approach described above with associated uncertainties, with the result for 1,000 trials being that the mean probability of pipe demand exceeding capacity (in tension) is 12%, with a standard deviation of 23%. If fines content are 15% rather than 40%, the probability of demand exceeding capacity (ie, failure) increases to 22%.

CONCLUSIONS

Assessing the reliability of a buried pipeline potentially subjected to large PGD is a process involving estimation of the occurrence of liquefaction, the extent of lateral spreading, and the capacity of the pipe to accommodate the resulting displacements while maintaining the integrity of the pressure boundary. A number of steps in this process involve considerable uncertainties, for which further research is required. While the geotechnical aspects are extremely difficult, an aspect on which relatively little work has been performed is the post-buckling capacity of internally pressurized pipe.

DEFINITION OF TERMS

a	soil adhesion factor,	L_{cr}	Length, critical (m)
σ_y	effective yield stress for the pipe material,	LSI	Liquefaction Severity Index (in)
a_{max}	maximum peak ground acceleration expected at the site	MLR	Multiple Linear Regression Analysis
β_p	Pipe burial parameter	MSF	magnitude-dependent scaling factor (dimensionless),
d	lateral spread displacement delta (m)	M_w	Earthquake moment magnitude
δ	interface friction angle, between pipe and soil	n and r	Ramberg-Osgood parameters for the pipe material
D	pipe diameter (units vary)	(N₁)₆₀	Normalized standard penetration resistance (blows per foot, or per 30 cm)
D50₁₅	Average median particle size (mm) in T ₁₅	ρ	mass density
d_w	depth to water table (m)	P	internal pressure (Mpa)
E	initial modules of elasticity for the pipe material, Young's modules MPa	r_d	stress reduction factor
ϵ	strain	s	applied stress
F₁₅	Average fines content (%) in T ₁₅	S	Ground slope (%)
f_m	axial friction force per unit length at the soil pipe interface	SPT	Standard Penetration Test
ϕ	soil friction angle	s_u	undrained shear strength (kN/m ²),
g	average unit weight of soil above depth d _w (kN/m ³)	t	pipe wall thickness (mm)
g'	soil (effective) unit weight (kN/m ³),	T₁₅	Thickness (m) of saturated cohesionless soils with (N ₁) ₆₀ < 15
$\bar{\gamma}$	average effective weight of soil between d _w and h	tan δ	interface friction angle between pipe and soil.
H	depth to pipe springline (m),	t_u	the axial resistance per unit length of pipe (kN/m)
h	depth of (N ₁) ₆₀ data (m)		
H_c	pipe burial depth from ground surface to the top of pipe (m)		

ACKNOWLEDGEMENTS

Discussions and technical contributions related to this topic, from Prof. T.D. O'Rourke (Cornell University), Prof. R. Dobry (Rensselaer Polytechnic Institute), Mr. D.G. Honegger (D.G. Honegger Associates), Dr. D. J. Nyman (D. J. Nyman and Associates), Prof. M. O'Rourke (Rensselaer Polytechnic Institute), Prof. H. Stewart (Cornell University), Prof. L.T. Youd (Brigham Young University), Dr. J. Arros and Mr. S.P. Harris (EQE) and Mr. W. Heubach (formerly EQE) are gratefully acknowledged.

REFERENCES

- ASCE Technical Council on Lifeline Earthquake Engineering Committee on Gas and Liquid Fuel Lifelines, 1984. Guidelines for the Seismic Design of Oil and Gas Pipeline Systems, American Society of Civil Engineers.
- Bartlett, S.F., and Youd, T.L., 1992. Empirical analysis of horizontal ground displacement generated by liquefaction-induced lateral spread: National Center for Earthquake Engineering Research, Technical Report NCEER-92-0021.
- Cornell, C.A. and Vanmarcke, E.H., 1969. "The Major Influences on Seismic Risk", in Proceedings of the Fourth World Conference on Earthquake Engineering, Santiago, Chile, p. 69-83.
- Hamada, M, Yasuda, S., Isoyama, R., and Emoto, K., 1986, "Study on Liquefaction Induced Permanent Ground Displacements," Association for the Development of Earthquake Prediction
- Iai, S., Matsunaga, Y. and Kameoka, T., 1992, "Analysis of Undrained Cyclic Behavior of Sand Under Anisotropic Consolidation," Soils and Foundations, 32(2), pp 16-20 .
- Kawasumi, H., 1951. "Measures of Earthquake Danger and Expectancy of Maximum Intensity Throughout Japan as Inferred from the Seismic Activity in Historical Times", Bulletin of Earthquake Research Institute, Vol. 29.
- Murray, D.W., 1997. "Local Buckling, strain localization, wrinkling and postbuckling response of line pipe", Engineering Structures, vol. 19, no. 5, pp. 360-371, Elsevier.
- National Aeronautics and Space Administration, 1968. Buckling of Thin-Walled Circular Cylinders, NASA Space Vehicle Design Criteria (Structures, NASA SP-8007).
- O'Rourke, M., Liu, X. and Flores-Berrones, R. 1995. "Steel Pipe Wrinkling Due to Longitudinal Permanent Ground Deformation, J. Transportation Engineering, Sept./October., Am. Soc. Civil Engineers.
- O'Rourke, T.D., 1996. Lessons Learned for Lifeline Engineering From Major Urban Earthquakes, Eleventh World Conference on Earthquake Engineering, ISBN 0 08 042822 3, Elsevier Science Ltd.
- O'Rourke, T.D., and Palmer, M.C., 1994, The Northridge, California Earthquake of January 17, 1994: Performance of Gas Transmission Pipelines, National Center for Earthquake Engineering Research, Technical Report NCEER-94-0011, May 16.
- O'Rourke, Tom D., Gailing, Richard W., Honneger, Douglas G., and Strand, Carl, 1995, "Gas Systems," Northquake Earthquake Lifeline Performance and Post-Earthquake Response

(edited by Anshel J. Schiff), American Society of Civil Engineers Technical Council on Lifeline Earthquake Engineering Monograph No. 8, August.

- Oka, Shojiro, 1996, "Damage of Gas Facilities by Great Hanshin Earthquake and Restoration Process," Program of the Sixth U.S.-Japan Workshop on Earthquake Resistant Design of Lifeline Facilities and Countermeasures Against Liquefaction, June, Tokyo, Japan.
- Phillips, Steven H., and Virostek, J. Kris, 1990, Natural Gas Disaster Planning and Recovery: The Loma Prieta Earthquake, Pacific Gas & Electric Company, April.
- Reiter, L., 1990. Earthquake Hazard Analysis, Issues and Insights, Columbia U. Press, N.Y.
- Seed, H.B. and Idriss, I.M., 1982. Ground Motions and Soil Liquefaction During Earthquakes, Earthquake Engineering Research Institute.
- Seed, H.B., Tokimatsu, K., Harder, L.F., and Chung, Riley M., 1985. "Influence of SPT Procedures in Soil Liquefaction Resistance Evaluations," Journal of Geotechnical Engineering, ASCE, Vol. 3, N. 12, pp. 1425-1446.
- Yamazaki, Fumio and Tong, Huanan, 1996, "Damage and Restoration of Natural Gas System in the 1995 Kobe Earthquake," The Hyogoken-Nanbu Earthquake, Committee of Earthquake Engineering, Japan Society of Civil Engineers, June.
- Youd, L., and Idriss, I.M., 1997. Liquefaction Resistance of Soils, Workshop Proceedings Conducted in salt lake City, UT, January 4-5, 1996, NCEER Technical Report, Forthcoming.
- Zimmerman, T.J.E., Stephens, M.J., DeGeer, D.D, and Chen, Q., 1995. "Compressive Strain Limits for Buried Pipelines," Proceedings 1995 Offshore Mechanics and Arctic Engineering Conference, Volume V, Pipeline Technology, American Society of Mechanical Engineers.

TABLE 1 EXAMPLE PARAMETERS, LAYOUT AND DIMENSIONS

Pipe	Material:	X60 Grade Steel
	Diameter, D:	600 mm
	Wall Thickness, t:	10 mm
	Depth of Burial, H _c :	1.5 m
	Pressure, P:	3 MPa
Soil	Material	Flood Plain deposits (alluvium)
	Water table depth	5m
	Ground surface Slope	0.5%
Liquefiable Layer	Depth	between 6.5 and 8m
	SPT blow count (normalized)	10
	Particle size (mm < 50%)	D _{50,15} = 0.4mm
	Fines content	40%
	Unit Wgt., g	18 kN/m ³
Seismicity	PGA (10 ⁻³ probability per yr)	0.32g

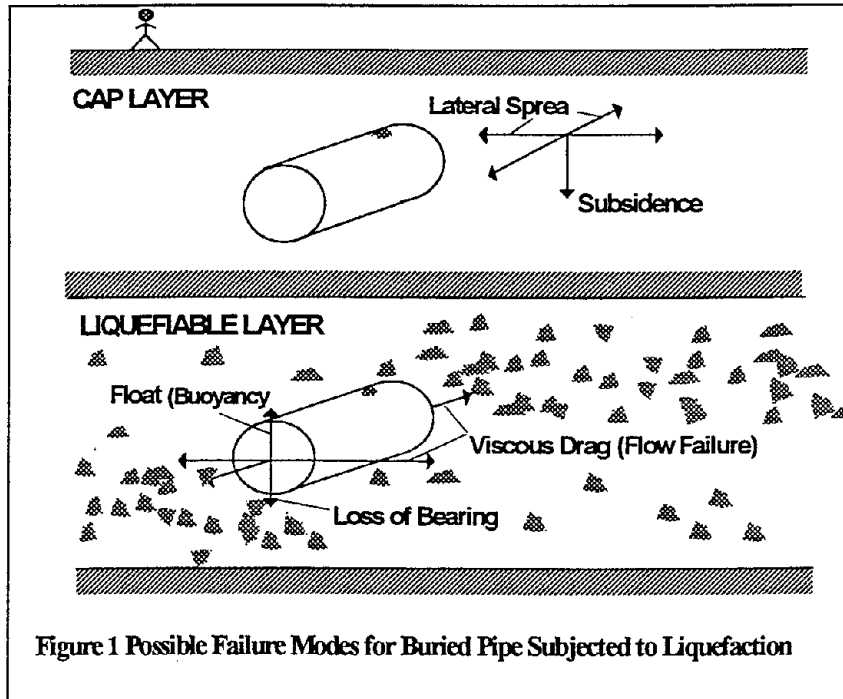


Figure 1 Possible Failure Modes for Buried Pipe Subjected to Liquefaction

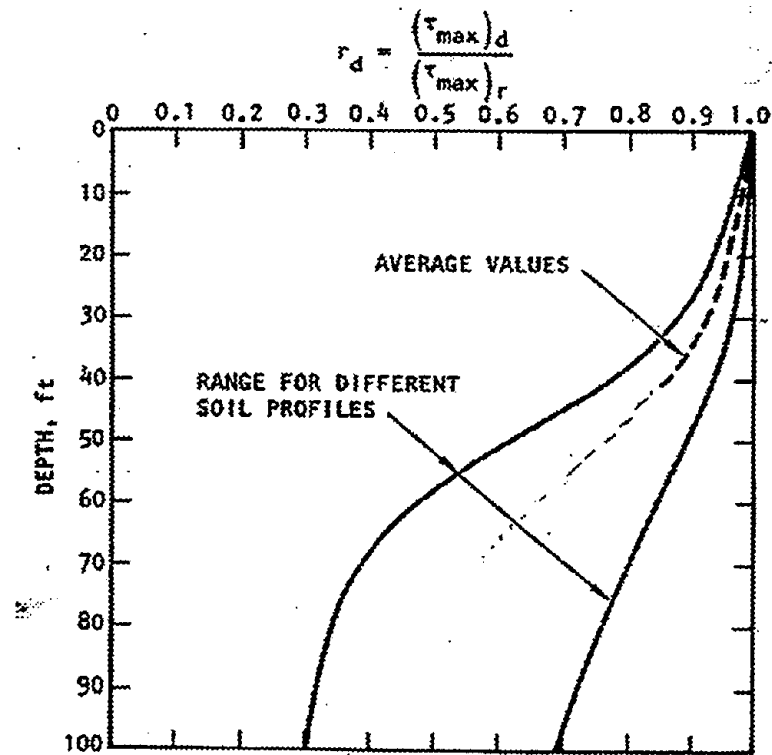


Figure 2. Range of values of r_d for different soil profiles.

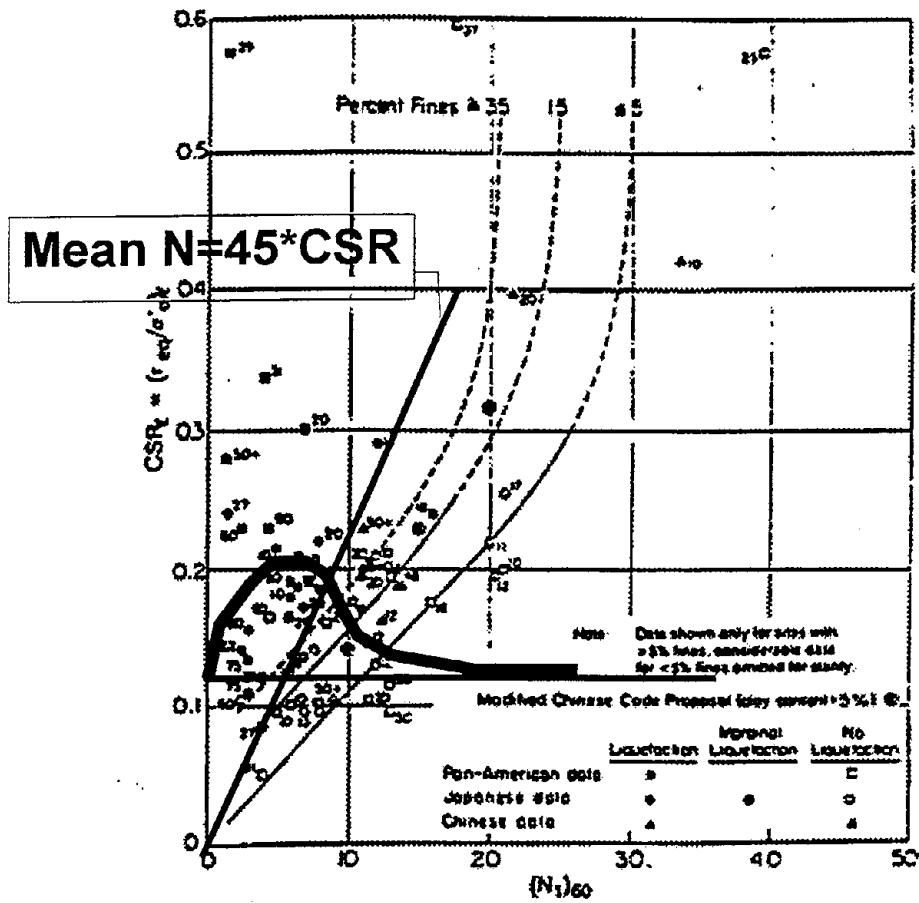


Figure 3 - Relationships between stress ratio causing liquefaction and $(N_1)_{60}$ values for silty sands for magnitude 7.5 earthquakes, with approximate probability distribution (superimposed by authors) for Fines $< 5\%$ (after Seed et al, 1985).

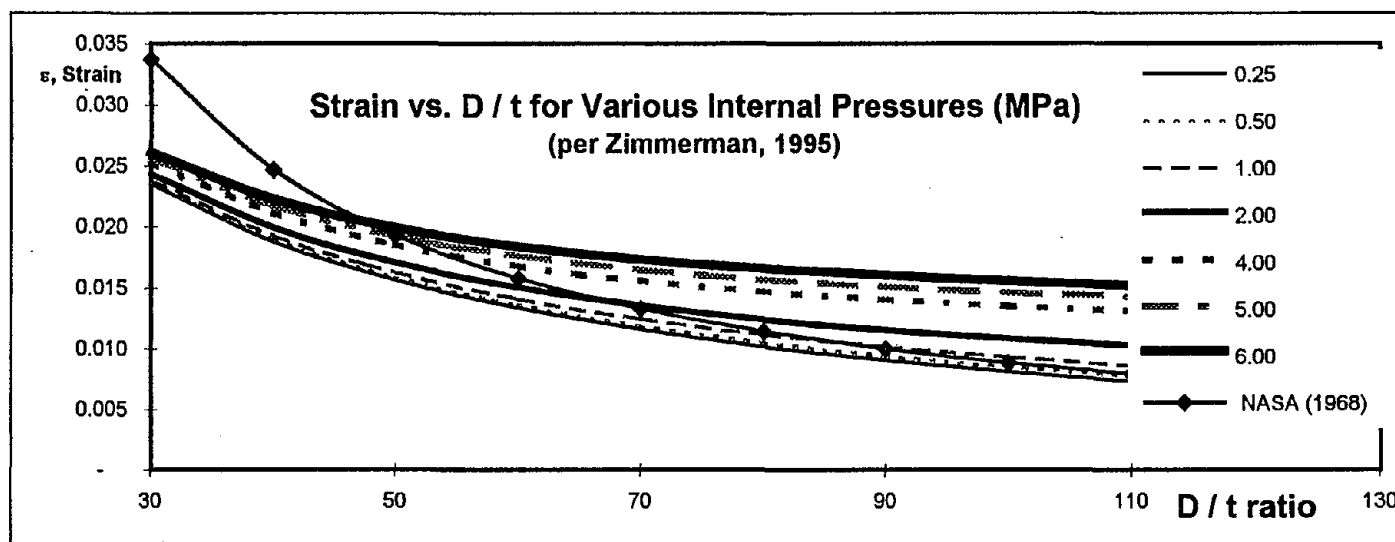
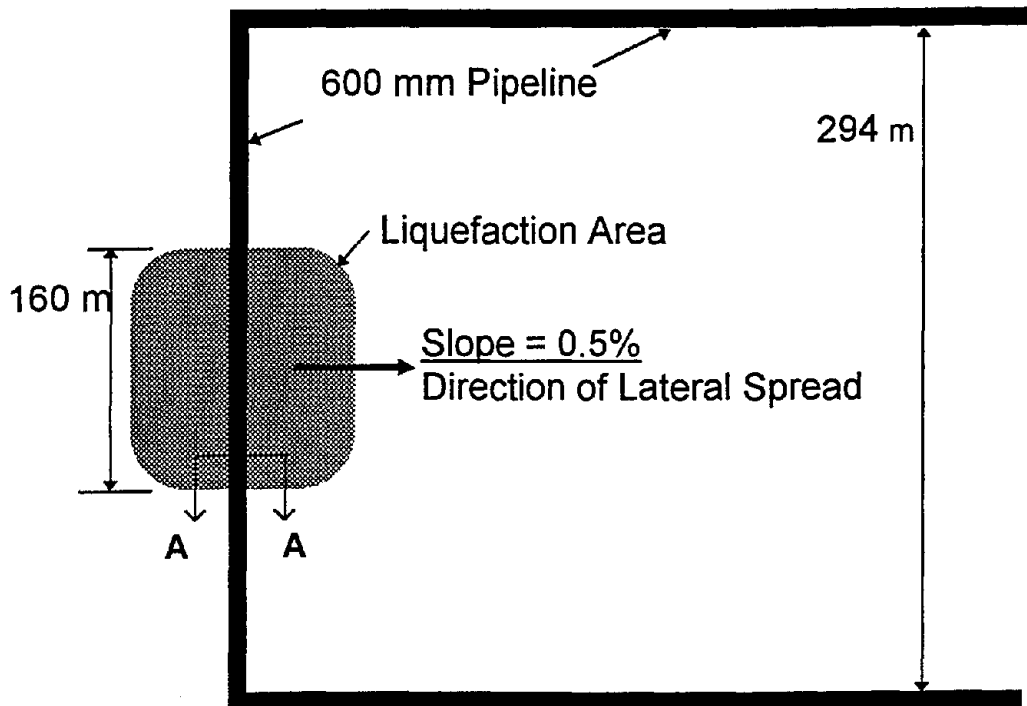
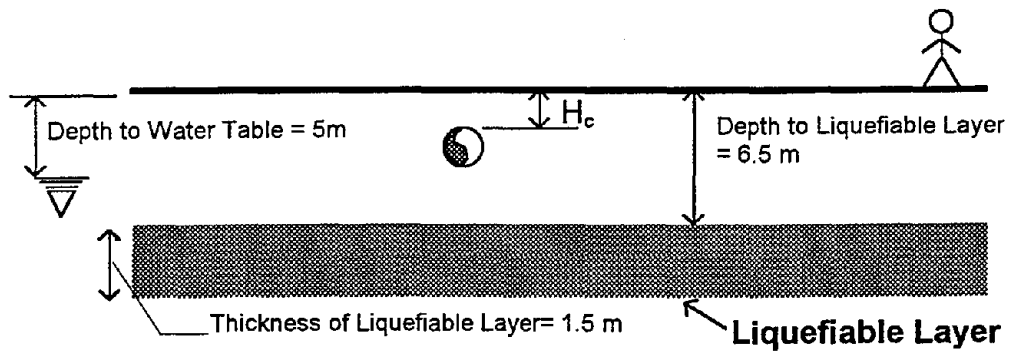


Figure 4 Strain vs. D/t for Various Internal Pressures (0.25~6 MPa) (per Zimmerman, 1995 and NASA 1968)



(a) Plan View



(b) Section A-A

Figure 5: Example Pipeline Layout

EFFECT OF SPATIAL VARIATION OF GROUND MOTION FOR ORDINARY BRIDGES

Masanobu Shinozuka

Fred Champion Professor
Department of Civil Engineering
University of Southern California, Los Angeles, CA

George Deodatis

Department of Civil Engineering and Operations Research
Princeton University, Princeton, NJ

ABSTRACT

A methodology is proposed to generate spatially varying seismic ground motion time histories at a number of prescribed locations on the ground surface, compatible with prescribed response spectra and duration of strong ground motion, and reflecting the wave propagation and loss of coherence effects. The prescribed locations can correspond to different local soil conditions and therefore different response spectra can be assigned to each location. In such a case, the generated ground motion time histories will have different frequency contents. In order to examine the effect of spatial variation of earthquake ground motion on the seismic response of bridges, three case studies are considered. First, two case studies of two bridges modeled linearly in three-dimensions and subjected to a variety of ground motion cases including different apparent velocities of wave propagation and different angles of incidence of the seismic waves with respect to the axis of the bridge are examined. The two bridges considered are the SR14/I-5 Interchange and a typical three-span concrete bridge designed by BERGER / ABAM Engineers Inc. for the Federal Highway Administration. The third case study is a comparative one of eight different bridges in order to quantify the effect of differential support ground motion as a function of the length of the largest span or the total length of the bridge. Linear as well as nonlinear dynamic analyses of these eight bridges are performed using two-dimensional finite element models. All eight bridges in this group are subjected to the same ground motion cases for comparison purposes.

METHODOLOGY TO GENERATE RESPONSE SPECTRUM COMPATIBLE AND CORRELATED SEISMIC GROUND MOTION TIME HISTORIES

The methodology is capable of generating acceleration time histories at several specified locations on the ground surface, according to user-supplied response spectra. It should be mentioned that different locations can correspond to different local soil conditions, and consequently different response spectra can be assigned to each location. In addition, a duration of strong ground motion can be specified through a modulating (envelope) function, and the simulated time histories will reflect a prescribed velocity of wave propagation and a specified loss of coherence law through a complex coherence function.

The methodology is now described following Deodatis (1996a), by considering three points on the ground surface (in general any number of points can be considered). The acceleration time histories at these three points are modeled as a uniformly modulated, tri-variate, non-stationary stochastic vector process. In general, the three points correspond to different local soil conditions. Consequently, a different target acceleration response spectrum $RSA_j(\omega)$; $j=1,2,3$ is assigned to each one of the three points. In addition, complex coherence functions $\Gamma_{jk}(\omega)$; $j,k=1,2,3$; $j \neq k$ are prescribed between pairs of points, and modulating functions $A_j(t)$; $j=1,2,3$ are assigned at each point. The simulation of the acceleration time histories is then performed according to the standard iterative scheme. As will be shown in the numerical example that follows, only a small number of iterations is usually needed (in most cases less than ten) for a sufficiently accurate convergence at every frequency. For more details about this iterative method, the reader is referred to Deodatis (1996a).

At this point it should be mentioned that the idea for upgrading the individual power spectral density functions depicted in Table 1 has been suggested by Gasparini and Vanmarcke (1976) for one-dimensional and uni-variate stochastic processes. Two alternative methodologies to generate ground motion time histories compatible with prescribed response spectra, coherence function, velocity of wave propagation, and duration of strong ground motion, have been suggested by Hao et al. (1989) and by Abrahamson (1993).

An example taken from Deodatis (1996a) is presented now to demonstrate the capabilities of the methodology. Three locations are considered on the ground surface as indicated in Fig. 1. Point 1 corresponds to rock or stiff soils (Uniform Building Code (UBC) Type 1), point 2 corresponds to deep cohesionless or stiff clay soils (UBC Type 2), and point 3 corresponds to soft to medium clays and sands (UBC Type 3). The corresponding acceleration response spectra specified by the Uniform Building Code (International Conference of Building Officials 1994) for a peak ground acceleration of 200 cm / sec^2 are plotted in Fig. 2. Acceleration time histories will be generated at the three points defined in Fig. 1 to be compatible with the corresponding three response spectra shown in Fig. 2. A velocity of wave propagation of 2 km / sec is prescribed with the direction indicated in Fig. 1. Abrahamson's coherence function (Abrahamson 1993) is

selected since it has the advantage that it can be used for a broad range of soil conditions. The duration of strong ground motion is controlled using the Jennings et al. model (Jennings et al. 1968) with parameters chosen.

The acceleration time histories are generated at 6,144 time instants, with a time step $\Delta t = 3.07 \cdot 10^{-3}$ sec, over a length equal to $6,144 \cdot 3.07 \cdot 10^{-3} = 18.85$ sec. They are plotted after ten iterations in Fig. 3. Their corresponding response spectra agreed with the prescribed UBC response spectra very well for all three locations. In addition, the three generated time histories shown in Fig. 3 reflect the prescribed velocity of wave propagation of 2 km / sec, Abrahamson's specified coherence law, and the modulating (envelope) function defined above.

CASE STUDIES

In order to examine the effect of spatial variation of earthquake ground motion on the seismic response of bridges, the following case studies have been considered. First, two case studies of two bridges modeled linearly in three-dimensions and subjected to a variety of ground motions cases including different apparent velocities of wave propagation and different angles of incidence of the seismic waves with respect to the axis of the bridge were examined. The two bridges considered were the SR14 / I-5 Interchange and a typical three-span concrete bridge designed by BERGER / ABAM Engineers Inc. for the Federal Highway Administration. These two case studies indicated that although only linear dynamic analyses were performed, the maximum stress at critical locations of the bridges when using differential support ground motion showed increases up to 18% for the SR14 / I-5 Interchange and up to 7% for the typical three-span concrete bridge, compared to the case of identical support ground motion. This was a strong indication that differential support ground motion can have a detrimental effect on the structural response of multi-span bridges. The third case study was a comparative one of eight different bridges in order to quantify the level of maximum stress increase due to differential support ground motion as a function of the length of the largest span or the total length of the bridge. Linear as well as nonlinear dynamic analyses of these eight bridges were performed using two-dimensional finite element models. All eight bridges in this group were subjected to the same ground motion cases for comparison purposes. The three case studies are described in the following.

Case Study I: The SR14 / I-5 Interchange

This case study is based on the thesis of Sanjay Arwade (Arwade 1996) that was completed at Princeton University, with the second author of this report serving as thesis advisor.

The southbound SR14 / I-5 separation and overhead structure is located at mile post 24.5 on Route 5 in Los Angeles County approximately 24 miles northwest of downtown Los Angeles and is generally aligned in the north-south direction. The bridge is a ten-span structure divided into five frames by four expansion joints. It has seat-type abutments and single column bents. The total length is 1582 ft with an overall width of 55 ft. The structure is curved to a radius of 2235 ft.

The viaduct failed spectacularly on January 17, 1994. The entire frame 1 from abutment 1 to the hinge in span 3-4 collapsed, with total disintegration of the column at pier 2, and an apparent punching through the superstructure of pier 3. The bridge unseated off abutment 1, moving about 5 ft north, and also unseated off the hinge adjacent to pier 4, again ending up in a final position some distance north of its original plan position. The right exterior shear key at abutment 1 was damaged. However, the left shear key had little visual damage. The pier 3 bent cap was inclined towards pier 4 and the measured ground separation from the column at pier 4 was approximately six inches north south and four inches east-west. The predominant motion of the structure appeared to be in the north-south direction.

In this case study, a linear three-dimensional finite element model of the viaduct was constructed based on the "as built plans" of the structure, and then this model was subjected to response spectrum compatible, spatially varying ground motions generated using the methodology described in the previous section. The purpose of this case study is to show that spatially varying ground motion can lead to increased bridge response when compared to spatially constant ground motion.

Ground Motion

A total of 18 scenario earthquakes were considered by varying the velocity of seismic wave propagation v , the angle of incidence of seismic waves with respect to the axis of the bridge θ ($\theta = 0$ when seismic waves propagate parallel to the axis of the bridge, and $\theta = 90^\circ$ when seismic waves propagate at an angle of 90° with respect to the axis of the bridge), and by considering combinations of horizontal and vertical components of ground motion.

The Caltrans acceleration design response spectrum for 80-150 ft alluvium, 5% damping, and 0.5g peak ground acceleration was selected for all supports of the bridge. Abrahamson's coherence law (Abrahamson 1993) was chosen to describe the coherence loss between pairs of supports. Finally, the Jennings et al. envelope (Jennings et al. 1968) was used to define the duration of strong ground motion.

Bridge Model

The motion of interest in this study is the motion of the center axis of the bridge. For this reason, the structure is modeled in three dimensions using 1-D frame elements running along the neutral axis of the superstructure box girder. The section properties of these elements are chosen to represent the full width and depth of the box girder. The ANSYS computer code was selected for the dynamic analysis.

Dynamic Analysis and Conclusions

For each of the 18 scenario earthquakes considered, the structure was analyzed using identical and differential support ground motion (linear dynamic time history analysis). The following ratio is computed for each section of the bridge (deck sections, pier sections) in order to quantify the effect of the spatial variation of ground motion on the dynamic response of the structure:

$$\rho = (\text{maximum value of stress computed using spatially varying ground motion}) / (\text{maximum value of stress computed using spatially constant ground motion})$$

(1)

It is obvious that the ratio ρ indicates the increase ($\rho > 1$) or decrease ($\rho < 1$) in the maximum value of the stress for a specific section of the bridge caused by differential support ground motion, compared to the corresponding case of identical support ground motion.

Values of ρ for the deck quantities showed that certain sections of the deck can experience maximum stress increases of the order of 16%-18% when analyzed using spatially varying ground motion (compared to a corresponding dynamic analysis using identical support ground motion). Since the "Standard Specifications for Highway Bridges" of AASHTO (1996) require either a response spectrum dynamic analysis or a time history dynamic analysis for bridges with more than 6 spans like the SR14 / I-5 Interchange, it is recommended to use the time history dynamic analysis option involving response spectrum compatible ground motion time histories that will reflect the wave propagation and loss of coherence effects. Such a dynamic analysis has to be performed by considering a few scenario earthquakes by varying the angle of incidence of seismic waves with respect to the axis of the bridge and by considering different (realistic) velocities of wave propagation. It is expected that one or more of these scenario earthquakes (that are design response spectrum compatible) will produce maximum stresses that will be higher than the corresponding maximum stresses obtained from a dynamic analysis using identical support ground motion. The set of dynamic analyses recommended here can be used to design new bridges or to analyze existing bridges for retrofitting and strengthening purposes.

CaseStudy II: A Typical Three-Span Concrete Bridge

This example (Kwan, 1997) involves a typical three-span continuous cast-in-place concrete box girder bridge that was designed by BERGER / ABAM Engineers Inc. for the Federal Highway Administration (FHWA 1996). The total span of the bridge is 320 feet, with the individual spans being equal to 100, 120 and 100 feet as indicated in Fig. 9, with a skew of 30° . The superstructure consists of a cast-in-place concrete box girder supported by two piers, each consisting of two circular cast-in-place concrete columns. For details about the geometry and materials of the bridge, the reader is referred to FHWA (1996).

The finite element model of the bridge developed by BERGER / ABAM Engineers (FHWA 1996) was used in this case study. It was subjected to response spectrum compatible, spatially varying ground motions to examine whether differential support ground motion can lead to increased bridge response, when compared to identical support ground motion. The methodology described in the beginning of this report is used again here to generate the ground motion time histories. The computer code SAP2000 was selected to perform the dynamic time history analyses.

Ground Motion

A total of 36 scenario earthquakes were examined by considering four different apparent velocities of seismic wave propagation v (1,000, 1,500, 2,000, and 2,500 m / sec), three different angles of incidence of the seismic waves with respect to the axis of the bridge θ (0° , 45° , and 90°), and by considering three different scenario earthquakes for each of the aforementioned $4 * 3 = 12$ cases, by varying the seed for the random number generator.

The Uniform Building Code (International Conference of Building Officials 1994) acceleration response spectrum for Type II soil, 5% damping, and 0.3g peak ground acceleration was selected for all supports of the bridge. Abrahamson's coherence law (Abrahamson 1993) was chosen to describe the coherence loss between pairs of supports. Finally, the Jennings et al. envelope (Jennings et al. 1968) was used to define the duration of strong ground motion.

Dynamic Analysis and Conclusions

For each of the 36 scenario earthquakes considered, the structure was analyzed using identical and differential support ground motion (linear dynamic time history analysis). The ratio defined in Eq. (1) is again computed for the deck and the columns of the bridge in order to quantify the effect of the spatial variation of ground motion on the dynamic response of the structure. The results of these dynamic analyses show that the deck and the columns can experience maximum stress increases up to 4.4% and 7.2% respectively, when analyzed using spatially varying ground motion (compared to a corresponding dynamic analysis using identical support ground motion).

Although these increases are smaller than the corresponding ones encountered in the previous case study involving the SR14 / I-5 viaduct, they indicate that differential support ground motion can have a detrimental effect even to relatively short-span bridges as the one considered here.

Case Study III: Comparative Analysis of Eight Bridges

The comparative analysis involves the eight bridges whose basic characteristics are summarized in Table 1. These eight bridges have total lengths ranging from 111 ft up to 1,584 ft, and number of spans ranging from 3 up to 10. All eight bridges are modeled in two-dimensions. The computer code SAP90 beta version was selected to perform the dynamic time history analyses. Both linear and nonlinear analyses are carried out. A relatively simple model is used to perform the nonlinear dynamic analyses. This appears quite appropriate considering the various types of approximation in modeling the structure, and the uncertainty involved in specifying the input ground motion. The model used here for the piers of all eight bridges (the only members considered to exhibit nonlinear behavior in this study) is, such that a pier is modeled as an elastic column of length $2H_e$, with a pair of plastic zones of length L_p at each end of the column. The total length H of the pier from the ground to the soffit of the girder is therefore equal to $2(H_e + L_p)$. The plastic zone is then modeled to consist of a nonlinear rotational spring and a rigid element of length L_p . These parameters are established using the *Column Ductility Program* COLx (Caltrans 1993). For those bridges with expansion joints, the joints are modeled by allowing the two sections of the bridge converging to the joint to move independently in the horizontal direction and to rotate independently, and by constraining them to move by the same amount in the vertical direction. Similar analysis was performed dealing with similar bridges by Shinozuka et al. (1997) in investigating the effect of viscous dampers at expansion joints on the suppression of the seismic vibration of bridges.

Ground Motion

All eight bridges were subjected to response spectrum compatible, spatially varying ground motions to examine whether differential support ground motion can lead to increased bridge response, when compared to identical support ground motion. The methodology described in the beginning of this report is used again here to generate the ground motion time histories.

A total of 15 scenario earthquakes were examined by considering three different apparent velocities of seismic wave propagation v (1,000, 1,500, and 2,000 m/sec), and five different scenario earthquakes for each value of v by varying the seed for the random number generator.

The Uniform Building Code (International Conference of Building Officials 1994) acceleration response spectrum for Type I soil, 5% damping, and 0.5g peak ground acceleration was selected

for all supports of each one of the eight bridges (with the exception of the FHWA / ABAM-No.2 bridge for which the UBC response spectrum for Type II soil was used for 5% damping and 0.3g peak ground acceleration). Abrahamson's coherence law (Abrahamson 1993) was chosen to describe the coherence loss between pairs of supports. The Jennings et al. envelope (Jennings et al. 1968) was used to define the duration of strong ground motion. Finally, as two-dimensional models of the eight bridges were selected, only the horizontal component of ground motion parallel to the axis of the bridge has been considered.

Dynamic Analysis and Conclusions

For each of the 15 scenario earthquakes considered (refer to Table 6), each one of the eight bridges was analyzed using identical and differential support ground motion. Linear as well as nonlinear dynamic analyses were carried out. The ratio defined in Eq. (1) is again computed for the deck and the piers of each bridge in order to quantify the effect of the spatial variation of ground motion on the dynamic response of the structure. The results of these linear and nonlinear dynamic analyses are provided in Tables 7-14.

Figure 4 plots the maximum response ratio ρ for the moment at the piers (linear dynamic analysis) as a function of the largest span length of the bridge. Figure 22 plots the maximum response ratio ρ for ductility demand (nonlinear dynamic analysis) as a function of the largest span length of the bridge. It should be mentioned that ductility demand is defined as the ratio of hinge rotation θ at the base of the pier over the yield rotation θ_y of the nonlinear rotational spring.

CONCLUSIONS, PRELIMINARY GUIDELINES, AND FURTHER WORK

There are very interesting conclusions that can be drawn from the three case studies, and especially from Figs. 4-5. It appears that in general the values of ρ_{\max} increase as the total length of the bridge or the longest span of the bridge increase. For bridges similar in configuration and span to the ones considered here, an increase in internal forces and ductility demands of up to 20% should be expected due to differential support ground motion. For the type of multi-span bridges like the SR14 / I-5 Interchange, this increase can be as high as 50%. Some preliminary results indicate that the effect of different local soil conditions at different supports of a bridge can produce even larger values for ρ_{\max} .

Although at this stage it is not possible to draw general conclusions because of the limited number of bridges examined, it has become obvious that differential support ground motion can have a highly detrimental effect on the seismic response of bridges, when compared to identical

support ground motion. This detrimental effect cannot be neglected and will have to be eventually included in the design of new bridges or the retrofit of existing ones.

An effort will be made to include in the final report results from further studies including the effect of restrainers, of pounding, of different local soil conditions, and of the large number of sample functions. Systematic further studies are also needed on the following topics: soil-structure interaction, vertical component of seismic ground motion, angle of incidence of seismic waves with respect to the axis of the bridge, stiffness of bridge structure, and effect of relative displacement at expansion joints.

Recommendations and guidelines in the final version of this report are expected to be provided in a form similar to that of codes like the AASHTO. Specifically, it will be recommended to perform a time history analysis using generated differential support ground motion for bridges with more than a certain number of spans, and / or longer than a specific total length, and/or with supports on different local soil conditions. Alternatively, new factors will be provided to increase the equivalent horizontal static loads for the analysis of bridges, depending on their total length and / or longest span.

ACKNOWLEDGMENTS

This work was supported by the NCEER Highway Project (FHWA Contract DTFH61-92-C-00106).

REFERENCES

- Abrahamson, N.A. (1993). "Spatial Variation of Multiple Support Inputs," Proceedings of 1st U.S. Seminar on Seismic Evaluation and Retrofit of Steel Bridges, a Caltrans & University of California at Berkeley Seminar, San Francisco, October 18.
- Arwade, S. (1996). "Analysis of the Effect of Differential Support Motion on a Typical Reinforced Concrete Highway Bridge," B.S.E. Thesis, Department of Civil Engineering and Operations Research, Princeton University.
- Buckle, I.G. (1994). "The Northridge, California Earthquake of January 17, 1994: Performance of Highway Bridges," Technical Report NCEER-94-0008, National Center for Earthquake Engineering Research, State University of New York at Buffalo.

California Department of Transportation - Division of Structures. (1993). "User's Manual for COLx -- Column Ductility Program."

Deodatis, G. (1996a). "Non-Stationary Stochastic Vector Processes: Seismic Ground Motion Applications," Probabilistic Engineering Mechanics, Vol. 11, No. 3, pp. 149-167.

Deodatis, G. (1996b). "Simulation of Ergodic Multi-Variate Stochastic Processes," Journal of Engineering Mechanics, ASCE, Vol. 122, No. 8, pp. 778-787.

Federal Highway Administration. (1996). "Seismic Design of Bridges," BERGER/ ABAM Engineers, Publication No. FHWA-SA-97-009.

Gasparini, D. and Vanmarcke, E.H. (1976). "Simulated Earthquake Motions Compatible With Prescribed Response Spectra," Technical Report, Department of Civil Engineering, Massachusetts Institute of Technology, Publication No. R76-4.

Hao, H., Oliveira, C.S. and Penzien, J. (1989). "Multiple-Station Ground Motion Processing and Simulation Based on SMART-1 Array Data," Nuclear Engineering and Design, Vol. 111, No. 3, pp. 293-310.

International Conference of Building Officials. (1994). "Uniform Building Code," Vol. 2.

Jennings, P.C., Housner, G.W. and Tsai, N.C. (1968). "Simulated Earthquake Motions," Technical Report, Earthquake Engineering Research Laboratory, California Institute of Technology.

Kwan, W-P. (1997). "The Effect of Spatially Differential Seismic Ground Motion on a Typical Three-Span Concrete Bridge," B.S.E. Thesis, Department of Civil Engineering and Operations Research, Princeton University.

Shinozuka, M., Kim, J-M. and Purasinghe, R. (1997). "Use of Visco-Elastic Dampers at Expansion Joints to Suppress Seismic Vibration of Bridges," Second National Seismic Conference on Bridges and Highways, Sacramento, California, July 8-11.

Table 1 Basic Characteristics of Eight Bridges
Considered in Case Study III

Bridge Analyzed	# of Span	Largest Span(ft)	Total length(ft)
Textbook Example Bridge	3	44	111
Aptos Creek Bridge	5	56	256
ABAM-No.2 Bridge	3	152	400
TYOH Example Bridge	5	175	525
TY1H Example Bridge	5	175	525
TY2H Example Bridge	5	175	525
Gavin Canyon (2D)	5	208	741
SR14/15 (2D)	10	206	1,584

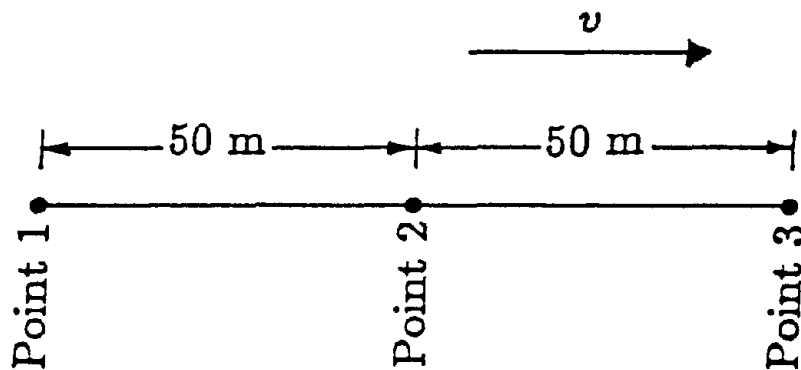


Fig. 1 Configuration of points 1, 2, and 3 on the ground surface along the line of main wave propagation.

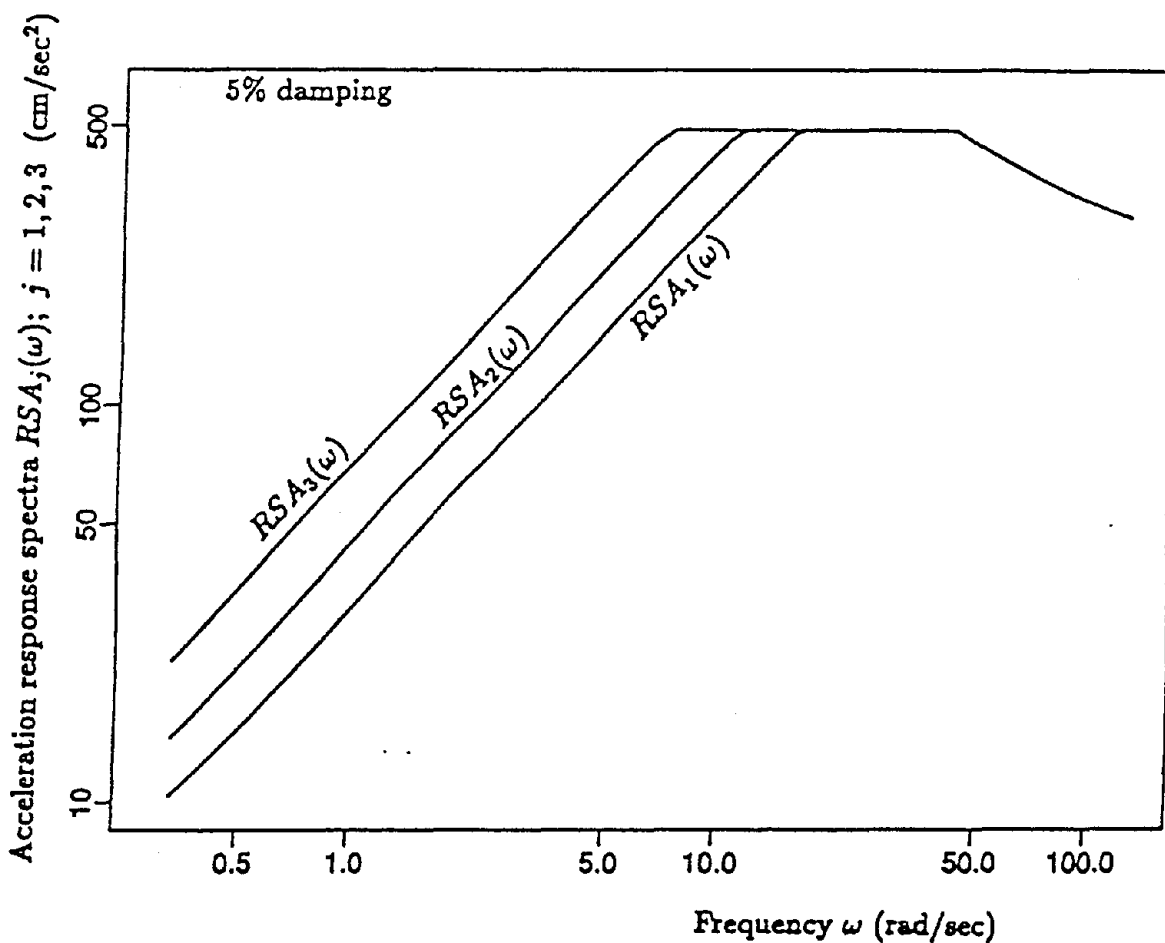


Fig. 2 Uniform Building Code acceleration response spectra assigned to points 1, 2, and 3, respectively (refer to Fig. 1 for location of three points).

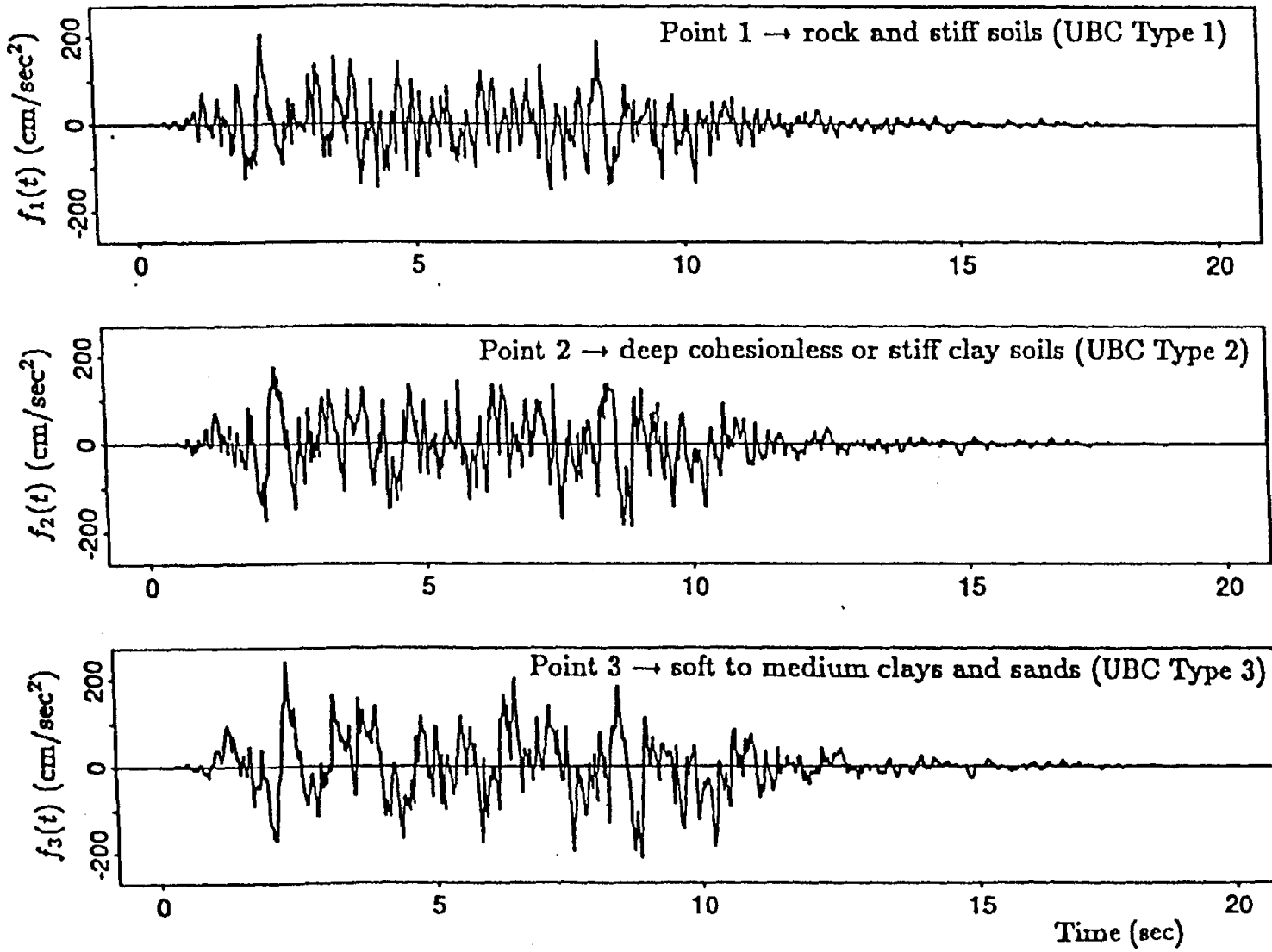


Fig. 3 Generated acceleration time histories at points 1, 2, and 3 defined in Fig. 1.

Fig. 4 Largest Span Length of Bridge
vs.

Maximum Response Ratio (ρ) for Moment at Piers (By Linear Analysis)

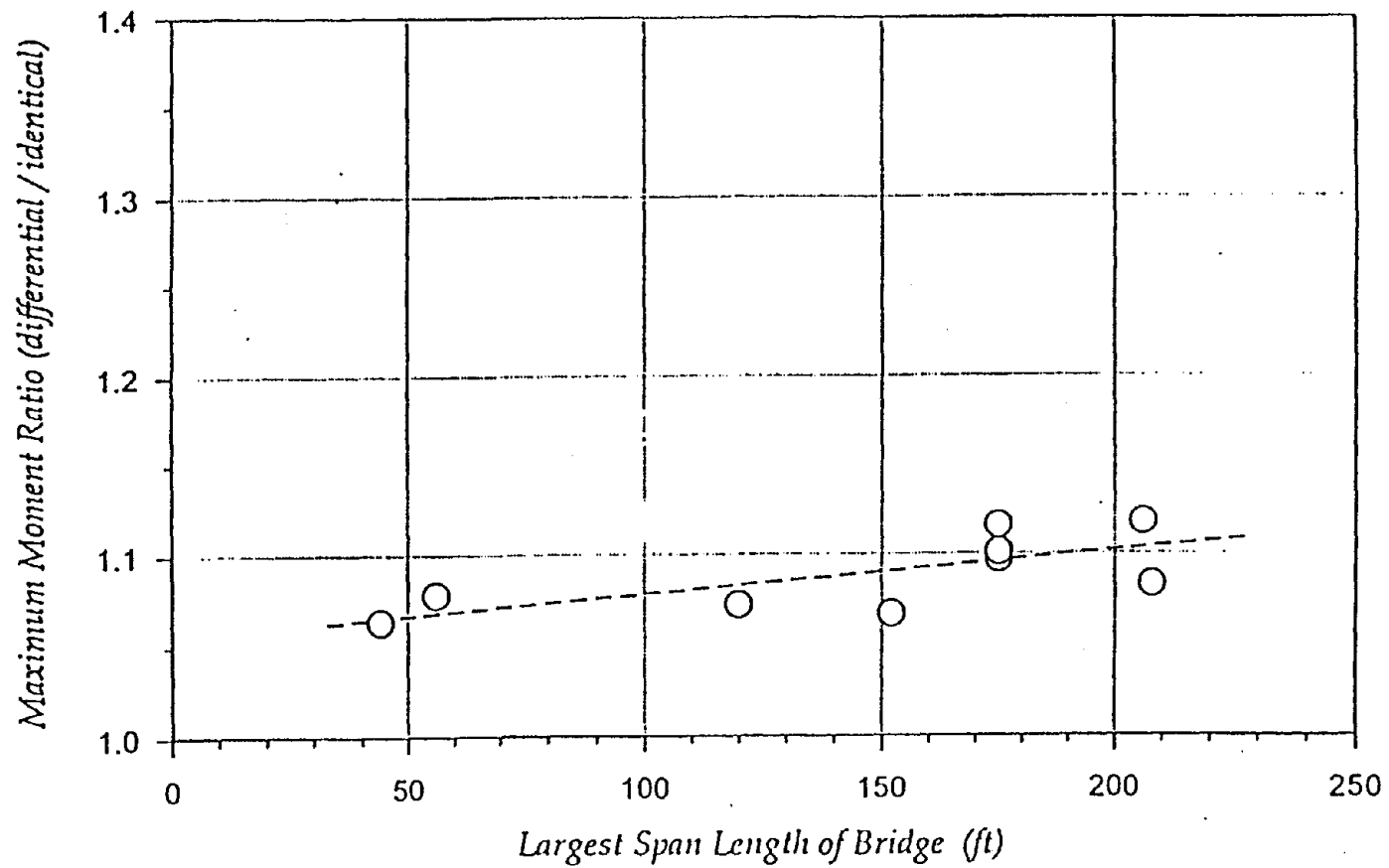
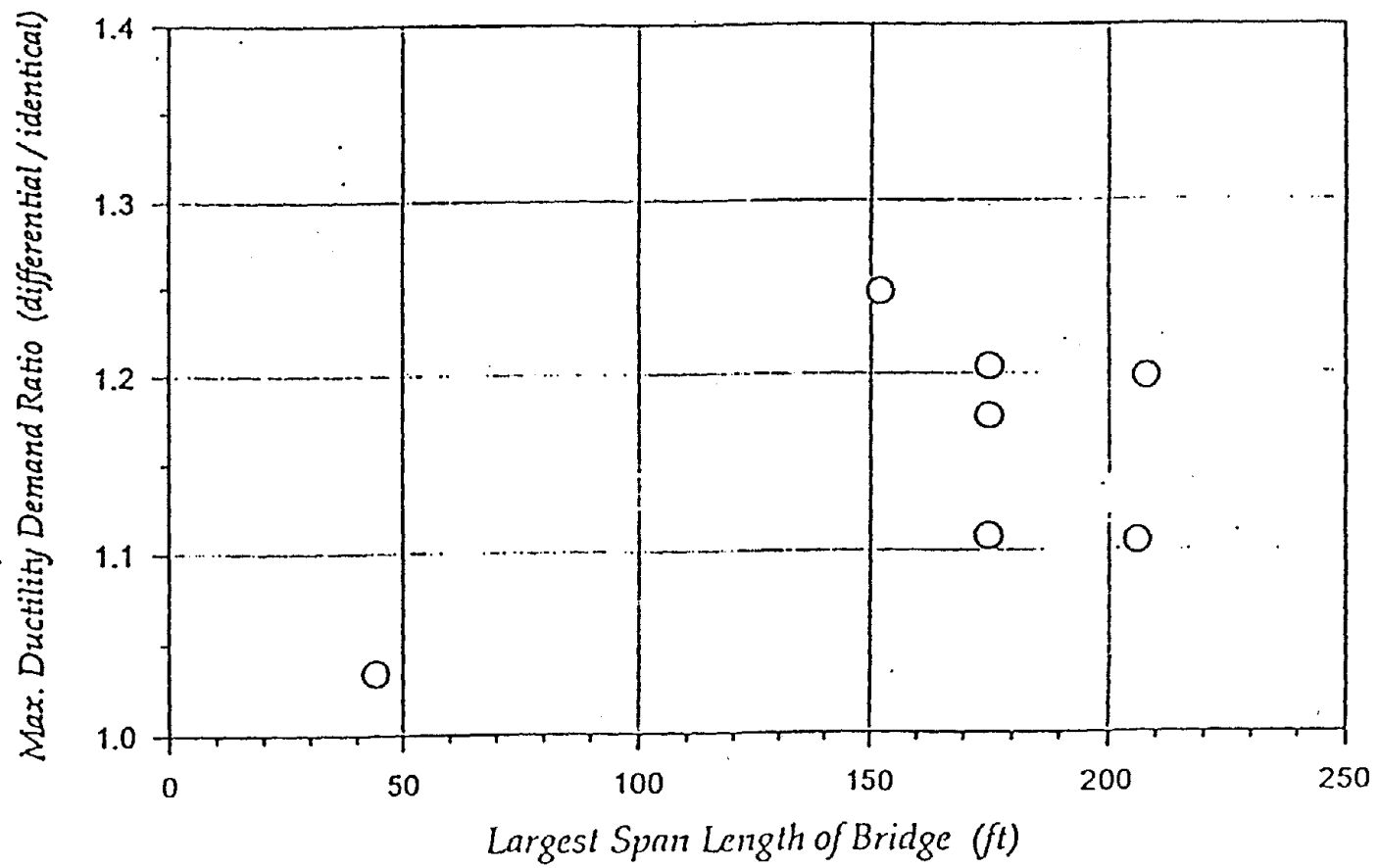


Fig. 5 Largest Span Length of Bridge
vs.

Maximum Response Ratio (ρ) for Ductility Demand (By Nonlinear Analysis)



BIOGRAPHICAL SKETCH

A. VITAE

NAME: Masanobu Shinozuka

Present Position: Fred Champion Chair in Civil Engineering
University of Southern California (1995-present)

Sollenberger Professor of Civil Engineering Emeritus,
Princeton University

Address: University of Southern California
Department of Civil Engineering
3620 South Vermont Avenue KAP 254
Los Angeles, CA 90089-2531
Phone : (213) 740-9528
Fax : (213) 740-9529
e-mail : shino@usc.edu

Education: Columbia University, Ph.D. (1960)
Kyoto University, M.S. (1955); B.S. (1953)

Professional License: P.E. #10115, Washington, D.C., 1994

Fields of Interest: Random Vibration, reliability of structural systems, structural dynamics, structural control, inelasticity, infrastructure system, lifeline systems

Professional Experience:

1988-1995	Sollenberger Professor of Civil Engineering Emeritus, Princeton University
1990-1992	Director, National Center for Earthquake Engineering Research at SUNY/Buffalo, (on leave from Princeton University)
1990-1992	Visiting Capen Professor of Civil Engineering, SUNY/Buffalo
1977-1988	Renwick Professor of Civil Engineering, Columbia University
1969-1977	Professor of Civil Engineering, Columbia University
1965-1969	Associate Professor of Civil Engineering, Columbia University
1961-1965	Assistant Professor of Civil Engineering, Columbia University

Professional Activities:

- Honorary Member ASCE; Fellow ASME, Senior Member AIAA
- Chairman, Research Committee, National Center for Earthquake Engineering Research (NCEER)
- Editor, Journal of Probabilistic Engineering Mechanics
- Associate Editor, Applied Mechanics Reviews, ASME
- Member, Editorial Board of International Journal of Earthquake Engineering & Soil Dynamics
- Member, Editorial Board of Journal of Structural Safety
- Member, U.S. Panel on Active Structural Control

Honors and Awards:

1994	ASCE Theodore von Karman Medal
1991	Wessex Institute of Technology Medal
1991	ASCE C. Martin Duke Award
1988	ASCE Moisseiff Award
1985	ASCE Nathan M. Newmark Medal
1985	Ticinense Medal, University of Pavia, Pavia, Italy
1978	ASCE Alfred M. Freudenthal Medal,
1978	Elected Member of the National Academy of Engineering
1972	ASCE Walter M. Huber Civil Engineering Research Prize

Patent:

U.S. Patent No. 4,228,759 "Pressure Sustaining Vessel"

Publications: More than 400 Journal and Conference papers.



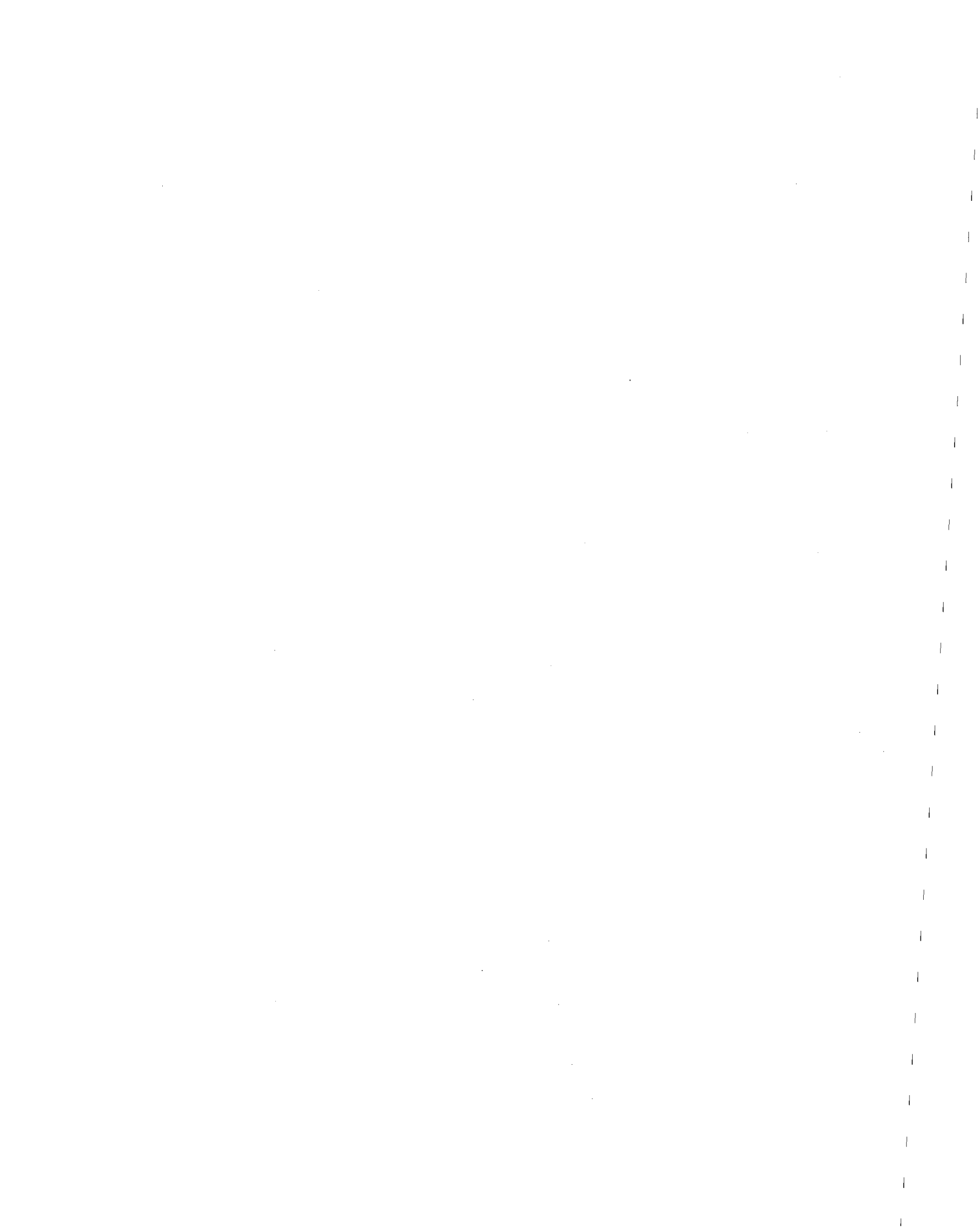
SPECIAL PRESENTATIONS AND PAPERS

**“Design Methods of Bridge Foundations Against Soil
Liquefaction and Liquefaction-Induced Ground Flow”**

K. Yokoyama, K. Tamura, O. Matsuo

**“Experimental Study of the Effects of Liquefaction-Induced
Ground Flow on Bridge Foundation”**

K. Tamura, T. Azuma



DESIGN METHODS OF BRIDGE FOUNDATIONS AGAINST SOIL LIQUEFACTION AND LIQUEFACTION-INDUCED GROUND FLOW

Koichi Yokoyama ¹ , Keiichi Tamura ² and Osamu Matsuo ³

1 Director, Earthquake Disaster Prevention Research Center, Public Works Research Institute, Ministry of Construction, 1 Asahi, Tsukuba-shi, Ibaraki-ken 305 Japan

2 Head, Ground Vibration Division, Earthquake Disaster Prevention Research Center, ditto

3 Head, Soil Dynamics Division, Earthquake Disaster Prevention Research Center, ditto

ABSTRACT

In this paper, a revised method to assess liquefaction potential of soils and a seismic design treatment of soil liquefaction for highway bridges are presented. The presented liquefaction potential assessment depends simply on the blow counts of a standard penetration test and soil gradation parameters. The design treatment of liquefaction for bridges verifies the ductility of foundation by the principle of conservation of energy. Also presented in this paper are the influence of liquefaction-induced ground flow on highway bridge foundations and its treatment in seismic design, in which the effect of ground flow is considered as static force acting to a bridge foundation.

INTRODUCTION

The Hyogo-ken Nanbu Earthquake of 1995 caused extensive soil liquefaction over a wide area of offshore reclaimed lands and natural deposits ^{1), 2)}. Besides that, near the water's edge, liquefaction induced ground flow with the movement of sea walls. Liquefaction and its associated ground flow exerted serious influence on various engineering structures. Although highway bridges did not suffer destructive damage due to liquefaction, liquefaction-induced ground flow caused large deformation of highway bridge foundations.

In the former "Specifications for Highway Bridges" ³⁾, the assessment of liquefaction was made mainly for loose sand against moderate ground motions, and a seismic design treatment of liquefaction was prescribed. However, the strong ground motions such as generated by the Hyogo-ken Nanbu Earthquake were not considered, and no concrete provision regarding the liquefaction-induced ground flow was given in the Specifications.

This paper first summarizes the newly proposed method to estimate liquefaction potential considering the feature of soil liquefaction caused by the Hyogo-ken Nanbu Earthquake⁴⁾. This method was calibrated by comparing with field performance data. The design treatment of liquefaction for bridge foundations that aims to ensure sufficient deformation capacity is also described.

Then, this paper presents a feature of the liquefaction-induced ground flow due to the Hyogo-ken Nanbu Earthquake, its influence on highway bridges which includes an estimation of ground flow force acting on a bridge foundation and an outline of seismic design treatment of the liquefaction-induced ground flow.

ESTIMATION OF LIQUEFACTION POTENTIAL

Soil Layers to Be Assessed

The Hyogo-ken Nanbu Earthquake of 1995 caused liquefaction even at coarse sand or gravel layers that had been regarded invulnerable to liquefy, and the design practice has been changed to include a gravel layer in the soil layers that require liquefaction potential estimation. Based on field performance data, the upper limit of mean grain size D_{50} , for which liquefaction potential estimation is necessary, has been changed from 2mm to 10mm.

Estimation of Liquefaction Potential

Liquefaction potential is estimated by the safety factor against liquefaction F_L as follows:³⁾

$$F_L = R/L \quad (1)$$

where

- F_L : liquefaction resistant ratio,
- R : dynamic shear strength ratio,
- L : shear stress ratio during an earthquake.

The dynamic shear strength ratio R may be expressed as

$$R = c_w R_L \quad (2)$$

where

c_w : corrective coefficient for ground motion characteristics,

R_L : cyclic triaxial strength ratio; a ratio of cyclic shear stress required to cause 5% double amplitude axial strain in 20 cycles of loading to the confining pressure.

The cyclic triaxial strength ratio was estimated by laboratory tests with undisturbed samples by in situ freezing method. The samples were formed into cylindrical specimens 10cm long and 5cm in diameter for sand, and 60cm long and 30cm in diameter for gravel, respectively. It should be noted that in this paper "sand" and "gravel" are defined as materials with a mean grain size $D_{50} < 2\text{mm}$ and $D_{50} \geq 2\text{mm}$, respectively. The specimens were set in a triaxial cell and undrained cyclic triaxial tests were performed. Isotropic consolidation were performed under the effective overburden pressure in situ. Sinusoidal load with a frequency of 0.1 Hz was applied to the specimens.

The undrained cyclic triaxial strength ratio R_L obtained from the laboratory tests is hereafter presented in correlation with the blow count per foot, N -value of a standard penetration test. This N -value is corrected by the overburden pressure as follows:

$$N_1 = 1.7N / (\sigma_v' + 0.7) \quad (3)$$

where

N_1 : corrected N -value to an effective overburden pressure of 1 kgf/cm²,
 σ_v' : effective overburden stress, in kgf/cm².

Sands

Figure 1 presents test results for clean sands i.e., sands with less than 10 % fine particles passing a 0.075mm sieve. The figure clearly demonstrates that for alluvial sands the cyclic triaxial strength ratio R_L increases significantly as N_1 exceeds 20 to 25, and the sand with N_1 greater than 30 is unlikely to liquefy even under very strong cyclic stresses. For diluvial sands, R_L is larger than that of alluvial sands and increases more rapidly with the increase of N_1 . Although the data for reclaimed soils are limited in number and are scattering, it seems that R_L is smaller than that of natural deposits. For alluvial clean sands, the relationship between R_L and N_1 may be expressed as

$$R_L = \begin{cases} 0.0882 \sqrt{N_1 / 1.7} & (N_1 < 14) \\ 0.0882 \sqrt{N_1 / 1.7} + 1.6 \times 10^{-6} \cdot (N_1 - 14)^{4.5} & (N_1 \geq 14) \end{cases} \quad (4)$$

Eq.(4) is also demonstrated in Figure 1.

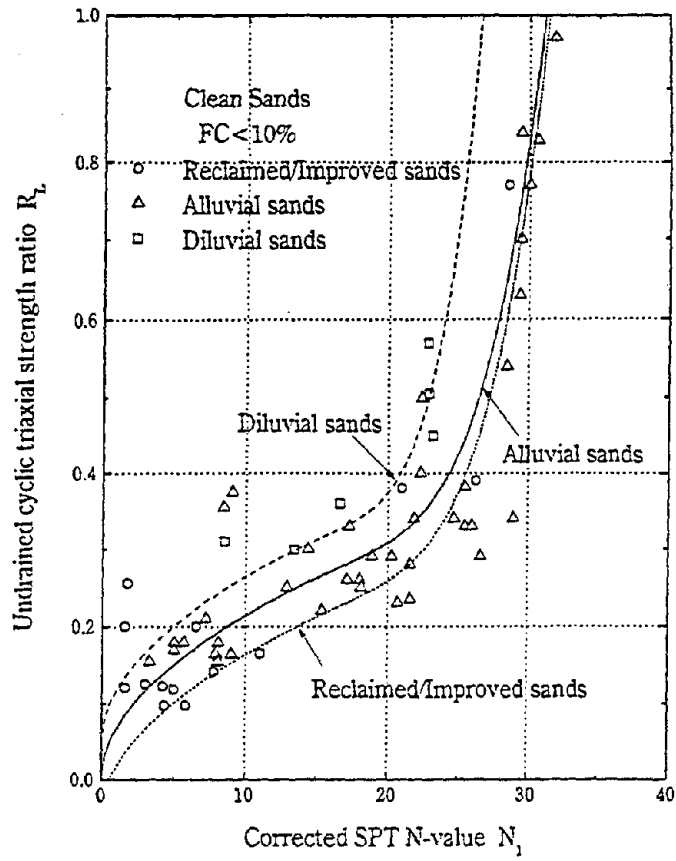


Figure 1 Relationship between R_L and N_1 for Clean Sands (FC < 10%)

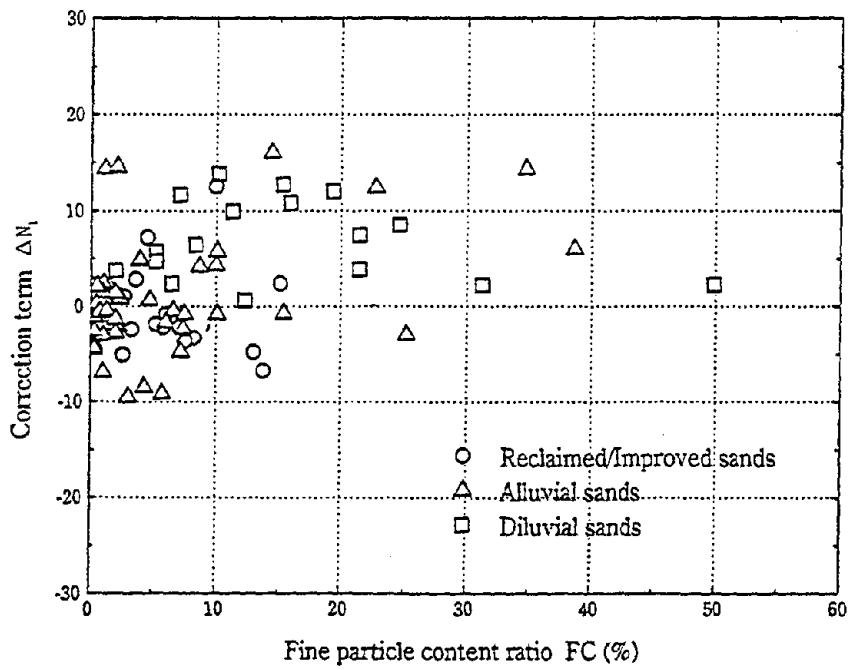


Figure 2 Relationship between ΔN_1 and FC(%)

The effect of soil gradation on the cyclic triaxial strength ratio R_L is studied by the following form

$$\begin{aligned} R_L &= R_{L1} (N_1 + \Delta N_1 \text{ (soil gradation parameters)}) \\ &= R_{L1} (N_a) \end{aligned} \quad (5)$$

where

R_{L1} : cyclic triaxial strength ratio of clean sand,

N_a : corrected N-value considering the effects of fine particles.

Figure 2 shows the relationship between the correction term ΔN_1 and fine particle content ratio FC, i.e., weight percentage of particles less than 0.074mm in diameter. It can be seen from Figure 2 that ΔN_1 increases with FC. In this study, N_a is estimated as

$$N_a = c_1 N_1 + c_2 \quad (6)$$

where c_1 and c_2 are parameters expressed by functions of FC as follows:

$$c_1 = \begin{cases} 1 & (0\% \leq FC < 10\%) \\ (FC+40)/50 & (10\% \leq FC < 60\%) \\ FC/20-1 & (60\% \leq FC) \end{cases} \quad (7)$$

$$c_2 = \begin{cases} 0 & (0\% \leq FC < 10\%) \\ (FC-10)/18 & (10\% \leq FC) \end{cases} \quad (8)$$

Gravels

Figure 3 plots test results for gravels on the relationship between the cyclic strength ratio R_L and the corrected N-value N_1 . In this figure, results for various blow count measurements other than N_1 are also presented. $N_{1(10)}$ represents the three times the minimum blow count among three of 10cm penetration. $N_{1(min)}$ represents the minimum value of (blow count)/(penetration length) and extrapolate this to 30cm. It is obvious that there is very weak correlation between R_L and N_1 or other N-values.

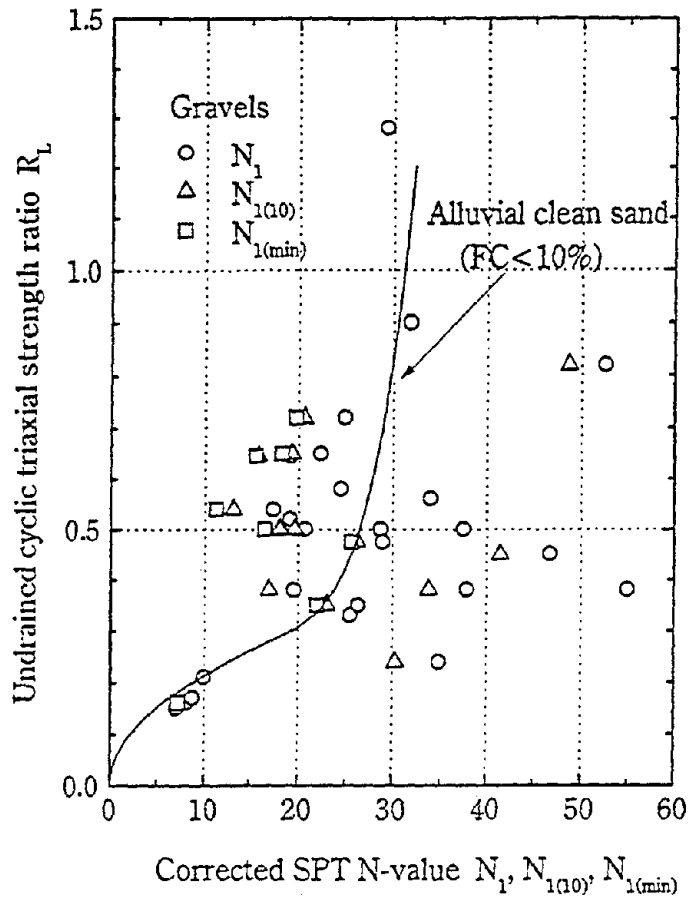


Figure 3 Relationship between R_L and Corrected N-values for Gravels

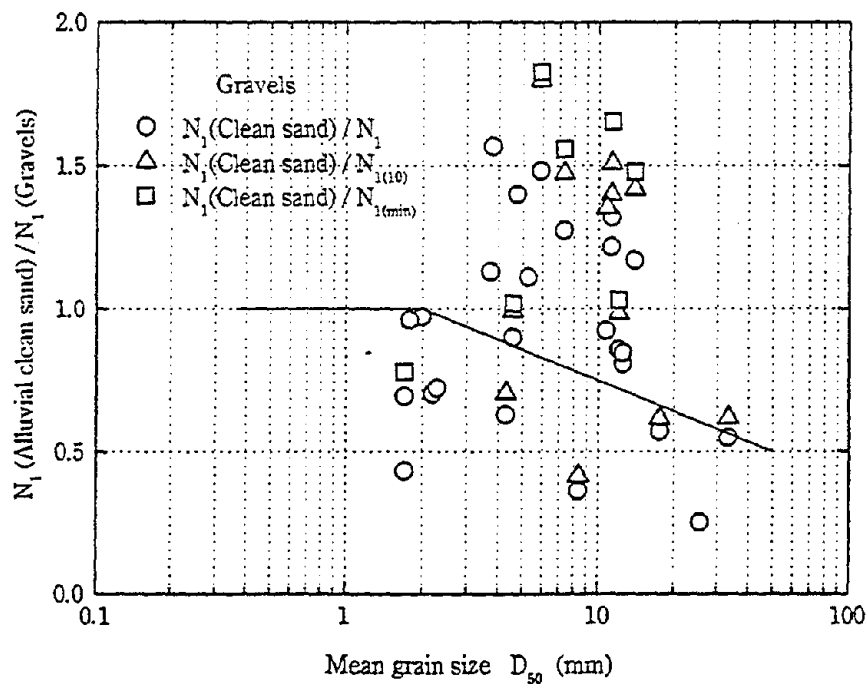


Figure 4 Relationship between the Ratio of Blow Count for Gravels to that for Clean Sand and the Mean Grain Size

Figure 4 shows the relationship between the ratio of blow count for gravels to that for clean sand with the same cyclic triaxial strength ratio and the mean grain size. Although considerable scattering exists, the ratio decreases as the mean grain size becomes large. The average relationship may be estimated as

$$N_1(\text{alluvial clean sand})/N_1(\text{gravels}) = 1 - 0.36 \log_{10}(D_{50}/2) \quad (D_{50} \geq 2) \quad (9)$$

in which the mean grain size D_{50} is measured in mm. Combining Eqs.(4) and (9), R_L for gravels can be estimated from blow counts of a standard penetration test.

Corrective Coefficient for Ground Motion Characteristics

When cyclic shear strength of a soil is compared with seismic shear stress induced by an irregular ground motion, it is necessary to convert the seismic shear stress time history to an equivalent cyclic shear stress time history. In this context, "equivalent" means that the both shear stress time histories yield the same degree of damage or degree of liquefaction. The modified accumulative damage concept developed by Tatsuoka et al.⁵⁾ was employed to estimate the corrective coefficient for ground motion characteristics c_w in Eq.(2).

The cyclic triaxial strength ratio curve was obtained by performing undrained cyclic triaxial tests for Toyoura sand over a wide density range. A total of 130 ground motion records from eight earthquakes were analyzed. The results on c_w obtained from records of each earthquake are finally averaged, and shown in Figure 5. As seen from this figure, the results for c_w seem to be divided into two groups. One is for the ground motions generated by interplate earthquakes (Type I), the other is for those generated by inland intraplate earthquakes (Type II). c_w may be expressed as

for Type I ground motions:

$$c_w = 1.0 \quad (10)$$

for Type II ground motions:

$$c_w = \begin{cases} 1.0 & (R_L \leq 0.1) \\ 3.3R_L + 0.67 & (0.1 < R_L \leq 0.4) \\ 2.0 & (0.4 < R_L) \end{cases} \quad (11)$$

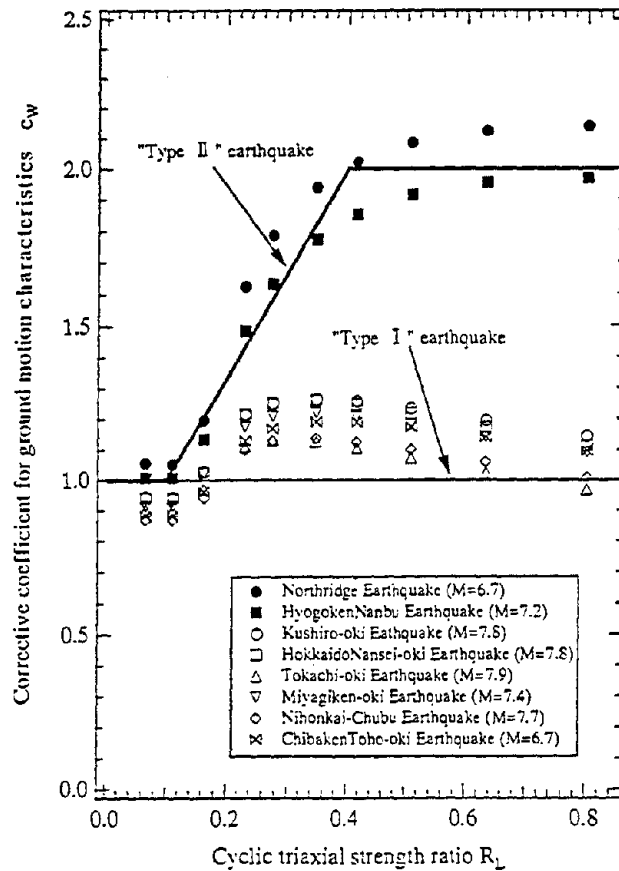
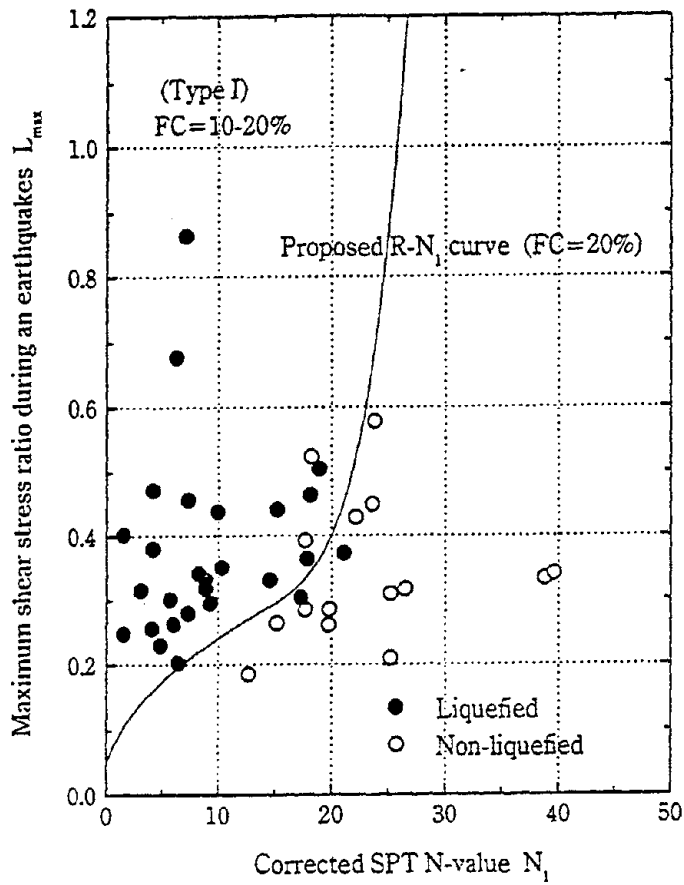


Figure 5 Corrective Coefficient for Ground Motion Characteristics c_w

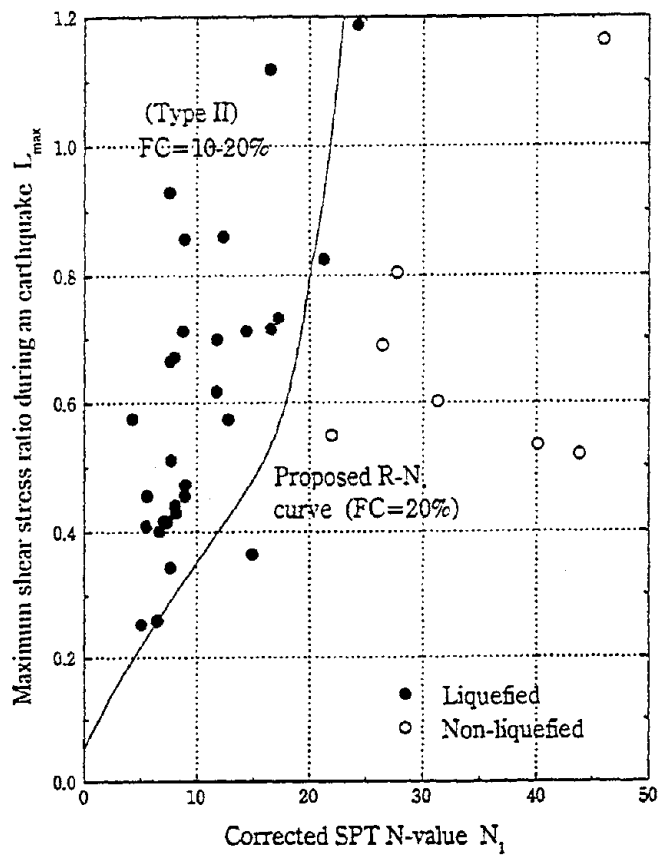
Calibration with Field Performance Data

The newly developed method for estimating the in situ liquefaction potential as presented in the above was examined by comparing with field performance data during past eight earthquakes⁴⁾. A total of 216 data include 145 of liquefied sites and 71 of non-liquefied sites. Judgement of liquefaction occurrence at a site was made primarily based on visual inspection of surface evidences such as sand boils, cracking or settlement.

Figure 6 shows an example of relationships between the corrected N-value N_1 and shear stress ratio during an earthquake L inferred from field performance data, where the dynamic shear strength ratio R estimated from the proposed method is superimposed. This figure indicates that the proposed dynamic shear strength ratio line classifies liquefied and non-liquefied data fairly well.



(a) $10\% \leq FC < 20\%$, Type I Ground Motion



(b) $10\% \leq FC < 20\%$, Type II Ground Motion

Figure 6 Comparison of Field Performance Data and the Proposed Method

SEISMIC DESIGN TREATMENT OF LIQUEFACTION FOR BRIDGE FOUNDATIONS

Soil Constants of Liquefiable Layer

The strength and the bearing capacity of a soil decreases when it liquefies. Based on this, for seismic design of highway bridges, soil constants of a sandy soil layer which is judged liable to liquefy are reduced according to the value of F_L , the liquefaction resistant ratio ³⁾. The reduced constants are calculated by multiplying the coefficient D_E in Table 1 to the soil constants estimated on an assumption that the soil layer does not liquefy ³⁾.

Table 1 Coefficient D_E to be Multiplied to Soil Constants

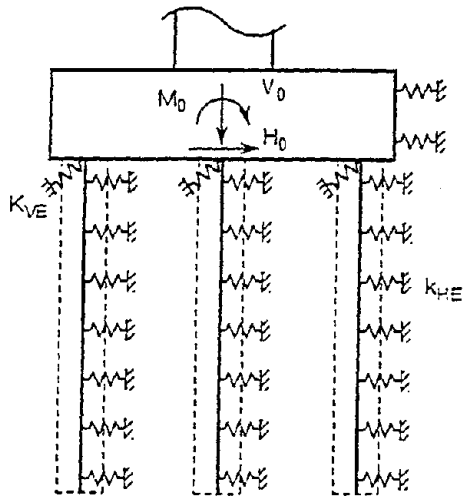
Range of F_L	Depth from the Present Ground Surface $x(m)$	Dynamic Shear Strength Ratio R	
		$R \leq 0.3$	$0.3 < R$
$F_L \leq 1/3$	$0 \leq x \leq 10$	0	1/6
	$10 < x \leq 20$	1/3	1/3
$1/3 < F_L \leq 2/3$	$0 \leq x \leq 10$	1/3	2/3
	$10 < x \leq 20$	2/3	2/3
$2/3 < F_L \leq 1$	$0 \leq x \leq 10$	2/3	1
	$10 < x \leq 20$	1	1

The coefficient D_E is based on the results of shaking table tests and analyses of bridge foundations damaged by earthquakes. The values of D_E are prescribed to be different for above and below the depth of 10m, because the ground vibration decreases as the depth increases and the cases in which soil layers totally liquefied below the depth of 10m are limited. The values of D_E are also different according to the dynamic shear strength ratio R of soil. This is because that the greater strength can be expected when R is large even if F_L is same.

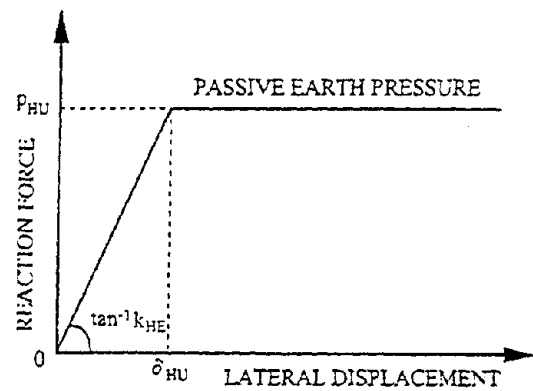
Seismic Design of Bridge Foundations against Liquefaction

Since a bridge foundation is built in the ground, it is more difficult to identify damage to it than to a bridge pier and it is also difficult to repair a foundation. For these reasons, a

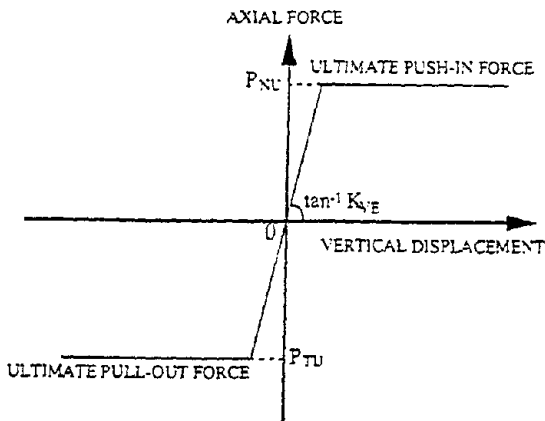
bridge foundation is to be designed so that it has greater dynamic strength than a bridge pier or that it has sufficient deformation capacity⁶⁾. When a sandy layer liquefies, the strength of foundation decreases with the decrease of strength and bearing capacity of the ground, it is not rational to ensure the strength of a foundation greater than that of a pier by excessively strengthening the foundation. For such a case, it may be rational to allow a foundation to go into a plastic zone whereby preventing to yield excessive damage to the foundation and absorbing earthquake motion energy at a foundation.



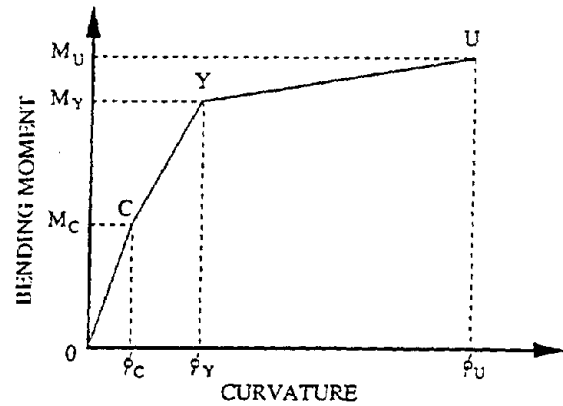
(a) Analytical Model



(b) Lateral Force vs. Lateral Displacement



(c) Vertical Force vs. Vertical Displacement



(d) Bending Moment vs. Curvature

Figure 7 Idealization of Pile Foundation for Analysis

For seismic design of highway bridges, the deformation capacity of a foundation is checked by confirming that the response ductility factor of a foundation is equal to or less than the allowable value⁶⁾, using the principle of conservation of energy by N. M. Newmark et al.⁷⁾. This principal assumes that the input energy of elasto-plastic response and elastic response is same when structure is subjected to an earthquake

motion. The allowable ductility factor for a pile foundation may be taken as 4 from model experiments ⁶⁾. To check the ductility of a bridge foundation, it is so idealized that a rigid footing is supported by piles that are supported by soils, considering nonlinear properties of pile bodies and the ground as shown in Figure 7 ⁸⁾.

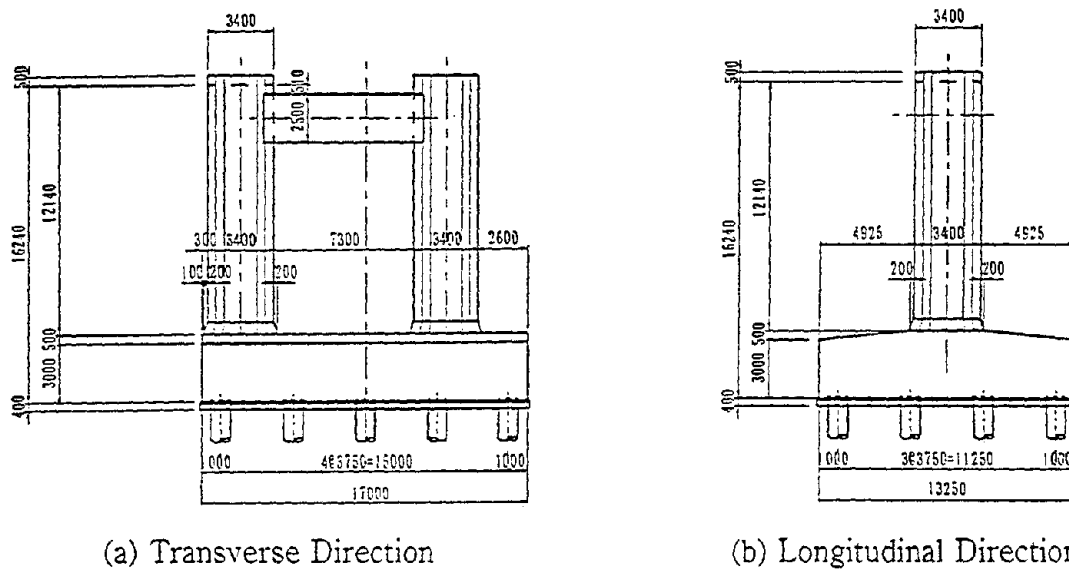


Figure 8 General View of the Analyzed Pier

An example of checking the ductility of a foundation is presented in Figure 8 through Figure 10. Figure 8 shows a general view of the pier analyzed. The superstructure for this pier is a 9-span continuous PC box girder. The girder is supported by movable bearings at this pier. Figure 9 shows a schematic view of the foundation and soil condition. The footing is supported by cast-in-place concrete piles 1.5m in diameter and 32.5 m long. The soil is alternation of sand and clay. A sandy soil layer beneath the footing is judged to liquefy, and soil constants of this layer are regarded to be 0 for seismic design. The relationship between lateral force and displacement for the foundation is presented in Figure 10. From this figure, the response ductility factor is calculated as 2.9, which means that this foundation is judged to have sufficient deformation capacity.

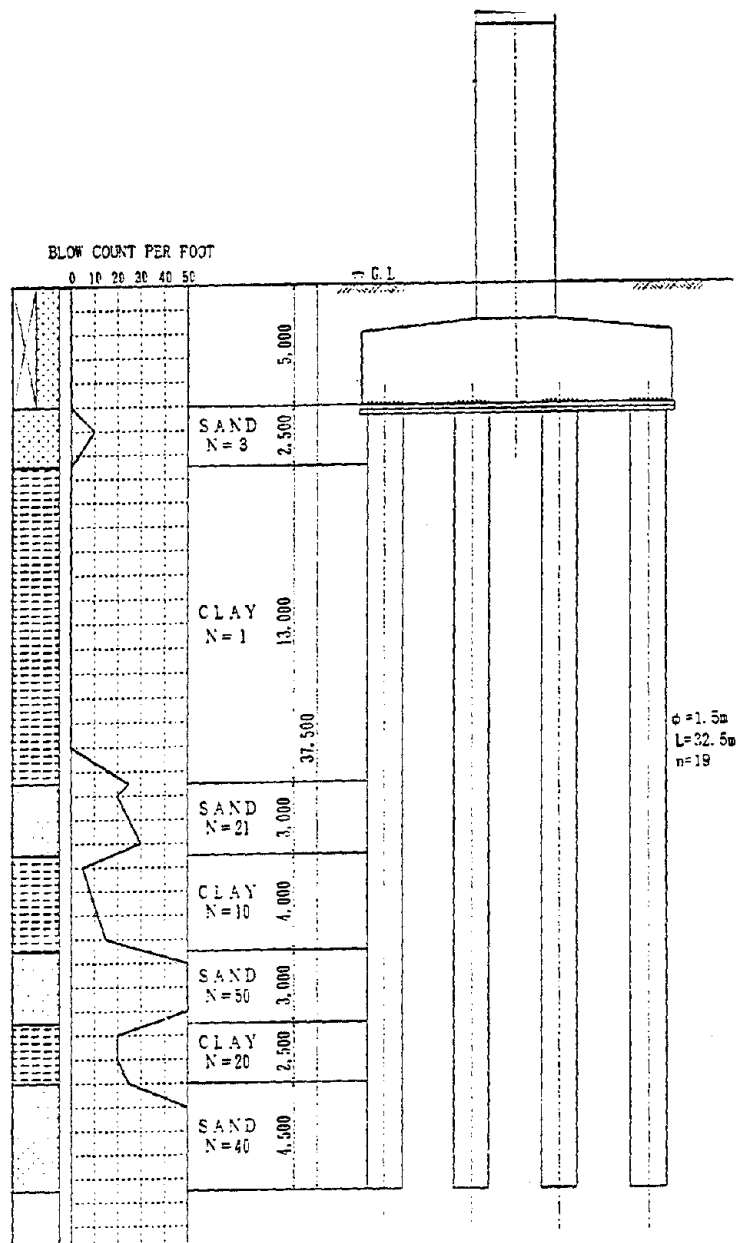


Figure 9 Schematic View of the Foundation

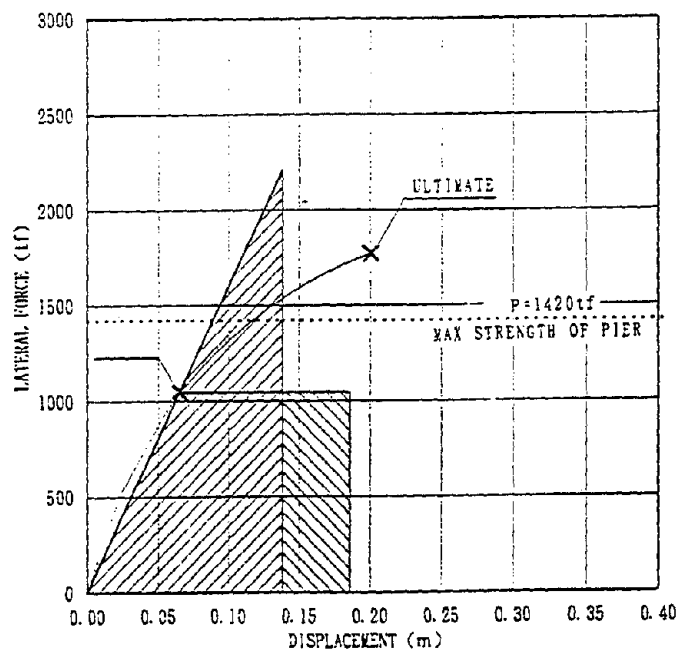


Figure 10 Relationship between Lateral Force and Displacement at Pile Top

INFLUENCE OF LIQUEFACTION-INDUCED GROUND FLOW ON HIGHWAY BRIDGES

Damage to Highway Bridges due to Liquefaction-Induced Ground Flow

No highway bridge suffered serious damage such as collapse of a superstructure directly due to the liquefaction-induced ground flow in the 1995 Hyogo-ken Nanbu Earthquake, however, the ground flow yielded large deformation of bridge foundations and related damage. As an example of damage to a highway bridge, the case of Shin-Shukugawa Bridge on Route 5, Bay Shore Line of the Hanshin Expressway is here presented⁹⁾.

The Shin-Shukugawa Bridge completed in 1993 is a 3-span cantilever box girder bridge which crosses a watercourse between reclaimed lands, i.e., Nishinomiya-hama and Minami Ashiya-hama. An overview of the damage to this bridge is shown in Figure 11. Since a toll gate is located on the P-134 pier on Minami Ashiya-hama, the width of the bridge varies from 28m to 69m. The bridge is supported by movable supports at its both ends on reclaimed lands, and by fixed supports on intermediate piers.

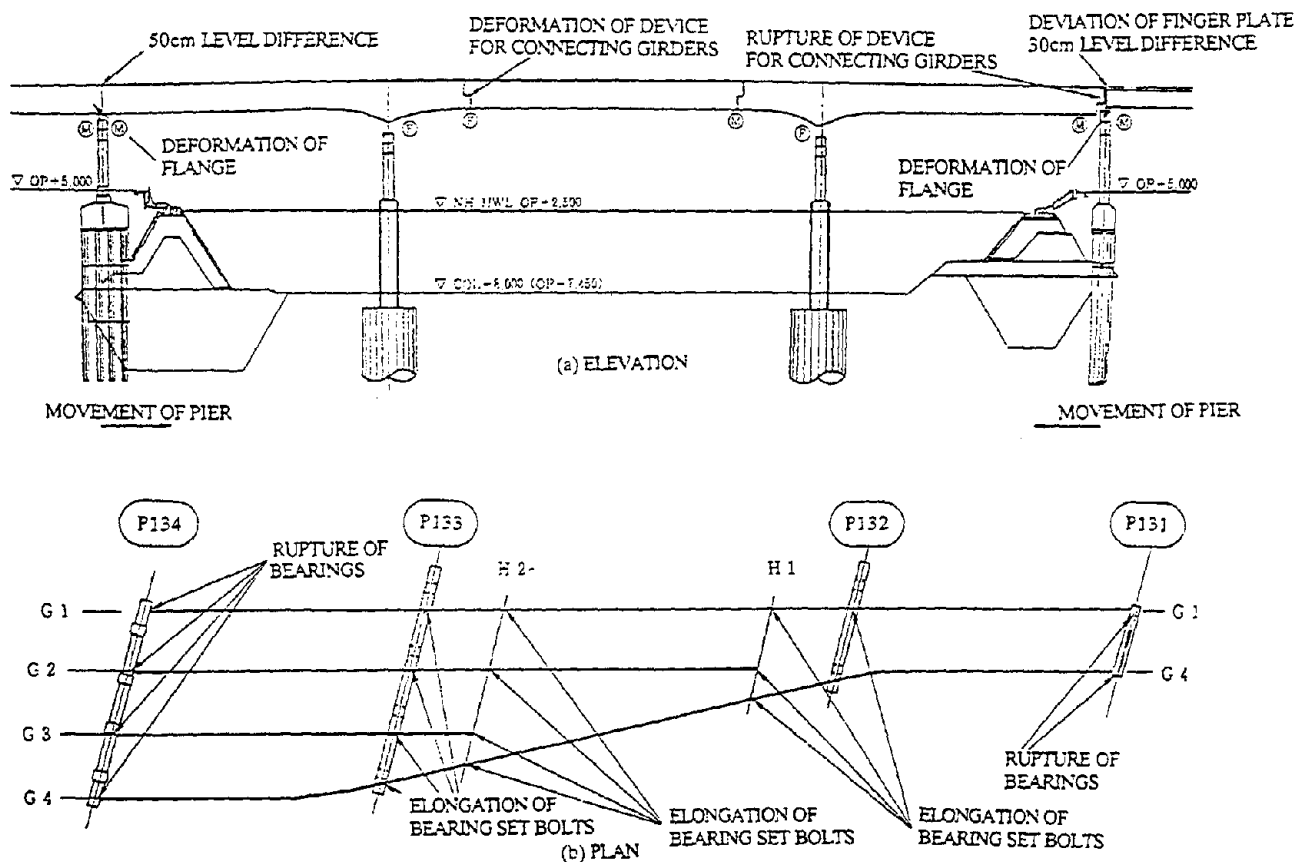


Figure 11 Overview of Damage to the Shin-Shukugawa Bridge

The P-131 pier on Nishinomiya-hama was a 2-column RC rigid frame pier with two caisson foundations, 6m in diameter. The P-134 pier on Minami Ashiya-hama was a 4-column steel rigid frame pier and was supported by cast-in-place concrete piles, 1.5m in diameter. The foundations were constructed in the reclaimed soil and supported by a diluvial sandy layer.

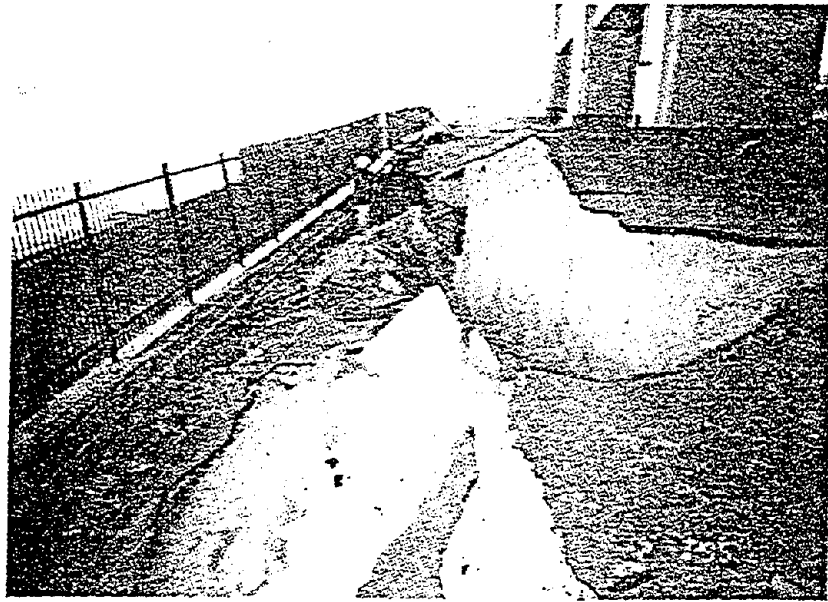


Photo 1 Ground Failure near the Shin-Shukugawa Bridge

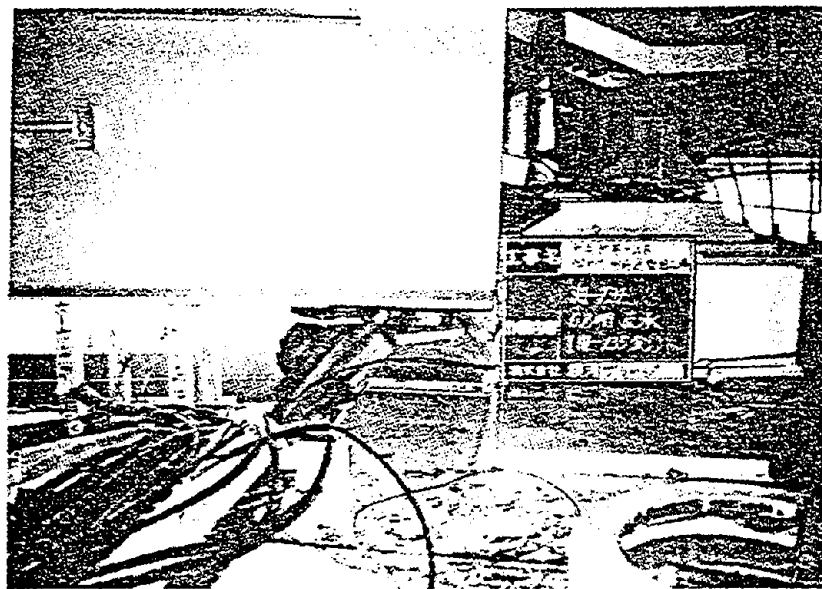


Photo 2 Damage to Bearing Support of the Shin-Shukugawa Bridge

Extensive liquefaction occurred around the bridge as shown in Photo 1, and both P-131 and P-134 piers moved toward the watercourse with the movement of sea walls. The damage was concentrated to the end piers on reclaimed lands. The piers were installed

with pivot roller supports, whose upper and lower shoes diverged as shown in Photo 2, which caused the difference in level between adjacent girders. A device for connecting girders on the P-131 pier was ruptured. A device for connecting girders was deformed at a cantilever hinge.

Ground Movement due to Ground Flow

The aerial photogrammetry was employed to estimate the ground movement vectors by comparing aerial photos taken before and after the earthquake¹⁰⁾. The result of aerial photogrammetry conducted by Hamada et al.¹¹⁾ was referred in this study. The main modifications from their study are as follows:

- 1) Hamada et al. used three survey points on Rokko Island as reference points for aerial photogrammetry, while six points established for surveying the bridge pier locations of the Route 5, Bay Shore Line of the Hanshin Expressway were used as reference points in this study.
- 2) Hamada et al. found displacement vectors of fixed objects on the ground surface such as manhole covers. In the present study, displacement vectors at intersection points of 20m interval grids were inferred from the movement of fixed objects. The residual horizontal displacements of bridge piers at the height of 1m above the ground level were also estimated in this study by another survey conducted after the earthquake.

The horizontal displacement vectors of the ground and bridge piers were found to include uniformly about 20cm component for the south-west direction. In addition to this, triangulation points near the Route 5 of the Hanshin Expressway shifted the same amount for the south-west direction. This displacement may be attributed to the base ground movement caused by fault movement or wide area ground movement. In the present study, this displacement is excluded from the result of aerial photogrammetry of the ground displacement and the residual displacement of bridge piers. The displacement vectors found may include a certain degree of error because of the errors associated with aerial survey and photographic interpretation. The accuracy of measurement is estimated as $\pm 30\text{cm}$ for the ground displacement and $\pm 10\text{cm}$ for residual displacement of bridge piers, respectively¹⁰⁾.

Figure 12 shows the vectors of the ground displacement and residual displacement of bridge piers near the north shore of Rokko Island. The sea walls moved toward the watercourse and the ground flow occurred, which caused the movement of the ground and bridge piers behind the walls. At the edge of the water, the ground moved more than 2m, and a bridge pier moved approximately 0.9m. The movements of the ground and bridge piers generally decrease as the distance from the watercourse increases.

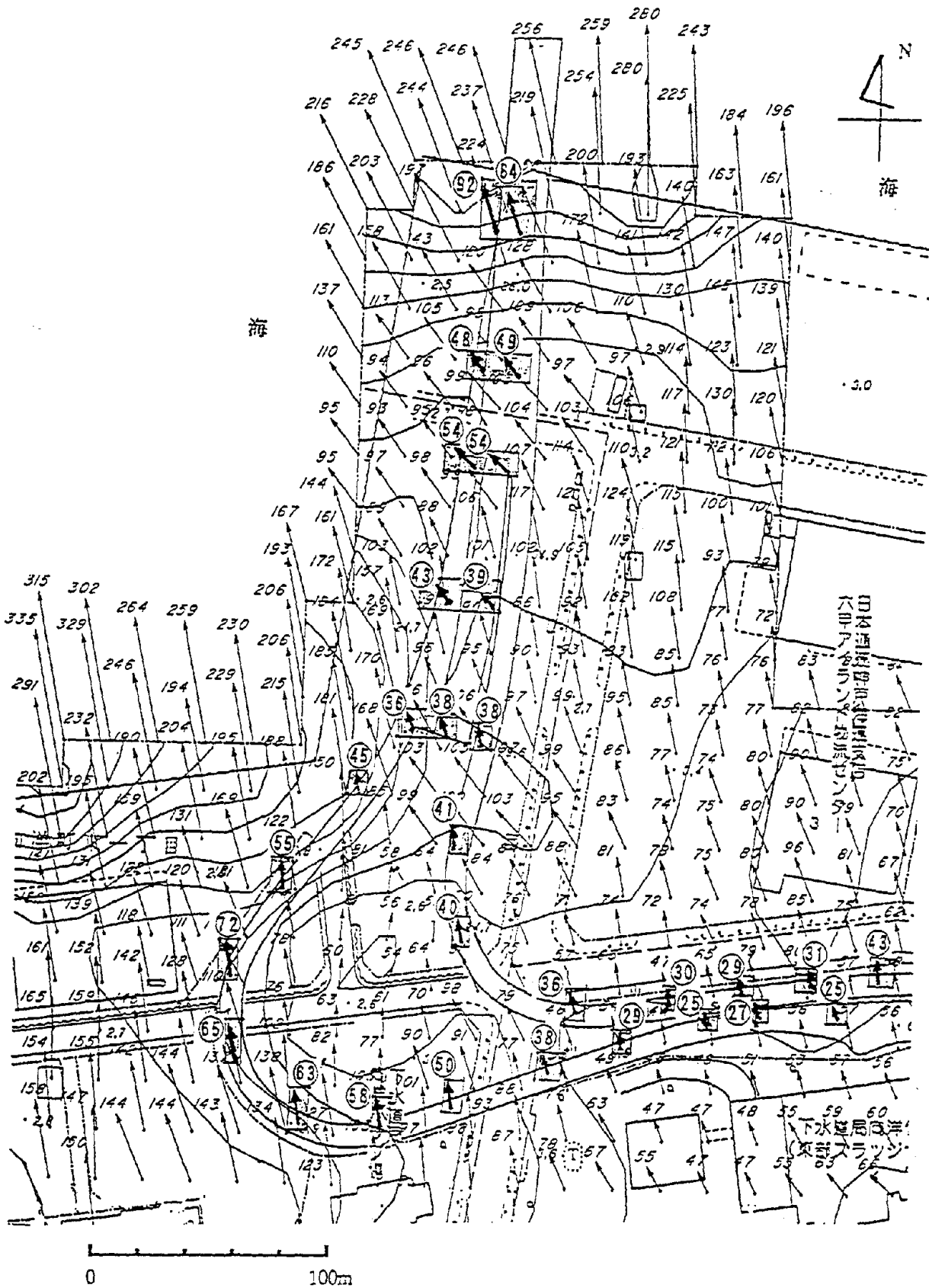


Figure 12 Horizontal Displacements of the Ground and Residual Displacements of Bridge Piers at Rokko Island

Figure 13 shows the relationship between the residual horizontal displacements of bridge piers and the horizontal displacements of the ground on the Route 5 of the Hanshin Expressway. Although the considerable scatters exist, the residual displacements of bridge piers tend to increase as the ground displacements increase, in general. The residual displacements of piers with rigid foundations, i.e., caisson and diaphragm wall foundations, are smaller than those with pile foundations for a certain amount of ground displacement.

The relationship between the residual horizontal displacements of bridge piers and the distance from the water's edge is shown in Figure 14. The residual displacement rapidly decreases with the increase of distance from the edge of the water. The range in which prominent residual displacement occurred is limited to approximately 100m from the water's edge.

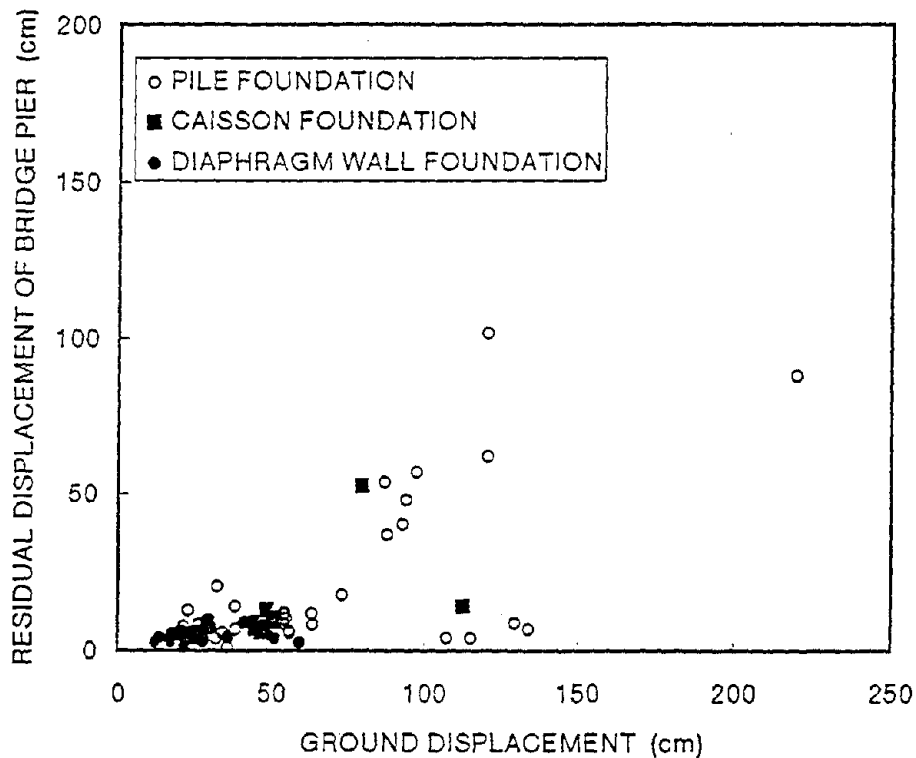


Figure 13 Relationship between Residual Horizontal Displacements of Bridge Piers and Horizontal Displacements of the Ground

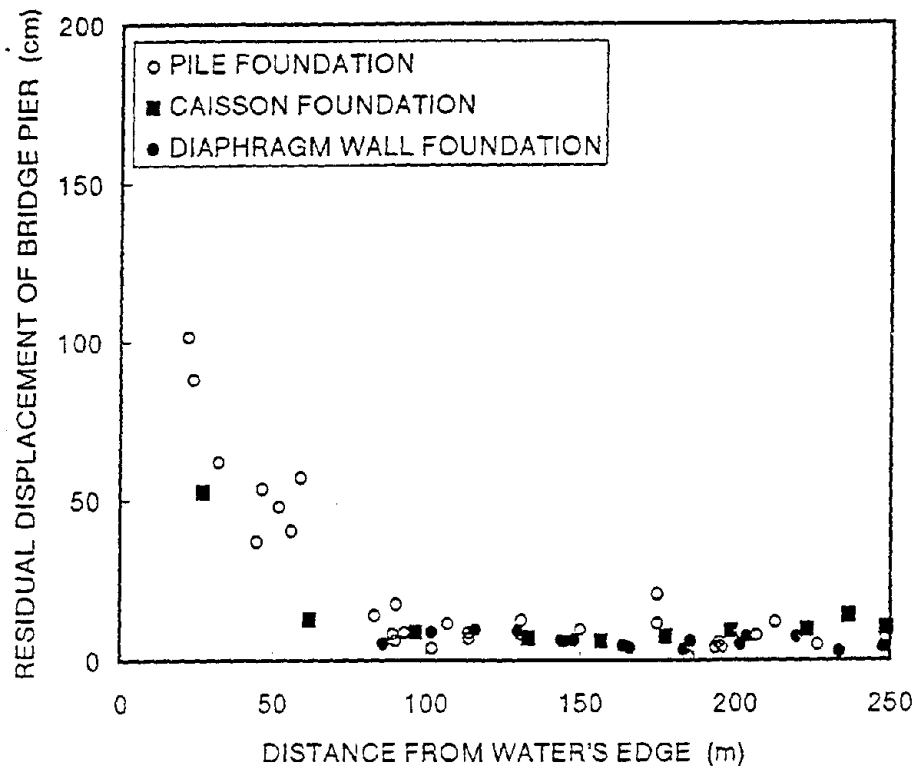


Figure 14 Relationship between Residual Horizontal Displacements of Bridge Piers and Distance from Water's Edge

Estimation of Ground Flow Force by Back Analysis

The force acted on a bridge foundation due to the liquefaction-induced ground flow was estimated by back analysis of bridges which suffered residual horizontal displacements. The result for P-216 pier, which is located at the north edge of Rokko Island, is here presented. The P-216 pier was a 2-story steel rigid frame pier and was supported by cast-in-place concrete piles, 1.5m in diameter. The bearings on this pier are fixed for the watercourse-side girder and movable for the inland-side girder. The soils are composed of sandy artificial fill, alluvial clay and alternation of diluvial sand and clay. The residual horizontal displacement of this pier was 0.9m, as shown in Figure 12. The ground water level of the site was 3.3m below the ground surface, and the liquefaction was judged to occur in the sandy artificial fill below the ground water level.

In the estimation of the force acted on a bridge foundation due to the ground flow, it was assumed that the layer near the ground surface which did not liquefy (non-liquefied layer) moved with the layer which liquefied (liquefied layer), and both layers caused force to a bridge foundation^{1,2)}. Since the non-liquefied layer was considered to move toward the structure and exert force on it, the force equivalent to the passive earth pressure was assumed to act on a bridge foundation in the non-liquefied layer. The

liquefied layer was considered to move fluidly around the structure, and the force corresponding to a certain portion of overburden pressure was assumed to act on a bridge foundation in the liquefied layer. This portion was estimated by back analysis of bridge piers with residual displacements.

An idealization of bridge foundation presented in Figure 7 was also employed in this analysis, except that the soil resistance were ignored for the non-liquefied and liquefied layers which were considered to move when the ground flow occurred. The width for which the ground flow force applied was set as the width of structure for a pier and footing, and the projected width between the end piles for pile bodies. Figure 15 shows an overview of the analyzed foundation and the applied force.

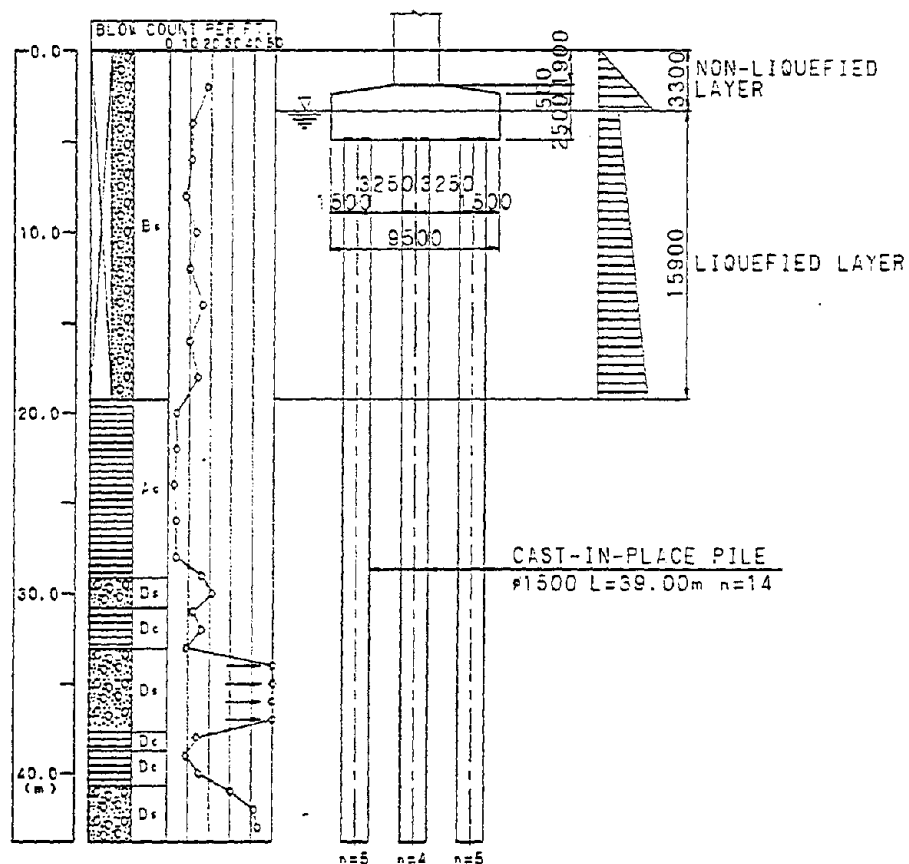


Figure 15 Overview of Analyzed Foundation and Applied Force

Since how much portion of the overburden pressure of the liquefied layer acted on a bridge foundation was unknown, varying this portion parametrically and calculating the relationship between lateral force and displacement, the amount of force that was consistent with the residual displacement was estimated. The result is shown in Figure 16. The total force which caused the residual displacement of 0.9m to the P-216 pier was estimated as 2,256tf; 578tf for non-liquefied layer and 1,678tf for liquefied layer.

The ratio of the force applied in the liquefied layer to the overburden pressure was calculated as 0.32 for this pier. Similar analysis was conducted for the four bridge piers on the Route 5 of the Hanshin Expressway, and the contribution factor of overburden pressure was estimated approximately as 0.3.

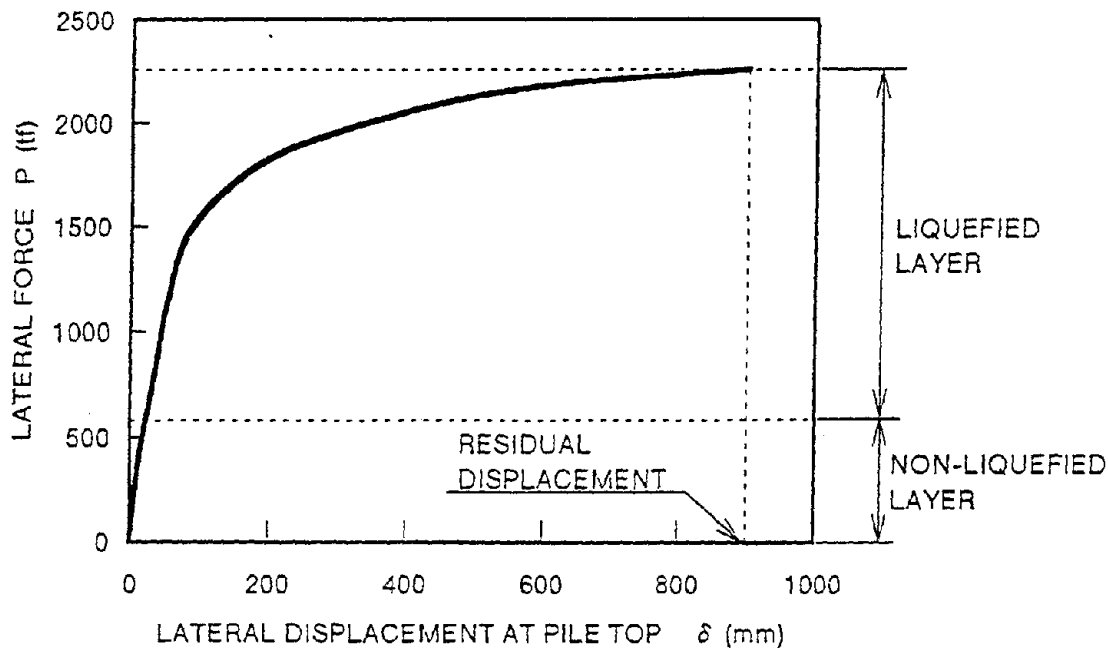


Figure 16 Relationship between Lateral Force and Displacement at Pile Top

SEISMIC DESIGN TREATMENT OF GROUND FLOW FOR BRIDGE FOUNDATIONS

When the liquefaction-induced ground flow that may affect bridge seismicity is likely to occur, this influence has become to be considered in the newly revised "Specifications for Highway Bridges" ⁶⁾. An outline of the seismic design treatment of liquefaction-induced ground flow is hereinafter introduced.

The case in which the ground flow that may affect bridge seismicity is likely to occur is generally that the ground is judged to be liquefiable and is exposed to biased earth pressure, e.g., the ground behind a sea wall. The effect of liquefaction-induced ground flow is considered as the static force acting on structure. This method premises that the surface soil is of the non-liquefiable and liquefiable layers, and the forces equivalent to the passive earth pressure and 30% of the overburden pressure are applied to the structure in the non-liquefiable layer and liquefiable layer, respectively. As seen from Figure 14, since the magnitude of ground flow decreases as the distance from the water's edge increases, modification by distance is incorporated in the estimation of the ground flow force. Modification by the degree of liquefaction is also established.

The seismic safety of a foundation is checked by confirming the displacement at the top of foundation caused by ground flow does not exceed an allowable value, in which a foundation and the ground are idealized as shown in Figure 7. The allowable displacement of foundation may be taken as two times the yield displacement of foundation. In this process, the inertia force of structure is not necessary to be considered simultaneously, because the liquefaction-induced ground flow may take place after the principal ground motion ends.

CONCLUSIONS

The following conclusions may be deduced from the present study.

- 1) A simple procedure to assess liquefaction potential of soils has been developed, in which the effects of soil gradation and ground motion irregularity are incorporated. This procedure is applicable up to gravelly soils.
- 2) A seismic design procedure of bridge foundations is demonstrated in which the effect of soil liquefaction is taken into account by reducing the soil constants and the deformation capacity of a foundation is checked by the principle of conservation of energy.
- 3) A simple design treatment of liquefaction-induced ground flow for bridge foundations is introduced, in which the ground flow force may be estimated as the sum of the passive earth pressure of the non-liquefied layer and 30% of the overburden pressure of the liquefied layer.

REFERENCES

- 1) Japanese Geotechnical Society: Special Issue on Geotechnical Aspects of the January 17 1995 Hyogoken-Nambu Earthquake, 1996
- 2) Japan Society of Civil Engineers: The 1995 Hyogoken-Nambu Earthquake - Investigation into Damage to Civil Engineering Structures -, 1996
- 3) Japan Road Association: Specifications for Highway Bridges, Part V Seismic Design, 1990
- 4) Matsuo, O. et al.: Revised Liquefaction Potential Procedure and Seismic Design Treatment of Liquefaction for Bridge Foundations, Proc. of Twelfth U.S.-Japan

Bridge Engineering Workshop, U.S.–Japan Panel on Wind and Seismic Effects, UJNR, 1996

- 5) Tatsuoka, F., Maeda, S., Ochi, K. and Fujii, S.: Prediction of Cyclic Undrained Strength of Sand Subjected to Irregular Loading, *Soils and Foundations*, Vol.26,^f No.2, 1986
- 6) Japan Road Association: Specifications for Highway Bridges, Part V Seismic Design, 1996 (in Japanese)
- 7) Veletsos, A. S. and Newmark, N. M.: Effect of Inelastic Behavior on the Response of Simple Systems to Earthquake Motion, *Proc. of Second World Conference on Earthquake Engineering*, 1960
- 8) Japan Road Association: Reference for Applying the Guide Specifications for Reconstruction and Repair of Highway Bridges which Suffered Damage due to the Hyogo–ken Nanbu Earthquake of 1995, 1995 (in Japanese)
- 9) Otsuka, H. et al.: Report on the Disaster Caused by the 1995 Hyogoken Nanbu Earthquake, Chapter 5, Damage to Highway Bridges, Report of PWRI, No.196, 1996
- 10) Committee for Investigation on the Damage of Highway Bridges by the Hyogo–ken Nanbu Earthquake, 1995: Report on the Damage of Highway Bridges by the Hyogo–ken Nanbu Earthquake, 1995 (in Japanese)
- 11) Hamada, M., Isoyama, R. and Wakamatsu, K.: The 1995 Hyogoken–Nanbu (Kobe) Earthquake, Liquefaction, Ground Displacement and Soil condition in Hanshin Area, Association for Development of Earthquake Prediction, 1995
- 12) Tamura, K., Hamada, T. and Azuma, T.: Seismic Design Treatment of Liquefaction –Induced Ground Flow, *Proc. of Third U.S.–Japan Workshop on Seismic Retrofit of Bridges*, U.S.–Japan Panel on Wind and Seismic Effects, UJNR, 1996

PERSONAL CAREER

NAME : Koichi Yokoyama

POSITION : Director
Earthquake Disaster Prevention Research Center
Public Works Research Institute
Ministry of Construction

ADDRESS : 1, Asahi, Tsukuba-shi
Ibaraki-ken
305 Japan
Tel. 0298-64-2829
Fax. 0298-64-0598



DATE OF BIRTH : July 8, 1945

EDUCATION : Bachelor of Engineering (1969, Tokyo Institute of Technology)
Master of Engineering (1971, Tokyo Institute of Technology)
Doctor of Engineering (1992, Tokyo Institute of Technology)

MAJOR SUBJECT : Structural Engineering, Wind Engineering, Wind resistant design of bridges

MAJOR AREAS OF EXPERIENCE :

1971-1979	Researcher, Structure Division Structure and Bridge Department, PWRI
1979-1980	Kyushu Regional Construction Bureau, M.O.C.
1980-1981	Technical Advisor, Prefectural Police Head-quarters, Fukuoka Prefecture
1982-1984	Colombo Plan Expert, Bridge Engineering Training Center in Burma
1984-1992	Head, Structure Division Structure and Bridge Department, PWRI
1992-1994	Director, First Research Department, Advanced Construction Technology Center
1994-1996	Director, Structure and Bridge Department, PWRI
1996	Director, Earthquake Disaster Prevention Research Center, PWRI

TRAVEL ABROAD : U.K., U.S.A., Burma, Canada, Sudan, Chile

MAJOR PUBLICATIONS :

- 1) "Aerodynamic Characteristics of Continuous Box-Girder Bridges relevant to their Vibration in Wind", 7th Int. Conf. on Wind Engineering, 1987
- 2) "Wind Resistant Design Manual for Highway Bridges", ASCE 7th Structures and Pacific Rim Engineering Congress, 1989
- 3) "Cooperative Research Program on Wind Tunnel Testing of Cable-Stayed Bridges" 8th Int. Conf. on Wind Engineering, 1991
- 4) "Future Projects for Highway Construction across Straits in Japan, and Technical Considerations, 3rd Symp. on Strait Crossings, 1994.

**EXPERIMENTAL STUDY OF THE EFFECTS OF
LIQUEFACTION-INDUCED GROUND FLOW
ON BRIDGE FOUNDATION**

by

**Keiichi TAMURA
and
Takuo AZUMA**

**Public Works Research Institute
Ministry of Construction, Japan**

**Thirteenth U.S.-Japan Bridge Engineering Workshop
U.S.-Japan Panel on Wind and Seismic Effects, UJNR
Tsukuba, Japan
October 2 and 3, 1997**

EXPERIMENTAL STUDY OF THE EFFECTS OF LIQUEFACTION-INDUCED GROUND FLOW ON BRIDGE FOUNDATION

Keiichi Tamura¹ and Takuo Azuma²

- 1 Head, Ground Vibration Division, Public Works Research Institute
Ministry of Construction, 1 Asahi, Tsukuba-shi, Ibaraki-ken 305 Japan
2 Research Engineer, ditto

ABSTRACT

The liquefaction-induced ground flow inflicted serious damage to various engineering structures including highway bridges in the Hyogo-ken Nanbu Earthquake of 1995. After this earthquake, the Specifications for Highway Bridges were revised, in which the effects of liquefaction-induced ground flow were incorporated. This was mainly based on the analytical study of damaged highway bridge foundations. From an experimental approach, shaking table tests are in progress at the Public Works Research Institute, Ministry of Construction. This paper presents the preliminary results of experiments on the liquefaction-induced ground flow. A quaywall and the ground behind it were modeled in a large container, and shaking table tests were carried out. Two different ground conditions were considered, and the effects of liquefaction-induced ground flow were studied.

INTRODUCTION

The Hyogo-ken Nanbu Earthquake, which occurred on January 17, 1995, caused extensive soil liquefaction over a wide area of offshore reclaimed lands and natural deposits [1, 2]. Besides that, near the water's edge, liquefaction induced ground flow with the movement of quaywalls and seawalls. Aerial photogrammetry revealed that the maximum residual displacement due to ground flow reached 3 to 4m [3, 4]. Liquefaction and its associated ground flow exerted serious influence on various engineering structures. Although highway bridges did not suffer fatal damage due to liquefaction, liquefaction-induced ground flow caused large deformation of bridge foundations. For example, a pier of the Shin-Shukugawa Bridge, which crosses a watercourse between reclaimed lands, was moved toward the watercourse by approximately 1m, which resulted in rupture of bearings on the pier [5]. This pier was supported by cast-in-place concrete piles, 1.5m in diameter. The piles were constructed in the reclaimed soil and supported by a diluvial sandy layer.

Considering large influence of the liquefaction-induced ground flow on the seismic safety of highway bridges, its seismic design treatment has been incorporated into the newly revised "Specifications for Highway Bridges" [6, 7], which was mainly based on the back analysis of bridges that suffered residual displacements by the Hyogo-ken Nanbu

Earthquake [8]. The effect of liquefaction-induced ground flow is idealized as the static force acting on structure in the Specifications. This premises that the surface soil is of the non-liquefiable and liquefiable layers, and the forces equivalent to the passive earth pressure and 30% of the overburden pressure are applied to the structure in the non-liquefiable layer and liquefiable layer, respectively, as shown in Figure 1. Since the magnitude of ground flow decreases as the distance from the water's edge increases, modification by distance is incorporated in the estimation of ground flow force. Modification by the degree of liquefaction is also introduced.

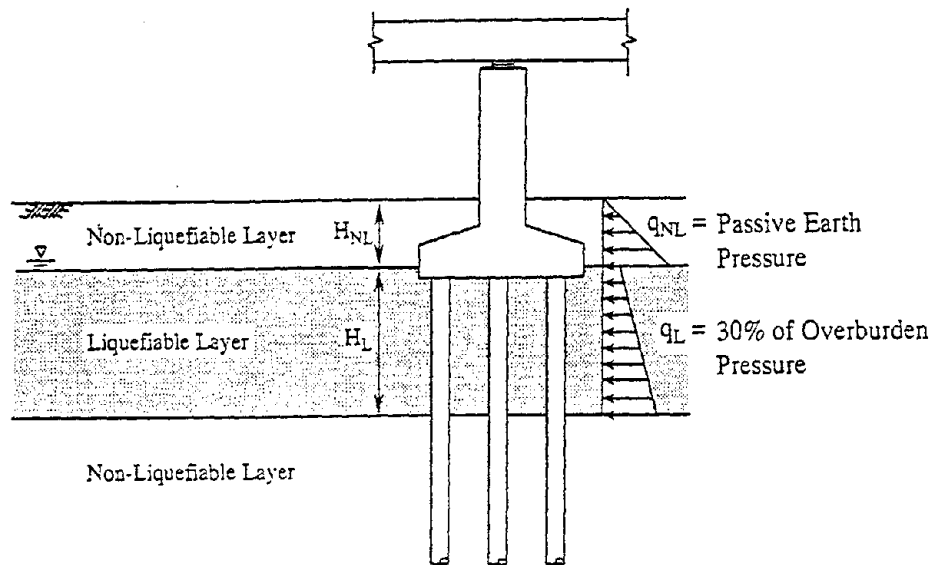


Figure 1 Idealization of Ground Flow Force for Seismic Design of Bridge Foundations

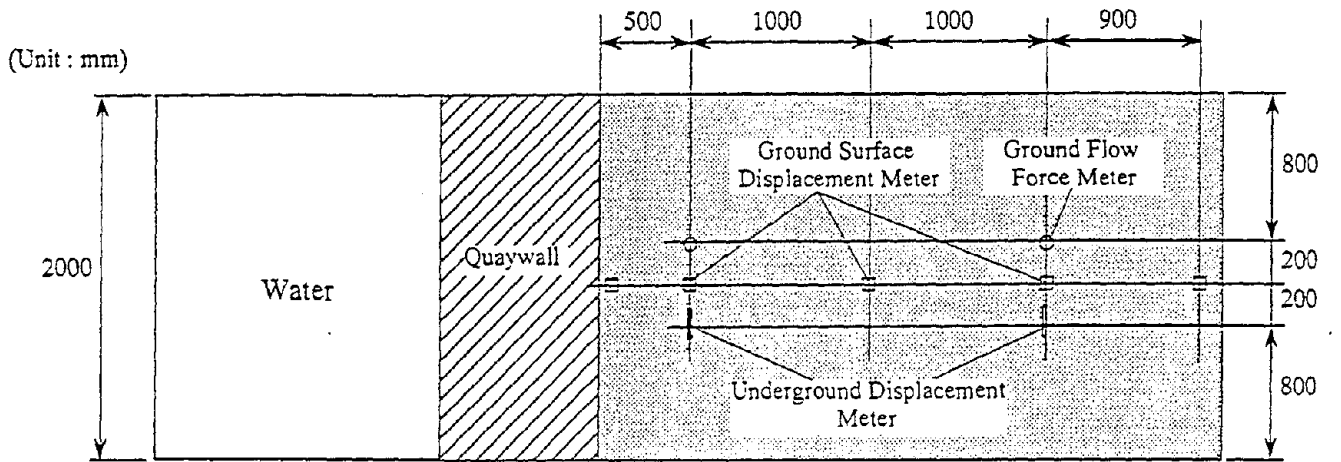
Presented in this paper are preliminary results of shaking table experiments on the liquefaction-induced ground flow [9]. Experiments were conducted for two different ground conditions and characteristics of ground displacement and ground flow force were analyzed.

METHODS OF EXPERIMENTS

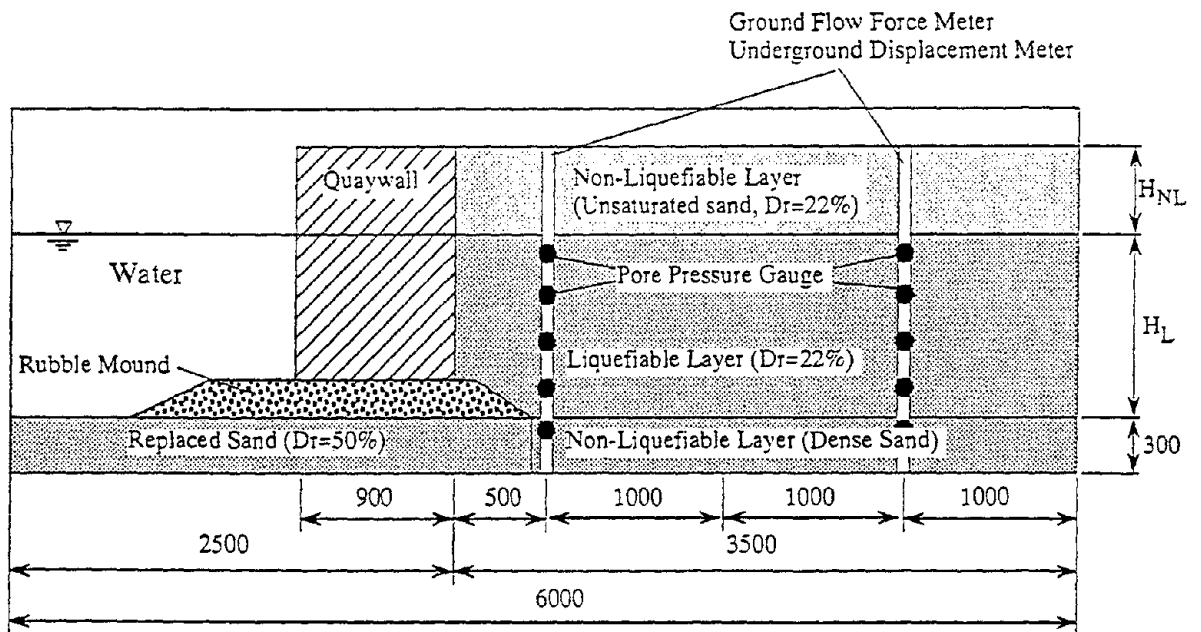
Experiment Models

A caisson type quaywall and the ground behind it were modeled in a large container (6m long, 2m wide and 2m deep), which was placed on a shaking table. An overall view of experiment model is given in Figure 2. The quaywall model was 0.9m wide, 2m long and 1.3m high. The ground model was composed of three layers, that is, base layer, liquefiable layer and non-liquefiable layer. The base layer was of dense sand. The upper two layers were of loose sand, and were made by putting clean sand into the water. The relative density of these layers was 22 %, and the other physical properties of the sand are listed in Table 1. The liquefiable and non-liquefiable layers were distinguished by adjusting the water level. Two cases of tests, i.e., Case 1 and Case 2, were carried out, in which the thicknesses of liquefiable layer H_L and non-liquefiable layer H_{NL} were

changed. H_L and H_{NL} were set as $H_L=100\text{cm}$, $H_{NL}=50\text{cm}$ in Case 1 and $H_L=50\text{cm}$, $H_{NL}=100\text{cm}$ in Case 2, respectively. The ground models had vertical lines on their sides so that ground deformation could be observed through the transparent glass of the container. These lines were made of colored sand. Photos 1 and 2 show the side views of experiment models.



(a) Plan



(b) Elevation

Figure 2 Overall View of Experiment Model

Table 1 Physical Properties of Sand

Specific Gravity of Soil Particle	2.633
Maximum Dry Density	1.350 gf/cm^3
Maximum Void Ratio	0.944
Minimum Void Ratio	0.593
60% Grain Size	0.195 mm
10% Grain Size	0.130 mm
Mean Grain Size	0.180 mm
Coefficient of Uniformity	1.500

Instrumentation

Acceleration, displacement, pore water pressure and ground flow force were measured in the experiments. An overall instrumentation layout was presented in Figure 2. Displacements on the ground surface were measured by wire-reel type displacement meters. Figure 3 shows the instruments to measure displacement in the ground and ground flow force. The displacement meter is of nine 2 mm thick stainless steel plates connected by hinges. These plates follow deformation of the ground. An accelerometer is attached to each plate, and the displacement is estimated from the change of gravity acceleration by incline of plate. The ground flow force meter consists of nine separate polyvinyl chloride pipes and a rigid shaft that goes through pipes. Each pipe is 20cm long. A load gauge is installed between pipe and shaft so that the force acted on each pipe can be measured.

Test Procedures

In the experiments, liquefaction and its induced ground flow were generated by shaking the container on a shaking table. Sinusoidal waves with frequency of 5Hz were inputted in both Case 1 and Case 2 tests. For each case, the test was first conducted with acceleration level of 0.15G on the shaking table, and the acceleration level was then increased to 0.5G, after confirming that the excess pore water pressure induced by the first test disappeared. The duration of excitation was 5 seconds for both tests with 0.15G and 0.5G.

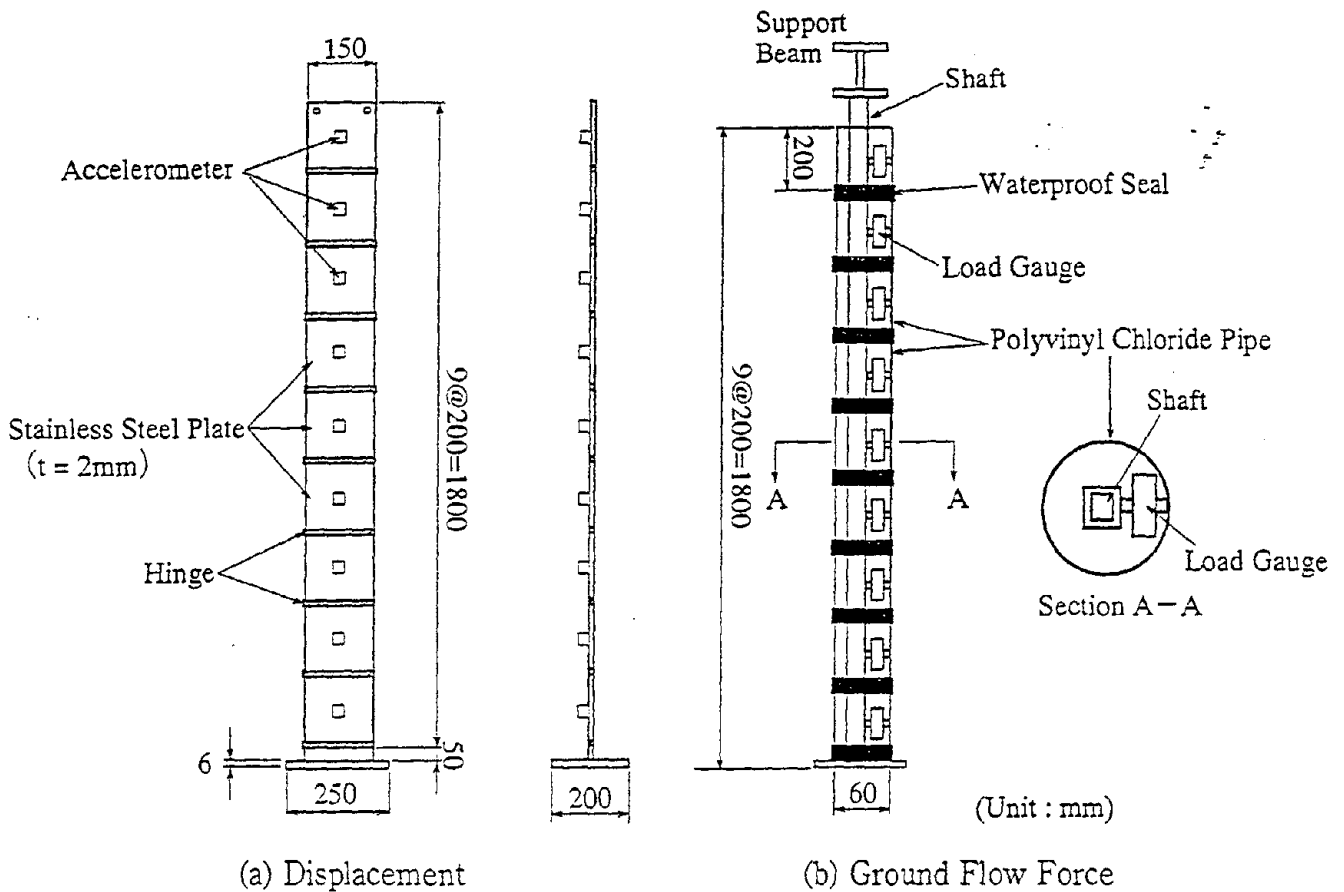
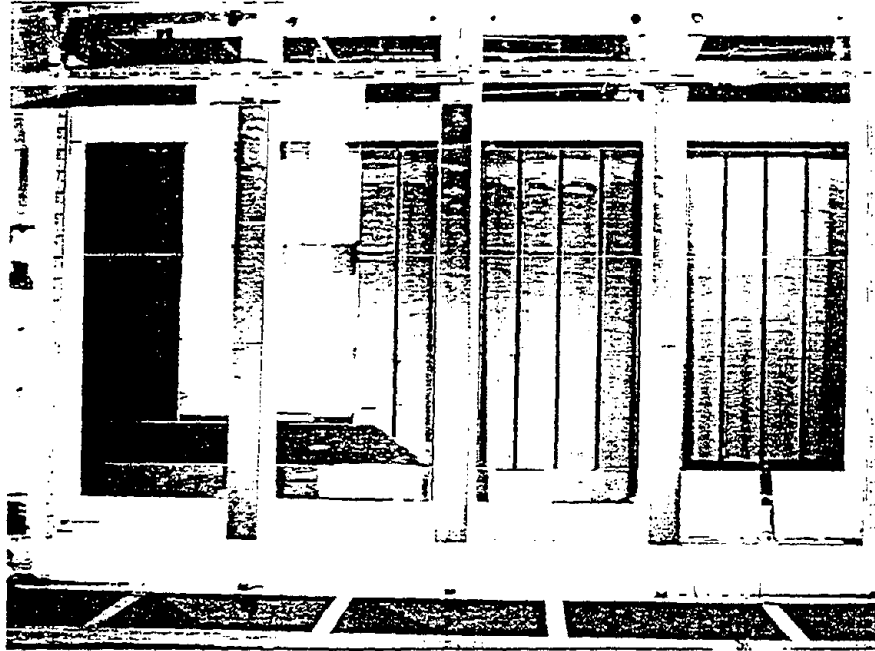


Figure 3 Instruments to Measure Displacement in the Ground and Ground Flow Force

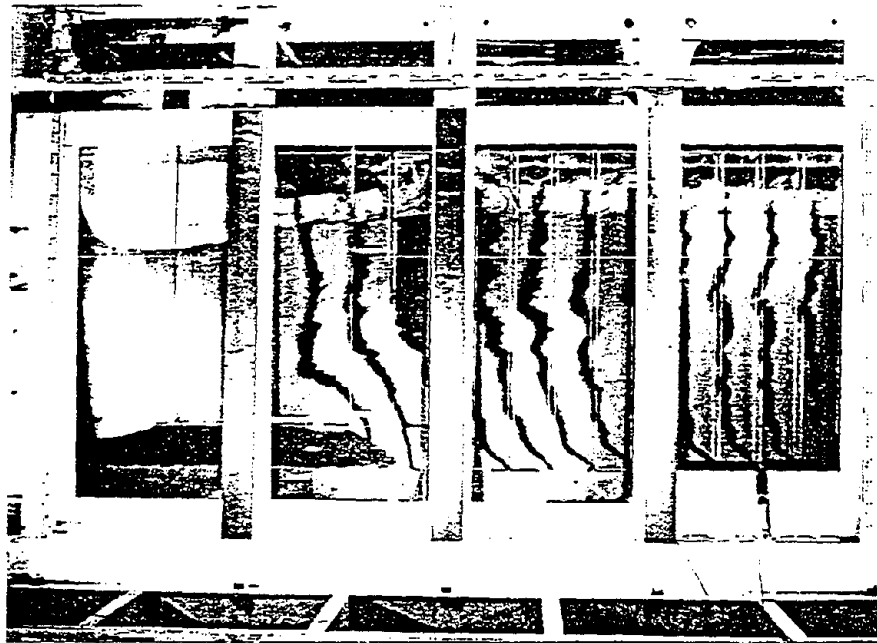
PRELIMINARY RESULTS OF EXPERIMENTS

Failure Modes

Photos 1 and 2 show the ground failure after 0.5G excitation for Case 1 and Case 2 tests, respectively. The quaywall was moved toward the water, and the liquefied layer with the overlain non-liquefied layer followed it. Deformation of vertical lines on the side of ground model indicates that lateral displacement of the ground increases from the bottom of the liquefied layer to the middle of it, and it is almost uniform for the upper part of the ground. Comparing the magnitude of ground deformation for Case 1 and Case 2, the former is larger than the latter. This may be attributed to the difference of the thickness of liquefied layer H_1 .



(a) Original Form

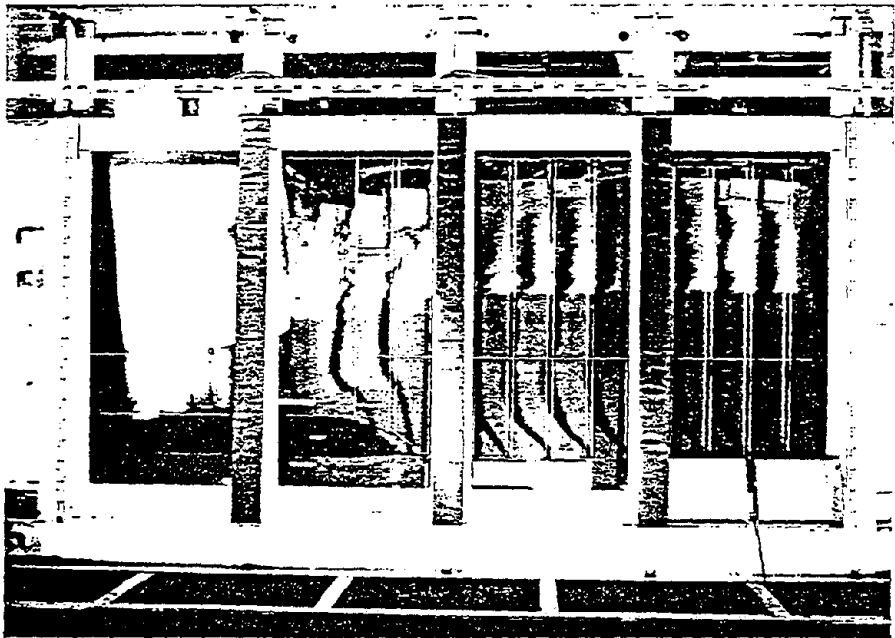


(b) After Excitation with 0.5G

Photo 1 Failure Mode of Case 1 Test ($H_c = 100\text{cm}$, $H_{NL} = 50\text{cm}$)



(a) Original Form

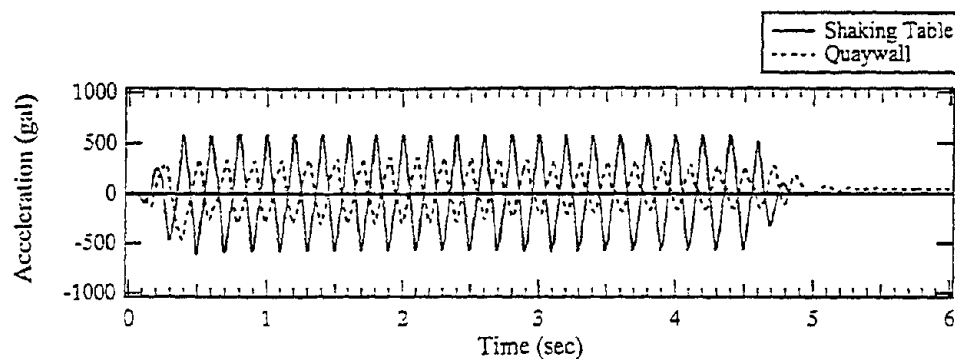


(b) After Excitation with 0.5G

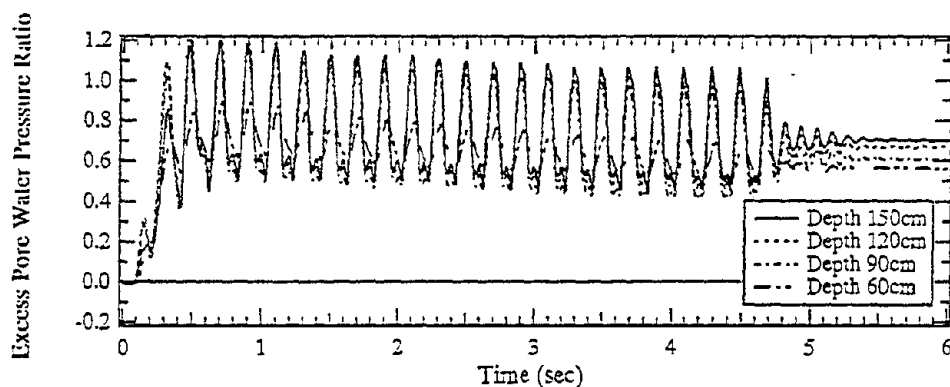
Photo 2 Failure Mode of Case 2 Test ($H_L = 50\text{cm}$, $H_{NL} = 100\text{cm}$)

Recorded Time Histories

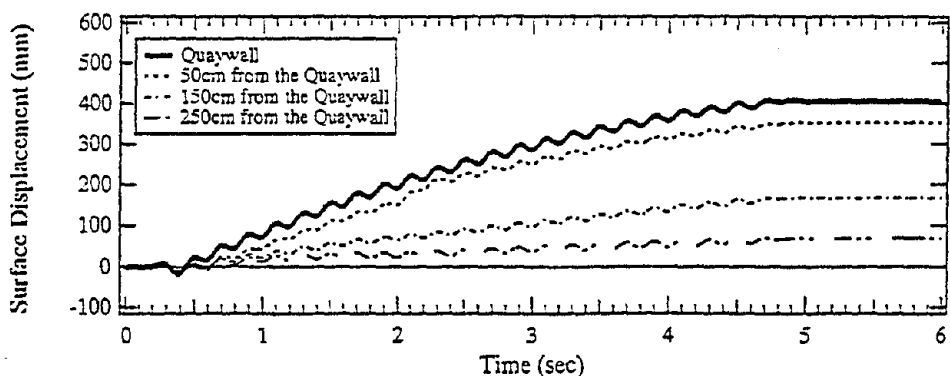
Time histories of acceleration, excess pore water pressure ratio which is the ratio of excess pore water pressure to effective overburden pressure, and ground surface displacement from Case 1 test with acceleration of 0.5G are shown in Figure 4: The accelerations were recorded on the shaking table and the quaywall. The excess pore water pressure ratios were measured at four depths, which were horizontally 150cm from the quaywall. The ground displacement begins to increase at about 0.5 seconds when the excess pore water pressure ratio becomes about 0.6 or greater. Displacement keeps to increase during excitation, and stops to increase when excitation ends. The residual displacement decreases as the distance from the quaywall increases.



(a) Acceleration



(b) Excess Pore Water Pressure Ratio



(c) Displacement

Figure 4 Time Histories of Case 1 Test with Acceleration of 0.5G

Ground Flow Displacement

Figure 5 illustrates the relationship between the residual displacement on the ground surface, which was caused by the ground flow, and the distance from the water's edge. The displacement at the left end indicates the residual displacement of quaywall. The ground flow displacement decreases as the distance from the water's edge increases. Comparing displacements for the same distance, it is larger as the thicknesses of liquefied layer H_L or level of input motion is larger.

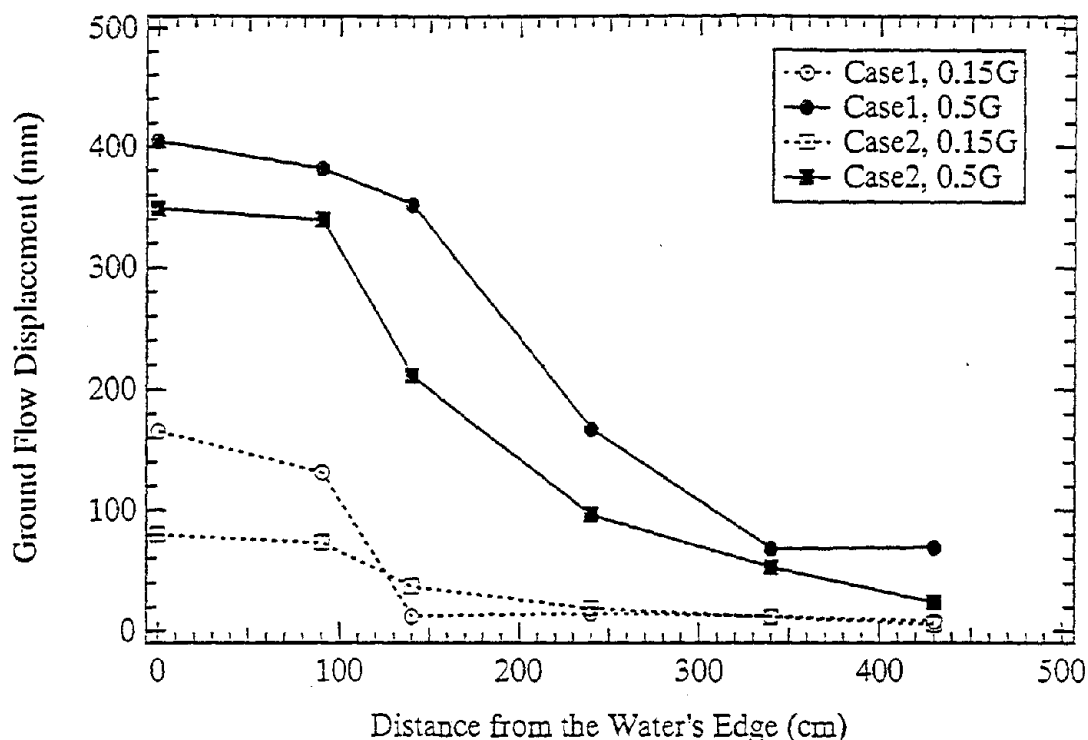


Figure 5 Relationship between the Ground Flow Displacement and the Distance from the Water's Edge

Based on Figure 5, Figure 6 shows the normalized relationship between the ground flow displacement and the distance from the water's edge, where the ground flow displacement and distance are normalized by the residual displacement of quaywall and the height of quaywall, respectively [10, 11]. The measured ground flow displacements at reclaimed lands in Kobe from the Hyogo-ken Nanbu Earthquake are also shown in this figure. They are also normalized by the same way. Although considerable scatter exists, the trends of ground flow displacement obtained from experiments agree with those estimated from the in situ measured data.

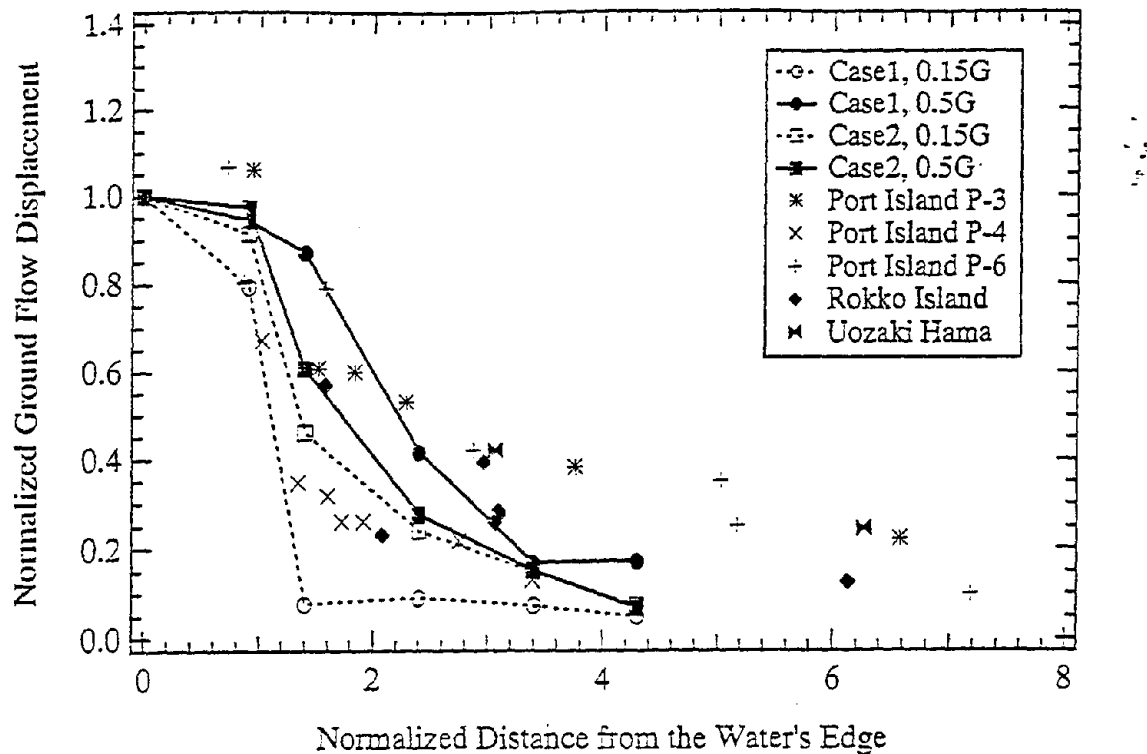
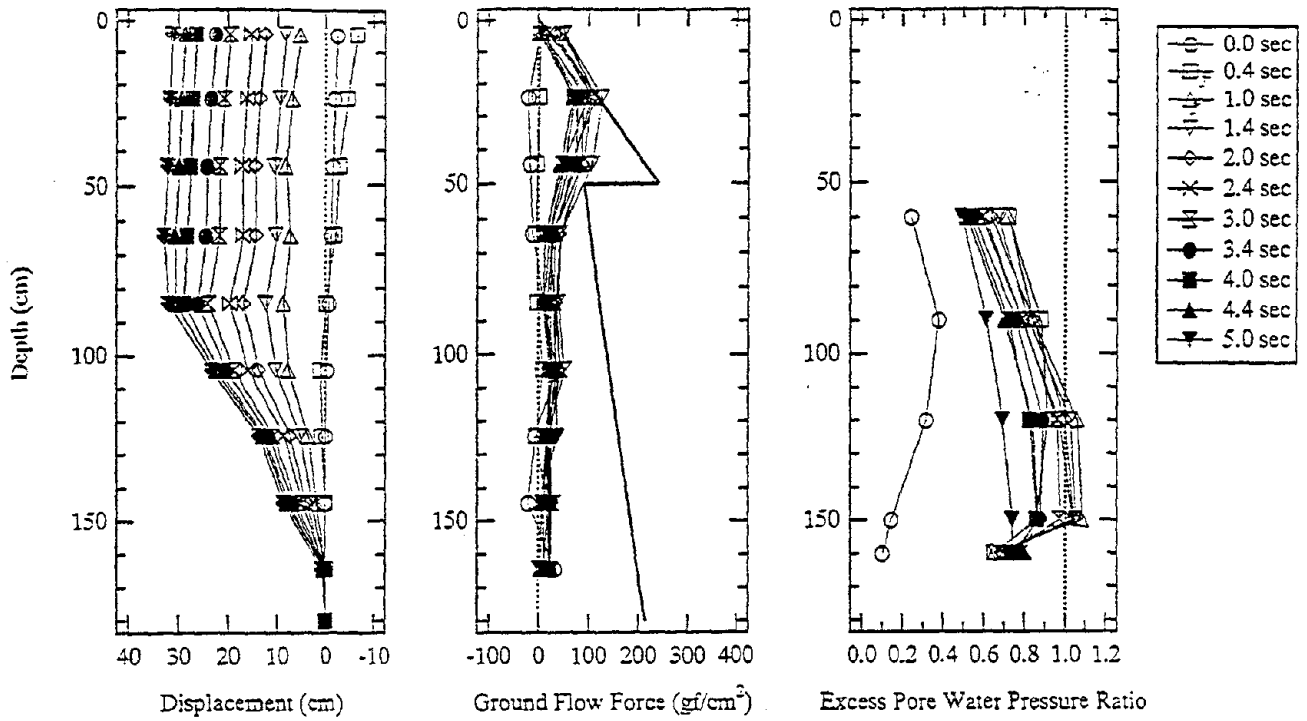


Figure 6 Normalized Relationship between the Ground Flow Displacement and the Distance from the Water's Edge

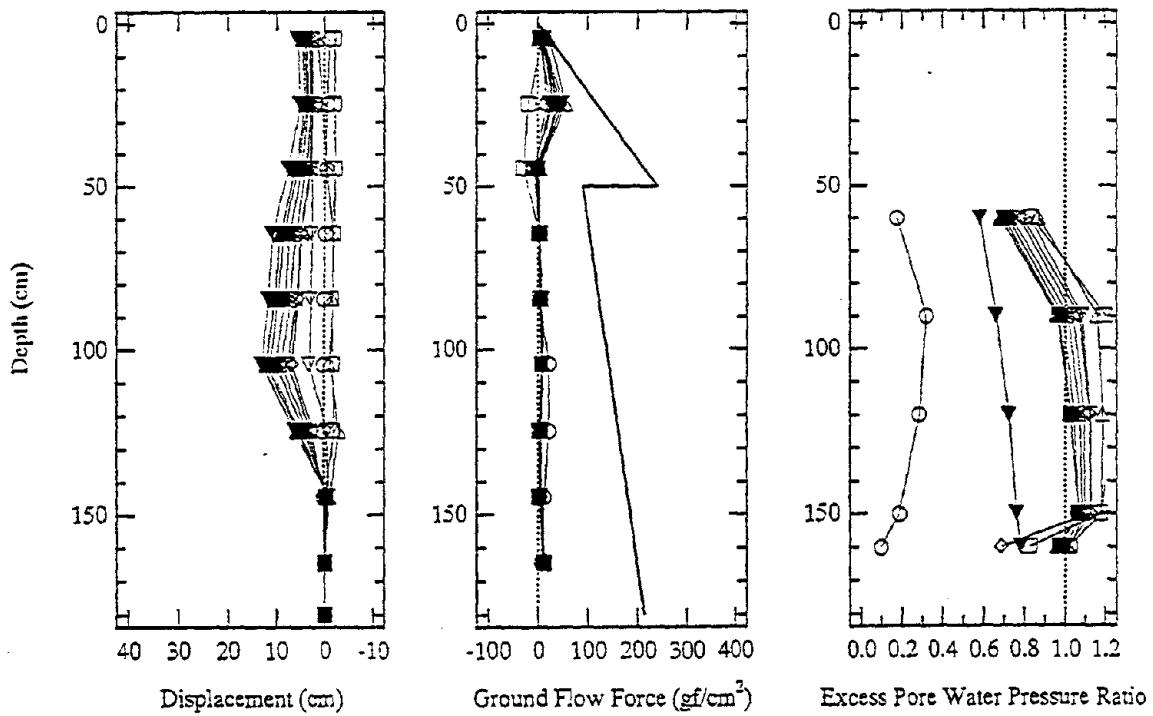
Ground Flow Displacement and Force in the Ground

Distributions of ground displacement, ground flow force and excess pore water pressure ratio in the ground are shown in Figures 7 and 8. These were recorded at 50cm and 250cm from the quaywall, and the results are presented for various times. Near the quaywall, the surface non-liquefied layer was moved toward the water with the underlain liquefied layer, on the other hand, the ground deformation far from the quaywall was mainly concentrated in the liquefied layer.

The ground flow force generated in the non-liquefied layer is larger than that in the liquefied layer. In the figures, the passive earth pressure and overburden pressure are also shown for the non-liquefied and liquefied layers, respectively. In case of 50cm from the quaywall, ground flow force in the non-liquefied layer almost reached the passive earth pressure, and it was smaller than the overburden pressure in the liquefied layer. In case of 250cm from the quaywall, however, the ground flow force was small and did not reach the passive earth pressure in the non-liquefied layer. It should be noted that the excess pore water pressure ratio for Case 2 did not exceed 1.0, which signifies that the complete liquefaction did not take place, nevertheless, large ground flow force was induced in the surface non-liquefied layer.

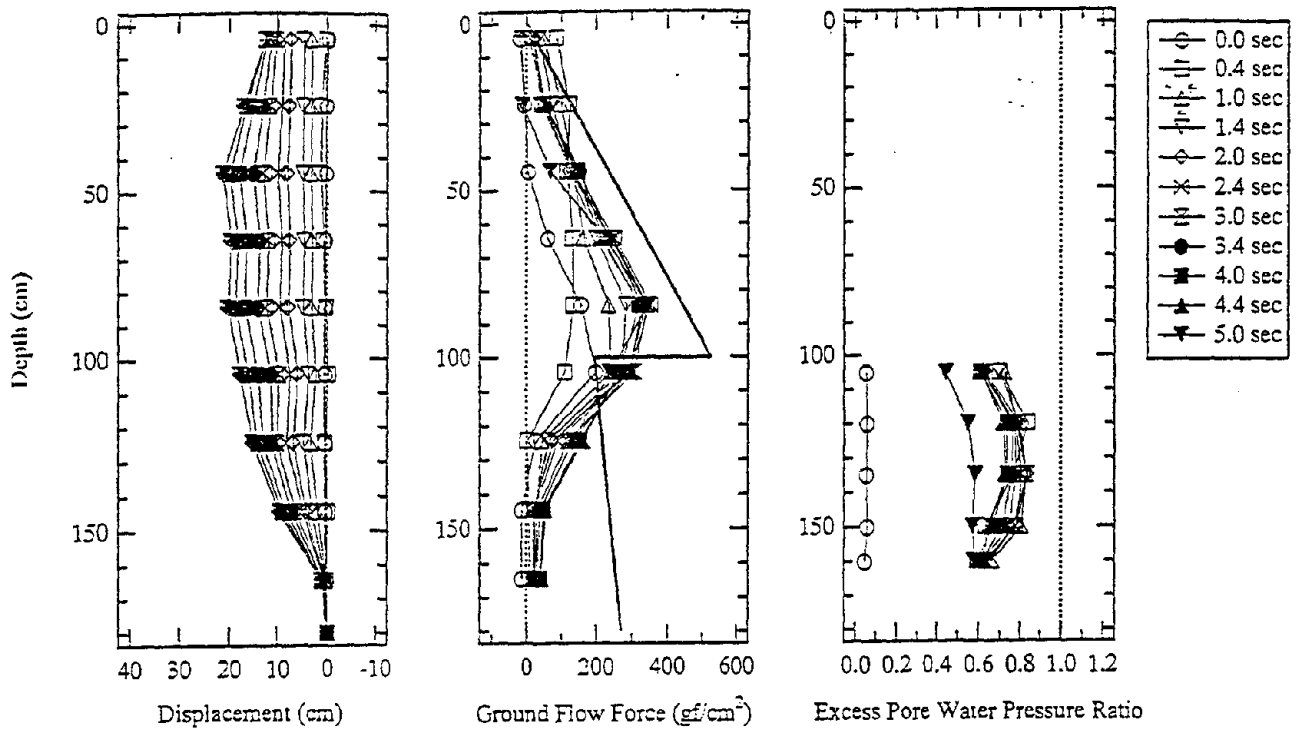


(a) 50cm from the Quaywall

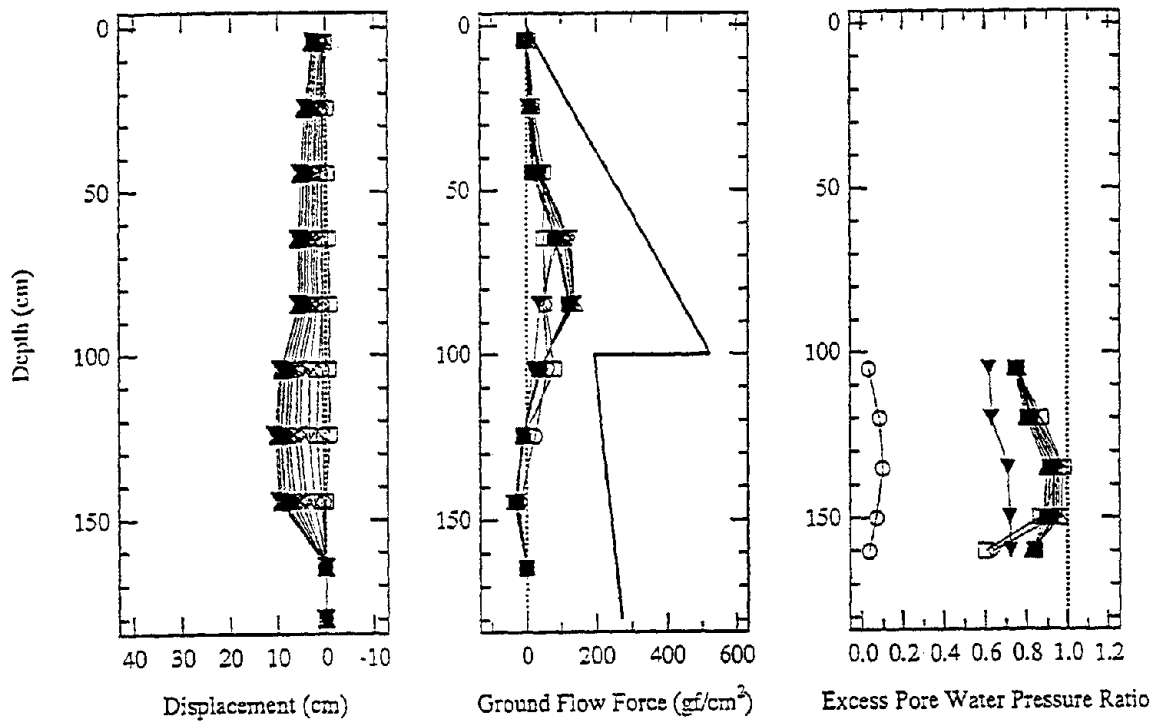


(b) 250cm from the Quaywall

Figure 7 Distribution of Displacement, Ground Flow Force and Excess Pore Water Pressure Ratio in the Ground of Case 1 Test ($H_L = 100cm$, $H_{NL} = 50cm$)



(a) 50cm from the Quaywall



(b) 250cm from the Quaywall

Figure 8 Distribution of Displacement, Ground Flow Force and Excess Pore Water Pressure Ratio in the Ground of Case 2 Test ($H_L = 50cm$, $H_{NL} = 100cm$)

CONCLUSIONS

The following conclusions may be deduced from the present study:

- 1) Ground flow was principally induced by the movement of liquefied layer with the overlain non-liquefied, following the movement of the quaywall. The normalized ground flow displacements obtained from experiments are consistent with those observed from the Hyogo-ken Nanbu Earthquake.
- 2) The ground flow force in the surface non-liquefied layer is almost equivalent with the passive earth pressure, and that in the liquefied layer is smaller than the overburden pressure.

REFERENCES

- 1) Japanese Geotechnical Society: Special Issue on Geotechnical Aspects of the January 17 1995 Hyogoken-Nambu Earthquake, 1996
- 2) Japan Society of Civil Engineers: The 1995 Hyogoken-Nambu Earthquake - Investigation into Damage to Civil Engineering Structures -, 1996
- 3) Hamada, M., Isoyama, R. and Wakamatsu, K.: The 1995 Hyogoken-Nambu (Kobe) Earthquake, Liquefaction, Ground Displacement and Soil condition in Hanshin Area, Association for Development of Earthquake Prediction, 1995
- 4) Committee for Investigation on the Damage of Highway Bridges by the Hyogo-ken Nanbu Earthquake, 1995: Report on the Damage of Highway Bridges by the Hyogo-ken Nanbu Earthquake, 1995 (in Japanese)
- 5) Otsuka, H. et al.: Report on the Disaster Caused by the 1995 Hyogoken Nanbu Earthquake, Chapter 5, Damage to Highway Bridges, Report of PWRI, No.196, 1996 (in Japanese)
- 6) Japan Road Association: Specifications for Highway Bridges, Part V Seismic Design, 1996 (in Japanese)
- 7) Kawashima, K. et al.: The 1996 Seismic Design Specifications of Highway Bridges, Proc. of 29th Joint Meeting, U.S.-Japan Panel on Wind and Seismic Effects, UJNR, 1997
- 8) Yokoyama, K., Tamura, K. and Matsuo O.: Design Method of Bridge Foundations against Soil Liquefaction and Liquefaction-Induced Ground Flow, Proc. of Second

Italy–Japan Workshop on Seismic Design and Retrofit of Bridges, 1997

- 9) Azuma, T. and Tamura, K.: Study on Ground Displacement and Force Acted on Bridge Foundations due to Liquefaction–Induced Ground Flow, Proc. of 24th JSCE Earthquake Engineering Symposium, 1997 (in Japanese)
- 10) Ishihara, K.: Soil Liquefaction and Effects of Lateral Flow on Foundations, 51st JSCE Annual Meeting, 1996 (in Japanese)
- 11) Inatomi, T. et al.: Mechanism of Damage to Port Facilities during 1995 Hyogo–ken Nanbu Earthquake, Technical Note of Port and Harbour Research Institute, No.813, 1995 (in Japanese)

PERSONAL CAREER

NAME: Keiichi TAMURA

POSITION: Head
Ground Vibration Division
Earthquake Disaster Prevention Research Center
Public Works Research Institute
Ministry of Construction

ADDRESS: 1 Asahi, Tsukuba-shi, Ibaraki-ken 305 Japan
Phone 0298-64-2926, Fax 0298-64-0598
E-mail tamura@pwri.go.jp



DATE OF BIRTH: December 12, 1956

EDUCATION: Bachelor of Engineering, University of Tokyo, 1980
Master of Engineering, University of Tokyo, 1982
Doctor of Engineering, University of Tokyo, 1992

MAJOR SUBJECT: Earthquake Engineering

MAJOR AREAS OF EXPERIENCE:

1982-1992 Research Engineer & Senior Research Engineer, Ground Vibration Division
Public Works Research Institute, Ministry of Construction

1989-1990 Visiting Scholar, Department of Civil Engineering, Stanford University

1993-1994 Assistant Director, Road Administration Division
Road Bureau, Ministry of Construction

1994-1995 Project Director, Stockpile Management Department
Japan National Oil Corporation

1995- Head, Ground Vibration Division
Public Works Research Institute, Ministry of Construction

TRAVEL ABROAD: Australia, Italy, U.S.A.

MAJOR PUBLICATIONS:

"Analysis on Phase Velocity of Ground Motion with Use of Array Records", Ninth World Conference on Earthquake Engineering, Tokyo-Kyoto, Japan, 1988

"Random Field Models of Spatially Varying Ground Motions", The John A. Blume Earthquake Engineering Center Report, No.92, Stanford University, 1990

"Spatially Varying Ground Motion Models and Their Application to the Estimation of Differential Ground Motion", Proc. of Japan Society of Civil Engineers, No.437, 1991

"Differential Ground Motion Estimation Using a Time-Space Stochastic Process Model", Proc. of Japan Society of Civil Engineers, No.441, 1992

"Effects of Geological Irregularities on Ground Motion Characteristics", Tenth World Conference on Earthquake Engineering, Madrid, Spain, 1992

"Ground Motion Characteristics of the Kobe Earthquake and Seismic Design Force for Highway Bridges", Second National Seismic Conference on Bridges and Highways, Sacramento, CA, U.S.A., 1997

III. SOCIO-ECONOMIC IMPACTS OF SEISMIC DAMAGE TO LIFELINE FACILITIES

“Highway System Performance Measures and Economic Impact”
S. Chang, N. Nojima

“System to Assess Socio-Economic Effect of Earthquake Disaster”
T. Nozaki, H. Sugita

“Influence of the Restoration of Hanshin Expressway Kobe Route
from the Earthquake upon the Surrounding Area”
N. Hamada, T. Yonekura, K. Yamamura

”Reliability and Restoration of Water Supply Systems for
Fire Suppression and Drinking Following Earthquakes”
D. Ballantyne

“Integrated Evaluation of Risks and Vulnerabilities for the Water System
at Portland, Oregon, Including Natural and Human Caused Hazards”
W. Elliott



HIGHWAY SYSTEM PERFORMANCE MEASURES AND ECONOMIC IMPACT

Stephanie E. Chang⁽¹⁾ and Nobuoto Nojima⁽²⁾

⁽¹⁾Project Engineering Economist
EQE International, Inc.

⁽²⁾Associate Professor
Department of Civil Engineering
Hiroshima Institute of Technology

ABSTRACT

As demonstrated in recent disasters such as the 1994 Northridge and 1995 Hyogoken-Nambu (Kobe) earthquakes, urban areas can suffer potentially large economic losses when highway transportation systems are damaged in seismic events. This paper addresses the development of performance measures for highway systems that are suitable for estimating the economic impact of earthquake damage. Economic impact is here defined as the loss of economic production or output levels (e.g., gross regional product) in the area affected by the disaster which may be caused either directly or indirectly by highway service disruption. It does not refer to the cost to repair physical damage. In this paper, summary measures of system performance are proposed and evaluated using data from Northridge and Kobe. Particular attention is paid to the improvement in system performance as damaged portions of the network are restored in the weeks and months following the earthquake. Using actual traffic volumes as an indicator of economic activity in the restoration period, an explanatory model is developed for the Kobe case using multiple regression analysis. Highway system performance is found to be the most important factor influencing traffic recovery, but its influence varies with the phase of restoration. A framework is then proposed by which this model can be used to estimate the reduction in economic losses associated with alternative post-earthquake restoration strategies and pre-earthquake mitigation measures.

INTRODUCTION

Recent earthquake disasters such as the 1989 Loma Prieta, 1994 Northridge, and 1995 Hyogoken-Nanbu (Kobe) events have demonstrated the seismic vulnerability of highway systems and the significance of the ensuing economic impact. In addition to engineering studies of highway bridge damage, several studies have investigated the consequences of the damage in terms of travel behavior and regional economic impacts (e.g., Giuliano et al. 1996, Gordon et al. 1996). However, few studies have utilized a systems perspective to analyze the link between structural damage and economic impact. While existing earthquake loss estimation models can indicate the likely pattern of damage to highway bridges, an evaluation of the entire system's performance is needed to estimate the economic consequences. Wakabayashi and Kameda (1992) perform network reliability analysis to explain traffic conditions in Loma Prieta but do not consider overall performance measures. Basoz and Kiremidjian (1995) utilize a bridge importance measure based on network connectivity analysis in their methodology for bridge retrofit prioritization but also do not measure system performance. Chang (1996) models the economic impact of transportation and other lifeline disruption in the Hyogoken-Nanbu earthquake but employs a simplified transportation measure that does not consider systems aspects.

This paper develops and applies performance measures for highway systems damaged by earthquakes. It focuses on developing summary measures that can be readily used for economic impact modeling, as well as for identifying effective mitigation and reconstruction prioritization strategies. Economic impact in this case refers to the loss of economic production or output levels (e.g., gross regional product or GRP) due directly and indirectly to highway system damage, rather than the actual cost to repair damage.

Figure 1 provides a conceptual framework for this analysis: earthquake damage to highway structures such as bridges provide the input to assessing system performance through summary measures, which in turn provide inputs to models of the ensuing economic loss. These disaster outcomes can be influenced by two types of policy options -- pre-earthquake seismic retrofit, which affects initial damage states, and restoration speed and prioritization strategies, which affect the system performance measures during the restoration period. This paper focuses on quantifying Links 1 and 2 in the figure, that is relating damage to system performance measures and relating performance measures to economic loss. Once these links are developed, the model can be used to evaluate the loss reduction impact of various risk reduction policy options. To establish Link 1, we use data from the Northridge and Hyogoken-Nanbu earthquakes in a comparative analysis. To investigate Link 2, we focus on the latter disaster only.

Summary highway system performance measures can potentially be advantageous for making comparisons across disaster events, thus leading toward generalized rather than case study evaluations of highway damage impact. They can also be useful for rapid, real-time earthquake loss estimation in a disaster. Such measures should therefore be simple to implement and require only data that will be readily available after a disaster. For utility lifelines such as water, electric

power, natural gas and telecommunications, some researchers have measured system restoration in terms of the percentage of households with service restored (e.g., Takada and Ueno 1995). This measure cannot, however, be directly applied to transportation systems.

The paper first provides a brief overview of highway damage and restoration in the Northridge and Hyogoken-Nanbu earthquakes. It then proposes measures of highway system performance and implements the measures for the two disasters. Further analysis develops a model for relating economic impact to highway system performance. The paper concludes with a discussion of potential applications and areas for future research.

HIGHWAY DAMAGE AND RESTORATION IN NORTHRIDGE AND KOBE

The January 17, 1994 Northridge earthquake ($M_w=6.7$) caused damage to 286 state highway bridges, of which seven major ones collapsed (Caltrans 1994). This caused severe disruption to four critical highway routes in the northwestern Los Angeles metropolitan area -- Interstate 5 (I-5), State Route 14 at the interchange with I-5, State Route 118, and Interstate 10. On I-5 at the Gavin Canyon crossing, a detour was opened on January 29 and the mainline was reopened on May 18, four months after the earthquake. At the I-5/SR-14 interchange, limited detours were implemented using undamaged connectors and truck bypasses. Contractors completed reconstruction of two of the four ramps in July and the remaining two in November. On SR-118, damage caused closure of over 9 miles of the highway west of the junction with I-210, and detours were implemented on local streets. In mid-February, partial restoration reopened about 5 miles of highway and allowed reduced-lane highway usage to replace detours on local streets. Reconstruction was completed in September. On I-10, bridge collapses occurred at La Cienega/Venice Boulevards and at Washington Boulevard/Fairfax Avenue. Detours on local arterial streets were implemented during reconstruction. The mainline was reopened on April 12, less than 3 months after the earthquake. (Caltrans, private communication, March 1997)

The January 17, 1995 Hyogoken-Nanbu earthquake ($M=7.2$ on the Japan Meteorological Agency (JMA) scale) caused severe damage to highway structures and disruption to the highway network in the Hanshin area including the Hanshin Expressway, Meishin National Expressway and Chugoku National Expressway. The most significant damage occurred to Hanshin Expressway Route 3. Before the earthquake, Route 3 shared approximately 40 percent of east-west corridor traffic at the Ashiya River screen line at the boundary between Kobe and Ashiya cities (average daily traffic (ADT)=252,800), providing an important connection between the Osaka and Kobe metropolitan areas. Approximately half of the 1,175 piers in Hyogo Prefecture suffered major to minor damage. Major damage included turnover of 18 spans at Higashinada-ward in Kobe city and collapse of 10 spans at disparate locations in Nishinomiya and Kobe cities, leaving 13 sections (approximately 28km) closed to traffic. Reopening of small isolated portions began in February 1996, but functional performance in terms of traffic volumes on Route 3 was not much improved because the east-west traffic connection was not yet

reestablished. Finally on September 30, 1996, more than 20 months after the earthquake, the entire route was reopened, completing restoration of damage to the entire regional highway system. National Route 43, a surface artery parallel to Route 3, was unfortunately degraded due to reconstruction work on Route 3. On Hanshin Expressway Route 5 (pre-quake ADT=28,300 at Ashiya River screen line), collapse of the Nishinomiya-ko Bridge and major damage to three bridges occurred. After partial reopening, Route 5 began to serve as a main alternative to Route 3, together with Routes 7 and 16, which did not experience physical damage. During the daytime, access was limited to emergency transportation for reconstruction work and disaster relief activities based on the Road Traffic Act.

On the Meishin National Expressway, viaducts suffered severe damage between Toyonaka Interchange(IC) and Nishinomiya IC. Pre-quake traffic volumes in the affected sections were approximately 50,000 to 70,000 in ADT. While even the worst-damaged sections were opened to traffic with reduced lanes after February 25, 1995, traffic volume was reduced to 30 to 55 percent of pre-quake levels because the direct connection with Hanshin Expressway Route 3 was lost and access was allowed for emergency transportation only during the daytime.

On the Chugoku National Expressway, damage to the viaduct between Toyonaka IC and Nishinomiya-kita IC (pre-quake ADT=98,700) caused closure of the main connector between the Chugoku/Kyusyu and Kansai/Kanto regions. Despite relatively short-term closure, the nationwide economy had been significantly affected because of additional origin-destination (OD) distance, OD travel time, and suspension of various activities. In mid-February 1995, 4 lanes were opened to traffic (out of 6). Since then, Chugoku National Expressway served as an alternate route to Hanshin Expressway Route 3, etc., carrying approximately 10 to 20 percent additional traffic volume.

MEASURES OF POST-DISASTER NETWORK PERFORMANCE

Proposed Measures

In order to effectively compare highway system performance across earthquake disasters, new measures or indices are needed. Performance measures traditionally used in transportation engineering are generally inappropriate for assessing post-disaster situations. These traditional measures typically address conditions at individual locations and focus on measuring traffic congestion. One measure of overall system performance that is sometimes used consists of total travel time on the network in vehicle-hours, that is the sum over all system links of the number of vehicles multiplied by travel time on each link. However, in a post-disaster situation, this measure is not practical because the availability of travel time data is very limited. In a post-disaster situation, performance measures are required which emphasize physical condition and network functionality.

Chang and Nojima (forthcoming) proposed and tested four measures of highway system performance. These measures were found to be promising, and two of them are utilized in the current analysis:

1. Total length of highway open (measure L);
2. Total “connected” length of highway open (measure C).

Each is estimated as the ratio of post-earthquake to pre-earthquake conditions and ranges from 0 (system non-functional) to 1 (system fully functional). Measure L reflects the length of highway in the network that is open to traffic. Measure C , defined in equation (1), attempts to capture the functionality of the highway system by recognizing the remaining degree of connectedness within the network. Note that in the case of a linear network, K is equal to 1.

$$C = \frac{1}{K} \sum_k \left(\frac{\sum_m l_{m,k}^2}{\sum_n \bar{l}_{n,k}^2} \right) \quad k = 1, 2, \dots, K \quad (1)$$

where l = connected length in damaged network (i.e., length between terminal nodes)
 \bar{l} = connected length in intact network
 m = index for connected segments of damaged network
 n = index for connected segments of intact network
 k = index for route directional group
 K = total number of route directional groups being considered.

These measures can be evaluated at regular time intervals following the earthquake. They require only information on pre-earthquake network configuration and post-earthquake physical damage and restoration patterns. As will be discussed below, adjustments can also be made to take into account the ameliorative effects of surface road detours around highway damage sites during reconstruction. Detours restore a portion of the connectedness of a damaged route.

A fundamental question concerns the relevant network to be analyzed. Too sparse or limited a network would not adequately capture the extent of damage or availability of alternate routes, thus overestimating the deterioration in system condition. Too extensive a network would dilute the significance of the damage and provide little useful information. One approach is to consider the area of physical damage to the highway system together with major alternate routes that are undamaged.

Application to Northridge and Kobe

Analysis of damage following the Northridge earthquake focused on the four areas of major highway bridge damage on I-5 (Gavin Canyon and SR-14 interchange), I-10, and SR-118. The relevant network was defined to include routes significantly impacted by the earthquake damage, either directly or indirectly by serving as major highway detour routes. This area was delimited in part by the ten highway locations where Caltrans regularly collected post-earthquake traffic

data. Routes were grouped into two categories, north-south and east-west. The former included: I-5 from Santa Clarita to downtown Los Angeles, SR-170/US-101 from the junction (Jct.) with I-5 to Jct. I-110, I-405 from Jct. I-5 (in L.A.) to Jct. I-105, and I-110 from Jct. I-5 to Jct. I-105. East-west routes included: SR-118 from Simi Valley to Jct. I-210, US-101/SR-134 from Thousand Oaks to Jct. I-5, and I-10 from Santa Monica to Jct. I-110. Highway length and normal average daily traffic (ADT) data were obtained from the Caltrans website (<http://www.dot.ca.gov/hq/traffops/traffsys/trafdata/trafdata.htm>). The effect of detours onto arterial or local streets was taken into account through the use of a detour factor (see Chang and Nojima, forthcoming). The performance measures were evaluated on a weekly basis following the earthquake. Results immediately after the earthquake show that $L=0.89$ and $C=0.84$. The measures provide very similar estimates of system degradation due to the highly redundant nature of the highway network and the distribution of damage.

Analysis of highway system performance in the Hyogoken-Nanbu earthquake focused on Hanshin Expressway Routes 3, 5, 7 and 16, Chugoku National Expressway (from Yokawa Jct. to Suita Jct.), and Meishin National Expressway (from Suita Jct. to Nishinomiya IC). Immediately after the earthquake, traffic was controlled in a wider area for damage inspection and emergency transport prioritization. However, because major interest herein is on more long-term impacts on the economy, the network under consideration was defined to include routes that suffered physical damage and/or served as major alternate highway routes, as listed above.

Configuration of the relevant network can be represented as a linear system because of geographic properties in the Hanshin area. Therefore, directional grouping was not applied in this case (i.e., $K=1$). Data on highway length, pre- and post-earthquake monthly ADT, and status of re-openings of damaged sections during the reconstruction period were obtained from the authorities concerned through private communications. Each measure was evaluated on a monthly rather than weekly basis. One of the reasons is data availability, and the other is the longer period of highway closure compared to Northridge, i.e., more than 20 months on Hanshin Expressway Route 3. Detour adjustments were not made to the measures since local arterial streets had insufficient capability to accommodate detouring vehicles due to damage, reconstruction work, and/or traffic control. Results immediately after the earthquake show the measures dropped to 0 due to full closure of highway networks. In February 1995, after non-damaged segments were made open to traffic, these measures rose to $L=0.67$ and $C=0.57$.

Correlation with Actual Traffic Volumes

As noted, these measures were estimated at regular time intervals as restoration of highway damage progressed. Northridge estimates were made on a weekly basis, and Kobe estimates on a monthly basis. The deterioration and restoration of system performance measures were then compared to changes in actual traffic volumes observed after the respective earthquakes.

Caltrans collected areal traffic count data at 10 locations for somewhat over 5 months following the Northridge earthquake using loop counters embedded in the highway pavement. These

included various locations on I-5, SR-134, SR-170, I-405, I-10, I-105, US-101, and SR-118. The unpublished data were made available for this study by the Caltrans District 7 office. Except for one case where monthly data were reported, these counts were provided on a weekly basis beginning about a week after the earthquake. Pre-earthquake daily traffic data at these locations were also provided for the corresponding months in 1993. Ratios of post- to pre-earthquake ADT were estimated for each count location, and assigned to segments of the study network. In some cases, averages of two nearby count locations were assigned. These ratios were applied to base-year ADT data to approximate post-disaster ADT for each section of the network, and weighted with section length data. The resulting weighted sum (V) indicates the ratio of system vehicle-miles of travel on a weekly basis. Base-year ADT data pertain to 1996 conditions, which are adequate for indicating "normal" traffic patterns.

Figure 2 shows the restoration of traffic in the L.A. area on a weekly basis starting from one week after the Northridge earthquake. The figure also plots the restoration of performance measures L and C over this period. Both measures show fairly good correlation with actual traffic restoration. However, traffic conditions are generally lower than the performance measures in the initial period and improve more rapidly than the measures would suggest. From week 19 (early June) onward, traffic actually exceeds pre-earthquake volumes.

Japan Highway Public Corporation (JH) monitors traffic count data on National Expressways at every interchange toll gate nation-wide. Hanshin Expressway Public Corporation monitors traffic count data at every on- and off-ramp on its own routes using traffic counters. Those data, stored as monthly average daily traffic volumes (ADT), were made available for this study. Based on the data, time series of ADT between interchanges or ramps were compiled on a monthly basis for the study network during the pre-earthquake ordinary period and post-earthquake reconstruction period from October 1994 through October 1996. The sum of section ADT multiplied by section length adds up to total vehicle-kilometers of transportation volumes over the entire study network. Normalized by pre-quake (from October through December 1994) average levels, the sum was compared with the highway performance measures.

Figure 3 shows the restoration of traffic on a monthly basis following the Hyogoken-Nanbu earthquake with plots of the two performance measures. Although the measures recovered to $L=0.81$ and $C=0.69$ by May 1995, progress stalled for over a year until July 1996, when the reopening of Hanshin Expressway Route 3 began to accelerate until full restoration was completed at the end of September 1996. While the performance measures exceed 0.9 after one month in Northridge, long-term degradation can be seen in the Kobe case, which clearly indicates significantly greater impact on the local and national economy.

Measure L is consistently higher than measure C in figure 3. As seen in Northridge, traffic is lower than the performance measures in the initial period. Once conditions become less confused, however, traffic conditions recover rapidly. While seasonal fluctuation is clearly observed on the Chugoku National Expressway in August, it can be seen that measures L and C serve as an upper bound and an approximate lower bound, respectively.

In both Northridge and Kobe, the system performance measures show good overall correlation with observed traffic patterns. Furthermore, the correlation patterns are similar except for the scale of the time axis. Figures 2 and 3 also suggest that the relationship between highway performance measures and traffic volume occurs over 3 phases in the restoration process. In the "emergency" phase, detours around highway damage are instituted and traffic may be controlled for emergency response. In this phase, traffic volume restoration is lower than the performance measures would imply. Several weeks later, a "rapid restoration" phase begins, in which lesser and/or critical repairs are made quickly to restore the network to a temporarily stable system. In this phase, measure *C* appears to most closely correlate with traffic restoration, indicating that the degree of connection within the network is important and highway capacity may to some extent constrain recovery. Following this, restoration reaches a lengthy plateau during which the most difficult repairs are made. Measure *L* appears to correlate most closely with observed traffic during this "final restoration" phase.

In the next section, we investigate some likely factors such as reconstruction activity and traffic control, in order to utilize the correlation between system performance and traffic restoration to model the economic impact of system degradation.

PERFORMANCE MEASURES AND ECONOMIC IMPACT

Methodology

The findings from the correlations above suggest that performance measures *C* and *L* may be useful in modeling the economic impact of highway system damage in earthquakes. To explore this further, a model of regional economic loss due to highway damage was developed for the case of the Hyogoken-Nanbu earthquake. The model is estimated using 21 monthly datapoints from February 1995 through October 1996.

The methodological approach consisted of applying multiple regression analysis to develop an explanatory model of observed traffic volumes over the course of the restoration period. It is assumed here that post-disaster traffic volumes provide a good general indicator of economic activity levels for this purpose. The objective of the analysis is to develop a model that is capable of explaining post-disaster traffic volumes through a number of causative factors. This model can then be used to gain insights into the economic impact of reduced highway system performance.

Model development begins with the assumption that post-disaster traffic volumes are influenced by four main factors: (1) highway system performance (i.e., damage and restoration levels); (2) stage of restoration/recovery; (3) non-highway reconstruction activity; and (4) seasonal factors. The performance variable consists of either measure *C* or *L*.

The restoration process is here divided into three phases, as discussed previously with reference to figures 2 and 3. The first, or "emergency phase," consists of the period of emergency response immediately after the earthquake, in which traffic control measures were imposed, and covers February 1995. The second, or "rapid restoration phase," extends from March 1995 through August 1995. The "final restoration phase" spans from September 1995 through October 1996. It is hypothesized that the parameters of the impact of highway damage on economic loss varies across these phases.

Non-highway restoration is represented by two variables, new housing starts and import/export trade through the Port of Kobe. Housing reconstruction commenced at a significant level in about June 1995 and remained high throughout the rest of the study period. Reconstruction at the Port of Kobe continued throughout the study period and had not yet been completed by October 1996. From virtually no import/export activity immediately after the earthquake, trade through the Port of Kobe recovered rapidly through the summer of 1995, but then leveled off at around 70-80 percent of pre-earthquake volumes. Data on housing starts and trade volumes were provided by various offices of the Kobe City government.

Seasonal factors were important to consider since the data on post-earthquake monthly traffic volumes was normalized against an average for the last quarter of 1994, rather than against the corresponding month in 1994. In particular, it is noted that travel behavior is anomalous in the month of August since this is the peak travel season in Japan.

In view of these considerations, the following model form was estimated using monthly data.

$$V = \alpha + \beta_1 H + \beta_2 M + \beta_3 D_A + \beta_4 D_E + \beta_5 X + \beta_6 (D_R X) + \varepsilon \quad (2)$$

where V = average daily traffic volume on highway network, normalized, $0 \leq V \leq 1$
 H = new housing starts in Kobe City, normalized, $0 \leq H \leq 1$
 M = import/export trade value through the Port of Kobe, normalized, $0 \leq M \leq 1$
 D_A = seasonal dummy variable (=1 for August, =0 otherwise)
 D_E = emergency phase dummy variable (=1 for Feb.'95, =0 otherwise)
 X = highway system performance measure (=C or L), $0 \leq X \leq 1$
 D_R = rapid restoration phase dummy variable (=1 for Feb.'95 through Aug.'95, =0 otherwise)
 α = constant, to be estimated
 β_i = parameters to be estimated
 ε = error term

Note that all explanatory variables (except dummy variables) are expressed in terms of percent of the value of the corresponding month in 1994. This model was estimated using both measures C and L , respectively, as the highway transportation performance index (X).

The model specification in equation (2) utilizes three dummy variables to reflect certain assumptions. The variables D_A and D_E serve to increase or decrease traffic volumes for the relevant months from what the model would otherwise predict due to exogenous factors of peak travel season and emergency traffic restrictions, respectively. The variable D_R , on the other hand, is used to allow for the possibility that highway system performance in the rapid restoration phase has a greater or lesser impact on traffic volumes than in the final restoration phase. That is, the impact parameter of X in the final restoration phase is β_5 ; in the rapid restoration phase, it is $\beta_5 + \beta_6$.

In this model, the focus is on obtaining the best estimates possible for parameters β_5 and β_6 . These parameters will provide some insights into the impact of highway system damage on economic activity.

As an alternative to equation (2), the following model was also estimated:

$$V = \alpha + \beta_1 H + \beta_2 M + \beta_3 D_A + \beta_4 D_E + \beta_5 (D_R C) + \beta_6 (D_F L) + \varepsilon \quad (3)$$

where D_F = final restoration phase dummy variable (=1 from Sept. '95 through Oct.'96, =0 otherwise)

Motivated by observations from figures 2 and 3, this specification assumes that C is the best measure of highway system performance in the emergency and rapid restoration phases, while L is the best measure during final restoration.

Results

Initial estimation of equations (2) and (3) yielded models with high statistical fit to the data on actual traffic volumes. However, the coefficient on the import/export variable M had a counter-theoretical negative sign. This implies that an increase in import/export trade through the Port of Kobe would decrease highway traffic volumes in the Kobe region, which is not a plausible result. The models were therefore reestimated without M .

The results suggested that the best model was equation (2) using C as the highway performance measure. While the alternatives, equation (2) using L and equation (3), had similarly high fits to the data, the statistical significance levels of the estimated parameters were notably lower, indicating that a lesser degree of confidence can be placed in these estimates. The final estimated model is:

$$V = 0.145 + 0.028 H + 0.124 D_A - 0.099 D_E + 0.788 C - 0.138 D_R C \quad (R^2=0.93) \quad (4)$$

(0.115) (0.037) (0.000) (0.030) (0.001) (0.000)

The t -test significance levels are shown in parentheses below each estimated coefficient. They indicate that the coefficient on each of the explanatory variables is statistically significant at least

at the 5 percent level of significance. The coefficients also have the expected signs (with the exception of $D_R C$, for which there was no *a priori* reason to expect either a negative or a positive coefficient). This model has an adjusted R-squared value of 0.93, indicating very high explanatory power. Furthermore, the Durbin-Watson test did not indicate the presence of serial autocorrelation in the error terms. Thus equation (4) appears to provide a very good explanatory model of post-disaster traffic volumes in the Hyogoken-Nanbu earthquake.

It is interesting to note that the effective coefficient on the highway performance variable C in the rapid restoration period is less than it is in the final restoration period, i.e. 0.65 (=0.788-0.138) as opposed to 0.788. This suggests that, all else being the same, a 1 percent improvement in highway performance (C) during this final restoration period actually has greater economic impact than a 1 percent improvement earlier in the process. This may be because in the Hyogoken-Nanbu earthquake, the highway segments that were restored last were central and critical to the functioning of the linear network system.

Note that since all of the variables in equation (4) are in percentage units, their coefficients can be compared directly. The equation suggests that highway system performance is by far the most important factor influencing post-disaster traffic volumes. The influence of the exogenous factors, that is peak travel season and emergency traffic controls, is about 15-20 percent that of system performance. Reconstruction activity has a much smaller impact, or only about 4 percent that of system performance. The following section discusses how Equation (4) can provide a means for potentially linking highway damage in earthquakes to the impact on the regional economy.

Economic Impact Framework

Unlike the cost to repair earthquake damage, economic losses due to impaired lifeline service occur over a length of time, that is over the duration of service disruption. If we continue to use total traffic volume as an indicator of economic activity levels, we can express total economic loss (Z) as shown in the following equation. Recall that V is the ratio of post-disaster traffic volume to pre-disaster or "normal" volume.

$$Z = k \cdot \sum_t (1 - V_t), \quad t=1,2,\dots,T \quad (5)$$

where k = constant

t = time index (e.g., month)

T = time to complete highway restoration

This concept is illustrated in Figure 4, which plots changes in total traffic volume over time. Assuming that traffic volumes after an earthquake drop and recover as indicated by restoration path "A" (full restoration at time T_A), the total traffic volume loss over the restoration period consists of the entire shaded portion in the figure. This shaded portion is equivalent to the

summation quantity in equation (5). Note that if highway damage repair proceeded more rapidly to shift the restoration path to "B" (full restoration at time T_B), economic loss could be reduced by an amount proportional to the area between restoration paths "A" and "B". Similarly, if initial highway damage could be reduced by pre-earthquake seismic retrofit to bridges, restoration path "C" might occur (full restoration at time T_C), in which case economic losses could be even more substantially reduced.

Equations (1) and (4) provide a promising means for estimating restoration paths such as "B" or "C" that would result from alternative mitigation and restoration policies. Holding all other variables constant, changes in individual bridge damage and restoration conditions can be summarized using equation (1) and predictions as to the change in traffic volumes can be made using equation (4), with traffic volumes being used as an indicator of economic activity as noted in equation (5).

CONCLUSIONS

This paper has developed a methodology for estimating economic loss from highway damage in earthquakes based on summary measures of highway system performance. The methodological approach emphasized simple measures that could be used to trace not only the immediate deterioration in system performance after the earthquake, but also the improvement of performance over the course of the reconstruction period. Tests using data from the Northridge and Hyogoken-Nanbu (Kobe) earthquake disasters showed that these measures demonstrate good correlation with actual highway traffic volumes in those events. Using these highway performance measures together with other variables to model changes in total traffic volume, a multiple regression model was developed for the Kobe case which demonstrated very high explanatory power ($R^2=0.93$). An approach was then suggested for relating system performance to economic loss by using traffic volume as an indicator of economic activity levels.

Several important issues remain for further research. First, while traffic volumes are expected to provide a reliable indicator in the short term of economic activity levels (e.g., in terms of GRP), the actual relationship should be quantified in further study. Second, as far as possible, the model of traffic volume developed for the Kobe case should be tested against Northridge or other earthquake data. This includes comparisons with loss results from other economic models that may be based on more sophisticated systems analysis. However, it is anticipated that developing a similarly effective model for Northridge may be difficult due to the smaller magnitude of impacts and greater degree of "noise" from exogenous factors.

Results suggest that the approach developed here could be advantageously applied for earthquake loss estimation as well as loss reduction. In particular, it can be used to estimate the potential reduction in economic loss deriving from alternative policy options ("what-if" scenarios) such as pre-earthquake mitigation and post-earthquake restoration prioritization.

ACKNOWLEDGMENTS

The authors appreciate the cooperation of Caltrans, Hanshin Expressway Public Corporation, and Japan Highway Public Corporation, and the kind advice of Prof. H. Kameda, Disaster Prevention Research Institute, Kyoto University. This study was supported on the U.S. side by the National Science Foundation (grant no. CMS-9531997) and on the Japanese side by the Monbusho Grant-in-Aid for International Scientific Research Program, Joint Research (grant no. 08044144).

REFERENCES

- Basoz, N. and A.S. Kiremidjian. 1995. "A Bridge Prioritization Method Based on Transportation System Performance Using GIS." *Proc. 6th U.S.-Japan Workshop on Earthquake Disaster Prevention for Lifeline Systems*. Tsukuba Science City, Japan: Public Works Research Institute, pp.437-449.
- Caltrans. 1994. *The Continuing Challenge: The Northridge Earthquake of January 17, 1994*, Seismic Advisory Board Report. Sacramento, Calif.: California Dept. of Transportation.
- Chang, S.E. 1996. "Economic Impact of Lifeline Disruption in the January 17, 1995 Hanshin-Awaji Earthquake." *Proc. Eleventh World Conference on Earthquake Engineering*, Acapulco, Mexico, paper no.357.
- Chang, S.E. and N. Nojima. "Measuring Lifeline System Performance: Highway Transportation Systems in Recent Earthquakes," forthcoming in *Proc. Sixth U.S. National Conference on Earthquake Engineering*.
- Giuliano, G., J. Golob, D. Bahl, W.Lee and Y.C. Liao. 1996. "Impacts of the Northridge Earthquake on Transit and Highway Use," Lusk Center Research Institute Research Report No. LCRI-96-03R. Los Angeles, Calif.: University of Southern California.
- Gordon, P., H.W. Richardson, and B. Davis. 1996. "Transport-Related Business Interruption Impacts of the Northridge Earthquake." Los Angeles, Calif.: Lusk Center Research Institute, University of Southern California.
- Takada, S. and J. Ueno. 1995. "Performance of Lifeline Systems during the 1995 Great Hanshin Earthquake." *Proc. 6th U.S.-Japan Workshop on Earthquake Disaster Prevention for Lifeline Systems*. Tsukuba Science City, Japan: Public Works Research Institute, pp.165-184.
- Wakabayashi, H. and H. Kameda. 1992. "Network Performance of Highway Systems under Earthquake Effects: A Case Study of the 1989 Loma Prieta Earthquake." *Proc. U.S.-Japan Workshop on Earthquake Disaster Prevention for Lifeline Systems*. Tsukuba Science City, Japan: Public Works Research Institute, pp.215-232.

FIGURES

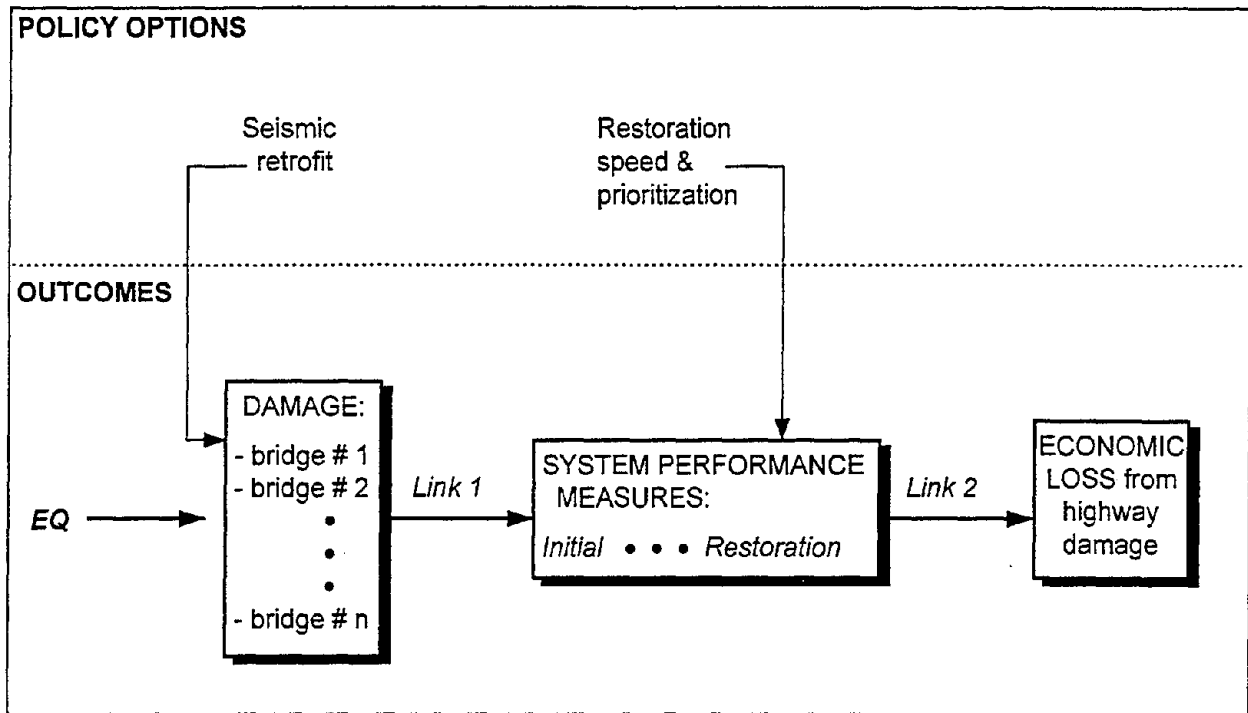


Figure 1. Conceptual Framework for Economic Impact of Highway Damage

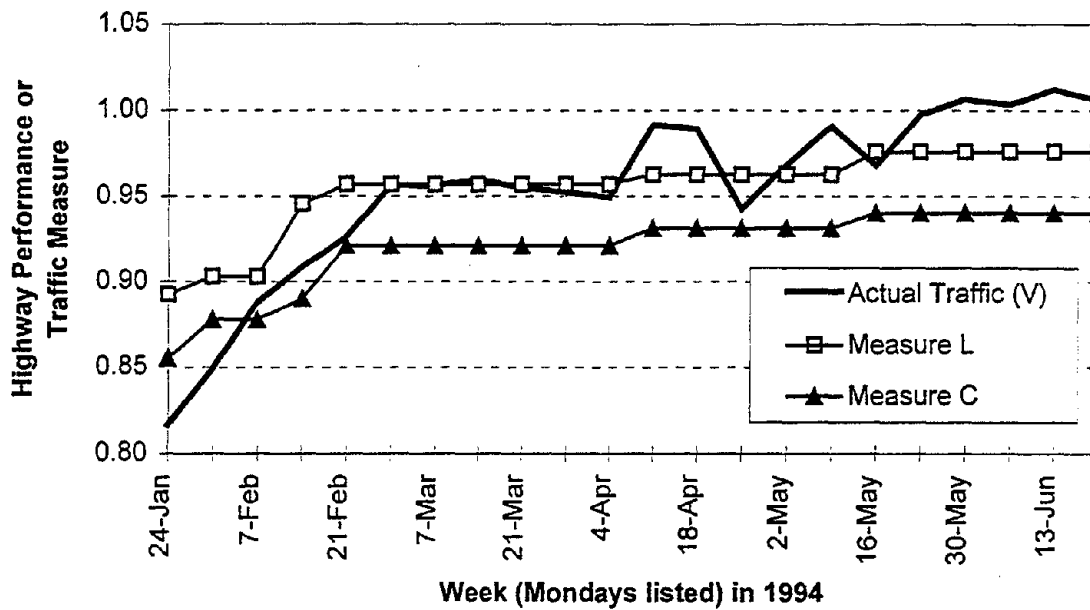


Figure 2. System Measures and Traffic Restoration, Northridge Earthquake

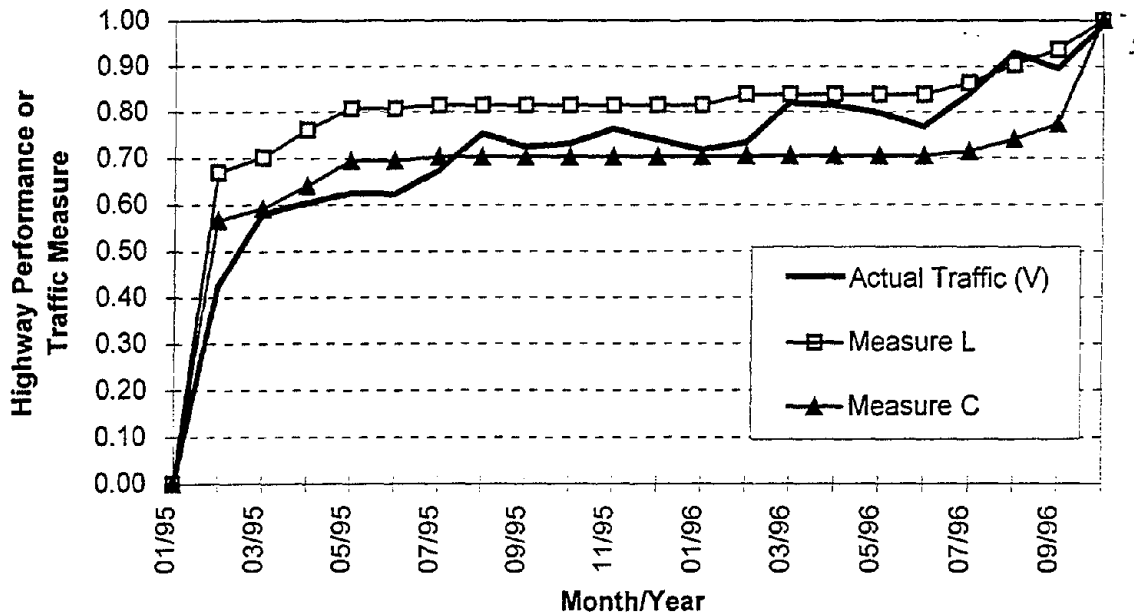


Figure 3. System Measures and Traffic Restoration, Hyogoken-Nanbu Earthquake

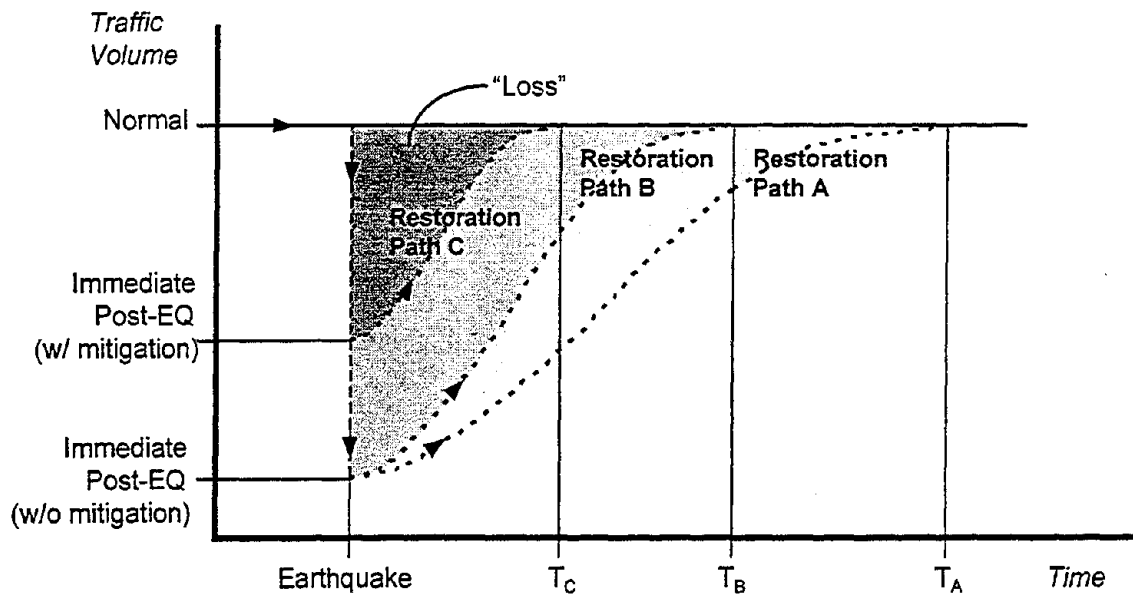


Figure 4. Schematic Illustration of Highway Restoration Impact

STEPHANIE E. CHANG

Position:

Project Engineering Economist (1996-present)
EQE International, Inc.

Address:

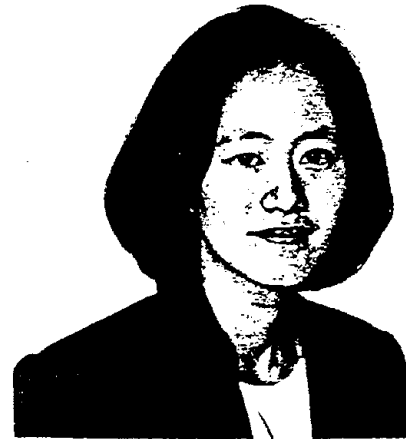
1411 4th Avenue, Suite 500
Seattle, Washington 98101, USA
tel. (206)623-7232
fax (206)470-4145
email: sec@eqe.com

Date of birth:

September 1, 1967

Education:

1994	Ph.D. (Regional Science)	Cornell University
1993	M.S. (Regional Science)	Cornell University
1989	B.S.E. (Civil Engineering)	Princeton University



Major subject:

Economic impact of earthquakes and other natural disasters; Engineering-economic issues in risk management; Regional economic modeling

Experience:

1994-96 Lead Engineering Economist, EQE International, Inc. (Irvine, Calif.)

Travel abroad:

Japan, Taiwan, China, Mexico, Canada, W. Europe

Major publications:

- A. Rose, J. Benavides, S.E. Chang, P. Szczesniak, and D. Lim. 1997. "The Regional Economic Impact of an Earthquake: Direct and Indirect Effects of Electricity Lifeline Disruptions." *Journal of Regional Science*, Vol.37, No.3, pp.437-458.
- S.E. Chang and M. Shinozuka. 1996. "Life-Cycle Cost Analysis with Natural Hazard Risk." *Journal of Infrastructure Systems*, Vol.2, No.3, pp.118-126.
- S.E. Chang. 1996. "Economic Impact of Lifeline Disruption in the January 17, 1995 Hanshin-Awaji Earthquake." *Proc. 11th World Conf. on Earthquake Engg.*, Acapulco, Mexico.
- S.E. Chang, H.A. Seligson, and R.T. Eguchi. 1996. *Estimation of the Economic Impact of Multiple Lifeline Disruption: Memphis Light, Gas and Water Division Case Study*. Buffalo, N.Y.: National Center for Earthquake Engineering Research Technical Report NCEER-96-0011.
- B.G. Jones and S.E. Chang. 1995. "Economic Aspects of Urban Vulnerability and Disaster Mitigation." In *Urban Disaster Mitigation: The Role of Engineering and Technology*, eds. F.Y. Cheng and M.S. Sheu. Oxford: Elsevier Science Ltd., pp.311-320.

SYSTEM TO ASSESS SOCIO-ECONOMIC EFFECT OF EARTHQUAKE DISASTER

NOZAKI Tomofumi⁽¹⁾, SUGITA Hideki⁽²⁾

(1) Senior Research Engineer, Earthquake Disaster Prevention Technology Division, PWRI

(2) Head, Earthquake Disaster Prevention Technology Division, PWRI

ABSTRACT

This article describes the structure and the method to assess the socio-economic effect of earthquake disaster in urban area. The methods are developed to be implemented on the application system which is used for practical planning uses. The system with the databases of socio-economic data and transportation network data is given with the damage data of production facilities and that of the transportation networks in a damaged area. The system utilizes the several methods to estimate the transportation state, to transform it to the change of production and to evaluate the economic effects in and out of the damaged area. Such system are useful for the personnel in charge of regional earthquake disaster prevention plans at public bodies to establish, revise and improve the designing/retrofit plans of transportation networks.

1. INTRODUCTION

Besides the direct damage on people's life, houses and civil infrastructures, 1995 Hanshin-Awaji earthquake disaster showed us various indirect effects such as traffic congestion and health problem. Among them the economical effect is one of the most important points to be considered carefully because the effect may spread over in and out of the damaged area and affect people's life lasting long time. Especially, the damage of highway networks have to do with such effect through the hindrance of production/ material transportation. Thus, those who plan the earthquake tolerating highway system and facilities must determine the portions of the network critical in terms of the influences on the economic effects. Also, such information is quite important when one considers the strategies of seismic retrofit or restoration of highway

facilities.

Estimations of such direct/ indirect economical effects were announced by several organizations⁽¹⁾. However, their amounts have large variation, and their definitions of indirect effects may differ one by one (Table 1-1). Also the effect due to the damage on highway network is not separated from the total amount of damage.

Table 1-1

Direct Damage	Indirect Damage
\$54 bil.	—
\$42 bil.	—
\$50 bil.	—
\$83 bil.	—
—	\$20 bil.
\$25-33 bil.	\$8 bil. on the local industry
\$21 bil. as stock damage	\$22 bil. as flow damage
—	\$8-21 bil. on business activities in damaged area
\$82 bil. in Hyogo	\$58 bil. of GDP decrease caused by delay of freight in damaged area
—	\$0.2 bil. by transport facility damage and \$5 bil. as repercussive economic effect
\$9 bil. on port facilities	\$5 bil. from decreased freight operation caused by damage on port facilities

In this article, first the mechanism of the economical effects of an earthquake is analyzed and clarified explicitly. The economical effect caused by the direct damage on production facilities and that induced by the damage of transportation facilities are taken into consideration. Each operation necessary for the estimation is divided and reorganized into “sub module.” Second, algorithm of each module is investigated, modeled and prepared ready for the system construction. Finally, a case study is tried in the particular area, namely the Kobe area suffered from Hanshin-Awaji earthquake disaster. The total amount and the portion due to the transportation network damage of the indirect effect is examined.

The system based on the methods introduced here is planned to be used for the practical use in public bodies such as construction bureaus and work offices in charge of highway networks. While many assumptions are used, it is concentrated that system has flexibility for revisions by dividing them into elemental modules. In the following sections, the fundamental issues from the point of the use of the system applying the methods. Then, the framework of the

estimation is shown. Explanations of three important parts of the methods follow; namely, transportation state estimation, its transformation to the economical analysis and estimation of its repercussion effect. Finally, results of the case study for the area damaged by Hanshin-Awaji earthquake disaster are discussed.

2. FUNDAMENTAL ISSUES

The final objective of the project is to construct an application system which estimates the economic effect of the damage on transportation facilities caused by an earthquake. Thus, the individual methods examined here are to be used in principal modules of the system. Several fundamental policies of the system design follow (See also Figure 2-1).

- a) Users of the system are supposed to be the ones in charge of planning and management of the highway network in an prefecture or a block which consists of several prefectures.
- b) The user inputs damaged portions of the highway network. The damage state is assumed when the system is used under normal condition before an earthquake, or it is investigated after an earthquake.
- c) Time period of the estimation is from one week to several years after the earthquake.
- d) In the development of the methods, it was considered that the problems and the possibilities of the modules must be clarified so that the system can be revised easily.

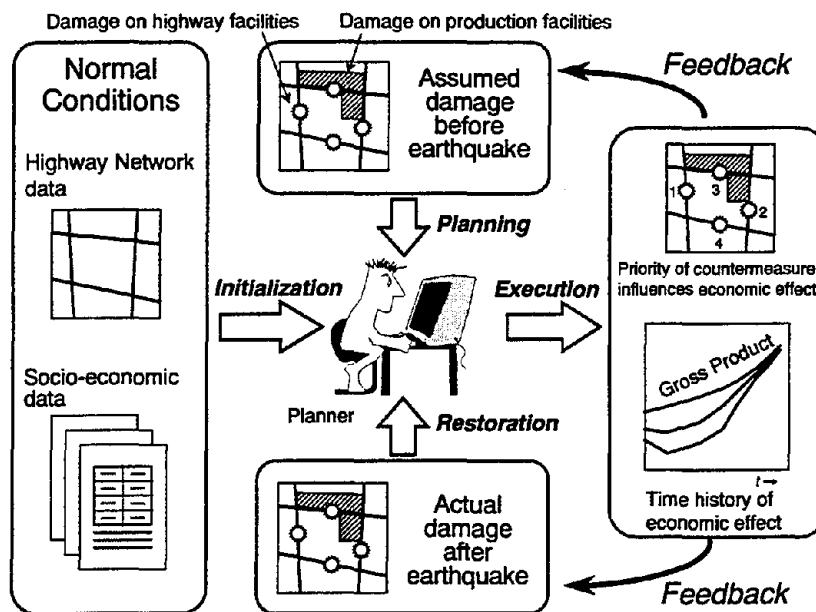


Figure 2-1

3. FRAMEWORK OF ESTIMATION

The estimation consists of following three methods (Figure 3-1).

- a) Transportation state estimation after earthquake: Transport times between all zones in the damaged area are calculated. Transportation analysis method is used (*Traffic estimation part*).
- b) Transformation of transport times to change of production: It determines the change of production affected by the direct damage on the production facilities themselves and by the indirect damage of transportation network (*Transformation part*).
- c) Economical effect estimation: The repercussion of the change of the production spread over in and out of the damaged area. This part deal with the calculation of indirect effect of the economy originated from the change of the production (*Economic estimation part*).

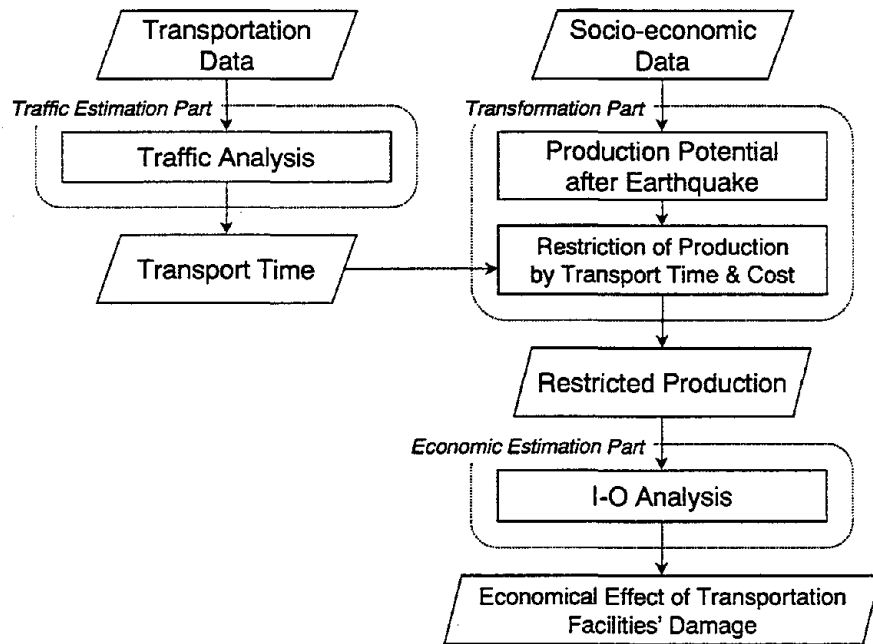


Figure 3-1

4. TRAFFICE ESTIMATION

(2) Outline

Transportation estimation part utilizes the four-step method to analyze the traffic state after an earthquake (Figure 4-1). In this part, the transport time between each zone is calculated based on the transportation network data and socio-economic data in each zone. The output result of this part is travel times from zones to another zones. They are provided to the transformation part to calculate the change of the production.

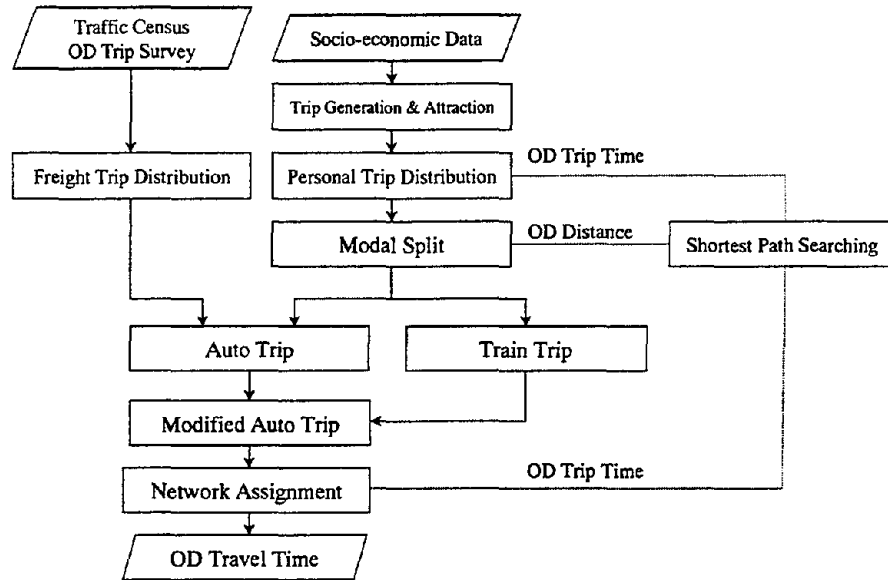


Figure 4-1

(2) Estimation of OD Trip Generation and Attraction

In the first step, the trip generation and attraction at each zone in the damaged area is estimated. The trip represents the source of traffic concerning the personal travel. Although these trips do not carry productions and materials, their traffic volume affect the transport time of freight trips. Personal trip generations and attractions are calculated from socio-economic data by using regression equations obtained from the person trip survey (PT survey).

$$\begin{aligned} G_i &= \text{func}(x_{i1}, x_{i2}, \dots) \\ A_i &= \text{func}(y_{i1}, y_{i2}, \dots) \end{aligned} \quad (4.1)$$

Where, G_i , A_i means the trip generation and attraction at zone i , respectively, and x_{ik} and y_{ik} correspond to the explanatory variables for generation and attraction at zone i .

(3) Trip Distribution

After the trip generations and attractions are calculated, they are assigned to the trip

from origin zones to destination zones. The method proposed here is the gravity model.

$$T_{ij} = \kappa \frac{G_i^\alpha A_j^\beta}{t_{ij}^\gamma} \quad (4.2)$$

In the above equation, T_{ij} is the trip from zone i to zone j , and G_i and A_j means trip generation at zone i and trip attraction at zone j . t_{ij} is the inter-zone resistance between zone i and j . To determine the equation completely, the coefficient κ and power numbers α , β and γ are determined by regressing the data from the PT survey.

(4) Modal Split

The trips derived through the step (1) and (2) does not include only those by automobiles, but also those by other modes such as walking and train. However, they do not include freight trips. In this stage, the personal trips are divided into several traffic modes, and then, the freight trips by trucks obtained directly from the traffic census data are added into the personal automobile trip (Figure 4-2). As a result, the automobile trips to be assigned on the highway network are obtained.

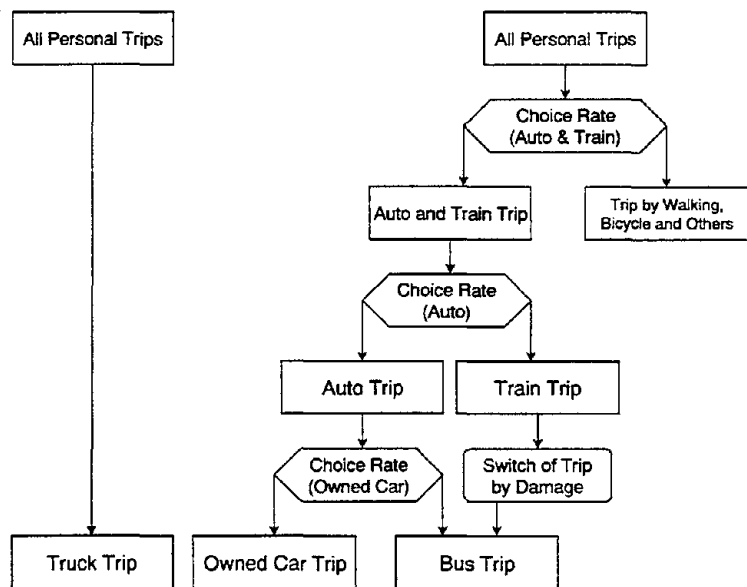


Figure 4-2

(5) Network Assignment

The trip from each zone to another zone is assigned on the given highway network here. For the pre-earthquake state, the network data without damage are used, and for the post-earthquake state, the network data with damage on the links corresponding to the designated time period are used. Assignment procedure is executed based on the user equilibrium (UE) theory. The trips are assigned in heuristic way; say, step-by-step assignment. Based on the traffic volume on each link in the network, the travel time on route from each zone to other zones is obtained. In other words, the travel time matrices of the normal conditions and each time period after the

earthquake are prepared for the input to the following transformation part.

5. TRANSFORMING THE RESULT OF TRANSPORTATION STATE INTO INFLUENCE ON PRODUCTION

(1) Outline

Given the travel time matrices, the change of travel times for a time period after the earthquake against the normal condition are obtained. In this part, the data are transformed into the change of production in the damaged area (Figure 5-1).

The part mainly consists of two steps. First, the production after the earthquake is calculated based on the input facility damage data. Although these data include the damage of the production facilities such as factories and stores, the effect of the damage on the highway network is not included. Thus, the result of this step means the possible production affected by the earthquake.

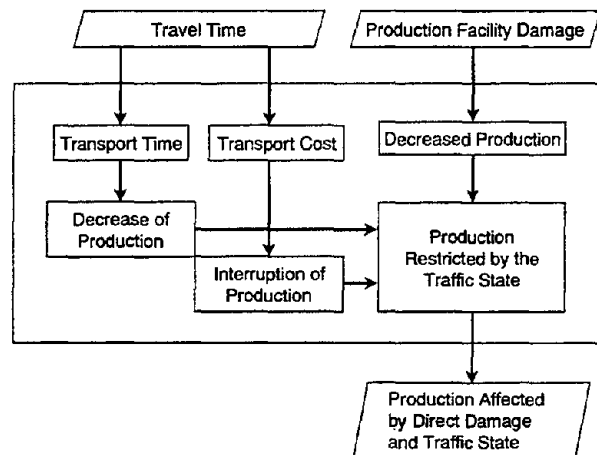


Figure 5-1

Next, the effect of the transportation network damage is taken into account. Two kinds of effects are examined: namely, the decrease of production caused by the increase of the transport time and the interruption of production caused by the increase of the transport cost. These effects are added on the possible production, and the decreased productions data are obtained. This set of data is used as the input data for the following economic estimation part.

(2) Possible Productions after the Earthquake

Possible Productions are determined for the production categories such as mining and manufacturing. For the initial data immediately after the earthquake, facility damage indices which mean the decreasing rate of each production category are input by the user. Then

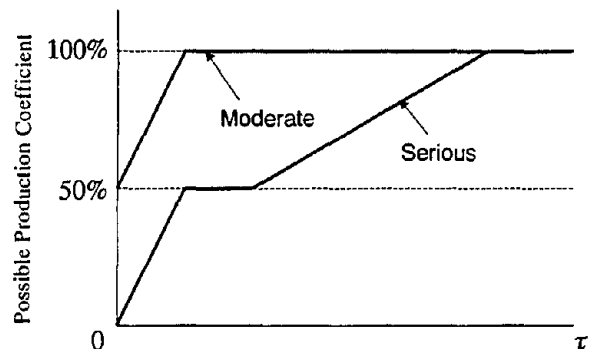


Figure 5-2

the decreasing rates recover as time goes. This situation is represented by two types of the production potential curves assumed as Figure 5-2 corresponding to the damage criteria: “serious” and “moderate”. These curves were derived by examining the results of the inquiries to the enterprises damaged in Hanshin-Awaji earthquake⁽²⁾.

(3) Effect of Transport Time

The possible production is affected by the transport time because its increase restricts the flow of products and materials. By comparing the travel time immediately after the earthquake and that of an arbitrary time period, the effect rate of the freight is determined.

$$\varepsilon_T(\tau) = \text{func} \left[\frac{t_c(\tau)}{t_c(0)} \right] \quad (5.1)$$

Here, the $\varepsilon_T(\tau)$ is the effect rate of the freight at time period τ based on the transport time, and $t_c(\tau)$ is the average travel time from the damaged zone to other zones at time period τ . Also, $\tau = 0$ means immediately after the earthquake. In this research, the function is assumed as the inverse proportion function. Thus, we obtain

$$\varepsilon_T(\tau) = \frac{t_c(0)}{t_c(\tau)} \quad (5.2)$$

The shape of the function is shown on the Figure 5-3.

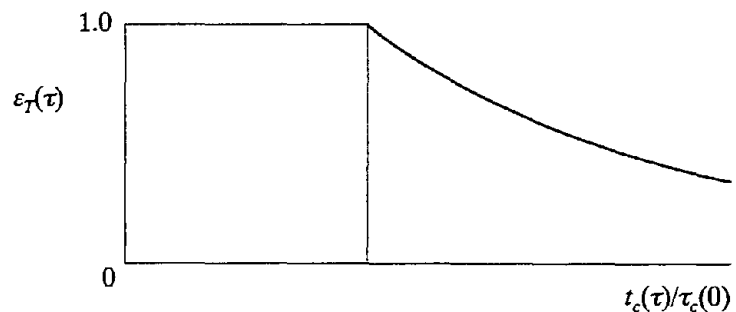


Figure 5-3

(4) Effect of Transport Cost

The productions are also affected by the transport cost when it becomes large against the total production cost. A producer may suspend his/her production activities while the transport cost is dominant and too much for him/her. The function curves of the transport cost effect rate is shown on Figure 5-4. Here, the effect rate is assumed to be explained by the certain coefficient: transport cost increase (ΔCs) divided by business surplus (Sr). In this research, three types of functions are assumed and

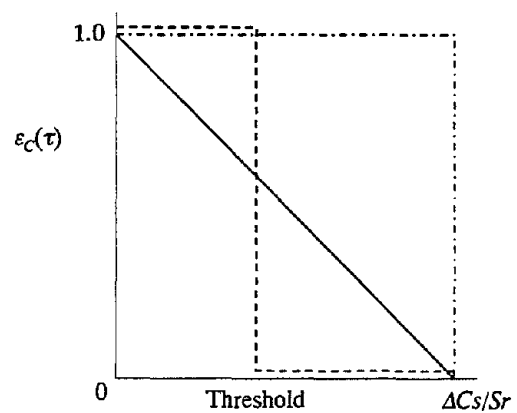


Figure 5-4

their effects are determined in the case study.

While the execution, the restricted production data are calculated for arbitrary time period based on the direct damage of production input to this module and the effect rates of production calculated here. The output data of this module is the production amount for each production category in the damaged area. They are submitted to the next economic estimation part and their repercussion effect is calculated.

6. ESTIMATION OF REPERCUSSION EFFECT OF ECONOMY IN AND OUT OF THE DAMAGED AREA

(1) Outline

After the calculation in the preceding two parts, the production vector for the instance immediately after the earthquake and that for arbitrary time period is derived.

$$\begin{aligned} p(0) &= (P_1(0), P_2(0), \dots, P_c(0)) \\ p(\tau) &= (P_1(\tau), P_2(\tau), \dots, P_c(\tau)) \end{aligned} \quad (6.1)$$

Here, C means the number of production categories, and $P_c(t)$ represents the production amount of category c at time period τ . Note that these vectors are column vectors. To approach the problem here, three conditions are set to solve the problem: namely, (a) the model must be the dynamic model to keep track of the phenomena after the earthquake, (b) the input data are the production amount restricted by the earthquake damage, (c) repercussion effect of a production category to other categories must be expressed.

Among the theories to deal with the economic effect, the input-output model (IO-model, Reontieff model) is generally used⁽³⁾. However, it usually has the production vector as the output value instead of the restricted input value.

$$p = (I - A)^{-1} f \quad (6.2)$$

In the equation above, f is the final demand vector, and I and A are the unit matrix and the input-output matrix (I-O matrix), respectively. Although there is a method which dynamically deal with the problem, the production vector is still used as a objective value.

(2) Alternatives

Here, we set the problem to input the restricted production vectors.

$$f_D(\tau) = f_D(\tau - 1) + \text{func}[p_D(\tau), p_D(\tau - 1), \text{parameters}] \quad (6.3)$$

τ means the discrete time period number, and the index D means that the variables are those of

the damaged area. In this research, three approaches examined, those include

- (a) *basic approach* that applies the fundamental balance equation of IO-model,
- (b) *primitive approach* in which the concept of supply and stock is introduced,
- (c) *possible-required balance approach* in which iterative calculations with IO-matrix and required IO-matrix.

(3) The method used for the case study

After some examinations, the simplest method (a) turned out to show better results. With the equation for the nationwide effect, it is written as below.

$$\begin{aligned}
 \Delta f_D(\tau) &= (I_D - A_D)\Delta p_D(\tau) \\
 \Delta p_N(\tau) &= (I_N - A_N)^{-1}\Delta f_N(\tau) \\
 \Delta f_D(\tau) &= \Delta f_N(\tau)
 \end{aligned}
 \tag{6.4}$$

Where, the index N represents the variables that are of whole nation. Although it is not really a dynamic approach, it gives better results than (b) or (c) without unclear parameters.

After this part is executed, the nationwide production effect caused by that in the damaged area is calculated for arbitrarily designated time period with input data.

7. CASE STUDY

(1) Outline

To examine the adequacy of the method, a case study was tried for the area damaged by Hanshin-Awaji earthquake disaster. The case study is divided into three parts: that is, (a) traffic estimation, (b) transformation, (c) economic estimation.

The target zone is Hyogo prefecture which includes cities and wards damaged in the earthquake. The highway routes for the

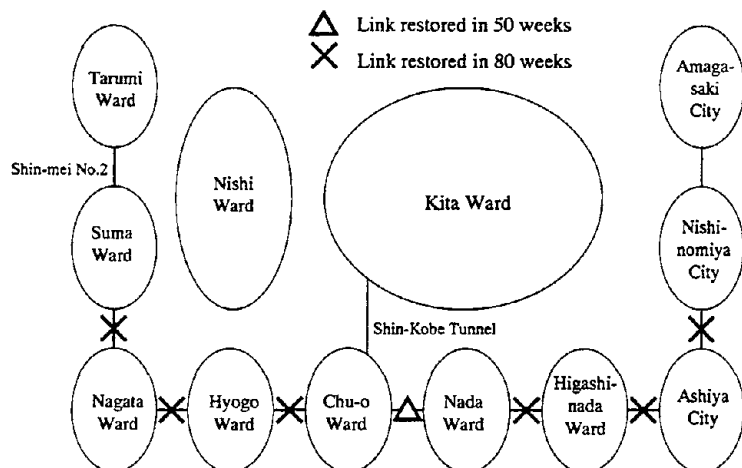


Figure 7-1

estimation is shown on Figure 7-1. The cities and wards are connected by several trunk routes such as national expressway/highways and Hanshin Expressway. Besides the routes in the figure, highway network with the level above the main prefecture load is included. To simulate the situation of the earthquake disaster, several highway links were cut off, and they were assumed to be restored in the certain time periods. Also, the damage on production facilities was assumed based on the acceleration distribution of the earthquake.

Starting from the settings above, the simulation calculations were conducted, and their results are shown for the three steps as stated above.

(2) Traffic Estimation Results

The damage on Hashin Expressway induces the increases of travel time between the cities and wards. Table 7-1 states the travel time and the traveling speed between Amagaski and Suma. The table indicates that the travel time immediately after the earthquake increases by one hour and six minutes (2.6 times) than that in the normal condition. Thus, the traffic along in the east-west direction is affected seriously, which is thought to coincide the state of the earthquake disaster. However, the calculated travel speeds are larger than that investigated after Hanshin-Awaji earthquake disaster⁽⁴⁾. To obtain more accurate results, the traffics unique for the situation immediately after an earthquake such as emergency relief and fire defense need to be included.

Table 7-1

		Normal	After Earthquake	After 50 weeks	After 80 weeks
Damage State	Nishinomiya - Nada	○	×	×	○
	Nada - Chu-o	○	×	○	○
	Chu-o - Suma	○	×	×	○
Estimates for Amagasaki-Suma	Travel Time (h)	0:41	1:47	0:59	0:41
	Travel Speed (km/h)	48.9	17.2	29.6	48.9
	Shortest Distance (km)	33.4	30.7	29.1	33.4

(3) Transformation Results

The estimated damages on the production facilities in Hyogo prefecture area are shown on Table 7-2. On the table, (a) the rate of direct damage without effect of the highway damage, (2) the rate of indirect damage caused by the increase of travel time and (3) the rate of indirect damage caused by the increase of travel cost are shown by the time period corresponding to the restoration. It can be said that the indirect effect induced by the increase of travel time dominates the direct damage. On the other hand, the indirect damage caused by the increase of travel cost does not indicates significant magnitude. Therefore, this method regarding the travel cost needs

to be modified if it is thought to show greater effect, or the final system may neglect it.

Table 7-2

	Normal	After Earthquake	After 50 weeks	After 80 weeks
Only direct damage on facility	100%	91%	97%	98%
Direct damage and the effect of travel time	100%	73%	93%	98%
Direct damage and the effect of travel cost	100%	91%	97%	98%

(3) Economic Estimation Results

As stated in the preceding chapter regarding the economic effect, only the basic approach showed the appropriate result (Table 7-3). The table shows that the repercussion effect of the damage on production facilities to the final demand in the damaged area (Hyogo) and that to the nationwide production. Corresponding to the damage level of the transformation result part, the final demand in Hyogo and the nationwide product decreases \$10-30 billion and \$20-70 billion, respectively. These results do not have excess differences compared to the results of past investigations. Thus the combination of the methods proposed here can be said to give appropriate results.

Table 7-3

		Normal	-5%	-10%	-20%
Hyogo	Product	0.00	-18.58	-37.15	-74.31
	Final demand	0.00	-9.23	-18.45	-36.91
Whole National	Product	0.00	-9.23	-18.45	-36.91
	Final demand	0.00	-18.85	-37.70	-75.40

(billion dollars)

CONCLUSIONS

The conclusions led from the research are stated as follows.

- (a) A method to estimate the socio-economic effect of the earthquake damage on transportation facilities was proposed by combining the three methods: traffic estimation, transformation of the result of traffic estimation to economic damage and economic estimation.
- (b) By examining the result of the case study of Hyogo, it was recognized

- that the post-earthquake specific traffic such as emergency relief and fire defense needs to be considered.
- that the indirect damage caused by the increase of transport time has larger effect than the direct damage. However, the indirect damage caused by the increase of transport cost may not have significant effect.
- that the basic approach showed the appropriate result among the economic estimation methods proposed in this research.

The method introduced here includes the modeled functions in which many assumptions and idealizations are applied. Although there are few well-organized socio-economic/ transportation data of the post-earthquake situation, the models in the method are needed to be improved from the theoretical and measurement points of view.

ACKNOWLEDGEMENT

We acknowledge that we are given quite many important suggestions by the “Committee on comprehensive earthquake preparedness measures to ensure the safety of residents’ life and to promote earthquake-resistant city planning” chaired by Dr. Tsuneo Katayama, head of National Research Institute for Earth Science and Disaster Prevention.

REFERENCES

- (1) Industrial Rehabilitation Plan, Industrial Rehabilitation Committee, Jun. 1996.
- (2) Effects on business activities caused by Hanshin-Awaji earthquake disaster, Kobe Chamber of Commerce & Industry, Mar. 1996.
- (3) “Evaluation of Economical Indirect Damage Caused by Earthquakes” , Kazuhiko KAWASHIMA, Hideki SUGITA, Tadashi KANO, Report of Public Works Research Institute, Vol. 186, pp.1-58, Jan. 1991.
- (4) “Analysis of Relief Goods Transportation to Shelters in the Great Hanshin-Awasji Earthquake”, Kouji NAKASHITA, Michiyasu ODANI, Kazuaki NAGAOKA, Proceedings of Infrastructures Planning Vol. 19 (2), Japan Society of Civil Engineering, Nov. 1996.

PERSONAL CAREER

NAME : TOMOFUMI NOZAKI

POSITION : Senior Research Engineer,
Earthquake Disaster Prevention
Technology Division,
Earthquake Disaster Prevention
Research Center,
Public Works Research Institute,
Ministry of Construction



ADDRESS : 1 Asahi, Tsukuba-shi, Ibaraki, 305 Japan
Tel. 0298-64-2211
Fax. 0298-64-0598

DATE OF BIRTH : April 22, 1964

EDUCATION : Bachelor (1977) and Master Degree (1989) of Engineering, Osaka
University

MAJOR SUBJECT : Earthquake Engineering, Disaster Mitigation Engineering

MAJOR AREA OF EXPERIENCE :

1989 - 1991 Engineer, Shikoku Regional Construction Bureau, MOC
1991 - 1993 Chief Official, Disaster Prevention and Restoration Division, River
Bureau, MOC
1993 - 1995 Chief Official, Regional Road Division, Road Bureau, MOC
1995 - 1996 Research Engineer, Earthquake Engineering Division, Earthquake
Disaster Prevention Department, PWRI, MOC
1995 - 1996 Scholar, The Ohio State University, USA
1996 - Senior Research Engineer, Earthquake Disaster Prevention
Technology Division, Earthquake Disaster Prevention Research
Center, PWRI, MOC

TRAVEL ABROAD: U.S.A

MAJOR PUBLICATIONS :

"A Method to Estimate Economic Effects Caused by Earthquake Damage on
Transportation Infrastructures" Journal of Research PWRI, Vol39-9, 1997

INFLUENCE OF THE RESTORATION OF HANSHIN EXPRESSWAY KOBE ROUTE FROM THE EARTHQUAKE UPON THE SURROUNDING AREA

Toru Yonekura, Nobuhiko Hamada and Kiyoshi Yamamura
Research Division, Planning Department, Hanshin Expressway Public Corporation

Abstract

After the disastrous Hyogoken Nanbu Earthquake, and during the course of rehabilitation of the damaged roads, several sessions of traffic fact-find surveys were conducted over major roads in the suffered areas and a questionnaire was also carried out over the users of the Hanshin Expressway Kobe Route after complete restoration of the route, which made us rediscover the roles and significance of this route.

The analyses of these surveys have verified that the restoration of trunk lines such as Kobe Route could contribute sharply to the recovery of traffic demand in the adjacent areas and curtailment of travel time. In addition, comparison of traffic flow between pre- and post-earthquake situations has clarified that the shares of the expressway and other general roads reversed on some cross sections, causing substantial changes in the dynamic traffic flow.

INTRODUCTION

On January 17 of 1995, the road infrastructure in Kobe City and other Hanshin (denoting "Osaka to Kobe") areas was given a mint of damage by the Hyogoken Nanbu Earthquake. Among others, Kobe Route (Route #3) of the Hanshin Expressway, which used to provide approximately 40 to 50 percent of major cross-section traffic volume in the Kobe urban area and the adjacent areas between Kobe and Osaka before the earthquake, suffered extensive damage and it could not resume providing full continuity for about one year and eight months until the end of September 1996, when the whole line eventually came to complete recovery (Fig. 1). The damage in the road infrastructure seriously affected not only the traffic for evacuation, rescue and salvage immediately after the earthquake in a drastic manner, but also the recovery efforts and economic activities as well as civilian life.

This paper reports the change in post-seismic traffic situations in a chronological system based on the traffic density survey in Kobe City and Hanshin region which was conducted since the time of immediately after the earthquake.¹⁾ It also summarizing the results of questionnaire survey to expressway users carried out after whole route resurrection of the Kobe Route, Hanshin Expressway.²⁾

Based on these two surveys, analysis has been conducted on the social effects of the damage and restoration of the road network on the vehicle traffic and other factors.

1. What Does Kobe Route of Hanshin Expressway Provide?
~ Why was early recovery demanded?

Soon after the earthquake, some intellects claimed to freeze the reconstruction work of Kobe Route in the form of elevated structure. They listed instances of underground reconstruction projects including the Central Artery of Boston in the USA, and the recovery plan of Embarcadero Elevated Bridge in San Francisco, which was damaged by the Loma Prieta earthquake, in the modified form of underground road. They claimed rehabilitation of the Kobe Route to be frozen in conjunction with the campaign against the air pollution by Kokudo No. 43 (or 43rd National Road, or Route 43)

which was in litigation in those days.

However, earliest restoration of the route had been strongly requested soon after the earthquake by the Governor of Hyogo Prefecture, the mayors of four cities of Kobe, Ashiya, Nishinomiya and Amagasaki, as well as the President of Kobe Chamber of Commerce, to secure one of the fundamental social facilities. Therefore, it was decided to recover the expressway in the elevated structure at the earliest stage as the most practicable, not spending time for structural modification, also for the purpose of supporting the general rehabilitation efforts.

(1) The role of Kobe Route

The Kobe Route has been bearing the crucial role of supporting civilian life and economic activities in the Hanshin (or Osaka to Kobe) areas. In particular, it accommodated the traffic demand to support various urban activities in the Osaka Bay area, and together with other highways including Kokudo No.2 and No. 43, played critical roles as the artery for east-west traffic in the Kobe and Hanshin region.

Before the earthquake, it shared approximately 40% of the east-west traffic for the Kobe and Hanshin districts (Fig. 2). Also, 80% or more of its total daily service traffic volume (i.e., 187,000 vehicles per day) located its origin or destination in Kobe City or other Hanshin cities, thus the traffic of Kobe Route was inevitably related to activities in these areas (Fig. 3).

(2) Time-saving value of Kobe Route

Hanshin Expressway, free of vehicle stop caused by traffic lights in comparison with other surface roads, can dramatically save travel time when one moves the same distance. This saved time can be assigned to other activities, yielding a sharp economic effects.

As shown in Fig. 4, trial calculation on Kobe Route as of pre-seismic days tells us it produced about ¥2,000 per vehicle. If totaled annually for all serviced vehicles, it could yield economic effects (time saving value) of about 140 billion yen.

2. Post-earthquake Traffic Fact-find Surveys

In order to determine the effects of road facility damage on the transportation, various surveys and analyses have been carried out. To investigate those of automobile traffic in particular, the Kinki Regional Construction Bureau continuously conducted, since February 1, just fortnight after the earthquake, traffic volume survey which covered typical cross sections in Kobe City and Hanshin region.³⁾ Another traffic survey was also carried out to examine traffic volume on highways in the damaged areas by transportation planning researchers and students.⁴⁾ This survey, taking the form of joint study by voluntary students from nine colleges, obtained video image data of traffic conditions and other noticeable findings. The results of these traffic fact-finds can be effectively used not only as the subject for analysis, but also as the background data for various studies related to the earthquake damage. They also provide the basic data to establish future urban projects and traffic plans through utilization of lessons given by the earthquake disaster.

Hanshin Expressway Public Corporation also conducted traffic fact-find surveys several times in Kobe City and Hanshin region to see the reality of traffic situations in the damaged road network, and for the purpose of collecting supporting data for resurrection work.

(1) Locations and date of surveys

Our traffic fact-finds are broadly divided into two phases, depending on the date and the body of performance. The first phase includes four sessions carried out by Hanshin Expressway Public

Corporation from March 1995 to March 1996. The second phase includes six survey sessions from July to November 1996 in harmony with the stepwise recovery of Kobe Route. These six sessions were carried out in a joint survey by the Ministry of Construction, Hanshin Expressway Public Corporation, Hyogo Prefecture and Kobe City, and they are positioned as impact surveys performed to the stepwise resurrection of Kobe Route.

In the first phase, each survey was conducted at eight cross sections in Kobe City and Hanshin region, although the details varied with the date of performance (Fig. 5). The cross sections were selected to focus on east-west traffic, taking into account the major origin/destination (OD) pattern which was characteristic and dominant in the damaged areas. Since general road networks inland of Kobe City and Hanshin districts had relatively less damage, and Chugoku Jidoshado (or Chugoku highway) was recovered to a certain extent at the end of January, the Rokko mountains cross section and the Mukogawa river inland cross section were added to the survey location in order to examine the detour traffic volume from the coastal areas. In addition, the cross section of man-made island was added to the group. This section is located on the road running from Naruohama to Rokko Island (or Rokko reclaimed island) via an over-sea bridges, the only gateways to several reclaimed islands from the existing urban areas, which was damaged by the earthquake. This cross section was selected to verify the function of Wangan Route (Route #5) to work as the alternative to that of Kobe Route. Most of the surveyed cross sections were used for the road traffic census to compare with the pre-earthquake situation. Also, traveling speed survey was conducted on the following three segments in order to collect data to determine the influence on east-west traffic through damaged areas: i) Between Kobe municipal office and Osaka municipal office, ii) Between Kobe municipal office and Kakogawa municipal office, and iii) Between Fukusaki IC and Suita IC of Chugoku highway which runs through the northern part to the damaged areas.

In the second phase, the following three cross sections were added to those in the first phase in order to collect more data of the impact by the stepwise recovery of Kobe Route: i) Iwaya cross section, ii) Higashi-kawasaki cross section, and iii) Minatogawa cross section. Traveling speed survey was also conducted on the same two segments as in the first phase: between Kobe and Osaka municipal offices and between Kobe and Kakogawa municipal offices. Another segment between Amagasaki West approach and Suma-rikyu-mae on Kobe Route was added to the above to directly check the impact of recovery work.

(2) Methods of surveys

Traffic fact-find consisted of the following surveys (Table 1):

- 1) Traffic volume
- 2) Travel time between major points
- 3) Traffic light indication at crossings

Our traffic volume survey was conducted at every one hour during a 24 hour period from seven in the morning till the same time in the next morning. Vehicles were classified into five types, i.e. passenger car, bus, small truck, ordinary truck and two wheeler, in the first phase, and two types, i.e. small vehicle and large vehicle in the second phase. Travel time survey between major locations was conducted by driving on a specified route accessible by general vehicles excluding recovery materials transportation routes. Record was kept on 1) departure time at the origin and arrival time at the destination, 2) time at major passing points, and 3) traveled distance from the origin and the destination. Examination of traffic light indication at crossings was conducted at the location

for the traffic volume surveys during typical time zones to record the signal cycle.

3. Effects on Traffic Volume Recovery

This section describes how traffic moving through the major cross sections in Kobe City and Hanshin region changed in time sequence by the damage of Hyogoken Nanbu Earthquake and rehabilitation of road networks. The focus is placed on the Mukogawa littoral cross section which is located in the eastern part of the damaged areas, and the Ishiyagawa cross section which is located at the ward boarder between Higashinada-ku (ku meaning a ward) and Nada-ku, Kobe city.

As shown in Fig. 6, as of March 1995, two months after the quake disaster, the traffic volume decreased about 50% that of pre-earthquake days at the Mukogawa cross section, and down to about 40% at the Ishiyagawa cross section. Regardless of traffic restrictions to general vehicles, the traffic volume at the Mukogawa cross section recovered up to 74% of the pre-earthquake level in November 1995 because of partial restoration between Amagasaki IC and Nishinomiya IC of Meishin Expressway on April 20, 1995 and because of total restoration of Wangan (or coastal) Route on July 1. Comparison of the November and the March-to-April period shows us no radical change in the traffic volume on the general roads, indicating that the traffic volume was near capacity level of general roads, and the restoration of expressways contributed much to the recovery of suppressed automobile traffic.

On the other hand, comparison at the same time points indicates that at the Ishiyagawa cross section where no remarkable change was observed in the road network, rehabilitation of traffic volume was rather slow, and at length the traffic recovered to about 50% of the pre-earthquake level in March 1996 when the traffic restrictions were released on the Kokudo (or national highway) No. 2. However, after July 1996, when Fukae junction and its west part on Kobe Route was recovered step by step, the traffic volume gradually increased and in September of the same year, a traffic volume equivalent to 74% of the pre-seismic level was observed.

In October 1996, when Kobe Route was completely resuscitated, the Mukogawa littoral cross section recovered its traffic volume to almost the same level as before the earthquake, and the Ishiyagawa cross section recovered up to about 90% of its pre-earthquake level. Here, we can notice that, at the Mukogawa littoral cross section, the shares between expressway and general roads reversed compared with those in pre-earthquake days. This can be attributed to the promoted use of the Wangan Route because of extended service interruption of Kobe Route. On the other hand, at the Ishiyagawa cross section, the traffic volume on the expressway kept at constant level, and decreased on general roads. It is not clear why this phenomenon occurred, but it can be caused by the construction work conducted on Kokudo No. 43 after the restoration of Kobe Route, and substantial decrement of traffic demand itself.

4. Effects on Travel Time

In this section we analyze the effects of the damage to road networks on travel time between major locations. Analysis is made on the segment between Kobe municipal office and Osaka municipal office in the morning peak time (departure at 8 a.m. for the first phase and at 9 a.m. for the second phase). The traveled route was accessible by general vehicles on the examination time.

As shown in Fig. 7, in April 1995 when Kobe Route was closed at Mukogawa and westward and

general vehicles were prohibited from using Kokudo No. 2 and 43 as they were designated as the route for restoration materials transportation, the travel time for the specified segment was about two hours both for eastbound and westbound. The possible factors for this remarkable increase in the travel time may include the fact that the traveling distance was longer than before for the same origin-destination (OD) because of the restriction over general vehicles of available route which was limited to the Rinko line, Yamate trunk line and others, and the concentration of general vehicles on the limited routes.

Sharp changes were noticed in the travel time for the specified segments in March 1996 when the traffic restrictions on Kokudo No. 2 were rescinded and in August 1996 soon after the clearance of restraint on Kokudo No. 43 resulted from resumed service between Yanagihara and Fukae, Kobe Route,. In March 1996, it took 104 minutes for westbound trip and 84 minutes for eastbound indicating substantial time shortening in comparison to the data for November 1995. Further, in August 1996, the required time was 57 minutes for westbound, indicating significant improvement. However, on September 10, when the section between Tsukimiyama and Yanagihara was turned back to service, the travel time increased both in westward and eastward directions. This was because Kobe Route and No.2 Shinmei road was directly connected at Tsukimiyama, which exacerbated traffic jam around the Fukae junction. Also in October soon after overall restoration of Kobe Route, travel time was substantially improved down to 43 minutes for eastbound and 59 minutes for westbound.

5. Change in Awareness of Kobe Route Users after Overall Restoration

A "Questionnaire survey for Actual User Conditions" was conducted over Kobe Route users on Wednesday, November 13, one month after the overall restoration of Kobe Route (September 30 1996).

In this survey, 50,000 questionnaires were distributed at the Ashiya tollgate and all other tollgates westward on Kobe Route. 5,700 sheets (11%) were returned.

(1) Need for Kobe Route

About 90% answered that Kobe Route "is absolutely necessary", and about 8% answered it "is somewhat necessary", which were totaled up to about 98% of users who thought it is necessary (Fig. 8).

(2) Required time to destination after overall restoration of Kobe Route

Mean required time of 112 minutes before the overall restoration decreased by 43 minutes down to 69 minutes by the restoration, proving sharp time shortening effects. The required time to the destination of one hour to two hours amounted to about 44% falling in the mode before entire continuity, but the mode was at the time zone of 30 minutes to one hour, amounting to about 38% after overall restoration (Fig. 9).

Regarding alternative routes available to users, about 26% took Wangan Route, about 21% took Kokudo No. 2, and about 16% named Sanroku Bypass and Nishi-Kobe turnpike (Fig. 10).

The ratio of decrement in required time by alternative routes before overall restoration is as high as about 46% for Kokudo No. 2, and as about 43% for Sanroku Bypass/Nishi-Kobe turnpike (Fig. 11).

(3) Time saving benefits for Kobe Route users

Service resuming of entire Kobe Route was advanced by three months to September 30, 1996 from the original scheduled date, the end of December 1996.

This advancement of reconstruction work brought users, by trial calculation, daily time saving benefit of about 600 million yen multiplied by three months resulting in about 53 billion yen (Fig. 12).

(4) Way of restoring Kobe Route

Regarding the practical form of restored route, about 77% users answered the route should be "restored as early as possible in the original form like this", and about 14% users answered it should be "constructed underground even if it would take 10 to 15 years" (Fig. 13).

Among those respondents for "restored as early as possible in the original form like this", about 94% felt the restoration of Kobe Route is "Absolutely necessary" and about 6% answered "somewhat necessary", indicating all of them were for the necessity (Fig. 14).

(5) Impression after total service resuming of Kobe Route

About 73% respondents answered the new route was "less vibratory when driving" and about 66% answered the route was "less noisy when driving", both confessing they felt amenity. Further, about 70% answered "road information boards are more conspicuous than before", showing high evaluation on the rehabilitation work. On the other hand, only about 45% answered they felt "reliance to disaster prevention" in the expressway, indicating concern about disaster (Fig. 15).

Regarding traffic jam, about 30% answered the total resuming "highly mitigated" of traffic congestion in Hanshin region, and about 46% "somewhat mitigated", both resulting in a total of about 76% for the contribution of overall service of Kobe Route to east-west traffic between Kobe and Osaka as well as its enhancement of local environment (Fig. 16).

For changes in level of service, as many people as about 88% felt "shorter travel time". In addition, 78% believed "improved accessibility to other highways", 71% felt a "further range of destination", 72% thought their "physical fatigue relieved" and 72% thought their "mental fatigue relieved". With all these percentages being 70% or higher, the total continuity in Kobe Route was proved to have contributed to improvement of traveling ability of car trips and consequent reduction of driving load (Fig. 17).

The total service resumption made 26% think their life and job "highly improved", and 51% think "somewhat improved", amounting to about 77% in total, showing the overall rehabilitation of Kobe Route has provided some good effects (Fig. 18).

6. Conclusion

This paper analyzed and summarized the effects on the regional automobile traffic of the damage and restoration of the road network based on the result of traffic fact-finds and the result of user questionnaires implemented after the Hanshin and Awaji Great Earthquake Disaster.

The analysis allowed us to verify the restoration of road networks, especially of expressways, gave great effects on the rehabilitation of traffic demand and travel time. In addition, the comparison of Mukogawa littoral cross section between pre-earthquake and post-restoration of entire Kobe Route, revealed that the shares of the expressway and general roads reversed although the total traffic volume remains almost the same, showing changes in traffic flow due to traffic discontinuity of

Kobe Route for one year and eight months.

This report focused chiefly on the analysis of the relation between the damage and restoration of road network and the traffic situations. In the future, the focus should be placed on the qualitative change of traffic⁵⁾ as well as the effects of damage to road network on the traffic conditions for further discussion.

References

- 1) Kiyoshi Yamamura, Toru Yonekura, Yasunobu Ishizaki: "Influence Analysis of Damage and Restoration Viewed from Traffic Situations in the Hanshin region", Japan Society for Civil Engineers; Symposium of Lessons from Hanshin and Awaji Great Earthquake Disaster: Approach from Civil Engineering Planning Theory, September 1997 (in Japanese).
- 2) Yasunobu Ishizaki: "Results of Questionnaire on Real Use of Kobe Route of Hanshin Expressway", Expressway and Automobile, No. 6, Vol. 40, June 1997 (in Japanese).
- 3) Road Economy Research Room, Planning Division, Road Bureau, Ministry of Construction: "Effects on Traffic of Road Closing and Traffic Restrictions", Road Traffic and Economy, '95-7, pp.13-17 (1995) (in Japanese).
- 4) Takashi Uchida: "Nine College Joint Survey - Observation of Traffic Volume in Highways in the Damaged Areas of Hyogo Prefecture Southern Earthquake, Traffic Science, vol. 25, Nos. 1 & 2 combined issue, pp.33-38, (1996) (in Japanese).
- 5) Satoshi Fujii, Ryuichi Kitamura, Akihide Tsuge, Takehiko Daito: "Panel Analysis over Effects on Traffic Behavior of Hanshin and Awaji Great Earthquake", Minutes of Civil Engineering Planning Theory Research and Lecture, No. 19 (1), pp.17-20, (1996) (in Japanese).

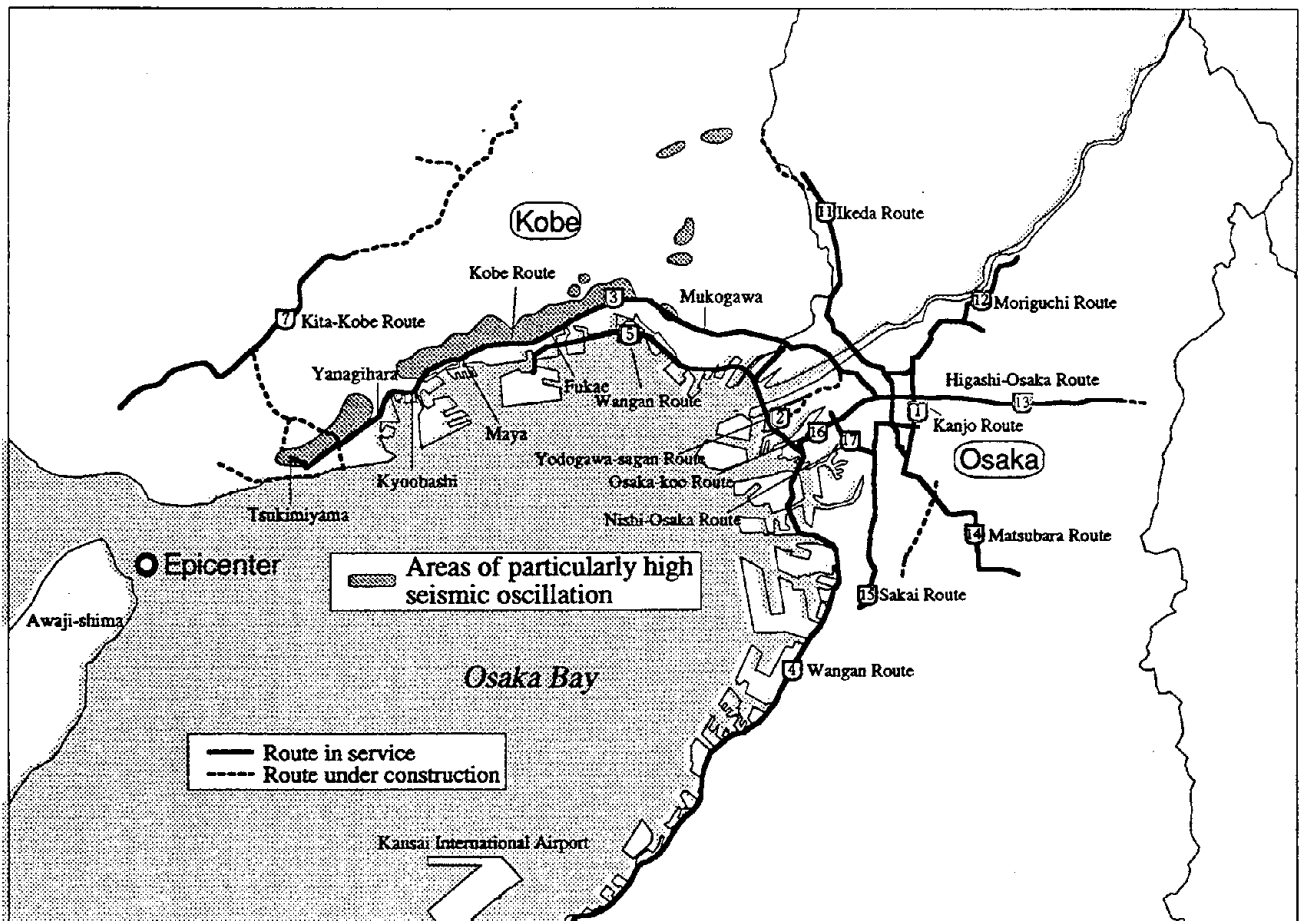
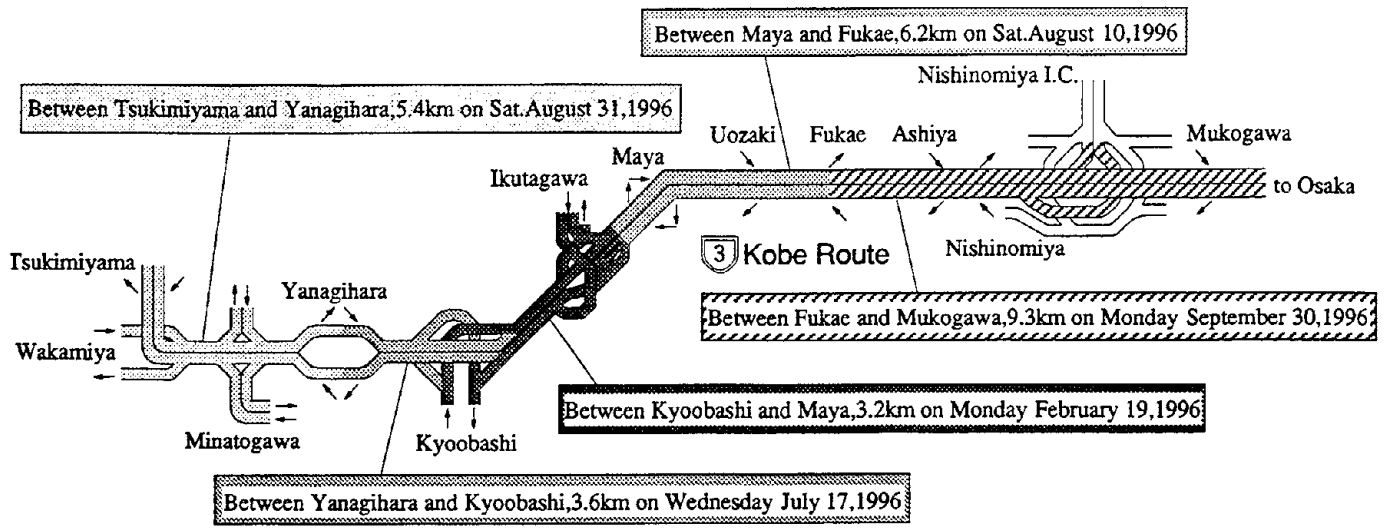


Fig.1 Footsteps of Kobe Route Restoration
220

Traffic Volume at Higashi-nada/Nada Ward
Border Cross Section, Kobe City

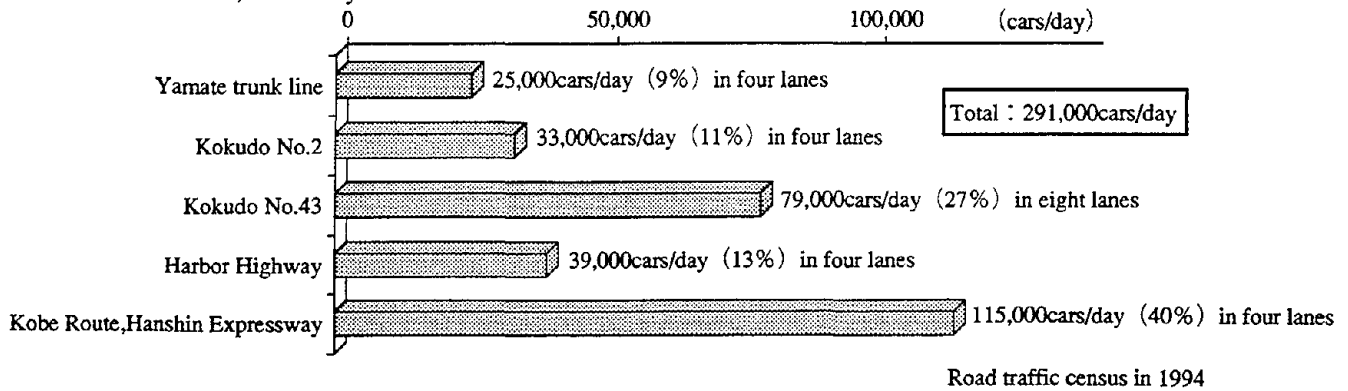


Fig.2 Percentage Share of Kobe Route in East-West Traffic Before Earthquake

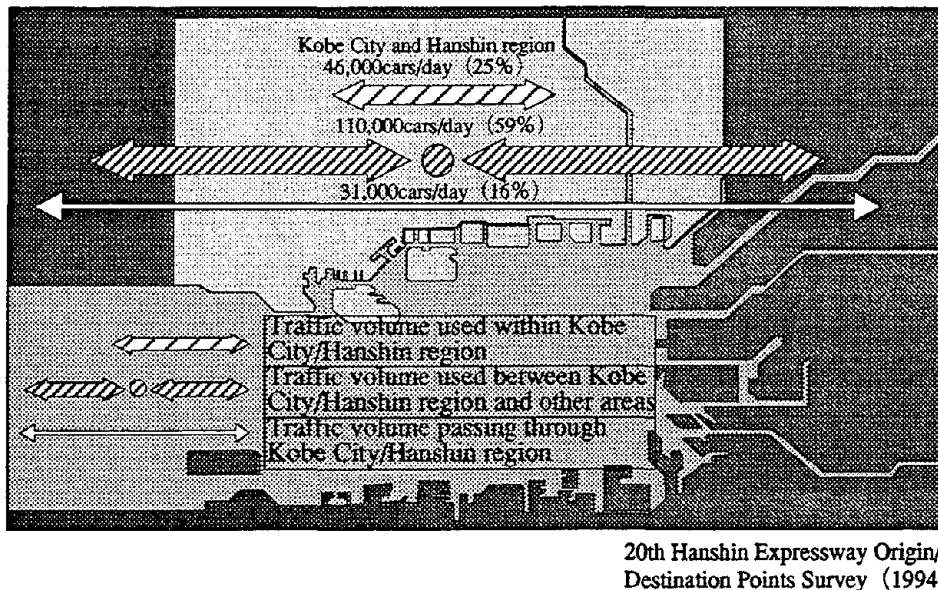


Fig.3 Origin Destination (OD) Characteristics in Pre-earthquake Kobe Route

Time saving benefit per vehicle (ca.¥2,000)	=	Value of time per minute (ca.¥80/min.)	×	Saved time per vehicle (ca.25minutes)
Annual time saving benefit (ca.¥140billion)	=	Time saving benefit per vehicle (ca.¥2,000/veh.)	×	Number of day-average user cars (ca.187,000veh./day) × 365days

Value of time:calculated from per capita national income in 1994.

Fig.4 Time Saving Benefit of Kobe Route

Name of Cross Sections	First Phase			Second Phase						
	1995			1996						
	3.8	4.19	11.8	3.6	7.10	7.24	8.21	9.11	10.2	11.6
A : Mukogawa littoral	○	○	○	○	○	○	○	○	○	○
B : Mukogawa inland	○	○	○	○	○	○	○	○	○	○
C : Ashiyagawa	○	○	○	○	○	○	○	○	○	○
D : Ishiyagawa	○	○	○	○	○	○	○	○	○	○
E : Kobe central	○	○	○	○	○	○	○	○	○	○
F : Nagata/Suma	○	○	○	○	○	○	○	○	○	○
G : Rokko mountain	○	○	○	○	○	○	○	○	○	○
H : Reclaimed islands	○	○	○	○	○	○	○	○	○	○
I : Iwaya					○	○	○	○		
J : Higashi-Kawasaki					○	○	○	○		
K : Minatogawa					○	○	○	○		

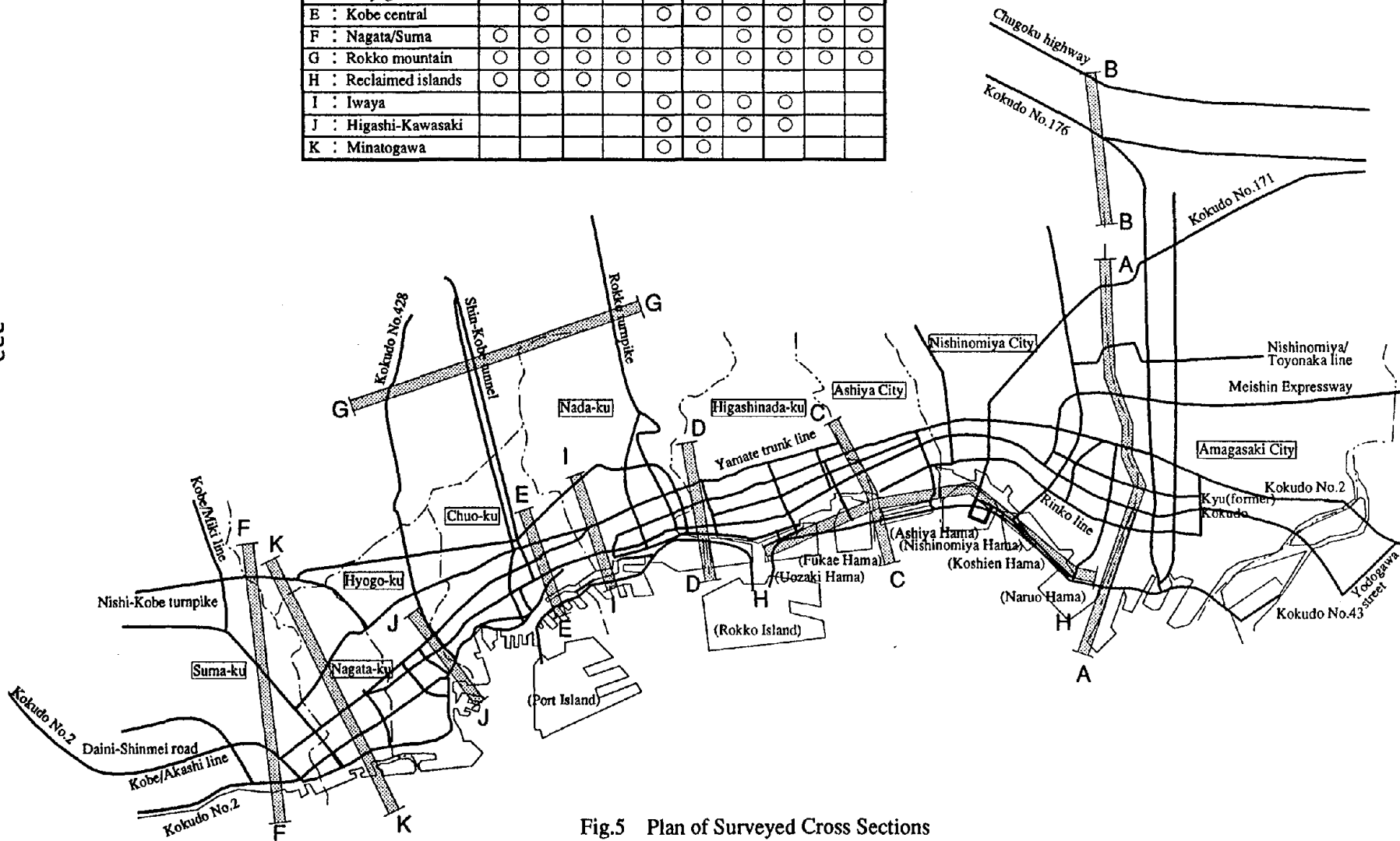


Fig.5 Plan of Surveyed Cross Sections

Table 1 Outline of Traffic Fact-find Surveys after Hanshin & Awaji Great Earthquake Disaster

Seq.	Date and time	Traffic volume	Signal indication	Traveling speed	Major closed routes	Remarks	
First phase	1	1995.3.8 (Wed)	23 points at 5 sections	14 crossing	—	<ul style="list-style-type: none"> Between Mukogawa and Tsukimiyama, Kobe Route Between Naruo-hama and Rokko Island-North, Wangan Route From Nishinomiya to Amagasaki, Meishin Expressway 	<ul style="list-style-type: none"> Traffic restrictions in Kokudo No.2 and 43
	2	4.19 (Wed)	38 points at 7 sections	11 crossing	1. Between Kobe and Osaka municipal offices 2. Between Kobe and Kakogawa municipal offices 3. Between Fukusaki IC and Suita junction (Departure at 08:00, 17:00 and 23:00)	<ul style="list-style-type: none"> Between Mukogawa and Tsukimiyama, Kobe Route Between Uozaki-hama and Rokko Island-North, Wangan Route From Nishinomiya to Amagasaki, Meishin Expressway 	<ul style="list-style-type: none"> Traffic restrictions in Kokudo No.2 and 43 JR Kobe line has entirely resumed service.
	3	11.8 (Wed)	35 points at 6 sections	11 crossing	1. Between Kobe and Osaka municipal offices (Departure at 08:00, 17:00 and 22:00)	<ul style="list-style-type: none"> Between Mukogawa and Tsukimiyama, Kobe Route 	<ul style="list-style-type: none"> Traffic restrictions in Kokudo No.2 and 43 Hankyu and Hanshin railroads have entirely resumed service.
	4	1996.3.6 (Wed)	32 points at 7 sections	17 crossing	1. Between Kobe and Osaka municipal offices 1) Via Kokudo No.2 2) Via Wangan Route (Departure at 08:00 and 17:00)	<ul style="list-style-type: none"> Between Mukogawa and Maya, Kobe Route Between Tsukimiyama and Kyoobashi, the same 	<ul style="list-style-type: none"> Traffic restrictions in Kokudo No.43
Second phase	5	7.10 (Wed)	35 points at 6 sections	13 crossing	1. Between Kobe and Osaka municipal offices 2. Between Kobe and Kakogawa municipal offices 3. Between Amagasaki West approach and Suma-rikyu (Departure at 07:00, 13:00 and 17:00)	<ul style="list-style-type: none"> Between Mukogawa and Maya, Kobe Route Between Tsukimiyama and Kyoobashi, the same 	(ditto)
	6	7.24 (Wed)	42 points at 8 sections	15 crossing	(ditto)	<ul style="list-style-type: none"> Between Mukogawa and Maya, Kobe Route Between Tsukimiyama and Yanagihara, the same 	(ditto)
	7	8.21 (Wed)	44 points at 8 sections	15 crossing	(ditto)	<ul style="list-style-type: none"> Between Mukogawa and Fukae, Kobe Route Between Tsukimiyama and Yanagihara, the same 	<ul style="list-style-type: none"> Traffic restrictions cleared in all routes and lines.
	8	9.11 (Wed)	56 points at 8 sections	18 crossing	(ditto)	<ul style="list-style-type: none"> Between Mukogawa and Fukae, Kobe Route 	
	9	10.2 (Wed)	48 points at 6 sections	16 crossing	(ditto)		
	10	11.6 (Wed)	51 points at 6 sections	16 crossing	(ditto)		

Note : Travel time survey selected those routes available to general vehicles

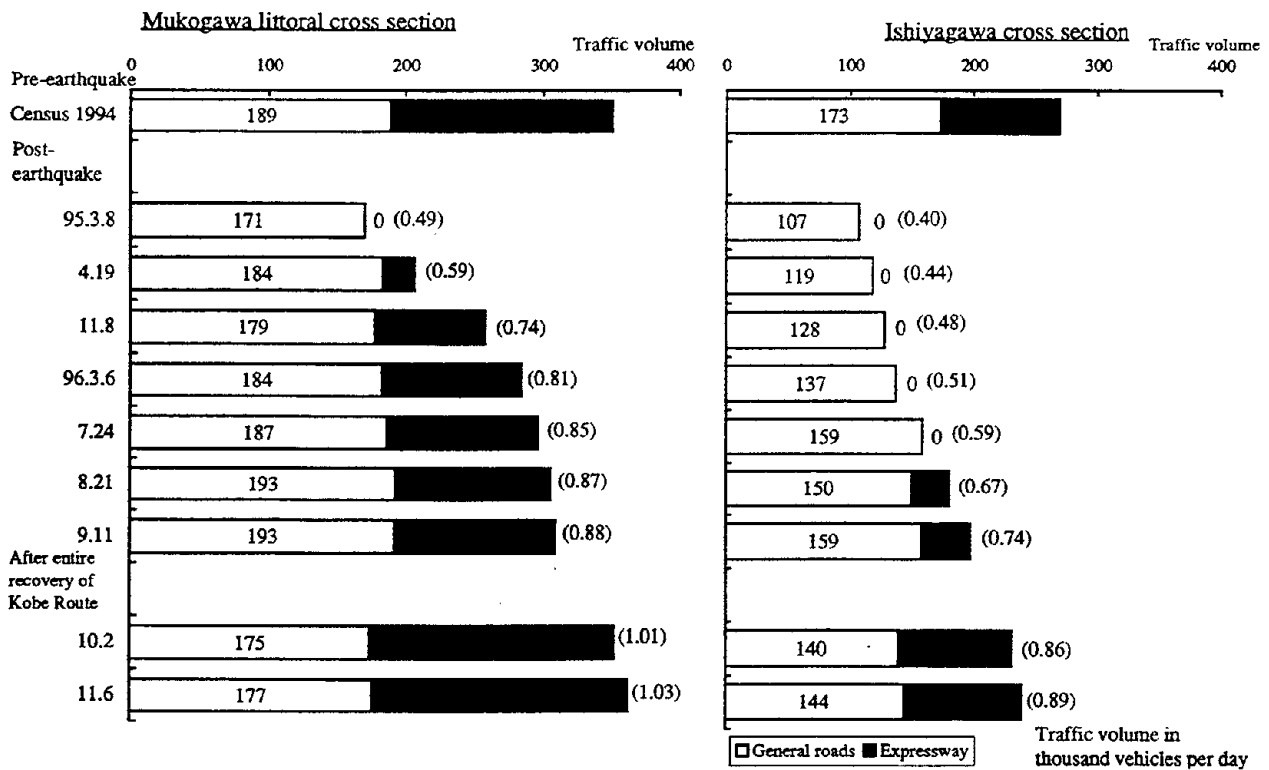
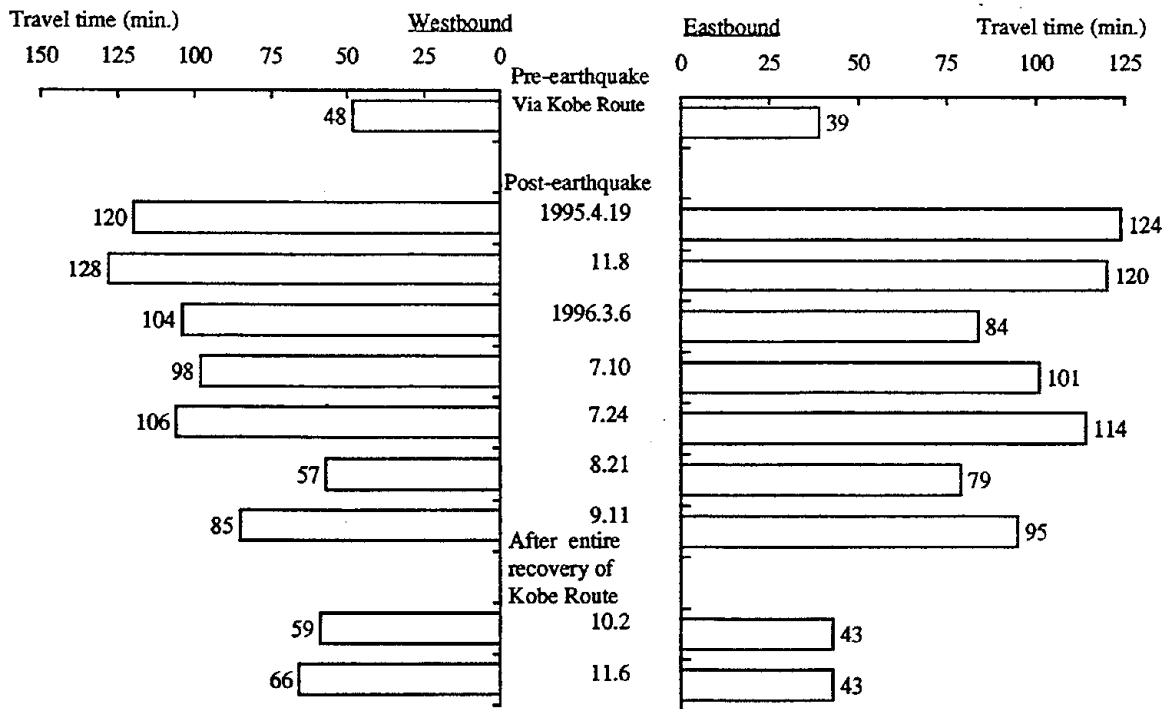


Fig.6 Change in Traffic Volume at Mukogawa Littoral and Ishiyagawa Cross Sections



Pre-earthquake survey was conducted on Wednesday April 17 1994 (Ten minutes'extra is added for access/egress time because the survey segment between Awaza and Kyoobashi was selected.)

Fig.7 Change of Travel Time (between Kobe and Osaka municipal offices in the morning peak zone)

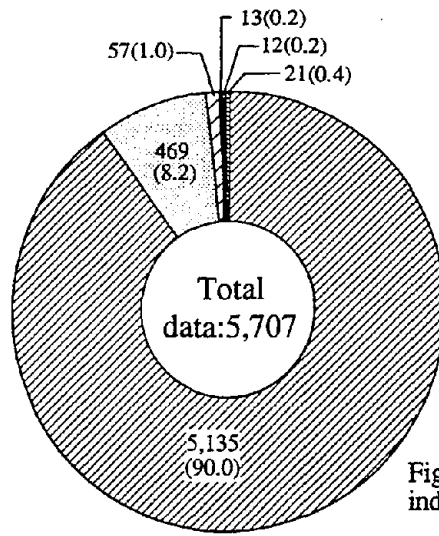


Figure in parentheses indicated in percentage

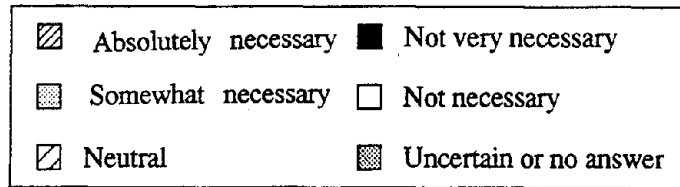


Fig.8 Necessity of Kobe Route

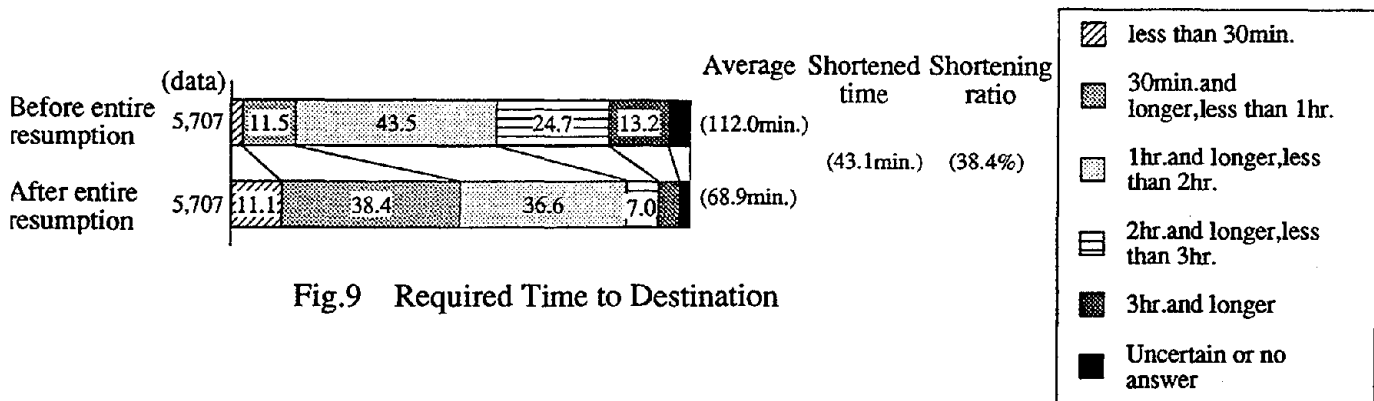


Fig.9 Required Time to Destination

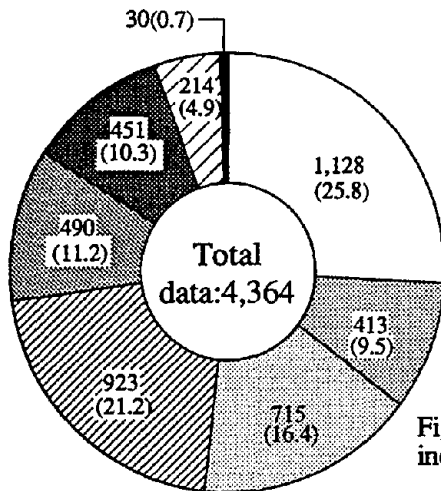


Figure in parentheses indicated in percentage

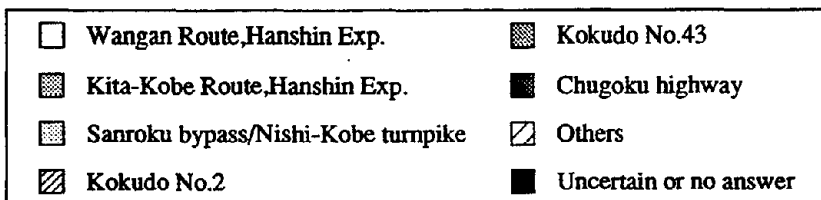
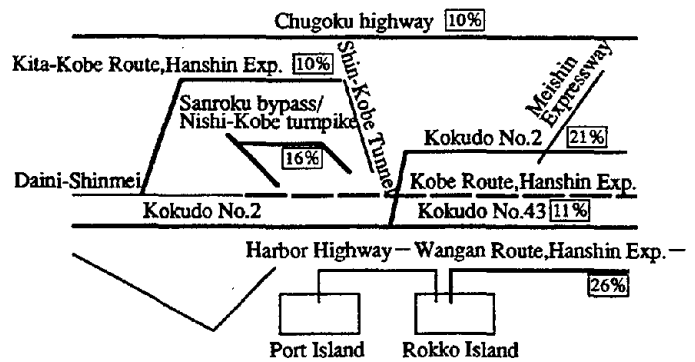


Fig.10 Alternative Routes Before Total Restoration

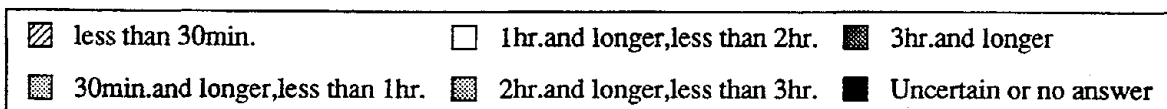
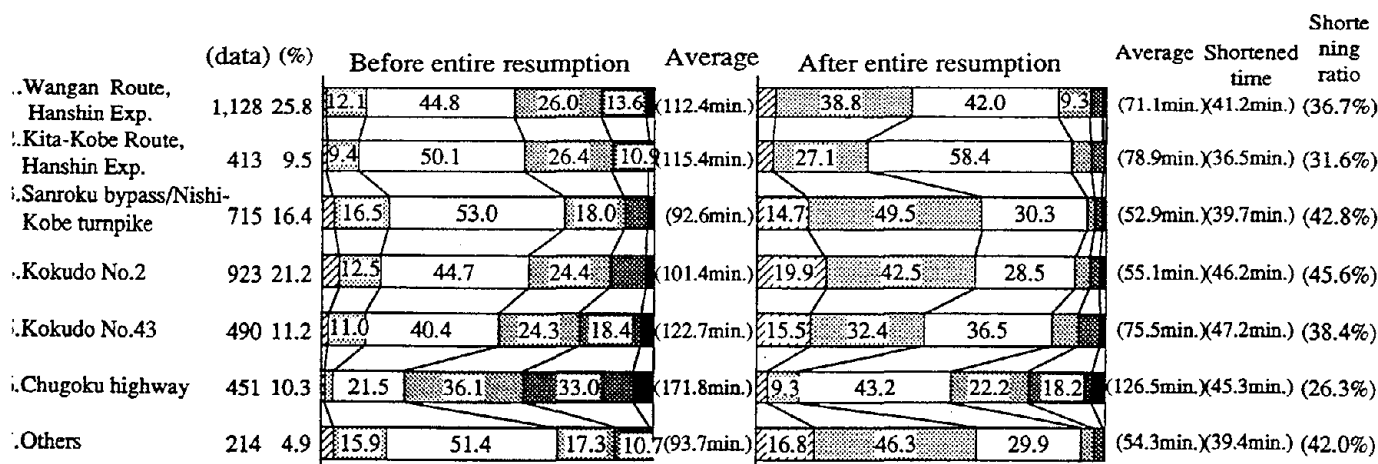
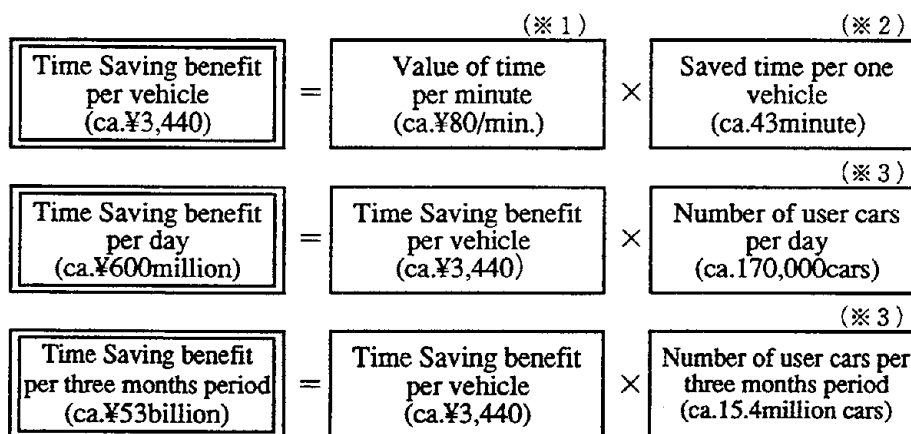


Fig.11 Required Time By Alternative Routes Before Entire Resuming



- (※ 1) Value of time:calculated from per capita national income in 1995.
- (※ 2) Saved time per vehicle:based on the results of "Fact-find Questionnaire for Kobe Route Users"
- (※ 3) Number of user vehicles after entire service resuming of Kobe Route.

	Overall user vehicles (cars)	Daily average user vehicles (cars/day)
October 1996	5,139,600	165,793
November 1996	5,045,500	168,182
December 1996	5,213,200	168,169
Total	15,398,300	167,373

Fig.12 Time Saving Benefit Owing to Advanced Restoration of Kobe Route

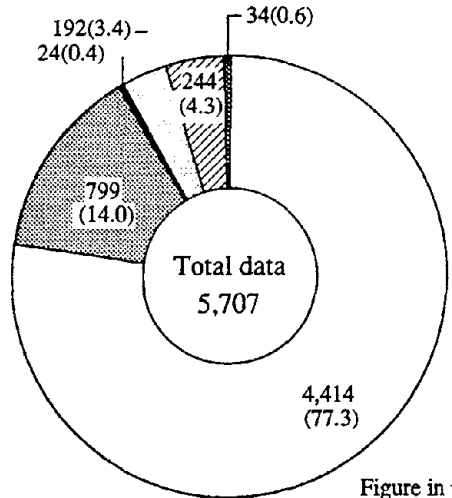


Figure in parentheses indicated in percentage

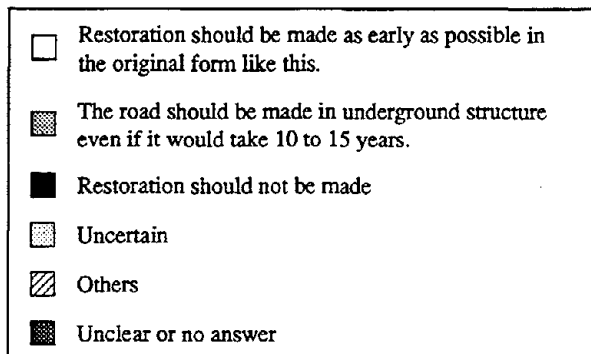


Fig.13 Restoration Manner of Kobe Route

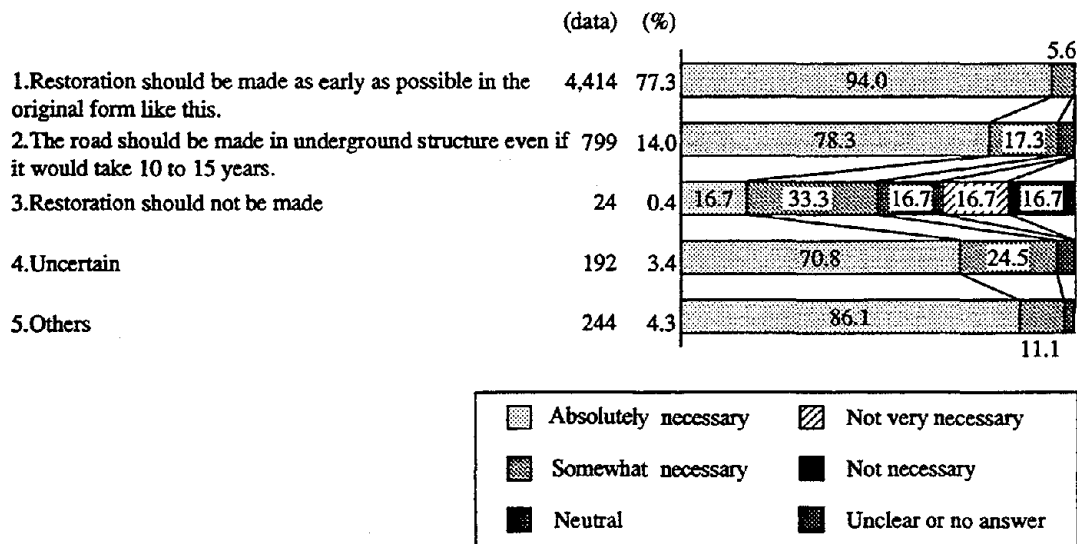


Fig.14 Necessity of Kobe Route by Restoration Manners

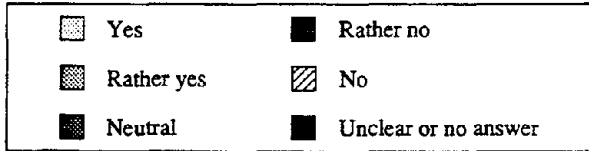
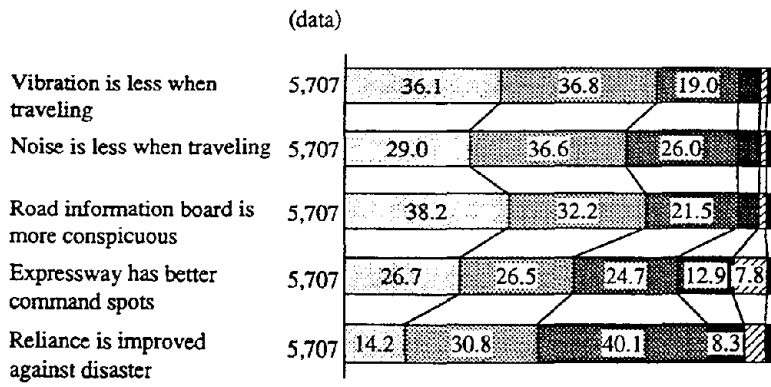


Fig.15 Impression of Kobe Route after Total Resumption

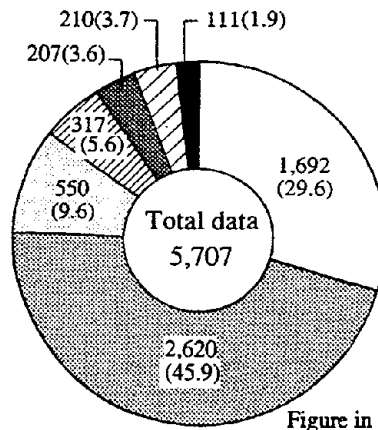


Figure in parentheses indicated in percentage

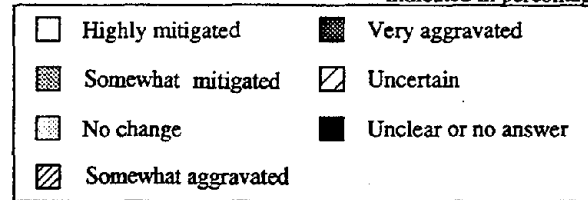


Fig.16 Traffic Congestion in Hanshin region after Total Resumption

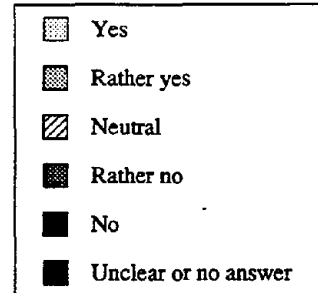
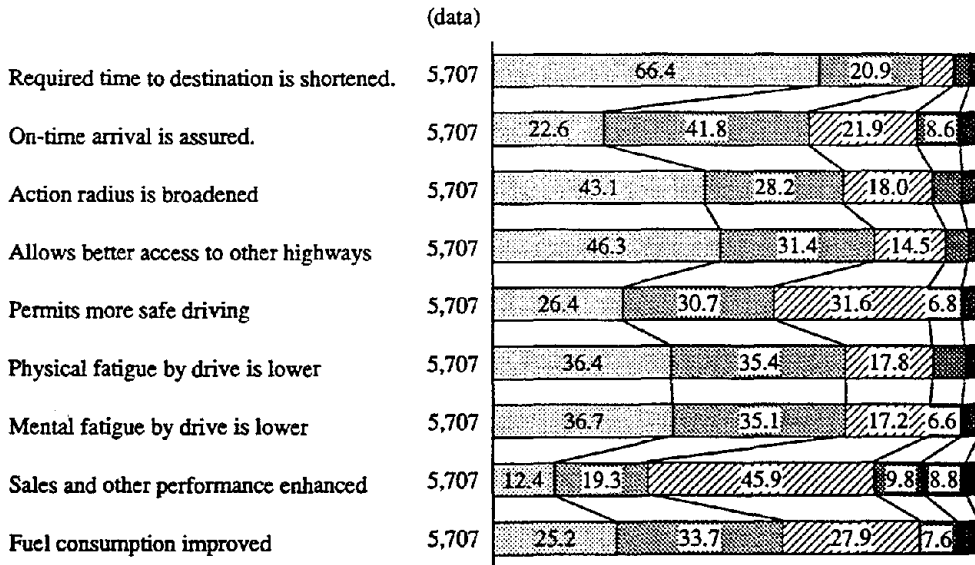


Fig.17 Change in Automobile Used owing to Entire Expressway Resumption

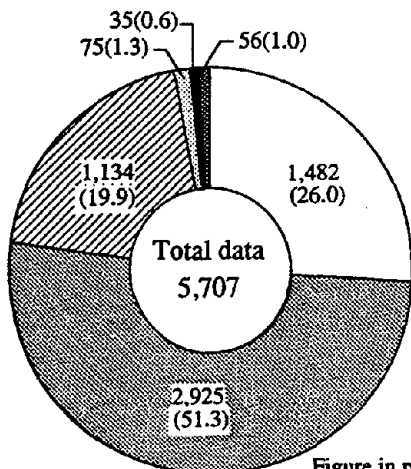


Figure in parentheses indicated in percentage

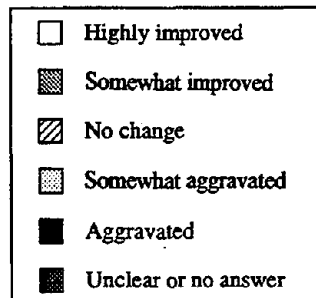


Fig.18 Changes in Life or Work owing to Entire Expressway Resumption

PERSONAL CAREER

NAME : Nobuhiko HAMADA

POSITION :

Assistant Manager,
Research Division, Planning Department,
Hanshin Expressway Public Corporation

ADDRESS :

4-1-3, Kyutaro-machi, Chuou-ku, Osaka, 541, JAPAN
(FAX : + 81-6-252-7414, TEL : + 81-6-252-8121, 3189)

PERMANENT ADDRESS :

2-3-5-407, Ayameike-minami, Nara, 631, JAPAN

E-mail : BXG00162@niftyserve.or.jp

DATE of BIRTH : May 30, 1958



EDUCATION :

Bachelor of Engineering in Civil Engineering, Kyoto University, Japan, 1981

Master of Engineering in Civil Engineering, Kyoto University, Japan, 1983

MAJOR AREA of EXPERIENCE :

1983-1988 Osaka Second & Third Construction Department
1988-1991 Design Division, Engineering Department
1991-1993 Visiting Researcher, University of California at San Diego
1993-1995 Design Division, Kobe Construction Department
1995- Planning Department

MAJOR SUBJECT and INTEREST :

Aseismic Design and Retrofit Method of Bridge, Soil Mechanics

TRAVEL ABROAD :

U.S.A., Mexico, Guatemala, Hong Kong, Australia, Malaysia, Singapore etc.

MAJOR PAPERS :

- 1) DAMAGE ASSESSMENT AND RECONSTRUCTION DESIGN OF HANSHIN EXPRESSWAY BAYSHORE "WANGAN" ROUTE, 11th U.S.-JAPAN BRIDGE WORKSHOP, May 1995, Tsukuba
- 2) RETROFIT OF BRIDGE FOOTINGS FOR IMPROVED SEISMIC PERFORMANCE, 9th U.S.-JAPAN BRIDGE WORKSHOP, May 1993, Tsukuba
- 3) ROCKING AND CAPACITY TEST OF MODEL BRIDGE PIER, Third NSF Workshop on BRIDGE ENGINEERING RESEARCH IN PROGRESS, November 1992, La Jolla

RELIABILITY AND RESTORATION OF WATER SUPPLY SYSTEMS FOR FIRE SUPPRESSION AND DRINKING FOLLOWING EARTHQUAKES

Donald Ballantyne, PE
EQE International, Seattle, Washington

ABSTRACT

This paper summarizes the report entitled "*Reliability and Restoration of Water Supply Systems for Fire Suppression and Drinking Following Earthquakes*", prepared for the National Institute of Standards and Technology (Ballantyne and Crouse, 1997). Elements of the report summarized in the paper include:

- Mutual Needs of Water and Fire Departments,
- Performance of Water Systems in Historic Earthquakes and Other Hazard Events
- Earthquake Hazards
- Post-Earthquake Performance Criteria
- System Component Damage, including Pipelines, Reservoirs, Treatment Plants, and Pump Stations
- Reliability Analyses
- Mitigation Alternatives
- Conclusions and Recommendations

OVERVIEW

Following the 1989 Loma Prieta and 1994 Northridge earthquakes in California, and the 1995 Kobe, Japan earthquake, major system water supply was lost for fire suppression and for domestic use. None of these recent events turned out to be as catastrophic as the fire storms following the 1906 San Francisco, California, and 1923 Kanto, Japan, earthquakes. The classic scenario occurred in the Loma Prieta, Northridge, and Kobe earthquakes where pipelines in both the transmission and distribution system failed. Reservoirs drained, and there was no water available for fire suppression or domestic use.

The report helps quantify the problem of water system reliability. It identifies system and component failure in historic events, and summarizes the results. Vulnerability evaluation techniques are developed for pipelines and reservoirs. Mitigation measures for system and components are discussed along with other alternatives such as developing alternative water supplies, optimizing system control, and use of geographic information systems (GIS).

The report, and the associated project is the result of recommendations from the Post-Earthquake Fire and Lifeline Workshop held in Long Beach, California, January 30 - 31, 1995. It includes research to assess earthquake reliability of municipal water supplies focusing on water for fire suppression. It considers experience from previous earthquakes, overall system operation, and performance of individual system components. Component and system failure mechanisms are addressed, and mitigation approaches identified and developed.

MUTUAL NEEDS OF WATER AND FIRE DEPARTMENTS

Fire departments and water purveyors are in many cases not part of the same governmental jurisdiction. However, fire departments are highly dependent on adequate water supplies to function effectively. Large fires reaching conflagration proportions have become common place. In many instances, water supply to meet large fire flow demands is insufficient, and liaison between water agencies and fire departments is poor or ineffective.

Legal and financial authorization governing the raising of capital to pay for facilities can be inconsistent with fire department needs. It is common for state regulations to require minimum fire flows for new facilities. As fire flow demands change, it may be difficult for water agencies to legally justify charging rate payers to build facilities to enhance fire flows.

Coordination between water and fire agencies must take place during pre-event planning, and should include operational procedures and priorities. Fire departments should attain a good working knowledge of the water system they use, and understand the earthquake vulnerability of that system.

PERFORMANCE OF WATER SYSTEMS IN HISTORIC EARTHQUAKES AND OTHER HAZARD EVENTS

Historic performance of water systems in earthquakes, as well as two instances of non-earthquake-related water system failures were reviewed to identify earthquake deficiencies that repeatedly occur, resulting in dysfunction of water systems. Hazard events reviewed include:

1. Key earthquakes - Kobe, Japan, 1995, Northridge, California, 1994, and Loma Prieta, California, 1989, earthquakes.
2. Less destructive earthquakes that caused water system damage - Landers/Big Bear, California, 1992, Cape Mendocino, (Petrolia), California, 1992, and Whittier, California, 1987, earthquakes.
3. Historic devastating earthquakes - Kanto, Japan, 1923, and San Francisco, California, 1906.
4. Potable water system outage from other natural disasters - Des Moines, Iowa, Flood, 1993, 12 days water outage resulting from flooding of a water treatment plant, and Oakland, California, Hills Fire, 1991, exacerbated by inadequate water supply for conditions.

These hazard events are summarized in Table 1, where ratings are shown (5-high; 1-low) for system failure consequences, and system component failures for each event.

There is a correlation between incidents where there was inadequate water for fire suppression, and where fire became a significant issue. The only two events where fire was a small or non-issue were Whittier, which was a relatively small earthquake, and Landers, where there is a sparse population and building density. There is also a strong correlation between the three most significant fires, San Francisco in 1906, Kanto, and Kobe, and the ineffective use/unavailability of an alternate water supply. System component failures can be grouped by significance of impact on system dysfunction as follows:

- Very High Impact - Pipe damage due to permanent ground deformation (PGD).
- High Impact - Pipe damage due to wave propagation and raw water transmission pipeline failure.
- Moderate Impact - Water treatment plant damage, loss of power, and tank inlet/outlet pipe damage.
- Low Impact - Tank shell/structure damage, surface supply failure, and well casing and equipment damage.

We conclude that pipeline damage due to PGD and wave propagation, in both transmission and distribution systems, had the greatest impact in most of these events.

EARTHQUAKES HAZARDS

Fault rupture results in earthquakes with a magnitude (measure of energy release), and site-specific intensity. Fault offsets can also cause tsunamis. Fault rupture may also result in PGD.

Ground motion, one measure of earthquake intensity, is often measured in terms of peak ground acceleration (PGA). Earthquake shaking intensity can be estimated deterministically or probabilistically. A deterministic ground motion estimate is based on a given earthquake scenario. Probabilistic estimates are often developed for “standard” return periods. Commonly used nomenclature and return periods are: operating basis earthquake (OBE) has a 72 year return period (50% chance of exceedance in 50 years), and a design basis earthquake (DBE) has a 475 year return period (10% chance of exceedance in 50 years).

Earthquake shaking can result in liquefaction, lateral spread resulting in PGD, and landslides that can be particularly damaging to buried water system components. Bartlett and Youd (1995) developed the multiple linear regression analysis (MLR) which has gained wide-spread acceptance for estimating PGD affecting buried pipelines.

POST-EARTHQUAKE PERFORMANCE CRITERIA

Performance criteria is needed to define the desired level of post-earthquake service. It ties five categories of water system performance to the probability of the defined earthquake ground motion being exceeded. OBE and DBE are set as reference points. Proposed post-earthquake performance criteria for these two probabilities are shown in Table 2.

SYSTEM COMPONENT DAMAGE

Damage to the key water system components including pipelines, reservoirs, treatment plants, and pump stations has resulted in water system failures.

Pipelines

The Northridge earthquake caused 1,500 pipeline failure in the Los Angeles system. The Kobe earthquake caused 1,600 distribution system failures. In both earthquakes, systems were quickly drained through damaged pipe, rendering the systems dysfunctional in many locations. Pipe joint damage is predominant for large diameter segmented pipe. For smaller diameter pipe, pipe barrels fail in addition to joint damage. Welded steel pipe damage sometimes fails due to localized wrinkling from compression, often concentrated at welded joints.

Analytical techniques have been developed to assess both continuous (welded joint) and segmented (bell and spigot joint) pipelines (Harding Lawson, 1991). PGD, often due to liquefaction/lateral spread, is the usual cause of damage to continuous welded steel pipelines. The steel's ductility helps minimize pipe damage due to wave propagation. Brittle segmented pipe with rigid joints, such as cast iron with leaded joints, is one of the most vulnerable segmented pipe systems, and is vulnerable to both wave propagation and PGD (Elhadi and O'Rourke, 1990). Use of ductile materials such as ductile iron, and joint restraint, greatly enhances pipe earthquake performance. Relationships between earthquake intensity parameters such as peak ground velocity and PGD, and unit failure rates have been developed for a variety of pipe materials, based primarily on empirical data. These relationships can be used to estimate pipeline damage for given earthquake scenarios. Damage estimates can be further used to predict water system hydraulic performance.

Reservoirs

Flat bottomed vertical steel water storage reservoirs (tanks) have been damaged in numerous earthquakes. The most common failure mechanism is damaged connection piping. This occurs when unanchored tanks rock, and inlet/outlet piping, rigidly attached to the tank and buried in the ground, breaks. In more severe cases, the tanks themselves are damaged. The tank wall lifts off the ground when the tank rocks. The tank wall then impacts the ground when the tank rocks in the opposite direction, causing severe compression loading, and results in wall buckling. This phenomena is often refereed to as elephants foot buckling. Steel tank damage mitigation methods include addition of connecting pipe flexibility, and anchoring the tank to its foundation. On occasion, the tank structure must be strengthened to accommodate seismic loading.

Wire-wrapped concrete tanks are less vulnerable to earthquakes than steel tanks, but have failed. Tanks that were constructed prior to use of "earthquake cables" used in current designs, are the most vulnerable. Corrosion of the wire wrapping is also a concern.

The American Water Works Association tank design standards incorporate seismic design methods (AWWA, 1985). Other analytical methods for analysis of existing tanks have been developed based on historic earthquake performance data.

Manos (1986) proposed tank evaluation method based on empirical data that was less conservative to be used for tank upgrades. Compared with AWWA for 11 tanks in the Landers and Northridge earthquakes. AWWA predicted 5 correct, and predicted 6 would suffer shell buckling, when they did not. Manos predicted 9 correct, and 2 incorrect; 1 predicted it would fail and didn't, and 1 predicted it would not fail and it did.

Treatment Plants and Pump Stations

Water treatment plants and pump stations have common earthquake failure mechanisms including damage to: foundations, process tanks, equipment and piping, electrical power systems, and building structures (Ballantyne, 1994). Tank structures and large conduits are subject to differential settlement, increased lateral soil pressures, and flotation. Reinforced concrete process tanks have performed well in earthquakes, but immersed elements such as tank baffles are commonly damaged due to earthquake induced hydraulic loading.

Buried yard piping is vulnerable to differential settlement. Inadequate braced plant piping can break due to differential movement, and depending on its contents and location, flood pipe galleries. Pipe flexibility can enhance earthquake performance. Anchored equipment, including office and lab equipment, seldom fails. Loss of power is the most common failure mechanism. Emergency generators are recommended if continuous operation is crucial.

RELIABILITY ANALYSES

There are a variety of approaches that have been used to assess post-earthquake water system reliability. Often, more than one of these approaches are used for a system evaluation.

- Conduct deterministic assessments of each water system component and use the component assessment results to develop a system performance scenario. Typically, three steps are involved. First, the seismic hazards are defined. Based on the seismic hazards and component characteristics, component vulnerability is then determined. The final step is use the component vulnerabilities to predict overall system performance.
- Express component vulnerability in probabilistic terms and use probabilistic techniques to evaluate system reliability. There is a significant amount of uncertainty associated with earthquake hazards and the response of facilities subjected to earthquake hazards. Although accurately modeling this uncertainty is difficult, probabilistic assessments can be used to assess the magnitude and likelihood of variations from the expected outcome.
- Use of system reliability assessment techniques such as fault tree analysis. Although fault trees have been used extensively in many applications such as the nuclear industry, fault trees have not been used as extensively by water utilities. Fault trees can be used to calculate failure probabilities, identify paths that may lead to failure, and to identify those events that are most likely to lead to failure.
- GIS, allows calculation and graphic presentation of system risk assessment results that can be easily used and interpreted by planners, emergency response personnel and engineers (Heubach, 1996). Pipeline construction materials and joint types can be electronically overlaid on the earthquake hazards. Damage algorithms, that relate pipe damage to ground shaking intensity and permanent ground displacement, can be used to determine pipe vulnerability using the GIS. Pipe criticality can be determined, and considered in the risk assessment determination.

MITIGATION ALTERNATIVES

There are a range of mitigation strategies that can be used to maintain or quickly restore water service following an earthquake.

Improve fire/water department communication. The objective is to overcome jurisdictional and institutional barriers to optimize water/fire department emergency operations.

Improve system hardware so it does not fail. Examples include replacing pipe, upgrading reservoirs, and providing emergency power. Improvement programs can be prioritized considering the importance of each component in operation of the overall system, and the desired performance objectives. Table 3 presents an approach for combining component vulnerability and criticality to prioritize mitigation projects (Kennedy/Jenks Consultants, et al, 1995). Vulnerability considers the probability of the hazard occurrence (and associated intensity), and the likelihood the component will become inoperable. Criticality or importance considers availability of redundant components and/or percent of the system capacity the component provides.

Provide post-earthquake system monitoring and control. Use it to isolate damaged sections of the system, so as to allow operation of other undamaged sections. Distribution system piping is vulnerable to earthquakes, and expensive to replace with piping resistant to seismic activity. Systems to monitor post-earthquake system performance, and isolate damaged sections can optimize overall post-earthquake system function. Table 4 lists systems which monitor: 1) seismic hazard parameters, 2) structural component/ soil parameters, and 3) system operational parameters.

Develop alternative sources/supplies such as those dedicated to fire protection. Provision of operational flexibility may provide the best opportunity of being able to provide post-earthquake service. Alternative water supplies to provide water for fire suppression can include: dedicated fire protection systems, portable water supply systems, cisterns distributed throughout the service area, planned use of swimming pools and/or other recreational water-containing facilities, and the planned and tested ability to draft water from local water bodies.

Further develop GIS applications. Use GIS as a tool to identify areas of water systems vulnerable to earthquakes, for use by fire suppression response personnel and engineers responsible for system earthquake mitigation. GIS can be used to map earthquake hazards and pipeline inventory. Vulnerability and criticality assessments can be performed within the GIS, and results effectively presented graphically to decision makers.

CONCLUSIONS AND RECOMMENDATIONS

From this study we conclude the following:

- Immediate post-earthquake water system function is crucial, particularly to suppress fires.
- Water system vulnerability must be understood by both water and fire departments so they can effectively plan for post earthquake response and restoration. Communication between fire and water departments becomes critical.

- Transmission and distribution pipeline damage has been the key element causing water systems to fail in historic earthquakes.
- An important initial step in developing a mitigation program is to define post earthquake performance criteria.
- Water system reliability can be assessed using deterministic, probabilistic, fault tree, and/or GIS techniques.
- Detailed evaluation methods are available for pipelines, reservoirs, and other system components.

Recommended mitigation strategies include:

- Improve the fire and water departments' understanding of the earthquake vulnerability of water systems, and enhance communication between the two organizations.
- Upgrade system hardware, prioritized considering the criticality and vulnerability of each component.
- Provide post-earthquake system monitoring and control to allow rapid isolation of damaged sections of the system.
- Develop alternative sources/supplies of water for fire suppression.
- Use GIS. It is a powerful tool, effective in performing earthquake mitigation programs, and responding to and recovering from earthquake events.

ACKNOWLEDGEMENTS

The author and project team gratefully acknowledge support from Dr. Riley Chung, representing the National Institute of Standards and Technology. Project investigators included:

D. Ballantyne – Co-Principal Investigator
 C.B. Crouse – Co-Principal Investigator
 N. Basoz
 F. Blackburn
 J. Eiding
 W. Heubach
 A. Kiremidjian
 A. Nissar
 M. O'Rourke
 C.R. Scawthorn
 P. Summers

SELECTED REFERENCES

American Water Works Association, 1985, ANSI/AWWA D100-84, *AWWA Standard for Welded Steel Tanks for Water Storage*.

Ballantyne, D.B., 1994, *Minimizing Earthquake Damage, A Guide for Water Utilities*, American Water Works Association, Denver, Colorado.

Ballantyne, D.B., and Crouse, C.B., 1997, *Reliability and Restoration of Water Supply Systems for Fire Suppression and Drinking Following Earthquakes*, prepared for the National Institute of Standards and Technology, R. Chung, program manager, in press.

Bartlett, S.F., and Youd, T.L., 1995, Empirical Prediction of Liquefaction-Induced Lateral Spread, *Journal of Geotechnical Engineering*, ASCE, v. 121, no. 4, p 316-329.

Elhmadi, K., and O'Rourke, M.J., 1990, Seismic Damage to Segmented Buried Pipelines, *Earthquake Engineering and Structural Dynamics*, v. 19, p. 529-539, May.

Harding Lawson Assoc., Dames & Moore, Kennedy/Jenks/Chilton, EQE Engineering, 1991, *Final Report, Liquefaction Study Marina District and Sullivan Marsh Area, San Francisco, CA*. Prepared for the City and County of San Francisco, Department of Public Works.

Heubach, W.F., 1996, Seismic Vulnerability Assessment of the Bellevue, Washington Water Pipeline System, Engineering and Construction Conference Proceedings, American Water Works Association, March.

Kennedy/Jenks Consultants in association with Dames & Moore, and William Lettis & Associates, 1995. *Integrated System Reliability Study*, prepared for the Marin Municipal Water District, Corte Madera, California, San Francisco, California.

Manos, G.W., 1986, Earthquake Tank Wall Stability of Unanchored Tanks, *Journal of Structural Engineering*, ASCE, v 112, no. 8, August, p 1863-1880.

Table 1
Summary - Performance of Water Systems in Earthquakes

Disaster Event	Year	Failure				System Component Failure										
		Consequences				Supply/Treatment				Tank		Pipe				
		Fire Suppression/ Lacked Water Supply	Fire	Used Alt. Supply	Cooling Telephone CO's and Computers	Surface Supply Failure	Raw Water Transmission	WTP Damage	Well Casing/ Equipment Damage	Loss of Power	Shell/Structure	Inlet/Outlet Pipe	PGD (lateral spread, landslide, fault offset)	Wave Propagation	Building Services	
Earthquakes																
San Francisco	1906	5	5	5	na	2	5	na	na	1	1	1	5	3	5	
Kanto	1923	5	5	5	na	4	5	3	1	1	1	1	5?	3?	5	
Whittier	1987	3	1	3	na	1	1	1	1	4	3	4	5?	3?	1	
Loma Prieta (San Francisco, EBMUD only)	1989	4	4	1	1	1	3	1	na	1	1	na	5	3	3	
Landers/Big Bear	1992	5	1	na	na	1	na	na	1	3	3	4	5	5	1	
Cape Mendecino	1993	5	3	1	na	1	na	na	na	1	1	1	5?	3?	1	
Northridge	1994	5	4	5	4	1	5	3	na	4	3	5	5	5	1	
Kobe	1995	5	5	3	?	1	5	3	na	3	1	2	5	5	5	
Other Disasters																
Oakland Hills Fire	1991	4	5	2	na	na	na	1	na	4	na	na	na	na	5	
Des Moines Flood	1993	5	3	2	4	1	1	5	na	4	1	1	2	1	1	
Average		4.6	3.6	3.0	3.0	1.4	3.6	2.4	1.0	2.6	1.7	2.4	4.7	3.4	2.8	

Table 2
Water Performance Objectives -
Acceptable Adverse Consequence Levels For Two Earthquake Levels

Performance Category	Acceptable Adverse Consequences	
	OBE (50% chance in 50 years)	DBE (10% chance in 50 years)
Life Safety	Minimal - Injury or loss of life are not acceptable consequences	Minimal - Injury or loss of life are not acceptable consequences
Fire Suppression	Minimal - With the exception of small isolated areas that are not densely populated, water for fire suppression should be available for entire service area.	Moderate - Water for fire suppression should be available for a minimum of 70% of the service area including all industrial areas and densely populated business and residential areas.
Public Health	Low - Water should be available for all but a few isolated areas. Boil water order acceptable for up to 48 hours.	Moderate - Provide service for at least 50% of system. Boil water order, or delivery by tanker truck acceptable. Restore 100% service in 1 week.
System Restoration	Low - Water should be available for all but a few isolated areas.	Moderate - Service should be available for at least 50% of system. Restoration to 100% service within one week.
Property Damage	Low - Any damage should not affect facility functionality and should be repairable.	Moderate - 100% loss of nonessential facilities acceptable if not cost-effective to upgrade, and other performance objectives are met.

Table 3
Risk Analysis Matrix Showing Seismic Retrofit

Overall Criticality Rating (5 is most critical)	Seismic Vulnerability Rating as Measured by Seismic Performance Estimate (5 is most vulnerable; A is highest priority)				
	5	4	3	2	1
5	A	A	B	C	Acceptable
4	A	B	C	D	Acceptable
3	B	C	D	Acceptable	Acceptable
2	C	D	Acceptable	Acceptable	Acceptable
1	Acceptable	Acceptable	Acceptable	Acceptable	Acceptable

TABLE 4
Examples of Lifeline Monitoring and Control Systems

Seismic Hazard Parameters	Structural Component/ Soil Parameters	System Operational Parameters
Water Reservoirs - earthquake valves close on PGA threshold exceedance	Water Pipe Joint Displacement – using strain gauges	Water Systems – control system on pressure, flow, rate of change of flow, or mass balance between points
Natural Gas - Transmission system and individual service shutdown on PGA threshold exceedance	Tokyo Water – tunnel monitored with strain gauges	Power and Communications – control system based on voltage, load
Electric Power - shut down services to control fire ignition source on re-energizing	Tokyo Gas – in-situ liquefaction monitoring	Natural Gas and Oil Transmission Systems – shut down on excess flow or pressure reduction
Trains – US & Japan – shut down power on PGA threshold exceedance	Building and Bridge Structures – strain gauges	Transportation – monitor traffic with video camera allowing quick dispatch of emergency equipment

DONALD B. BALLANTYNE

Position:

Senior Consultant (1995-present)
EQE International, Inc.

Address:

1411 4th Avenue, Suite 500
Seattle, Washington 98101, USA
tel. (206)623-7232
fax (206)470-4145
email: dbballantyne@eqe.com



Date of birth:

October 9, 1952

Education:

1977	M.S. (Civil/Sanitary Engineer)	SUNY at Buffalo
1974	B.S. (Civil Engineering)	Rensselaer Polytechnic Institute

Major subject:

Water system reliability

Experience:

1995-Present	Senior Consultant, EQE International, Inc. (Seattle, Wash.)
1994-1995	Associate, Dames & Moore (Seattle, Wash.)
1980-1994	Senior Consultant, Kennedy/Jenks Consultants (Seattle, Wash. & San Francisco, Calif.)
1979-1980	Project Engineer, EQSI (Rockville, Maryland)
1974-1979	Project Engineer, E.R. Cotton Associates (Gowanda, New York)

Travel abroad:

Japan, Philippines, Turkey, Costa Rica, Israel, New Zealand

Major publications:

The January 17, 1995 Hyogoken-Nanbu (Kobe) Earthquake - Performance of Structures, Lifelines, and Fire Protection Systems, chapter titled "Performance of Lifeline Systems", National Institute of Standards and Technology, 1996.

National Center for Earthquake Engineering Research, *The Hanshin-Awaji Earthquake of January 17, 1995 Performance of Lifelines*. Chapter 8 "Water and Wastewater."

"An Overview of Lifeline Earthquake Engineering of Water and Wastewater Systems, Focusing on the Pacific Northwest", *Proceedings of the American Public Works Association National Conference*, Seattle, WA, April 1995.

"Estimation of System Reliability for Lifeline Standards and Example Using the City of Everett, Washington, Lifelines," *Proceedings of the 4th U.S.-Japan Workshop on Earthquake Disaster Prevention for Lifeline Systems*, August 19-21, 1991, Los Angeles, California.

**INTEGRATED EVALUATION OF RISKS AND VULNERABILITIES FOR THE
WATER SYSTEM AT PORTLAND, OREGON INCLUDING NATURAL AND HUMAN
CAUSED HAZARDS**

William M. Elliott, P.E.

Senior Engineer
Portland Bureau of Water Works
1120 SW Fifth Avenue
Portland, Oregon 97204-1926

ABSTRACT

The Portland Water Bureau is a municipal water supply entity in the State of Oregon located at the confluence of the Columbia and Willamette Rivers. The Portland water system serves a population of nearly 1.2 million in 3 counties that make up the Portland Metropolitan Area. A study is about to begin that will evaluate the risks and vulnerabilities to the water supply and delivery system. Concerns for seismic risk will be considered along with all other risks including natural hazards and human caused hazards so that a clear picture of overall system vulnerability is possible. This paper presents the background and general approach that will be taken in this study and how it relates to other integrated planning efforts currently underway.

INTRODUCTION

Water Supply Facilities

The municipal water supply for the City of Portland, Oregon includes a forested watershed, long pipelines and terminal reservoirs. In addition there is a groundwater system developed to provide emergency backup and peaking supplies. The primary source for the water system is the entire watershed of the Bull Run River including 102 sq. miles (265 sq. km) that is closed to entry and mostly owned by the Federal Government. The City operates 2 major dams in the watershed, each about 120 ft. (36 meters) high. Total storage available is 60,000 acre feet (74 million cubic meters) of which 45,000 acre feet (55.5 million cubic meters) is available for use. Hydro Electric power facilities exist for the generation of electricity at both dams under strict controls that preclude draw down of the reservoirs. From the Headworks facilities below the dams, there are three large pipelines ranging in size from 48 to 60 inches (1200 to 1500 mm), each 25 miles (40 km) long. These three pipelines deliver an average annual demand of 140 MGD (6.1 cubic meters per second) to the Portland Metropolitan Area.

In addition to the surface water supply, Portland maintains an emergency backup system of 22 wells, collection mains and a pump station for use during emergencies and occasional peaking needs. A terminal reservoir receives surface water and groundwater for blending. The reservoir is 50 million gallons in size (189,500 cubic meters) and is the key storage for gravity supply to the majority of customers.

Regional Water Supply

The municipal system serves the majority of the Metropolitan area including the residents of Portland (456,000) and water providers receiving wholesale service (319,000) for over 750,000 population total served.

The regional providers working together recently completed a Regional Water Supply Plan using the Integrated Resource Planning Model approaches. A heavy reliance on conservation and use of other resources by our regional partners precludes expansion of service for approximately 20 years. (Water Providers, 1996)

Portland is about to commence an integrated planning effort to develop an Infrastructure Master Plan (IMP) that will help determine the courses of action to improve reliability and meet future needs. The Portland system consists of an aging infrastructure in areas of vulnerability that are of concern.

Figure No. 1 is a system sketch that shows the key elements for the City of Portland system in relationship to the watershed area.

PORTLAND HAZARD HISTORY

Emergency Incidents

Portland has experienced several different types of incidents that have impacted our ability to provide water to our customers. For example, floods in the watershed in 1964 caused the failure of two of our three pipelines for an extended period of time. Extreme weather and landslides in 1972 impacted our water quality and led to the decision to build a backup groundwater supply system independent from our watershed.

Figure No. 2 shows the service area for Portland's customers. Our entire service area is twice as large. In 1996 heavy rains and a small landslide caused the collapse of a bridge carrying two pipelines and caused the failure of two of the three conduits for a five week period of time. Because of the well field we were able to provide water to all our customers. The figure does not show the wholesale providers that also receive water from Portland.

Seismic Risks Identified

In the last 15 years scientific research by seismologists and geologists has brought to the attention of the people of the State of Oregon the seismic risks from several source zones. Building codes have been modified and facility owners and public agencies are taking seriously the seismic threat posed here in the State of Oregon. The Bureau has strengthened a number of water tanks including ground level storage and elevated reservoirs. (Anoushiravani, 1986) Improved anchorage and cross bracing has been completed on several reservoirs. A recently completed seismic vulnerability assessment of key facilities at our groundwater source and at our maintenance and operations location has shown shortcomings that need to be addressed. In order to understand the full spectrum of hazards facing the Bureau and the vulnerabilities they posed, we are initiating a system vulnerability assessment that will be described further below.

PORTLAND WATER SYSTEM VULNERABILITY

The Portland water system is vulnerable to many types of hazard. Episodes of damage and loss can be recalled for every facet of our operation. In order to understand current actions the following is presented as background.

Early Portland Mitigations and Studies

Much of the Portland system currently in operation was built before the turn of the century and continues to perform well. However, current knowledge and design practices are such that we now recognize the vulnerability of the many aspects of the system. For example, following the 1972 flood and landslide problems in the watershed, a study looking at disaster related aspects of the watershed and mitigation opportunities resulted in several studies and activities to improve reliability. The addition of Hydro Electric facilities and the oversight of the Federal Energy Regulatory Commission

has caused review of several facilities using modern approaches to analysis. For example our two dams (one concrete gravity arch and the other earth and rockfill) have been evaluated for seismic capability, as well as the outlet towers from the lower reservoir. As the state of seismology improves these studies will be revisited.

As noted earlier tanks and standpipes have been strengthened, although this work is not yet complete. The efforts of other cities in strengthening large elevated reservoirs using base isolation techniques are being reviewed for applicability to our situation. An earlier pilot project used GIS techniques to look at water and sewage systems in two pilot test areas, and develop an inventory and seismic loss estimation model.

Recent State-wide Studies

In response to concern for earthquake risk in Oregon, two significant studies have been completed by state agencies. The Department of Geology has completed several seismic hazard maps in the Portland Metropolitan area and other urban areas of the state. These maps combine several aspects including site amplification potential, liquefaction potential, and landslide susceptibility to produce generalized hazard maps. A second effort by the State Department of Transportation to develop probabilistic seismic hazard maps for the entire state has been completed. (Geomatrix, 1995) These maps provide ground motions for 500 year, 1000 year, and 2,500 year return periods. The maps utilize all known sources including crustal interface, intra plate, and subduction that are believed to exist in the state.

Bureau Key Facilities Studied

The Bureau has completed a Seismic Vulnerability Study focusing on our groundwater emergency system and our maintenance headquarters facilities. The study details opportunities for strengthening pipelines, buildings, and system components (including non-structural aspects). This effort serves as the springboard for the system-wide vulnerability assessment work to be described below.

HAZARD EVALUATIONS

The System Vulnerability Assessment (SVA) project is intended to look at all hazard situations that could affect the Bureau. This includes natural hazards, human caused hazards and service losses affecting our ability to perform. Table 1 details natural hazards that will be considered in the study. Table 2 details the human caused hazards, and Table 3 identifies the service loss hazards that will be reviewed and be considered in multi-attribute utility modeling efforts.

Vulnerabilities Identified

Previous studies have identified several vulnerabilities to concentrated and distributed facilities including non-structural aspects, electric power supply problems, and structural needs including potential building collapse. Table 4 provides a breakdown of Bureau processes, systems and

Risk Assessment and Consequences of Failure

The study will include decision analysis techniques including multi-attribute utility models and expert opinion in the data gathering phase. Performance expectations from various stakeholders is an important aspect of the work so that future activities meet the greatest need and most pressing problems. The consequences of individual and multiple failures will be modeled with event diagrams and fault trees. Once risks and hazards are identified and linked to the PSC's we will be able to develop order of magnitude cost estimates to reduce vulnerability. We will be able to identify constraints to implementation of projects, identify quick fixes that can be undertaken, and prioritize and sequence the work in our Infrastructure Master Plan.

The relationship of earthquake risk to losses is apparent in several recent studies (Chung, 1996; Housner, 1997; NRC 1989). The importance of relating earthquake risks to other risks is becoming an important planning objective (Davidson, 1997; NRC 1985). Successful integrated planning efforts require the involvement of all stakeholders, i.e., those with an interest or "stake" in the result or expected outcome (Stern 1996; Kerr, 1996, Lang 1997).

Further, the risk perception of the public plays an important role in risk decisions (Flynn, 1996). Therefore, Portland believes this study will provide the information needed to put earthquake risk and other risk concerns in context for further stakeholder deliberations

INTEGRATED EVALUATION

The goal of the work is to integrate all of the aspects of hazard and risk with all of the elements of our infrastructure system, so that performance can be improved and water delivery reliability enhanced. The three elements of work include: Regional Water Supply Plan (RWSP); Infrastructure Master Plan (IMP); and System Vulnerability Assessment (SVA) described above.

Regional Water Supply Planning

The recently completed RWSP utilized an Integrated Resource Planning (IRP) effort. This resulted in a consensus on which sources should be developed in which time frames. These include sources of other providers and a reliance on conservation to delay needed resource enhancements. Close cooperation and involvement with all stakeholders has resulted in successful source identification.

Infrastructure Plan

In order to deal with the aging infrastructure of the Portland system and improve reliability, the Infrastructure Master Planning effort (IMP) is being pursued presently. A key aspect of that work is the System Vulnerability Assessment (SVA). We are not aware that such a broad look at all hazard aspects, and all elements of public water delivery system, has been completed in such a comprehensive manner.

CONCLUSIONS

The City of Portland has decided to pursue a system-wide, comprehensive hazards and vulnerability effort. This study may be a model for others to follow. We wish to understand the significance of seismic risk (low probability-high impact) events along with other types of hazards (high probability-lower impact). We believe this approach will validate the need for seismic strengthening and will show that such work can improve reliability and public awareness for other hazard situations also.

ACKNOWLEDGMENTS

Several of these studies will be conducted by the firm of EQE International, under the guidance of Donald Ballantyne. The team includes experts in a number of natural hazards and human caused hazards areas, and will draw heavily on expert opinion from the Portland Water Bureau and other stakeholders. In particular, earlier work by the San Francisco Water Department and by the East Bay Municipal Utility District in Oakland have been inspirations for this work.

REFERENCES

- Anoushiravani, M. and Bader, C.G., 1986, Seismic Resistance of an Elevated Water Tank - a Case Study: found in Lifeline Seismic Risk Analysis Case Studies, TCLEE proceedings April 6, 1986, ASCE, Technical Council on Lifeline Earthquake Engineering, pp. 51-69.
- Ballantyne, D.B., 1993, *Minimizing Earthquake Damage a Guide for Water Utilities*, AWWA, 1993.
- Bernstein, P.L., 1996, *Against the Gods: The Remarkable Story of Risk*, John Wiley & Sons .
- Bolt, B.A., 1993, *Earthquakes*, W.H. Freeman & Company.
- Chung, R.M., Editor, 1996, The January 17, 1995 Hyogoken-Nanbu (Kobe) Earthquake, U.S. Department of Commerce, National Institute of Standards and Technology, NIST Special Publication 901 (ICSSC TR18).
- Cohrssen, J.J., and Covello, V.T., 1989, United States Council on Environmental Quality , Executive Office of the President, 397p.
- Davidson, R., 1997, A Multidisciplinary Urban Earthquake Disaster Risk Index: found in *Earthquake Spectra*, v.13, no. 2, May 1997, Earthquake Engineering Research Institute, pp. 211-223.
- Dijkers, R.D., Chung, R.M. and others, 1996, Proceedings of a Workshop on Developing and Adopting Seismic Design and Construction Standards for Lifelines, September 1991 at Denver, Colorado, NISTIR 5907, National Institute of Standards and Technology, Gaithersburg, MD, 210p.
- Earthquake Engineering Research Institute, 1986, *Reducing Earthquake Hazards: Lessons Learned from Earthquakes*, EERI Publication 86-02, pp. 167-187.
- Flynn, J., Slovic, P. and Mertz, C.K., 1996, Final Report - City of Portland Risk Survey, for Portland Bureau of Buildings by Decision Research, Eugene, OR., 34p.
- Geomatrix Consultants, for Oregon Department of Transportation, 1995, *Seismic Design Mapping*, State of Oregon, Oregon Department of Transportation, 300p.
- Hinman, E.E. and Hammond, D.J. , 1997, *Lessons from the Oklahoma City Bombing - Defensive Design Techniques*, ASCE Press, New York, 48p.
- Housner, G.W. and Chung, R.M., 1997, Natural Disaster Reduction, ASCE conference proceedings, December 1996, Washington, D.C., 407p.
- Kempner, L. and Brown, C.B., 1997, *Building to Last*, ASCE conference proceedings, April 1997, ASCE Structural Engineering Institute, Portland, OR., 1064p.

Kerr, P.A., 1996, "A New Way to Ask Experts: Rating Radioactive Waste Risks", article in Science, v.274, 8 November 1996, pp. 913-914.

Lang, S., 1997, "Moving Forward - Risk Management Meets the Information Age", in Risk Management magazine, September 1997, pp. 43-47.

National Research Council, 1989, Estimating Losses from Future Earthquakes - Panel Report, National Academy Press, Washington, D.C., 82p.

National Research Council, 1985, Safety of Dams - Flood and Earthquake Criteria, National Academy Press, Washington, D.C., 276p.

Oregon Department of Transportation, 1997, Prioritization of Oregon Bridges for Seismic Retrofit - Final Report, January 1997, 47p.

Parmalee, M.A., 1997, "Water Resources Meeting Makes Business Sense", in Mainstream magazine, American Water Works Association, September 1997, pp. 1-2.

Stern, P.C. and Fineberg, H.B., 1996, Understanding Risk: Informing Decisions in a Democratic Society, National Academy Press, Washington, D.C., 249p.

Water Providers of the Portland Metropolitan Area, 1996, Regional Water Supply Plan - Final Report, Barakat & Chamberlain, Montgomery Watson and others, 278p.

Table 1. Natural Hazards to be Considered

Floods	Fire Following Earthquake	Drought
Snow Melt	Tsunami/Seiche	Heat Wave
Storm Series	Volcanic Activity	Turbidity Event
Land and Rock Slides	Lightening	Microbial Contamination
Debris Flows	Fire in the Watershed	Public Health Catastrophe
High Winds	Urban Park Fires	
Winter Storm	Urban Fire Storms	
Snow and Ice		
Prolonged Freezing		
Earthquake		

Table 2. Human Caused Hazards to be Considered

<u>Intentional</u>	<u>Technological</u>	<u>Transportation Accidents</u>
Sabotage	Piping Flood/Bureau Building	Airplane
Vandalism	Facility Fire/Bureau Building	Marine
Kidnap/Ransom/Extortion	Explosion/Bureau Facility	Rail
Civil Disturbances	Computer Disruption	Light Rail
Arsons/Riots/Strikes	Hazardous Materials Release	Truck/Car
Terrorism/Nuclear	Hazardous Materials Containment	
Terrorism/Chemical	Watershed Dam Failure	
Terrorism/Biological	Columbia River Dike Failure	
Terrorism/Bomb	Operational Error	
Terrorism/Computer		

Table 3. Service Loss Hazards

<u>Lifeline Losses</u>		<u>Societal Losses</u>
Water		Banking
Electrical		Insurance
Wire Communications		Food
Wireless Communications		Shelter
Media		Confinement/Detention
Sewerage		Hospitals
Natural Gas		Health Care
Liquid Fuel		Fire Service
Air Transport		Police Service
Rail Service		Emergency Centers
Light Rail Service		
Marine Operations		
Vehicle Service		

Table 4. Processes, Systems and Components to be Considered

<u>Process</u>	<u>System</u>	<u>Component</u>
Water Resource	Watershed	Lands/Roads
	Aquifers	Well Source Areas
Raw Water Production	Dams	2 Large Dams/Spillways
	Lakes	Natural Lakes/Reservoir Impoundments
	Wells	22 Well Sites
Raw Water Transmission	Hydro Generation	2 Power Plants & Power Transmission and Switching
	Headworks	Diversion Facilities / Headworks Buildings
	Groundwater	Collection Mains
Water Treatment	Disinfection Facilities	Headworks Chlorination / Downstream Chemical Addition
		Laboratory Facilities / Services
	Groundwater	Treatment / Disinfection
		Storage
Finished Water	Transmission	3 Existing Conduits, Interties, Future Conduit
		Conduit Bridges
		Pipe Line Appurtenances
	Terminal Storage	6 Large Terminal Reservoirs
	Supply Mains	River Crossings, Large Supply Mains, Pressure Regulation
	Water Providers	Customer Delivery Facilities, Dedicated Supply Mains

Process	System	Component
Distribution	Maintenance/Operation	Water Control Center, Operations Building, Maintenance Building, Fleet Maintenance Building
	Local Piping	86 Pump Units and 34 Pump Stations
	Local Storage	71 Locations including concrete (34) and steel (37)
	Pipelines	Buried, on bridges, under rivers
	Customer Services	Services, valves, fire hydrants
Business Support	Customer Base	Industrial, commercial, residential, wholesale, institutional
	Business Affairs	Records, computer system, key locations
Shared Services	Service Providers	Communications, control, utilities, materials, supplies
	City Services	Elected officials, attorneys, risk, fleet, general services, communications.
	Internal Services	Customer, laboratory, construction, maintenance, engineering, stores, public information, operating engineers, field forces, emergency management
	City Other	Police, fire, maintenance, transportation, environmental

WME:sms ENG:9710E523

SYSTEM SKETCH

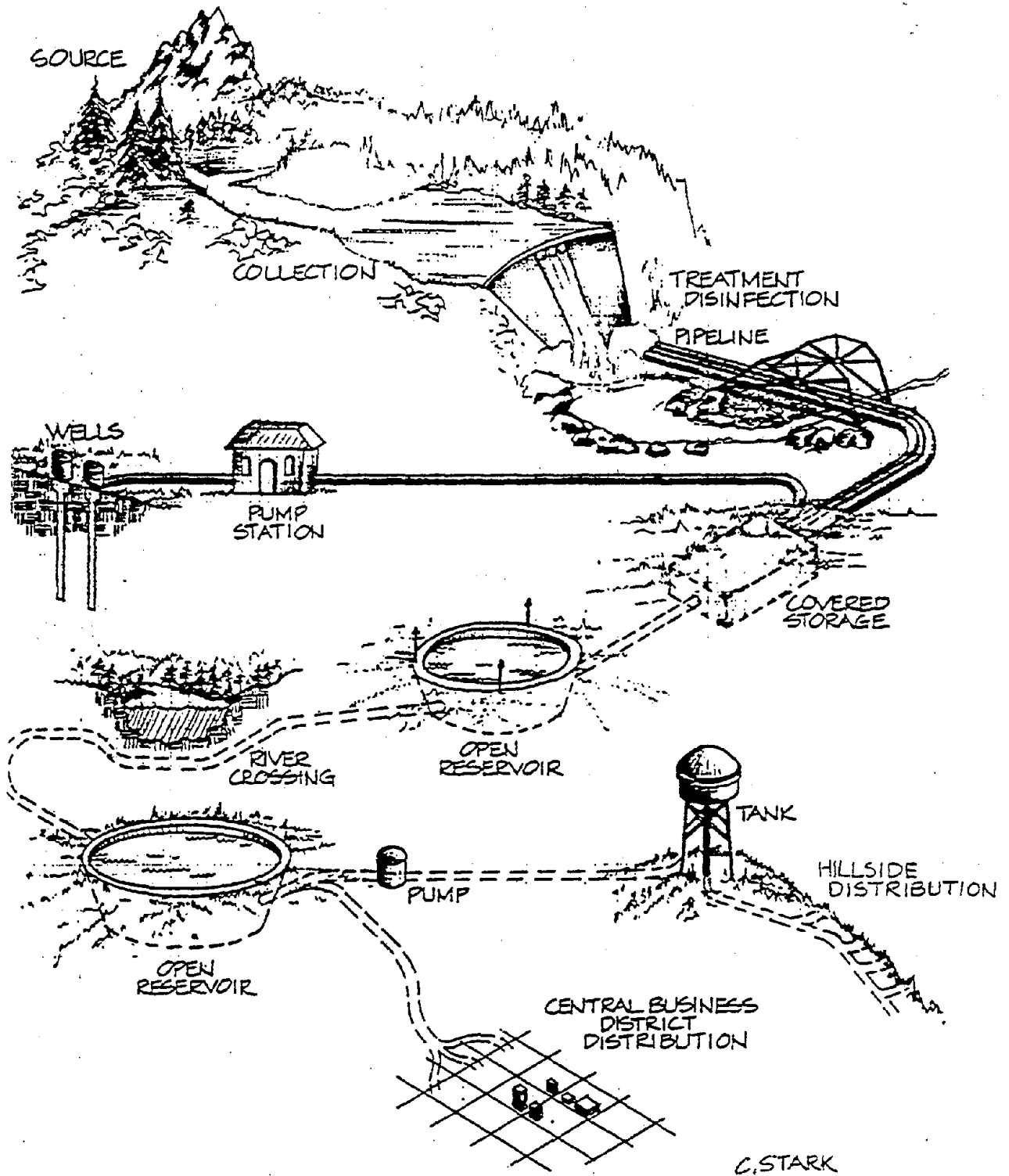


Figure 1. Generalized Portland Water Supply schematic.

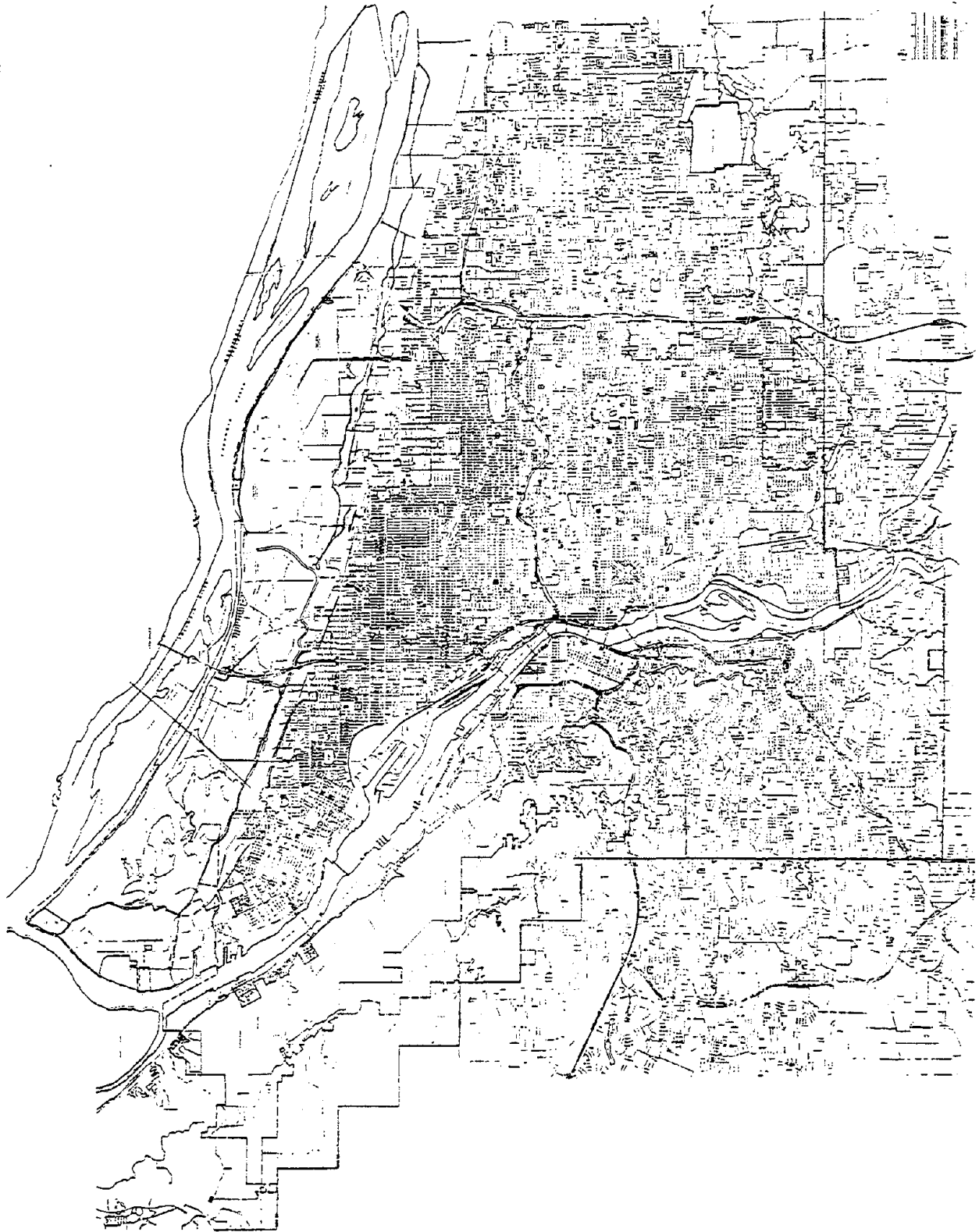


Figure 2. City of Portland portion of the Water Service Area

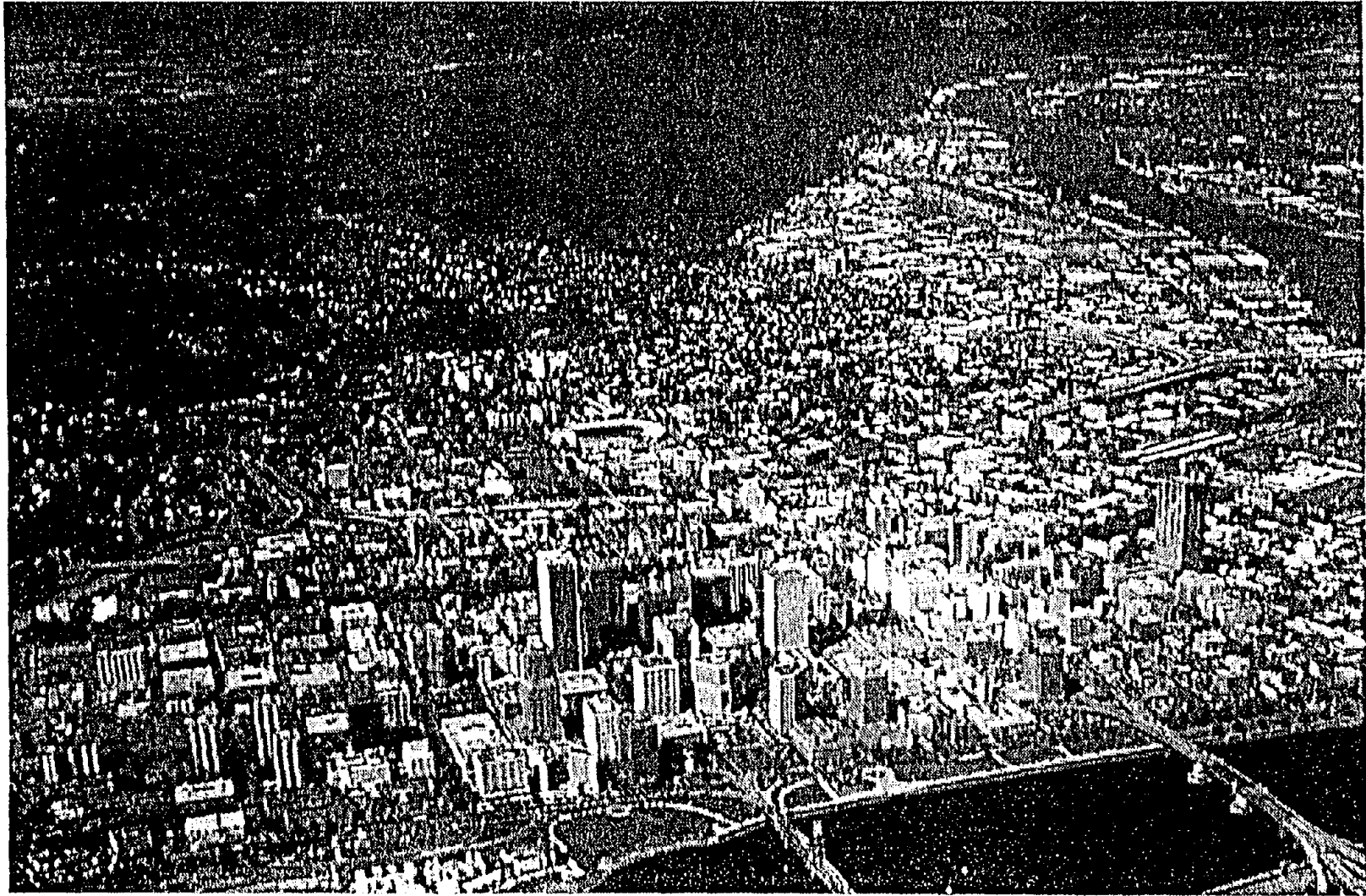


Figure 3. Aerial view of Portland central business district including Portland hills fault lineament

WILLIAM M. ELLIOTT, P.E.

Date of Birth: December 19, 1940

Birthplace: Los Angeles, California

Education: Degrees

University of Southern California, B.S., M.S., M.B.A.

B.S. Civil Engineering, 1963

M.S. Civil (Hydraulics, Soil Mechanics) Engineering, 1966

M.B.A. Business Administration, 1970

Member of Chi Epsilon, Civil Engineering Honorary Society

Registered Professional Engineer in California and Oregon



Position:

Senior Engineer, Water Engineering Section

Portland Bureau of Water Works - Portland, Oregon

Address:

Portland Water Bureau

1120 SW Fifth Avenue, 6th Floor

Portland, OR 97204-1926

Ph: (503) 823-7486

Fax: (503) 823-4500

E-Mail: bellott@water.ci.portland.or.us

Mr. Elliott is responsible for long range planning in special projects for the Portland Water Bureau including a study of system wide vulnerability to natural and man caused hazards.

Mr. Elliott has worked in the public sector, including the City of Los Angeles Department of Water and Power (6 yrs), and building and safety (2 yrs), before joining the Portland Water Bureau (25yrs). He has worked in the private sector for a large construction company on industrial construction of paper making facilities.

Mr. Elliott has been involved with disaster response and recovery situations including disaster counter measures, and is currently a member of the Portland team responding to disaster situations.

Professional:

Mr. Elliott is a member of ASCE and AWWA. He is an EXCOM member of TCLEE/ASCE, and is vice-chair of the Oregon Seismic Safety Policy Advisory Commission, being appointed by the Governor of the State of Oregon.

Travel Abroad:

Mr. Elliott has been to Manila, the Philippines on a ASCE/TCLEE follow up to the 1990 Luzon earthquake.

Publications:

Mr. Elliott was co-principal investigator on a U.S.G.S. study "Development of Inventory and Seismic Loss Estimation Model for Portland Water and Sewer Systems" completed in 1990. Other publications include papers for the AWWA Distribution System Symposium and ASCE Earthquake Engineering Conferences.

**IV. SEISMIC DAMAGE ESTIMATION AND PREDICTION
FOR LIFELINE FACILITIES**

“Earthquake Loss Estimation for Transportation and Utility Lifelines”

M. O'Rourke

“Development of Real-Time Damage Estimation System for Road Facilities”

H. Sugita, T. Hamada

“Seismic Hazard Mapping in Eugene-Springfield, Oregon”

Y. Wang, D. Keefer, Z. Wang

“Seismic Risk Evaluation and Improvement Program for the Metropolitan
Wastewater Department, City of San Diego”

D. Hu, P. Wong, R. Eguchi, K. Mertz, D. Ballantyne

“Mapping Predictions of Liquefaction Induced Lateral Spread Displacements”

M. Mabey

“Integrated Real-Time Disaster Information Systems:
The Application of New Technologies”

R. Eguchi, J. Goltz, H. Seligson

EARTHQUAKE LOSS ESTIMATION FOR TRANSPORTATION & UTILITY LIFELINES

M. J. O' Rourke

Department of Civil Engineering, Rensselaer Polytechnic Institute
Troy, New York, 12180-3590, USA

ABSTRACT

Typically the first step in the seismic upgrade of an existing lifeline system is an evaluation of the potential losses due to future earthquakes. This paper describes HAZUS, a recently developed Earthquake Loss Estimation tool. The purpose and objectives of HAZUS and a brief review of its overall capabilities are presented. Detailed description of the transportation and utility lifeline modules follow. This includes information on the required input, internal fragility relations and restoration curves. Finally a sample of HAZUS analysis results for various possible events along the Hayward fault are presented for potable water and electric power systems.

INTRODUCTION

When transportation departments and/or utility system operators are planning a seismic retrofit or upgrade program for an existing system, an evaluation of the potential losses (e.g., direct repair costs and temporary system outages) due to future earthquakes is often the first task in the project. This initial loss estimation task provides a benchmark of the current, unimproved, status of the system in question. The probable benefits (e.g., reduced repair costs and shortened outage intervals) of various retrofit or upgrade strategies are then estimated in order to provide a rational basis for selecting which specific proposed improvements are actually implemented. Both of these tasks require loss estimation tools.

This paper focuses on one such loss estimation tool, namely HAZUS, the NIBS/FEMA Earthquake Loss Estimation Methodology. The HAZUS project was organized and directed by the National Institute of Building Sciences (NIBS) for the Federal Emergency Management Agency (FEMA). Technical supervision and review was provided by a seven person Project Working Group (PWG) chaired by Prof. Robert Whitman of MIT. The author served on the PWG. The GIS based HAZUS software was developed by Risk Management Solutions (RMS), and tested in two pilot studies. The first pilot study was conducted in Portland, OR, by Danes and Moore while the second was done by EQE for Boston, MA.

HAZUS is designed to produce loss estimates for use by state, regional and local governments in planning for earthquake loss mitigation, emergency preparedness, as well as response and recovery. The methodology deals with nearly all aspects of the built environment and with a

wide range of different types of losses. Elements of the built environment considered by HAZUS include the general building stock, essential facilities (e.g., fire, police and emergency operations centers), transportation lifelines (e.g., highway, rail, bus and airports), and utility lifelines (e.g., potable water, wastewater, oil, natural gas, electric power and communications systems). The types of losses considered by HAZUS include: damage to structural and non-structural components for the general building stock; potential exposure to inundation, hazardous material release and fire following earthquake; estimates of debris, casualties, displaced households and short-term shelter needs; direct economic losses (e.g., business inventory, relocation expenses and rental income losses); and indirect economic losses (e.g., post-earthquake changes in general business activity).

For the ground shaking and ground failure (i.e., liquefaction, landslide and surface fault rupture) hazards, the seismic environment is initially characterized by an user selected earthquake magnitude located at a user selected epicenter. Based upon an attenuation relation (either a default or a user selected relation) and local soil conditions, the software calculates and can display the ground shaking intensity. For lifeline system components, the peak ground accelerations (PGA) and peak ground velocity (PGV) are currently provided. For ground failure hazards, the amount of Permanent Ground Deformation (PGD) is provided.

The following sections will describe in some detail the component classification systems, damage states, fragility relations and restoration curves for highway bridges and potable water systems. Finally a sample of HAZUS results for potable water and electric power in the San Francisco Bay region for various magnitude events along the Hayward fault are presented as well as plans for upgrades to HAZUS in the near future.

HIGHWAY BRIDGES

Highway bridges are classified based upon three criterion; type, design and special risk attributes. The three types are major (at least one span over 500 ft.), continuous, and simply supported. The design criteria distinguishes between bridges original designed with seismic considerations (or retrofitted to comply with seismic provisions), and these designed without seismic considerations. Special risk attributes include, among others, skewed and curved bridges.

There are four damage states for highway bridges; slight , moderate, extensive and complete damage. Slight damage means minor cracking and spalling to the abutment, as well as similar damage to support columns and the deck, which require no more than cosmetic repair. Extensive damage means major approach settlement, loss of some bearing support, and degradation of columns such that they are structurally unsafe.

Fragility relations provide the connection between the seismic hazard (e.g., PGA for ground shaking) and the probability of various damage states. For example, Figure 1 is the fragility curve for conventionally (i.e., non-seismic) designed continuous bridges subject to the ground shaking hazard, while Table 1 provides the medium PGA for each damage state and bridge type.

For bridges with special risk attributes, these medians are increased by 20%. For the ground failure hazard, median PGD's range from 5 inches for slight damage, up to 24 inches for complete damage, irrespective of bridge type.

Restoration curves quantify the expected repair time for various damage states. HAZUS bases its restoration relations upon information in ATC-13 (1985). Figure 2 shows the restoration curve for highway bridges. For example, there is a 50% probability a bridge in the moderate damage state will be functional 2.5 days after the event.

POTABLE WATER

Potable Water Systems consists of a number of components including treatment plants, pump plants, wells, storage tanks as well as transmission and distribution piping. Many of these components are classified by size (treatment plants with 50 million gallons per day or less capacity are small, plants with capacity of 200 mgd or more are large; pump plants with capacity less than 10 mgd are small) and by subcomponent anchorage. "Anchored" means equipment designed with seismic tie downs and/or tie backs while "unanchored" means equipment only meeting manufacturers normal requirements. Storage tanks are further classified by material (concrete, steel or wood), location (buried, on grade or elevated) and anchorage. For storage tanks, anchored means a positive connection to the supporting ring wall. Buried pipe is classified as either brittle (e.g., asbestos cement, concrete and cast iron) or ductile (e.g., ductile iron, and PVC). Steel pipe with arc-welded joints are classified as ductile while gas-welded joints (typically pre-1935) are classified as brittle.

There are four damage states (slight, moderate, extensive and complete) for water system components other than pipeline. For wells, slight damage means malfunction of the well pump and motor due to loss of electric power and/or backup power while extensive damage means the vertical shaft is badly distorted and nonfunctional. For storage tanks, slight damage means minor cracks in concrete tanks, localized wrinkles in steel tanks or minor roof damage due to water sloshing. Elephant foot buckling of a steel tank with loss of contents would be extensive damage. For pipeline components there are only two damage states; a leak or a break.

Table 2 provides for selected, non-pipeline, water system component the median PGA for each damage state. For treatment plants and pump stations, the lower median PGA's are for smaller facilities. Note that the higher damage states, extensive and complete, are not strongly influenced by equipment anchorage. Figure 3 shows a typical fragility relation, in this case for a medium size water treatment plant with unanchored components.

Table 3 provides median PGA's for on-grade and elevated storage tanks. For buried concrete tanks, damage is related solely to the PGD at the site (median PGD of 2 inches for slight damage, 12 inches for complete damage.)

For buried pipeline, damage is characterized by the number of repairs per kilometer of pipe. For brittle pipe subject to ground shaking (i.e., wave propagation effects) the fragility relation in

terms of PGV is based upon work by O'Rourke and Ayala (1993) and is shown in Figure 4. For PGD damage, again for brittle pipe, the fragility relation in terms of PGD in inches is based upon work by Honegger and Eguchi (1992) and is shown in Figure 5. In HAZUS, ductile pipe is assumed to sustain about a third of the corresponding brittle pipe damage.

A restoration curve for non-pipeline water system components are based upon ATC-13. For example Figure 6 shows the restoration curve for storage tanks. That is, an extensively damaged tank is expected to be 50% functional after 93 days, or more precisely, there is a 50% probability that the tank is functional after 93 days. Table 4 presents the mean restoration times for selected water systems components. Restoration for buried pipe components is based upon an assumed 16 hour work day and the number of available workers (utility personnel plus mutual aid volunteers) or a default value of 0.02% of the study region population. In addition, a 4 person crew takes 4 hours to fix a leak in a small pipe (20 inch diameter or less) and 6 hours for a leak in a large pipe. These repair times are doubled for breaks.

SAMPLE RESULTS

In this section, sample results from a HAZUS analysis for selected lifeline components in the San Francisco Bay region are presented. Four scenario events, with magnitudes ranging from 5.5 to 7.0, along the Hayward Fault are considered. Figure 7 shows the study region and the Hayward fault. The nine county region has of a total area of about 7300 square miles, a population of roughly 5.7 million people and about 2.1 million households. The inventory of roughly 34,000 km of water pipe is based on the assumption that water lines closely follow the streets. The inventory of 34 electric power substations is based upon California Division of Mines and Geology (CDMG) and Earthquake Engineering Research Institute (EERI) reports. Table 5 presents water pipe damage and electric power restoration. Specifically, the number of leaks, breaks, total repairs, as well as the break rate (breaks per km) are presented for each of the four scenario events. Also presented are the number of households without electric power at days one, three and seven after the event.

FUTURE PLANS

Annual updates to HAZUS are planned. In 1998, one year after its initial release, two upgrades are planned for the transportation and utility lifeline modules. After a comparison of actual damage in the 1994 Northridge event with losses estimated by HAZUS, it was decided to revise the bridge fragility relations using newly developed information from the NCEER Highway project. For potable water, HAZUS currently contains a somewhat generic functionally relation, that is the percentage of households without water as a function of pipe break rate. This relation is based upon previous simulations for systems in the US and Japan. In the coming year, a system specific model will be used to evaluate functionally.

REFERENCES

Applied Technology Council, (1985), "Earthquake Damage Evaluation Data for California," ATC-13, Redwood, CA

Honegger D. and Eguchi, R., (1992), "Determination of Relative Vulnerability to Seismic Damage for San Diego County Water Authority (SDCWA) Water Transmission Pipeline," EQE International, San Francisco, CA

O'Rourke, M. and Ayala, G., (1993), "Pipeline Damage due to Wave Propagation," J. Geotechnical Engineering, ASCE Vol. 119, No. 9, Sept.

Table 1 Median PGA's and Bridge Damage States for Ground Shaking Hazard

Bridge Class	Damage State	Median PGA(g) Seismic Design	Median PGA (g) Conventional Design
Simple Support	Slight	.22	.11
	Moderate	.34	.22
	Extensive	.39	.26
	Complete	.85	.60
Continuous	Slight	.28	.18
	Moderate	.42	.37
	Extensive	.55	.48
	Complete	1.2	.90
Major	Slight	.38	.32
	Moderate	.46	.43
	Extensive	.62	.55
	Complete	1.5	1.25

Table 2 Median PGA's for selected Water System Components for Ground Shaking Hazard

Water System Component	Damage State	Median PGA (g) anchored sub.	Median PGA (g) unanchored sub.
Treatment Plant	Slight	.25-.44	.16-.22
	Moderate	.38-.58	.27-.35
	Extensive	.53-.87	.53-.87
	Complete	.83-1.57	.83-1.57
Pump plants	Slight	.15	.13
	Moderate	.36	.28
	Extensive	.66-.77	.66-.75
	Complete	1.50	1.50
Wells	Slight	.15	.15
	Moderate	.36	.36
	Extensive	.72	.72
	Complete	1.5	1.5

Table 3 Median PGA's for Water Storage Tanks for Ground Shaking Hazard

Tank Class	Damage State	Median PGA (g) Anchored Tank	Median PGA (g) Unanchored Tank
On-Grade Concrete	Slight	.25	.18
	Moderate	.52	.42
	Extensive	.95	.70
	Complete	1.64	1.04
On-Grade Steel	Slight	.30	.15
	Moderate	.70	.35
	Extensive	1.25	.62
	Complete	1.60	.95
On-Grade Wood	Slight	.15	
	Moderate	.40	
	Extensive	.70	
	Complete	.90	
Elevated Steel	Slight	.18	
	Moderate	.55	
	Extensive	1.15	
	Complete	1.50	

Table 4 Mean Restoration Times for selected Water Systems Components

Water system Components	Damage State	Mean Restoration Time (days)
Treatment Plants	Slight	0.9
	Moderate	1.9
	Extensive	32.0
	Complete	95.0
Pump Plants	Slight	0.9
	Moderate	3.1
	Extensive	13.5
	Complete	35.0
Wells	Slight	0.8
	Moderate	1.5
	Extensive	10.5
	Complete	26.0
Storage Tanks	Slight	1.2
	Moderate	3.1
	Extensive	93.0
	Complete	155.0

Table 5 Sample Results for Various Magnitude Events along the Hayward Fault

Magnitude	5.5	6	6.5	7
Potable Water Pipelines				
Number of Leaks	390	1177	3196	6816
Number of Breaks	771	1593	3009	5336
Total Repairs	1161	2770	6205	12152
Repair Rate (/km)	0.0343	0.0819	0.1834	0.3592
Break Rate (/km)	0.0228	0.0471	0.0889	0.1577
Electric Power System Performance - Households without Power				
Day 1	702,750	945,350	1,200,600	1,422,950
Day 3	189,000	298,000	428,000	578,000
Day 7	48,000	90,500	144,000	210,350

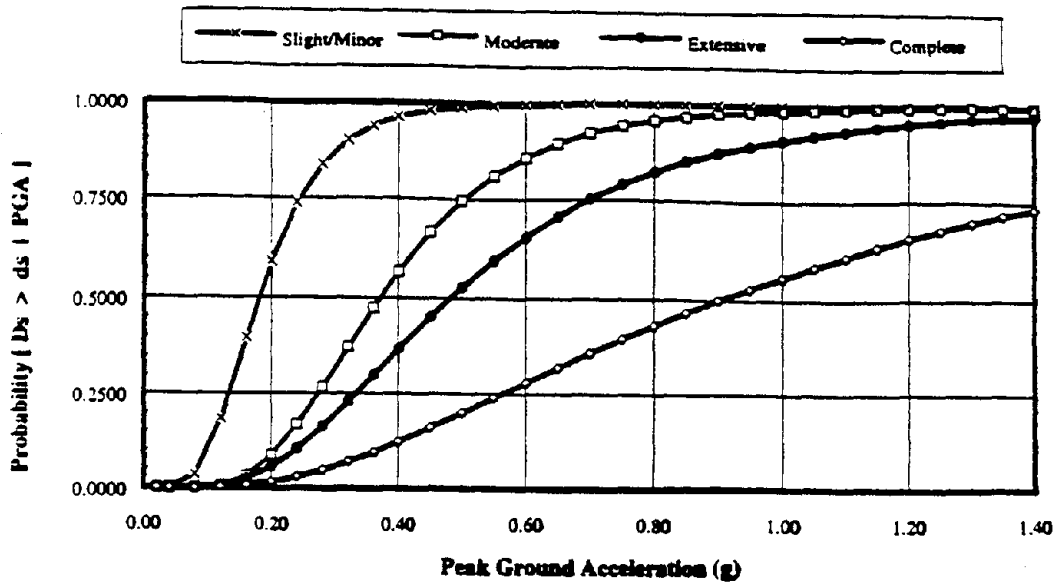


Figure 1 Fragility Curve for Conventional Design, Continuous Bridge

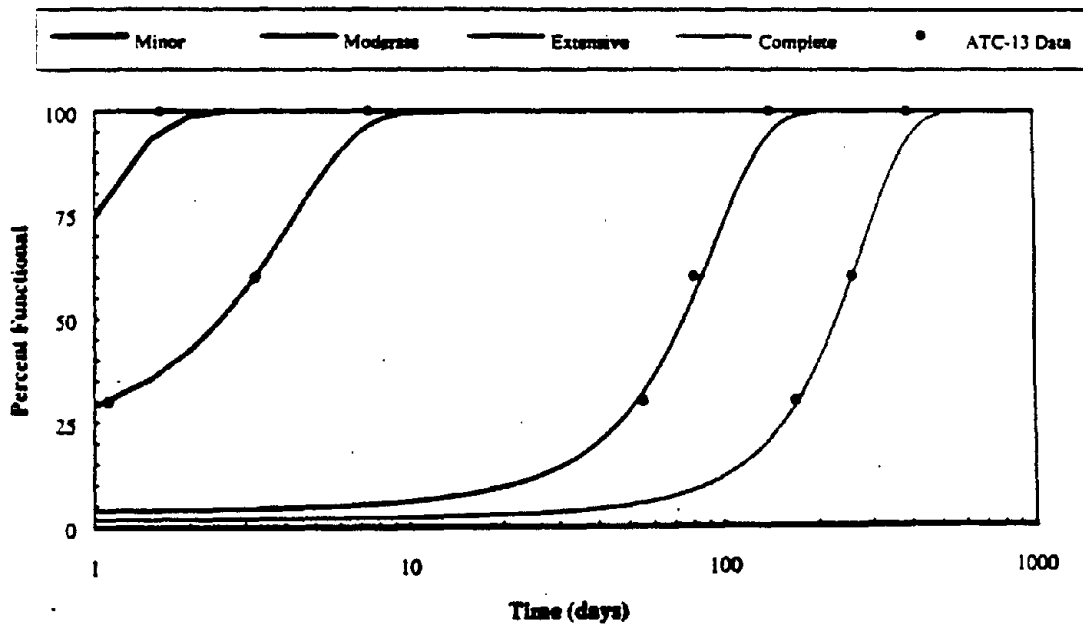


Figure 2 Restoration Curve for Highway Bridges

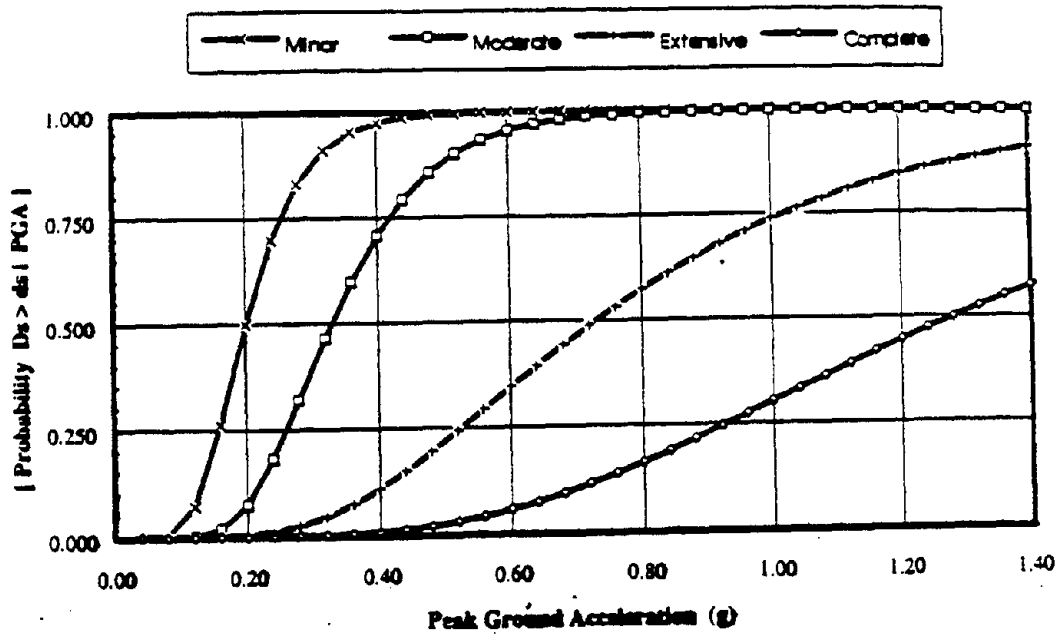


Figure 3 Fragility Curve for Meduis Size Water Treatment Plant with unanchored Components

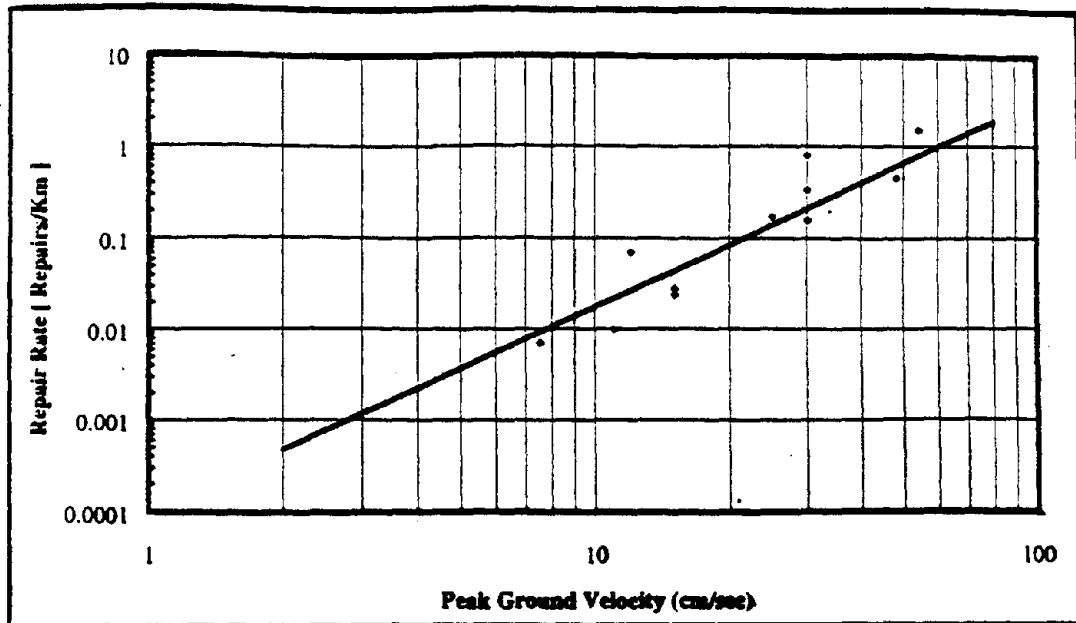


Figure 4 Wave Propagation Fragility Relation for Brittle Pipe

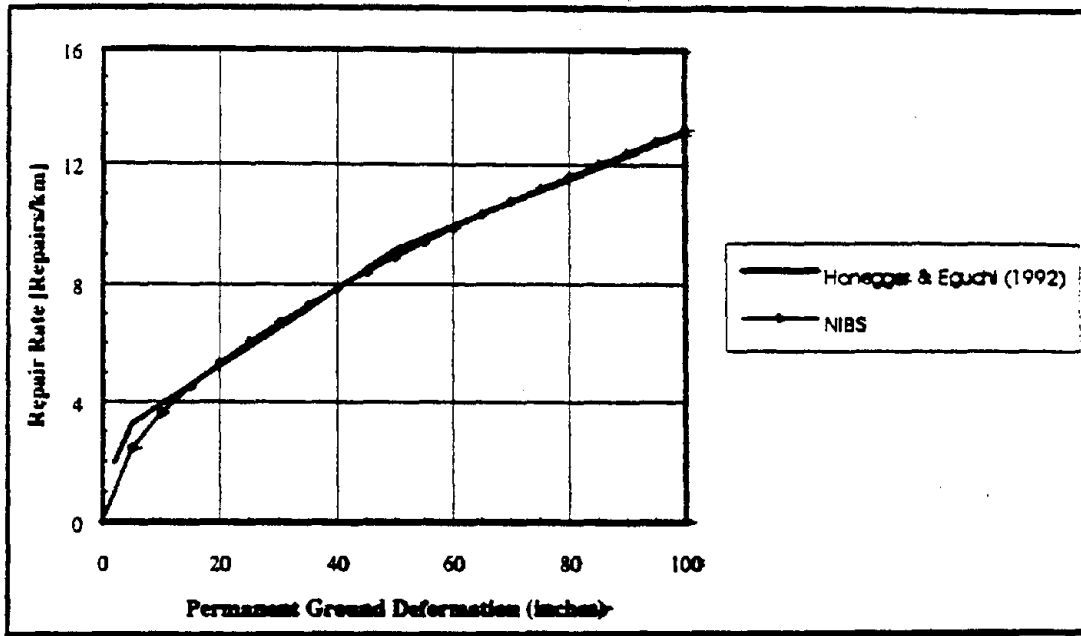


Figure 5 PGD Fragility Relation for Brittle Pipe

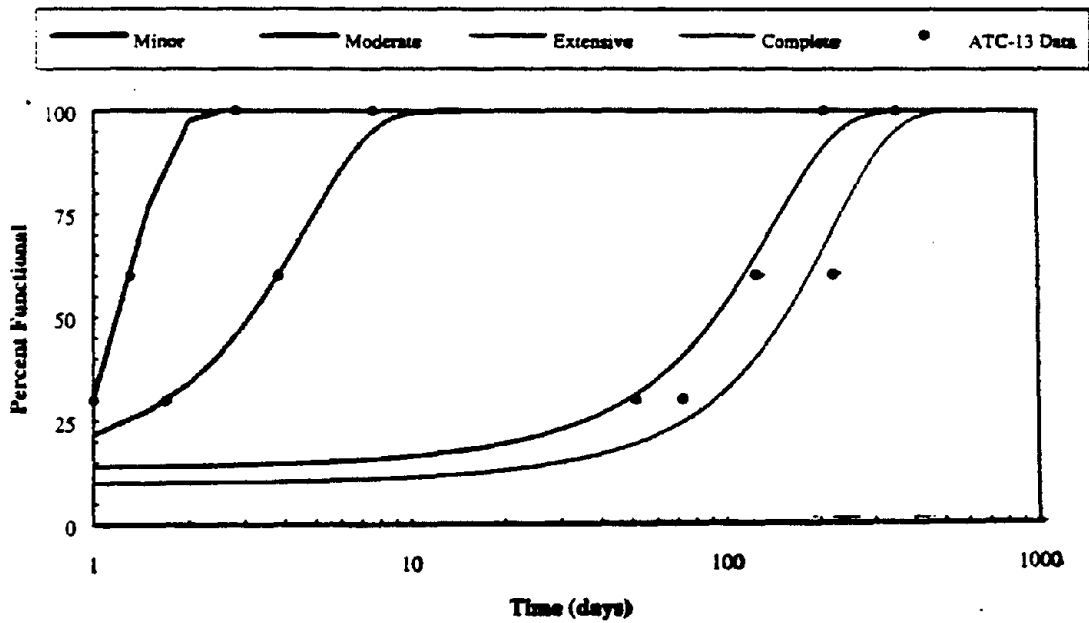


Figure 6 Restoration Curve for Water Storage Tanks



Figure 7 San Francisco Bay Study Design

DEVELOPMENT OF REAL-TIME EARTHQUAKE DAMAGE ESTIMATION SYSTEM FOR ROAD FACILITIES

by

Hideki SUGITA¹⁾ and Tadashi HAMADA²⁾

- 1) Head, Earthquake Disaster Prevention Technology Div., Earthquake Disaster Prevention Research Center, Public Works Research Institute, Ministry of Construction, Tsukuba, Japan
- 2) Research Engineer, ditto

ABSTRACT

Earthquake damage of road facilities does not only reduce their functions but affects the socio-economic activities in and around the damaged area. Therefore, besides improving the seismic performance of road facilities, post-earthquake emergency activities to reduce the damage effects must be jointly promoted.

This paper presents a Real-time Earthquake Damage Estimation System for Road Facilities, which is developed at Public Works Research Institute, Ministry of Construction. By providing rough estimation on damage states and damage distributions in a short time, the system will support decision-makers to facilitate emergency actions immediately after earthquakes.

Key Words: Real-time Information System, Emergency Activity, Damage Estimation, Ground Liquefaction, and Highway Bridge

INTRODUCTION

Emergency activities at sections that are in charge of road facilities can be classified into four stages¹⁾; i.e. assuming magnitude of the earthquake, grasping a damage outline in a whole affected area, conducting temporary repair works to secure transportation functions and conducting permanent restorations. To establish a scope of works for a series of emergency activities, it is quite important to conduct the second stage of grasping a damage outline as fast as possible.

1995 Hyogo-ken Nanbu Earthquake was a first destructive earthquake attacked a highly integrated urban area in Japan²⁾. Based on that disaster experience, following difficulties were pointed out for grasping a damage outline;

- 1) Much time was required for setting-up damage inspection teams,
- 2) Much time was required for investigations of widely spread severe damages, and
- 3) Adequate amount of damage information was not assembled at the headquarter due to disruptions/congestion of telecommunication lines.

Table 1 shows the required time for grasping damage outline at the headquarter. The table also describes the time required in 1994 Sanriku Haruka-oki Earthquake, in which severe damage was not developed on road facilities. For promoting a series of emergency activities against a destructive

event, quick decision-making is indispensable in spite of the difficulty of assembling damage information. Applications of information systems to support the decision-making of sectors are therefore considered to be essential.

Table 1 Required Time for Grasping Damage Outline at Headquarter

	Hyogo-ken Nanbu EQ (1995)*	Sanriku Haruka-oki EQ (1994)**
EQ Occurrence	05:46 1/17	21:19 12/28
Damage Inspection	08:00 – 8:00 1/18	21:50 – 23:22
Time Period for Grasping	Approx. 24 hours	Approx. 30 minutes

* : Kinki Regional Construction Bureau

** : Hokuriku Regional Construction Bureau

REAL-TIME DAMAGE ESTIMATION SYSTEM

1. Scope of Work

Based on the past disaster experiences, development of information systems to support emergency activities has been conducted in PWRI^{3),4)}. The Real-time Damage Estimation System is developed as a major system component for grasping damage outline automatically immediately after an earthquake by providing rough estimations on damage states and damage distributions of road facilities.

Fundamental policies for developing the system are as follows;

- 1) Ground liquefaction state and bridge damage state are to be estimated in the system,
- 2) Damage estimation is to be conducted by a combination of pre-stored ground/ structural condition database and real-timely observed earthquake ground motion data,
- 3) Damage estimation is to be completed within 15 min., by that time emergency investigation team can be set-up, and
- 4) Estimated information is to be visually displayed on the CRT using digital maps.

Implementation of the system is considered to be effective in the following aspects;

- 1) Severely damaged area can be assumed in a short time. Damage inspections can be effectively engaged by a restricted amount of inspectors,
- 2) Damage outline can be understood smoothly based on damage inspections, and
- 3) Decision-making on the back-up organization and stuffs/ devices management can be initiated from the early period of emergency responses.

2. System Configuration

Fig.1 show a system configuration of the Real-time Damage Estimation System. The system works by fabricating three major components; i.e. 1) Seismograph Network, 2) Microwave Communication Network, and 3) Engineering Workstation.

1) Seismograph Network

The Ministry of Construction initiated construction of Seismograph Network in 1995. Approximately 700 strong motion seismographs are to be installed along highways and rivers with an interval of 20-40 km. Ground motion data can be transmitted real-timely to the headquarter and

sectors in charge of emergency activities.

2) Microwave Communication Network

The Microwave Communication Network connects headquarter and sectors in Ministry of Construction. Maximum acceleration values, seismic intensity values and equivalent JMA (Japan Meteorological Agency) SI values observed by each seismograph can be transmitted to these offices simultaneously.

3) Engineering Workstation

Damage estimation is performed by an Engineering Workstation implemented at headquarter and sectors. Ground/ structural condition database has to be installed prior to earthquakes. Transmitted ground motion data can be assembled by the WS. Estimated damage can be displayed using GIS software.

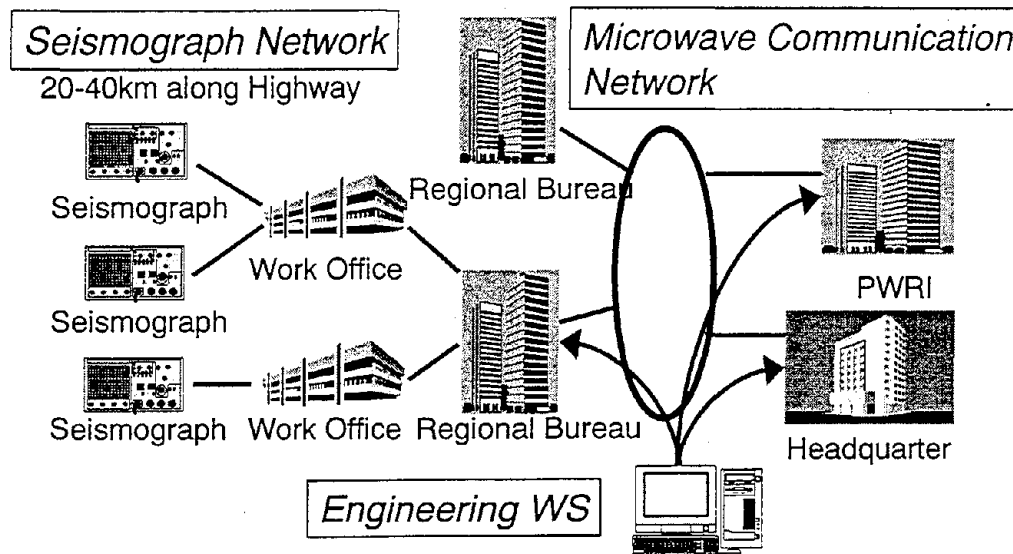
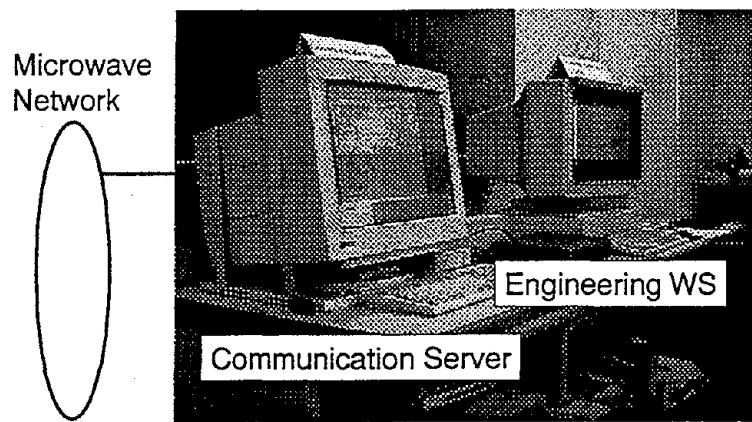


Fig.1 System Configuration of Real-time Damage Estimation System



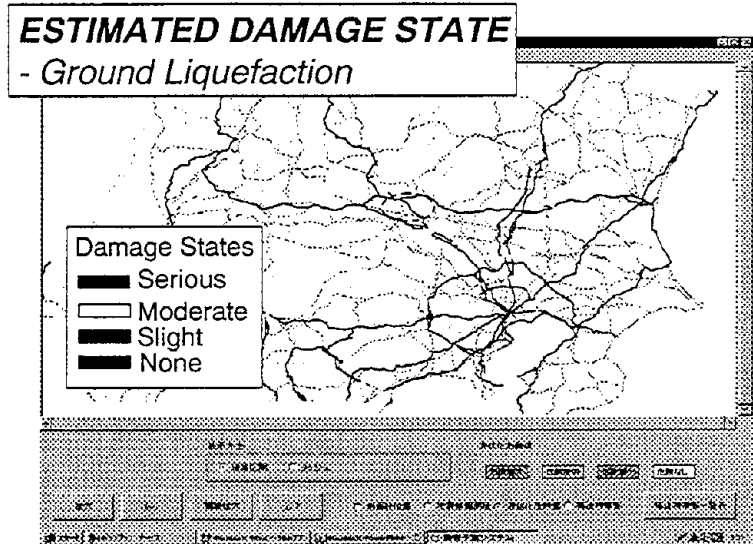
- Covers Kanto Area (Tokyo and 8 Prefectures)
- Liquefaction (6,028 Highway Sites)
- Bridge Damage (368 Bridges)

Photo 1 Hardware Configuration of Prototype System

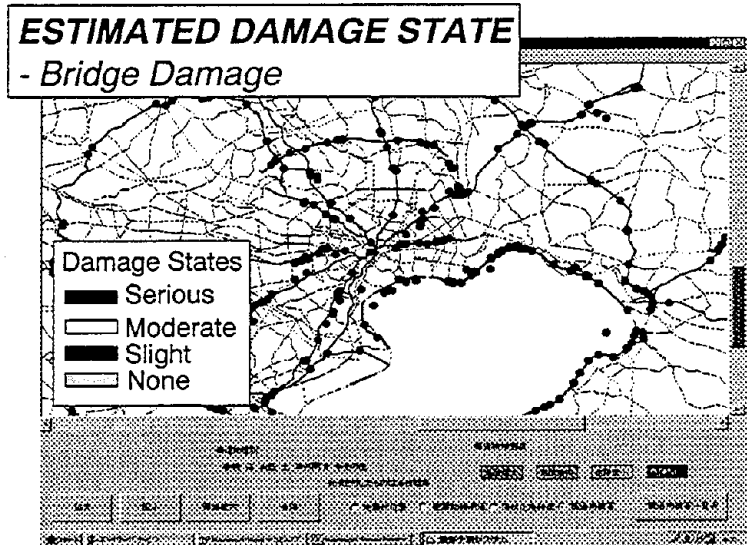
3. Prototype System

Photo 1 shows the hardware configuration of a prototype system. The system, which does not cover whole Japan but Kanto region (Tokyo and other 8 prefectures), is scheduled to be set-up at the Kanto Regional Construction Bureau of MOC in 1997.

Fig.2 Shows the estimated ground liquefaction states and bridge damage states by the prototype system. Rough estimation of ground liquefaction states (at 6,028 highway sites) and bridge damage states (368 highway bridges) is available at this time. Maximum acceleration values and SI values



(a) Ground Liquefaction States



(b) Bridge Damage States

Fig.2 Estimated Damage States by Prototype System

(designated hereinafter as ground motion characteristic values) observed by 100 seismographs installed in the Kanto region is adopted for the estimation.

ESTIMATION OF DAMAGE STATES

1. Flowchart of Estimation

Damage estimation is performed through three steps as shown in **Fig.3**. Fundamental policies of each estimation steps are as follows;

1) Estimation of Ground Motion Characteristic Values

For the judgement of ground liquefaction states and bridge damage states, ground motion characteristic values at the very site where the judgement is to be performed (designated hereinafter as a judgement site) are required. Because the locations of observation sites are different from judgement sites, ground motion characteristic values have to be estimated analytically.

2) Estimation of Ground Liquefaction States along Highways

Ground liquefaction states are judged in each divided highway section. Division of highway sections is carried out so that the ground condition is assumed to be uniform in each section. Judgement of ground liquefaction states can be performed based on a P_L value evaluated in each highway section. The P_L value can be evaluated by eq.(1), where a liquefaction resistant ratio F_L ⁵⁾ can be evaluated by a ground condition and an estimated maximum acceleration value in each highway section.

$$P_L = \int_0^{20} (1 - F_L)(10 - 0.5x)dx \dots \dots \dots (1)$$

$$F_L = R / L$$

where,

- x : Depth from the surface (m)
- FL : Liquefaction resistant ratio
- PL : Potential of liquefaction
- R : Dynamic shear strength ratio
- L : Shear stress ratio during an earthquake

3) Estimation of Bridge Damage States

Judgement of bridge damage states is performed individually based on the structural database. As the structural database, bridge maintenance data accumulated at sectors are adopted in this estimation. Damage states of whole bridge can be judged by comparing damage states of major bridge components. Damage states of major bridge components can be judged by the SI value estimated at the judgement site. By using the SI value, it is possible to consider the cyclic effect of ground motion to bridges. The SI value can be evaluated by eq.(2), where S_{wi} means the i (sec) component of velocity response spectrum.

$$SI = \frac{1}{2.5} \sum_{i=0.1}^{2.5} S_{wi} \dots \dots \dots (2)$$

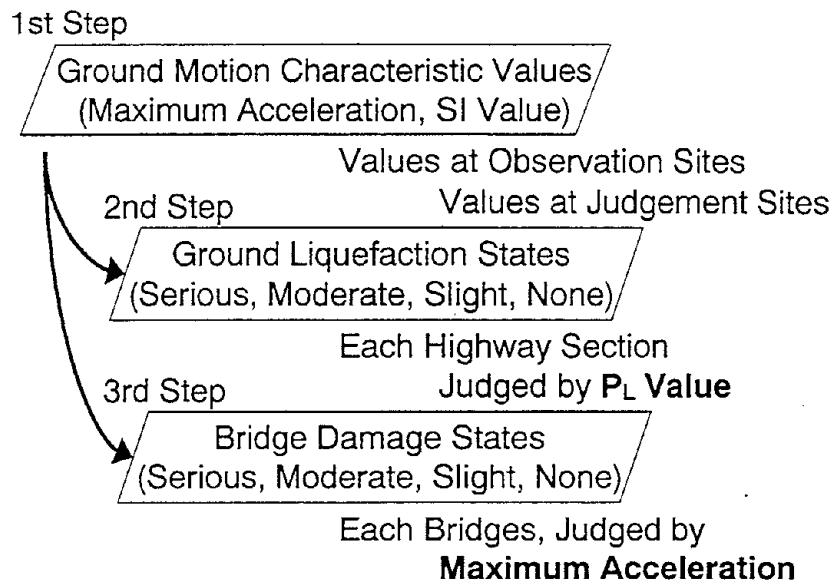


Fig.3 Flowchart of Damage Estimation

2. Classification of Damage States

Estimated ground liquefaction states and bridge damage states are displayed in four categories of "Serious", "Moderate", "Slight" and "None". Although there are other quantitative ways to display the estimated states using probabilities (%), qualitative four categories are adopted in the system. This is because; 1) qualitative expression is more understandable for decision-makers, 2) estimation accuracy is not enough for the quantitative expression, and 3) time period for the estimation can be reduced by the qualitative expression.

Table 2 shows the definitions of each category. Categories were defined as a combination of an assumed loss of transportation functions and a necessity of emergency repair works.

Table 2 Categories of Damage States

Damage States	Function Loss of Transportation	Required Activities
Serious	Interruption for Weeks	Restoration
Moderate	Interruption/ Restriction for Days	Temporary Repair
Slight	Restriction for Hours	Temporary Repair
None	No Restriction	None

3. Estimation of ground motion Characteristic Values

3.1 procedures

Fig.4 shows the estimation steps of ground motion characteristic values at judgement sites. Although a 3-D dynamic response analysis of ground model with a real-timely observed input ground motion is desirable, following simplified procedure was adopted in this system for minimizing the estimation time period with enough accuracy.

- 1) Ground motion characteristic values at the engineering bedrock: A characteristic value right under a observation site can be estimated by assuming a ground response amplification ratio.
- 2) Interpolation at the engineering bedrock: A characteristic value right under a judgement site can be estimated by an interpolation.
- 3) Ground motion characteristic values at judgement sites: a characteristic value can be estimated by assuming a ground response amplification ratio.

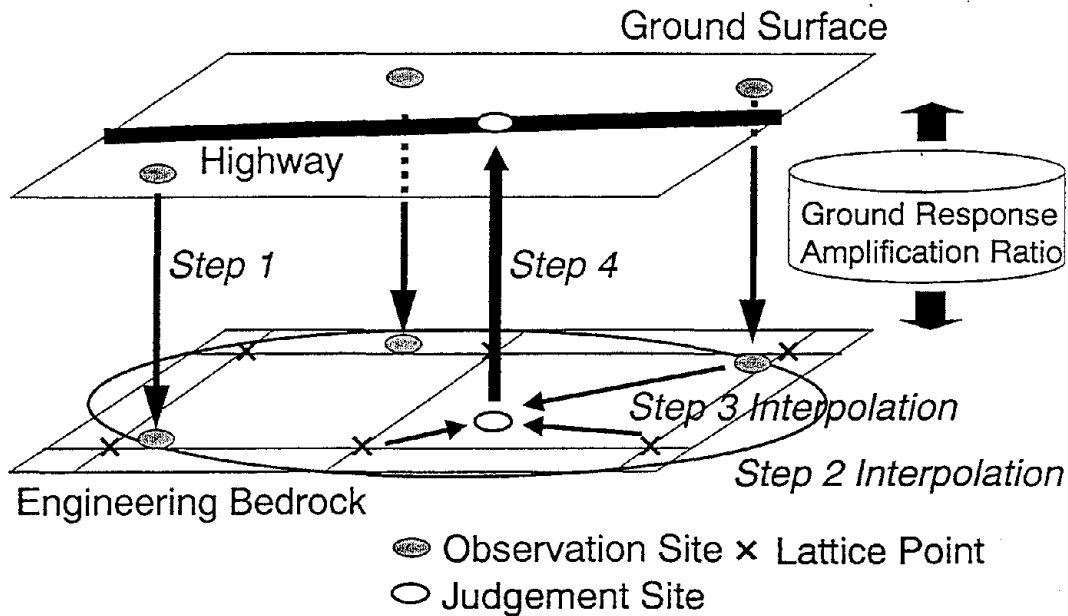


Fig.4 Estimation Steps of Ground Motion Characteristic Values

3.2 Ground Response Amplification Ratio

The ground response amplification ratio varies according to the cyclic characteristics of ground motions and non-linear property of ground. The amplification ratio is, therefore, desirable to be assumed for each observed ground motion. But because the seismograph network does not transmit a time history of ground motion, a standard amplification ratio was calculated in advance by a standard time history observed in the past earthquake. Calculation of the standard amplification ratio was carried out by the "SHAKE" for each observation/ judgement site.

The Kaihoku Bridge record detected in 1978 Miyagiken-oki Earthquake was adopted as a standard time history because it provided the most average amplification ratio in trial calculations using five

other typical records observed during past earthquakes. The non-linear property of ground can also be considered by eq.(3).

$$\alpha = a \times b^{-x} \dots\dots\dots(3)$$

where, α :Ground response amplification ratio for each observation/ judgement site
 x :Maximum acceleration value (SI value) at engineering bedrock
 a, b :Coefficients which represent the non-linear property of ground

Fig.5 shows an example of fixing the coefficients a and b . These coefficients were determined by a regression analysis of amplification ratios. Four input ground motions obtained by adjusting the maximum acceleration value of the Kaihoku Bridge record to 50, 100, 300 and 500 gals were adapted to the analysis.

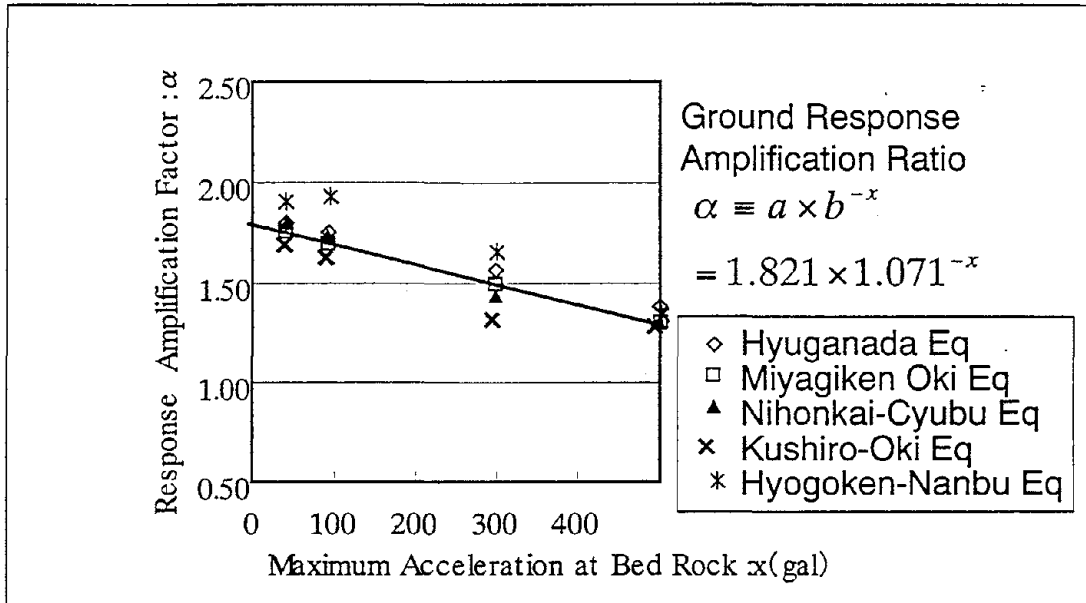


Fig.5 Coefficient a and b for Non-linear Property of Ground

3.3 Interpolation at Engineering Bedrock

Fig.6 shows an image of the interpolation at the engineering bedrock. Ground Motion Characteristic values right under judgement sites can be estimated by the following steps;

- 1) Dividing a whole region into 10m*10m square sections,
- 2) Definition of a co-ordinate system, in which system (x, y) represents the horizontal location of each observation site, and z -axis represents the ground motion characteristic value,
- 3) Definition of a curve surface which includes characteristic values of all observation sites,
- 4) Estimating characteristic values at each lattice point using the curve surface,
- 5) Estimating characteristic values at each judgement site by weighting the distance from closest four lattice points.

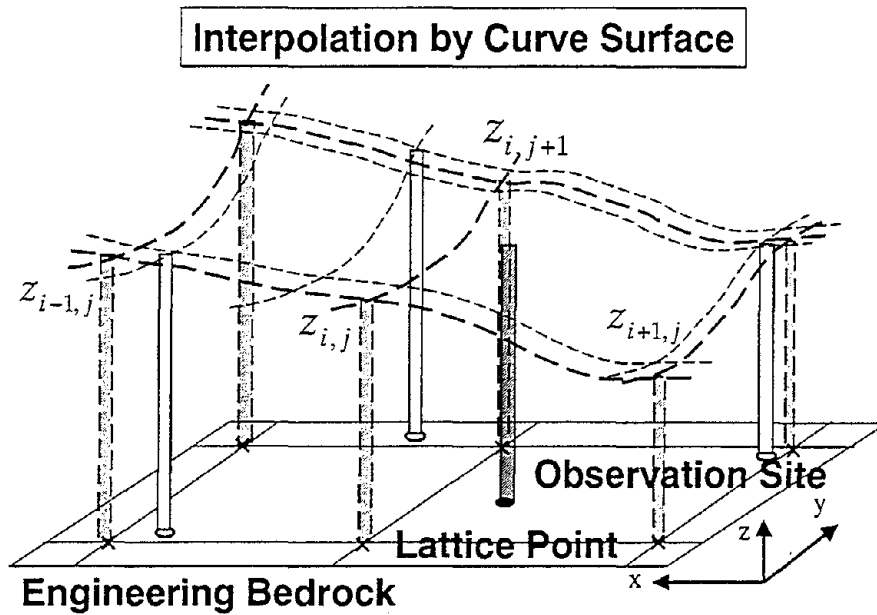


Fig.6 Interpolation at Engineering Bedrock

The highlight of this procedure is a definition of a curve surface. Because a curve surface is defined for the whole region, the characteristic value at each lattice point can be surely estimated. The characteristic value at each judgement point can be surely estimated if characteristic values at some observation sites could not be obtained by accidents.

4. Estimation of Ground Liquefaction States along Highways

4.1 $P_L \sim$ Ground Liquefaction States Matrix

Table 3 shows a $P_L \sim$ Ground Liquefaction States Matrix. Ground liquefaction states can be judged with the Matrix by P_L value that is estimated for each highway sections. The Matrix was developed based on a series of experimental studies of past earthquake disasters in PWRI. By modifying the Matrix in accordance with the future research development, judgement accuracy of ground liquefaction states can be easily upgraded.

Table 3 $P_L \sim$ Ground Liquefaction States Matrix

Ground Liquefaction States	Serious	Moderate	Slight	None
P_L Value	-----	$P_L > 15$	$15 \geq P_L > 5$	$5 \geq P_L$

The P_L value for the Damage State "Serious" was not set-up in the Matrix. This is because ground liquefaction is hardly considered to induce serious damages to road facilities that would interrupt the transportation for a long time period.

4.2 Procedures

Fig.7 shows the estimation steps of a ground liquefaction state at each highway section. The highlight of this procedure is a setting-up of maximum acceleration levels for each damage state as judgement indices. By setting-up the judgement indices prior to an earthquake, time period required for the judgement can be much reduced.

- 1) Calculation of a dynamic shear strength ratio R : R ratios, which is defined in eq.(1), for each soil layer can be calculated with pre-stored ground condition database.
- 2) Setting-up of judgement indices: P_L values for each Damage State "Serious", "Moderate" and "Slight" can be determined by **Table 3**. Maximum acceleration levels for each P_L value can be set-up at each highway section by eq.(2).
- 3) Judgement of damage states: By comparing the estimated maximum acceleration value with the maximum acceleration levels, judgement of damage state can be performed.

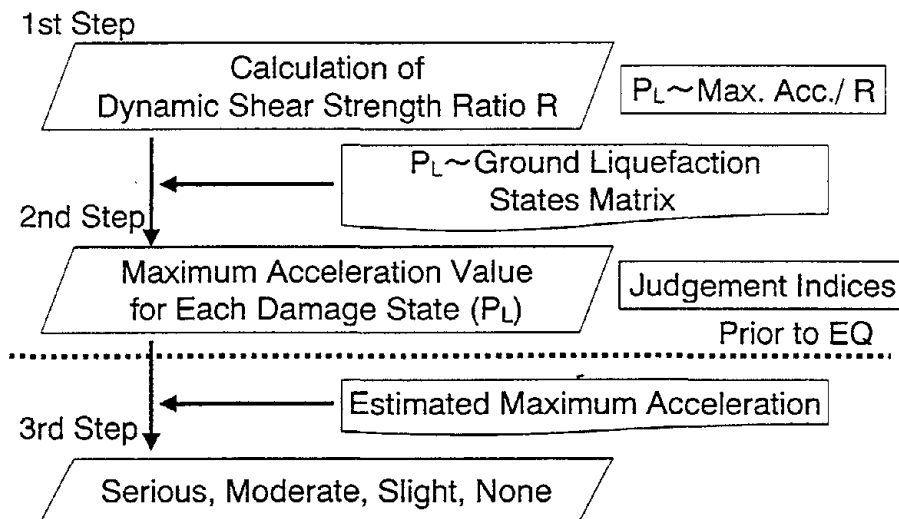


Fig.7 Estimation Steps of Ground Liquefaction States

5. Estimation of Bridge Damage States

5.1 SI Value ~ Bridge Component Damage States Matrix

Table 4 shows the SI Value ~ Bridge Component Damage Matrix. Damage States of the major bridge components can be judged with the Matrix by SI value that is estimated for each highway section including a bridge site. As the Damage States of major bridge components, following five states were selected due to their large effects on a whole bridge system, i.e. 1) Bending failure of RC column, 2) Shear failure of RC column, 3) Buckling of ST column, 4) Failure of bearing and 5)

Movement of foundation due to the liquefaction-induced ground flow.

Table 4 SI Value~Bridge Component Damage States Matrix

Damage States of Component	Damage States of Bridge			
	Serious	Moderate	Slight	None
Bending Failure of RC Column	Ultimate	Before Ultimate	Yielding	Before Yielding
Shear Failure of RC Column	Failure	Before Failure	Shear Cracking	Before Cracking
Buckling of ST Column	Buckling	Before Buckling	Slight Deformation	Before Deformation
Failure of Bearing	Failure	Damage (tall one)	Damage (short one)	Slight Damage
Movement of Foundation	-----	Large Displacement	Small Displacement	Slight Displacement

The Matrix was developed based on both a series of experimental studies and dynamic response analyses in PWRI. Basic concepts for the judgement of damage states are as follows;

1) Bending failure of RC column:

Relationships between SI value and damage states were set-up for several column types. Relationships were determined by the dynamic response analyses on approximately 400 columns. Column types were classified by structural specifications such as section size and weight. Damage states for each column type can be judged by the SI value.

2) Shear failure of RC column:

By a combination of h/D value and design year, a possibility of shear failure to be developed prior to the bending failure is estimated. h/D value is a ratio of a column height against a section size. Damage states can be judged by the SI value based on a series of experimental studies of past earthquake disasters.

3) Buckling of ST column:

A possibility of buckling is estimated by design year. Damage states can be judged experimentally by the SI value.

4) Failure of bearing:

A possibility of failure is estimated experimentally by the SI value. Because a failure of bearing induces a gap of road surface, the damage states are to be judged by the bearing height.

5) Movement of foundation due to lateral ground spread:

Verifying the distance between foundation sites and water lines, a possibility of the liquefaction-induced ground flow is estimated. Damage states can be judged by a combination of the distance and a ground liquefaction state.

5.2 Bridge Component Damage States~Bridge Damage States Matrix

Table 5 shows a Bridge Component Damage States~Bridge Damage States Matrix. The Damage State of a whole bridge system can be judged by comparing the damage states of major bridge components, i.e. the maximum damage state among those of major bridge components represents the

damage state of a whole bridge system.

Table 5 Bridge Component Damage States Matrix~Bridge Damage States Matrix

Bending Failure of RC Column

Design Code	Yield Seismic Coefficient	Damage States of Component			
		Ultimate	Before Ultimate	Yielding	Before Yielding
1979	-----	SI>50	SI>30	SI>10	10≥SI
1990	-----	SI>50	SI>30	SI>10	10≥SI
1995	0.6>k _{hy}	SI>50	-----	-----	50≥SI
	k _{hy} ≥0.6	SI>100	SI>50	-----	50≥SI

5.3 Procedures

Fig.8 shows the estimation steps of the damage states for each bridge. The highlights of this procedure are; 1) setting-up of SI value levels for each damage state as judgement indices, 2) verifying a bridge component that represents the damage state of a whole bridge system. By these pre-earthquake works, time period required for the judgement can be much reduced.

- 1) Setting-up of judgement indices for each major bridge component: SI value levels for each Damage State "Serious", "Moderate" and "Slight" can be determined by **Table 5**.
- 2) Setting-up of judgement indices for a whole bridge system: SI value levels for each Damage State can be determined by verifying a minimum SI value level among those of major components.

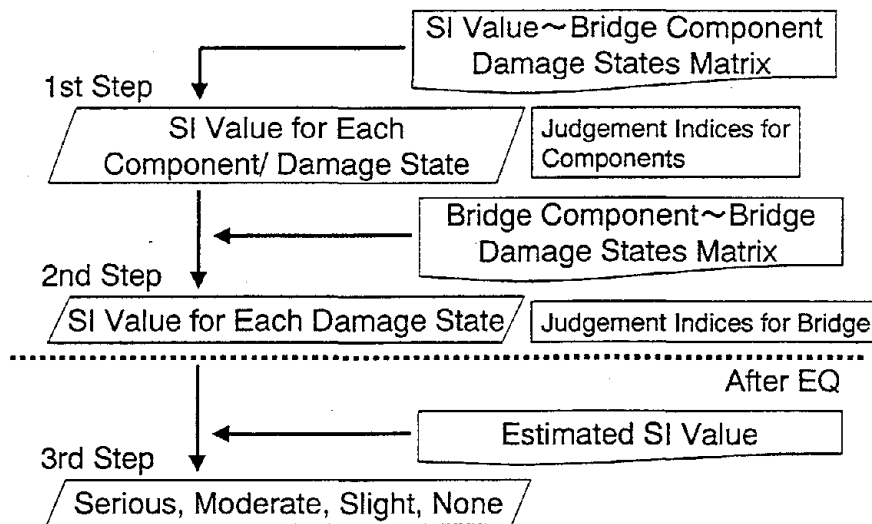


Fig.8 Estimation Steps of Bridge Damage States

- 3) Judgement of damage state: By comparing the estimated SI value with the SI value levels, judgement of damage state can be performed.

CONCLUSIONS

The Real-time Earthquake Damage Estimation System for Road Facilities was introduced. By providing rough estimations on damage states and damage distributions of road facilities immediately after an earthquake, the System will support quick decision-making on emergency activities, i.e. efficient damage inspections with restricted amount of inspectors, management of buck-up organization management and construction stuffs/ devices control.

For the implementation to the emergency practice, further research is required on the following points;

- 1) Accumulation of ground/ structural condition data, and construction of databases
- 2) Upgrade of damage estimation accuracy based on disaster experiences
- 3) Development of damage estimation procedures for the other road facilities
- 4) System cooperation with the other individual systems for the road management activities

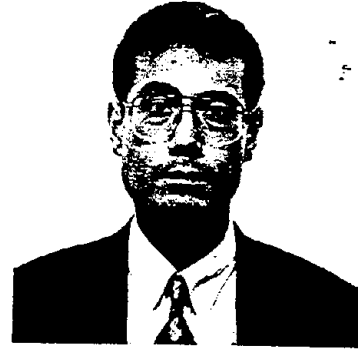
REFERENCES

- 1) Public Works Research Institute: Manual for Repair Methods of Civil Engineering Structures Damaged by Earthquakes, Technical Note of PWRI, Vol. 45, 1986.12
- 2) Public Works Research Institute: Report on the Disaster caused by the 1995 Hyogo-ken Nanbu Earthquake, Report of PWRI, Vol. 196, 1996.3
- 3) Public Works Research Institute: Guidelines for Disaster Information Systems for Important Infrastructures (draft), Technical Note of PWRI, Vol. 58, 1992.4
- 4) H. Sugita, S. Odagiri and M. Kaneko: Development of Real-time Seismic Information System for MOC, 29th UJNR Joint Panel on Wind and Seismic Effects, 1997.5
- 5) Japan Road Association: Design Specification of Highway Bridges; Part V Seismic Design, 1996.12

PERSONAL CAREER

NAME: Hideki SUGITA

POSITION: Head,
Earthquake Disaster Prevention
Technology Division, Earthquake
Disaster Prevention Research Center,
Public Works Research Institute,
Ministry of Construction



ADDRESS: 1 Asahi, Tsukuba-shi, 305 Japan

DATE OF BIRTH: May 7, 1964

EDUCATION: 1987 Bachelor of Civil Engineering, Osaka University
1995 Doctor of Engineering, Osaka University

MAJOR SUBJECT: Earthquake Engineering

MAJOR AREA OF EXPERIENCE:

1987-1994 Research Engineer, Earthquake Engineering Div., PWRI
1993-1994 Visiting Scholar, University of California at Berkeley
1994-1996 Planning and Administration Div., PWRI
1996- Head, Earthquake Disaster Prevention Technology Div., PWRI

TRAVEL ABROAD: U.S.A, Italy

MAJOR PUBLICATIONS:

- (1) "Loading Test of Shield Tunnel Specimens subjected to Alternative Axial Loading", U.S. National Conference on Earthquake Engineering, 1990
- (2) "Seismic Behavior of Buried Pipelines through Field Observation", U.S.-Japan Workshop on Earthquake Disaster Prevention for Lifeline Systems, 1992
- (3) "Guidelines for Seismic Design Methods of Large Underground Structures", UJNR Joint Panel on Wind and Seismic Effects, 1992
- (4) "Dynamic Strength and Ductility Characteristics of Steel Bridge Piers", U.S.-Japan Workshop on Bridges, 1993
- (5) "Guideline for Disaster Information Systems for Important Infra-structures", UJNR Joint Panel on Wind and Seismic Effects, 1993
- (6) "Development of Real-time Seismic Information Systems for MOC", UJNR Joint Panel on Wind and Seismic Effects, 1997

Seismic hazard mapping in Eugene-Springfield, Oregon

Yumei Wang¹, David K. Keefer², and Zhenming Wang¹

Abstract

The Oregon Department of Geology and Mineral Industries (DOGAMI) and the U.S. Geological Survey (USGS) are developing earthquake hazard maps for the Eugene-Springfield area, in Lane County, Oregon. The method for producing the map is derived from state-of-practice dynamic analyses for ground response, slope stability and liquefaction analyses, empirical correlations of slope stability with engineering properties of materials, and manipulation of data on local topography, engineering geology, and hydrology using geographic information system (GIS) tools. Specific types of data used to produce the map include: (1) distribution of geologic units; (2) engineering properties of materials in each geologic unit; (3) slope inclinations; (4) regional hydrology; (5) distribution of existing landslide deposits; (6) distribution of artificial slope alterations; and (7) ground motions from design scenario earthquakes (M6.5 shallow crustal and M8.3 subduction zone event).

Seismically-induced ground deformation is evaluated as follows: slopes steeper than 25 degrees are analyzed using empirical criteria that relate slope stability to degree of weathering, strength of cementation, spacing and openness of rock fractures, and hydrologic conditions. Slopes between 5 and 25 degrees, which in the project area are commonly mantled with aprons of heterogeneous colluvium, are evaluated with a dynamic slope stability analysis that uses slope inclinations, engineering geologic characteristics of geologic units, and shaking parameters from design earthquakes as inputs. Slopes gentler than 5 degrees are analyzed for liquefaction and resultant lateral spreading. Results of these analyses are then combined to produce a ground deformation map with five slope instability categories (Very High, High, Medium, Low, and Nil potential for slope failure). Site periods and maximum spectral ratio are also shown on the ground deformation hazards map. Site effects of local geology on ground shaking are evaluated using SHAKE91. Site periods and maximum amplification of spectral accelerations were determined and used to produce a ground response map.

The 1:24,000-scale maps resulting from this study are intended for use by local communities for regional planning and mitigation purposes. Techniques developed in this study are intended to be applicable to regional-scale mapping in other areas with a wide variety of topographic, geologic, and hydrologic characteristics.

¹ Oregon Department of Geology and Mineral Industries, 800 NE Oregon St., #28, Portland, OR 97232, USA

² U. S. Geological Survey, 345 Middlefield Rd., MS 977, Menlo Park, CA 94025, USA

Introduction and Purpose

Many types of earthquake hazards can be evaluated and mitigated to an acceptable level of risk in advance of future damaging earthquakes. Ground failures from slope instability can be a significant threat, especially in urban areas with concentrated development on unstable slopes. Amplified ground shaking can be destructive, intensifying and prolonging ground shaking. Many recent earthquakes have caused significant loss of life and property damage from earthquake-induced landslides and amplified ground shaking.

This paper presents a preliminary method for producing an earthquake hazard map showing (1) dynamic (i.e. earthquake-induced) slope stability for slopes that range from steep to gentle, and (2) dynamic ground response. Dynamic slope stability is evaluated for a wide spectrum of landslide failure types. Steep slopes (> 25 deg.) are most susceptible to rockfalls and other fast moving landslides, moderate slopes (5 - 25 deg.) are susceptible to deep seated rotational and translational block slides, and even gentle slopes (< 5 deg.) may be susceptible to liquefaction-induced lateral spreading. Ground response results show site periods and maximum spectral ratio. Site periods and maximum spectral ratios are shown as 0.1 second and 1.0 contour intervals, respectively.

The method described here for producing a hazard map is derived from dynamic ground response, slope stability and liquefaction analyses, empirical correlations of slope stability with engineering properties of materials, and manipulation of data on local topography, engineering geology, and hydrology using geographic information system (GIS) tools. The final map will be produced at a 1:24,000 scale, using 30-ft grid digital elevation model (DEM) data, and will provide information for regional planning, design, and mitigation. The map should serve as a useful tool to reduce hazards through effective land-use and emergency planning, regional vulnerability studies, identifying areas that would benefit from site specific studies, and providing a means to prioritize mitigation efforts.

The project area encompasses three 7 1/2 minute U.S. Geological Survey quadrangles (Eugene West, Eugene East, and Springfield) and totals about 200 square miles (Figure 1). The project area is rectangular and includes the Metro plan boundary and extends beyond the three quadrangles. This project involves working closely with an advisory task force composed of local community members. It also includes establishing a temporary local seismograph network to monitor local and distant earthquakes to gain a better understanding of local sources and ground response, and performing an evaluation of structural seismic vulnerability on a limited number of selected buildings.

Background

From its beginnings in the 1840s, the population of the Eugene-Springfield metropolitan area is now approaching 200,000 and continues to increase. The population within the metro plan boundary (Figure 1), which covers an area slightly larger than both the city and urban growth boundaries, is projected to increase by approximately 57 percent between 1990 and 2020 (Meacham, 1990).

Building expansion continues to penetrate the hillslope and urban development areas, which tend to be difficult areas to build. Due to the nature of the geology, topography, and climate, certain areas are prone to ground failure and amplified ground shaking, which threaten both existing and new developments.

Geographic Setting

The project area is located in the southern reach of the upper Willamette basin near the confluence of the Coast and Middle Fork Willamette Rivers and the McKenzie River. It includes hills bounding the valley, with the Cascades on the east flank and the Coast Range on the west and south. The climate is moderate in temperature and has an average annual precipitation of 40 inches. Generally, the elevation of central Eugene and Springfield is about 400 ft.

Geologic Setting

The Willamette Valley geomorphic province is a broad lowland separating the Oregon Coast Range from the Cascade Range. This terrain is part of the forearc basin associated with the Cascadia subduction zone and consists of interfingering, gently-dipping, Tertiary rocks ranging from Eocene to Miocene age, including volcanic flows and intrusions, tuffaceous sediments, and sedimentary rocks (Walker and Duncan, 1989, Figure 2). In the Willamette Valley, bedrock units are overlain by Quaternary age alluvium and thus are not well understood in detail. The smooth alluvial plain of the Willamette Valley is interrupted by occasional flood and stream channels. Table 1 describes the geologic units found in the test area (Figure 2), which is discussed later in Slope Analyses (Walker and Duncan, 1989).

Table 1. Geologic units

Symbol	Age	Description
Qal	Holocene	Alluvium - Clay, silt, sand, and gravel in river and stream channels.
Qoal	Holocene/ Pleistocene	Older alluvium - Poorly consolidated clay, silt, sand, and gravel marginal to active stream channels and filling lowland plains of Willamette River Basin and tributary drainages.
Qt	Holocene/Pleistocene	Terrace and fan deposits - Elevated deposits of alluvial silt, sand, and gravel along main drainages in the Coast Range and in the western Cascade Range.
Tub	Miocene	Basalt and basaltic andesite flows and flow breccias - Grades laterally into palagonitic tuff and breccia and into clastic sedimentary rocks (Tus).
Ti	Oligocene	Mafic intrusions - Sheets, sills, and dikes of massive granophyric ferrogabbro; some bodies strongly differentiated and include pegmatitic gabbro, ferrogranophyre, and granophyre.
Tf	Oligocene/Eocene	Fisher Formation, undivided - Predominantly continental volcanoclastic rocks, including andesitic lapilli tuff, breccia, water-laid and air-fall silicic ash, and interbedded basaltic flows.

Te	Oligocene/Eocene	Eugene Formation - Thin to moderately thick bedded, coarse-to fine-grained arkosic, micaceous, and, locally, palagonitic sandstone and siltstone, locally highly pumiceous, assigned to the upper Eocene to middle Oligocene, marine Eugene Formation.
Tfb	Eocene	Basaltic flows - Flows, some of which may be invasive into the undivided Fisher Formation (Tf), and undivided and questionable sills that may intrude the undivided Fisher.

Seismic Setting

The physiographic setting of the Pacific Northwest results from its plate tectonic setting. From northern California to British Columbia, oceanic plates, including the Juan de Fuca plate, are being subducted beneath the North American plate along the Cascadia subduction zone. Earthquakes can occur within the subducting Juan de Fuca plate (oceanic intraplate earthquakes), within the overriding North American plate (crustal earthquakes), or along the interface between the two plates (subduction zone earthquakes). All three possible earthquake types (subduction, oceanic intraplate, and crustal) can severely impact the project area, and each was considered as part of this study.

Although no damaging earthquakes have occurred during historic times, small local earthquakes have been recorded. A recent study that focused on evaluating ground response in Eugene and Springfield (R. Weldon and S. Perry-Huston, University of Oregon Geological Sciences Department, unpublished data) included the recording of several very small local earthquakes. In January 1996, a cluster of small earthquakes occurred about 25 km east of Eugene. Later, in May 1996, a small earthquake occurred about 5 km north-northwest of downtown Eugene. These earthquakes have not been identified with any specific fault structure (S. Perry-Huston, personal communication, 1997) but indicate zones of potential threat to local communities. The project area is located about 100 km east of the Cascadia subduction zone, where several large-magnitude subduction zone earthquakes are thought to have occurred in the past few thousand years (Atwater, 1996). A strong local crustal earthquake or great subduction zone earthquake would likely produce strong ground shaking for all geologic units in the project area. Bedrock ground motions incorporated in the study were developed by Geomatrix Consultants (1995).

Data Collection

The method used to evaluate earthquake-induced ground failure and local ground response requires information on the geologic units (their distribution and engineering characteristics), slope angles, hydrology, and the occurrence of existing landslides and large artificial slope alterations. The distribution of geologic units was determined from published geologic maps (Walker and Duncan, 1989; Vokes and others, 1951) and from additional mapping carried out as part of the study. The engineering properties of materials in each geologic unit were determined from field mapping, laboratory testing of selected materials, in-situ tests, and engineering judgment. Field work included the mapping of over 200 outcrops considered to be reasonably representative of the geologic units. In situ tests included downhole shear wave velocity profiling, surface refraction profiling, and standard penetration testing. Slope inclinations were determined using geographic information system (GIS) tools and digital elevation models (DEMs) with a grid spacing of 30 ft. Regional hydrology was determined from borehole and well data, mapping of

springs and seeps, and also hydrologic modeling conducted by the local water departments. Existing landslide deposits were mapped as part of the study. Input on active landslides was provided by local consultants and public works department staff. Lastly, artificial slope alterations, such as large road- and railroad cuts were identified. The method does not specifically address slope aspect, vegetation, and human effects (such as logging and grading practices).

Slope Analyses

Preliminary analyses were conducted in a test area, which covers about 20 square miles of the project area (Figure 1). Slopes in the test area are divided into four groups: (A) existing landslides; (B) steep slopes, greater than 25 degrees; (C) moderate slopes, ranging from 5 to 25 degrees; and (D) gentle slopes, less than 5 degrees (Figure 3). It was assumed that groups (B), (C) and (D) have fundamentally different modes of dynamic failure. Consequently, different analytical techniques were applied to these groups as shown on Figure 4.

(a) Existing landslides

The movement characteristics of existing landslides are highly variable and range from actively moving to stable. To understand the nature of each existing landslide would require numerous site-specific evaluations. In the absence of this landslide information, it was assumed that the slip planes are at reduced shear strengths of unknown values, and that existing landslide masses are inherently unstable under earthquake loading. Thus, existing landslides were assigned to the very high susceptibility rating. No analytical techniques were applied.

(b) Steep slopes

Bedrock slopes greater than 25 degrees are particularly susceptible to slope failures (Keefer, 1993). Consequently, slopes greater than 25 degrees were assigned to Group B, steep slopes. Engineering properties of geologic units, including degree of weathering, strength of cementation, spacing and openness of rock fractures, and hydrologic conditions, were mapped in outcrops. Each outcrop was assigned to a mapped geologic unit. Then, each geologic unit was evaluated for susceptibility to slope failure using a decision tree outlined in Keefer (1993) and shown in Figure 5.

For each geologic unit, the average value from the rating category was analyzed using empirical criteria that relate slope instability to area (Keefer, 1993). Keefer (1993) related engineering properties observable in outcrop to landslide concentrations, expressed as number of landslides per square kilometer (LS/km²). For the geologic units within the test area, each outcrop was rated according to Figure 5. Then, the results were averaged for each geologic unit, using the following landslide concentration relationship: $LS/km^2 = (32)(\% \text{ extremely high}) + (8)(\% \text{ very high}) + (2)(\% \text{ high}) + (0.125)(\% \text{ low})$, where the multipliers (32, 8, 2 and 0.125) are taken from landslide concentrations used to assign ratings in Keefer (1993). Landslide concentration results are shown on Table 2, column 3. Then, each geology unit was assigned a new susceptibility rating compatible with the DOGAMI earthquake hazard rating system of high, medium, or low on the basis of calculated landslides per square kilometer value as follows: High > 2 LS/km² > Medium > 1 LS/km² > Low. The results on dynamic landslide susceptibility for each geologic unit is shown on Table 2, column 4.

Table 2 Landslide concentration and ratings for geologic units

Geologic unit	Lithology	LS/km ²	DOGAMI Rating
Basalt flows, Tfb	Basalt	10.82	High
Eugene Formation, Te	Sandstone	5.34	High
Fisher Formation, Tf	Volcaniclastics	2.73	High
Basalt flow breccias, Tub	Breccias	1.83	Medium
Mafic intrusions, Ti	Gabbro	1.30	Medium

The following illustrates how the susceptibility was determined for a specific geologic unit, Tub, which consists of predominantly basalt and basaltic andesite flows and flow breccias. A total of 34 outcrops were mapped and evaluated in accordance to Keefer's method (1993): Thirty-one of 34 of the outcrops, or 91%, were assigned a susceptibility rating of high, and 3 of 34, or 9%, were assigned a rating of low. Landslide concentration is determined as follows ($2 \times 0.91 + 0.125 \times 0.09 = 1.83$) and gives a result of 1.83 landslides per square kilometer. This value falls into the medium susceptibility rating.

(c) Moderate slopes

Slopes ranging from 5 to 25 degrees were assigned to Group C, moderate slopes. For moderate slopes, we assume that coherent, relatively deep-seated translational and rotational slides are the most common modes of failure (Keefer, 1984). Moderate slopes in the project area are commonly mantled with aprons of heterogeneous colluvium. Our method for rating these slopes is based on the dynamic slope stability analysis of Newmark (1965), as verified and extended to regional-scale use by Wilson and Keefer (1983, 1985), Wieczorek and others (1985), Jibson (1993, 1996), and Jibson and Keefer (1993).

The selected earthquake input parameters included two controlling events: A magnitude 8.5 subduction zone earthquake at a 100-km distance from the earthquake source and a magnitude 6.5 event at 10-km distance. Arias Intensity (I_a) values were determined based on magnitude and distance from the source according to the equation developed by Wilson and Keefer (1985): $\log(I_a) = M - 2\log R - 4.1$ where I_a is in meters per second, M is moment magnitude, and R is earthquake source distance in kilometers. Next, assuming an infinite slope failure, an equation by Newmark (1965): $a_c = (FS - 1)g \sin \alpha$ is used to calculate a the critical acceleration (a_c). Here, a_c is the acceleration required to overcome frictional resistance and initiate sliding in terms of g , the acceleration due to Earth's gravity; FS is the static factor of safety, and α is the angle from the horizontal that the center of the mass of the potential landslide block first moves. The Newmark displacement (D_N in cm) was then determined from the relationship (Jibson, 1993; Jibson and Keefer, 1993): $\log(D_N) = 1.460\log I_a - 6.642 a_c + 1.546$. Finally, each slope is assigned a DOGAMI susceptibility rating of high, medium, or low based on the calculated D_N using High > 100 cm > Medium > 10 cm > Low (Figure 4).

(d) Gentle slopes

Slopes less than 5 degrees are assigned to Group D, gentle slopes. For gentle slopes, we calculated lateral spreading (i.e. slope instability) susceptibility for Quaternary-aged geologic units

that are prone to liquefaction failure. Gentle slopes underlain by pre-Quaternary geologic units are assumed to be stable and were automatically given a susceptibility rating of nil. Areas of Quaternary-aged units are separated in order of depositional age, with artificial fill and the youngest deposits generally being the most vulnerable to slope movement. The selected earthquakes include a M6.5 event at a 10-km distance and M8.5 subduction zone earthquake at 100-km, and were taken from an Oregon Department of Transportation study (Geomatrix Consultants, Inc., 1995).

To evaluate for lateral spreading susceptibility, we first estimate the site effects of local geology on ground shaking using SHAKE91, which is a commercially available program for analyzing one-dimensional site-response of vertically propagating (normally incident) shear waves at a level site (Idriss and Sun, 1992). Peak rock accelerations on the synthetic acceleration time history were scaled to 0.34g and used as input parameters in SHAKE91. The peak surface accelerations determined from SHAKE91 analysis were used as input accelerations in the liquefaction analyses.

Next, initial liquefaction was analyzed using two methods: The first by Robertson and Fear (1996), which is an improvement of a method developed by Seed and others (1984) and is based on standard penetration test (SPT) measurements, and the second by Andrus and Stokoe (1996), which is based on shear wave velocity measurements. Both methods were used to maximize the available in-situ data in the project area and account for the uncertainties associated with evaluating the predominantly gravelly soils.

For soils that are prone to liquefaction, lateral spreading was estimated using Barlett and Youd (1992). According to Barlett and Youd (1992), lateral spreading due to liquefaction satisfies: $\log(D_H) = -15.787 + 1.178M - 0.927 \log R - 0.013R + 0.429 \log S + 0.348 \log T_{15} + 4.527 \log (100 - F_{15}) - 0.922D_{50_{15}}$, where, D_H is lateral spreading, in meters; M is moment magnitude; R is horizontal distance to the nearest seismic energy source, in kilometers; S is ground slope, in percent; T_{15} is the cumulative thickness, in meters, of saturated cohesionless soils with $N_{1_{60}}$ value ≤ 15 ; F_{15} is the average fines content, in percent; $D_{50_{15}}$ is mean grain size.

To illustrate this method, we use drill hole data from Test Site ES-2, which is located in the Eugene West quadrangle (Figure 1). SHAKE 91 was run and a peak surface acceleration of 0.40g was achieved. Liquefaction was analyzed using methods of Robertson and Fear (1996) and Andrus and Stokoe (1996). Next, for soils that liquefy, lateral spreading is calculated using Barlett and Youd (1992). We assume: $M=8.5$, $R=100$ (km), $D_{50_{15}}=1.0$ (mm), $F_{15}=5\%$, $T_{15}=5$ m and S that range from 1 to 5 degrees. Results, shown on Table 4, indicate that for the given liquefiable deposit, steeper slopes have the tendency for greater lateral spreading displacements (0.56 m) than for gentler slopes (0.28m).

Table 4. Lateral Spreading Displacements for Test Site ES-2

Slope, S (deg)	D _H (m) (Bartlett and Youd, 1992)
1	0.28
2	0.38
3	0.45
4	0.51
5	0.56

A susceptibility rating will be assigned a rating of high, medium, low or nil according to possible lateral spreading displacements in a relative sense.

Slope Susceptibility Ratings

Applying susceptibility ratings within each of the four groups (A. existing landslides, B. steep, C. moderate and D. gentle slopes) requires professional judgment. The last step involves combining the independent analytical results from each group together to produce a coherent, uniform, relative hazard susceptibility map. Results from each group fall within one of five susceptibility ratings for dynamic slope instability: very high, high, medium, low, and nil (Figure 4).

Dynamic Ground Response Analyses

For the local geologic conditions in valley areas with about 10 ft or more of soil deposits (Figure 6), site period and maximum spectral ratio are evaluated. Site effects on ground shaking were determined using SHAKE91. Design earthquake for M6.5 crustal and M8.3 subduction zone events were modeled assuming epicentral distances of 10 km and 100 km, respectively.

Preliminary results of site period, which was determined for 26 site-specific soil locations, was contoured at 0.1 intervals (Figure 7). At these locations, amplification curves and Fourier response spectra were plotted to determine maximum spectral ratios, that is, maximum amplification of spectral accelerations. Figure 8 illustrates the process of determining maximum spectral ratios, including the input parameters (e.g. initial damping, density, shear wave velocity), input and output acceleration time histories, and spectral response showing the maximum spectral ratios. Figure 9 shows preliminary results of maximum spectral amplification contours. These amplification factors can be correlated with site period (shown on Figure 7) to indicate areas of potential soil-structure resonance that can cause structural damage. Higher damage also occurs in areas with prolonged strong shaking, which can be generally related to areas with longer site period.

Discussion

The method described in this paper is still under development and preliminary results using this method is scheduled to undergo additional review in early 1998. The tentative final product is one 1:24,000-scaled color map showing ground failure hazards, site period and maximum spectral ratios. These data were selected by community representatives with the assistance of DOGAMI and USGS staff on the basis of predicting high damage areas for a wide range of users.

Additional research is needed to more accurately predict dynamic ground response on a regional basis. To calibrate the reliability of this method, more post-earthquake field calibrations should be performed. Special focus should be given to determining dynamic slope stability hazards for moderate slopes.

Acknowledgments

Special thanks to Stephen E. Dickenson of Oregon State University Civil Engineering Department and Robert E. Kayen of U.S. Geological Survey for their helpful reviews. Thanks to Gerald Black for technical advice; Donald Hull and John Beaulieu for supporting this study; Klaus Neuendorf for editorial assistance; Tom Wiley and Robert Murray for geologic assistance; and Neva Beck for assisting in the preparation of this paper.

References

Andrus, R.D., and Stokoe, K.H., 1996. "Guidelines for Evaluation of Liquefaction Resistance Using Shear Wave Velocity", Proc. NCEER Workshop on Evaluation of Liquefaction Resistance, Jan. 4-5, 1996, Salt Lake City, Utah.

Atwater, B.F., 1996, Coastal evidence for great earthquakes in western Washington, in Rogers, A.M., Walsh, T.J., Kockelman, W.J., and Priest, G.R., eds., Assessing earthquake hazards and reducing risk in the Pacific Northwest: U.S. Geological Survey Professional Paper 1560, v. 1, P. 75-90.

Bartlett, S. F. and Youd, T. L., 1992, Empirical Prediction of Liquefaction-Induced Lateral Spread, *Journal of Geotechnical Engineering*, v. 121, No. 4, pp. 316-329

Geomatrix Consultants, Inc., 1995, Seismic design mapping, State of Oregon: Final report to Oregon Department of Transportation, Project no. 2442, var. pag.

Idriss, I.M., and Sun, J., 1992, User's manual for SHAKE 91, a computer program for conducting equivalent linear seismic response analyses of horizontally layered soil deposits: National Institute of Standards and Technology, Building and Fire Research Laboratory, Structures Division, Gaithersburg, Maryland, and Center for Geotechnical Modeling, Department of Civil & Environmental Engineering, University of California, Davis, Calif., var. pag.

Jibson, R.W., 1993, Predicting earthquake-induced landslide displacements using Newmark's sliding block analysis: Washington DC., National Research Council Transportation Research Record 1411, p. 9-17.

Jibson, R.W., 1996, Use of landslides for paleoseismic analysis: *Engineering Geology*, v. 43, p. 291-323.

Jibson, R.W., and Keefer, D.K., 1993, Analysis of the seismic origin of landslides: Examples from the New Madrid seismic zone, *Geological Society of America Bulletin*, Vol. 105, pp. 521-536.

Keefer, D.K., 1984, Landslides caused by earthquakes, *Geological Society of America Bulletin*, v. 95, p. 406-421.

Keefer, D.K., 1993, The Susceptibility of Rock Slopes to Earthquake-Induced Failure, *Technical Notes in the Bulletin of the Association of Engineering Geologists*, pp. 353-361.

Meacham, J.E., Editor, Atlas of Lane County, Oregon, 1990, QSL Printing Company, Eugene, Oregon, 73 p.

Newmark, N. N., 1965, "Effects of Earthquakes on Dams and Embankments", *Geotechnique*, vol. 5, no. 2.

Robertson, P.K. and Fear, C.E., 1996. "Soil Liquefaction and its Evaluation Based on SPT and CPT", Proc. NCEER Workshop on Evaluation of Liquefaction Resistance, Jan. 4-5, 1996, Salt Lake City, Utah.

Seed, H.B., Tokimatsu, K., Harder, L.F., and Chung, R.M., 1984, The influence of SPT procedures in soil liquefaction resistance evaluations: Berkeley, Calif., University of California, College of Engineering, Earthquake Engineering Research Center Report UCB/EERC-84/15, 50 p.

Vokes, H.E., Snavely, P.D., and Myers, D.A., 1951, Geology of the southern and Southwestern Boarder area of the Willamette Valley, Oregon, U.S.G.S. Oil and Gas Investigation Map OM 110.

Walker, G.W., and Duncan, R.A., 1989, Geologic Map of the Salem 1° by 2° Quadrangle, Western Oregon, Miscellaneous Investigation Series I-1893, U.S. Geological Survey.

Wieczorek, G.F., Wilson, R.C., and Harp, E. L., 1985, Map of slope stability during earthquakes in San Mateo County, California: U.S. Geological Survey Miscellaneous Investigations Map I-1257-E, scale 1:62,500.

Wilson, R. C., and Keefer, D. K., 1983, Dynamic analysis of a slope failure from the August 6, 1979, Coyote Lake, California, earthquake: *Seismological Society of America Bulletin*, v. 73, no. 3, p. 863-877.

Wilson, R. C., and Keefer, D.K., 1985, Predicting Areal Limits of Earthquake-Induced Landsliding, in Ziony, J.I., ed., in *Evaluating Earthquake Hazards in the Los Angeles Region— An Earth-Science Perspective*, U.S. Geological Survey Professional Paper 1360, pp. 317-494.

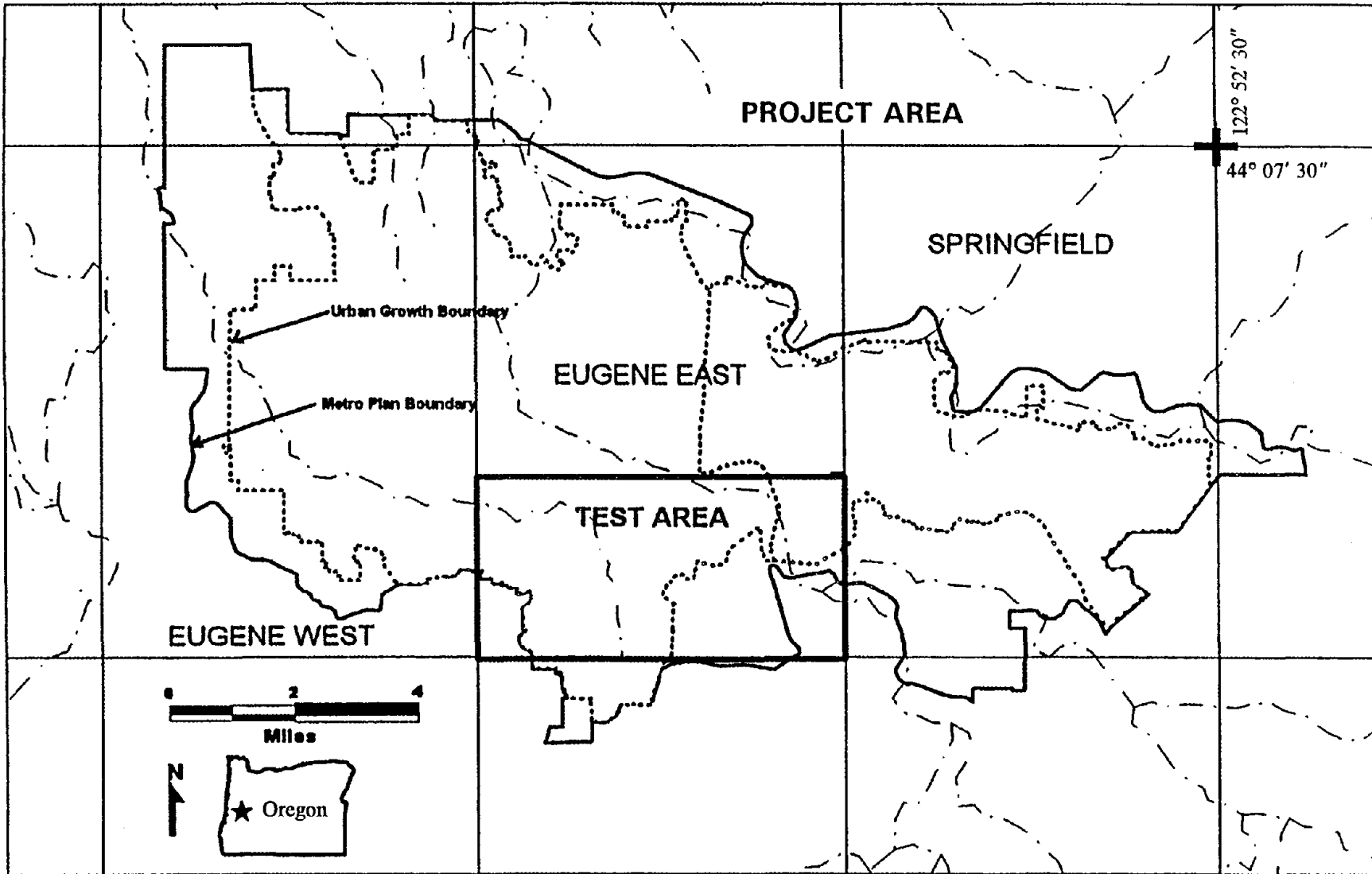
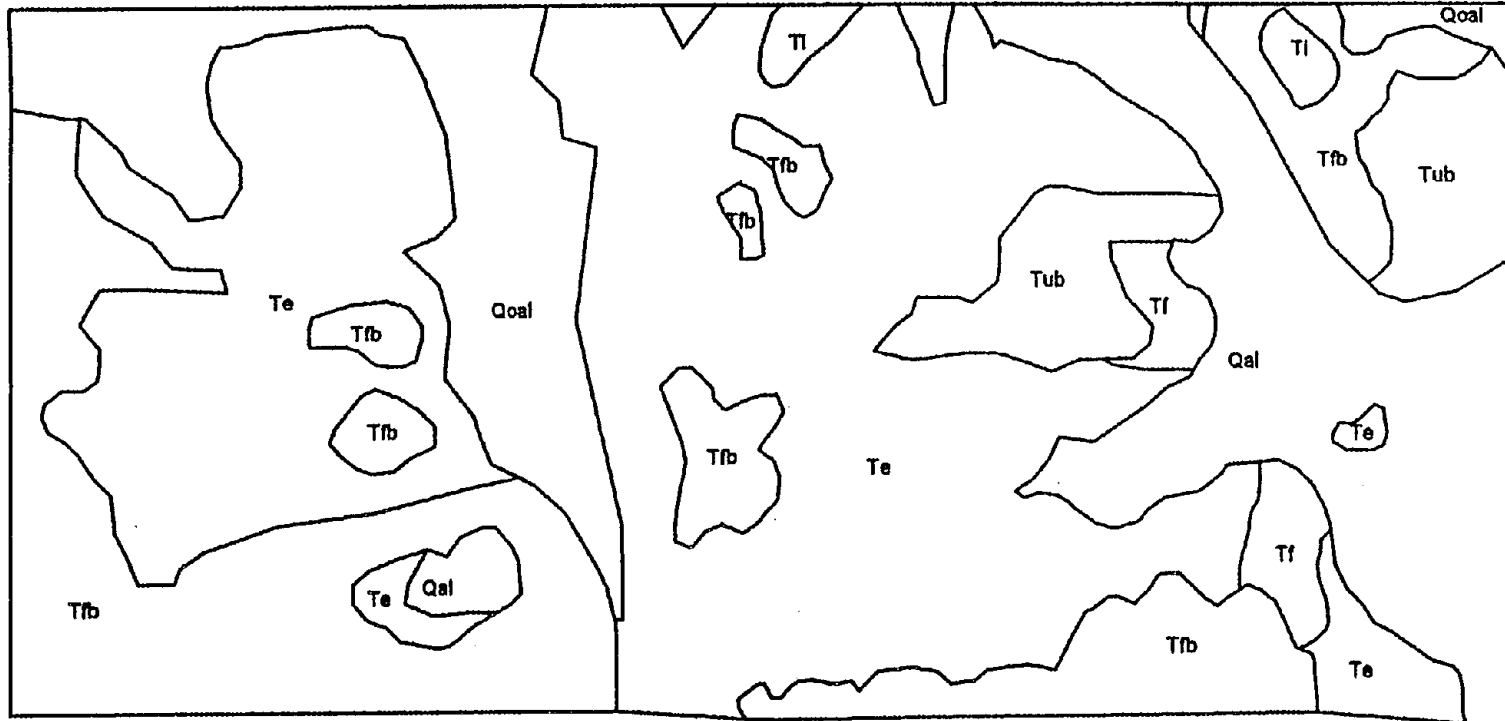


Figure 1. Project area for the Eugene-Springfield earthquake hazard map. Also shown are the slope test area, major drainages (dash-dotted lines), and project location (star) with the state of Oregon.



EXPLANATION

Qal	Alluvium
Qoal	Older alluvium
Qt	Terrace and fan deposits
Tub	Basaltic flow breccias
Tf	Fisher Formation
Tfb	Basaltic lava flows
Te	Eugene Formation
Ti	Mafic intrusions

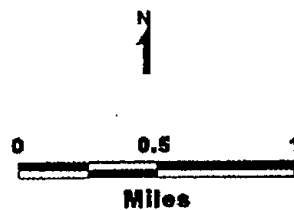
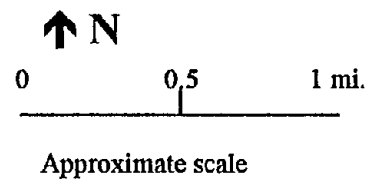
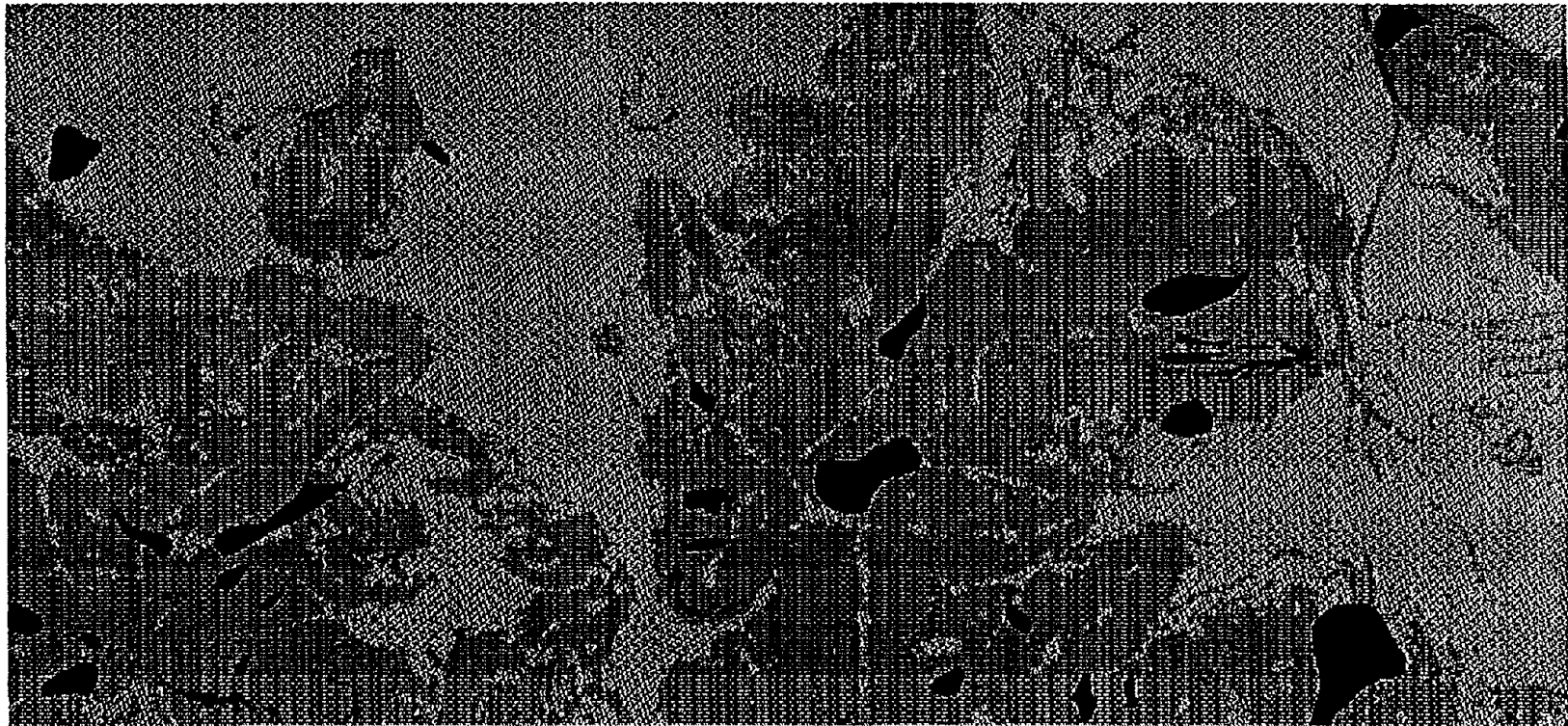


Figure 2. Geologic map of test area (Modified from Walker and Duncan, 1989)



Explanation





- | | |
|---|---------------------------------|
|  | Group A. Existing Landslides |
|  | Group B. Steep Slopes, 25 deg. |
|  | Group C. Mod. Slopes, 5-25 deg. |
|  | Group D. Gentle Slopes, <5 deg. |

Figure 3
A, B, C and D Groups

Different analytical techniques were applied to these groups.

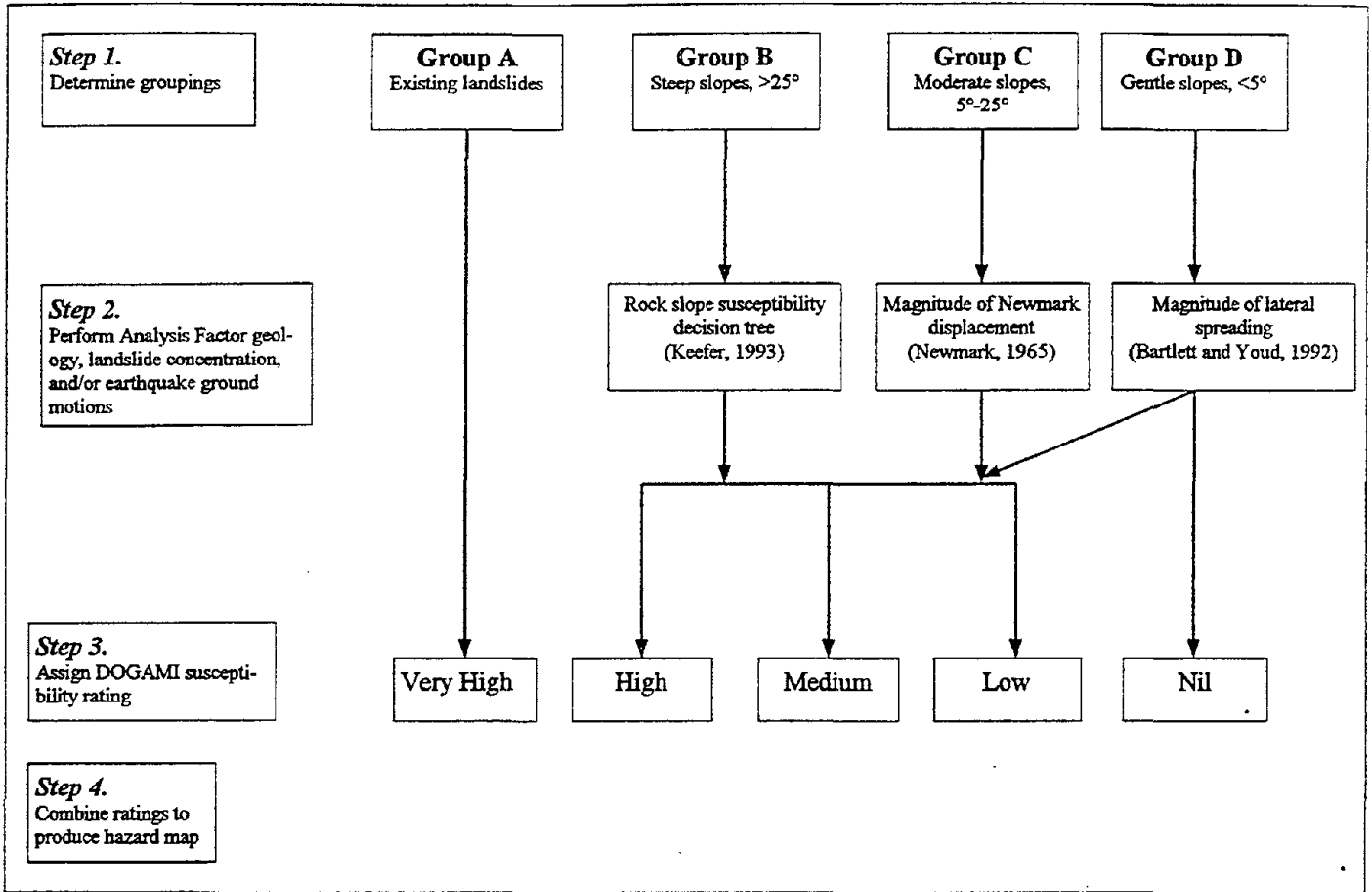


Figure 4. Method of slope ratings flow chart

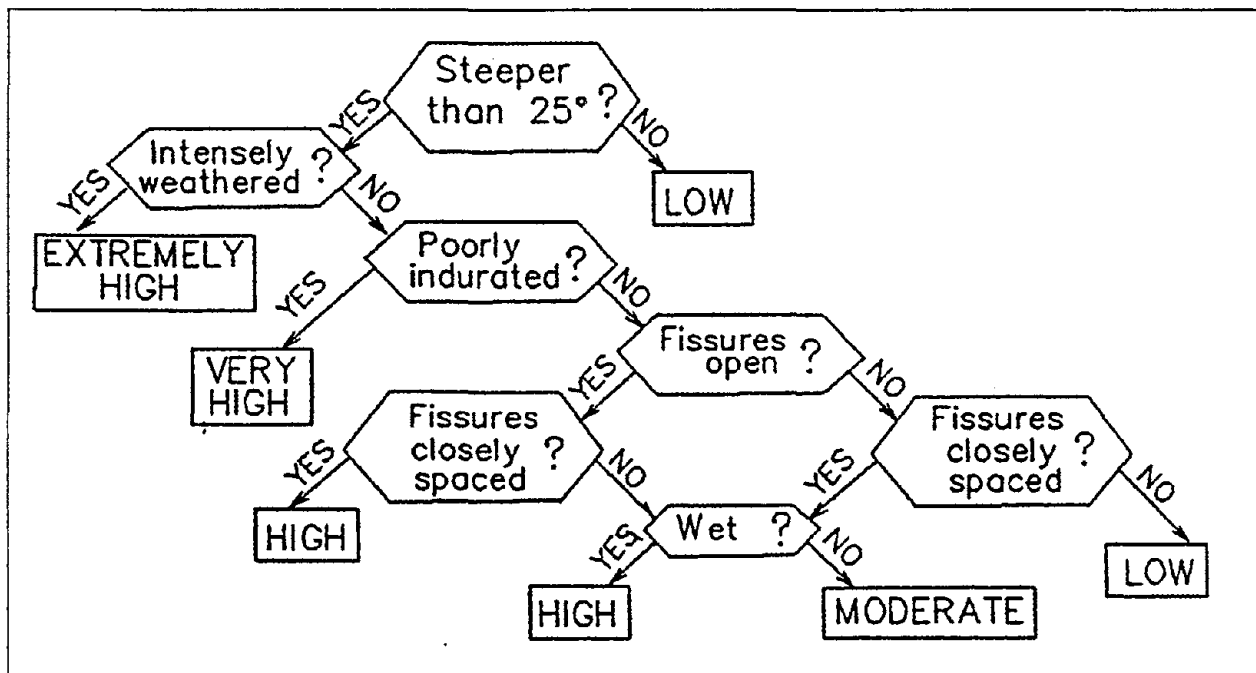


Figure 5. Decision tree for susceptibility of rock slopes to earthquake-induced landslides (from Keefer, 1993). For the test area, all slopes were assumed to be wet.

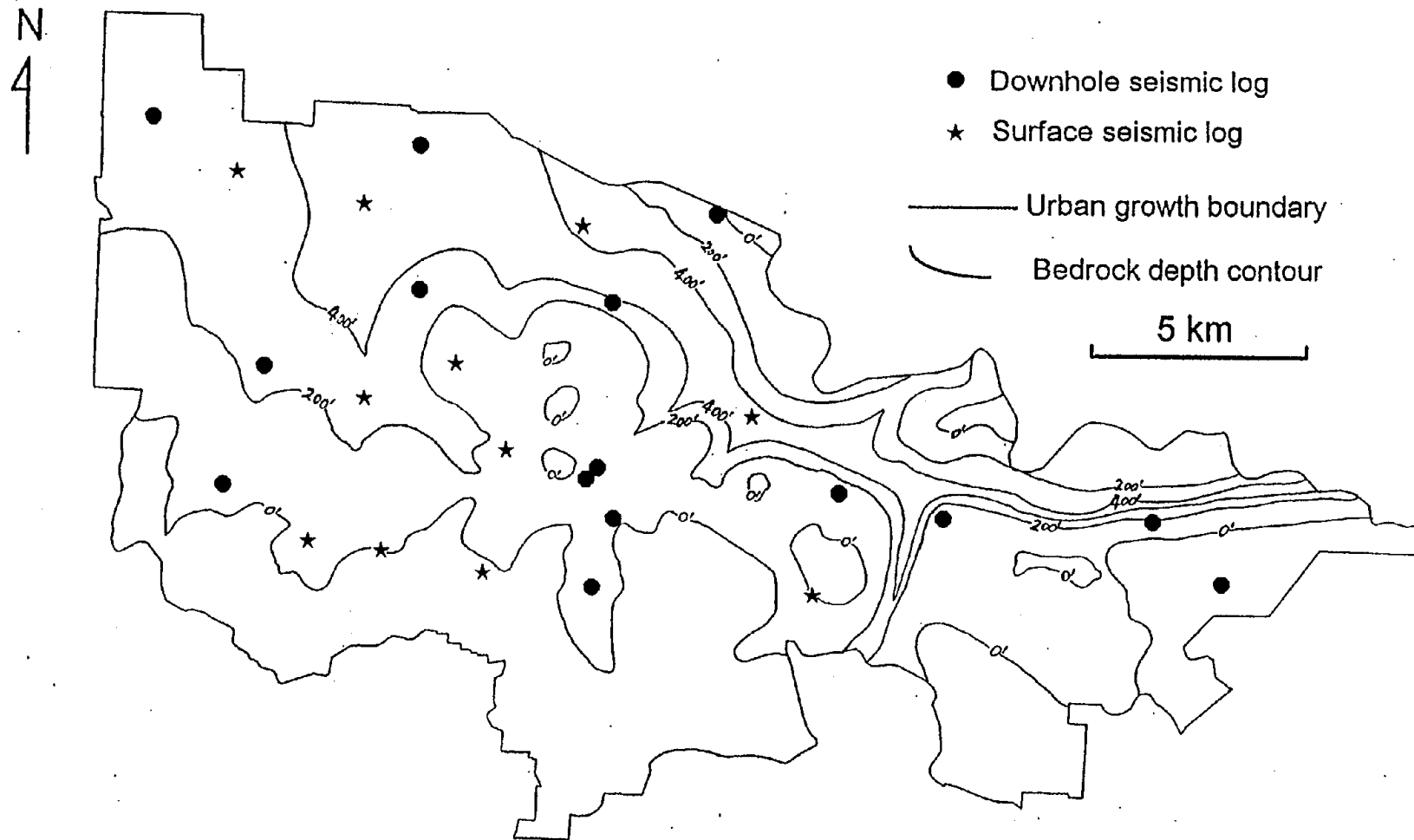


Figure 6. Location of seismic log and generalized depth to bedrock contours in the Eugene-Springfield urban growth boundary (contours in 200 feet intervals).

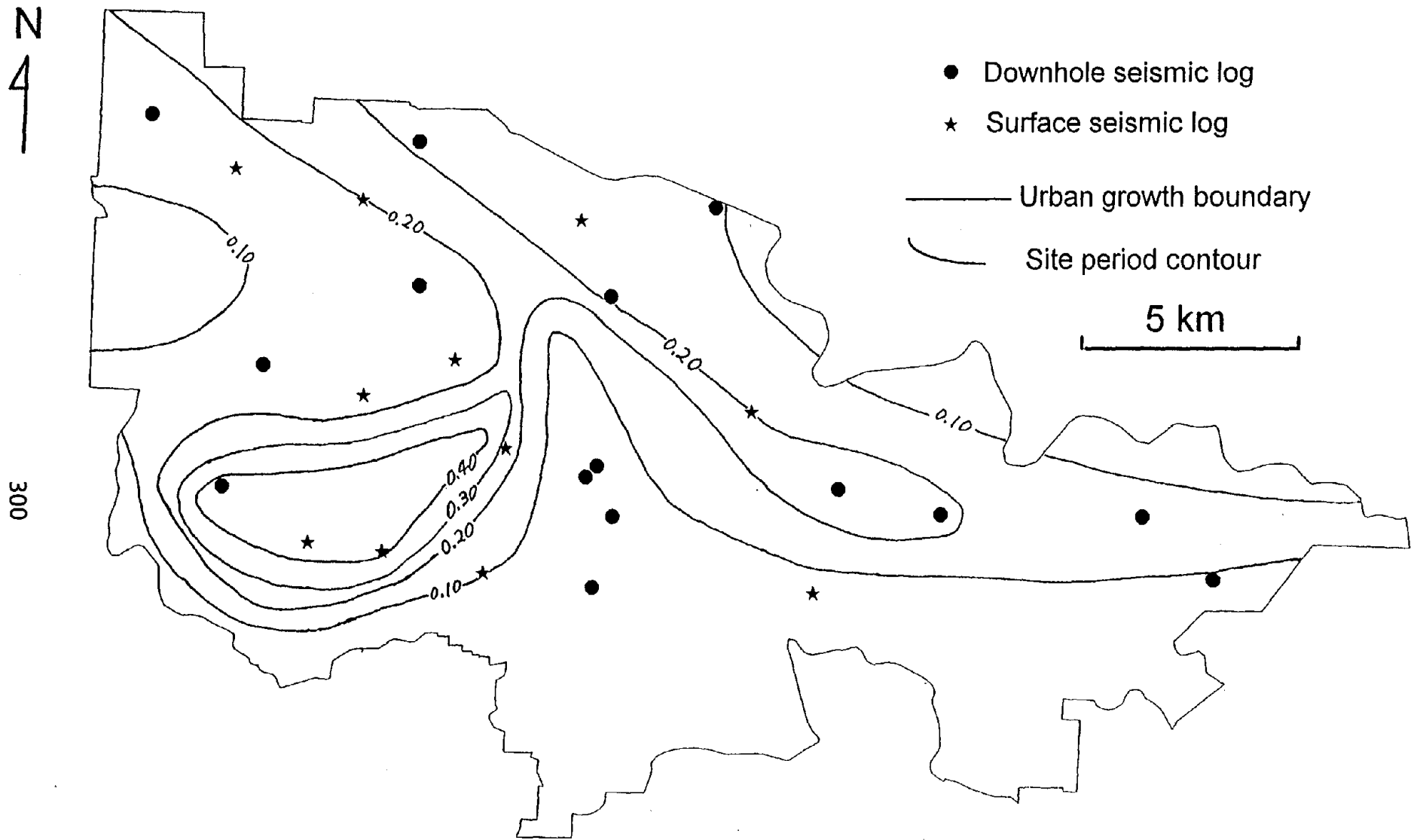


Figure 7. Site period, preliminary results (contours in 0.1 intervals).

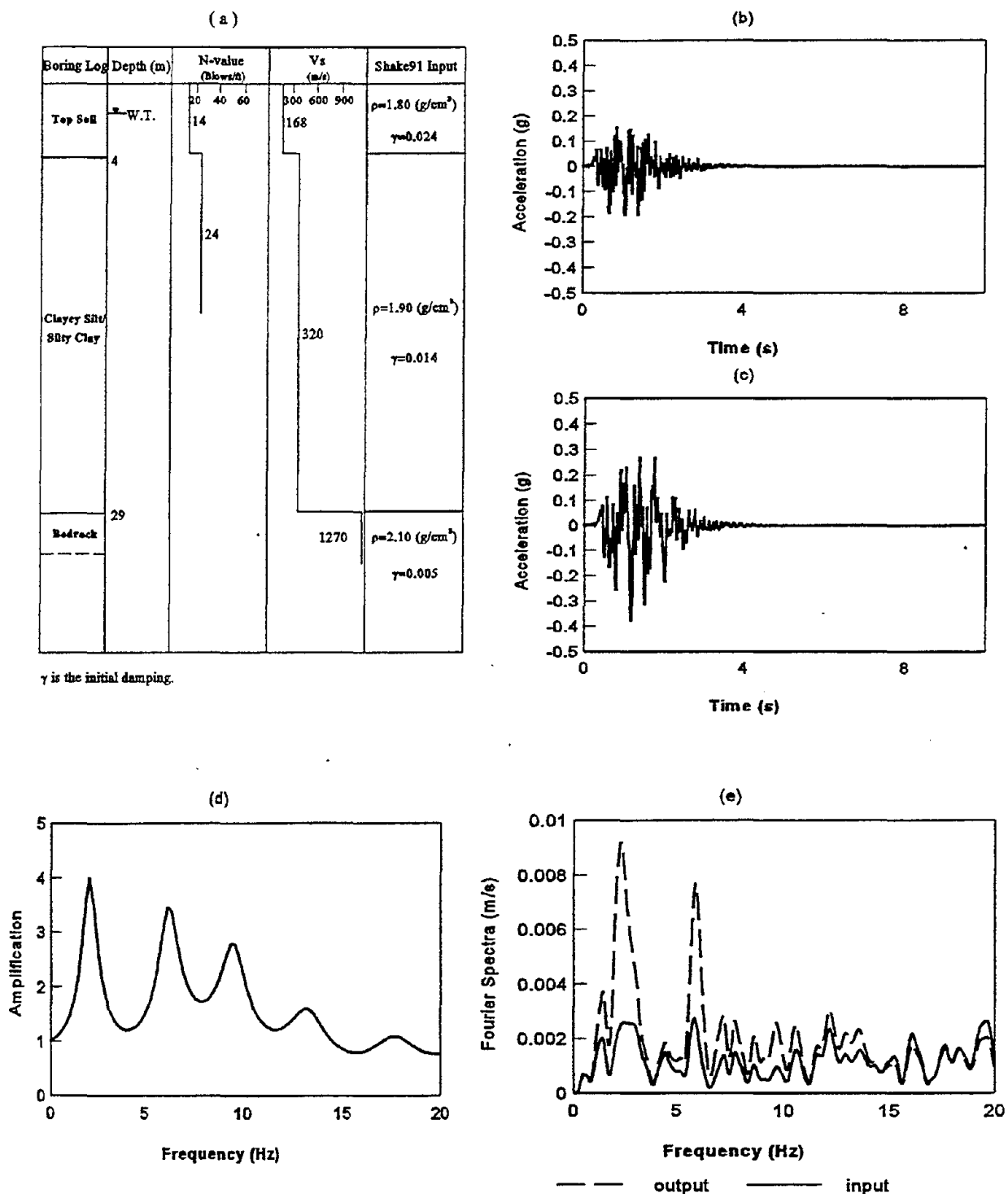


Figure 8. Soil column and SHAKE91 modeling at Site ES-2. (a) soil column and SHAKE91 input parameters; (b) input ground motion (M6.5 crustal earthquake) at bedrock; (c) output ground motion on free surface; (d) amplification curve; (e) input and output Fourier spectra.

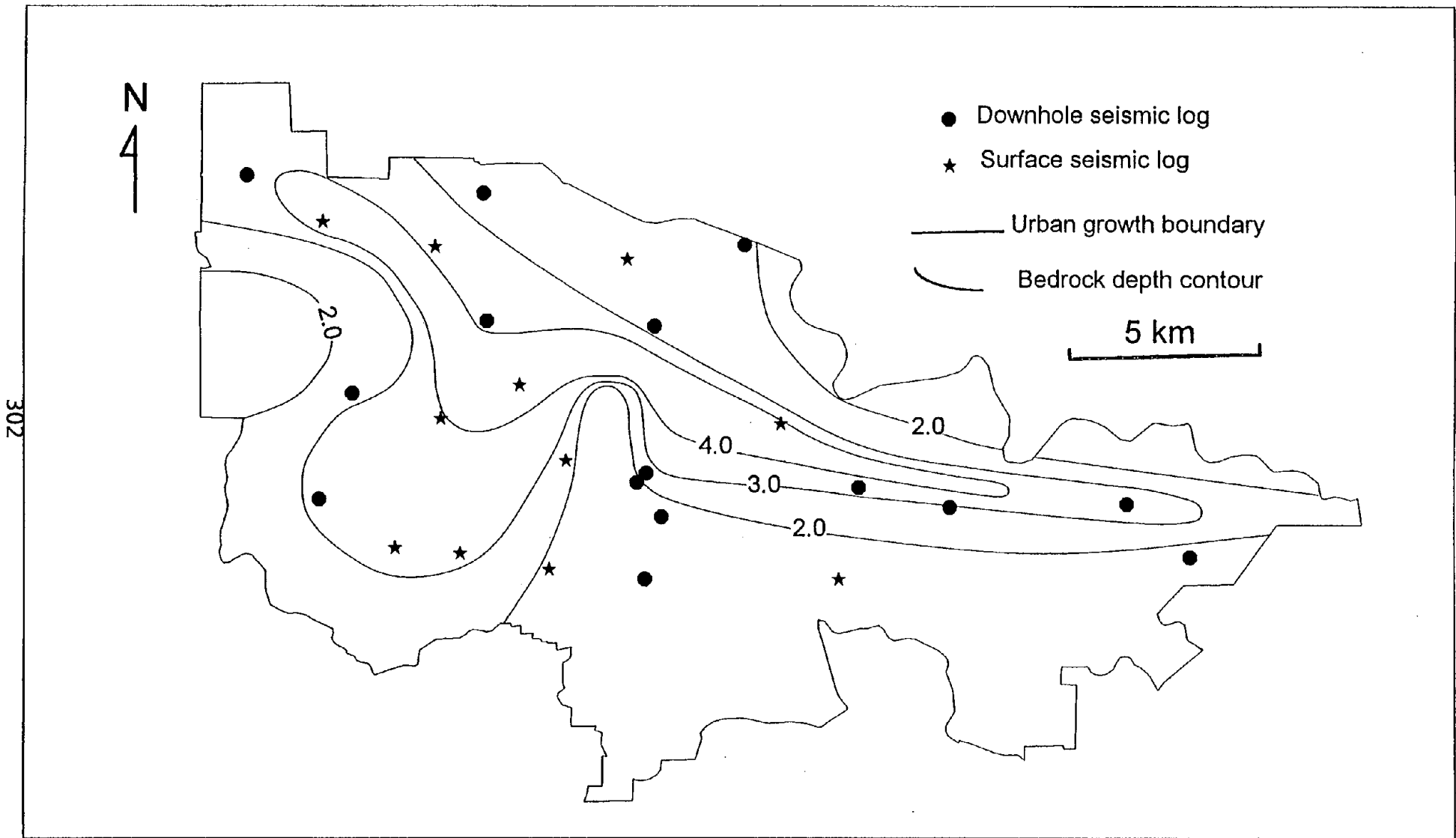


Figure 9. Spectral amplification, preliminary results (contours in 1.0 intervals)

Yumei Wang

Position

Director of Earthquake Programs
Oregon Department of Geology and Mineral Industries (DOGAMI)

800 NE Oregon St., #28, Suite 965
Portland, Oregon 97232 USA
Tel. 503-731-4100 Fax. 503-731-4066
email. meimei.wang@state.or.us

Date of birth

January 28, 1962

Education

University of California at Berkeley, M.S.
in Civil Engineering, Geotechnical emphasis, 1988
University of California at Santa Barbara, B.A.
in Geological Sciences, Computer Science minor, 1985



Major area of experience

Ms. Wang directs the earthquake mitigation activities for DOGAMI. A main focus is developing earthquake hazard maps that identify areas of potential earthquake damage related to geologic conditions. Other duties include formulation of earthquake hazard reduction policy, including as a member of the Oregon Seismic Safety Policy Advisory Commission, and educating the professional, public and private sectors on earthquake hazards in Oregon.

Between 1988 and 1994, Ms. Wang worked in the private sector as an independent geotechnical consultant mainly in the San Francisco Bay Area. Past projects involve seismic ground response, landslides, dam stability, and foundation engineering and construction.

Ms. Wang is a licensed professional engineer (PE), the current Vice President of American Society of Civil Engineers (ASCE) Oregon section geotechnical group, and a member of Earthquake Engineering Research Institute (EERI), Association of Engineering Geologists (AEG), and Seismological Society of America (SSA).

Travel abroad

Personal travels in Eurasia, Americas, Australia, South Pacific, Indonesia, and extensively in China.

Selected publications

Keefer, D.K., and Wang, Y., 1997, "A method for predicting slope instability for earthquake hazard maps: preliminary report," in *Earthquakes— Converging at Cascadia symposia proceedings*, Oregon Department of Mineral Industries Special Paper 28, p. 39 - 52.

Wang, Y., 1997, "Earthquake Risks and Mitigation in Oregon," in *Environmental, Engineering, and Groundwater Geology of Oregon*, Association of Engineering Geologists, Star Press: Belmont, California.

Wang, Y., and Leonard, W.J., 1996, *Relative Earthquake Hazard Map Series of the Salem East and West Quadrangles, Marion and Polk Counties, Oregon*: Oregon Department of Geology and Mineral Industries Geological Map Series GMS 105.

Wang, Y., and Priest, G.P., 1995, *Relative Earthquake Hazard Maps of the Siletz Bay Area, Coastal Lincoln County, Oregon*: Oregon Department of Geology and Mineral Industries Geological Map Series GMS-93.

**SEISMIC RISK EVALUATION AND IMPROVEMENT PROGRAM
FOR THE METROPOLITAN WASTEWATER DEPARTMENT
CITY OF SAN DIEGO**

DAVID HU
PETE WONG
CITY OF SAN DIEGO

RONALD T. EGUCHI
KELLY L. MERZ
DONALD B. BALLANTYNE
EQE INTERNATIONAL, INC.

ABSTRACT

The Metropolitan Wastewater Department (MWWD) of the City of San Diego currently collects, treats and disposes of waste and sewage for the entire San Diego Metropolitan area. The system is comprised of a network of treatment facilities, pump stations and large diameter pipelines. In total, over 80 pump stations are used to transfer waste throughout the city. Like many regions of California, San Diego is also subject to numerous natural hazards including earthquakes. For example, the seismically-active Rose Canyon fault traverses through the most populated areas of San Diego.

Since 1988, MWWD has been implementing an aggressive upgrade and replacement program of existing wastewater pump station facilities and forced mains. This program has been multi-year effort and has concentrated on facilities that are located in the coastal areas of San Diego. As part of this program, MWWD has commissioned several studies to evaluate the seismic vulnerability of its key pump stations. The results of these studies are being integrated into the longer-range capital improvement program (CIP) which has been given the name CARP (Condition Assessment and Rehabilitation Program).

MWWD is currently using a systems approach to define important seismic performance criteria that can be translated into facility-specific criteria. In general, the system performance criteria seeks to (1) minimize public health and safety consequences through effective preparedness, mitigation and response planning, (2) minimize system disruption through increased design requirements or retrofit of vulnerable facilities or improved emergency response measures, and (3) minimize expected damage to key MWWD facilities in moderate and major earthquakes. This paper outlines the approach being used by MWWD to perform seismic vulnerability assessments of its system.

INTRODUCTION

Several years ago, the Metropolitan Wastewater Department (MWWD) of the City of San Diego launched a multi-year effort to study the overall condition of its major pump stations. This program has been referred to as the CARP program (Condition Assessment and Rehabilitation Program). As part of this effort, EQE has evaluated the seismic vulnerability of three major pump stations and has recommended corrective actions for each station to enhance seismic reliability. The results of this study are summarized in a series of technical memoranda (EQE, 1996a,b,c), which conclude that the stations are essentially rugged, with the exception of unanchored or unbraced equipment.

An important product from the CARP effort is a report entitled “Pump Station and Force Main Audit Report.” This report describes the current condition of each MWWD pump station based on a variety of factors, including design capacity, operability status and age of equipment, emergency holding capacity, standby power supplies, and force main corrosion susceptibility. Where necessary, improvements in design or operations have been recommended in order to achieve overall system performance goals.

Based on the results of the Pump Station Audit Report, and the results of the first EQE study, MWWD has decided that a comprehensive seismic evaluation of all of its all pump station facilities is needed in order to complete its condition assessment study. The results from this seismic evaluation would then feed into the development of a system-wide emergency response plan. The remaining sections of this paper focus on the approach that will be used by MWWD to perform its system seismic vulnerability assessments. First, a general discussion is provided on the approach; later sections list the tasks that will be performed in order to meet the goals of the study, as well as implementation issues that all water and wastewater agencies face when starting long-term earthquake risk reduction programs.

APPROACH

In order to perform this study, the project team will be using a systems analysis approach, as outlined in Chapter 8 of the ASCE/TCLEE Monograph entitled “Guidelines for the Seismic Upgrade of Existing Water Transmission Facilities,” (ASCE/TCLEE, to be published). This approach is based on defining, from MWWD’s perspective, important system performance criteria that can be translated into facility-specific criteria. In general, the system performance criteria will seek to (1) minimize public health and safety consequences through effective preparedness, mitigation and response planning, (2) minimize system disruption through increased design requirements or retrofit of vulnerable facilities or improved emergency response measures, and (3) minimize expected damage to key MWWD facilities in moderate and major earthquakes.

The approach utilizes systems analysis techniques to quantify the seismic vulnerability of individual elements first, and then translates this information into an assessment of how the overall system will perform. The key feature of this approach is that it allows the analyst to identify the relative importance of each facility or pipeline segment in helping to achieve the system goal, e.g., continuity of service. In this way, the evaluation criteria for each facility is weighted by its relative importance to the system. For example, redundancy of elements may help to achieve overall system goals, thus eliminating the need for overly robust design requirements for each facility. In this manner, the results of a system analysis will identify those elements that are not redundant, and are extremely key to systems operations. In these cases, special design or operational criteria may be necessary.

Basic Overview of Seismic Risk Evaluation Elements

Figure 1 illustrates the basic elements of a systems seismic risk evaluation. These models include seismic hazard, component vulnerability, network, performance criteria, and final system risk models.

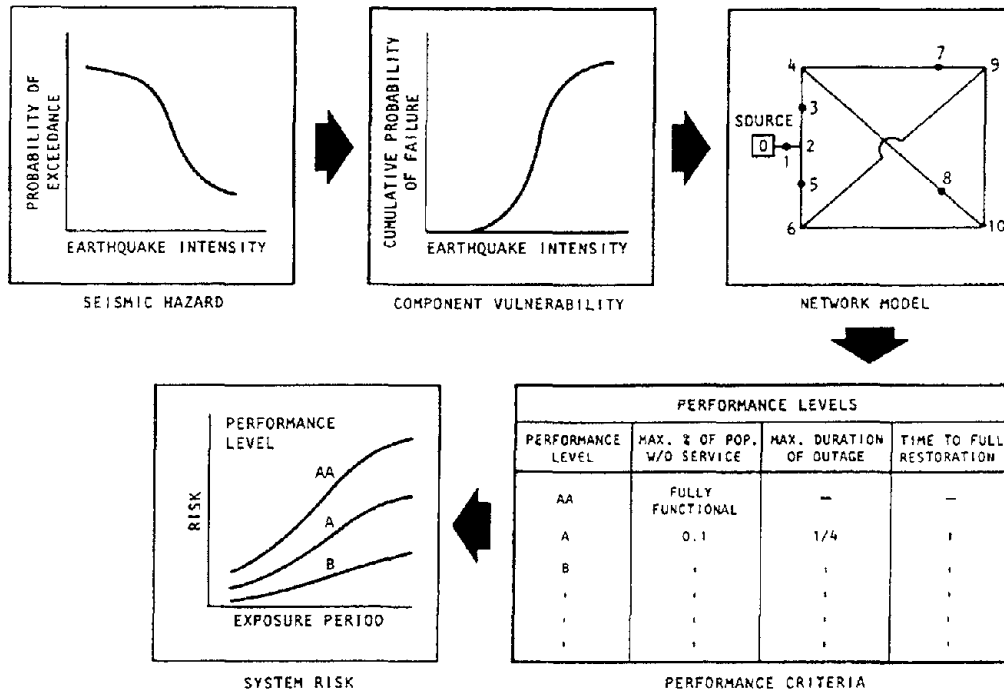


Figure 1 Relevant Models for a Lifeline Seismic Risk Analysis

The seismic hazard model expresses the likelihood of experiencing or exceeding various levels of earthquake hazard or intensity. This assessment could be based on a particular earthquake scenario or on a probabilistic analysis for a specified time period, e.g., 50 years. Intensity measures should characterize the effects from seismic shaking and ground failure hazards such as surface fault rupture, liquefaction ground failure or landslide/subsidence. Assessing the likelihood of these hazards occurring, excluding fault rupture, requires an estimate of the level and duration of ground shaking at the site of interest. The likelihood of fault rupture depends on the source characteristics, such as the size and depth of the earthquake.

Published probabilistic hazard maps showing the expected ground shaking level for a particular return period, are not completely applicable to systems risk analysis. These maps are designed to reflect the effects at a site over many potential events, rather than the effects at many sites from one or several events. Therefore, a map of relevant seismic parameters for every earthquake that can be expected to significantly damage the system, together with an assessment of their probabilities of occurrence, is required.

Once the earthquake hazard is specified, the seismic performance of discrete components must be assessed. Required in these assessments are seismic vulnerability or fragility models that relate cumulative probability of failure or damage to some measure of earthquake intensity. Seismic vulnerability models should reflect those earthquake hazard effects that contribute most to the damage of a component. For instance, recent studies have generally shown that the performance of underground pipes during earthquakes is strongly correlated to differential ground movements. Vibratory effects

appear significant only when pipes are already in degraded states, e.g., corroded, or have been designed or constructed with vulnerable elements such as oxyacetylene welded joints. Similar assessments of failure or damageability are made for other components (treatment facilities, pump stations, etc.)

Depending upon the objectives of the analysis, different sets of elements may be prescribed in the network model. For instance, an emphasis on operational performance may lead to a different set of system components than that prescribed by vulnerability analyses. Regulator valves, for example, are essential elements in hydraulic analyses for water supply and distribution. However, with regard to earthquake vulnerability studies, these components are sometimes omitted because of their resistance to earthquake effects.

In order to assess the performance of a wastewater system during earthquake, it is necessary that performance be measured against nominal standards. The ASCE/TCLÉE monograph mentioned earlier introduces a number of different schemes for measuring water and wastewater system performance, several of which involve the amount of service that can be provided under different earthquake situations, and the maximum restoration time allowable before indirect impacts resulting from a disruption of service occurs.

The final system risk model expresses the likelihood of meeting the various levels of performance, within some time period or under a particular earthquake scenario. Normally, this model is presented in the form of a risk curve that increases with exposure period and higher performance standards or requirements, or with earthquake size. Risk, in this case, may be defined by the probability of not being able to provide a certain level of service, or the probability that the system will not be restored to full operation within some acceptable number of days. Depending on the criticality of the system, these standards could vary considerably. The next section discusses the procedure that will be used to assess the seismic vulnerability of the MWWD system.

Procedure for Seismic Vulnerability Analysis

The objectives of this analysis are five-fold: (1) to quantify the long-term seismic vulnerability of all key MWWD pump station facilities, (2) to quantify the seismic vulnerability of major pipeline elements, (3) to estimate the potential for system disruption based on plausible earthquake scenarios, (4) to identify key facilities requiring corrective actions to improve seismic performance, and (5) to develop a detailed plan for how this information can be incorporated in the development of a system-wide emergency response plan, to address earthquake hazards.

In order to achieve these objectives, eight major tasks have been identified. These include:

Task 1: Establish system performance objectives for the MWWD system

Task 2: Perform seismic hazard analysis for the MWWD service region

Task 3: Compile facility database on all key MWWD pump station facilities

Task 4: Compile database on all key MWWD pipeline elements

Task 5: Perform seismic vulnerability analysis on all key pump stations and pipeline elements

Task 6: Review the projected performance of all facilities relative to the desired facility-specific performance goals

Task 7: Develop a detailed system-wide emergency response program for MWWD

System Performance Objectives. In this task, MWWD will establish the post-earthquake performance requirements for the entire MWWD system. In general, these requirements will vary depending upon the size and seriousness of the postulated disaster. In all cases, however, the objective of any response or mitigation plan is to reduce (1) any serious safety and health hazards to the public, (2) the potential for significant system disruption or downtime, and (3) the potential for direct physical damage to system elements. The preliminary requirements for system performance will be developed through a series of discussions and interviews with MWWD management personnel, and facility operators. It is the intent to use these preliminary system performance criteria to quantify the relative importance of all MWWD facilities and to define individual performance criteria for key MWWD facilities.

Individual performance criteria will be based on qualitative rankings that account for (1) the relative importance of the facility to overall system functions, (2) the degree of seismic hazard assigned to the site based on probabilistic studies (e.g., 475-year return period event) and different earthquake scenarios, and (3) the degree of redundancy associated with that type of facility within the MWWD network. The results of this analysis will be used to compare expected performance with desired performance.

Seismic Hazard Analysis. In this task, several different analyses will be conducted. The first analysis will be a probabilistic study of the seismic hazard potential of the MWWD service region. Specifically, for each key site and pipeline alignment, the expected ground motion level based on a 475-year return period (or equivalently, a 10% probability of exceedance in a 50 year time period) will be calculated. This analysis will take into consideration the location and magnitude potential of all major faults that can affect facilities in the MWWD service region. Furthermore, to the extent that local soil conditions will modify this potential, these will be considered in the analysis.

A second set of seismic hazard data will be provided in the form of expected ground motions for earthquake scenarios large enough to cause significant system-wide damage to the MWWD network. Possible fault sources that could create damaging earthquakes in the San Diego region include the Elsinore, the Rose Canyon and San Andreas fault systems.

In addition to ground motions, liquefaction ground failure effects will be addressed for key pipeline alignments. As a minimum, areas of moderate, high and very high liquefaction susceptibility will be identified, and probabilities of ground failure occurrence with these zones will be calculated.

Pump Station Database. According to MWWD's pump station and force main audit report, there are 82 pump stations located throughout the MWWD system. Three of the largest and most important stations were analyzed as part of EQE's first study (pump stations 1, 2 and 64). The remaining stations vary considerably in terms of size and importance. Some of the data that are used in individual assessments include: facility type, size and age; capacity; on-site emergency backup power capabilities; and key facility contacts.

Pipeline Database. In this task, key information on the pipeline system will be compiled. In particular, for each element, pipeline type, size and age; joint type; and pipeline location will be sought. An important task here will be to compile this information in a Geographic Information System (GIS) format. By creating this data in a GIS format, numerous analytical calculations can be performed including assessments of liquefaction potential for each pipeline segment, estimation of total pipeline lengths by ground shaking levels, etc.

Seismic Vulnerability Analysis. Based largely on the results of previous studies, general vulnerability relationships for all pump stations will be used to estimate the expected level of damage and downtime associated with various levels of ground motion. These relationships will address structural, nonstructural and equipment vulnerabilities. For this study, ground motion levels will be defined based on the results of the 475-year event and the selected earthquake scenarios. The results from the 475-year analysis will be used to prioritize corrective measures; the results from the scenario analyses will be helpful in identifying operational weaknesses that should be addressed through emergency response or preparedness measures.

The same type of analyses will be applied to pipeline elements. In addition to ground shaking effects, we will also estimate the impact of liquefaction ground failures on key pipeline segments. Specifically, GIS software tools will be used to overlay liquefaction susceptibility and ground motion maps onto maps of the MWWD system. The output from this analysis will be (1) an identification of seismically-vulnerable pipeline alignments, based on the results of the 475-year analysis and, and (2) expected number of breaks and projected downtimes associated with the repair of key pipelines, as a result of the postulated scenarios.

Acceptable System and Facility Performance. Based on the results of the previous task and the projected performance goals for the system, the next step will be to identify facilities or pipeline elements that appear to be deficient with respect to desired performance. The results from this task will form the basis for corrective actions for each facility, if needed. Along with this assessment, we will also estimate industry standard costs for performing basic corrective actions.

System-Wide Emergency Response Program. Based on the results of the two previous tasks, a detailed system-wide emergency response plan will be developed. It is important to conduct interviews with knowledgeable operations personnel in order to develop a complete understanding of the roles and responsibilities of key individuals (for individual facilities as well as general department operations) during a large-scale disaster. These plans must be flexible to allow for continuous updating. They must also be tested through regular training exercises to allow staff to identify deficiencies that may not have been considered in the development of these plans.

IMPLEMENTATION ISSUES

Seismic risk reduction programs, such as the one discussed in this paper, are not without impediments or implementation issues. Even in areas of high seismicity, such as San Diego, mitigation programs to reduce seismic risks must be balanced with other agency programs that focus on other daily hazards or risks. For example, the CARP program mentioned earlier addresses a variety of concerns that have very little to do with seismic hazards, e.g., pipeline corrosion.

In order for seismic risk reduction programs to be effective, they must be integrated with other agency programs. One strategy that has been successfully used by many California water and wastewater agencies is to address seismic concerns as part of long-term capital improvement programs (CIP). In this way, large costs associated with the retrofit of seismically-vulnerable facilities can be spread over many years and be absorbed within other costs to improve or maintain these facilities.

Some of the key strategies that are used by water and wastewater agencies to affect seismic hazard reduction programs include:

1. *Educate the public or rate paying community on the hazards and risks associated with earthquakes.* Perhaps the most effective means of conveying this information is to build on the experiences of recent damaging events. For example, in California, there is ample experience and history on the effects of earthquake on water and wastewater systems. The Loma Prieta earthquake in 1989 and the Northridge earthquake in 1994 created a myriad of problems and concerns for water and wastewater systems. Agency operators have used these experiences to justify retrofit programs for critical facilities and have generally passed the costs of these programs onto their customers. In areas that have been affected by recent events, these costs are usually not questioned, particularly if they are designed to improve the reliability of these systems in non-earthquake situations.
2. *Include the costs of seismic retrofit programs as part of long-term capital improvement programs.* There are numerous advantages to this kind of strategy. First, the cost of the seismic programs will be small relative to the overall budget. Second, improvements designed to prolong the life of the facility will often involve those elements that are also seismically vulnerable. Therefore, replacing old elements with seismically rugged ones addresses two concerns at one time. A good example of this would be the replacement of old pipe.
3. *Use a variety of instruments to fund seismic retrofit programs.* One interesting strategy that has been used by the Fire Department in the City of San Francisco has been to put forward bond issues to improve the seismic safety and reliability of their system. San Francisco has been successful in using this strategy to upgrade its earthquake fire support system (i.e., the Auxiliary Water Supply System). Close to \$50 million was approved by the public to implement this initiative.
4. *Use cost/benefit studies to demonstrate the cost-effectiveness of seismic retrofit measures.* For many mitigation activities, the benefits associated with implementation far outweigh the costs. This is particularly true for those activities that have far-reaching benefits to the public or community. For example, enhancing the reliability of water supply systems has the indirect benefits of improving post-earthquake fire response, insuring public health after a disaster and minimizing community disruption. If these benefits are quantified and compared to the initial costs of mitigation, then those paying for the mitigation activities will more likely approve their implementation.
5. *Address earthquake hazards as part of a multi-hazard program.* Obviously, earthquakes are but one hazard that may affect a water and wastewater agency. In California, floods, fires, environmental hazards, sabotage, all create problems for water and wastewater agencies.

Having a comprehensive hazard reduction plan that addresses as many of these hazards as possible has both economic and political benefits. Many agencies are now finding that in order to gain political support for its programs (even from federal initiatives such as those supported by the Federal Emergency Management Agency), it must reach a larger base of constituents. These agencies have also found out that addressing many concerns with the same initiative can expand the support for the initiative. Therefore, broad-based programs have been popular, particularly in California.

REFERENCES

ASCE/TCLEE (to be published), "Guidelines for the Seismic Upgrade of Existing Water Transmission Facilities," TCLEE Monograph.

City of San Diego (1997), Wastewater Collection Division, Metropolitan Wastewater Department, "Pump Station and Force Main Audit Report," June 1997.

EQE International, Inc.(1996a), "Earthquake Risk Evaluation of Pump Station No. 1," Metropolitan Wastewater Department , Condition Assessment & Rehabilitation Program, Technical Memorandum TM 1.2, October 15, 1996.

EQE International, Inc.(1996b), "Earthquake Risk Evaluation of Pump Station No. 2," Metropolitan Wastewater Department , Condition Assessment & Rehabilitation Program, Technical Memorandum TM 2.2, October 15, 1996.

EQE International, Inc.(1996c), "Earthquake Risk Evaluation of Pump Station No. 64," Metropolitan Wastewater Department , Condition Assessment & Rehabilitation Program, Technical Memorandum TM 1.5, October 31, 1996.

David P. Hu

Date of Birth: September 27, 1939
Birth place: Kwangshi, China
Education: Degrees
National Taiwan University, B.S.
Civil Engineering, 1961
Colorado State University, M.S.
Structural Engineering, 1965
University of Wisconsin, Ph.D.,
Engineering Mechanics, 1972
Position: Chief Structural Engineer and Senior Project Manager
Metropolitan Wastewater Department (MWWD)
City of San Diego, CA



Dr. Hu is responsible for the planning, technical support, project management of the Clean Water Program, MWWD, in the area of structural engineering, earthquake and geotechnical engineering, computer aided design and drafting, QA/QC, and GIS applications.

Dr. Hu has extensive engineering management experience in the private industry prior to joining MWWD, City of San Diego in 1991. His consulting experiences include technical consultation in design, engineering and management as president of Pacific Versatech, Inc. and DDH Enterprise, Inc., 1987 to 1989; Structural Engineering Department Manager, M&E, Inc., 1989 to 1991; Project Manager, Jaykim Engineering 1987 to 1989; Engineering Supervisor in Structural and Earthquake Engineering, SDG&E, 1976 to 1987; Senior Structural Engineer, United Engineers and Constructors, 1973 to 1976; Senior Engineer, Bechtel Power Corporation 1972 to 1973; Research Fellow, Department of Engineering Mechanics, University of Wisconsin, Madison, 1968 to 1972; Civil Engineer, BES Engineering Corporation, 1962 to 1964.

Dr. Hu has extensive knowledge of domestic and international markets in engineering and design and has provided effective consultation services in transportation, energy related projects, environmental engineering and earthquake engineering. He developed and conducted seminars on earthquake engineering, land-use management, wastewater facilities design for the private companies and other agencies both domestic and abroad. He has published technical papers involved in structural and earthquake engineering. Selected papers are listed as follows:

* "A Higher Order Theory for Circular Cylindrical Shells", The Fourth Canadian Congress of Applied Mechanics, Montreal, 1973; * "Repair of Deteriorated Power Plant Circulating Water Structures", ACI Fall Convention, 1982, Detroit, Michigan; * "Retrofit of Turning Vanes in the Combined Units Chimney System", ASCE, Fall Convention, 1982; * "Computer Modeling of Width Formation for Alluvial Rivers", ASCE, Special Conference, 1983; * "Seismic Risk Assessment of LNG Storage Tanks", Eighth World Conference on Earthquake Engineering, 1984; * "Cylindrical Shells Subjected to Tangential Surface Loads", The Southeastern Conference on Theoretical and Applied Mechanics, 1984; * "Seismic Risk Analysis of LNG Tanks", ASCE Spring Convention, 1986; * "Dynamic Tests of LNG Storage Tanks for Earthquake Analysis of Liquid-Tank-Pile-Soil Interaction", The Third ASCE Engineering Mechanics Specialty Conference, UCLA, March 1986; * "Seismic Design and Retrofit of Tunnels and Highway Bridges", Joint Conference on Transportation, NACTPA 1994; * "Earthquake Vulnerability and Seismic Resistant Design of Highway Bridges", The First Asian Pacific Transportation Development Conference, 1995; * "Seismic Resistant Design of Highway Bridges", Transportation Development and Technology Transfer Conference, 1997.

Dr. Hu is a member of ACI, ASCE, EERI, PMI, TCLEE/ASCE and is registered as Civil Engineer and Professional Engineer in the States of California and Wisconsin, and Adjunct Faculty Member, San Diego State University.

MAPPING PREDICTIONS OF LIQUEFACTION INDUCED LATERAL SPREAD DISPLACEMENT

Dr. Matthew A. Mabey

Assistant Professor
Brigham Young University, Department of Geology

ABSTRACT

In recent years a number of techniques, both analytical and empirical, have been developed for the predictions of liquefaction induced lateral spread displacements. While these techniques continue to be refined they have been applied to regional liquefaction hazard mapping. Liquefaction hazard maps that quantitatively present the hazard in terms of displacement are extremely useful for damage and loss estimation and vulnerability analyses. They also provide information useful in the design and rehabilitation of lifeline systems. The methodology for making such maps continues to be refined in parallel with both the techniques for predicting displacements as well as the computer hardware and software used in the process.

INTRODUCTION

It has long been recognized that the damage caused by liquefaction is related to the displacements that are induced by the liquefaction (Youd, 1978 and 1980). It has become relatively common to construct liquefaction hazard maps which indicate the areas of liquefaction susceptibility or liquefaction potential. Such information is an important part of the overall hazard picture. For understanding the potential for damage to lifelines, information regarding the displacements, which the occurrence of liquefaction is likely to induce, is needed. In the past decade a small, but significant, body of research has been completed in this area. Glaser (1994) provides a summary of the various research up to that point in time. Some of these techniques have been applied to hazard mapping. This ability is a result of both the development of the displacement prediction techniques and the advancement of computer hardware and software tools which allow them to be applied to hazard mapping efforts. Mapping predicted displacements is especially useful for application to lifelines, given their areal distributed nature. These early mapping efforts have begun to be incorporated into damage and loss estimation efforts and vulnerability assessments as well as earthquake response planning. The continued evolution of displacement prediction techniques and computer capabilities is being combined with refinements of the mapping methodologies and improved data sets to increase the accuracy and reliability of displacement prediction maps.

TECHNIQUES FOR DISPLACEMENT PREDICTION

Given the importance of the displacements induced by the occurrence of liquefaction, a number of researchers have been working on techniques for predicting the magnitudes of the displacements (see Glaser, 1994). Here three techniques (covering most of the spectrum of approaches) which have been applied to hazard mapping will be briefly reviewed.

Youd and Perkins (1987) proposed the Liquefaction Severity Index as a measure of the damage potential due to liquefaction-induced horizontal displacements. A regression equation for estimating the displacements was developed based on case histories of past displacement. The equation they developed was:

$$\text{Log LSI} = -3.49 - 1.86 \log R + 0.98 M_w$$

The independent variables in this equation are, R , the horizontal distance from the energy source in kilometers, and M_w , the moment magnitude of the earthquake. The equation was developed for gently sloping, saturated, late Holocene fluvial deposits, thus restricting the range of geometry of the setting and material properties. The dependent variable, LSI, is the maximum horizontal displacement in inches (or mm divided by 25). The strength of this approach is the simplicity of the terms involved. The short comings of this approach are that it does not deal explicitly with the liquefiable materials or the geometry of the setting.

Bartlett and Youd (1996) published a regression equation which was again based on case history data but included independent variables dealing with the liquefiable materials and the

geometry of the setting. They developed two equations, one dealing with continuous ground slopes and the other dealing with free face situations. The equations they developed are:

For ground-slope conditions,

$$\text{LOG } D_H = - 15.787 + 1.178 M - 0.927 \text{ LOG } R - 0.0133 R + 0.429 \text{ LOG } S \\ + 0.348 \text{ Log } T_{15} + 4.527 \text{ Log } (100 - F_{15}) - 0.922 D50_{15}$$

For free-face conditions,

$$\text{LOG } D_H = - 16.366 + 1.178 M - 0.927 \text{ LOG } R - 0.0133 R + 0.657 \text{ LOG } W + \\ 0.348 \text{ Log } T_{15} + 4.527 \text{ Log } (100 - F_{15}) - 0.922 D50_{15}$$

where:

- D_H = Estimated horizontal ground displacement in meters
- $D50_{15}$ = Average mean grain size of sediments within layers included in T_{15} , in mm.
- F_{15} = Average fines content (percent passing No. 200 sieve) of saturated granular layers included in T_{15} .
- M = Earthquake magnitude (moment magnitude).
- R = Horizontal distance from the seismic energy source, in kilometers.
- S = Ground slope, in percent.
- T_{15} = Cumulative thickness of saturated granular layers with a corrected blow count, $(N1)_{60}$, less than 15, in meters.
- W = Ratio of the height (H) of the free face to the distance (L) measured from the base of the face to the point in question, in percent.

At the same time, and working with the same case history data set, Mabey and Youd (1992) developed a technique based on the sliding block analysis technique proposed by Newmark (1965). In this case a strength value for the liquefied soil layer was needed. The residual strength of the liquefied soil was assumed to become effective essentially at the beginning of shaking. The residual strengths for the case history data were back-calculated by varying the residual strength term until the observed displacement was matched. Using these back-calculated residual strengths, a correlation between $(N1)_{60}$ and residual strength for lateral spreading of natural material was developed (Mabey and Youd, in press).

EXAMPLES OF DISPLACEMENT HAZARD MAPS

These three techniques, each anchored to past observations of lateral spread displacements have subsequently been applied to liquefaction hazard mapping projects.

Youd and Perkins (1978) demonstrated how the LSI equation could be applied to displacement hazard mapping, using southern California as a test case. A National LSI map was constructed by Youd and others (1989) using the LSI equation. In doing this it was recognized that the "attenuation" of ground displacements, as one moved away from the source of the earthquake, would be different in the eastern United States than in the west in the same way that ground shaking differs. (the western U.S. is where the case history data and original equation were developed). The LSI equation was adjusted based on the way in which ground shaking differs. This map was developed using the LSI equation just like an attenuation equation with the same methodology and source models that had been used in the national map of probable ground shaking hazard. This map merely showed the probable LSI values throughout the

country, assuming the gently sloping, saturated late Holocene fluvial deposits were everywhere present.

The LSI equation was again applied to make a hazard map in Utah (Mabey and Youd, 1989a and 1989b). For this map the LSI equation was again adjusted to account for the regional attenuation characteristics and a more detailed and up-to-date seismic source model was used. Again, maps of probable LSI, assuming the gently sloping, saturated late Holocene fluvial deposits were everywhere present were the result. A further refinement was added by using an existing map of the extent of shallow ground water for the state (Figure 1). In this way the LSI for areas where the saturated condition did not exist was set to zero. Combining the LSI maps with existing maps of liquefaction potential for some parts of the state was considered. However, a state-wide map was the desired product and both scale and partial coverage precluded this additional refinement.

As part of the sliding block technique (Mabey and Youd, 1992) a liquefaction-induced lateral spread displacement map of the Seattle South 7-1/2 minute, 1:24,000 Quadrangle was constructed. This map was built upon an existing liquefaction susceptibility map (Grant and others, in press). Given the liquefaction susceptibilities of the soils as described on the map, maximum likely displacements were calculated. This was done using the same two scenario earthquakes used for the susceptibility map. The residual strengths used were based on the $(N1)_{60}$ previously mentioned. The analysis was performed for a range of ground slope conditions. The map shown in Figure 2 was constructed by assigning a displacement magnitude based on the ground slope and susceptibility category present at any given location. Because the sliding block technique can be repeated with any of the input parameters being varied, separately or jointly, it is possible to explore the areas of probability and uncertainty, both quantitatively and qualitatively, when this technique is employed. The time history or acceleration, residual strength and ground slope are three areas of uncertainty that could be considered. Because of the prior occurrence of liquefaction within the map area the results of the methodology were also validated against the historically observed displacements.

Mabey and others (1993, Jones and others 1994) published a liquefaction displacement hazard map for the Portland 7-1/2 minute, 1:24,000 Quadrangle (Figure 3) as part of the Portland Relative Earthquake Hazard Mapping Project. This map was based on the technique of Bartlett and Youd (1996) and again displacements were calculated for a range of soil and ground slope conditions. Then displacement hazards were assigned to areas of the map based on the soil and slope conditions present. Again a liquefaction susceptibility map was used for this process to describe the soil conditions which should apply for displacement estimation.

As the Portland Relative Earthquake Hazard Mapping Project progressed to additional quadrangles the methodology has been refined so that the liquefaction displacement hazard is calculated based on the detailed model of the soil and slope conditions on a 30 m grid rather than on the generalized conditions from susceptibility and slope categories (Mabey, 1997, Mabey and Madin, 1996) (Figure 4). In this way a displacement was calculated for each 30 grid cell based on the thickness of various geologic units in the cell and the unit's average geotechnical properties. These newest maps benefit from expanded data sets and better computer tools. Also of benefit is a more rigorous assessment of the seismicity of the region (Geomatrix, 1995; Madin and Mabey, 1996) which facilitates the selection of scenario earthquakes and allows probabilities to be attached to them.

UTILITY OF DISPLACEMENT HAZARD MAPS

To anticipate, plan for, and design for the damage an earthquake may cause one of the key factors needed is an estimate of the displacements which will result from liquefaction-induced lateral spreading (Ballantyne, 1994; Ballantyne and Heubach, 1996, Youd, 1978 and 1980). The sliding block type analysis was used in the design of the Kern River Pipeline (Keaton and others, 1991) on a site specific basis.

The Seattle South Quadrangle is part of the City of Seattle's GIS database as one part of the city's ability to mitigate the earthquake hazards Seattle faces. In the Portland Metropolitan Area an aggressive effort is underway to inventory both the hazards, building stock and lifelines in the area to be able to work toward effective mitigation and response planning.

The use of earthquake hazard maps was begun with a pilot feasibility study for damage and loss estimation (Mabey and others, 1993). The effort has since been carried forward with the liquefaction displacement maps being explicitly included in the damage and loss estimation and mitigation optimization methodology developed by McCormick (1996). This project is still underway with funding from the Federal Emergency Management Agency (Mabey, 1997).

While the hazard maps for the Portland Relative Earthquake Hazard Mapping Project were still being completed the City of Portland contracted to have a vulnerability study done on their sewer system. As part of this study (D. Ballantyne, personal communication) the results of the Portland Quadrangle displacement hazard map were extrapolated to other areas of the city.

The State of Oregon organized a task force to study the problems and needs regarding seismic rehabilitation of all "structures" in the state. While the task forces report (Bowmen and others, 1996) focused on buildings and not lifelines, one of their key findings was that for rehabilitation to be undertaken rationally, realistic assessments of the hazard and the magnitude of the potential losses were essential.

FUTURE REFINEMENTS

At this point in time refinements in four areas are under way related to the mapping of predictions of liquefaction-induced lateral spread displacements. The first is the improvement of displacement prediction techniques. Additional approaches are being investigated and the existing approaches are being refined with additional case history data sets.

Secondly, the problem of the spatial variation of the soil properties and ground slope are being addressed. The mapping efforts to date have all involved some degree of averaging of properties and have used relatively crude digital elevation models for ground slope. Efforts are underway to improve our ability to model geologic and topographic conditions more accurately and to make explicit expressions of uncertainty. Yamamoto and Hoshiya (1996) and Yoshida and others (1995) are examples of published work relating to this area. The data sets available in the Portland area are extensive enough to allow a number of statistical and modeling approaches to be investigated.

Thirdly, as geographic information systems improve the ability to store and review spatial data sets with greater resolution. Errors in data sets will be more easily found and corrected and improved quality will be the result

Lastly, improved hardware and software for computation and modeling capability will allow for more detailed and accurate use of the improvements in the three previous areas.

CONCLUSION

Mapping of predictions of liquefaction-induced lateral spread displacements, based on published techniques for making such predictions, has been demonstrated to be feasible. These estimates of displacement are important to understanding a significant component of the earthquake hazard and mitigating it. Mapping displacement hazards is especially important for lifelines given their widely distributed nature. Useful maps have resulted, but continuing refinements in a number of areas will improve both the accuracy and the utility of future maps.

ACKNOWLEDGMENTS

This paper and the publications leading to it have been made possible by the research of many workers in this area. Of particular importance has been the willingness of consultants to open their files and their discussions to an outsider working in the public sector and academia.

The Portland Relative Earthquake Hazard Project and the Metro Earthquake Hazard Mitigation Projects have benefited from funding and other forms of support from the Federal Emergency Management Agency. Staff of the U.S. Geologic Survey have also contributed in a number of roles.

The Liquefaction Severity Index Maps of the State of Utah were funded by the then Utah Geological and Mineral Survey, now know as the Utah Geological Survey.

Research supported, in part, by the U.S. Geological Survey (USGS), Department of the Interior, under USGS award numbers 14-08-0001-G1985 and 14-08-001-G2132. The views and conclusions contained in this document are those of the authors and should not be interpreted as necessarily representing the official policies, either expressed or implied, of the U.S. Government.

REFERENCES

- Bowman, R.W., Bugni, D.A., Cliburn, M.A., Collins, P.A., Eppstein, R.J., Hellesvig, D.D., Isham, D., Little, D.C., Lorenzini, P.G., Mabey, M.A., McMillan, R.C., Sjostrom, T.O., Tess, J.M., Theoderson, R., Tibbatts, R.B. (1996). Seismic rehabilitation of existing buildings in Oregon, Report to the Sixty-Ninth Oregon Legislative Assembly, Sept. 30, 1996. Seismic Rehabilitation Task Force created by Senate Bill 1057.
- Ballantyne, D. (1994). Changing needs for hazard information for pipeline loss estimation, *in*: Proceedings from the Sixth Japan-US Workshop on Earthquake Resistant Design of Lifeline Facilities and Countermeasures Against Soil Liquefaction, Snowbird Resort and Conference Center, Snowbird, Utah, September 29-October 1, 1994. O'Rourke, T.D., et al eds. National Center for Earthquake Engineering Research, Buffalo, November 1994, p. 653-661.
- Ballantyne, D. and Heubach, W. (1996). Use of GIS to evaluate earthquake hazard effects and mitigation on pipeline systems: case studies, *in*: Proceedings from the Sixth Japan-US

- Workshop on Earthquake Resistant Design of Lifeline Facilities and Countermeasures Against Soil Liquefaction, Waseda University, Tokyo, June 11-13, 1996. Hamada, M. and O'Rourke, T. eds. National Center for Earthquake Engineering Research, Buffalo, September 1996, p. 685-696.
- Bartlett, S.E. and Youd, T.L. (1996). Empirical prediction of horizontal ground displacement generated by liquefaction-induced lateral spread, *Journal of Geotechnical Engineering*, ASCE, vol. 121, no. 4, p. 316-329.
- Geomatrix Consultants. (1995). Seismic design mapping, State of Oregon: Final report prepared for the Oregon Department of Transportation, Salem, Oregon.
- Glaser, S.D. (1994). Estimation of surface displacements due to earthquake excitation of saturated sands. *Earthquake Spectra*, vol. 10, no. 3, p.489-517.
- Grant, W.P., Perkins, W.J., and Youd, T.L., (in press) Evaluation of Liquefaction Potential Seattle, Washington, U.S. Geological Survey Professional Paper.
- Jones, C.F., Youd, T.L., and Mabey, M.A. (1994). Liquefaction hazard maps for the Portland, Oregon, Quadrangle, in *Proceeding of the U.S. Fifth National Conference on Earthquake Engineering*, Chicago, Illinois., Earthquake Engineering Research Institute, p. 209-218.
- Keaton, J.R., Bischoff, J.E., Youd, T.L. and Mabey, M.A. (1991). Liquefaction hazard analysis for the Kern River Pipeline crossing of the Muddy River, Southern Nevada, in *Proceedings of ASCE 3rd U.S. Conference on Lifeline Earthquake Engineering*.
- Mabey, M.A. (1997). Regional versus site specific spatial analysis, *in: Spatial Analysis in Soil Dynamics and Earthquake Engineering*, Geotechnical Special Publication No. 67, ASCE, New York City, p. 29-41.
- Mabey, M.A., (1997). Earthquake ground response mapping: a tool for earthquake hazard mitigation in the Portland Metropolitan Area, *in: Building to Last: Proceedings of the XV Structures Congress*, edited by Leon Kempner Jr. And Colin B. Brown, American Society of Civil Engineers, New York City.
- Mabey, M.A. and Madin, I.P. (1996). Assessing the local geologic component of the earthquake hazard in the Portland Metropolitan Area, *in: Natural Disaster Reduction: Proceedings of the Conference*, edited by George W. Housner and Riley M. Chung, American Society of Civil Engineers, New York City, p.177-178.
- Mabey, M.A. Madin, I.P., Drescher, D.E., Uba, O.G., and Bosworth, M. (1993). Earthquake scenario pilot project assessment of damages and losses, Metro, Portland, Oregon, 19 p.
- Mabey, M.A., Madin, I.P., Youd, T.L. and Jones, C.F. (1993). Earthquake hazard maps of the Portland Quadrangle, Multnomah and Washington Counties, Oregon, and Clark County, Washington, Oregon. Department of Geology and Mineral Industries, Portland, Oregon, GMS-79.
- Mabey, M.A. and Youd, T.L. (in press). Development of a correlation between residual strength and $(N_1)_{60}$ for lateral Spreads in Natural Materials, NSF Workshop on Post-Liquefaction Shear Strength of Granular Soils.
- Mabey, M.A. and Youd, T.L. (1992). Prediction of displacements due to liquefaction induced lateral spreading, Brigham Young University Department of Civil Engineering Report No. CEG 92-02.
- Mabey, M.A. and Youd, T.L., (1989). Probabilistic liquefaction severity index maps for the state of Utah: Utah Geological and Mineral Survey Open File Report 159, 28 p.

- Mabey, M.A. and Youd, T.L., (1989). Liquefaction severity index maps of the state of Utah, in Watters, R.J., ed., Proceedings of the 25th Symposium on Engineering Geology and Geotechnical Engineering: Reno, Nevada, A.A. Balkema, Rotterdam, Netherlands.
- Madin, I.P., and Mabey, M.A., eds. (1996). Earthquake hazard maps for Oregon. Oregon Department of Geology and Mineral Industries, Portland Oregon, GMS-100.
- McCormack, T.C. (1996). "A Methodology for Regional Seismic Damage Assessment and Rehabilitation of Existing Buildings." Ph.D. Dissertation, Portland State University, Portland, Oregon.
- Newmark, N.M. (1965) Effects of Earthquakes on Dams and Embankments, 5th Rankine Lecture, Geotechnique, vol. 15, no. 2, June, p. 139-160.
- Yamamoto, K. and Hoshiya, M. (1996). Application of conditional stochastic field to mapping of ground vertical displacement, *in*: Proceedings from the Sixth Japan-US Workshop on Earthquake Resistant Design of Lifeline Facilities and Countermeasures Against Soil Liquefaction, Waseda University, Tokyo, June 11-13, 1996. Hamada, M. and O'Rourke, T. eds. National Center for Earthquake Engineering Research, Buffalo, September 1996, p. 153-162.
- Yoshida, M. Miyajima, M., Kitaura, M. and Fukushima, S. (1995). Estimation of spatial liquefaction potential using kriging technique, *in*: Earthquake Geotechnical Engineering: Proceedings of the IS-Tokyo '95 –The First International Conference on Earthquake Geotechnical Engineering; Tokyo , 14-16 November 1995, Ishihara, K. ed., A.A. Balkema, Rotterdam, 1995, volume 2, pages 911-916.
- Youd, T.L., (1978) Major Cause of Earthquake Damage is Ground Failure: Civil Engineering, vol. 48, no. 4, p.47-51.
- Youd, T.L., (1980) Ground Failure Displacement and Earthquake Damage to Buildings: in Vol. II Geotechnical Topics, ASCE Conference on Civil Engineering and Nuclear Power, 2nd, p.7-6-1 - 7-6-26.
- Youd, T.L., and Perkins, D.M. (1978). "Mapping liquefaction-induced ground failure potential." Journal of the Geotechnical Engineering Division, ASCE, 104(GT4), 433-446.
- Youd, T.L. and Perkins, D.M. (1987) Mapping of Liquefaction Severity Index, Journal of Geotechnical Engineering, ASCE, vol. 113, no. 11, November 1987, p.1374-1392.
- Youd, T.L., Perkins, D.M., and Turner, W.G. (1989). Liquefaction severity index attenuation for the Eastern United States: Proceedings, 2nd US-Japan Workshop on Liquefaction, Large Ground Deformation and Their Effects on Lifelines, Buffalo, NY, National Center for Earthquake Engineering Research Technical Rept. NCEER-89-0032, p. 438-452.

FIGURES

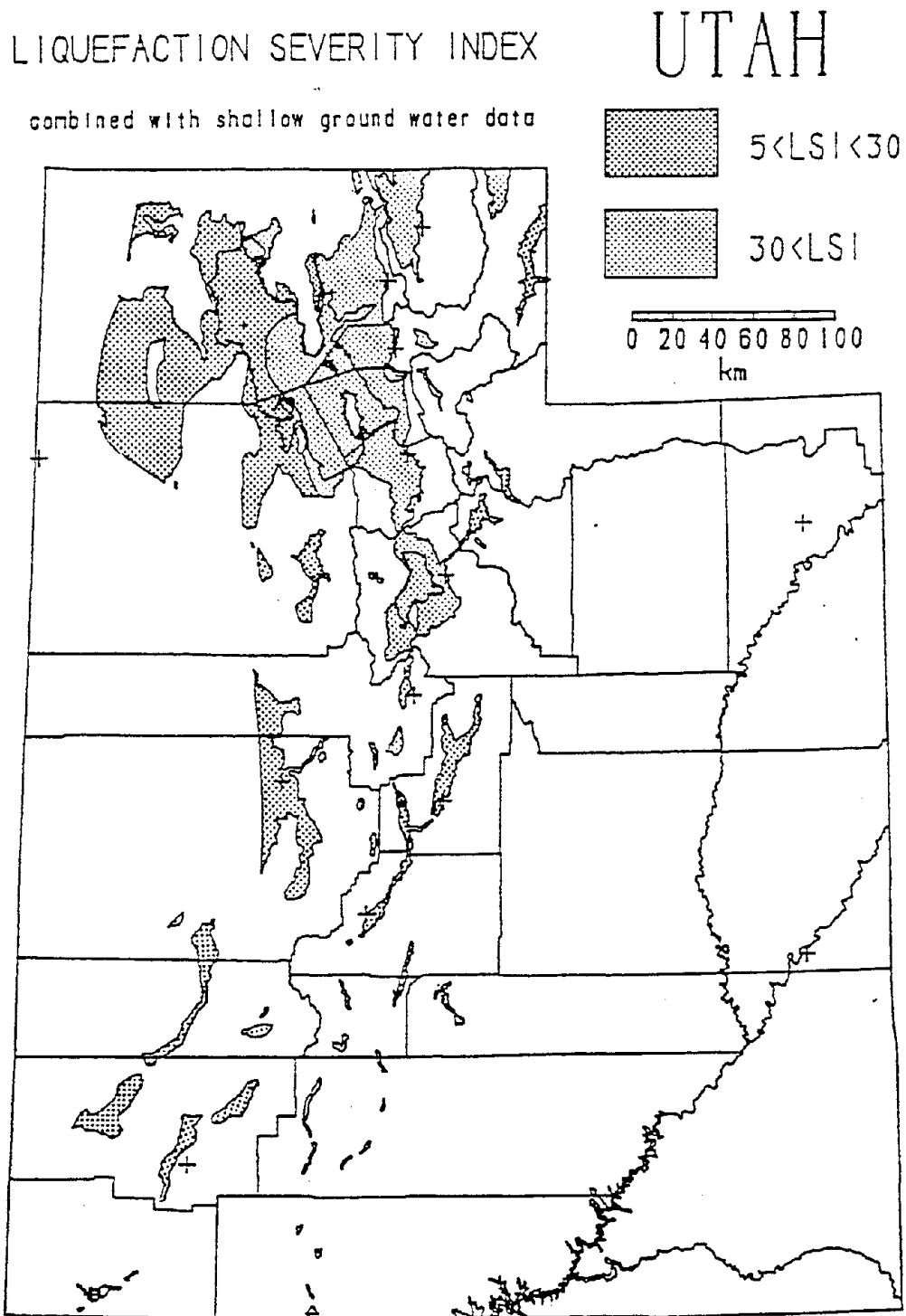


Figure 1. Liquefaction Severity Index Map of Utah, including extent of shallow ground water. LSI values have 10% probability of being exceeded in 250 years.

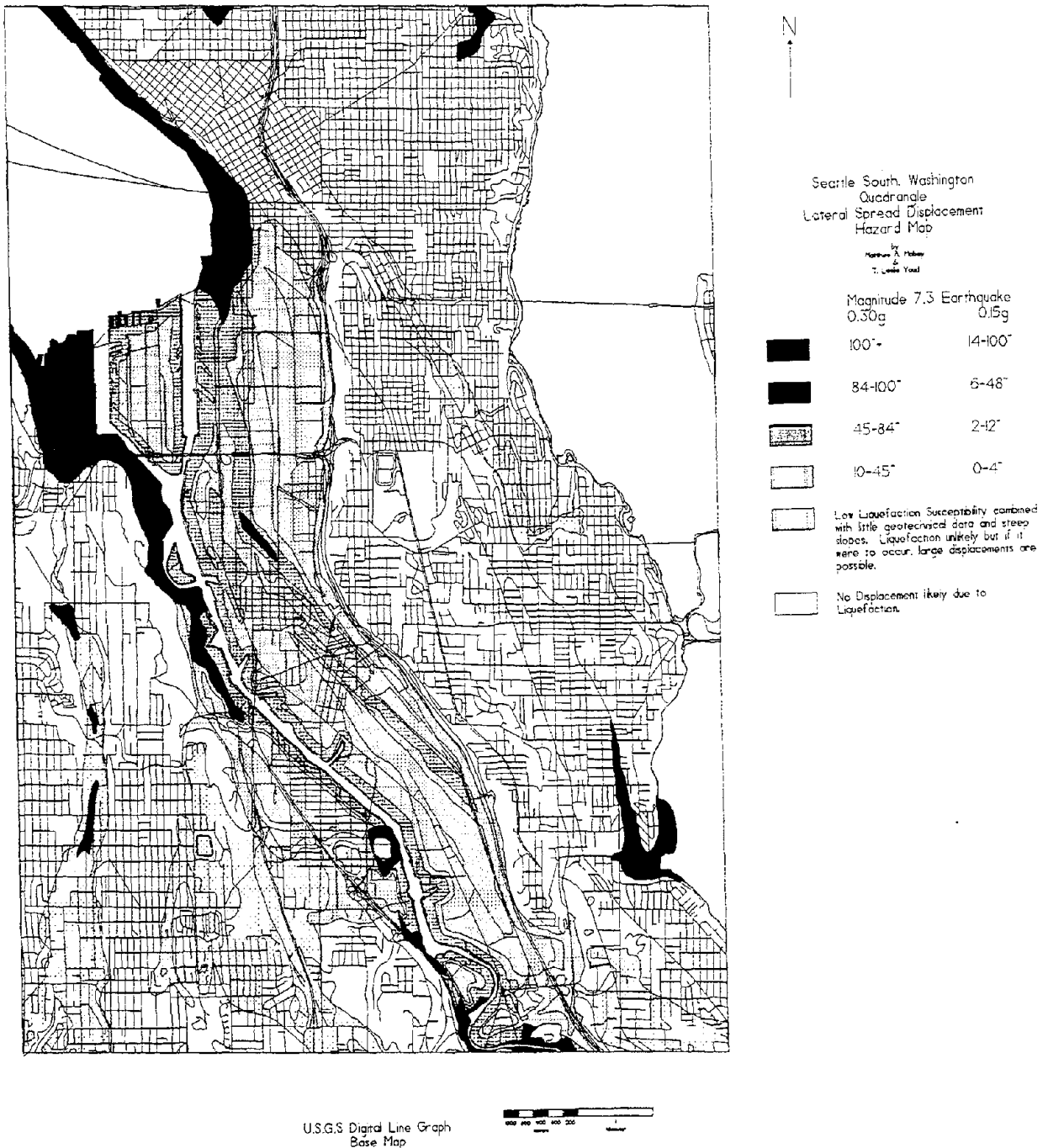
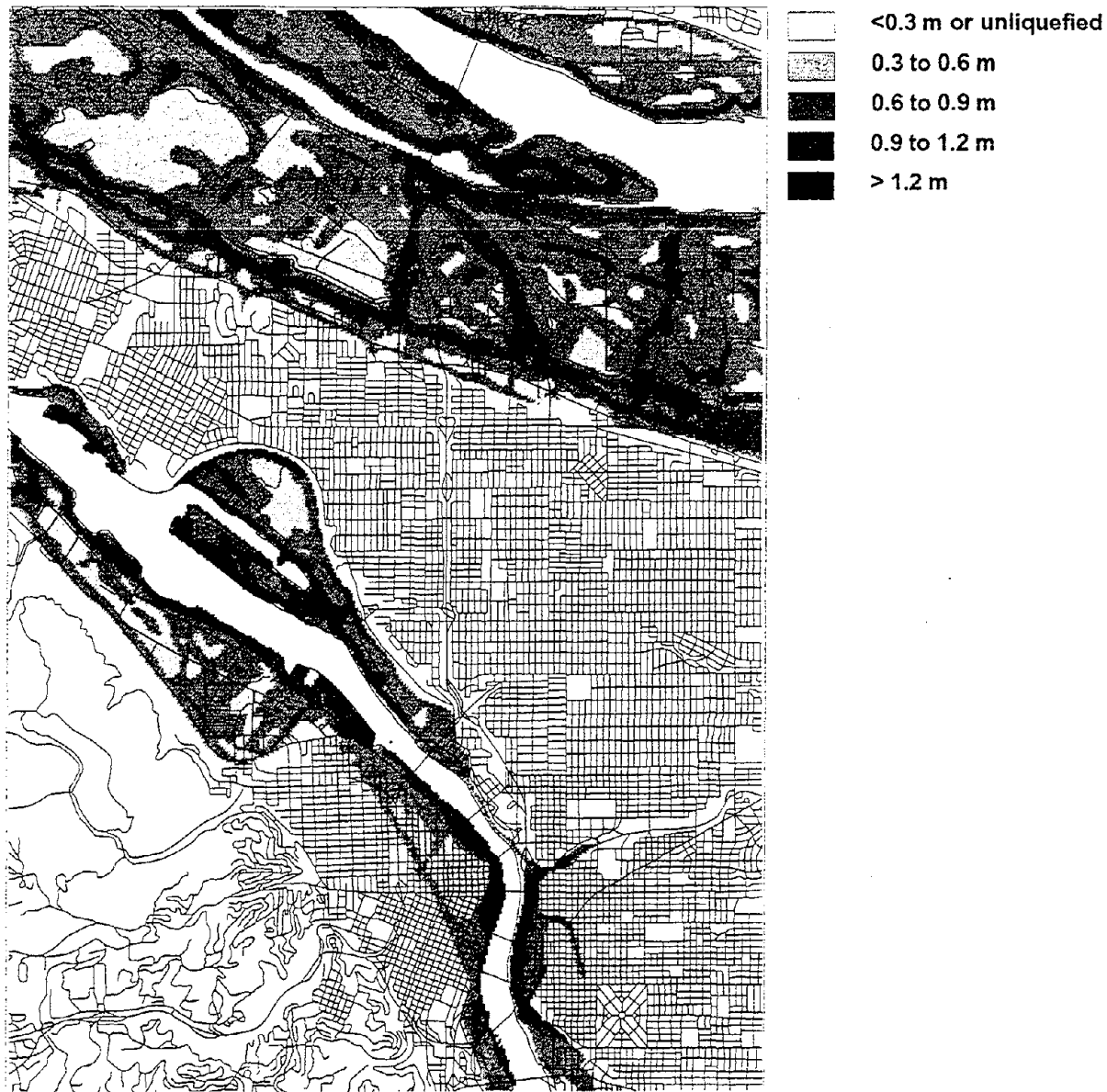


Figure 2. Lateral Spread Displacement Hazard Map, Seattle South, Washington Quadrangle.

Lateral Spread Displacement Map, Portland, Oregon



Meters
2920.00

Idrisi

Figure 3. Lateral Spread Displacement Map Portland, Oregon Quadrangle.

Draft Liquefaction Displacement Map Portland Metro Area

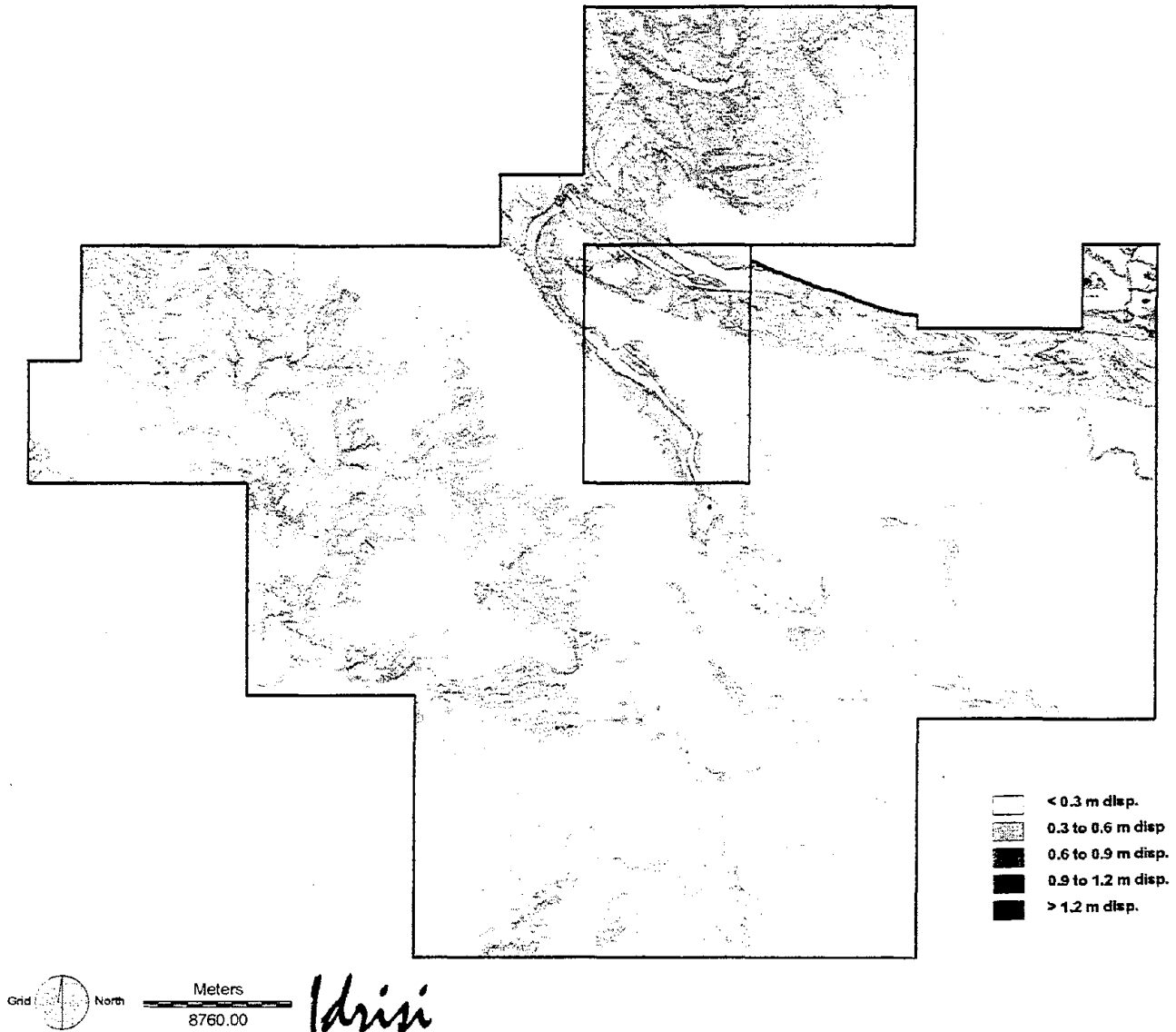


Figure 4. Preliminary Lateral Spread Displacement Hazard Map of Portland Metropolitan Area.

Dr. Matthew A. Mabey

Assistant Professor
Brigham Young University
Department of Geology
P.O. Box 25111
687 WIDB
Provo, UT 84663
phone: (801) 378-5248
fax: (801) 378-8143
e-mail: Matthew_Mabey@byu.edu



Education

Ph.D. in Civil Engineering, Brigham Young University, 1992.
MS in Civil Engineering, Brigham Young University, 1989.
BS in Geophysics, University of Utah, 1981.
BS in Geology, University of Utah, 1981.

Experience

Dr. Mabey is currently teaching geology and conducting research at Brigham Young University.

Before joining the faculty at Brigham Young University in 1996 he worked as the Geotechnical Earthquake Specialist at the Oregon Department of Geology and Mineral Industries, as well as an Adjunct Professor at Portland State University, for 6 years. While in this position he developed the Relative Earthquake Hazard Mapping methodology which is being applied to cities throughout Oregon and is also the basis for hazard mapping projects at various stages in Washington, Utah and British Columbia. The hazard information of the Relative Earthquake Hazard Mapping project in Oregon also served as the basis for several damage and loss estimation projects including FEMA's HAZUS project.

Dr. Mabey received both his Ph.D. and Masters degrees from the Civil Engineering Department at Brigham Young University. The research he performed as part of completing these degrees centered around predicting liquefaction induced lateral spreading displacements and using these displacements to construct hazard maps both in Utah and the Seattle, Washington area.

Dr. Mabey took a sabbatical from his professional career to serve as a volunteer missionary for the Church of Jesus Christ of Latter-day Saints from 1984 to 1986. He worked with the Spanish speaking community of Orange County, California.

Dr. Mabey began his professional career working as an exploration geophysicist for Marathon Oil Company. He worked with a variety of geophysical tools while with Marathon, but primarily with seismic data. Before starting with Marathon Dr. Mabey received dual Bachelors degrees from the University of Utah. While at the University of Utah he worked as an undergraduate research assistant performing micro-earthquake surveys, deep crustal seismic refraction surveys, and measuring seismic velocity delays across the Yellowstone Caldera.

Dr. Mabey has been involved in four post earthquake field investigations in the United States. He has served on two task forces regarding earthquake hazards and building codes. He is a member of the American Society of Civil Engineers, the Earthquake Engineering Research Institute, the Seismological Society of America, the Geological Society of America, the Society of Exploration Geophysicists, and the American Geophysical Union.

Selected Publications

- Mabey, M.A. and Youd, T.L., (in press), Development of a correlation between residual strength and (N1)60 for lateral Spreads in Natural Materials, NSF Workshop on Post-Liquefaction Shear Strength of Granular Soils.
- Mabey, M.A., 1997, Regional versus site specific spatial analysis, *in*: Spatial Analysis in Soil Dynamics and Earthquake Engineering, Geotechnical Special Publication No. 67, ASCE, New York City, p. 29-41.
- Mabey, M.A., 1997, Earthquake ground response mapping: a tool for earthquake hazard mitigation in the Portland Metropolitan Area, *in*: Building to Last: Proceedings of the XV Structures Congress, edited by Leon Kempner Jr. And Colin B. Brown, ASCE, New York City.
- Wong, I., Silva, W., Bott, J., Anderson, D., Mabey, M.A., Meier, D., Olig, S., Sanford, A., and Wright, D., (1997), Microzonation for earthquake ground shaking in three urban areas in the western United States, poster at the 1997 Annual Meeting of the Earthquake Engineering Research Institute, held in Austin, Texas.
- Mabey, M.A. and Madin, I.P., 1996, Assessing the local geologic component of the earthquake hazard in the Portland Metropolitan Area, *in*: Natural Disaster Reduction: Proceedings of the Conference, edited by George W. Housner and Riley M. Chung, American Society of Civil Engineers, New York City, p.177-178.
- Whelan, R.M. and Mabey, M.A., 1996, The expected financial losses due to building damage caused by severe earthquakes in Oregon, Oregon Geology, vol. 58, no. 6, p. 146-149.
- Mabey, M.A., Madin, I.P., Youd, T.L. and Jones, C.F., 1993, Earthquake hazard maps of the Portland Quadrangle, Multnomah and Washington Counties, Oregon, and Clark County, Washington, Oregon Department of Geology and Mineral Industries, GMS-79, 3 plates, 104 p.

Integrated Real-Time Disaster Information Systems The Application Of New Technologies

Ronald T. Eguchi
James D. Goltz
Hope A. Seligson
EQE International, Inc.
Newport Beach, California 92660-9027

ABSTRACT

This paper provides a brief overview of how new technologies were used after the Northridge earthquake to improve lifeline response and recovery. Technologies that are discussed include real-time availability of earthquake source data, improved loss estimation techniques, Geographic Information Systems and satellite-based monitoring systems. This paper also identifies areas in which further integration of these methods into emergency response would improve the survivability or reliability of lifeline facilities or services.

INTRODUCTION

At the time of the Northridge earthquake, a number of new technologies, including real-time availability of earthquake source data, improved loss estimation techniques, Geographic Information Systems and various satellite-based monitoring systems, were either available or under consideration as emergency management resources. The potential benefits from these technologies for earthquake hazard mitigation, response and recovery however, was largely conceptual. One of the major lessons learned from the January 17, 1994 earthquake was that these technologies could confer significant advantages in understanding and managing a major disaster, and that their integration would contribute a significant additional increment of utility.

The technologies discussed in this paper developed as discrete entities, in diverse disciplines and at different rates relative to one another. At the time of the Northridge earthquake, near real-time broadcasts of earthquakes had been available to utility and lifeline operators in southern California since 1990, although emergency management application of this information remained mainly experimental. Loss estimation, on the other hand, has been in use for two or three decades by both government and the private sector but has evolved, in recent years from a single event scenario format to a more versatile automated one.

Geographic Information Systems (GIS), like loss estimation, have a history spanning the last quarter century but only within the last several years have they been applied as an emergency management tool, and only in the Northridge earthquake were they used extensively in disaster response and recovery. As part of the "defense conversion" in the aftermath of the Cold War, satellite monitoring systems have been made available for peacetime purposes and have already been successfully applied in weather and storm surveillance and have been applied, to a limited extent, in other natural hazard analysis.

In this paper, we will examine these various new technologies, their contributions to response and recovery after Northridge and their actual or potential application to improving lifeline performance. Although this discussion will treat these technologies as discrete scientific developments, we will attempt

to identify areas in which there has been convergence and where further integration could produce significant improvements in the survivability and continued functionality of lifeline facilities and services.

NEW TECHNOLOGIES

REAL-TIME SEISMOLOGY

Although real-time seismic monitoring has been applied to promote public safety in Japan, similar applications have been slow to materialize in the United States. Following the Loma Prieta earthquake, a survey was conducted to assess the perceived utility of an earthquake early warning system which would provide a few seconds of warning in advance of damaging levels of shaking. Researchers found that most groups which were expected to enthusiastically endorse this new technology were luke-warm, at best, considering a few seconds warning too little time to take meaningful action in advance of a major earthquake. Nor was such a system regarded as a cost-effective strategy for hazard reduction and thus, unlikely to receive much support from users (Holden et al., 1989).

Despite this somewhat disappointing beginning for real-time monitoring, Caltech and the U.S. Geological Survey pushed ahead with plans to upgrade the Southern California Seismic Network (SCSN) to provide real-time broadcasts of earthquakes and seek the support of government agencies, large utilities and corporations for the potential post-event benefits these broadcasts might provide. Gradually, participants were recruited to participation in the Caltech-USGS Broadcast of Earthquakes (CUBE) and by the time of the Northridge earthquake, there were 18 Level III participants in the Earthquake Research Affiliates of Caltech (ERA), the organizational vehicle for provision of real-time earthquake broadcasts from SCSN. These participants made an annual contribution of \$25,000 to the Caltech Development Fund (which helped support the purchase of new seismic monitoring equipment) and received reports of earthquakes via pagers which carried the magnitude, location, time and other earthquake data within 2-5 minutes of occurrence.

For approximately four years, CUBE reliably broadcasted earthquakes up to about M5.5 to participants. At 4:31 a.m. on January 17, however, the CUBE system experienced both hardware and software difficulties which resulted in delays of approximately one hour in providing information on the Northridge earthquake. A study currently under way is designed to determine how response of CUBE participants was affected by the performance of CUBE after the Northridge earthquake, and in general, how receipt of real-time earthquake information from SCSN has been integrated into the response plans of these organizations (Goltz, 1995).

Preliminary results from this study indicate that the CUBE system usually provides the first data upon which action may be taken. To assist in determining whether a response is justified, many CUBE participants have customized the Q-pager software (which displays spatial and other data on an earthquake) by adding overlays to the basic southern California map on which earthquake epicenters are plotted. These overlays include facilities such as transmission lines, dams, power stations or other critical structures. In a few instances, participants reported monitoring the patterns of small earthquakes in a particularly critical location under the assumption that these earthquakes may be precursors to a large damaging event.

Statewide real-time broadcasts are now available and have been adopted by those agencies (OES and Caltrans) and companies (utilities and railways) with statewide jurisdiction, facilities or distribution networks. These statewide broadcasts are available through a cooperative agreement between Caltech (CUBE) and the University of California at Berkeley (REDI or Rapid Earthquake Data Integration). In March, 1995, CUBE participants received software which permits the mapping of ground acceleration data broadcast in real-time from the SCSN. Most users consider this to be a very important development in that

the potential impact on facilities can be more precisely estimated and mobilizations of personnel for inspections can be expedited.

The development of real-time monitoring and broadcast of seismic information appears to be in transition from concept and pilot project to a practical operational system. Under the strictest definition of real-time availability, the Northridge earthquake must be considered a missed event. It appears, however, that the January 17 event exposed a plethora of technical vulnerabilities in the CUBE system and triggered a concerted effort to remedy most, if not all of them. It does not appear that the failure of the CUBE system to provide rapid and accurate information on the earthquake had a dampening effect on the interest and enthusiasm of users.

LOSS ESTIMATION

The Northridge earthquake was the first earthquake disaster to occur in the United States in which important emergency response and early recovery decisions were based on loss estimates as well as actual data gathered through standard reconnaissance procedures. The utilization of loss estimation techniques in the immediate post-earthquake context is a key development and marks a significant departure from conventional applications. For the last two decades, earthquake loss studies have addressed the pre-earthquake planning needs of utility operators and government agencies. Although the needs of these users vary, understanding risks and maintaining public safety have generally required similar scenario events, that is, those with the greatest impacts on the local population and economy.

Historically loss estimation studies for planning purposes have identified scenario earthquakes as the focal point of estimate development. These studies use existing knowledge of regional geology and seismology to generate maps with estimated intensities and, based on projected ground motion and other factors, estimate damage to buildings and structures, lifelines and impacts on population. Some studies also address potential secondary hazards such as fire, flood and hazardous materials releases. Presented in report or document form, often with fold-out and sometimes overlay maps, these earthquake scenarios have been employed by government and utilities to prepare and mitigate potential earthquake losses. Thus, the typical loss study has been single-event focused, applied in the long-term pre-event period and utilized primarily by those concerned with seismic safety planning and risk management.

Even before the Northridge earthquake, technological developments were rapidly rendering these scenarios and the formats in which they are presented obsolete. The advent of high speed computing, satellite telemetry and Geographic Information Systems (GIS) have made it possible to electronically generate loss estimates for multiple earthquake scenarios, provide a nearly unlimited mapping capability, and perhaps most important, develop estimates for an actual earthquake in near real-time given the source parameters of magnitude and location. For the last five years, real-time broadcasts of earthquake data including magnitude, location, depth and time of occurrence, have been available in southern California on an experimental basis from the Southern California Seismic Network operated jointly by the California Institute of Technology and the United States Geological Survey.

Currently under development for the California Governor's Office of Emergency Services (OES) is a GIS-based system capable of modeling building and lifeline damage and estimating casualties in near real-time given the source parameters of an earthquake (Eguchi, et al, 1994). The Early Post-Earthquake Damage Assessment Tool (EPEDAT) utilizes real-time seismic information from the Southern California Seismic Network and operates on a personal computer. EPEDAT utilizes fault and seismicity data to locate the most likely source of an earthquake, as broadcast by CUBE. Applicable ground motion and soil amplification models are employed to estimate the expected intensity patterns in the affected area. These intensities are then overlaid onto the computerized data files containing an aggregate listing of buildings

and lifelines in the region. Based on damage and casualty models already developed under contract with the State of California, and the intensity patterns computed, building and lifeline damage as well as casualties are estimated for the impacted area. EPEDAT also allows the user to update early estimates with actual reconnaissance data. Thus, as more accurate and specific data become available, they can be incorporated to refine or correct initial predictions.

Real-time loss estimation offers direct and tangible benefits over conventional loss studies. For the first time, loss estimation can be used in the emergency response and early recovery phases of a disaster as a decision support tool. Based on rapid receipt of magnitude and location, estimates of ground shaking and intensity can be calculated and mapped giving emergency responders a sense of the overall scope of an event minutes after it has occurred. Reconnaissance efforts can focus on those areas projected to be hardest hit based on estimates of intensity. Inspection teams can be dispatched, staging areas can be identified, medical emergency resources mobilized and sheltering needs considered, as responders are guided by estimates of damage, casualties and displaced persons. Recovery can be hastened by calculation of total dollar loss estimates and breakdowns of losses by facility or structural type, usage or other categorizations expedite governmental disaster assistance.

Immediately following the January 17 earthquake, data and models which are the basis for EPEDAT in Southern California were utilized and, though the system was not fully operational at the time, produced timely and accurate information which was used by state and federal officials to support key policy and program decisions. Estimates of dollar losses and ground shaking intensity were used by the California Office of Emergency Services to define the general regional scope of the disaster during the critical 24-48 hours after the event. The shaking intensity map was instrumental in approximating the locations of heaviest damage, used in briefing state agency executives, including the Governor, and in making decisions regarding shelter needs, locating Disaster Application Centers and "fast-tracking" the federal Disaster Housing Assistance Program. A total dollar loss estimate of \$15 billion, generated within 24 hours of the earthquake, served as the basis for negotiation of a supplemental Congressional appropriation of \$8.6 billion in federal disaster assistance.

GEOGRAPHIC INFORMATION SYSTEMS (GIS)

In the context of emergency management, GIS technology has rapidly evolved over the last decade and, in the aftermath of the Northridge earthquake, is regarded as a vital response and recovery decision support system. An obvious advantage for response and recovery officials is the ability to gain both a regional and highly localized assessment of situations requiring rapid decision making. Such decisions are facilitated by the interrelationship of structural, demographic, economic and environmental data in mapped as well as tabular formats. The utility of GIS has been enhanced by technological developments in related areas including remote sensing, global positioning, software and hardware improvements and desktop applications (Topping, 1993).

A GIS unit had been established within the California Governor's Office of Emergency Services prior to the Northridge earthquake; after the January disaster, however, this unit was greatly enhanced with additional personnel, new equipment and technical expertise available on a consulting basis. Co-located in the Pasadena Disaster Field Office with its GIS counterpart in the Federal Emergency Management Agency, this unit provided an important source of information in both the response and recovery phases of the Northridge earthquake. In addition, this unit has taken major strides toward development of a disaster management database for California.

In the immediate aftermath of the Northridge earthquake, GIS was used to develop a shaking intensity map based on model estimates. This map was instrumental in gaining a rapid assessment of the regional scope

of the disaster and supported key decisions regarding the location of shelters and disaster application centers and documenting the state's request for a presidential disaster declaration (Goltz, 1995). As recovery programs were initiated, GIS was instrumental in identifying and displaying language and demographic characteristics, geographically locating disaster assistance applications and in hazard mitigation planning (Topping, 1994).

For lifeline operators, GIS also played an important role in Northridge response and recovery. The wastewater collection system for the City of Los Angeles consists of a complex network of underground sewers, both gravity driven and forced mains. In total, over 7,000 miles of sewer pipe traverse the City of Los Angeles. As in past earthquakes, damage to underground sewer pipes has been difficult to detect because the effects are not immediately visible, unless ground failure has occurred. In some cases, leaks and breaks are only detected when adjacent water mains are filled and wastewater spills onto the ground and street because of blockages caused by internal damage or collapse. Other indicators of severe sewer damage include street settlement, crushed or buckled curbs, damage to sidewalks and failed water mains.

In an attempt to quickly identify areas of severe sewer damage after the Northridge earthquake, the City of Los Angeles relied on GIS (Solorzano et al., 1994). First, GIS was used by the Bureau of Engineering to identify areas of extensive building damage, water main repair and surface disruption (i.e., damage to sidewalks, roads, etc.). This information was then overlaid onto maps of the sewer system in order to prioritize close circuit television (CCTV) surveys. Areas that fell within relative high risk areas (e.g., areas with extensive building damage) were surveyed first. This assessment revealed that approximately 16% of the inspected sewers required emergency repair, 49% sustained some damage and the remaining 35% sustained no damage.

Similarly, the Los Angeles Department of Transportation used a GIS-based Automated Traffic Surveillance and Control system (ATSAC), installed several months prior to the earthquake to monitor traffic flow, to plan detour routes and implement signal timing strategies in the Santa Monica I-10 Freeway corridor. The ATSAC system is also used to control the message signs along the freeways and, after the earthquake, these signs were used to advise motorists of the various detour routes and traffic conditions (LADOT, 1994).

AERIAL AND SATELLITE-BASED MONITORING SYSTEMS

Images, measurements and other data obtained from the vantage point of high altitude aircraft and satellites has recently entered the technological arsenal of emergency managers. These technologies have been employed to monitor geological changes and as a source of damage assessment during and after major emergencies including fires, bombings and flooding. These technologies including aerial photography and satellite imagery have recently been proposed for assessing the effects of large earthquakes (Crippen, 1992; Crippen and Blom, 1993). Using SPOT satellite images acquired approximately one month after the 1992 Landers earthquake, the Jet Propulsion Laboratory in Pasadena was able to capture spatial details of terrain movements along fault breaks associated with the earthquake that were virtually undetectable by any other means.

The Japanese have used aerial photographs to identify areas of significant ground failure after several large earthquakes. By comparing pre- and post-earthquake aerial photos of liquefaction affected areas, they have successfully mapped areas of ground movement including both magnitude and overall displacement (Hamada and O'Rourke, 1992).

Another example of aerial reconnaissance after an earthquake is shown in Figure 1. This photograph shows earthquake damage detected after the 1971 San Fernando earthquake. Explosion craters resulting

from gas leakage along Glen Oaks Boulevard in Sylmar can be clearly detected. Also visible in the center of this photo are ground cracks that resulted from extensive ground shaking during the earthquake. In this particular area, over 100 pipeline breaks were recorded in water and natural gas pipelines (Eguchi, 1982). It has been demonstrated historically that extensive ground distortion generally leads to significant damage to underground lifeline components (Eguchi, 1991).

Until recently, it was not clear how satellite data could be used effectively to identify areas of earthquake impact. In general, the data that are publicly available are limited by the level of resolution possible. For example, the SPOT image pixel size used to detect ground movement during the 1992 Landers earthquake is 10 meters (Crippen and Blom, 1992), which is larger than many of the displacements observed during the event. However, through the use of image matching by correlation analysis, JPL has been able to computationally detect displacement vectors revealing horizontal ground strain patterns. The most effective means of using this data in a post-earthquake situation is in identifying large areas of tectonic ground movement. Data resulting from satellite imaging may suggest areas for detailed aerial reconnaissance. A technique derived by Gabriel and others (1989) has been used to map small elevation changes over large areas using differential radar interferometry. This technique could be used to supplement satellite imaging (which only estimates horizontal changes) to identify areas of significant tectonic changes or perhaps ground failure settlement.

Global Positioning Satellite (GPS) systems were employed after the Northridge earthquake to assess the extent of crustal deformation and displacement. Based on measurements taken before and after the earthquake, the extent and nature of co-seismic displacements were determined. These data indicated that measurable displacements were produced over a 4,000 square kilometer area including much of the San Fernando Valley and adjacent mountainous areas (Hudnut et al, publication pending). Although these measurements were not available immediately following the earthquake, they could be made within sufficient time in future earthquakes for lifeline organizations to make response decisions based on the probable location and magnitude of displacements.

DISCUSSION AND CONCLUSIONS

Lifeline operators, both public and private, have been receptive and, in many cases enthusiastic, users of new emergency management technologies. The application of these technologies in the Northridge earthquake was, for many organizations, the first real test of their actual or potential utility in a major regional crisis. In some cases, existing systems proved to be successful and of critical importance, in others, performance was disappointing but important lessons were learned and vulnerabilities exposed. In addition, many new applications were discovered and the potential integration of these technologies moved from the conceptual to actual pilot testing. In this final section, we will identify areas in which the further application or integration of technologies could improve lifeline performance.

Expanded application of real-time earthquake monitoring holds considerable promise in improving performance during and hastening recovery after an earthquake for lifeline organizations. Most of the participants in the Caltech USGS Broadcast of Earthquakes are utilities and rail transportation providers. While most CUBE users, including lifeline organizations, have used the receipt of real-time source data for determining response needs, some have worked toward linkage of real-time notification with automated shutdown or other procedures which would ensure continued service after a major earthquake. Telecommunications companies, for example, have developed methods of rerouting network traffic away from areas likely to have sustained earthquake damage based on real-time broadcasts. Lifeline organizations have also been advocates of expanded real-time information including strong ground motion, estimates of displacement and early warning systems.

Earthquake loss estimation studies and scenarios such as those developed by the California Division of Mines and Geology have been used by lifeline organizations for planning and hazard mitigation purposes. Most, if not all, of these planning scenarios have included relevant vulnerability information which specifically address transportation and utility lifelines. Although new rapid loss estimation techniques which are linked to real-time earthquake monitoring systems have been developed for state and federal agencies, lifeline organizations, both in the United States and Japan, have expressed considerable interest in these new systems which provide a range of geotechnical, economic (e.g. damage, dollar loss) and population impact (e.g. casualties, displaced persons) data within minutes of the occurrence of a major earthquake.

In our earlier discussion of the application of GIS technology, we cited two examples of the use of GIS systems by lifeline operators in the Northridge earthquake. The experience of the two Los Angeles city agencies suggests that GIS-based systems in lifeline organizations are more fully integrated with operational processes than is the case in other organizations. Recall that the Department of Transportation used their GIS-based system to assess traffic conditions, implement control mechanisms and provide public information in one operation. This level of system integration suggests that lifeline organizations are likely to provide key innovations in the application of GIS technology to the management of emergencies.

Aerial surveillance and satellite imagery could be potentially beneficial sources of rapid information on above ground lifeline systems. Although high altitude aerial reconnaissance was attempted in the Northridge earthquake, neither the mission nor the results of this effort are known and to date have not appeared in after action assessments or other media known to the authors. The value of aerial photography and remote imaging are questionable for underground lifelines. The potential benefits of GPS data for pipelines and other underground systems, however, is quite significant.

The convergence of these new technologies after the Northridge earthquake mark an important development for emergency management in general, and for the performance of lifelines in particular. Of particular significance is the integration of real-time monitoring of seismic activity, loss estimation methodologies and GIS systems. The potential benefit lies in the ability of lifeline operators to obtain early warning of potentially damaging ground motion and implement procedures to lessen impacts and to respond rapidly to an earthquake, based on both empirical information and model estimates.



Figure 1. Cratering caused by gas leakage and explosions along Glenoaks Blvd. After the 1971 San Fernando Earthquake

REFERENCES

- Crippen, R.E. (1992). Measurement of Subresolution Terrain Displacements Using SPOT Panchromatic Imagery, *Episodes*, Vol. 15, No. 1.
- Crippen, R.E. and Blom, R.G. (1993). Observation and Measurement of Horizontal Terrain Displacements Associated with the Landers Earthquake of 28 June 1992 Using SPOT Panchromatic Imagery. Presentation to the Geological Society of America Meetings, Reno, May, 1993.
- Eguchi, R.T. (1982), Earthquake Performance of Water Supply Components During the 1971 San Fernando Earthquake, Prepared for the National Science Foundation, J.H. Wiggins Report No. 82-1396-2a.

- Eguchi, R. T. (1991), "Seismic Hazard Input for Lifeline Systems," *Structural Safety*, 10, Elsevier, p. 193-198.
- Eguchi, R. T., J.D. Goltz, H.A. Seligson, and T.H. Heaton (1994). Real-Time Earthquake Hazard Assessment in California: The Early Post-Earthquake Hazard Assessment Tool and the Caltech-USGS Broadcast of Earthquakes, *Proceedings of the Fifth U.S. National Conference on Earthquake Engineering*, July 10-14, 1994.
- Gabriel, A.K., R.M. Goldstein, and H.A. Zebker (1989), Mapping Small Elevation Changes Over Large Areas: Differential Radar Interferometry, *Journal of Geophysical Research*, Vol. 94, no. B7, p. 9183-9191.
- Goltz, J.D. (1995). The Use of Real-Time Seismic Information by Government, Utilities and Corporations. Presentation at the California Institute of Technology, Seminar on Real-Time Seismology, April 20, 1995.
- Hamada, M. and T.D. O'Rourke (1992), Case Studies of Liquefaction and Lifeline Performance During Past Earthquakes, Technical Report NCEER-92-0001, Vols. 1 and 2.
- Holden, R., R. Lee, and M. Reichle (1989). Technical and Economic Feasibility of an Earthquake Early Warning System in California, report to the California Legislature. California Division of Mines and Geology.
- Hudnut, K.W., Z. Shen, M. Murray, S. McClusky, R. King, T. Herring, B. Hager, Y. Feng, P. Fang, A. Donnellan, and Y. Bock (1995). Co-Seismic Displacements of the 1994 Northridge, California Earthquake. Publication pending in the *Bulletin of the Seismological Society of America*.
- Los Angeles Department of Transportation (1994). Northridge Earthquake Transportation Response: After Action Report. City of Los Angeles.
- Solorzano, R., D. Parikh, R. Price, and A. Hagekhalil (1994). Sewer Damage from the Northridge Earthquake. Presentation to the U.S.-New Zealand Workshop on the Northridge Earthquake, Los Angeles, August 15-16, 1994
- Topping, Kenneth C. Implications of GIS Applications Following the Northridge Earthquake, Abstract for the Fourth Japan-United States Workshop on Urban Earthquake Hazard Reduction, Osaka, Japan January 17-20, 1995.

V. **RESEARCH AND DEVELOPMENT IN EARTHQUAKE DISASTER
PREVENTION TECHNOLOGY AFTER THE NORTHRIDGE
AND KOBE EARTHQUAKES**

“Development of Seismic Risk Analysis of Power Systems”

J. Tohma, S. Higashi, Y. Shumuta

“Current Developments in Seismic Design Criteria and Mitigation
Efforts for Electric Power Transmission Systems”

L. Kempner

“The 1996 Seismic Design Specifications for Highway Bridges”

T. Terayama, K. Yokoyama, K. Tamura, S. Unjoh, J. Hoshikuma

“Aseismic Countermeasure Technologies for Outdoor Telecommunication
Facilities Implemented Following the 1995 Hyogo-ken Nanbu Earthquake”

M. Okutsu, K. Honda, Y. Yamaguchi, A. Sawaguchi, K. Ikeda

“Comparison of Recovery and Reconstruction Strategies in Water Supply
Systems Between the 1994 Northridge and the 1995 Kobe Earthquakes-
Emphasizing on an Emergency Response”

J. Ueno, S. Takada, R. Ozaki



DEVELOPMENT OF SEISMIC RISK ANALYSIS OF POWER SYSTEMS

by

Jun'ichi Tohma
Sadanori Higashi
Yoshiharu Shumuta

Geotechnical and Earthquake Engineering Department,
Central Research Institute of Electric Power Industry
Abiko, Japan

ABSTRACT

Older substation components are vulnerable in power systems. They would cause widespread power failure just after the earthquake hit. It was pointed out by the government commission report after the Hyogo-ken Nambu earthquake that seismic retrofit is needed for those components which do not satisfy the existing guide for seismic design. To make an upgrading plan for preexisting components under economically rational condition, evaluation on seismic input and associated retrofit cost should be considered. In this paper, our on-going researches on these subjects are described.

DEVELOPMENT OF A 3-D ANALYSIS METHOD FOR WAVE PROPAGATION

Determining the spatial distribution of seismic motion for a region affected by scenario earthquakes is fundamental to the seismic retrofit planning process. Until now, seismic motion has typically been estimated using empirical formulations based on the statistical analysis of seismic records, or through response analysis of simplified soil models, but the limitations of such techniques have become apparent as phenomena which cannot readily be analyzed under such a framework have been observed during recent large earthquakes. However, recent years have seen a rapid development in seismic simulation techniques on both the software and hardware fronts, and it is becoming possible to make estimations of seismic motion based on more physical models.

An analysis code for seismic wave propagation was developed by Higashi and Satoh (1997) using the pseudo-spectral method. The analysis area is discretized, and an equation of motion is solved for each grid point. The spatial differentiation of the displacement and stress is solved on the wavenumber domain using FFT, while the temporal differentiation of the displacement is solved using a finite difference approximation. Despite having less degrees of freedom than

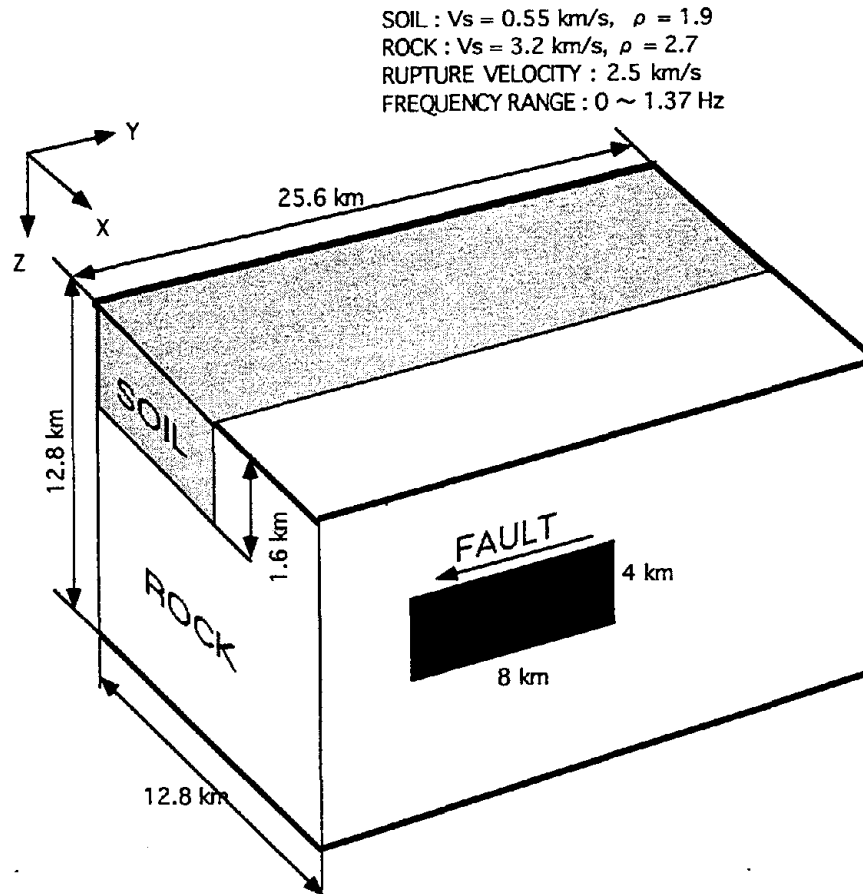


Fig.1 A three-dimensional model of underground structure and fault

other methods such as the finite difference method, this method is advantageous in that a large domain of analysis can be handled without losing accuracy. The newly-developed analysis code improves artificial and free-surface boundary conditions, and thus has a high level of applicability as a 3-D analysis method for seismic wave propagation.

When estimating seismic ground motion for a near-field earthquake, the location of faults relative to the relevant topography is particularly important. To demonstrate the applicability of the developed 3-D analysis, numerical simulation for a simple geological model was carried out. An active fault with a vertical fault plane (length 8 km, width 4 km, depth 4 km) situated within rock was assumed for the model. The underground structure used for the model assumed that the basement rock lied at a depth of 1.6 km with a very steep gradient (Fig.1). The analysis found that the region of strong ground motion was not located in the rock surface directly above the fault, but occurred at the ground surface of the sedimentary layer some distance away from the fault, and that the region of strong ground motion had the same directivity as the rupture direction of the fault (Fig.2).

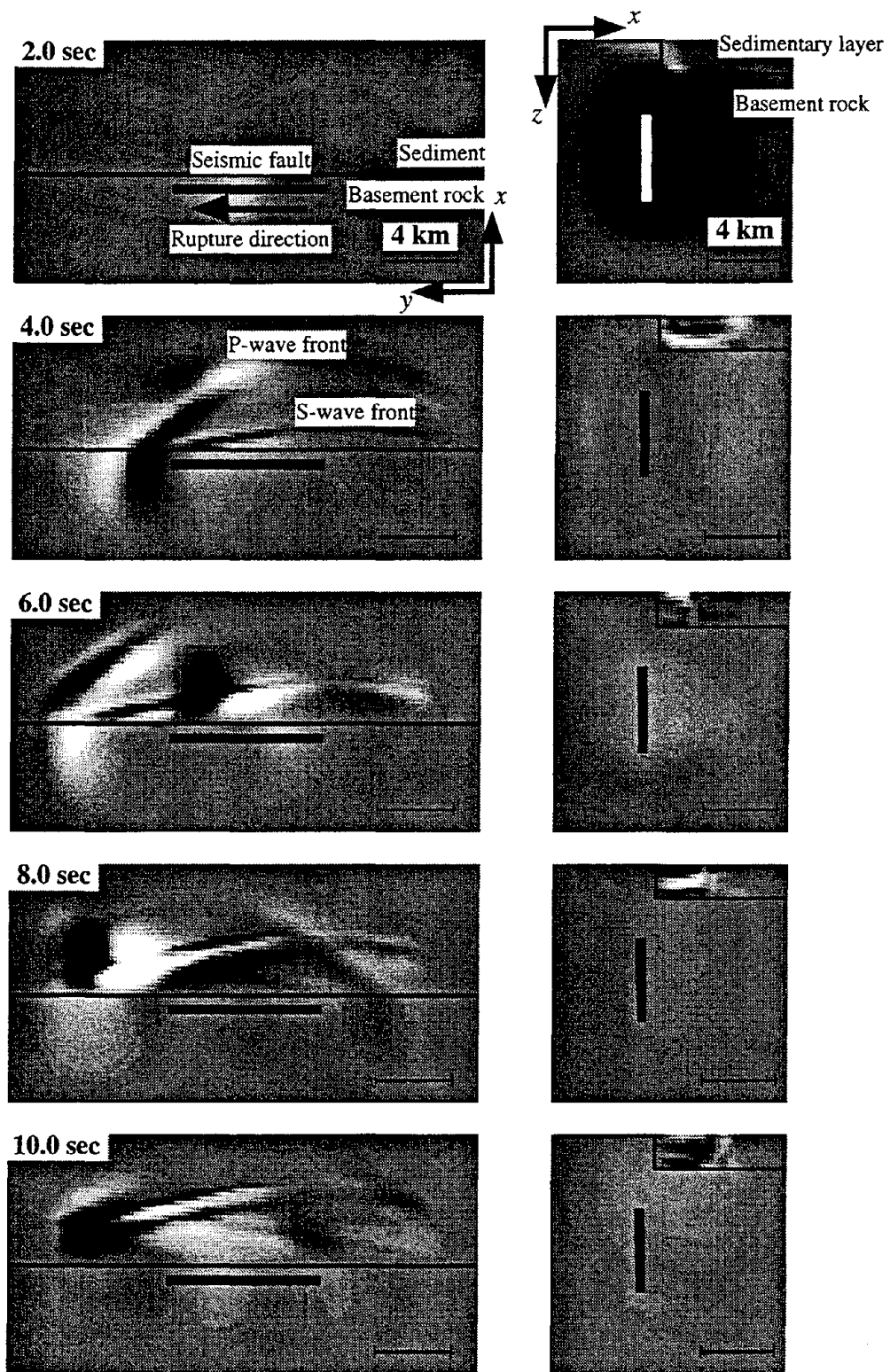


Fig.2 Snapshots of seismic wave field after fault rupture started
left : X-Y plane
right : X-Z section

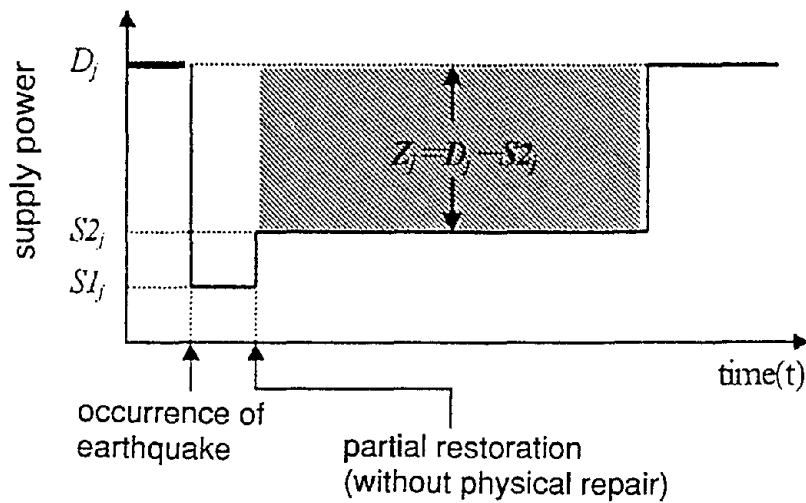


Fig.3 Determination of the capacity deficiency function

Although this analysis code is still in the preliminary research stages, simulation results are in accordance with phenomena observed as a result of the Hyogo-ken Nanbu earthquake, suggesting that the analysis code will be of significant value as a method for predicting seismic ground motion for 3-D underground structures with faults. In order to achieve a comprehensive seismic risk analysis of power systems, we are planning to introduce geographic information system (GIS) in the project .

DEVELOPMENT OF BENEFIT-COST ANALYSIS METHOD FOR SEISMIC RETROFIT

An optimum seismic upgrading method for older substation components is developed by Shumuta and Tohma (1997) considering network reliability of power systems and expected economical loss. The developed method consists of three steps. The seismic damage probability for substation component is evaluated in the first step. The seismic reliability of power systems is estimated in the second step on the basis of the component damage probability. The power loss in damaged power system is divided into two levels (Fig.3). Power system damage due to an earthquake reduces performance to $S1$, the supply power just after the earthquake. $S2$ indicates possible supply power after partial restoration by corrective switching without physical repair. System redundancy allows operators to quickly improve the supply power ability from $S1$ to $S2$, without replacing the damaged components. Thus, power loss is estimated by a capacity deficiency function Z .

$$Z = D - S2 \quad (\geq 0) \quad (1)$$

Where, D indicates the demand power just before an earthquake. To estimate the expected power loss, seismic reliability analysis for power systems is executed. Each substation is modeled as a sub-network consisting of buses, line switches, circuit breakers, and transformers. These components are modeled as nodes, while lead lines connected to each component are modeled as links. On the basis of the damaged probability of each node, the damaged nodes are determined for every trial in the Monte Carlo simulation. Power loss is calculated for each substation including damaged nodes using the connectivity analysis. Then, the power loss of each substation is used as the input data for the seismic reliability analysis of the main network. Physical connectivity, properties of electricity, effects of flow control are considered in the analysis of loop type primary systems. Effects of system switching are considered in the analysis of radial type lower systems.

In the third step, total cost is expressed as

$$\text{Total Cost} = \text{Company Loss} + \text{Retrofit Cost} \quad (2)$$

Where,

$$\text{Company Loss} = \text{Capital Loss} + \text{Revenue Loss} + \text{Chargeable Cost} \quad (3)$$

Capital Loss is determined by

$$\text{Capital Loss} = \sum_{i=1}^n P_{f_i} \times (\text{Repair Cost})_i \quad (4)$$

Where, i and n indicate substation components and number of damaged components; P_{f_i} indicates the damage probability of substation components i ; $(\text{Repair Cost})_i$ indicates repair cost of damaged component i .

Revenue Loss is determined by

$$\text{Revenue Loss} = \frac{1}{m} \sum_{n=1}^m \left\{ Z_n \times T_{Rn} \times \int_0^1 f_L(t) dt \right\} \times \text{Profit Cost / Unit} \quad (5)$$

Where, n and m indicate trial and total trial number of the Monte Carlo simulation; Z_n indicates the total power loss of the power system at trial n in the Monte Carlo simulation; T_{Rn} indicates the restoration time for the power system at trial n ; $f_L(t)$ indicates power loss rate in the local area (L) with the elapsed time t . Profit Cost / Unit indicates the profit cost due to the sale of electric power unit.

Chargeable cost indicates the cost which a power company in charge of the power loss has to pay to customers.

Retrofit Cost is determined by

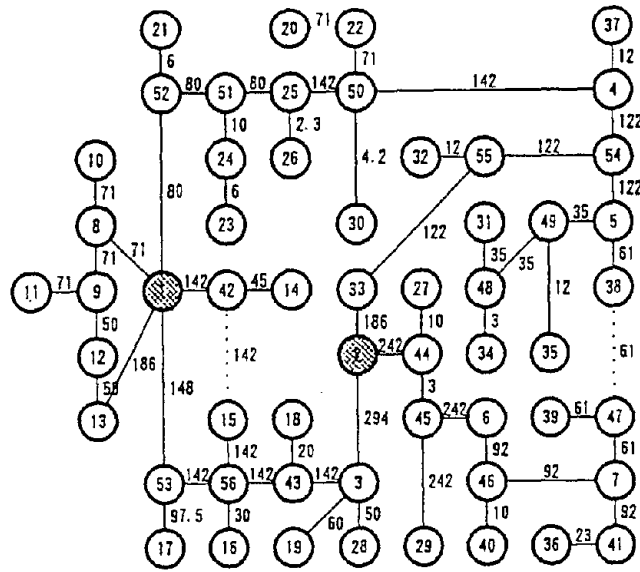


Fig.4 A main network model of secondary system
 ○ : substation with serial number
 — : transmission line with capacity (MVA)

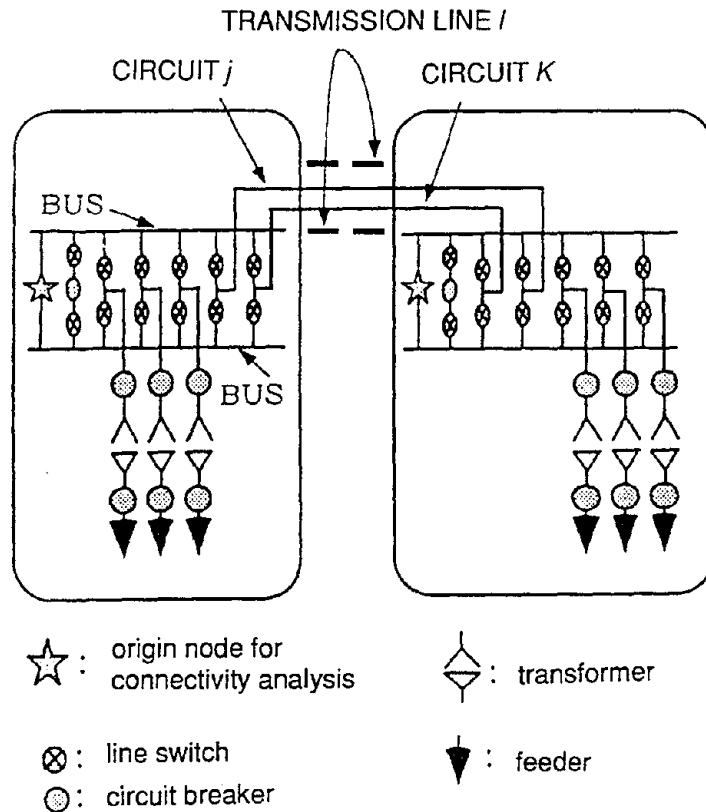


Fig.5 Subnetwork models for substation systems

$$\text{Retrofit Cost} = \sum_{i=1}^m (\text{Retrofit Cost})_i \quad (6)$$

Where, i indicates substation components and m indicates the total number of components with retrofit. Even if the number of retrofitted components is the same, the expected power loss with changes in the retrofit order of substation components. We have developed a method for determining the retrofit order for substation components introducing Coefficient of Supply Power Constraint(CSPC).

To demonstrate the developed method, a network model with 56 nodes for substations and 59 links for transmission lines was constructed (Fig.4). Each node in the main network has a sub-network consisting of nodes for transformers, buses, circuit breakers, line switches, and links for lead lines (Fig.5). The total number of nodes and links for all sub-network models is 864. This power system supply about 660MW in a model city.

Under a scenario earthquake (magnitude 7.8, hypocentral distance 100km) condition, peak ground accelerations are given to the substation. A total of 474 line switches and a total of 53 circuit breakers were targeted for seismic retrofit. The relation between expected power loss and associated costs are obtained. It is understood that the retrofit of 34.2% of the targets minimize the total cost. The expected power loss for this measure is equal to 16.9 MW. The results also suggest that the retrofit of 43 circuit breakers would be effective for the improvement of the reliability of the power system. However, the retrofiting of remaining circuits breakers would not be effective.

CONCLUDING REMARKS

On-going researches on our seismic risk assessment of power systems are described in this paper; A 3-D analysis method for wave propagation and a benefit-cost analysis method for seismic retrofit are developed. Retrofit policies which are economically rational would be adopted based on the benefit-cost analysis under more realistic seismic input condition. The methods described here would be helpful for this purpose. GIS technology would be a powerful tool for combining input data and results of these methods.

REFERENCES

- S. Higashi and K. Satoh, "Development of an analysis method for seismic wave propagation in 3-D underground structure including faults", Central Research Institute of Electric Power Industry, Research Report U96043, March 1997 (in Japanese).
- Y. Shumuta and J. Tohma, "A seismic retrofit method for substation components on the basis of the cost-benefit analysis", Central Research Institute of Electric Power Industry, Research Report U97015, July 1997 (in Japanese).

PERSONAL CAREER

NAME:

Jun'ichi Tohma

POSITION :

Research Fellow
Geotechnical & Earthquake Engineering Department
Abiko Research Laboratory
Central Research Institute of Electric Power Industry

ADDRESS:

1646 Abiko, Abiko-shi, Chiba-ken 270-11 Japan
Tel. 0471-82-1181
Fax. 0471-84-2941



DATE OF BIRTH :

June 2, 1954

EDUCATION :

Bachelor(1977) and Master Degree(1979) of Engineering, Waseda University

MAJOR SUBJECT :

Dynamic Soil - Structure Interaction

MAJOR AREA OF EXPERIENCE :

1979 - 1985 Research Engineer, Geotechnical & Earthquake Engineering Department, CRIEPI
1985 - 1986 Reserach Collaborator, Structural Analysis Division, Brookhaven National Laboratory
1986 - 1990 Senior Research Engineer, Earthquake Engineering Department, CRIEPI
1990 - 1993 Principal Research Engineer, Earthquake Engineering Department, CRIEPI
1993 - 1995 Manager, Management Advisory Dept., Planning Div., CRIEPI
1994 Doctor of Engineering, Waseda University
1995 - 1996 Group Leader, Seismic Motion Group, Earthquake Engineering Department, CRIEPI
1997 - Research Fellow, Geotechnical & Earthquake Engineering Department, CRIEPI

TRAVEL ABROAD : USA, Australia, Taiwan, Thailand, Spain, Portugal

MAJOR PUBLICATIONS :

" Forced Vibration Tests and Earthquake Observation on the Dynamic Response of Rigid Embedded Foundations" Journal of Structural Mech./Earthquake Eng., JSCE, 1992.

" Model Shaking Test and Numerical Simulation on Nonlinear Response of Rigid Embedded Foundations" Journal of Structural Mech./Earthquake Eng., JSCE, 1992.

**CURRENT DEVELOPMENTS IN SEISMIC DESIGN CRITERIA
AND
MITIGATION EFFORTS FOR ELECTRIC POWER TRANSMISSION SYSTEMS**

Leon Kempner, Jr., Ph.D., P.E.

**Structural Engineer
Bonneville Power Administration
Portland, Oregon**

ABSTRACT

A brief summary of seismic design and mitigation documents being developed to provide criteria and guidance for electric power transmission line facilities is presented. The basic elements of a seismic mitigation program are discussed. It is recommended that an electric power utility's seismic mitigation program consider the advantages of investment protection and power system recovery. Investment protection is the seismic hardening of critical components such as power transformers that require extensive lead time for replacement. Power system recovery involves the seismic hardening of a critical electric power flow path through an electric power substation facility. Cost effective mitigation of critical components of an electric substation will provide for a timely recovery after a significant earthquake. The cost of replacing older electric power high voltage equipment can be prohibitive. A mitigation solution for a 500 kV live-tank power circuit breaker is presented.

INTRODUCTION

The level of seismic readiness of electric power utilities in the US varies significantly. California electric utilities experience major earthquakes on a frequent basis. Their facilities have been tested by actual earthquake events and weak components are replaced with more seismically hardened and less vulnerable equipment. Less seismically prepared electric power transmission line facilities are located in the Midwest and East Coast. The earthquake events in this part of the US have significantly longer return periods and therefore the electric power transmission line facilities typically have not considered seismic design criteria. The Pacific Northwest (PNW) seismic readiness falls somewhere between the prepared California utilities and the seismically vulnerable Midwest and East Coast electric utilities. The PNW has

experienced several significant earthquakes in the last 100 years. Recent research on the Cascadia subduction zone has determined that the seismic hazard in the PNW is greater than that indicated by the last 100 years. Information presented in this paper can help the seismically vulnerable electric power utilities initiate the seismic hardening of their facilities.

SEISMIC DESIGN AND MITIGATION REPORTS - WORK IN PROGRESS

Five new or revised seismic design and mitigation documents for electric power facilities are either in draft format or being balloted for publication, see Table 1. A brief discussion of the contents of these documents is presented in the following paragraphs.

The Institute of Electrical and Electronics Engineers' (IEEE) Standard 693, "Recommended Practices for Seismic Design of Substations," has been updated, 1997 revision. This document addresses the seismic qualification and installation of new electric power transmission substation equipment (power circuit breakers, transformers, switches, instrument transformers, air core reactors, suspended equipment, battery systems, arrestors, capacitors, control devices, metalclad switch gear, and cable terminators). The intent of the document is to provide standard methods of analysis and testing for seismic qualification of electrical substation high voltage equipment. Three levels of seismic qualification are presented: Low, Moderate, and High. Seismic qualification methods of substation equipment are based on either a static analysis, dynamic analysis, or shake table testing. The qualification method for a particular type of equipment is determined on its earthquake performance history and voltage level. High voltage (230 and 500 kV) substation equipment is typically more seismically vulnerable. Committee balloting of this IEEE standard is complete and the document is being forwarded for publication. (Mr. Rulon Fronk - Chair, Los Angeles Department of Water and Power, Los Angeles, California)

Another IEEE committee is writing a document titled "Recommended Design Practice for Flexible Buswork Located in a Seismically Active Area." This report addresses the seismic design of flexible conductors for substation bus and electrical power substation equipment connections. Guidance for designing flexible conductor equipment connections is provided that represents the current state of knowledge concerning the dynamic effects of conductors and flexible high current bus interconnections. Guidance for determining seismically induced equipment motion, conductor flexibility and sag/span limits are presented. The information discussed in this document can be applied to both new construction and the retrofit of existing electrical power substation equipment connections. This IEEE document is currently a committee draft. (Mr. Robert Stewart - Chair, BCHydro, Burnaby, B.C., Canada)

The American Society of Civil Engineers (ASCE) Technical Council on Lifeline Earthquake Engineering (TCLEE) is writing a document titled "Methods for Achieving Improved Seismic Performance of Electric Power Systems." The document provides earthquake performance based information and guidance for seismic mitigation options that can be applied to existing electrical power facilities. The seismic performance base data used in this document is primarily obtained from earthquakes in California and international (Japan 1978, 1996, and Chile 1985) earthquake experiences. The earthquake performance of electrical power generating plants, electrical substations, and transmission and distribution wire support structures are discussed. Mitigation options mainly focused on major electrical substation components that have demonstrated to be seismically vulnerable; power transformer, lightning arresters, instrumentation transformers, power circuit breakers, disconnect switches, circuit switches, wave traps, voltage support and power factor correction devices, station power, station control structures, communications and control equipment. The earthquake performance of transmission and distribution wire support structures has been good. Damage to these structures is typically caused by foundation failures due to soil liquefaction, lateral spreading, ground displacement, and ridge shatter. Most US electrical power generation plants have performed well during the earthquakes studied. (Dr. Anshel J. Schiff - Chair, Stanford University, Stanford, California)

The seismic design of structures used to support substation conductor and rigid bus is discussed in the American Society of Civil Engineers (ASCE) document titled "Guide for the Design of Substation Structures." An ASCE Substation Structures subcommittee of the Committee on Electrical Transmission Structures (CETS) is developing this substation structure design guide (draft, 1997). The primary purpose of this design guide is to document current electrical substation structural engineering practice and to give guidance and recommendations for the design of outdoor electrical substation structures. The design guide presents a review of structure types and typical electrical equipment. Guidelines for analysis methods, loading and deflection criteria, member and connection design, structure testing, quality control and quality assurance, and connections used in foundations, detailing and fabrication, construction and maintenance issues are discussed. (Dr. Leon Kempner Jr. - Chair, Bonneville Power Administration, Portland, Oregon).

The National Earthquake Hazards Reduction Program (NEHRP) "Recommended Provisions for Seismic Regulations for New Buildings" has been revised (1997) with the addition of a new chapter giving seismic design criteria for nonbuilding structures. Nonbuilding structures are categorized by structural systems that are building-like (storage racks, electrical power generating facilities, piers and wharves, structural towers for tanks and vessels) and non-building like (tanks and vessels, electrical transmission, substation, distribution, and earth retaining structures, telecommunication towers, stacks and chimneys, signs and billboards, amusement structures, conveyors, special hydraulic structures, inverted pendulums, and monuments).

Electrical transmission and distribution conductor support structures, and telecommunication towers are considered by the NEHRP document as nonbuilding structures with building-like structural systems. The seismic performance of the structural systems used in these towers have been good. Typical problems have been related to foundation issues caused by liquefaction, lateral spreading, ground displacement, and ridge shatter. One reason for the good performance is that these towers are designed for extreme wind and ice loading combinations that typically exceed potential seismic loads. The intent of the NEHRP seismic criteria are to provide a tower designed to resist a minimum seismic lateral load as a baseline for special cases when the selected design extreme wind and ice loads do not exceed the seismic loads. A simplified static analysis using Response Modification Factors (R) is specified to determine the seismic lateral load capacity for comparison with the design extreme wind and ice loads. The R values account for the inelastic reserve strength of the structural systems during an earthquake event. If it is determined that seismic loads are significant enough to control the design of main load carrying members then a more detailed lateral force distribution and/or a modal analysis is recommended. Guyed telecommunication towers are required to be evaluated with a more detailed computer analysis that takes into account nonlinear analysis and guy-tower interaction effects. The NEHRP document is maintained by the Building Seismic Safety Council (BSSC), National Institute of Building Sciences, and is published by the Federal Emergency Management Agency (FEMA). The revised 1997 NEHRP document is currently in the balloting process. (Mr. Harold O. Sprague, Chair - Nonbuilding Structures Committee TS-13, Black & Veatch Consultants, Overland Park, Kansas)

SEISMIC RISK REDUCTION PROGRAM

A seismic risk reduction program has five basic elements. The first element in a seismic risk reduction program is to identify **earthquake hazards** within the electric power transmission system's service area. Typically as a minimum the Uniform Building Code (UBC) seismic zone map is used. In very special cases, a site specific study may be performed to determine the earthquake risk.

The **seismic design criteria** for new facilities should result in facilities that have structural capacity to provide for life safety and to remain functional after an earthquake event. This level of design should be based on a benefit-cost analysis that will provide the accepted level of risk within reasonable costs.

An assessment of the **seismic vulnerability** of the electric power transmission system's existing facilities should be performed. This assessment should include identification of critical facilities for operation of the power system. Also included in this assessment should be identification of facilities that provide electrical power to lifeline systems. The electric utility should conduct seismic walkdown training for identifying

seismic vulnerability of electrical substation components. This training should include engineering, maintenance, and operation personnel.

The following information is an overview of the seismic vulnerability based on the performance experiences of US electrical utility facilities (transmission, substation, distribution, and microwave communications) to major earthquake events. In general, the following performance experiences are for facilities designed to some level of earthquake resistance. **Generation Plants:** Overall performance has been good. **Buildings (Control Houses, Maintenance Buildings and Offices):** Earthquake response of these facilities is similar to that of the "engineered" building population. **Microwave Communication:** Generally, there has been good performance of these systems with only bent structural members of ground mounted towers. **Transmission and Substation Structures:** Worldwide performance of these structures has been very good. Damage has been limited to bent structural members, broken porcelain wire supports, and foundation failures caused by landslides, ground fracture, and liquefaction. **Substation Electrical Equipment:** The damage of electrical equipment is directly related to Voltage levels. This is typically represented by slight damage at 115 kV and below; moderate damage at 230 kV; and significant damage at 500 kV and above. Porcelain components (brittle material) of electrical equipment are very susceptible to earthquake damage. Failures have also resulted from rigid bus and tight (inadequate slack) flexible aluminum conductor connections between substation equipment. Experience has shown that the following equipment are vulnerable to seismic events: disconnect switches (broken porcelain), transformers (broken porcelain, bushing seal failure, radiator leaks, and triggering of protective relays), live-tank power circuit breakers (broken porcelain and seal leakage), instrument transformers (broken porcelain), and unrestrained batteries (spilled acid and cracked cell cases). Dead-tank and bulk oil power circuit breakers have performed well during earthquakes. A dead-tank circuit breaker is a circuit breaker with a "tank" (the chamber that houses the interrupter mechanism) at electrical ground potential that is supported by a structural frame. The more seismically vulnerable Live-tank circuit breaker (Figure 1) is a circuit breaker with a "tank" at electrical line potential that is supported on a tall porcelain insulating column. **Distribution Systems:** Typical damage has been associated with unanchored pole top and platform mounted transformers. Earthquake induced distribution line motions have caused contact between lines that resulted in burn-down (wire failure), blown fuses, and triggering of line reclosers.

Seismic mitigation of existing facilities should be prioritized and when possible schedule during routine maintenance. Experience has shown that electrical power equipment should be anchored. Connection between equipment should be flexible and have sufficient slack to accommodate movement of the equipment. Equipment should be adequately braced to prevent damage during an earthquake event.

The electric power utility should have a current **emergency response plan**. The plan should be reviewed and exercised on an annual basis.

SEISMIC MITIGATION PROGRAM - THE BONNEVILLE POWER ADMINISTRATION

On January 13, 1994, (the Friday before the Northridge earthquake) the Bonneville Power Administration (BPA) Assistant Administrator for Engineering charged a task force with the review of BPA's then-current seismic policy and the development of recommendations for prudent actions that BPA should be taking to address changing seismic requirements and risks to BPA's electric power transmission system.

The Seismic Task Force developed a mitigation plan, comprised of a set of recommendations for seismically hardening the BPA system (reinforcing it against damage) through a series of cost-effective, short- and long-term actions. The plan had three goals: to inform, to identify problems, and to propose mitigation options. The seismic mitigation plan provides steps recommended by the Seismic Task Force for protecting the BPA electric power grid facilities from unacceptable earthquake damage.

The Task Force evaluated what level of mitigation would be required for different components of the electric power system. Of particular concern was support of lifeline services, since the electric power system lifeline provides the critical element for operation of other local and regional lifeline systems or components following an earthquake. The purpose and results of a seismic mitigation program are well stated in the following paragraphs that were modified from a paper titled "Policy on Acceptable Levels of Earthquake Risk for California Gas and Electric Utilities."

An electrical transmission system shall withstand earthquakes in order to protect lives, to limit damage to property, and to provide for resumption of utility system functions in a reasonable and timely manner. An acceptable level of earthquake risk is the residual risk that remains after a seismic policy has been implemented and seismic mitigation tasks completed.

The goal of a seismic policy and mitigation program is to protect the public and to provide reliable customer service in the face of possible earthquake effects. Although compliance with a seismic policy and mitigation program will provide reasonable public safety and customer service, it will not prevent all loss of life, property damage, or loss of utility function.

An electric power transmission utility should consider seismic design issues for new construction and develop and implement a

long-term seismic mitigation program for existing facilities. A mitigation program should be based on the current understanding of earthquake hazards and risk, the current technical capabilities and practices of the industry, and the need to optimize results obtained from resources expended.

The contents of these paragraphs are very important in that there is no absolute guarantee that damage will not occur to the electric power system after a significant earthquake. This is particularly true for older electric power systems where seismic mitigation options are directed to limit damage levels and not to eliminate them completely.

BPA's Seismic Design Criteria History

Up until 1971, BPA's electrical substation seismic design criterion was a static analysis with 0.2g horizontal ground acceleration. BPA buildings were designed to meet the seismic loads specified in the Uniform Building Code (UBC), which at that time characterized much of the Pacific Northwest as Zones 1 and 2 (except for the Puget Sound region and the western region of BPA's service area that were designated UBC Zone 3) . The 0.2g requirement was determined from experience gained during the 1933 Long Beach, California earthquake, and was a common seismic design criterion for US electric power utilities.

In 1971, after the San Fernando, California earthquake (magnitude 6.6), BPA undertook a major review of the earthquake potential and electric power system vulnerability in its service area. BPA contracted with Agabian Associates and Shannon & Wilson Inc. to develop a regional seismic intensity map and performed a seismic risk assessment of its service area--Washington, Oregon, Idaho, and western Montana. Earthquake hazard data collected indicated a minimum Modified Mercalli Intensity (MMI) level of IV, and a recurrence interval of 130 years, with an approximate 2 percent probability of being exceeded. This study recommended a horizontal ground motion of 0.36g for facilities in the Puget Sound region. A BPA seismic review committee, upon reviewing the report, felt that the recommended horizontal ground acceleration levels were too conservative in estimates of ground motion, in part because relatively little data existed for the Pacific Northwest and much had to be extrapolated from a California data base where geology differed significantly. Consequently, BPA developed its seismic policy by modifying the Agabian average peak ground motion accelerations. The ground motion acceleration values were reduced to 67 percent of the recommended values. Therefore a 0.24g horizontal ground acceleration was recommended for the Puget Sound area. Even with this new information transferable equipment such as transformers and power circuit breakers

were still designed for 0.2g horizontal ground acceleration regardless of their location within BPA's service area.

In 1990 the Structural Engineering Section began to review the existing policy for its application to a new Static Var Compensator (SVC's) facilities to be installed both in Portland, Oregon, and Puget Sound, Washington. It was decided at that time that BPA's seismic policy needed updating to reflect current seismic risk information for the Pacific Northwest. Since the 1970's, the UBC map had significantly changed in BPA's service area. All of Oregon and most of Washington were upgraded to UBC Zone 2; the UBC Zone 3 area in Puget Sound was enlarged; the Yellowstone area was changed to a UBC Zone 4; and UBC Zone 3 was redrawn to include larger portions of Montana.

In 1991 a new policy was developed. Transferable equipment such as transformers and power circuit breakers were to be seismically qualified using a standard 0.4g minimum horizontal ground motion acceleration, regardless of the seismic zone. A simultaneous vertical ground motion acceleration equal to 67 percent of the design horizontal ground motion acceleration was to be used. These ground motion accelerations were to be applied in the direction that produced the most severe equipment stresses.

This policy was to be applied to new installations only (not retroactively to existing facilities). However, when a modification was applied to an existing installation, it was desirable to carry out the modification in conformity with the 1991 policy.

Buildings would be designed in accordance with the latest UBC, as adopted and/or modified by the State where the building would be located. Buildings essential for the operation and maintenance of the electrical transmission system were to be designed for UBC occupancy category "Essential Facilities." All other buildings were to use the appropriate category and importance factors as specified in the UBC.

The 1994 UBC was been revised to reflect the (higher) UBC Seismic Zone 3 west of the Cascade Mountains for both the States of Oregon and Washington. BPA's new criteria are based on the 1997 UBC seismic hazard map with substation electrical equipment seismic qualification to a minimum of 0.4g for Zone 3 and 0.3g for Zone 2B.

The method for seismic qualification (static or dynamic analysis, dynamic testing - sine beat or time history) of substation structures, electrical equipment supports, and electrical equipment will be determined by the seismic qualification requirements of the 1997 revised IEEE 693 Standard "Recommended Practices for Seismic Design of Substations."

BPA's Seismic Experience

BPA's electric power facilities have had limited experience with significant earthquakes. The following is a summary of earthquake effects on BPA substations. The 1949 Olympia, Washington, magnitude 7.1 earthquake shifted (maximum of 1.5 feet, 0.46 meters) transformers on their foundations, damaged transformer bushings, and failed the porcelain supports of instrument transformers. The Seattle, Washington, 1965 magnitude 6.5 earthquake caused misalignment of several disconnect switches, damaged two power circuit breakers, and failed post insulator supports mounted on a substation deadend tower. These two events represent damage to electric power substations with a voltage of 230 kV and below. The 1993 Scotts Mills, Oregon, magnitude 5.6 earthquake caused no damage to substation equipment but did trip transformer relay protection systems. A BPA maintenance building was also reported to have minor cracking in a reinforced concrete structural support system. The 1996 Duvall, Washington, magnitude 5.3 earthquake caused the failure of a 500 kV disconnect switch and numerous porcelain resistors mounted on the disconnect switches, damaged two 500 kV live-tank power circuit breakers, failed 500 kV rigid bus line raisers, a 230 kV rigid bus connection, and an instrument transformer. The substation control building also experienced minor structural damage. The Duvall earthquake caused problems with the "weakest of the weak" substation equipment components. BPA's 500 kV electric power system still has not been tested by a significant earthquake.

Seismic Mitigation Of BPA Facilities

The following discussion will address BPA's seismically vulnerable facilities: substations and telecommunication facilities. BPA has approximately 360 high voltage electrical substations and 120 telecommunication sites. These facilities were design to the 0.2g static analysis level. The substation and telecommunication facilities were evaluated, weighted, and priority ranked to help identify a cost effective mitigation strategy.

The ranking of BPA's substations was based on nine categories. The categories in order of ranking (high to low) are customer lifeline service, major generation (megawatt, MW, greater than or equal to 200), major transmission hub, large step-down transformers, major intertie connections, regional source lines (i.e., cross-mountain generation line), other generation (MW less than 200), lost energy transactions, and intermediate load service. The sum of weighting factors is multiplied by one of five bus voltage weighting factors (500 kV = 1.0, 345 - 230 kV = 0.5, 161- 115 kV = 0.25, 69 - 46 kV = 0.13, less than 46 kV = 0.08) ; these in turn are multiplied by the bus fault mega-volt-amperes, MVA, at that voltage. For each voltage level at the substation, these

individual factors are summed to a total and then normalized with respect to the highest value.

Communication sites include radio stations, substations, maintenance facilities, and customer service points. Eleven key communication parameters were used to prioritize these facilities: microwave hub main grid, microwave repeater main grid, microwave repeater, microwave spur terminal, Ultra High Frequency (UHF) data and control, Very High Frequency (VHF) repeater, VHF voice base station, power-line carrier (data and control), fiber optic, and telephone communication.

Seismic hardening of BPA facilities start by conducting walkthroughs of the facilities beginning with the highest ranking score and continuing until all facilities have been evaluated. The walkthrough is used to identify unanchored equipment, inadequate bracing of equipment, structural load path and integrity, and equipment interaction problems that require seismic mitigation. The information collected during the walkthroughs is used to develop an action plan for mitigation activities to be accomplished at each facility. Mitigation items include anchorage of power transformers, reactors, and station service transformers beginning with high-risk 230-kV and 500-kV facilities and continuing until all facilities have been completed. Also, substation and communication battery banks and emergency engine generator systems, are hardened by providing adequate anchorage, bracing, and flexible connections to electrical, oil, and fuel supply lines.

Additional short-term seismic mitigation efforts include the evaluation of spare equipment storage facilities for seismic resistant methods. Long-term seismic mitigation will include the evaluation of building facilities and critical transmission line components. Transmission line river crossing towers will be evaluated for soil liquefaction effects and key segments of cross-mountain transmission lines for earthquake generated landslide potential.

Substation Investment Protect / Critical Path Power System Recovery Approaches

Seismic mitigation of existing power system facilities is very expensive, particularly in a deregulated competitive environment. Therefore cost effective methods with high benefit-to-cost ratios that satisfy the seismic policy and mitigation goal objectives previously discussed need to be implemented. Two approaches to accomplish this are the investment protection and critical path power system recovery approaches.

The investment protection approach is the seismic mitigation of only equipment and components that are very expensive and/or have very long replacement times, and have a high benefit-to-cost ratio. An electric power substation component that satisfies

all three criteria is high voltage power transformers. The mitigation issues for this equipment type are anchorage, and bracing of the cooling radiators and oil conservator. Power transformers are necessary and critical to provide lower voltage electric power to the distribution system if the electric power system remains functional. The investment protection approach does not consider the capability to maintain electric power system function during and after an earthquake or a timely recovery from potential earthquake damage.

The critical path power system recovery approach focuses on the ability of the electric utility to either maintain the electric power system function during an earthquake or to provide for a timely electric power system recovery. In this approach only the key electric power transformers and electrical transmission systems would be hardened. A cost effective approach is the hardening of components with high benefit-to-cost ratios and not hardening components that can be bypassed during emergency operations, such as disconnect switches and in special cases live-tank power circuit breakers. Highest ranking priority substations are being seismically hardened using a critical path approach. The critical path approach is based on hardening only selected critical substation components through a facility so that a minimal effort would be required to restore damage to the electric power system grid. The critical path may evolve the hardening of only one bay of a multi-bay substation.

The best solution with the most benefit to an electric utility and the lifelines served is a seismic mitigation program that combines the two approaches, investment protection and critical path power system recovery. The very large benefit-to-cost ratio for anchoring power transformers justifies this mitigation task. The additional cost of hardening electric power system components that are low cost items can allow continued operation or a timely power system recovery. The combination of the two approaches will allow the electric utility to continue its lifeline function at a critical time.

500 kV Live-Tank Power Circuit Breaker Seismic Upgrade

Earthquake performance of power circuit breakers has demonstrated that high voltage live-tank power circuit breakers are seismically vulnerable and dead-tank power circuit breakers are seismically rugged. Older electric power substations that have not been subjected to major seismic events may have a significant number of high voltage live-tank power circuit breakers. The cost to replace a live-tank power circuit breaker is too prohibitive. Therefore, cost effective seismic hardening retrofit solutions are required. The Bonneville Power Administration with assistance from Asea Brown Boveri (ABB), Greensburg, Pennsylvania, developed a retrofit solution for an ABB 500 kV live-tank power circuit breaker. The goal of the seismic hardening retrofit project was to increase the power circuit breaker seismic capacity from 0.2g to 0.4g.

A spring friction-damper system is installed at the base of the power circuit breaker. The spring friction-damper is made of concentric rings that are stacked and overlaid so that movement of the rings causes friction damping at their interface. The rings are installed in a weather-tight steel tube that is installed between the power circuit breaker foundation and the legs of the support structure. The power circuit breaker and the damping system were shake-table tested. Shake-table testing was conducted to determine the seismic capability of the installed live-tank power circuit breakers and the increase in seismic capacity of the power circuit breaker spring friction-damper system.

The power circuit breaker was tested with and without closing resistors. The closing resistors added an additional 1000 pounds (4450 N) to the top of the porcelain support column. The results of measured strains at the base of the porcelain support column are summarized in Figure 2. The strains are plotted with respect to the percent of required input response level, 0.4g. The tests on the undamped power circuit breaker were limited to 50 percent (480 microstrain) of the recommended maximum porcelain strain that was calculated to be 960 microstrain. The 70 percent strain level (672 microstrain) is the maximum allowable porcelain strain for any test and the maximum accepted level for qualification of this retrofit option. The plot nomenclature for the individual tests are "SS" - Side-to-Side, no dampers, no closing resistors, "45" - 45 degree orientation, no dampers, no closing resistors, "RSS" - Side-to-Side, no dampers, with closing resistors, "FBWD" - Front-to-Back, with dampers, no closing resistors, "SSWD" - Side-to-Side, with dampers, no closing resistors, "45WD" - 45 degree orientation, with dampers, no closing resistors, and "RSSWD" - Side-to-Side, with dampers, with closing resistors.

The test data for the power circuit breaker without the dampers were curve fit with a linear function. There are only 2 to 3 data points for these tests. It is expected that as the input response level is increased the porcelain strains will deviate from a linear curve and provide lower strain levels with increase of the input response level. This would be the case if the power circuit breaker responded with higher damping as the input level increases. Therefore using a linear function to predict the maximum accepted qualification level (g's) could be conservative.

The power circuit breaker with dampers installed was tested to higher input levels and therefore more data points were obtained. The data was curve fit with a polynomial function. These curves show that the porcelain strain levels appear to be nonlinear with the input level, as expected with increase in effects of damping. The test results show an approximate 3 to 1 seismic capacity increase with the power circuit breaker/damper system compared to without the dampers. Ten live-tank power circuit breakers have been retrofitted with this damper design. The benefit-to-cost ratio based on equipment replacement cost for this mitigation option is approximately 6. Additional power circuit breakers are being evaluated for the spring friction-damper system.

CONCLUSIONS

Current works in progress reports were presented for the seismic design and mitigation of electric power facilities. The reports discussed are not published at this time. They are either working drafts or balloted documents. The chairpersons can be contacted to obtain the status of these documents and their availability. The seismic design, analysis, qualification, and mitigation criteria and guidance provided by these documents will improve the earthquake performance of electric power systems. An electric utility's seismic policy should require new facilities and components to be designed to current seismic hazard levels. An active seismic mitigation program based on the combination of investment protection and critical path power system recovery hardening will increase the ability of an electric power system to either remain function during an earthquake or assist in a timely recovery. Proven cost effective and high benefit-to-cost ratio seismic mitigation options are available to the electric power industry.

REFERENCES

- Kempner , L., Jr., "BPA's Seismic Risk Mitigation Plan", CREW - 2nd. Annual Conference, Mitigation: The Bottom Line, Portland, Oregon, 1997
- Kempner, L., Jr., Jordan, P., ABB 500 kV Type ELF Breaker Seismic Test, Bonneville Power Administration Report, 1995.
- Kempner, L., Jr., "BPA's Seismic design Criteria - PAST, PRESENT, and FUTURE," BPA Engineering Symposium, Portland, Oregon, 1992.
- Lyver T., Mueller, W. H., Kempner, L., Jr., "Seismic Response Modification Factor for Lattice Steel Electrical Transmission Tower," ASCE Structures Congress Preprint, Portland, Oregon, 1997.
- Miller, M., Kempner, L., Burley, T., Hill, J.R., and Sommer, S.C., "Seismic Mitigation Within The Power Marketing Administrations," Fifth DOE Natural Phenomena Hazards Mitigation Symposium, Denver, Colorado, 1995.
- Ostrom, D.K., Crouse, C.B., Seismic Walk-Through Training: Observations and Comments of Several BPA Substations in Puget Sound, Washington, Bonneville Power Administration Report, 1994.

Savage, W., Cluff, L., Gailing, R., et al., "Policy on Acceptable Levels of Earthquake Risk for California Gas and Electric Utilities," Forth US Conference on Lifeline Earthquake Engineering, San Francisco, California, August, 1995.

Schiff, A.J., Seismic Vulnerability of Bonneville Power Administration Communication and Power Facilities - Observations from Walkdown of Facilities in the Portland Area, Bonneville Power Administration Report, 1995.

Seismic Task Force, Seismic Risk Mitigation Plan, Bonneville Power Administration, Draft, 1994.

TABLES

Table 1 - Seismic Design and Mitigation Reports - Work in Progress

Document Title	Purpose	Organization
Recommended Practices for Seismic Design of Substations	Seismic Qualification of Electrical Substation Equipment	IEEE
Recommended Design Practice for Flexible Buswork Located in a Seismically Active Area	Seismic design criteria for flexible conductor electrical equipment connections and bus	IEEE
Methods for Achieving Improved Seismic Performance of Electric Power Systems	Seismic performance and mitigation options for new and existing electrical power facilities	ASCE
Guide for the Design of Substation Structures	Seismic design criteria for substation wire support and rigid bus structures	ASCE
The National Earthquake Hazards Reduction Program (NEHRP), Chapter 13, NonBuilding Structures	Baseline evaluation of the seismic lateral load capacity of transmission and distribution wire support structures and telecommunication towers	BSCC/FEMA

FIGURES

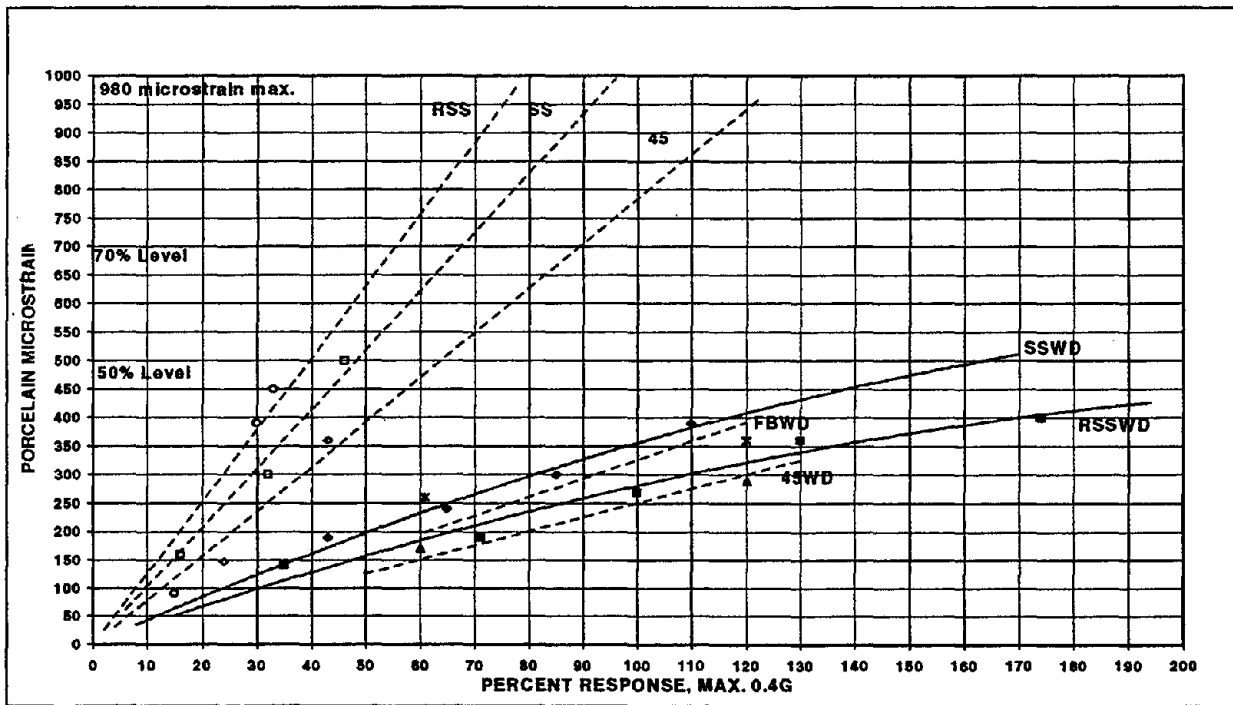
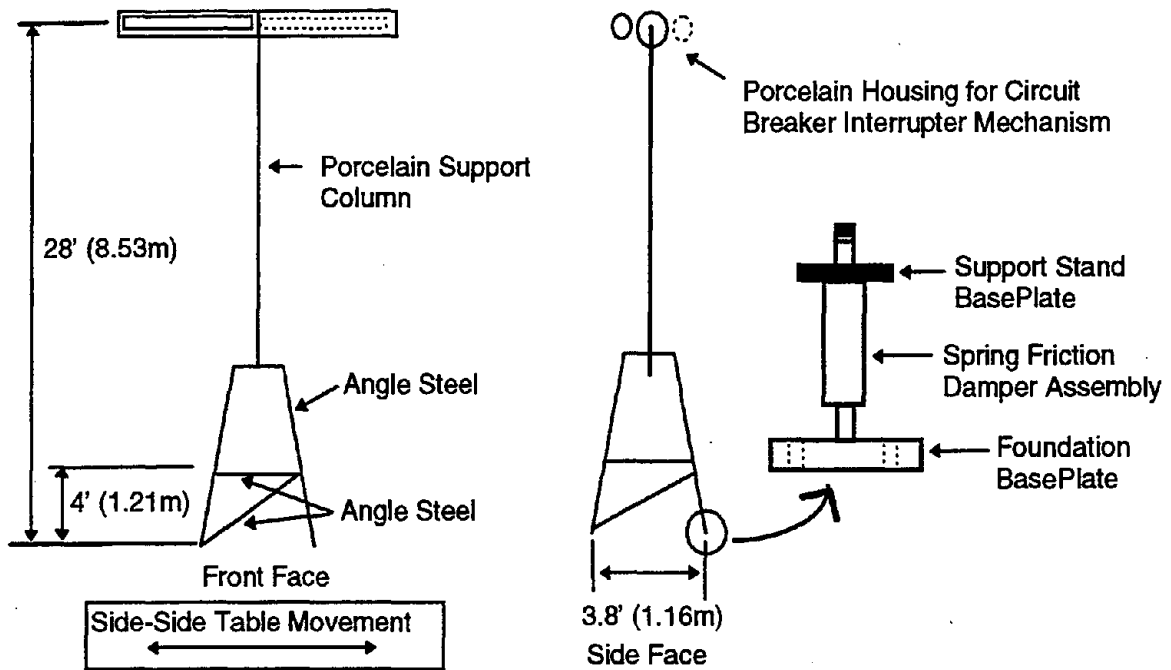


Figure 2 - 500 kV Live-Tank Power Circuit Breaker Shake-Table Test Results

LEON KEMPNER, JR.

Date of Birth: September 30, 1946

Birthplace: Jamaica, New York

Education: Degrees

University of Nebraska, Omaha, B.S.C.E.,
Civil (Structural) Engineering, 1972,
Oregon State University, M.S.,
Civil (Structural) Engineering, 1974
Portland State University, Ph.D.,
System Science: Civil (Structural) Engineering, 1997



Position:

Structural Engineer
Lines and Facilities (TNF-3)
Bonneville Power Administration
Portland, Oregon, 97208
Phone: 503-230-5563
Fax: 503-230-3984
E-mail: lkempnerjr@bpa.gov

Dr. Kempner has over 23 years experience as a structural engineer for the Bonneville Power Administration. His assignments have included structural engineering analysis, design, and research of transmission line facilities (transmission line towers, substations, and microwave structures). The last five years Dr. Kempner has been performing seismic evaluation, qualification, shake-table testing, standards development, and mitigation design of the Bonneville Power Administration transmission line facilities.

Dr. Kempner is a member of the following professional societies; American Society of Civil Engineers (ASCE), Structural Engineers of Oregon (SEAO), American Association of Wind Engineering (AAWE), International Conference on Large High Voltage Electric Systems (CIGRE), American Concrete Institute (ACI), International Conference of Building Officials (ICBO), and the Earthquake Engineering Research Institute (EERI). He is an active member of the following technical committees; American National Standards Institute (ANSI)/ASCE Standard - Design of Transmission Pole Structures, Institute of Electrical and Electronic Engineers Standard 693 - Seismic Design of Substation Structures, National Electrical Safety Code Subcommittee 5 - Overhead Lines (Strength and Loadings), US Representative to CIGRE Study Committee 22 (Overhead Line) Working Group 08 (Towers), and National Earthquake Hazards Reduction Program, TS-13 Non-building Structures committee. Dr. Kempner also serves as the Secretary of ANSI/ASCE 10 Standard - Design of Latticed Steel Transmission Structures, and Chairperson of ASCE's Technical Committee for Electrical Transmission Structures and Subcommittee for Design of Electrical Substation Structures.

Dr. Kempner has over forty technical papers discussing structural engineering (analysis, design, and research) of transmission line facilities. He is a registered Professional Civil Engineer (P.E.) in the State of Washington.

THE 1996 SEISMIC DESIGN SPECIFICATIONS OF HIGHWAY BRIDGES

Koichi YOKOYAMA, Director of Earthquake Disaster Prevention Research Center,
Public Works Research Institute, Ministry of Construction
Keiichi TAMURA, Head of Ground Vibration Division, ditto
Shigeki UNJOH, Head of Earthquake Engineering Division, ditto
Toru TERAYAMA, Senior Research Engineer, Earthquake Engineering Division, ditto
Jun-ichi HOSHIKUMA, Research Engineer, Earthquake Engineering Division, ditto

ABSTRACT

This paper presents the revised Seismic Design Specifications of Highway Bridges in 1996^{1), 2)} as well as the background of the revision. Damage features of bridges in the 1995 Hyogo-ken Nanbu Earthquake is firstly described with emphasis on the lessons learned from the earthquake. Seismic performance levels and design methods as well as the seismic design force introduced in the 1996 Design Specifications are then described. The ductility design methods for reinforced concrete piers, steel piers, foundations, and bearings are also briefly described.

INTRODUCTION

Highway bridges in Japan had been considered safe even against extreme earthquake such as the Great Kanto Earthquake (M7.9) in 1923, because various past bitter experiences have been accumulated to formulate the seismic design method (Kawashima³⁾). Large seismic lateral force ranging from 0.2g to 0.3g has been adopted in the allowable stress design approach. Various provisions for preventing damage due to instability of soils such as soil liquefaction have been adopted. Furthermore, design details including the unseating prevention devices have been implemented.

In fact, reflecting those provisions, number of highway bridges which suffered complete collapse of superstructures was only 15 since 1923 Great Kanto Earthquake. Based on such evidence, it had been regarded that the seismic damage of highway bridges had been decreasing in recent years.

However, the Hyogo-ken Nanbu Earthquake of January 17, 1995, exactly one year after the Northridge earthquake in California, USA, caused destructive damage to highway bridges. Collapse and nearly collapse of superstructures occurred at 9 sites, and other destructive damage occurred at 16 sites (Ministry of Construction,⁴⁾). The earthquake revealed that there are a number of critical issues to be revised in the seismic design and seismic strengthening of bridges in urban areas.

After the earthquake the "Committee for Investigation on the Damage of Highway Bridges Caused by the Hyogo-ken Nanbu Earthquake" (chairman : Toshio IWASAKI, Executive Director, Civil Engineering Research Laboratory) was formulated in the Ministry of Construction to survey the damage and clarify the factors which contributed to the damage.

On February 27, 1995, the Committee approved the "Guide Specifications for Reconstruction and Repair of Highway Bridges which suffered Damage due to the Hyogo-ken Nanbu Earthquake,"⁵⁾ and the Ministry of Construction noticed on the same day that the reconstruction and repair of the highway bridges which suffered damage in the Hyogo-ken Nanbu earthquake should be made by the Guide Specifications. It was decided by the Ministry of Construction on May 25, 1995 that the Guide Specifications should be tentatively used in all sections of Japan as emergency measures for seismic design of new highway bridges and seismic strengthening of existing highway bridges until the Design Specifications of Highway Bridges was revised.

In May, 1995, the "Special Sub-Committee for Seismic Countermeasures for Highway Bridges" (chairman : Kazuhiko KAWASHIMA, Professor of the Tokyo Institute of Technology) was formulated in the "Bridge Committee" (chairman : Nobuyuki NARITA, Professor of the Tokyo Metropolitan University), Japan Road Association, to draft the revision of the Design Specifications of Highway Bridges. The Special Sub-Committee drafted the new Design Specifications of Highway Bridges, and after the approval of the Bridges Committee, the Ministry of Construction released it November 1, 1996.

This paper summarizes the damage feature of highway bridges by the Hyogo-ken Nanbu earthquake and the new Design Specifications of Highway Bridges issued in November 1996.

DAMAGE FEATURES OF BRIDGES IN THE HYOGO-KEN NANBU EARTHQUAKE

Hyogo-ken Nanbu earthquake was the first earthquake which hit an urban area in Japan since the 1948 Fukui Earthquake. Although the magnitude of the earthquake was moderate (M7.2), the ground motion was much larger than anticipated in the codes. It occurred very close to the Kobe City with shallow focal depth.

Damage was developed at highway bridges on Routes 2, 43, 171 and 176 of the National Highway, Route 3 (Kobe Line) and Route 5 (Bay Shore Line) of the Hanshin Expressway, the Meishin and Chugoku Expressway. Damage was surveyed for all bridges on National Highways, Hanshin Expressways and Expressways in the area where destructive damage occurred. Total number of piers surveyed reached 3,396 (Ministry of Construction, ⁴⁾). Fig.1 shows Design Specifications referred to in design of the 3,396 piers. Most of piers (bridges) which suffered damage were designed according to the 1964 Design Specifications or older Design Specifications. Although the seismic design methods have been improved and amended several times since 1926 based on damage experience and progress of bridge earthquake engineering, only a requirement for lateral force coefficient was provided in the 1964 Design Specifications or older Specifications.

Fig.2 compares damage of piers on the Route 3 (Kobe Line) and Route 5 (Bay Shore Line) of the Hanshin Expressway. Damage degree was classified as AS (collapse), A (nearly collapse), B (moderate damage), C (damage of secondary members) and D (minor or no damage). Substructures of the Route 3 and Route 5 were designed with the 1964 Design Specifications and 1980 Design Specifications, respectively. It

should be noted in this comparison that the intensity of ground motion in terms of response spectra was smaller at the Bay Area than the narrow rectangular area where JMA Seismic Intensity was VII (equivalent to Modified Mercalli Intensity of X-XI). The Route 3 was located in the narrow rectangular area while the Route 5 was located in the Bay Area. Keeping in mind such difference of ground motion, it is apparent in Fig.2 that about 14% of the piers on Route 3 suffered As or A damage while no such damage was developed in the piers on the Route 5.

Although damage concentrated on the bridges designed with the older Design Specifications, it was thought that essential revision was required even in the recent Design Specifications to prevent damage against destructive earthquakes such as the Hyogo-ken Nanbu earthquake. The main points requiring modifications were;

- 1) it was required to increase lateral capacity and ductility of all structural components in which seismic force is predominant so that ductility of a total bridge system be enhanced. For such purpose, it was required to upgrade the "Check of Ductility of Reinforced Concrete Piers," which has been used since 1990, to a "Ductility Design Method," and to apply the Ductility Design Method to all structural components. It should be noted here that "check" and "design" is different; the check is only to verify the safety of a structural member designed by other design method, and is effective only to increase the size or reinforcements if required, while the design is an essential procedure to determine the size and reinforcements,
- 2) it was required to include the ground motion developed at Kobe in the earthquake as a design force in the Ductility Design Method,
- 3) it was required to specify input ground motions in terms of acceleration response spectra for dynamic response analysis more actively,

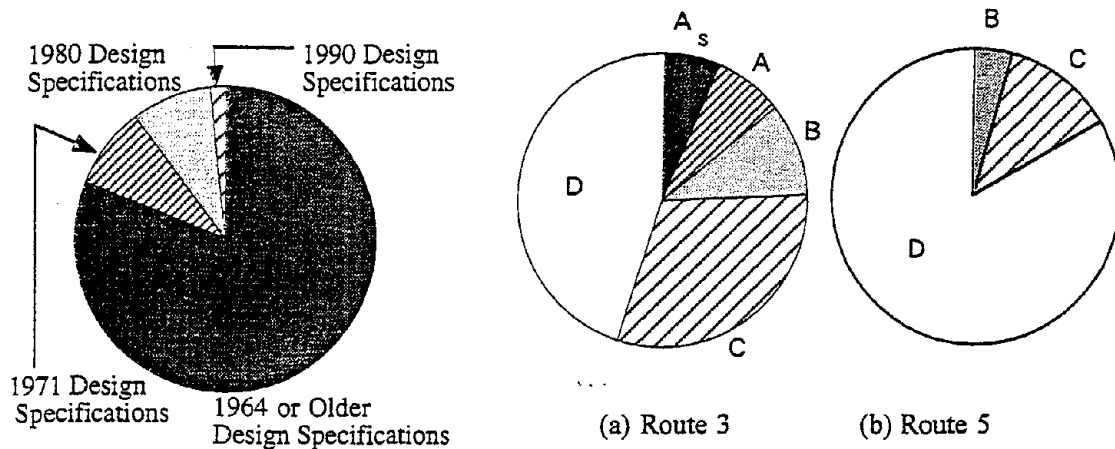


Fig.1 Design Specifications Referred to in Design of Hanshin Expressway

Fig.2 Comparison of Damage Degree between Route 3 and Route 5 (As : Collapse, A : Nearly Collapse, B : Moderate Damage, C : Damage of Secondary Members, D : Minor or No Damage)

- 4) it was required to increase tie reinforcements and to introduce intermediate ties for increasing ductility of piers. It was decided not to terminate main reinforcements at mid-height for preventing premature shear failure, in principle,
- 5) it was suggested to adopt multi-span continuous bridge for increasing number of indeterminate of a total bridge system,
- 6) it was suggested to adopt rubber bearings for absorbing lateral displacement between a superstructure and substructures. It was important to consider correct mechanism of force transfer from a superstructure to substructures,
- 7) it was suggested to include the Menshin design (seismic isolation),
- 8) it was required to increase strength, ductility and energy dissipation capacity of unseating prevention devices, and
- 9) it was required to consider the effect of lateral spreading associated with soil liquefaction in design of foundations at the site vulnerable to lateral spreading.

BASIC PRINCIPLE OF SEISMIC DESIGN

Table 1 shows the seismic performance level provided in the revised Design Specifications in 1996. The bridges are categorized into two groups depending on their importance; standard bridges (Type-A bridges) and important bridges (Type-B bridges). Seismic performance level depends on the importance of bridges. For moderate ground motions induced in the earthquakes with high probability to occur, both A and B bridges should behave in an elastic manner without essential structural damage. For extreme ground motions induced in the earthquakes with low probability to occur, the Type-A bridges should prevent critical failure, while the Type-B bridges should perform with limited damage .

Table 1 Seismic Performance Levels

Type of Design Ground Motion		Importance of Bridges		Design Methods	
		Type-A (Standard Bridges)	Type-B (Important Bridges)	Equivalent Static Lateral Force Method	Dynamic Analysis
Ground Motions with High Probability to Occur		Prevent Damages		Seismic Coefficient Method	Step by Step Analysis
Ground Motions with Low Probability to Occur	Type-I (Plate Boundary Earthquake)	Prevent Critical Damages	Limited Damages	Ductility Design Method	Or Response Spectrum Analysis
	Type-II (Inland Earthquake)				

In the Ductility Design Method, two types of ground motions must be considered. The first is the ground motion which could be induced in the plate boundary-type earthquakes with magnitude of about 8. The ground motion at Tokyo in the 1923 Kanto Earthquake is a typical target of this type of ground motion. The second is the ground motion developed in earthquakes with magnitude of about 7-7.2 at very close distance. Obviously the ground motions at Kobe in the Hyogo-ken Nambu earthquake is a typical target of this type of ground motion. The first and the second ground motions are called as Type-I and Type-II ground motions, respectively. The recurrence time of the Type-II ground motion may be longer than that of the Type-I ground motion, although the estimation is very difficult.

DESIGN METHODS

Bridges are designed by both the Seismic Coefficient Method and the Ductility Design Method as shown in Fig.3. In the Seismic Coefficient Method, a lateral force coefficient ranging from 0.2 to 0.3 has been used based on the allowable stress design approach. No change was introduced since the 1990 Specifications in the Seismic Coefficient Method.

In the Ductility Design Method, assuming a principle plastic hinge formed at the bottom of pier as shown in Fig.4(a) and the equal energy assumption, a bridge is designed so that the following requirement is satisfied.

$$Pa > khe \cdot W \quad (1)$$

where

$$khe = \frac{khc}{\sqrt{2\mu a - 1}} \quad (2)$$

$$W = Wu + cpWp \quad (3)$$

in which, Pa = lateral capacity of a pier, khe = equivalent lateral force coefficient, W = equivalent weight, khc = lateral force coefficient, μa = allowable displacement ductility factor of a pier, Wu = weight of a part of superstructure supported by the pier, Wp = weight of a pier, and cp = coefficient depending on the type of failure mode. cp is 0.5 for a pier in which either flexural failure or shear failure after flexural cracks are developed, and 1.0 for a pier in which shear failure is developed. The lateral capacity of a pier Pa is defined as a lateral force at the gravity center of a superstructure.

In the Type-B bridges, residual displacement developed at a pier after an earthquake must be checked as

$$\delta R < \delta Ra \quad (4)$$

where

$$\delta R = cR(\mu R - 1)(1 - r)\delta y \quad (5)$$

$$\mu R = \frac{1}{2} \left\{ (khcW / Pa)^2 + 1 \right\} \quad (6)$$

in which δR = residual displacement of a pier after an earthquake, δRa = allowable residual displacement of a pier, r = bilinear factor defined as a ratio between the first stiffness (yield stiffness) and the second stiffness (post-yield stiffness) of a pier, cR = factor depending on the bilinear factor r , μR =

response ductility factor of a pier, and δ_y = yield displacement of a pier. The δRa should be 1/100 of a distance between the bottom of a pier and a gravity center of a superstructure.

In a bridge with complex dynamic response, the dynamic response analysis is required to check the safety of a bridge after it is designed by the Seismic Coefficient Method and the Ductility Design Method. Because this is only for a check of the design, the size and reinforcements of structural members once determined by the Seismic Coefficient Method and the Ductility Design Methods can only be increased if necessary. It should be noted however that under the following conditions in which the Ductility Design Method is not directly applied, the size and reinforcements can be determined based on the results of a dynamic response analysis as shown in Fig.3. The conditions when the Ductility Design Method should not be directly used include:

- 1) principle mode shapes which contribute to bridge response are different from the ones assumed in the Ductility Design Methods,
- 2) more than two modes significantly contribute to bridge response,
- 3) principle plastic hinges form at more than two locations, or principle plastic hinges are not known where to be formed, and
- 4) response modes for which the equal energy assumption are not applied.

In the seismic design of a foundation, a lateral force equivalent to the ultimate lateral capacity of a pier P_u is assumed to be a design force as

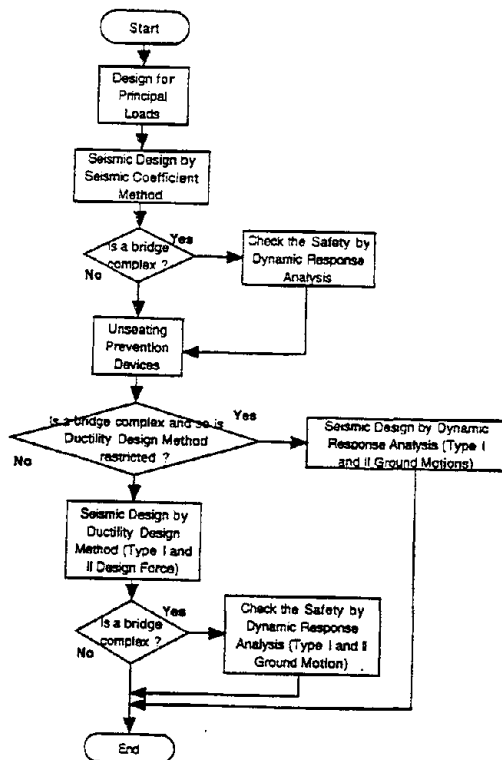


Fig.3 Flowchart of Seismic Design

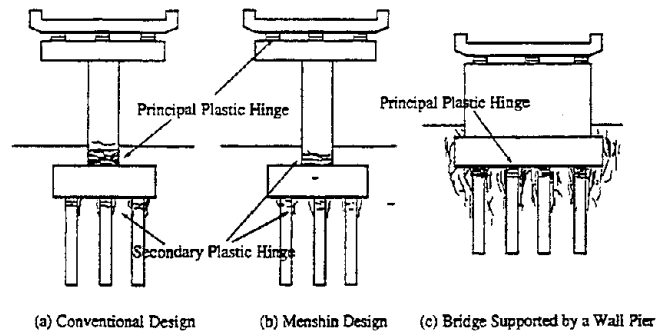


Fig.4 Location of Primary Plastic Hinge

$$khp = cdf Pu / W \quad (7)$$

in which khp = lateral force coefficient for a foundation, cdf = modification coefficient (=1.1), and W = equivalent weight by Eq.(3). Because the lateral capacity of a wall-type pier is very large in transverse direction, the lateral seismic force evaluated by Eq.(7) becomes in most cases excessive. Therefore if a foundation has sufficiently large lateral capacity compared with the lateral seismic force, the foundation is designed assuming a plastic hinge at the foundation and surrounding soils as shown in Fig.4(c).

DESIGN SEISMIC FORCE

Lateral force coefficient khc in Eq.(2) is given as

$$khc = c_z \cdot khco \quad (8)$$

in which c_z = modification coefficient for zone, and is 0.7, 0.85 and 1.0 depending on zone, and $khco$ = standard modification coefficient. Fig.5 shows the standard lateral force coefficients $khco$ for the Type-I and the Type-II ground motions. The Type-I ground motions have been used since 1990 (1990 Specifications), while the Type-II ground motions were newly introduced in the 1996 Specifications. It should be noted here that the $khco$ at stiff site (Group I) has been assumed smaller than the $khco$ at moderate (Group II) and soft soil (Group III) sites in the Type-I ground motions as well as the seismic coefficients used for the Seismic Coefficient Method. The Type-I ground motions were essentially estimated from an attenuation equation for response spectra that was derived from a statistical analysis of 394 components of strong motion records. Although the response spectral accelerations at short natural period are larger at stiff sites than at soft soil sites, the tendency has not been explicitly included in the past. This was because damage has been more developed at soft sites than at stiff sites. To consider such fact, the design force at stiff sites has been assumed smaller than that at soft sites even at short natural period. However being different from such a traditional consideration, the Type-II ground motions were determined by simply taking envelopes of response accelerations of major strong motions recorded at Kobe in the Hyogo-ken nanbu Earthquake. It was considered appropriate to set realistic ground motions.

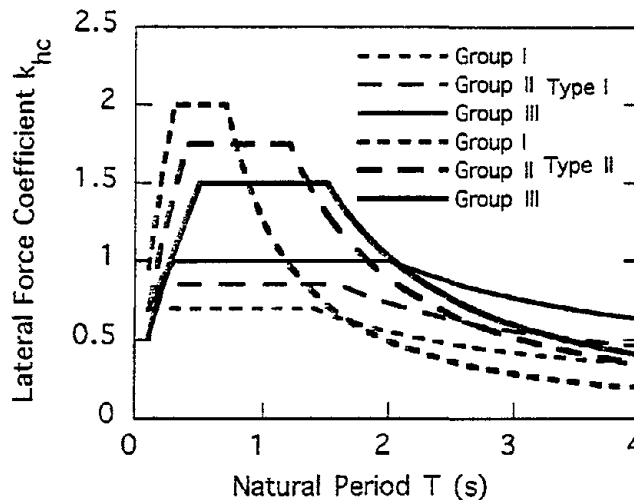


Fig.5 Type I and Type II Ground Motions in the Ductility Design Method

Although the acceleration response spectral intensity at short natural period is higher in the Type-II ground motions than in the Type-I ground motions, the duration of extreme accelerations excursion is longer in the Type-I ground motions than the Type-II ground motions. As will be described later, such a difference of the duration has been taken into account to evaluate the allowable displacement ductility factor of a pier. Details were discussed by Tamura et. al.⁶⁾

EVALUATION OF DISPLACEMENT DUCTILITY FACTOR OF A REINFORCED CONCRETE PIER

Evaluation of Failure Mode

In the ductility design of reinforced concrete piers, the failure mode of the pier is evaluated as the first step. Failure modes is categorized to 3 types based on the flexural capacity and shear capacity of the pier as

- 1) $P_u \leq P_s$: flexural failure
- 2) $P_s < P_u \leq P_{s0}$: flexural to shear failure
- 3) $P_{s0} < P_u$: shear failure

in which P_u = flexural capacity, P_s = shear capacity in consideration of the effect of cyclic loading, and P_{s0} = shear capacity without consideration of the effect of cyclic loading.

The ductility factor and capacity of the reinforced concrete piers are determined according to the failure mode as described later.

Displacement Ductility Factor

The allowable displacement ductility factor of a pier μ_a in Eq.(2) is evaluated as

$$\mu_a = 1 + \frac{\delta_u - \delta_y}{\alpha \delta_y} \quad (9)$$

in which α = safety factor, see Table 3, δ_y = yield displacement of a pier, and δ_u = ultimate displacement of a pier. As well as the lateral capacity of a pier P_a in Eq.(1), the δ_y and δ_u are defined at the gravity center of a superstructure. In a reinforced concrete single pier as shown in Fig.4(a), the ultimate displacement δ_u is evaluated as

$$\delta_u = \delta_y + (\phi_u - \phi_y)L_p(h - L_p/2) \quad (10)$$

in which ϕ_y = yield curvature of a pier at the bottom, ϕ_u = ultimate curvature of a pier at the bottom, h = height of a pier, and L_p = plastic hinge length of a pier. The plastic hinge length is given as

$$L_p = 0.2h - 0.1D \cdots (0.1D \leq L_p \leq 0.5D) \quad (11)$$

in which D is a width or a diameter of a pier.

Table 3 Safety Factor α in Eq.(9)

Type of Bridges	Type-I Ground Motion	Type-II Ground Motion
Type-A	3.0	1.5
Type-B	2.4	1.2

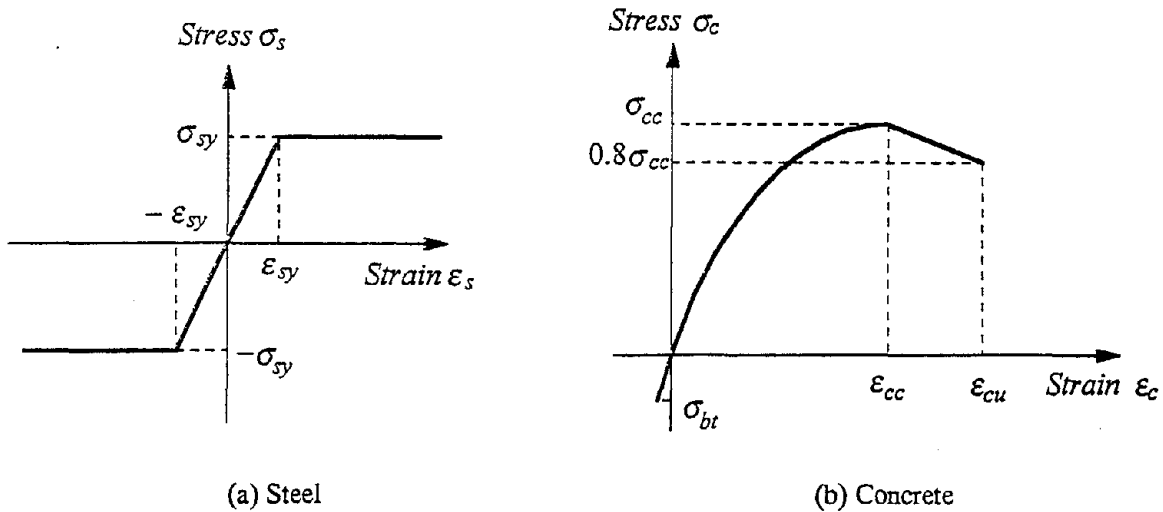


Fig.6 Stress and Strain Relation of Confined Concrete and Reinforcement

The yield curvature ϕ_y and ultimate curvature ϕ_u in Eq.(10) are evaluated assuming a stress-strain relation of reinforcements and concrete as shown in Fig.6. The stress σ_c - strain ϵ_c relation of concrete were developed by Hoshikuma et. al.⁷⁾

The ultimate curvature ϕ_u is defined as a curvature when concrete strain at the longitudinal reinforcement in compression reaches an ultimate strain ϵ_{cu} , which is defined as

$$\epsilon_{cu} = \begin{cases} \epsilon_{cc} & \text{For Type I ground motion} \\ \epsilon_{cc} + \frac{0.2\sigma_{cc}}{E_{des}} & \text{For Type II ground motion} \end{cases} \quad (12)$$

It is important to note here that the ultimate strain ϵ_{cu} depends on the types of ground motions; the ϵ_{cu} for the Type-II ground motions is larger than that for the Type-I ground motions. Based on a loading test, it is known that a certain level of failure in a pier such as a sudden decrease of lateral capacity occurs at smaller lateral displacement in a pier subjected to a loading hysteresis with more number of load reversals. To reflect such a fact, it was decided that the ultimate strain ϵ_{cu} should be evaluated by Eq.(12), depending on the type of ground motions. Therefore, the allowable ductility factor μ_a depends on the type of ground motions; the μ_a is larger in a pier subjected to the Type-II ground motions than a pier subjected to the Type-I ground motions.

It should be noted that the safety factor α in Eq.(9) depends on the type of bridges as well as the type of ground motions as shown in Table 3. This is to preserve higher seismic safety in the important bridges, and to take account of the difference of recurrent time between the Type-I and the Type-II ground motions.

Shear Capacity

Shear capacity of reinforced concrete piers is evaluated by a conventional method as

$$P_s = S_c + S_s \quad (13)$$

$$S_c = 10 \cdot cc \cdot ce \cdot cpt \cdot \tau_c \cdot b \cdot d \quad (14)$$

$$S_s = \frac{A_w \cdot \sigma_{sy} \cdot d (\sin \theta + \cos \theta)}{10 \cdot 1.15a} \quad (15)$$

in which P_s = shear capacity, S_c = shear capacity shared by concrete, S_s = shear capacity shared by tie reinforcements, τ_c = shear stress capacity shared by concrete, cc = modification factor for cyclic loading (0.6 for Type-I ground motions, 0.8 for Type-II ground motions), ce = modification factor for scale effect of effective width, cpt = modification factor for longitudinal reinforcement ratio, b, d = width and height of section, A_w = sectional area of tie reinforcement, σ_{sy} = yield strength of tie reinforcement, θ = angle between vertical axis and tie reinforcement, and a = spacing of tie reinforcement. Details were described by Kawano et. al.⁸⁾

Arrangement of Reinforcement

Fig.7 shows suggested arrangement of tie reinforcement. Tie reinforcement should be deformed bars with a diameter equal or larger than 13 mm, and it should be placed in most bridges at a distance of no longer than 150mm. In special cases such as the bridges with pier height taller than 30m, the distance of tie reinforcement may be increased at height so that pier strength should not be sharply decreased at the section. Intermediate ties should be also provided with the same distance with the ties to confine the concrete. Horizontal spacing of the intermediate ties should be less than 1m.

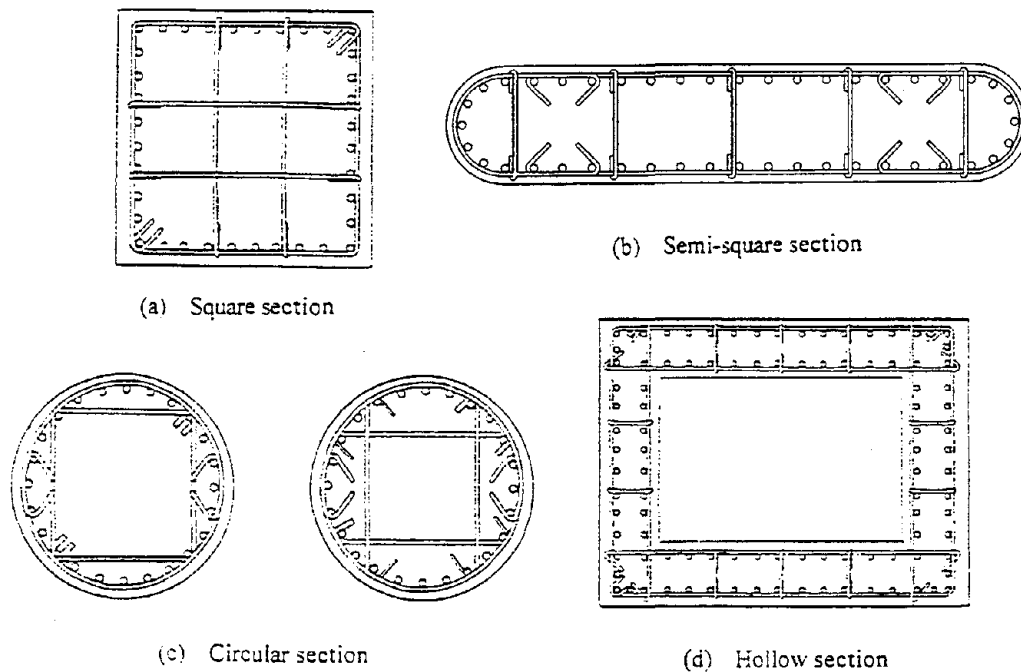


Fig.7 Confinement of Core-concrete by Tie Reinforcement

Two-Column Bent

To determine the ultimate strength and ductility factor for two-column bents, it is modeled as the frame model with plastic hinges at the both end of lateral cap beam and columns as shown in Fig.8. Each elastic frame member has the yield stiffness which is obtained based on the axial load by the dead load of the superstructure and the column. The plastic hinge is assumed to be placed at the end part of a cap beam and the top and bottom part of each column. The plastic hinges are modeled as spring elements with bilinear moment-curvature relation. The locations of plastic hinges are half distance of the plastic hinge length off from the end edge of each member, where plastic hinge length L_p is given by Eq.(11).

When the two-column bent is subjected to the lateral force in the transverse direction, axial force developed in the beam and columns is affected by the applied lateral force. Therefore, the horizontal force-displacement relation is obtained through the static push-over analysis considering axial force N - moment M interaction relation. The ultimate state of each plastic hinges is obtained by the ultimate plastic angle θ_{pu} as

$$\theta_{pu} = (\phi_u / \phi_y - 1)L_p \cdot \phi_y \quad (16)$$

in which ϕ_u = ultimate curvature and ϕ_y = yield curvature. The ultimate state of the whole two-bent column is determined so that all 4 plastic hinges developed reach the ultimate plastic angle. Details were described by Terayama et. al.⁹⁾

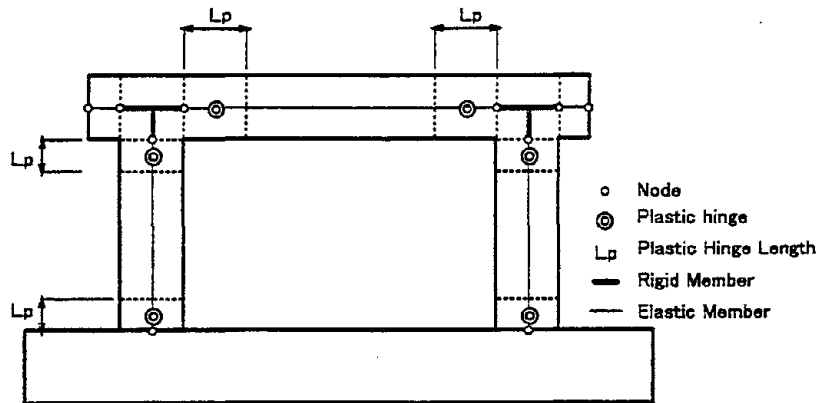


Fig.8 Analytical Idealization of A Two-Column Bent

EVALUATION OF DISPLACEMENT DUCTILITY OF A STEEL PIER

Basic Concept

To improve seismic performance of a steel piers, it is important to avoid specific brittle failure modes. Fig.9 shows the typical brittle failure mode for rectangular and circular steel piers. The followings are the

countermeasures to avoid such brittle failure modes and to improve seismic performance of steel piers:

- 1) fill the steel column with concrete
- 2) improve structural parameters related to buckling strength
 - decrease the width/thickness ratio of stiffened palates of rectangular piers or the diameter/thickness ratio of steel pipes
 - increase the stiffness of stiffeners
 - reduce the diaphragm spacing
 - strengthen corners using the corner plates
- 3) improve welding section at the corners of rectangular section
- 4) eliminate welding section at the corners by using round corners

Concrete In-filled Steel Pier

In a concrete in-filled steel pier, the lateral capacity P_a and the allowable displacement ductility factor μ_a in Eqs.(1) and (2) are evaluated as

$$P_a = P_y + \frac{P_u - P_y}{\alpha} \quad (17)$$

$$\mu_a = \left(1 + \frac{\delta_u - \delta_y}{\alpha \delta_y} \right) \frac{P_u}{P_a} \quad (18)$$

which P_y and P_u = yield and ultimate lateral capacity of a pier, δ_y and δ_u = yield and ultimate displacement of a pier, and α = safety factor, see Table 3. The P_a and the μ_a are evaluated idealizing that a concrete in-filled steel pier resists flexural moment and shear force as a reinforced concrete pier. It is assumed in this evaluation that the steel section be idealized as reinforcing bars and that only steel section resists axial force. The height of in-filled concrete has to be decided so that buckling is not developed above the in-filled concrete.

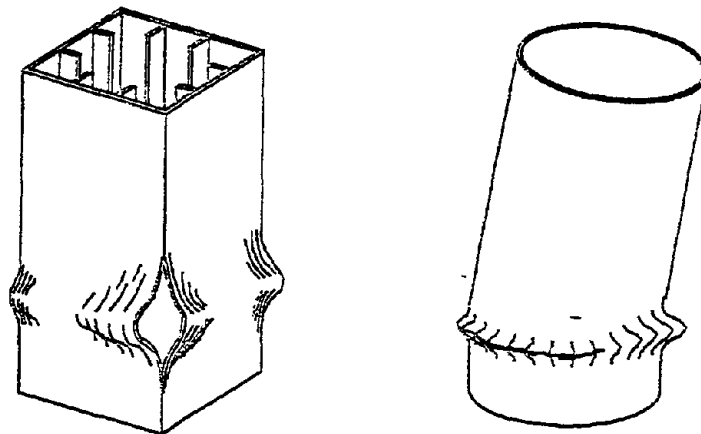


Fig.9 Typical Brittle Failure Modes of Steel Piers

Steel Pier without In-filled Concrete

A steel pier without in-filled concrete must be designed with the dynamic response analysis. Properties of the pier need to be decided based on a cyclic loading test. Arrangement of stiffness and welding at corner must be precisely evaluated so that brittle failure should be avoided.

DYNAMIC RESPONSE ANALYSIS

Dynamic response analysis is required in the bridges with complex dynamic response to check the safety factor of the static design. Dynamic response analysis is also required as a "design" tool in the bridges for which the Ductility Design Method is not directly applied. In dynamic response analysis, ground motions which are spectral fitted to the following response spectra are used;

$$SI = c_z \cdot c_D \cdot SI_0 \quad (19)$$

$$SII = c_z \cdot c_D \cdot SII_0 \quad (20)$$

in which SI and SII = acceleration response spectrum for Type-I and Type-II ground motions, SI_0 and SII_0 = standard acceleration response spectrum for Type-I and Type-II ground motions, respectively, c_z = modification coefficient for zone, see Eq.(8), and c_D = modification coefficient for damping ratio given as

$$c_D = \frac{1.5}{40h + 1} + 0.5 \quad (21)$$

Fig.10 shows the standard acceleration response spectra (damping ratio $h=0.05$) for the Type-I and Type-II ground motions. It is recommended to use at least three ground motions per analysis, and take an average to evaluate the response. Details were discussed by Tamura, et. al ⁶⁾.

In the dynamic analysis, modal damping ratios have to be carefully evaluated. To determine the modal damping ratios, a bridge may be divided into several sub-structures in which energy dissipating

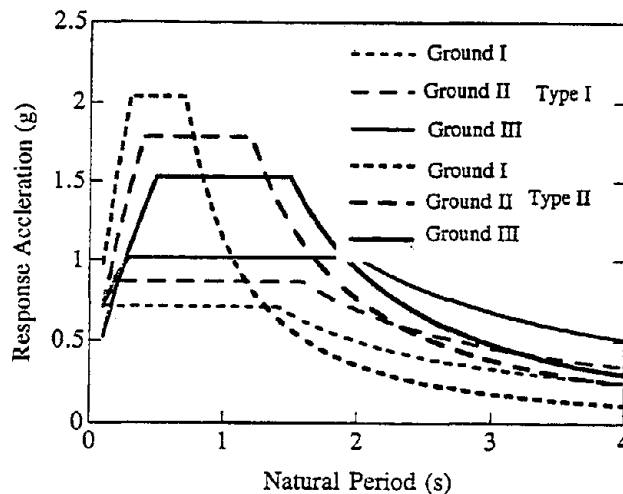


Fig.10 Type I and Type II Standard Acceleration Response Spectra

mechanism is essentially the same. If one can specify a damping ratio of each sub-structure for a given mode shape, the modal damping ratio for i-th mode, h_i , may be evaluated as

$$h_i = \frac{\sum_{j=1}^n \phi_{ij}^T \cdot h_{ij} \cdot K_j \cdot \phi_{ij}}{\phi_i^T \cdot K \cdot \phi_i} \quad (22)$$

in which h_{ij} = damping ratio of j-th substructure in i-th mode, ϕ_{ij} = mode vector of j-th substructure in i-th mode, K_j = stiffness matrix of j-th substructure, K = stiffness matrix of a bridge, and ϕ_i = mode vector of a bridge in i-th mode, and is given as

$$\phi_i^T = \{ \phi_{i1}^T, \phi_{i2}^T, \dots, \phi_{in}^T \} \quad (23)$$

Table 4 shows recommended damping ratios for major structural components.

Table 4 Recommended Damping Ratios for Major Structural Components

Structural Components	Elastic Response		Nonlinear Response	
	Steel	Concrete	Steel	Concrete
Superstructure	0.02 – 0.03	0.03 – 0.05	0.02 – 0.03	0.03 – 0.05
Rubber Bearing	0.02		0.02	
Menshin Bearing	Equivalent Damping		Equivalent Damping	
Substructure	0.03 – 0.05	0.05 – 0.1	0.1 – 0.2	0.12 – 0.2
Foundation	0.1 – 0.3		0.2 – 0.4	

MENSHIN DESIGN

Implementation of the Menshin bridges should be carefully decided from not only seismic performance but function for traffic and maintenance point of view, based on the advantage and disadvantage of increasing natural period. The Menshin design should not be adopted at the following conditions;

- 1) sites vulnerable to lose bearing capacity due to the soil liquefaction and the lateral spreading,
- 2) bridges supported by flexible columns,
- 3) soft soil sites where potential resonance with surrounding soils could be developed by increasing the fundamental natural period, and
- 4) bridges with uplift force at bearings.

It is suggested that the design should be made with an emphasis on an increase of energy dissipating capability and a distribution of lateral force to as many substructures as possible. To concentrate the hysteretic deformation at not piers but bearings, the fundamental natural period of a Menshin bridge should be about 2 times or longer than the fundamental natural period of the same bridge supported by the conventional bearings. It should be noted that an elongation of natural period aiming to decrease the lateral force should not be attempted. Details were described by Kawashima et. al. ¹⁰⁾

DESIGN OF FOUNDATION

The evaluation methods of ductility and strength of foundations such as pile foundations and caisson foundations was newly introduced in the 1996 Specifications.

In a pile foundation, a foundation is so idealized that a rigid footing is supported by piles which are supported by soils. The flexural strength of a pier defined by Eq.(7) shall be applied as a seismic force to foundations at the bottom of the footing together with the dead weight superstructure, pier and soils on the footing. Fig.11 shows the idealized nonlinear model of a pile foundation. The non-linearity of soils and piles is considered in the analysis.

The safety of the foundation shall be checked so that 1) the foundation shall not reach the yield point of a foundation, 2) if the primary non-linearity is developed in the foundations, the response displacement shall be less than displacement ductility limit, and 3) the displacement developed in the foundation shall

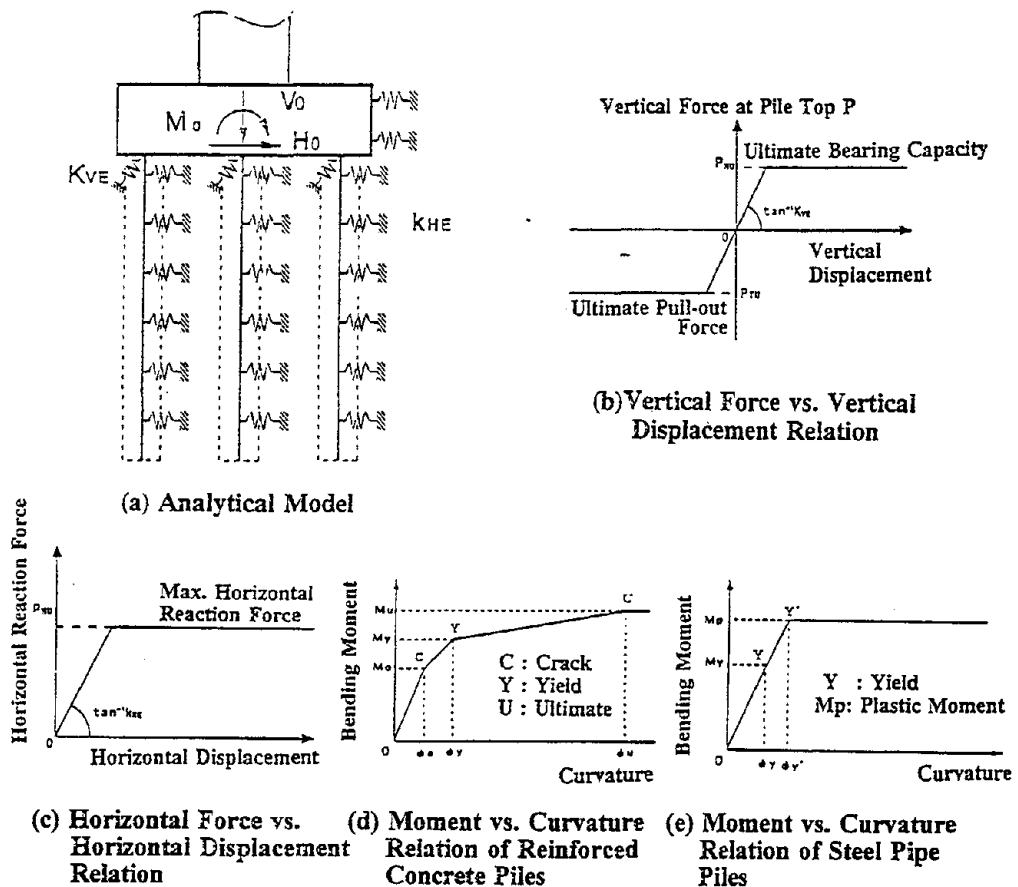


Fig.11 Idealized Nonlinear Model of A Pile Foundation

be less than allowable limit. The allowable ductility and allowable limit of displacement were commented as 4 in displacement ductility, 40cm in horizontal displacement and 0.025rad in rotation angle. More details were discussed by Fukui et. al.¹¹⁾

DESIGN AGAINST SOIL LIQUEFACTION AND LIQUEFACTION-INDUCED GROUND FLOW

Estimation of Liquefaction Potential

Since the Hyogo-ken Nanbu Earthquake of 1995 caused liquefaction even at coarse sand or gravel layers which had been regarded invulnerable to liquefy, a gravel layer was included in the soil layers that require liquefaction potential estimation. Soil layers that satisfies the following conditions is estimated to be potential liquefaction layers:

- 1) saturated soil layer which is located within 20m deep under the ground surface and in which ground water level is within 10m deep.
- 2) soil layer in which fine particle content ratio FC is equal or less than 35% or plasticity index IP is equal or less than 15.
- 3) soil layer in which mean grain size D50 is equal or less than 10mm and 10% grain size D10 is equal or less than 1mm.

The design procedure to evaluate the seismic safety of bridges against liquefaction is described by Yokoyama et. al.¹²⁾

Design Treatment of Liquefaction-Induced Ground Flow for Bridge Foundations

When the liquefaction-induced ground flow that may affect the seismic safety of bridges is likely to occur, this influence was included in the revised Design Specifications in 1996. The case in which the ground flow that may affect the seismic safety of bridges is likely to occur is generally that the ground is judged to be liquefiable and is exposed to biased earth pressure, for example, the ground behind a seaside protection wall. The effect of liquefaction-induced ground flow is considered as the static force acting on structure. This method premises that the surface soil is of the non-liquefiable and liquefiable layers, and the forces equivalent to the passive earth pressure and 30% of the overburden pressure are applied to the structure in the non-liquefiable layer and liquefiable layer, respectively.

The seismic safety of a foundation is checked by confirming the displacement at the top of foundation caused by ground flow does not exceed an allowable value, in which a foundation and the ground are idealized as shown in Fig.11. The allowable displacement of a foundation may be taken as two times the yield displacement of a foundation. In this process, the inertia force of structure is not necessary to be considered simultaneously, because the liquefaction-induced ground flow may take place after the principle ground motion.

BEARING SUPPORTS

The bearings are classified into two groups; the first is the bearings which resist the seismic force of

Eq.(2), and the second is the bearings which resist the seismic force considered in the Seismic Coefficient Method. The first and the second bearings are called as the Type-B bearings and the Type-A bearings, respectively. Seismic performance of the Type-B bearings is, of course, much higher than the Type-A bearings. In the Type-A bearings, a displacement limiting device, which will be described later, has to be co-installed in both longitudinal and transverse directions, while it is not required in the Type-B bearings. Because of the importance of bearings as one of the main structural components, the Type-B bearings should be used in the Menshin bridges.

UNSEATING PREVENTION SYSTEMS

Unseating prevention measures are required for the highway bridges. The measures required for the highway bridges are as:

- 1) the unseating prevention systems have to be so designed that unseating of a superstructure from their supports can be prevented even if unpredictable failures of the structural members occur,
- 2) the unseating prevention systems consist of providing enough seat length, a falling-down prevention device, a displacement limiting device, and a settlement prevention device,
- 3) enough seat length must be provided and a falling-down prevention device must be installed at the ends of a superstructures against longitudinal response. If the Type-A bearings are used, a displacement limiting device has to be further installed at not only the ends of a superstructure but each intermediate support in a continuous bridge, and
- 4) if the Type-A bearings are used, a displacement limiting device is requested at each support against transverse response. The displacement limiting device is not generally required if the Type-B bearings are used. But, even if the Type-B bearing is adopted, it is required in skewed bridges, curved bridges, bridges supported by columns with narrow crest, bridges supported by few bearings per piers, and bridges constructed at the sites vulnerable to lateral spreading associated with soil liquefaction.

The seat length S_E is evaluated as

$$S_E = u_R + u_G \geq S_{EM} \quad (24)$$

$$S_{EM} = 70 + 0.5l \quad (25)$$

$$u_G = 100 \cdot \varepsilon_G \cdot L \quad (26)$$

in which u_R = relative displacement (cm) developed between a superstructure and a substructure subjected to a seismic force equivalent to the equivalent lateral force coefficient khc by Eq.(2), u_G = relative displacement of ground along the bridge axis, S_{EM} = minimum seat length (cm), ε_G = ground strain induced during an earthquake along the bridge axis, and is 0.0025, 0.00375, and 0.005 for Group-I, II and III sites, respectively, L = distance which contributes to the relative displacement of ground (m), and l = span length (m). If two adjacent deck are supported by a pier, the larger span length should be l in evaluating the seat length.

CONCLUDING REMARKS

The preceding pages presented an outline of the new Seismic Design Specifications of Highway Bridges issued in 1996 as well as the damage features of highway bridges in the Hyogo-ken Nanbu earthquake. The Hyogo-ken Nanbu earthquake was the first earthquake which developed destructive damage in an urban area since the 1948 Fukui Earthquake. Because it had been considered that such destructive damage could be prevented due to the progress of construction technology in recent years, it provided a large impact on the earthquake disaster prevention measures in various fields. The "Part V Seismic Design" of the "Design Specifications of Highway Bridges" (Japan Road Association) was totally revised in 1996, and the design procedure moved from the traditional Seismic Coefficient Method to the Ductility Design Method.

Major point of the revision was the introduction of explicit two-level seismic design consisting of the Seismic Coefficient Method and the Ductility Design Method. Because the Type-I and the Type-II ground motions are considered in the Ductility Design Method, three design seismic forces are totally used in design. Seismic performance for each design force was clearly stated in the Specifications.

The fact that lack of near-field strong motion records prevented to seriously evaluate the validity of recent seismic design codes is important. The Hyogo-ken Nanbu earthquake revealed that history of strong motion recording is very short, and that no near-field records have yet been measured by an earthquake with magnitude on the order of 8. It is therefore essential to have enough redundancy and ductility in a total bridge system. It is hoped that the revised Seismic Design Specifications of Highway Bridges contributes to enhance seismic safety of highway bridges.

ACKNOWLEDGEMENTS

Drafting of the revised version of the "Part V Seismic Design" of the "Design Specifications of Highway Bridges" was conducted at the "Special Sub-committee for Seismic Countermeasures for Highway Bridges" (chairman : Prof. K. Kawashima of Tokyo Institute of Technology) and was approved by the Bridge Committee, Japan Road Association. The authors would like to express sincere gratitude to Prof. K. Kawashima for his continuous and intensive guidance through the beneficial discussion in the committee. The authors also thank all members of the Special Sub-Committee and the Bridge Committee.

REFERENCES

- 1) K. Kawashima, M. Nakano, K. Nishikawa, J. Fukui, K. Tamura, S. Unjoh : The 1996 Seismic Design Specifications of Highway Bridges, Proceedings of the 29th Joint Meeting of Unites States – Japan Panel on Wind and Science Effects, Japan, May, 1997
- 2) Japan Road Association : Design Specifications of Highway Bridges, Part I Common Part, Part II Steel Bridges, Part III Concrete Bridges, Part IV Foundations, and Part V Seismic Design, 1996
- 3) K. Kawashima : Impact of Hanshin/Awaji Earthquake on Seismic Design and Seismic Strengthening of Highway Bridges, Report No. TIT/EERG 95-2, Tokyo Institute of Technology., 1995

- 4) Ministry of Construction: Report on the Damage of Highway Bridges by the Hyogo-ken Nanbu Earthquake, Committee for Investigation on the Damage of Highway Bridges Caused by the Hyogo-ken Nanbu Earthquake, 1995
- 5) Ministry of Construction: Guide Specifications for Reconstruction and Repair of Highway Bridges Which Suffered Damage due to the Hyogo-ken Nanbu Earthquake, 1995
- 6) K. Tamura, R. Honda, A. Chiba, K. Yamamoto : Ground Motion Characteristics for Seismic Design of Highway Bridges, Proceedings of 2nd Italy-Japan Workshop on Seismic Design and Retrofit of Bridges, Italy, February, 1997
- 7) J. Hoshikuma, K. Kawashima, K. Nagaya, A. W. Taylor : Stress-Strain Model for Confined Reinforced Concrete in Bridge Piers, Journal of Struc. Engineering pp624-pp633, ASCE, May, 1997
- 8) H. Kawano, H. Watanabe : Shear Strength of Reinforced Concrete Columns –Effect of Specimen Size and Load Reversals, Proceedings of 2nd Italy-Japan Workshop on Seismic Design and Retrofit of Bridges, Italy, February, 1997
- 9) T. Terayama, H. Otsuka, K. Nagaya : Strength and Ductility Characteristics of Two-Column Bents, Proceedings of 2nd Italy-Japan Workshop on Seismic Design and Retrofit of Bridges, Italy, February, 1997
- 10) K. Kawashima, S. Unjoh : Menshin Design for Highway Bridges, Proceedings of 2nd Italy-Japan Workshop on Seismic Design and Retrofit of Bridges, Italy, February, 1997
- 11) J. Fukui, Y. Kimura, M. Okoshi : Strength and Ductility Characteristics of Pile Foundation, Proceedings of 2nd Italy-Japan Workshop on Seismic Design and Retrofit of Bridges, Italy, February, 1997
- 12) K. Yokoyama, K. Tamura, O. Matsuo : Design Methods of Bridge Foundation against Soil Liquefaction and Liquefaction-Induced Ground Flow, Proceedings of 2nd Italy-Japan Workshop on Seismic Design and Retrofit of Bridges, Italy, February

APPENDIX

TABLE OF CONTENTS OF "Part V : SEISMIC DESIGN" OF "DESIGN SPECIFICATIONS FOR HIGHWAY BRIDGES," JAPAN ROAD ASSOCIATION, 1996

<ol style="list-style-type: none"> 1 General <ol style="list-style-type: none"> 1.1 Scope 1.2 Definition of Terms 2 Basic Principle of Seismic Design 3 Loads and Design Conditions Considered in Seismic Design <ol style="list-style-type: none"> 3.1 Loads and Combinations 3.2 Effects of an Earthquake 3.3 Inertia Force 3.4 Importance 	<ol style="list-style-type: none"> 3.5 Modification Factor for Zone 3.6 Modification Factor for Ground Condition 3.7 Ground Surface Assumed in Seismic Design 4 Seismic Design by Seismic Coefficient Method <ol style="list-style-type: none"> 4.1 Lateral Force Coefficient 4.2 Dynamic Earth Pressure 4.3 Dynamic Hydraulic Pressure 5 Seismic Design by Ductility Design Method <ol style="list-style-type: none"> 5.1 General 5.2 Evaluation of Safety
---	---

	5.3	Lateral Force Coefficient		9.8	Lateral Capacity and Ductility of Frame Piers
6		Check of Safety by Dynamic Response Analysis		9.9	Effect of Eccentricity of Vertical Load in Inverted L-Shaped Piers
	6.1	General			
	6.2	Analytical Models and Analytical Procedures	10		Lateral Capacity and Ductility of Steel Piers
	6.3	Ground Motions		10.1	General
	6.4	Evaluation of Safety		10.2	Steel Piers with In-filled Concrete
7		7. Seismic Design of Foundations at the Soils Vulnerable to Instability		10.3	Steel Piers without In-filled Concrete
	7.1	General		10.4	Seismic Design of Anchor
	7.2	Seismic Design of Foundations at the Sites Vulnerable to Failure of Clayey Materials or Soil Liquefaction		10.5	Effect of Eccentricity of Vertical Load in Inverted L-Shaped Steel Piers with In-filled Concrete
	7.3	Seismic Design of Foundations at the Sites Vulnerable to Lateral Spreading	11		Lateral Capacity of Foundations
	7.4	Evaluation of Soft Clay or Silty Clay with Potential Failure		11.1	General
	7.5	Evaluation of Sandy Soils with Potential to Develop Soil Liquefaction		11.2	Evaluation of Seismic Force, Reaction Force and Displacement of Foundations
	7.6	Soil Layers whose Bearing Capacity Should be Decreased		11.3	Yield of Foundations
8		Menshin Design		11.4	Evaluation of Response of Foundations when Principle Plastic Hinge Occurs at Foundations, and Allowable Maximum Response Displacement
	8.1	General	12	11.5	Check of Safety
	8.2	Menshin Design			Bearings and Their Surrounding Structures
	8.3	Seismic Force in Menshin Design		12.1	General
	8.4	Design of Devices		12.2	Seismic Design Force for Bearings and Their Surroundings
	8.5	Evaluation of Natural Period of a Menshin Bridge		12.3	Evaluation of Safety
	8.6	Evaluation of Damping Ratio of a Menshin Bridge	13	12.4	Structures of Bearings and Their Surroundings
	8.7	Design Detailings in Menshin Design			Unseating Prevention Systems
9		Capacity and Ductility of Reinforced Concrete Piers		13.1	General
	9.1	General		13.2	Seat Length
	9.2	Lateral Capacity and Ductility		13.3	Unseating Prevention Devices
	9.3	Lateral Force and Lateral Displacement at Yield and Ultimate		13.4	Excessive Displacement Limiting Devices
	9.4	Stress-Strain Relation Assumed in Concrete		13.5	Devices for Preventing Settlement of a Superstructure
	9.5	Shear capacity		13.6	Joint Protector
	9.6	Design Detailings to Enhance Ductility		13.7	Strengthening of Portion of Superstructure where Unseating Prevention Devices is Connected
	9.7	Termination of Main Reinforcement at Mid-height	14	13.8	Unseating Prevention Systems in Transverse Direction
					Devices to Reduce Bridge Response

Personal Career

Name : Toru Terayama

Position : Senior Research Engineer
Earthquake Engineering Division
Earthquake Disaster Prevention
Research Center
Public Works Research Institute
Ministry of Construction



Address : 1, Asahi, Tsukuba-shi, Ibaraki-ken,
Japan 305
Tel. +81-298-64-4966
Fax. +81-298-64-4424
email terayama@pwri.go.jp

Date of Birth : November 27, 1959

Education: Bachelor of Engineering in Civil Engineering, Tokyo University
(1983)
M.S. in Structural Course in Applied Mechanics and Engineering
Sciences, University of California, San Diego (1993)

Major Area of Experience :

- 1983-1991 Practical Design Work at Metropolitan Expressway Public Corporation
- 1991-1993 Graduate Study at University of California, San Diego
- 1993-1995 Practical Design Work at Metropolitan Expressway Public Corporation
- 1995- Earthquake Engineering Division, Public Works Research Institute, Ministry of Construction

Major Subjects: Structural Engineering, Seismic Design of Bridges

Travel Abroad: U.S.A., Mexico, Canada, New Zealand, Australia, Thailand, France, Italy

Major Publications :

- 1) "Seismic Evaluation and Strengthening of Reinforced Concrete Bridge Piers of Metropolitan Expressway", Second International Workshop on Seismic Design and Retrofit of Reinforced Concrete Bridges, Queenstown, August 1994
- 2) "Shaking Table Tests of Bridge Columns, Designed by Japan and US Codes", 12th US-Japan Bridge Engineering Workshop, Buffalo, October, 1996
- 3) "Strength and Ductility Characteristics of Two-Column Bents", 2nd Italy-Japan Workshop on Seismic Design and Retrofit of Bridges, Rome, February 1997

Aseismic Countermeasure Technologies for Outdoor Telecommunication Facilities Implemented Following the 1995 Hyogo-ken Nanbu Earthquake

by Kenichi Honda, Yuzo Yamaguchi, Akira Sawaguchi, Kazuharu Ikeda and Masaru Okutsu
NTT Access Network System Laboratories

ABSTRACT

Civil facilities containing underground cables sustained damage from the Hyogo-ken Nanbu Earthquake, but the cables themselves were relatively undamaged, indicating that these facilities were for the most part effective at protecting cables. This is thought to be due to aseismic countermeasures implemented based on the experiences and lessons obtained from past earthquake disasters. On the other hand, aerial facilities were severely damaged due to the effects of fire and collapsed houses, etc. The damage to underground cables was approximately 1/9 that of aerial cables at the service level, and 1/30 at the facility level. This indicates that underground telecommunication facilities are highly reliable and confirmed once again that burying telecommunication cables is effective from the perspective of ensuring telecommunication reliability. Nevertheless, some weak spots such as connections between different structural systems were confirmed, and new aseismic countermeasure for the three locations of open-cut telephone tunnel joints, manhole ducts and building access facilities were developed quickly following the disaster. In addition, a cable damage estimation and understanding system capable of estimating macro damage conditions of access facilities in about half a day and understanding micro damage conditions in about four days after a disaster has occurred was developed based on the lessons of the need to understand damage conditions.

These aseismic countermeasure technologies have been introduced successively since July 1996.

COMPOSITION OF TELECOMMUNICATION FACILITIES

NTT provides telecommunication services by laying telecommunication cables from telecommunication center buildings containing switchboards to customer houses through outdoor facilities consisting of civil and line facilities. Civil telecommunication facilities are broadly classified into the two types of telephone tunnel and conduit facilities, and are used to house and protect underground telecommunication cables. In metropolitan areas, these cables are laid to customer buildings through underground distribution conduits, and in residential and other areas, cables are raised on telephone poles and led into customer houses using aerial distribution lines. An outline of NTT's outdoor telecommunication facilities is shown in Fig. 1.

Of these outdoor telecommunication facilities, telephone tunnel facilities are tunnels with a diameter of 3 to 5 m which are used exclusively for telecommunication cables. These facilities are constructed at relatively deep levels about 20 to 40 m below the ground surface, and house dozens of telecommunication cables.

Conduit facilities are divided by conduit diameter into the two types of free-space conduits and $\phi 75$ mm conduits (main line conduits). Free-space conduits are steel or cast iron pipes with a nominal

diameter of 300 to 600 mm which are buried using the microtunneling method, and contain from about 7 to 27 spacers for housing telecommunication cables. On the other hand, main line conduit facilities consist of multiple layers of multiple $\phi 75$ mm pipes that are buried at shallow depths of about 1 to 2 m below the ground surface, with each conduit housing a single telecommunication cable. $\phi 75$ mm conduits are generally polyvinyl pipes (hereafter "PV pipes") in consideration of cost efficiency, but metal pipes are used in sections where countermeasures against ground liquefaction and induction are necessary.

Underground distribution conduits are mainly pipes with a nominal diameter of 25 mm and 50 mm.

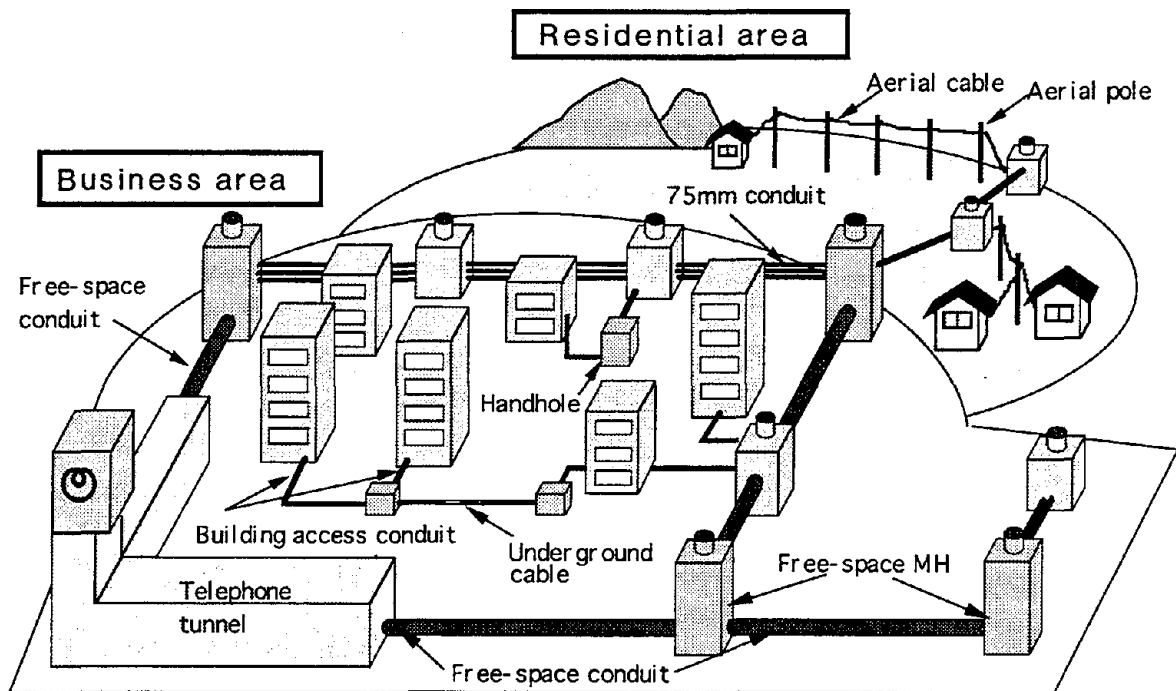


Fig.1 Outline of outside telecommunication facilities

ASEISMIC COUNTERMEASURE TECHNOLOGIES Implemented FOLLOWING THE HYOGO-KEN NANBU EARTHQUAKE

Underground cable facilities sustained only light damage during the Hyogo-ken Nanbu Earthquake, so it could be said that these civil facilities were fairly effective in terms of protecting cables. However, some weak spots such as joints between different structural systems were confirmed, so countermeasures for these areas were investigated. The priority issues arising from these investigations were the three locations of open-cut telephone tunnel expansion joints, manhole ducts and building access facilities. (Fig. 2) The damage conditions in these locations were as follows.

Cables housed in telephone tunnels sustained no damage whatsoever, indicating that these facilities fulfilled their expected functions. For open-cut telephone tunnels located in ground where liquefaction occurred, however, the expansion joints connecting these tunnels to buildings or shafts experienced

level differences of up to 18 cm in both the vertical and horizontal planes, resulting in water leakage and flooding. Therefore, the decision was made to apply flexible joints as aseismic countermeasures for the joints of open-cut telephone tunnels in ground subject to liquefaction, and technology for upgrading existing expansion joints to flexible joints was developed in consideration of cost efficiency and ease of work.

Manhole ducts are the connections between the different structural systems of manholes and conduits. During earthquakes, ground deformation and other factors produce relative displacement between these structures, applying enormous force on the ducts. This caused the duct concrete to crack and concrete clumps to peel away from the duct in locations experiencing severe damage. There were some cases where falling concrete clumps damaged the cables inside manholes, so countermeasures to prevent concrete peeling in manhole ducts were investigated.

Building access facilities are used to connect handholes under public roads to customer buildings using building access conduits. Building access conduits are classified into two cases: where NTT conduits are connected to building distribution conduits at the boundary between public and private property and where buildings and handholes are connected by a single conduit. Building access conduits are shorter than general conduits, so if ground subsidence or other factors produce rather large relative displacement between handholes and customer buildings, they are unable to absorb this displacement and suffer damage such as separation or breakage. Based on the damage conditions produced by the Hyogo-ken Nanbu earthquake, a flexible facility format capable of absorbing large displacement

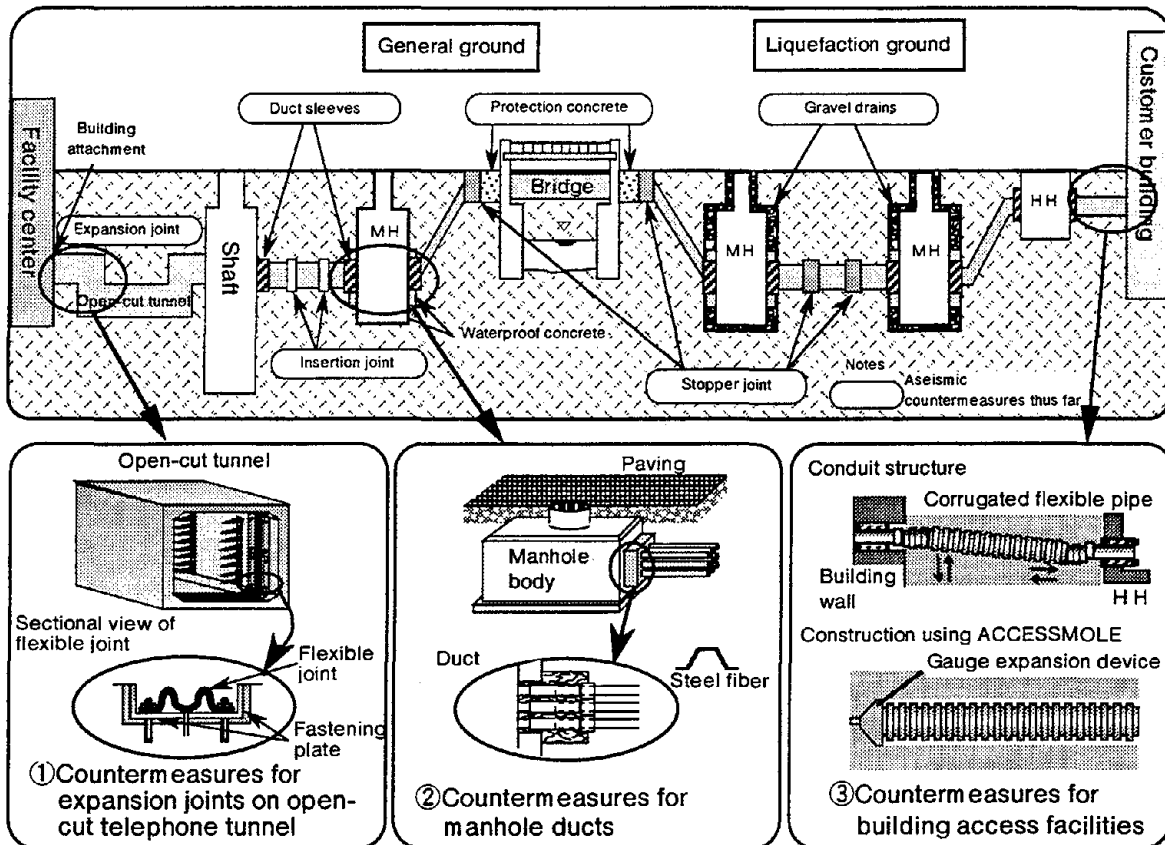


Fig.2 New aseismic countermeasures implemented following the Hyogo-ken Nanbu Earthquake

near buildings and in the joint portions was judged necessary in order to improve the aseismic performance of building access conduit facilities. Regarding work methods, the development of technologies allowing construction using NO-DIG method system was also desired in order to protect the pavement around customer buildings.

The following sections describe the countermeasure technologies concerning these three areas, as well as the development of a system for estimating macro damage conditions and understanding micro damage conditions in order to efficiently survey, inspect and repair facilities.

REPLACING TELEPHONE TUNNEL EXPANSION JOINTS WITH FLEXIBLE JOINTS

Joint structure

Joints are installed in open-cut telephone tunnels in order to locally stop open-cut telephone tunnel cracking when unanticipated external force is applied as a result of temperature-induced expansion or contraction, uneven ground subsidence or earthquakes, etc. There are two types of joint structures: flexible joints (Fig. 3) and expansion joints. Flexible joints are used as countermeasures against uneven subsidence, and expansion joints are used in places where the amount of uneven subsidence is judged to be within a certain standard. The allowable displacement amount for the water stopping plates of expansion joints is 3 mm, so flooding and other problems occurred during the Hyogo-ken Nanbu Earthquake.

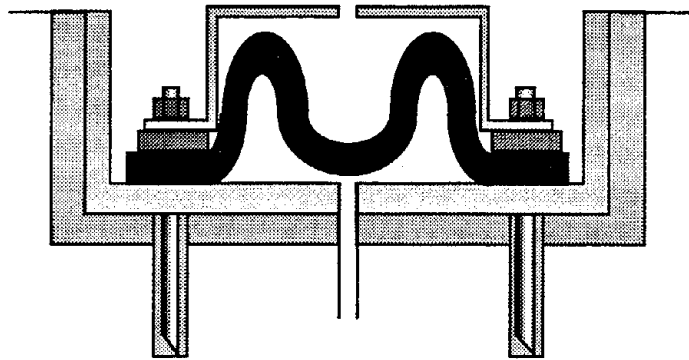


Fig.3 Flexible joint structure

Issues for application to existing telephone tunnels

When attaching flexible joints to existing telephone tunnels, the current work method assumes the construction of new telephone tunnels, so the anchor bolt fastening interval is about 20 cm and all cables must be moved. Accordingly, when flexible joints are installed using the current work method, the cable movement costs are approximately 2.5 times the joint installation costs, and account for the majority of the overall construction costs.

Therefore, revising the attachment structure to involve as little cable movement as possible and reducing costs became important issues, and investigations were undertaken to widen the anchor bolt fastening interval in order to solve these issues.

Experimental verification

The pressure applied to the installation surface was investigated using the elastic foundation beam theory in order to widen the anchor bolt fastening interval. These results showed that increasing the fastening plate rigidity and axial force (tightening torque) were effective methods, so experiments were conducted to verify these methods.

(1) Basic experiments

The experimental apparatus consisted of an M-shaped joint made from a straight rubber sheet and held by fastening plates secured at four points on each side by hydraulic jacks. Here, the presence of water leaks from the fastenings was confirmed visually.

These experiments confirmed the relationship between the axial force and water pressure resistance (water pressure just before water leaked) for different fastening intervals. The results showed that the fastening interval could be widened by using steel materials with a higher rigidity for the fastening plates and by increasing the axial force (tightening torque).

(2) Actual-size experiments

Pressurized tests were conducted on full-size test pieces that used the fastening plates selected in the basic experiments in order to confirm performance at the actual-size level. These experiments consisted of producing hypothetical earthquake displacement and then applying the design water pressure of 1.0 kgf/cm².

Improvement method points

(1) Outline of countermeasures

Current countermeasures for uneven subsidence consist of applying the flexible joints used when newly constructing conduits to existing joints as well.

(2) Bolt fastening interval

The fastening interval of 20 cm for commercial flexible joints was widened up to 80 cm. Widening the fastening interval makes it possible to reduce the existing cable movement work accompanying anchor bolt installation and other operations. (Fig. 4)

(3) Cost analysis

- 1) Cable movement costs are reduced by approximately 80%.
- 2) Joint installation costs are reduced by approximately 20%.
- 3) This makes it possible to reduce overall construction costs by approximately 70%.

(4) Attachment specifications

As a result of these investigations, the fastening plate material was changed to SS400 flat steel (l max: 1000 mm, w : 75 mm, t : 25 mm) and the fastening interval was increased to a maximum of 800 mm as noted above. Also, the rubber shape was changed to a structure that prevents fastening plate separation, the bolts were upgraded to SUS304 M24 bolts, and the axial torque was set at 2000 kg·cm.

Business introduction

NTT introduced these technologies to business operations in November 1996. Based on damage conditions from the Hyogo-ken Nanbu Earthquake, application is scheduled over the next five years

with priority given mainly to the expansion joints of open-cut telephone tunnels installed at the ground water level or deeper in ground subject to liquefaction and which are expected to suffer water leaks or other damage in the event of earthquakes.

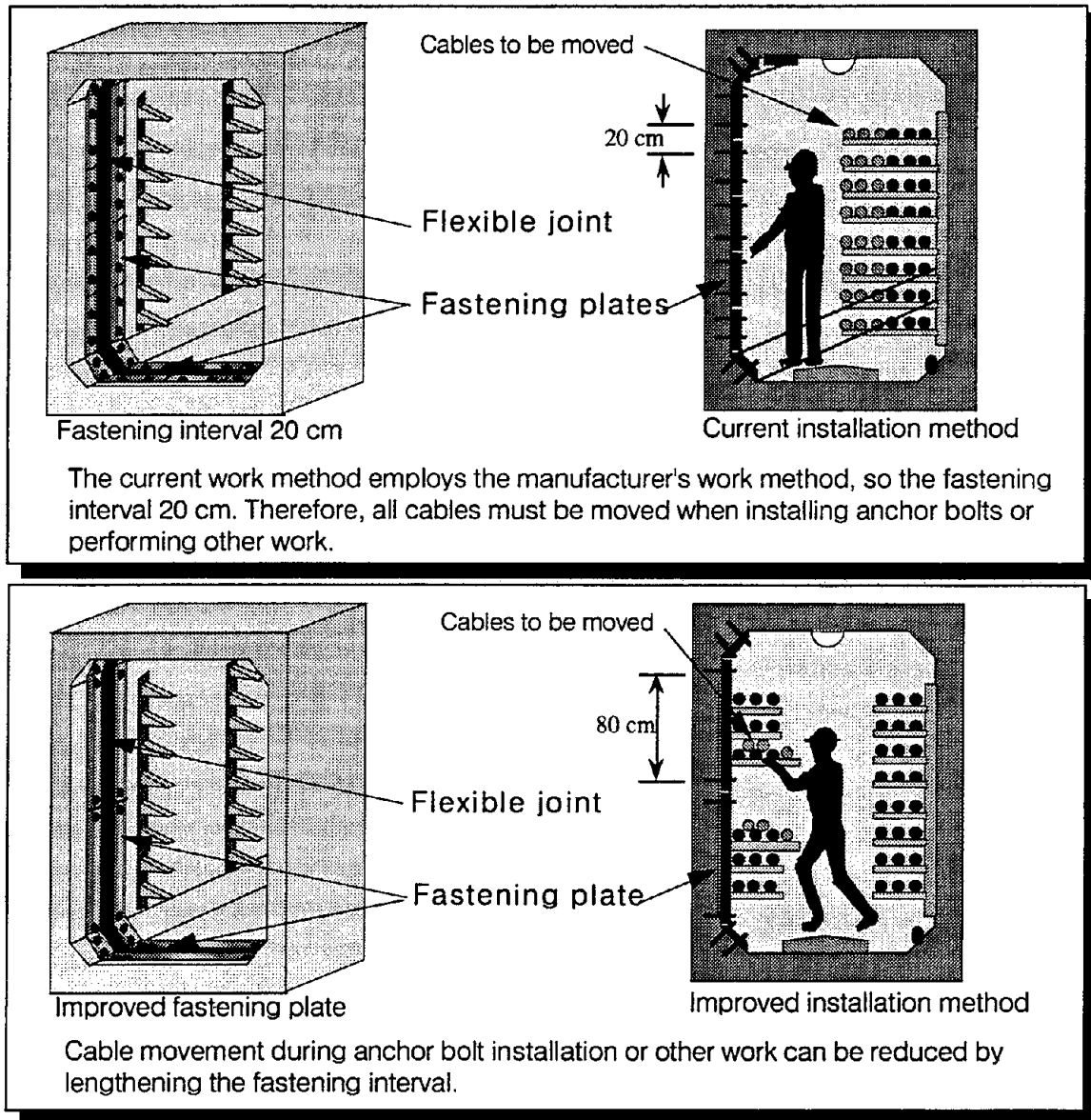


Fig.4 Comparison of structures and movement work before and after the improvement

COUNTERMEASURES TO PREVENT MANHOLE DUCT PEELING

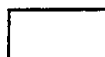
Requirements of waterproof concrete for ducts

Current and additional requirements for the waterproof concrete of manhole ducts are shown in Table 1. Whereas current requirements stress strength, work safety and durability, additional requirements are characterized by enhanced cracking load resistance with respect to Hyogo-ken Nanbu class earthquakes and preventing cable damage caused by concrete clump peeling. Here, the earthquake load is calculated through model analysis that assumes a Hyogo-ken Nanbu class earthquake.

Table 1 Requirements for the waterproof concrete of manhole ducts

Item		Requirements
Strength	Duct	Concrete design standard strength $\sigma_{28}=150\text{kgf/cm}^2$ or better
	Seismic load	Cables are protected under a load of 12 t in the direction of the conduit axis and 8 t in the direction perpendicular to the conduit axis.(4.5 t for resin block MH)
Toughness		Cracking load resistance during earthquakes is better than for current method.
Cost efficiency		Approximately +10,000 yen per MH
Ease of work		Roughly the same as for the current method
Safety		Safety is ensured during the concrete casting work and the surface condition after casting does not hinder line work
Durability		Adding fibrous reinforcing materials does not worsen concrete quality or cause deterioration.

Notes



Current requirements



Additional requirements

Outline of countermeasures

Steel fibers are added to duct concrete to convert the current concrete to steel fiber reinforced concrete (hereafter "SFRC") as shown in Fig. 5. This increases the concrete toughness and provides load resistance (tenacity) even after cracking occurs, thus preventing peeling and cable damage.

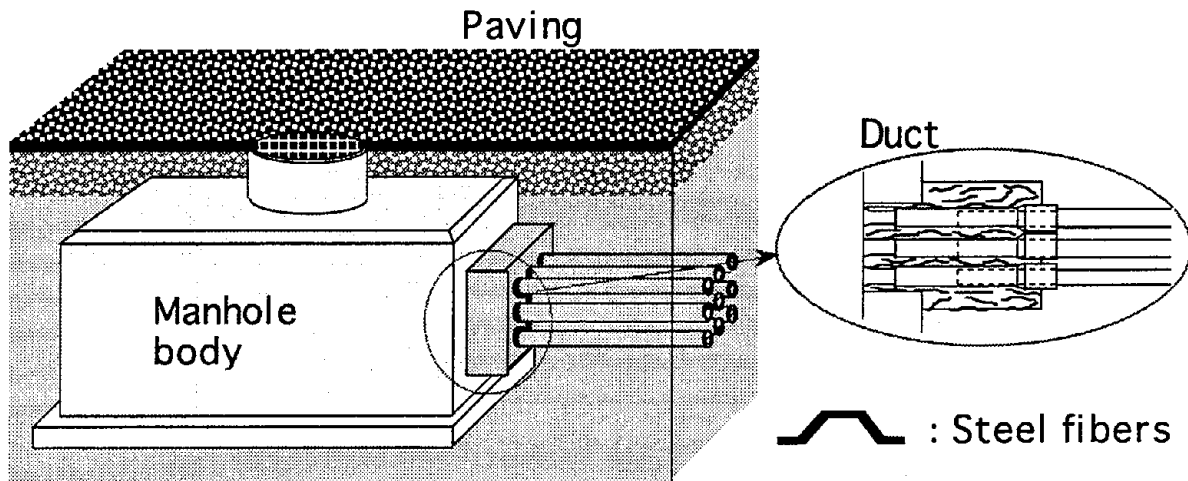


Fig.5 Waterproof concrete of SFRC manhole duct

Investigations and results

Steel fibers were selected from among commercially available fibrous reinforcing materials as a result of theoretical investigations and basic experiments. Then, experiments were carried out to confirm ease of work and strength in the directions of and perpendicular to the conduit axis based on the requirements in order to determine the steel fiber content.

(1) Loading experiments in the directions of and perpendicular to the conduit axis and results

Actual-size duct models were constructed and experiments were conducted to confirm the strength using large-scale structure testing facilities. Then, loading experiments in the directions of and perpendicular to the conduit axis were carried out with a steel fiber content of 1% for concrete and 2% for resin concrete duct blocks, and it was confirmed that cracking was suppressed with respect to a Hyogo-ken Nanbu class earthquake. In addition, these experiments also revealed the need to add duct sleeves to old-specification vinyl pipes with fixed duct portions.

(2) Experiments to confirm ease of work and results

Experiments were performed to verify casting and removal work conditions using a SFRC duct model based on on-site conditions. These results confirmed that the time required to mix and cast SFRC duct concrete was roughly the same as that for the current method. However, the removal work time was found to increase by about 50% compared to the current method.

Steel fiber content and application range

(1) Steel fiber content

As a result of the above investigations and in overall consideration of technical requirements and cost efficiency, bound type fibrous reinforcing materials with hooks on both ends and a size of $\phi 06 \times 30$ (mm) were selected, and the content was set at 1% for cement concrete and 2% for resin concrete.

(2) SFRC application range

This technology will be applied to all newly constructed manholes in the future regardless of conduit

type. For existing manholes, however, this technology will be applied as necessary, and also when adding duct sleeves to older manholes that do not use duct sleeves.

INCREASING THE FLEXIBILITY OF BUILDING ACCESS CONDUITS

New building access conduits

New building access conduits must be able to absorb horizontal and vertical displacement of 10 and 20 cm, respectively, so the decision was made to use corrugated flexible pipes. Experiments were carried out concerning the following investigation items in order to evaluate the aseismic performance of corrugated flexible pipes.

- 1) Behavior when NTT conduits are attached to building distribution conduits
- 2) Behavior when installing a single conduit from the building wall to the handhole wall
- 3) Stress adsorption properties

(1) Outline of experiments

Conduits were buried in steel model soil tanks under conditions simulating a structure connected to building and handhole walls. The building side end was then lifted up to produce the maximum displacement of 20 cm assumed to occur during earthquakes, and the stress generated on the conduits at this time was measured to evaluate aseismic performance.

(2) Experimental results

Experiments were performed with a building distribution conduit present using four cases of connections between different types of conduits (steel pipe + corrugated flexible pipe, steel pipe + vinyl pipe, steel pipe + steel pipe, and corrugated flexible pipe only). The results of these experiments showed that the ratio of the generated stress to the yield stress with respect to corrugated flexible pipe displacement was a small value, thus confirming sufficient aseismic performance. For steel pipes, however, the duct concrete sustained damage even though the stress was within the tolerance value, and vinyl pipes broke before the maximum displacement was reached.

Experiments for the case without a building distribution conduit used only a corrugated flexible pipe. These results showed that the ratio of the generated stress to the yield stress with respect to corrugated flexible pipe displacement was a small value and that almost no stress was generated even over short distances of about 50 cm from the building wall, thus confirming sufficient aseismic performance.

These experiments confirmed that corrugated flexible pipes are the most effective aseismic structure both with and without a building distribution conduit.

Development of driving technologies using NO-DIG method

(1) Development conditions

In consideration of protecting the pavement around buildings and of realizing economical construction in urban areas, the decision was made to develop technologies capable of installing corrugated flexible pipe without excavation. Based on investigation results concerning building access conditions, development conditions were defined as a maximum driving distance of 10 m, application to clayey to sandy soil with an N value of 15 or less, and a work efficiency of one location per day.

(2) Technical issues and driving method

As development themes, the applicable corrugated flexible pipes have a small allowable tensile force of 140 kgf, so measures were necessary to reduce the tensile stress produced on the pipe during pulling. In

addition, since work is performed inside customer buildings, work methods using compact and lightweight machines that can execute work quickly with as little effect on customer facilities as possible were also required. Ultimately, these issues were resolved by improving the conventional ACCESSMOLE CB system.

Therefore, a three-process method was investigated in order to reduce the peripheral friction resistance of the ground during conduit installation. These three processes are first auger boring with the ACCESSMOLE method (CB), then press insertion gauge expansion using a gauge expansion tool, and finally pulling through the corrugated flexible pipe.

The work procedures are shown in Fig. 6.

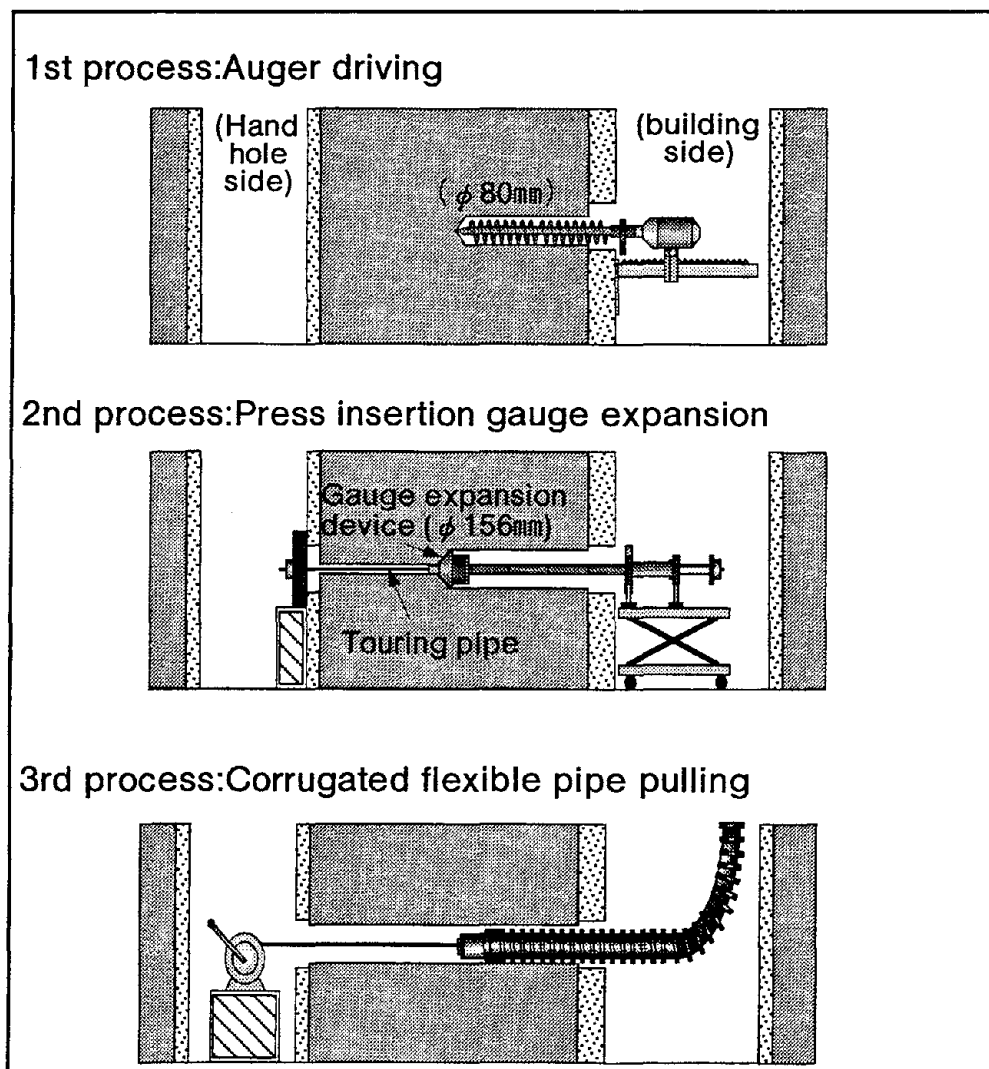


Fig.6 Outline drawing of work method

A jacking machine is fixed to the wall of the customer building with suction pads and auger driving is performed to open a ϕ 80 mm hole.

2) Second process

A PC steel cable is passed through the hole opened by auger driving, and then a pushing machine is set up in the customer building and reaction materials are set up in the handhole via the PC steel cable to take the driving reaction force on the handhole side.

A ϕ 156 mm (when installing a ϕ 100 mm pipe) gauge expansion tool is attached to the tip of the pushing machine and press insertion gauge expansion is performed by driving hollow tooling pipes one after another with the pushing machine using the PC steel cable as a guide.

3) Third process

A wire is passed through the gauge-expanded hole and connected to a ϕ 100 mm corrugated flexible pipe, then the pipe is pulled through the hole from the building side by a winch set up in the handhole.

(3) Experimental results

Experiments were carried out using the selected driving method to investigate the pulling force on the corrugated flexible pipe, the thrust during press insertion gauge expansion, and the applicability in terms of work efficiency.

1) Pulling force on the corrugated flexible pipe

ϕ 156 mm holes (for ϕ 100 mm pipes) were opened in experimental soil tanks and corrugated flexible pipes were pulled through these holes to measure the pulling force in clayey and sandy soils. The results showed that the force required for a pipe pulling length of 10 m was 12 kgf in clayey soil and 11 kgf in sandy soil, thus confirming that pulling can be performed at less than the allowable tension of 140 kgf.

2) Thrust during gauge expansion

The thrust required to drive the gauge expansion tool in the second process was confirmed using experimental soil tanks containing clayey and sandy soils with an N value of 10.

These results showed that the maximum tip resistance was 5.1 tf which was measured for sandy soil. Using the formula for calculating the thrust during press insertion, the estimated thrust for soil with an N value of 15 is 7.2 tf, indicating that gauge expansion can be performed at less than the allowable thrust of 8 tf (80% of the equipment capacity of 10 tf).

3) Work efficiency

This method was confirmed to have a work efficiency enabling construction of one location to be completed within one day (8 hours).

Summary

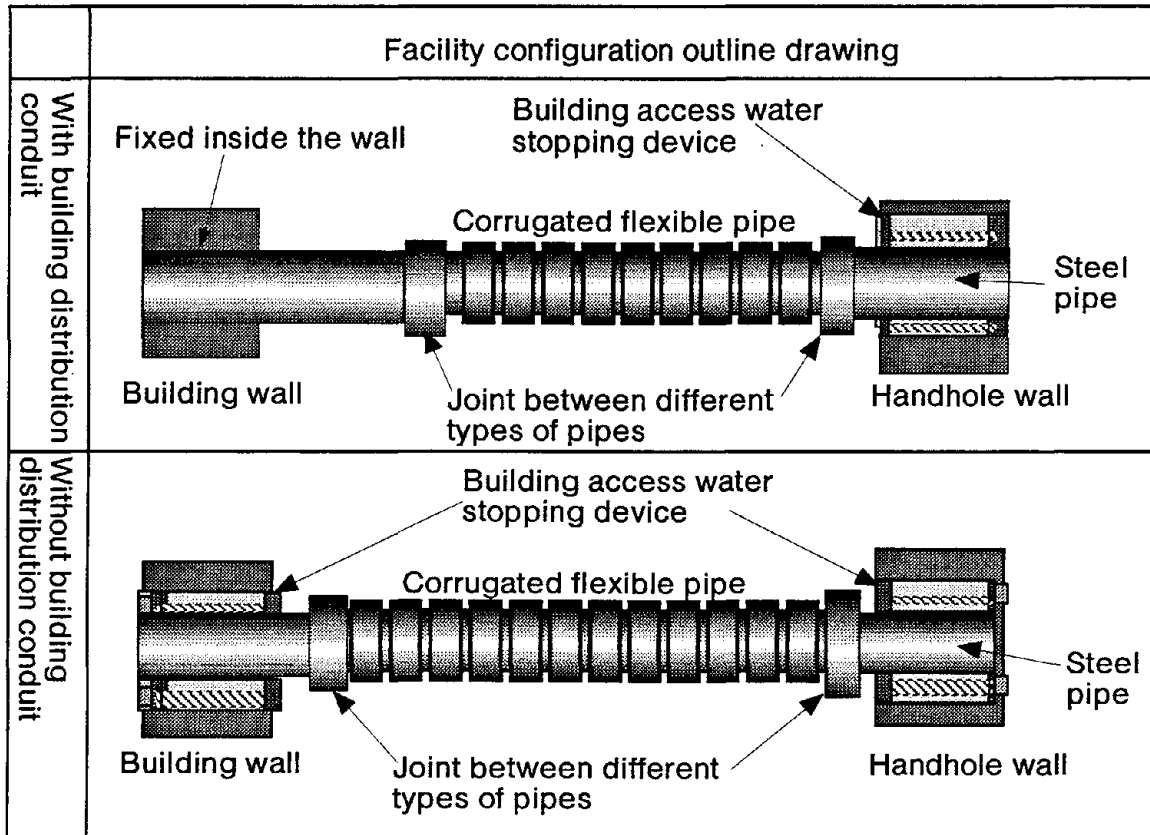
The results of the above investigations show that aseismic performance can be improved by employing flexible building access conduits that use corrugated flexible pipes.

In addition, corrugated flexible pipes also satisfy the requirements for ease of cable installation and overload strength properties, and can be constructed at about the same cost as for current methods. Building access conduits have the two facility configurations with and without a building distribution conduit as shown in Table 2, and are applied to locations subject to liquefaction which are highly likely to experience major earthquake displacement.

Business introduction

These technologies have been introduced from the first quarter of fiscal 1997, and are being progressively applied to the construction of highly reliable civil facilities which support the opticalization of the access network.

Table 2 Building access conduit facility configuration



SYSTEM FOR UNDERSTANDING METALLIC ACCESS FACILITY DAMAGE CONDITIONS USING THE MARIOS *2 PLATFORM

Development background and purpose

Currently, if a large-scale disaster such as the Hyogo-ken Nanbu Earthquake strikes an urban area, it takes quite some time to inspect underground telecommunication facilities which are spread out over a wide area, thus extending the recovery period. Therefore, when large-scale disasters occur, it is vital that initial disaster measures be carried out accurately and that recovery work and the lifeline mission of announcing disaster conditions to local residents and other concerned parties be performed efficiently and quickly. The concept behind understanding damage conditions and the policies during each phase are shown in Fig. 7. Of these, a system that performs metal access facility tests using order lines and displays affected regions by fixed distribution area using MARIOS has been developed as a method for quickly understanding access system macro damage conditions (Fig. 8).

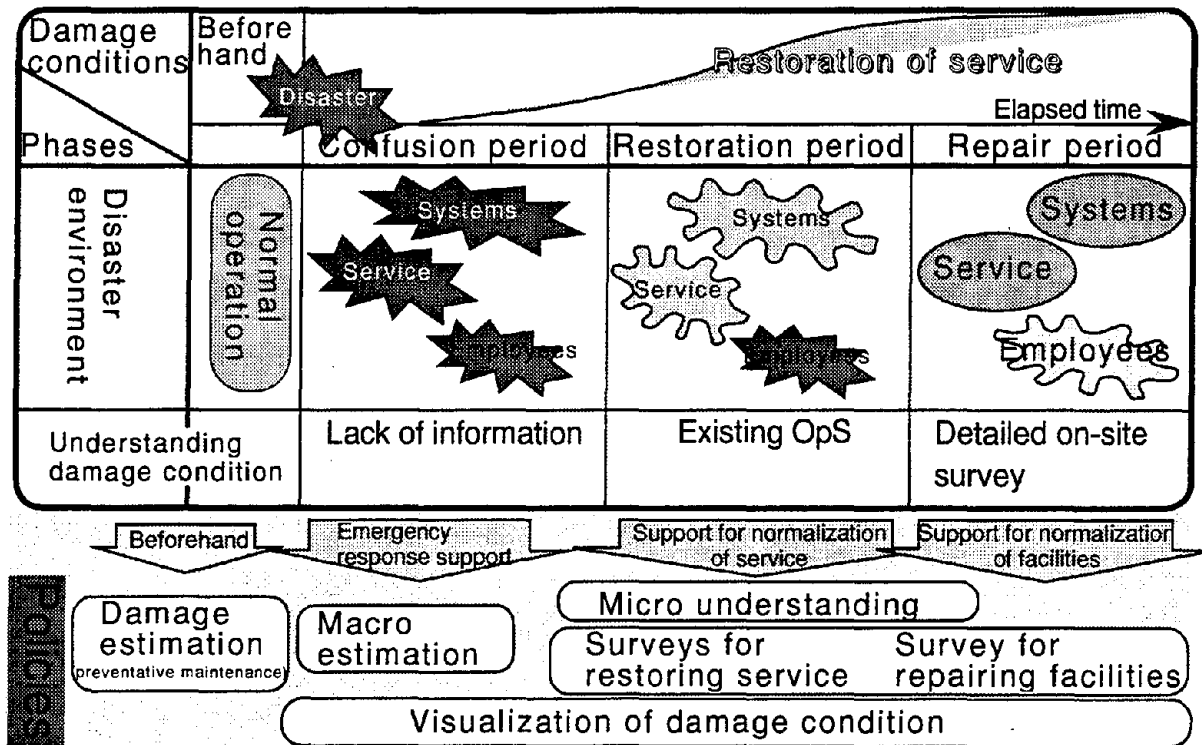


Fig.7 Concept behind understanding damage condition

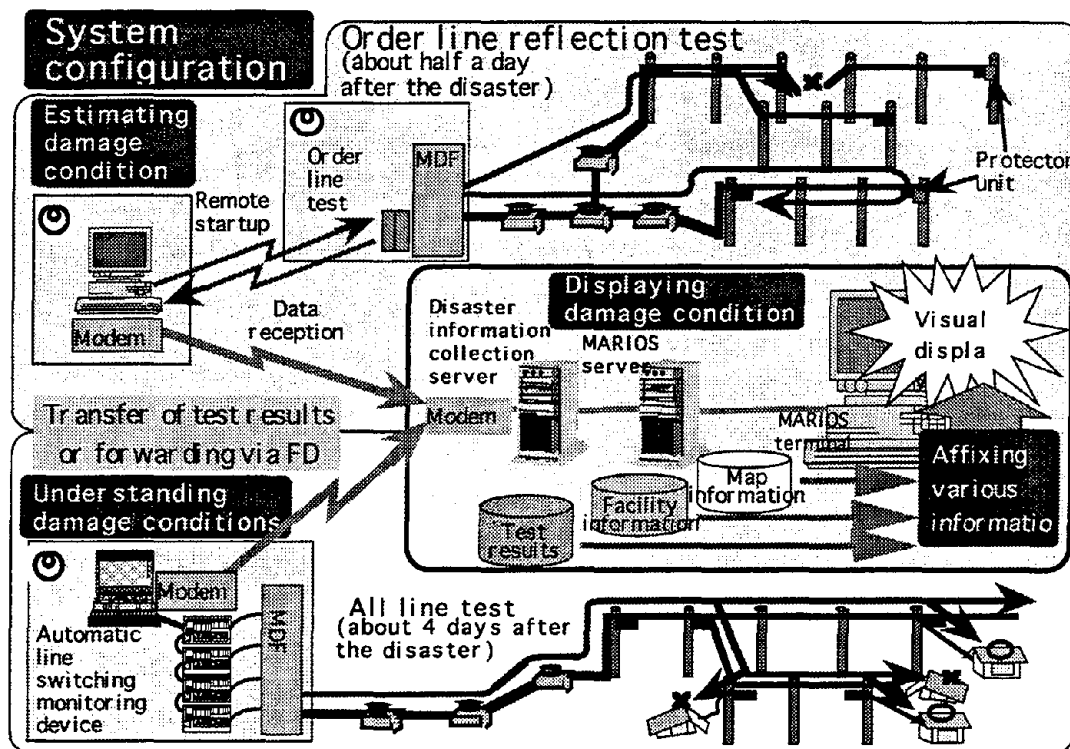


Fig.8 Outline of system for understanding cable damage

Outline

Understanding damage conditions can be divided into 1) estimating macro damage conditions in about half a day immediately after a disaster strikes, and 2) understanding damage conditions during the restoration period.

Estimating macro damage conditions consists of first GO/NO GO testing the order lines installed in each fixed distribution area using an order line tester, and then accumulating these results in the disaster information collection server. These test results are then combined with the facility information in the MARIOS server and the map information in the MARIOS terminals to estimate the macro damage conditions for each fixed distribution area and display the results on maps and ledgers. This makes it possible to understand the conditions for even the largest class of buildings in about an hour and a half.

On the other hand, understanding damage conditions during the restoration period consists of performing all core tests directly from the MDF using portable automatic line switching monitoring devices and accumulating these results in the disaster information collection server. Like macro estimates, the damage conditions are displayed on maps and ledgers using MARIOS. This makes it possible to understand the conditions for even the largest class of buildings in about twelve hours.

Open transfer technology has been established to allow reliable data transfer even under disaster conditions for both macro estimations immediately following disasters and understanding damage conditions during the restoration period. This technology can be supported by multiple means of communication including general public lines, leased lines and cellular telephones, and has a high degree of freedom with respect to terminal type, OS and communication software. This increases access freedom while at the same time ensuring security, and realizes a real-time database using the disaster information collection server.

This system employs the MARIOS platform, allowing full use of the powerful data processing technology and versatile display functions. In addition, this system is also equipped with diverse and advanced analysis functions that combine the MARIOS facility data, customer data and damage data, and is capable of flexibly expanding functions in the future.

CONCLUSION

The Hyogo-ken Nanbu Earthquake is said to have been the first major disaster to strike Japan since the establishment of a telecommunication society, and served to remind us once again of the importance of "information" for crisis management and initial response during disasters. In light of the damage to underground telecommunication facilities, these facilities could be said to have fulfilled their appointed role to protect telecommunication cables. This supports the view that aseismic technology development and improvement have thus far proceeded in the correct direction.

However, telecommunications are playing an ever increasing role in the multimedia society, making it more and more important to ensure telecommunication reliability. NTT intends to continue its efforts to improve the aseismic performance of facilities and to more accurately estimate and understand damage in the future in order to meet these social needs.

REFERENCES

- Damage of Underground Telecommunication Facilities in the 1995 Great Hanshin Earthquake
Honda, K., et al., 6th U.S.-Japan Workshop, Earthquake Disaster Prevntion for Lifeline Systems,
July 18-19, 1995

*1) ACCESSMOLE Method

A NO-DIG construction method used to construct building access conduits that link customer buildings and handholes using microtunneling technology.

*2)MARIOS (Management support system for Access task Reengineering Innovation Objects)

MARIOS is a system developed to improve the efficiency of some complex facility management operations such as facility investment and the establishment of maintenance strategies.

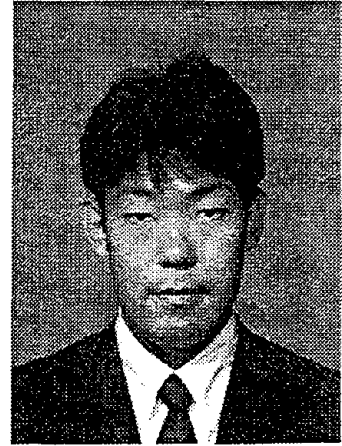
MARIOS uses the client-server method in which the server and clients (terminals) are linked via an ISDN network, allowing the integration of database sites which had thus far remained scattered.

Basic functions include compound operation processing for various databases, making it possible to display analyzed information as drawings and in other formats using work applications developed through object-oriented programming. This increases the efficiency of operations which had thus far been performed while comparing drawings and ledgers.

PERSONAL CAREER

NAME: Masaru Okutsu

POSITION: Research Engineer
Facility Design Systems Group
Civil Engineering Systems Project
Nippon Telegraph and Telephone
Access Network Systems Laboratories



ADDRESS: 1-7-1, Hanabatake, Tsukuba
305 JAPAN
Tel. 81-298-52-2543
Fax. 81-298-52-2676

DATE OF BIRTH: April, 21, 1971

EDUCATION: Bachelor (1994) and Master (1996) of Engineering, Waseda University

MAJOR SUBJECT: Tunnel Engineering
Earthquake Engineering

MAJOR AREA OF EXPERIENCE:

1996- Research Engineer, Facility Design Systems Group
Civil Engineering Systems Project
NTT, Access Network Systems Laboratories

TRAVEL ABROAD: Western Europe

MAJOR PUBLICATION:

**COMPARISON OF RECOVERY AND RECONSTRUCTION STRATEGIES
IN WATER SUPPLY SYSTEMS BETWEEN THE 1994 NORTHRIDGE
AND THE 1995 KOBE EARTHQUAKES
-EMPHASIZING ON AN EMERGENCY RESPONSE-**

Shiro Takada¹, Ryuzo Ozaki² and Junichi Ueno³

- 1 - Professor, Department of Architecture and Civil Engineering, Kobe University**
2 - Graduate Student, Department of Science and Technology, Kobe University
3 - Chief Engineer, Civil Engineering Division, Konoike Construction Co., Ltd.

ABSTRACT

In this paper, the comparison of the emergency response in water supply systems during the 1994 Northridge and the 1995 Kobe Earthquakes is conducted. As a result, it is considered that the emergency response of the Kobe Water Department was inferior to that of the Los Angeles Department of Water and Power. Also the problems and what should be in future in terms of the emergency response are quoted.

INTRODUCTION

The Hyogo-ken Nanbu (Kobe) Earthquake, 5:46 (JST) Jan. 17, 95 attacked the central areas of Kobe City and Hanshin (southern Hyogo-ken and Osaka) districts, which killed more than 6,000 victims and caused severe damage for residential houses, highway bridges, harbor facilities as well as functional interruption of lifelines in wide areas. Just one year before, 4:31 (PST) Jan. 17, 94, the Northridge Earthquake occurred in Orange and Ventura Counties in Los Angeles, which caused severe damage in the central area of the Northridge City. Both the Kobe and the Northridge Earthquakes were typical near field earthquakes which occurred under the highly populated urban areas and caused stop of lifeline function. Present paper deals with recovery and reconstruction of water supply systems in Kobe Water Department (hereafter KWD) and Los Angeles Department of Water and Power (hereafter LADWP), emphasizing on the comparison of emergency response in both organizations.

OUTLINE OF EARTHQUAKES AND DAMAGE^{(1),(2),(3)}

Table 1 lists the outline of earthquakes and damage statistics of killed and injured persons, residential houses, fires and number of customers subjected to supply stop of water, electricity and gas. An extent of damage is much severe in the Kobe Earthquake even for the almost

same level of earthquake magnitude, which is now explained by the difference for the direction of the fault rupture propagation and topographical ground conditions. Several problems to be solved and many lessons for disaster prevention and mitigation of lifelines has been made clear especially in the strategy of recovery and reconstruction and emergency response in these two earthquakes.

Table 1 Outline of earthquakes and damages

		1994 Northridge Earthquake	1995 Kobe Earthquake
Date		4:31 (PST) Jan. 17, 1994	5:46 (JST) Jan. 17, 1995
Richter Scale		6.7	7.3
Epicenter		N 34 ° 12.93 W 118 ° 32.28	N 34 ° 36 E 135 ° 02
Focal depth		17.34 km	16 km
Killed		61	6,312
Injured		about 20,000	43,188
Residential Houses	Total	92,952	439,405
	Completely collapsed	2,132	100,301
	Half collapsed	9,284	108,786
	Partly collapsed	81,536	230,318
Water stop (customers)		about 0.20 millions	about 1.30 millions
Electricity stop (customers)		about 0.65 millions	about 2.60 millions
Gas stop (customers)		about 0.01 millions	about 0.86 millions
Fire		about 100	294

PHYSICAL DAMAGE IN WATER SUPPLY FACILITIES

Kobe Water Department⁴⁾

Three fourths of drinking water in KWD is supplied by Yodo River operated by Hanshin Water Enterprise and the remains are given by Hyogo Prefecture Water Business. Damage in the reservoirs was very slight such as crack in embankments and partly fell down of retaining wall and cliffs along the managing roads. The Sengari inlet went to malfunction due to break

of the secondary cover concrete in the tunnel. Purification plants in Uegahara and Motoyama had slight damage. Transmission pipelines in Uegahara, Egeyama, Jyumonji and Konan had severe water leakage and a water transmission tunnel had been partly broken in the tunnel body and joints.

Among the 119 water distribution ponds, cracks and separations of wells only at Egeyama lower lever distribution ponds were observed at joint parts causing water leakage. The severest damage in water supply facilities was that for water distribution and supply pipelines resulting in 2,283 repairs and 1,757 breaks with failure modes of joint separation, break of pipe body, hydrants and valves. The total number of breaks in supply pipes were 89,854, in which 14,561 under public street and 75,023 inside house areas. The collapse of residential houses were closely related with the break of water pipelines. Moreover, the city office building where the KWD located and the branch offices of Western and Eastern Centers were completely destroyed, which caused so much confusion in emergency activities and restoration workings.

Los Angeles Department of Water and Power^{2),5),6),7)}

A 75% of a drinking water in southern California is transmitted by Los Angeles Aqueduct System from the water source in Eastern Sierra Nevada. The remaining 15% is provided by ground water in three districts and 10% by State Water Project and Metropolitan Water District (MWD) from Colorado River Aqueduct. Five water transmission pipelines had severe damage, which transmitted the water to San Fernando Valley, Simi Valley and Santa Clarita Valley from North California. Three purification plants located on the way of the above transmission lines were sustained water leakage at joints due to ground subsidence. Distribution pipes had severe damage due to strong shaking and permanent displacements in the vicinity of epicenter areas such as about 1,400 breaks in San Fernando Valley and about 300 breaks in Simi Valley and Santa Clarita Valley. Pumping stations and wells had not physical damage, but malfunction by a break down of electricity. On the other hand, reservoir tanks failed at valves, roofs and elephant foot buckling. Hundred twenty dams were located within 74 km from the epicenter, but damage was such slight as ground subsidence and crack on embankments.

FUNCTIONAL DAMAGE IN WATER SUPPLY FACILITIES

Kobe Water Department⁴⁾

As time passed after the occurrence of the earthquake, it turned out the damage was too enormous and spreading in wide areas to grasp the situation of water facilities. Collection and transmission of damage information among the responsible organizations were so difficult due to the collapse of central office building of the water department, interruption of public telecommunication, hackle of road systems, traffic jams and huge amounts of failure of residential houses. However, Okuhirano Control Center kept the function even though the water supply were interrupted from the Hanshin Water Enterprise due to several breaks of large diameter pipes. A large quantity of water was lost in a short time because the water in

Kobe city was provided by using natural down slopes in topography and couldn't be controlled the outflow of the water to the broken pipe networks. Water for fire fighting was tried to transmit preferentially to the Nagata Ward (burnt area) under the extreme low water pressures. 0.58 million customers lost water within total customers of 0.65 million in Kobe City and it was completely recovered after 10 weeks.

Los Angeles Department of Water and Power⁶⁾

The Los Angeles Aqueduct System stopped transmitting water to Los Angeles City to check the leakage points just after the earthquake. Water distribution systems in Western San Fernando Valley and Sherman Oaks were severely damaged and partly damaged in Western Los Angeles and Eastern San Fernando Valley. More than a hundred thousand customers lost water lasting almost one week. It took 13 days for complete recovery of a drinking water. Purification plants started working 4 hours after the earthquake with the aid of emergency electric generators. However, regular water supply to Los Angeles City came back 3 days after the earthquake supported by recovery of electricity in 11 hours later.

CONTENTS OF EMERGENCY RESPONSE

Response of Kobe Water Department^{4),8)}

(1) First response in the organization

It was very difficult to cope with lost of function at first because of collapse of city office building and loss of a means of communication and transportation for staff. Table 2 shows the list of emergency response actions in Kobe Water Department on 17th, January. Injury or death of staff or their families, damage for their house and stopped transport facilities had become obstacles for attending. Table 3 shows the state of condition for attending. It was after PM 8:00 that 67% of staff, which is necessary for establishing minimum emergency operation system, had attended as shown in Table 3. Manuals for emergency operation such as Kobe City's District Disaster Mitigation Plan or Disaster Mitigation Organization Plan of Water Department was issued before the earthquake but supposed earthquakes in these manuals were far smaller than the earthquake. So it was impossible to cope with and unsolved problem, such as loss of a means of communication, had exposed. As 6th floor of No.2 city government building where the KWD located was collapsed, the document and drawing were lost and the operation center of water system had to moved to meeting room in No.1 city government building. It was very difficult for this operation center to grasp the condition of damage under the congestion of telephone. As emergency relief request plan (mutual aid program), there were the memorandum of department of water works in 12 major cities and agreement between 3 surrounding cities (Ashiya, Nishinomiya and Sanda). Following these plans, The KWD requested emergency water delivery for major cities on 17th, 13:00 and aid of restoring work for Japan Water Association on 18th, 9:00. Other than these, many personnel had come from all over the Japan to help or support.

Table 2 Emergency response of Kobe Water Department

Time	Action/Response in Kobe water Department (1995.1.17)
1/17	
5:46	Occurrence of E.Q., Collapse of City office building, power failure and malfunction of telecommunication
5:47	Backup generator on Okuhirano water purification plant started.
6:10	Tobu (eastern) business office ordered the staff to attend via telephone network.
7:00	The staff began to arrive at their office.
7:35	Water supply stop from Hanshin Water Enterprise.
8:00	Water supply stop from Hyogo Prefecture Water Business.
	Tarumi center began to carry water for shelters.
8:45	Sengari water purification plant restarted by power recovery.
9:00	Telecommunication for Seibu (western) center was still suspended.
	The operation center of water system was set up.
9:30	The state of damages for water system was reported to headquarters of city government office and fire department.
10:45	Water from Hanshin Water Enterprise recovered partially (1,500m ³ /h).
11:58	Arima water purification plant restarted.
13:00	Relief for emergency water supply was requested to major cities, organizations via the ministry of welfare or prefectures and Japan Water Association.
13:30	Tarumi center began to deliver water for base of temporary water supply.
14:00	Seibu (western) center was burned down in a spreading fire.
	Kita (northern) center was asked to supply water from a hospital.
	Tobu (eastern) center designate Higasinada low layer distribution pond as base of temporary water supply.
14:30	Kita (northern) center began to carry water for hospitals and schools with shelters.
15:15	Chuo (central) center began to carry water for schools with shelters.
16:00	Tobu (eastern) center began to carry water.
	Okuhirano water purification plant recovered partially (2,000m ³ /h).
17:00	Chuo (central) center began to deliver water for base of temporary water supply.
17:20	Party for water supply from Kyoto City arrived.
17:45	Tarumi center notified locations of the base of temporary water supply to ward office.
18:50	Seibu (western) center failed to notify locations of the base of temporary water supply to ward office.
19:50	Party for water delivery from Sanda city arrived at Tobu distribution control office.
21:00	Tarumi center was asked to supply water from a ward office.
22:35	Seibu (western) center began to delivery water for base of temporary water supply.
22:45	The volume of water from Hanshin Water Enterprise was increased to 9,500m ³ /h.
23:30	Tarumi center was asked to supply water from a hospital.
23:40	Western center began to delivery water for refuge places.

(2) Temporary emergency water supply

Emergency water supply had started on 17th, afternoon. Before the earthquake, some distribution reservoirs were equipped with emergency shut-off valve and they were designated as water supply point. They could hold about 42,000 tons of a drinking water and it was supplied into water tank trucks and portable tank. Water tank trucks were mainly delivered to hospital doing artificial dialysis and 170 of elementary schools where served as refuge places. A permanent water supply point per a ward was placed for citizens. Traffic jam was the biggest obstacle for water supply plan. Seriously damaged area has more demand for emergency water supply but also has more traffic congestion. So it was difficult to keep pace with initial plan. According with requests for relief operation, 804 of workers and 432 of water tank trucks from 83 cities, 20 of private parties and the Self-Defense Forces had come to help for water supply at its peak on 25th, January. As the progress of restoration for distribution line, water supply with water tank trucks was shifted to that with a fire hydrant gradually. These temporary water supply was continued until 17th, April.

Table 3 Number of attending staff

	Head office		Branch office		Total			All Total
	Place of work	Other	Place of work	Other	Place of work	Other	Total	
Occurrence-7:00	1	2	58	1	59	3	62	62
7:00-8:00	3	9	99	6	102	15	117	179
8:00-9:00	11	12	169	25	180	37	217	396
9:00-10:00	13	6	51	9	64	15	79	475
10:00-11:00	4	6	32	4	36	10	46	521
11:00-12:00	4	4	36	5	40	9	49	570
12:00-14:00	6	6	28	6	34	12	46	616
14:00-16:00	5	6	22	3	27	9	36	652
16:00-18:00	1	2	16	1	17	3	20	672
18:00-20:00	0	1	6	0	6	1	7	679
After 20:00	0	1	2	6	2	7	9	688
1st day total	48	55	519	66	567	121	688	688 (66.5%)
2nd day	8	50	74	30	82	80	162	850 (82.2%)
3rd day	3	18	44	10	47	28	75	925 (89.5%)
4th day	3	4	21	4	24	8	32	957 (92.5%)
5th day	0	0	9	0	9	0	9	966 (93.4%)
6th day	1	1	6	2	7	3	10	976 (94.4%)
7th day		3	19	0	19	3	22	998 (96.5%)
After 8th day	2	1	28	5	30	6	36	1034 (100%)
Total	17	77	201	51	218	128	346	
All Total	65	132	720	117	785	249	1034	1034

(3) Temporary restoration work

When the earthquake, many leakages had occurred at a time, so water pressure dropped suddenly and it became difficult to find leaked points. Restoration works had started on 18th, Jan. from the area where water supply from Hanshin Water Enterprise was recovered.

Procedures of restoring works were followings: (a) Storing water for distribution reservoir, (b) Filling the pipe for testing and detection of leakage point, (c) Repairing of distribution and service pipe. For an objective area, unit area for restoration works was set small, necessary volume of water was secured and above procedures were repeated. With these works, restored area become enlarged gradually. Although detection of leakages were done carefully, undiscovered leakages were found after resupply. Collapsed building and banking for road or heavy traffic jam were also the reason for delay of restoration work.

Support party from other areas had started restoration works from 22nd, Jan. and contributed to the performance. 735 of workers from 38 cities were attended to restoration works on the road at a peak. 272 of workers from 53 cities were attended to works within private property at a peak.

End of February, temporary restoration was over except for following areas: (a) Area where most of the building were collapsed or burnt down, (b) Area where land slide or collapse of road banking occurred, (c) Waterfront area where liquefaction or subsidence occurred.

End of March, it was over except for some waterfront area with cave-in. Finally restoration work for whole Kobe City area was over on 17th, April.

Response of Los Angeles Department of Water and Power⁶⁾

(1) First response in the organization

The ground motion was very strong and it was clear that enough damages for establishing Water Emergency Coordination Center (hereafter WECC) prescribed by Emergency Response Plan (hereafter ERP) had occurred. Just after its establishment, WECC called managers and their staff. Following the ERP, site staff directly went to the field where assigned in advance to do damage investigation or closing down of damaged facilities. Because of system failure of telecommunication, these activities were done without contact each other. Collecting information had started via restored telecommunication or emergency communication equipment and much information had become gathered.

Table 4 shows the number of recorded information which were reported to WECC from 17th to 24th, January. Table 5 shows the list of emergency response actions of the LADWP on 17th, January.

Table 4 Number of information collected

Information / Date	Total	Damage of facility / function loss	Restoration of function	Resource of restoration work	Relief for restoration work	Water supply	Other lifeline service	Boil water notice / water quality	Others
1/17	58	37	6	1	2	2	6	1	3
1/18	2	0	0	0	0	1	0	0	1
1/19	7	0	3	0	0	1	2	0	1
1/20	13	2	5	0	0	2	0	2	2
1/21	20	0	8	4	1	0	2	2	3
1/22	59	9	17	10	1	2	8	5	7
1/23	48	2	19	5	0	4	2	8	8
1/24	15	4	2	0	0	4	1	0	4

From Table 4, it is clear that the contents of the reports had shifted from the hardware damages into the system function such as restoration or boiled water notice. LADWP placed first priority on the check of 5 major reservoirs. Within a few minutes, manager being stationed at reservoirs finished the inspection and reported to Central Supervisory Control Center via radio that there were no serious damage. Other site staff began to inspect 68 of

pumping station, 95 of small reservoirs/tanks and 200 of pressure regulating station. Another priority matter is to announce Boil Water Notice to whole Los Angeles City area for public health within 3 hours after the earthquake. This decision was made with consideration on amplitude of earthquake, state of chlorination on reservoir and so on. Water examination for major facilities had finished within 12 hours. Consequently, Boil Water Notice for a half area of Los Angeles city had lifted in the evening of 17th, January.

Table 5 List of emergency response actions of LADWP on 17th, January

Time	Action/Response in Los Angeles Department of Water and Power
1/17	
4:31	Occurrence of E.Q. , Power failure / cut off on phone and fax
Just after EQ	Installation of WECC by ERP
	Work for emergency case began. Report from major reservoir (slight damage)
6:00	Function stop of San Pedro pumping station by power failure.
6:30	LA treatment plant lost function of purification and ozonation
7:00	Water leakage on Saugas Speedway
	Information of damage from staff on site had continued to come successively until 21:25.
	Report of pipe failure on Melrose and Crescent north from LAPD
7:20	Boil water notice was broadcasted via KFWB radio station.
8:20	Most of pumping station lost function by power failure.
10:50	Inquiry on sewer facility damage by Dept. of public health
10:51	Inquiry on tank truck from its staff
11:00	Inquiry from Emergency Operation Board
11:05	Confirmation on stock of resource for restoration
11:10	Decision of the water supplying location after investigation.
	Corresponding to media (water supply started from 18th)
11:26	2 cranes (75 ton,125ton) were dispatched for power facility repairing.
12:30	Offer from governor for meeting at 3pm
12:56	MWD restarted to send water with low pressure.
13:05	Request for rescheduling of meeting to governor
13:10	Offer of personnel from Fulton County, GA
15:30	Volume of water from No.1 pumping station, Van Norman was 30CFS
15:35	Offer of source for restoration (personnel and material) from East Bay MUD (Oakland)
17:20	Recovery of No.2 pumping station, Van Norman
17:20	Penstock pumping station works on 12 CFS
evening	Boil water notice for a half area of Los Angeles city had lifted after water examination.

(2) Temporary emergency water supply

One day after the Earthquake of 17th January 1994, Water tank trucks owned by the department were dispatched and 10 rented trucks were also dispatched. These trucks were donated by the U.S. Army Corps of Engineers, the U.S. Army National Guard, and the Metropolitan Water District of Southern California (MWDSC). The Department's General Services Truesdale Yard was designated as the main base for these trucks.

At the peak of the temporary water supply, 72 water tank trucks were dispatched and more than 100,000 gallons of water per day were distributed. Besides truck drivers, 36 persons were engaged in this work for the arrangement of trucks, the monitoring of the designated locations and accumulation of field informations. During the 13-days of operation, the department was committed to provide continuous water service from 7 a.m. to midnight at published locations including most of high schools and large parks in the San Fernando Valley. In response to additional requests from the Red Cross, State Office of Emergency Services and City

Emergency Operations Center, over 50 sites were also served throughout the operation. Although the first priority was placed for providing potable water to the public, the department tried to provide water to any customer that made a special request. The Olive View Hospital, the Pacific Bell Receiving Station, the Borden Foods, and the Los Angeles Airport were a few examples of these special requests. On the weekend of January 28-30, when normal water service was resumed to the entire city, the temporary water supply was phased out completely.

(3) Temporary restoration work

LADWP was confronted with the difficulties in restoration process because epicenter was quite close to many facilities of their large and complex water system for Los Angeles area. The repair works were very time-consuming because such processes as drainage before repair, the repair itself, pressured the pipe with water for testing, and chlorination were inevitable. In the case that another leak was observed after this process, same process had to be repeated. This kind of repetition had occurred in many cases.

The initial goals established by the LADWP for restoration works were followings: (a) Restoration of water service to many people as quickly as possible, (b) To lift the Boil Water Notice as soon as possible, (c) No interruption of water service to areas in which supply has been returned, and (d) Not to degrade water quality in areas once the Boil Water Notice has been lifted.

Originally WECC was created to help coordinate the major decisions and activities that have to be undertaken after a major disaster. WECC took the initiative in the restoration planning. Managing personnel was convened in WECC room to receive updated information and to discuss the emergency strategy. The WECC room had several city-wide distribution maps, emergency telephone lines, TV monitors, and other necessary emergency-related logistic equipment. All damage reports were received in this room and evaluated within the context of the effect on customers. The whole western and southern parts of San Fernando Valley were without water because the city trunk lines for these areas were ruptured in many places. However, MWDC had been able to restart the water supply three days after the Earthquake. In this way LADWP could provide water to about 250,000 people who were without water in the West Valley area. However another 150,000 people living at elevated locations in the West Valley were still suffering the water shortage. About 20 fire department truck pumpers were used to pump across fire hydrants to supply water to about 70 percent of these people. After five days, the trunk lines for this area were repaired, and normal service was restored. Repairs of the distribution system, less critical trunk lines and damaged tanks continued for months. The water service was fully restored nine days after the earthquake.

COMPARISON OF THE EMERGENCY RESPONSE

Fig.1 shows the time history of emergency response both in the KWD and the LADWP after the earthquake. In terms of the establishment of the operation center, the LADWP set up the WECC following the Emergency Response Plan for earthquake disaster. However, in the case of Kobe, the KWD couldn't operate for three hours after the earthquake because of the collapse of the office building, it obligated to set up the operation center in another location. It was the night of January, 18th that telephone service was installed in the operation center of

the KWD. In other word, most important facility was lost. Therefore, there were much difference of logistic equipments between these water departments.

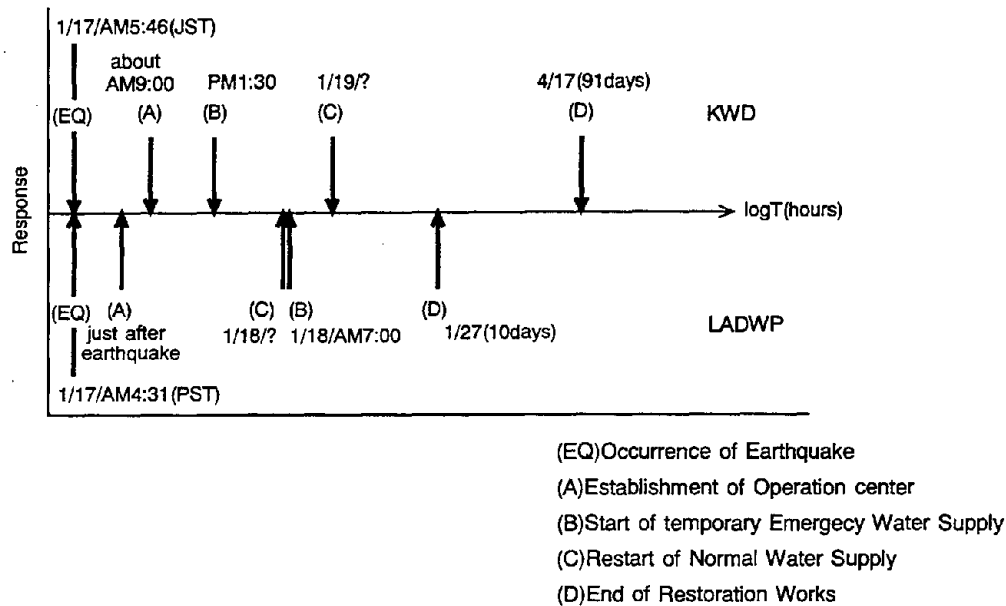


Fig.1 Time history of emergency response and restoration both in the KWD and the LADWP

The temporary emergency water supply provided by the KWD to the refuge places such as elementary and high schools had started some hours after the earthquake. However, undoubtedly it was impossible to deliver the required volume of water and consequently the number of the place where people could get potable water was limited. But there was no way to inform the location of these points for public, so the operation was thrown into confusion. In case of the LADWP, the operation started on the next day of the earthquake but the arrangement of the water tank trucks was broadcasted through the mass media on the day of earthquake. In both cases, the broadcasting by the mass media was used to inform the locations of the temporary water supply, however the problem remained regarding with the way for people who lost their houses and access to broadcasted information.

The process for temporary restoration works, such as getting some informations on damage, gathering resources and arrangement of resources is similar in both case. But there were much difference in the time consumed for repairing works. As shown in Table 6, the damage ratio of the distribution pipes of the LADWP is lower than that of the KWD.

Table 6 Damage and damage ratio of distribution pipelines

Organization \ Damage	Total length of distribution pipes (km)	Number of damages	Damage ratio (number of damages/km)
KWD	4,000	1,757	0.44
LADWP	11,200	about 1,700	0.15

It can be explained due to the fact that the total pipe length of the LADWP is longer than that of the KWD, however there is no much difference in the total number of the damage. Some reasons why the KWD consumed much time for repairing works can be attributed to the following facts: traffic jam, destruction of houses, collapse of roads, the large number of damaged service connections and the difference of the specification of materials. In Japan, some of specification of materials for water works is unique from city to city.

It also took long time to decide the strategy, the prioritization and arrangement the resources (i.e. materials, aid, etc.) for repair works. Because the way to get enough information regarding with damages toward the operation center and the method to judge the reliability of them were not yet established before earthquake. Therefore, it is considered that the well organized information systems between the operation center and the field was not enough in both cases, especially in Kobe.

As concerning to the waterworks facilities of KWD, the construction of emergency shut-off valve system was in progress, valves of 21 service reservoirs were in operation before the Earthquake, 18 sites' valves functioned at the time of the Earthquake. The system consists of three seismometers at the control center, an electric butterfly valve which is equipped in either of paired service reservoirs, and a control system. The system was intended to secure water in the reservoir functioning as the source of the temporary emergency water supply. It can be judged that the system was very effective during the Kobe Earthquake. The LADWP didn't have such a system when the earthquake, but it was considered as the subject to have this kind of system before the earthquake. This kind of system not only for reservoirs but also for tank of the important public institution such as hospitals will be effective for both areas.

Table 7 Earthquake preparedness by LADWP and KWD concerned emergency response

Organization Earthquake preparedness	LADWP	KWD
Concept of disaster countermeasures	The concept prioritized firstly the quick help and survival of people suffered from earthquake and restoration efforts work after that.	The countermeasures were focused on the concept to prevent facility damage. After 1995 Kobe Earthquake concept towards earthquake has changed.
Recognition for earthquake in disaster mitigation plan	In 1971, San Fernando Earthquake had occurred and then many lessons were learned.	Major earthquake hadn't occurred and the level of recognition to presumed earthquake hazard was low.
Emergency Operations Organization (EOO)	EOO was established in 1980 in Los Angeles City.	Not only Kobe City but also Hyogo Prefecture didn't have organization such as EOO.
Training for emergency response	Emergency Response Plan (ERP) had been established after the 1971 San Fernando EQ which was similar level to the Northridge EQ and functioned effectively.	Training for the emergency response based on the Manual was insufficient.
Mutual aid program	Mutual aid program worked sufficiently and large aid were offered.	Mutual aid program did work but not sufficiently, because it was request-basis and very troublesome in procedure.

Table 7 shows earthquake preparedness by the LADWP and the KWD concerned with emergency response. They are different obviously. It is assumed that the conception or

recognition for natural disaster are different, so the philosophy of countermeasures, provided in regulation is also different. The emergency countermeasures in the Japan are based on the concept to prevent physical damage by strengthening the seismic code which prompts to the improvement of facilities. In contrary, the concept in U.S. prioritize firstly for the quick help and survival of people suffered from the earthquake and how restoration effort works after that. In Japan, concept towards earthquake has changed. The idea that certain damage is inevitable, similar to U.S. is accepted for the philosophy of regulation, then revision of the seismic code for lifeline system has begun.

The city of Los Angeles had detailed emergency response plan which was based on the lessons learned from the 1971 San Fernando Earthquake. In the case of Hanshin Area including Kobe city, the current system didn't have such an experience, so the level of the recognition to earthquake hazard had been much lower than U.S.. Within Japan, public consciousness for earthquake is generally lower than Kanto and Tokai Area. Therefore, Hyogo Prefecture as well as Kobe City had not Emergency Operations Organization⁹⁾ (hereafter EOO). This made the emergency response to be so slow. On the other hand, the rescue and restoration operation during emergency in the city of Los Angeles were conducted smoothly since the EOO was established in 1980 in Los Angeles.

In terms of the response plan during emergency, Kobe City had "Kobe City's District Disaster Mitigation Plan" and "Disaster Mitigation Organization Plan of Water Department" and the city of Los Angeles set up "Emergency Response Plan". The plan of Kobe City hadn't considered this kind of large earthquake such as the 1995 Kobe Earthquake, the emergency response of the KWD was thrown into confusion. On the other hand the plan of Los Angeles had been established after the 1971 San Fernando Earthquake which is similar to Northridge and the emergency response of LADWP was conducted smoothly according to the plan. This plan is as follows. When the communication systems doesn't work just after earthquakes, every personnel who takes part in the Emergency Response Plan will follow previously given instructions on when and how to act, which is specified based on the broadcasted information on intensity and the location of epicenter. If earthquake is so large that there is no way to get any information including broadcasting, every personnel has to attend their own position in principle and some designated personnel has to carry out inspection and repair activities directly. With this plan, LADWP could deploy a large number of personnel throughout the city.

Concerning to the mutual aid, Kobe City had the memorandum of department of water works in 12 major cities and the agreement between 3 surrounding cities. At the 1995 Kobe Earthquake the mutual aid programs did work but not sufficiently because it was regulated that an aid should be performed on request-basis. On the other hand, in the 1994 Northridge Earthquake, large aid from neighboring utilities in Southern California, from Northern California and other states according to the Mutual Aid Agreement were offered.

According to the facts above-explained, the response of the KWD was disordered severely. It could serve as a lesson on how to avoid confusing by providing instructions on when and how to respond for every personnel in the emergency response manual. On this way, it was very useful in the case that communication systems were not in operation just after earthquake, not only to set up the response plan during the emergency but also to train the personnel as the plan and to improve the plan is indispensable. Moreover, it may be effective for the emergency response that the EOO be established at city level or prefecture level in order to cooperate in water system and to cooperate with the other lifeline utilities. According to the mutual aid it is necessary to improve the request-basis procedure in Japan. Two major plans as

the preparedness for the post earthquake emergency response in Kobe City has been revised. One is related to the Lifeline Information System and the other is about Liaison Board of Excavation Works of Roads, both of which are prepared for the strategies in emergency response and restoration works after earthquakes. The former is the plan which exchanges information on damage and restoration works among organizations of lifeline business, city office, mass media and citizens. As shown in Fig.2, the lifeline organizations send the information to the operation center through a FAX service, which in turn provides such information to the mass media and public. The latter is established in order to prevent unnecessary inconvenience on the roads (traffic jams, etc.) for emergency response and also prevent economic losses on the road system due to complications in the excavation works of roads as well as laying underground works of lifelines such as water and gas supply systems.

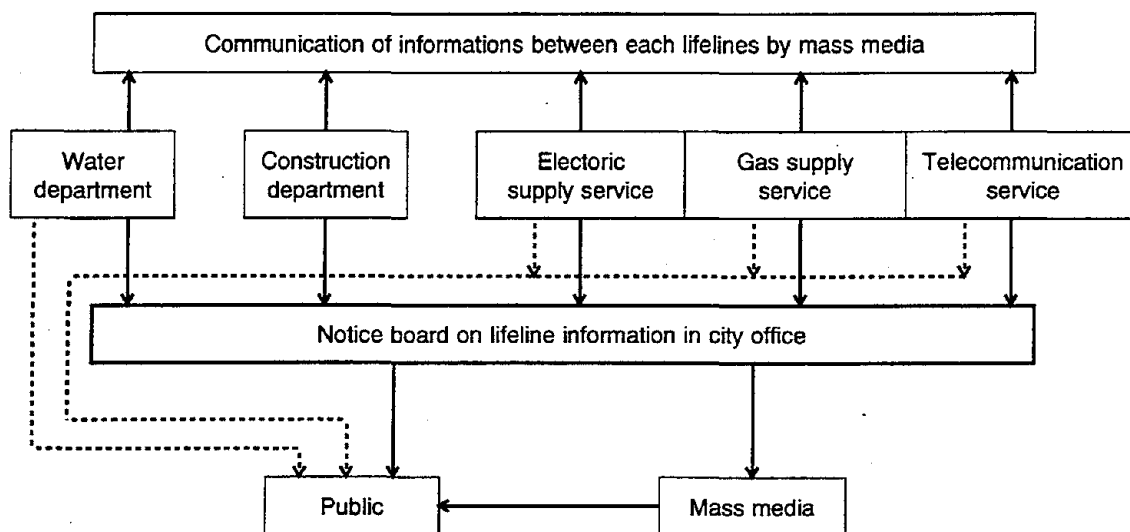


Fig.2 Information flow in Lifeline Information System during disasters

CONCLUSIONS

In this paper, the comparison of the emergency response in water supply systems between the 1994 Northridge and the 1995 Kobe Earthquakes has been conducted. Results shows followings.

- (1) Outline of earthquake, physical and functional damages and time dependent emergency response in the KWD and the LADWP have been compared during the 1994 Northridge and the 1995 Kobe earthquakes.
- (2) It took much more time for complete recovery of a drinking water in the KWD compared with the LADWP due to traffic jam, destruction of many houses, collapse of roads, damaged service of other lifelines and poor training for emergency response.
- (3) The countermeasures in the KWD were focused on strengthening the water facilities and didn't pay so much attention to training for the emergency response in spite of the existence of emergency action manuals. The reason is considered that the KWD had not experienced

- so destructive earthquakes as the Kobe Earthquake.
- (4) Los Angeles city established EOO (Emergency Operations Organization) in 1980 learned by the 1971 San Fernando Earthquake, which worked sufficiently during the 1994 Northridge Earthquake.
 - (5) Emergency response organizations such as EOO and EOC would be indispensable in Japan to organize the different many sections related to emergency response after earthquakes, which would be able to manage disaster information, personnel and others smoothly and exactly.
 - (6) A smart system such as an automatic shut off valve in reservoir tanks in the KWD would be effective countermeasures under the cost performance disaster mitigation plans for water supply systems.

REFERENCES

- 1) Field Investigation Team on Great Hanshin Earthquake, Department of Civil Engineering, Faculty of Engineering, Kobe University: 2nd report on great Hanshin Earthquake, 1995.3.
- 2) Le Val Lund: Lifelines, Northridge Earthquake reconnaissance report, Earthquake Spectra, Vol.1, pp.143-243, 1995.4.
- 3) FEMA: The Northridge Earthquake one year later, 1995.1.
- 4) Kobe Water Department: Document of restoration in water supply system during the 1995 Kobe Earthquake, 1996.2.
- 5) Los Angeles Department of Water and Power: The Los Angeles aqueduct filtration plant, 1990.3.
- 6) Larry McReynolds and Robert L. Simmons: LA's rehearsal for the big one, Journal of AWWA, pp.65-70, 1995.5.
- 7) Le Val Lund: Lifeline utilities performance in the 17 January 1994 Northridge, California, Earthquake, Bulletin of the Seismological Society of America, Vol.86, No.1B, pp.S350-S361, 1996.2.
- 8) Lifeline Network, Kansai: Lessons learned from the 1995 Kobe Earthquake, pp.141-170, pp.483-493, 1997.6.
- 9) City of Los Angeles: Emergency operations organization, 1996.3.

PERSONAL CAREER

Name: Junichi Ueno

Position: Chief Engineer
Civil Engineering Div.
Konoike Construction Co., Ltd.

Address: 3-6-1, Kitakyuhoji-machi
Chuo-ku, OSAKA
541, Japan
Tel. 81-6-244-3670
Fax. 81-6-244-3676
E-mail ueno_ji@konoike.co.jp



Date of birth: May 21st, 1957

Education: BS in civil engineering:Kobe University(1981)
MS in civil engineering:Kobe University(1983)
ME in civil engineering:Columbia University(1992)

Major Subject: Lifeline Earthquake Engineering

Major area of experience

1992-present	Chief Engineer Civil Engineering Div. Konoike Construction Co.,Ltd.
1983-1990	Engineer Civil Engineering Div. Konoike Construction Co.,Ltd.

Travel Abroad: US, Canada, Greece, Turkey etc

Major Publication:

"The Kobe Earthquake:Geodynamical Aspects"
Computational Mechanics Publications,1996

VI. LIFELINE FACILITIES AND URBAN EARTHQUAKE DISASTER PREVENTION

“Development of Seismic Isolation Systems for Underground Structures
and the Mechanism of Seismic Isolation”

J. Hoshikuma, S. Unjoh, K. Nagaya, K. Murai

“Seismic Design of Liquid Storage Tanks”

D. Hu, B. Hendrickson

“Research and Development on the Seismic Isolation System Applied
to Urban Tunnels (Part-1: Development of Seismic Isolation Materials
and Construction Methods)

T. Suzuki, T. Tanaka

“Research and Development on the Seismic Isolation System Applied
to Urban Tunnels (Part-2: Effects of Seismic Isolation and Seismic Design)

T. Tanaka, T. Suzuki

“Translating Earthquake Damage Data into New Performance Requirements
for Earthquake Actuated Automatic Gas Shutoff Devices”

Douglas Honegger



DEVELOPMENT OF SEISMIC ISOLATION SYSTEMS FOR UNDERGROUND STRUCTURES AND THE MECHANISM OF SEISMIC ISOLATION

Shigeki Unjoh¹, Jun-ichi Hoshikuma², Kazuhiro Nagaya² and Kazuhiko Murai³

1) Head, Earthquake Engineering Division, Public Works Research Institute,
Ministry of Construction, Tsukuba Science City, Japan

2) Research Engineer, ditto

3) Visiting Research Engineer, ditto

ABSTRACT

Underground structures are often constructed in the seismically high risk condition. To enhance the seismic safety of such underground structures, a new structural system for reducing the seismic effect in the underground structures is being developed in this paper. It is interesting in the system that the underground structures is cased by an isolation material with a smaller shear stiffness than the surrounding soil to isolate the underground structures from the effect of earthquake ground motion. This system is expected to be effective for the tunnels through a transition section of geological conditions, a connection section between tunnel and the vertical shaft, a wide box structure in the soft soil. The Public Works Research Institute has conducted a 3-year joint research program on the development of seismic isolation systems for underground structures with the Public Works Research Center and 17 private firms since 1995. This paper presents an outline of the joint research program and the seismic isolation mechanism of the system through the 3-dimensional finite element analysis.

INTRODUCTION

The underground structures have often been constructed in geological transition or soft soil, where are seismically high risk conditions. Furthermore, the cross section of the underground structures has recently become large, so that seismic effect has been required to consider in their design.

The underground structures deform following the deformation of the subsurface soil during the earthquake. Therefore, seismic forces increase as the structure becomes stiffer. When the seismic effect to the underground structures is significant, it would not be advisable that the sectional area and/or the reinforcing bars shall be increased. In such case, it would be effective to apply the system to be able to reduce the seismic effect. There are two mechanisms for reducing the seismic effect in the underground structures; to decrease the

equivalent stiffness of the underground structures by installing flexible joints; and to isolate them from the seismic deformation of the subsurface soil by the isolation layer injected into a gap between the underground structures and the subsurface soil. The former technique has already been used in practice in the construction of submerged tunnels, common utility ducts and shield tunnels. However, the seismic deformation developing in the underground structures with flexible joints become large, which may sometimes cause functional damage in important structures. It should also be noted that the flexible joint is effective in the only longitudinal direction, thus the reduction of seismic effect is not expected for the response in the transversal direction. On the other hand, seismic forces developed in underground structures with the isolation layer would reduce for both longitudinal and transversal direction without excessive deformation, because the isolation layer absorbs the seismic deformation of the subsurface soil¹⁾.

The Public Works Research Institute has conducted a 3-year joint research program on the development of seismic isolation system for underground structures with the Public Works Research Center and 17 firms since 1995. The private firms consist of material makers, general construction companies and design consulting companies. The objectives of the program is to develop appropriate materials for the isolation layer, construction methods for injection of the isolation materials and design recommendations for the seismic isolation system. This paper introduces an outline of the joint research program and the seismically isolated underground structures. The mechanism of the seismic isolation is also discussed based on the 3-dimensional finite element analysis. For reference, developments of the isolation materials, construction methods and the design models for the seismic isolation system are presented in companion papers^{2,3)}.

JOINT RESEARCH PROGRAM

Fig. 1 illustrates the seismic isolation system for underground structures. It should be noted that the underground structures are isolated from the subsurface soil by the isolation layer at vulnerable sections during earthquakes. The seismic isolation system presented here would be applicable to both the shield driven tunnel and the cut-and-cover tunnel. In the joint research program, the following technical issues have been studied for the development of the seismic isolation system.

Development of Isolation Materials

The shield driven tunnel with the isolation layer is constructed by injecting the isolation materials into the tail void. The isolation layer for the cut-and-cover tunnel is set up around the section. Therefore, the isolation materials for those tunnels are required not only to have the appropriate property for the seismic isolation but also to be stable during static situation. Furthermore, the isolation materials for the shield driven tunnel must function as the conventional infill material injected into the tail void. Followings are required properties for the isolation materials.

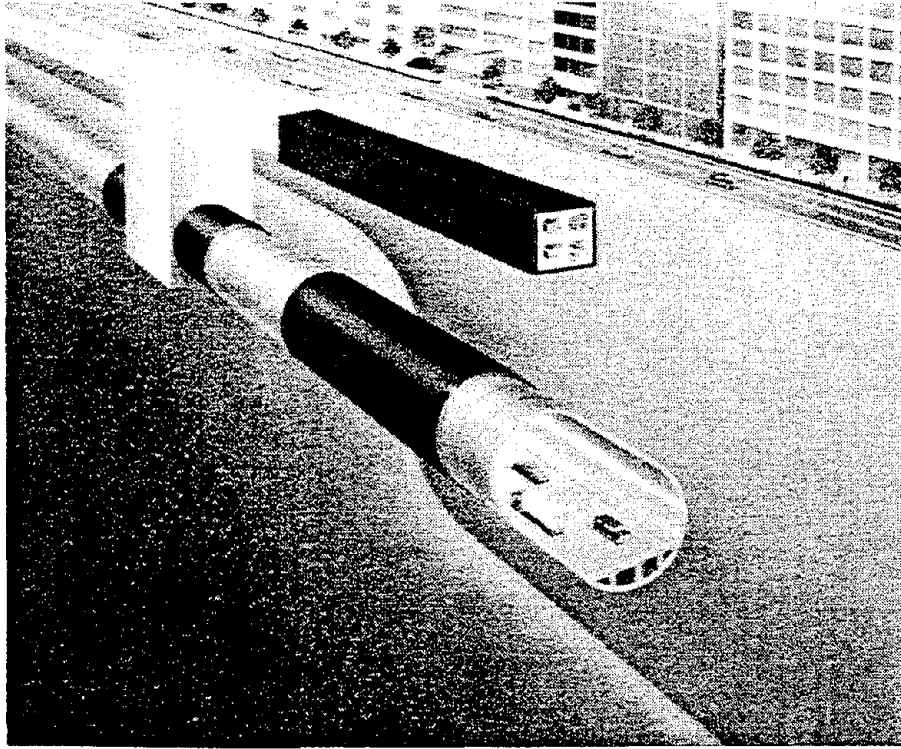


Fig.1 Seismic Isolation System for Underground Structures

- much lower shear modulus than subsurface soil
- high shear deformation capacity
- durable and stable
- small volumetric change from injection through solidification
- waterproof
- able to supply by compressor (for shield driven tunnel)
- able to fill up the tail void (for shield driven tunnel)
- not be diluted with underground water
- not develop harmful substances during injection and solidification

Based on above requirements, the isolation materials were proposed by the joint research program as shown in Table 1. The hollow cylindrical cyclic shear test were carried out, and the shear modulus and its strain-dependency of proposed materials were investigated²⁾.

Table 1 Isolation Materials for Underground Structures

Shield Driven Tunnel	Cut-and-cover Tunnel
asphalt-based material urethane-based material silicone-based material	Liquid Rubber Precast Rubber Panel

Development of Construction of Isolation Layer

To inject the isolation materials (asphalt-based, urethane-based, silicone-based) into the tail void of the shield driven tunnel, new injection systems have been developed for each isolation material. An applicability of these systems was verified based on model tests²⁾. Furthermore, a minor improvement is required for the shield machine to prevent the isolation material from flowing backward during the injection. Details of the improved shield machine for the seismic isolation system have been studied in the joint research program.

The liquid rubber for the cut-and-cover tunnel is able to be constructed by using the similar injection system for the shield tunnel, which was examined by the construction test²⁾. On the other hand, the precast rubber panels are put around sections during the construction of tunnel body²⁾.

Development of Design Recommendations

At first, dominant factors for controlling the seismic isolation effect were studied based on parametric analyses. It was found out from analyses that the shear modulus ratio of the isolation material to subsurface soil is the most important factor and the efficient one would be around 0.01 to reduce the seismic force³⁾. Furthermore, the seismic response were analyzed for various seismic isolation system so that appropriate geological/ structural condition for the seismic isolation be found out. Analytical results show that the seismic isolation would be effective in the underground structures, where the seismic effect is significant; underground structures constructed through a transition of geological condition; connection of the shield tunnel to the vertical shaft; laterally wide underground structures in a soft soil condition.

Appropriate analytical models were studied for the seismic isolation system. For the transverse direction, the static 2-dimensional finite element analysis was recommended, because the static soil-isolation-structure interaction could be accurately taken into account by the finite element model. On the other hand, it is a 3-dimensional issue to analyze the seismic response in the longitudinal direction. The 3-dimensional analysis would be so complicated method for design practice that some simplified models were developed³⁾.

The effect of the isolation layer on ordinary behavior of the subsurface soil and underground structures has also studied based on the static 2-dimensional finite element analysis. It was found that the effect of the isolation layer on static soil pressure and deformation was not so significant that the conventional evaluation method would be applicable to the seismic isolation system, if proposed materials listed in Table 1 were used for the isolation materials³⁾. However, it should be noted that significant effect on ordinary behavior would be developed when the shear modulus ratio of the isolation material to subsurface soil is less than 0.001.

ANALYTICAL MODEL FOR 3-DIMENSIONAL DYNAMIC FEM ANALYSIS

As described above, the efficient shear modulus ratio of the isolation material to subsurface soil is around 0.01 to reduce the seismic forces³³. To make clear a mechanism of the seismic isolation system and develop a theoretical design model, the seismic behavior in the longitudinal direction was studied for the isolated shield driven tunnel constructed through the geological transition based on the 3-dimensional finite element analysis.

Fig. 2 shows an analytical model for 3-dimensional dynamic finite element analysis. A 1/2 model is used for the analysis and a model width is 16.5m. An analytical length in the longitudinal direction is 87.75m. The geological transition plane crosses the horizontal plane at an angle of 45 degree. All of elementary boundaries in the model are the viscous ones. The structural component of shield driven tunnel is modeled by shell element, and the solid element is used for modelling both the subsurface soil and the isolation layer. As a consequence, numbers of solid element, shell element and node in total are 6235, 232 and 7350, respectively. Node restraint is adequately made so as to express the symmetrical model.

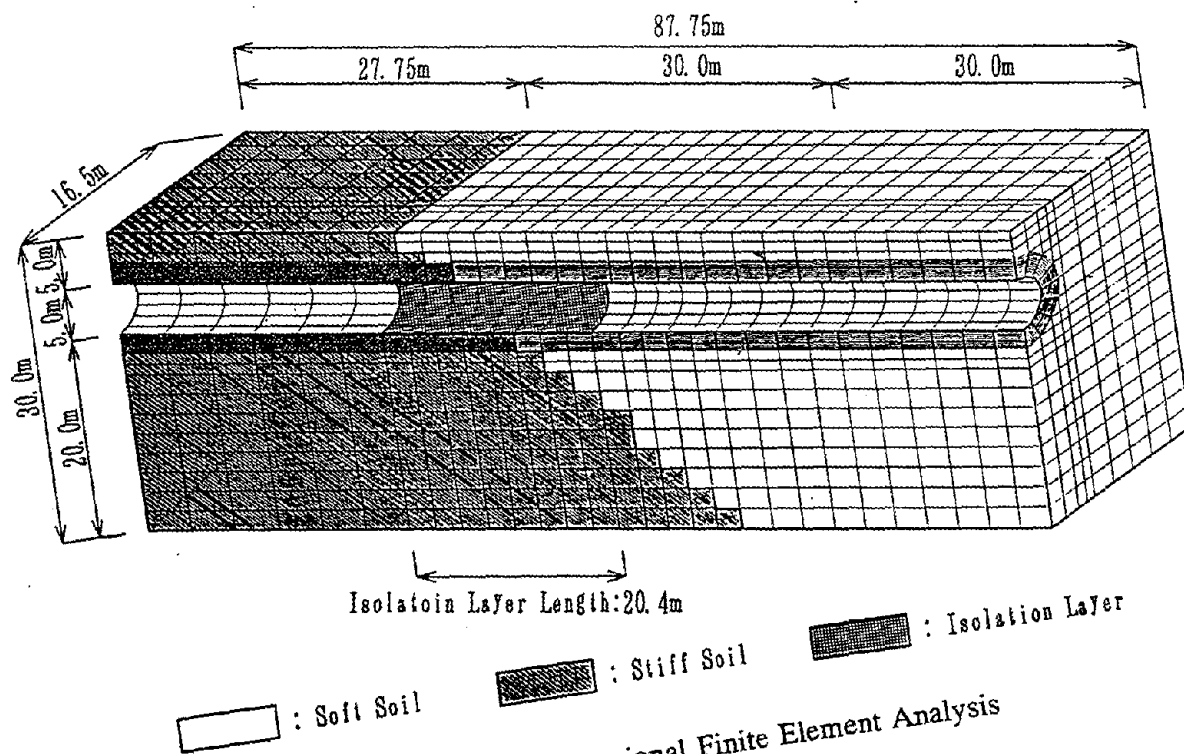


Fig.2 Model of 3-Dimensional Finite Element Analysis

Geological conditions and properties of the isolation layer used in the analysis are shown in Table 2. The properties of the soft and stiff soil correspond with clayey alluvium and sandy diluvium, respectively. The shear modulus ratio of the isolation layer to stiff soil is 0.01, so that the shear modulus of the isolation layer be 55.6 tf/m^2 . The poisson's ratio and the damping ratio of the isolation layer is assumed here to be 0.3 and 0.03, respectively, based on experimental results. The thickness of the isolation layer is 100mm, which is able to be constructed without enlargement of the tail void. The shield driven tunnel is isolated from the subsurface soil around the section of the geological transition, and total length of the isolation layer is 20.4m.

Table 3 shows structural conditions of the shield driven tunnel analyzed. The external diameter of the shield driven tunnel is 5.0m and the thickness of soil cover is 5.0m. The shield driven tunnel is fabricated by reinforced concrete segments with 225mm in thickness. It should be noted that the equivalent stiffness of the shield tunnel in the longitudinal direction is different from one in the transverse direction. To take account of such effect, the equivalent stiffness for the longitudinal (or transverse) direction was used for analyses in the longitudinal (or transverse) excitation.

An acceleration ground motion shown in Fig. 3 is used as an input into the base rock. The analyses were carried out for both longitudinal and transverse excitations. Analytical results were compared between isolated tunnel and unisolated.

Table 2 Geological Condition and Isolation Layer for Analysis

	Soft Soil	Stiff Soil	Isolation Layer
Shear Modulus tf/m^2	2,160	5,560	55.6
Unit Weight tf/m^3	1.6	1.8	1.0
Shear Elastic Wave Modulus m/s	115	174	23
Poisson's ratio	0.49	0.45	0.30
Damping	0.03	0.03	0.03

Table 3 Structural Condition of Tunnel

	Longitudinal Excitation	Transversal Excitation
Modulus t/m^2	195,000	3,000,000
Shear Modulus t/m^2	84,000	1,285,700
Unit Weight t/m^3	2.5	
Poisson's ratio	0.167	
Damping	0.03	

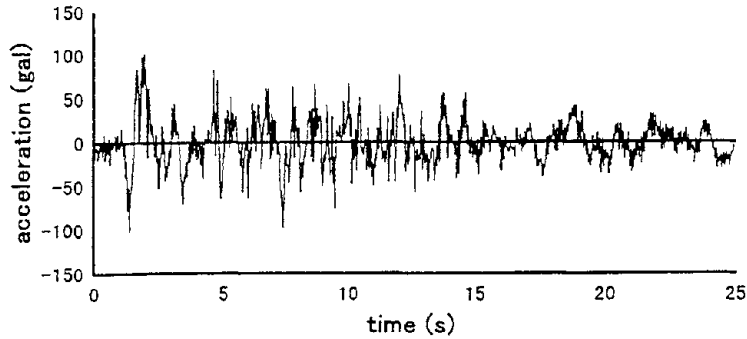


Fig.3 Input Acceleration Motion

ANALYTICAL RESULTS AND MECHANISM OF SEISMIC ISOLATION

Longitudinal Excitation

This paper focuses on the seismic response at the side of the shield tunnel, as illustrated in Fig. 4. Discussions are made based on peak response distributions in the longitudinal direction. Fig. 5 shows a difference of peak response acceleration between isolated and unisolated tunnel. Results of the free field analysis are also shown in the figure for comparison. It can be observed that the analytical result for the isolated is close to that for the unisolated, therefore the effect of the isolation layer on response acceleration is less significant. The peak response velocity is shown in Fig. 6, which also indicates the effect of the isolation is negligible.

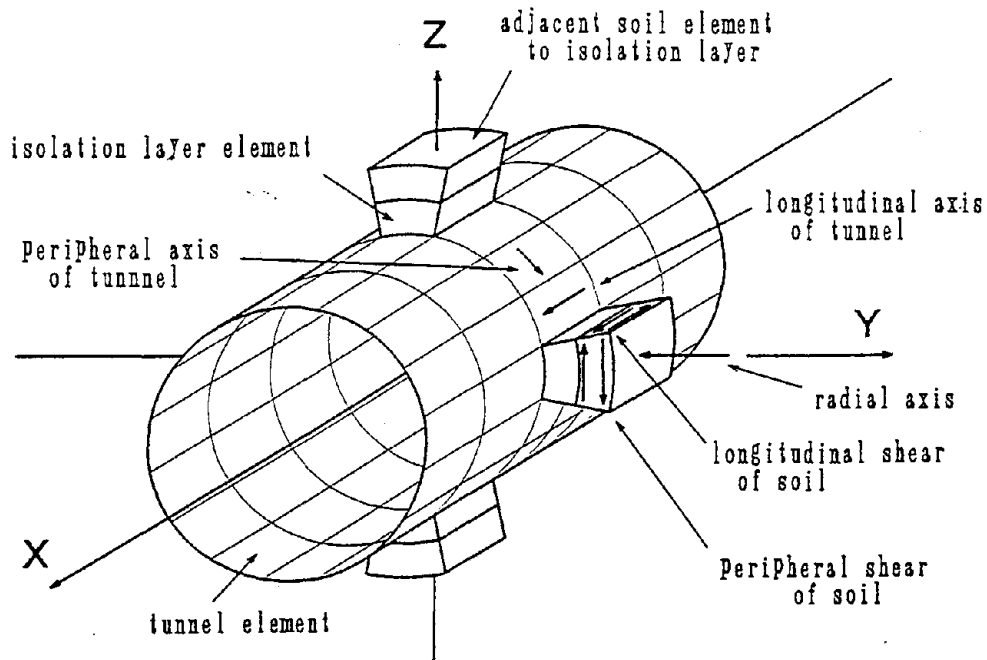


Fig.4 Elements of Tunnel, Isolation Layer and Soil

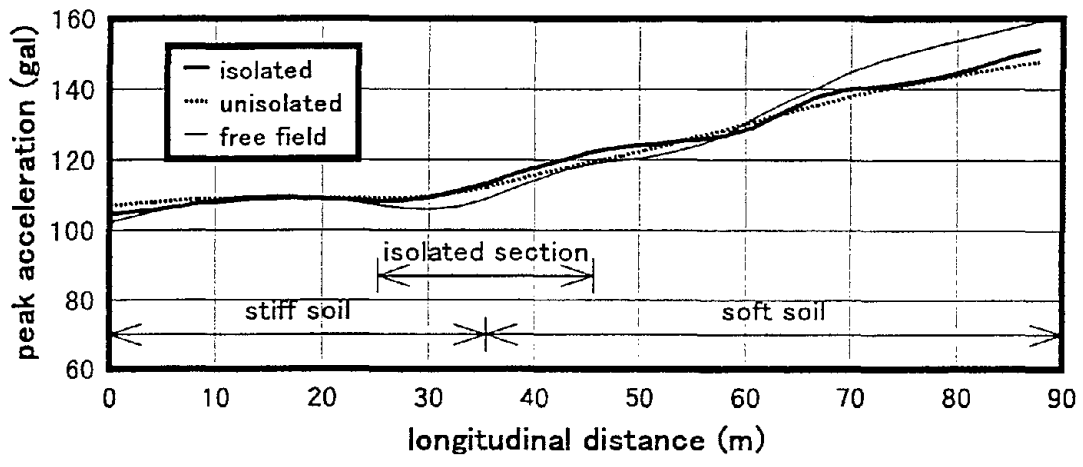


Fig.5 Response Acceleration Distribution

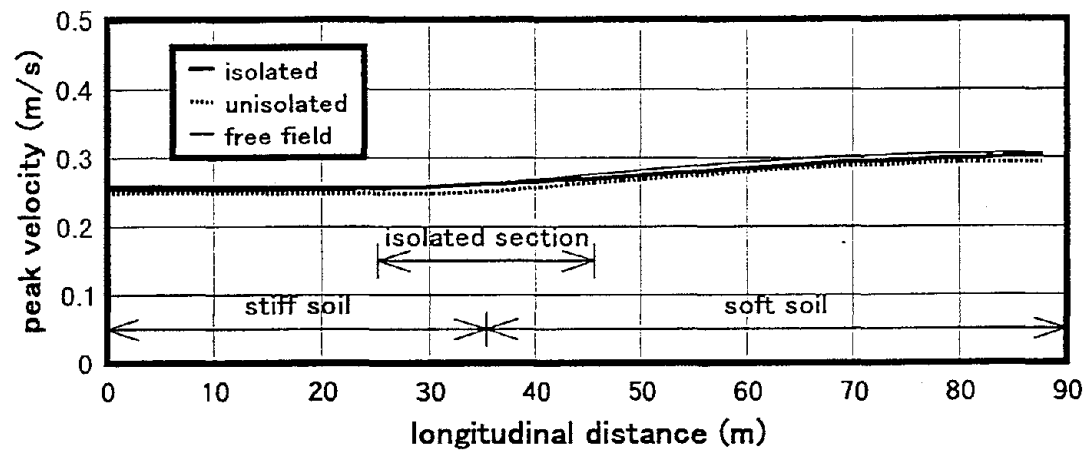


Fig.6 Response Velocity Distribution

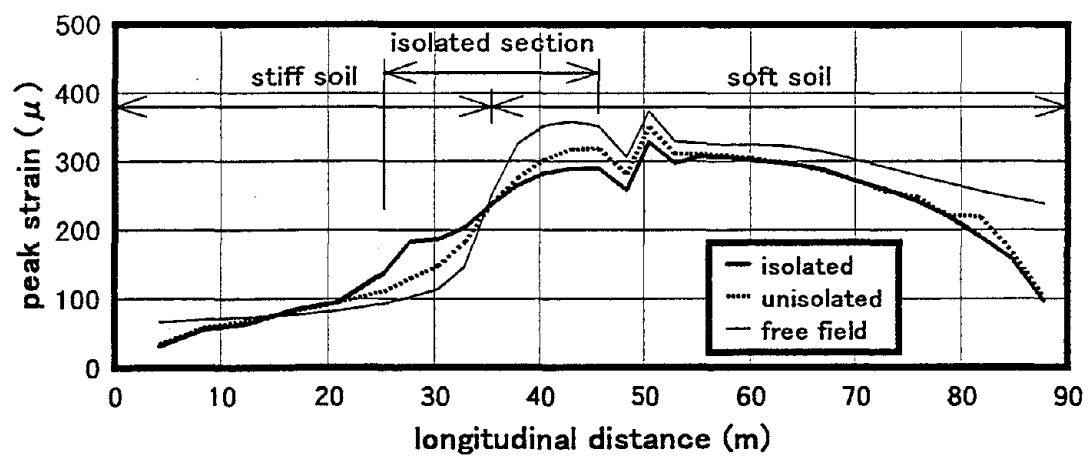


Fig.7 Longitudinal Strain Distribution

Fig. 7 shows a peak axial strain of tunnel in the longitudinal direction. It can be seen from the result for free field analysis that the largest axial strain is developed at the element in soft soil side. The distribution of the peak axial strain for the unisolated tunnel is similar to that for the free field, which means the unisolated tunnel deforms following the deformation of the free field. On the other hand, the axial strain of the isolated tunnel in the soft soil side decreases, as compared with unisolated. Also, the axial strain in the stiff soil side increases due to the isolation. Therefore, the isolation layer restrains a sharp peak of the axial strain.

Fig. 8 compares the shear strain in the longitudinal direction at the element for the isolation layer position between the isolated and unisolated tunnel. Comparison of the shear stress in the longitudinal direction is made in Fig. 9. The shear strain of the isolation layer is 10 to 20 times as much as that of the unisolated soil corresponding to the isolation layer position. On the other hand, it can be observed that the shear stress of the element is reduced by isolation, because the shear modulus ratio of the isolation layer to subsurface soil is as small as 0.01. It is noted that the peak shear stress is developed locally in sections of termination of the isolation layer. This is because the interaction forces were developed due to a significant difference of shear modulus between isolated and unisolated section.

Fig. 10 compares the axial force developed at tunnel shell elements. It can be seen that the peak axial force is reduced by the isolation. The reduction of axial force would be caused by following mechanism: the interaction between soil and tunnel would be mitigated due to large shear deformation of the isolation layer, and seismic deformation of the subsurface soil is not transmitted to the tunnel in the isolated section, so that seismic force would be reduced. However, it is noted that the reduction of the axial force is not significant in this analysis. This is because the longitudinal length of the isolation layer may be too short to produce the significant reduction. Based on the peak axial strain distribution in the longitudinal direction shown in Fig. 7, the isolation layer would be required to put into the soft soil side as long as possible.

Transversal Excitation

In transversal excitation for the tunnel crossing the geological transition as analyzed here, bending deformation would be developed at the tunnel section where the geological condition changes. Therefore, discussion was made for the shear behavior of the isolation layer at side and the axial force of the tunnel shell element at side.

Fig. 11 compares the shear strain in the longitudinal direction at the element of the isolation layer position between the isolated and unisolated tunnel. Comparison of the shear stress in the longitudinal direction is also shown in Fig. 12. The shear strain of the isolation layer is much larger than that of the soil at unisolated tunnel corresponding to the isolation layer position, which means the peripheral shear force transmitted to the tunnel would be reduced.

The axial forces developed at the tunnel side are compared between the isolated and unisolated in Fig. 13. It can be observed that the axial force at the element of tunnel side

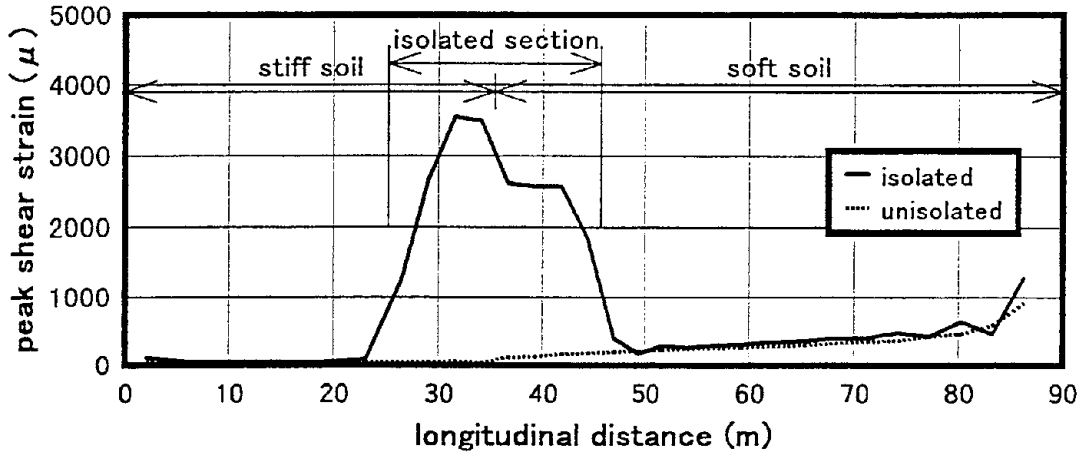


Fig.8 Distribution of Shear Strain at Element of Isolation layer Position

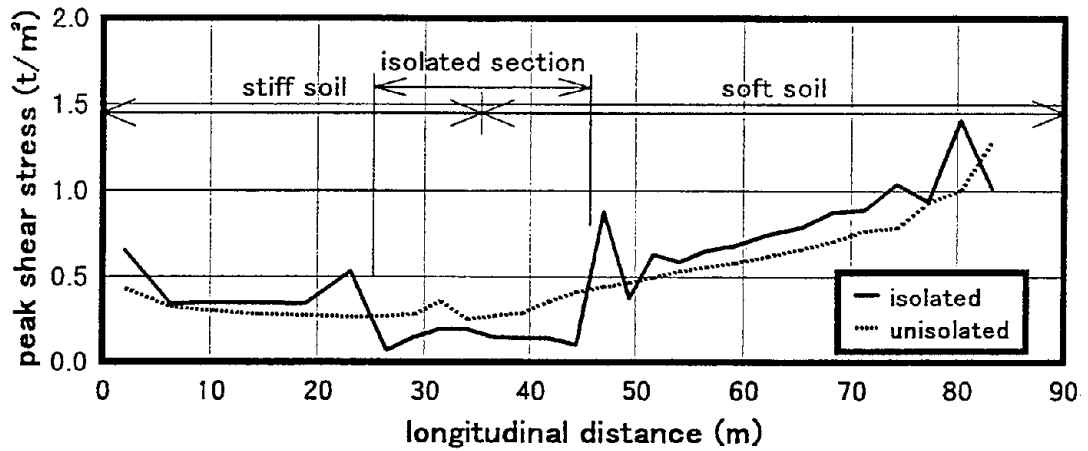


Fig.9 Distribution of Shear Strain at Element of Isolation layer Position

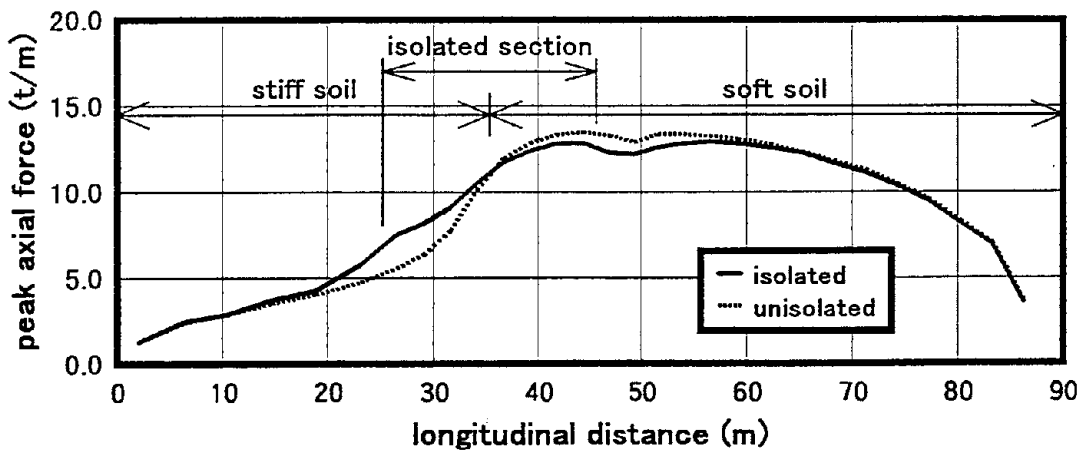


Fig.10 Distribution of Axial Force at Element of Tunnel Body

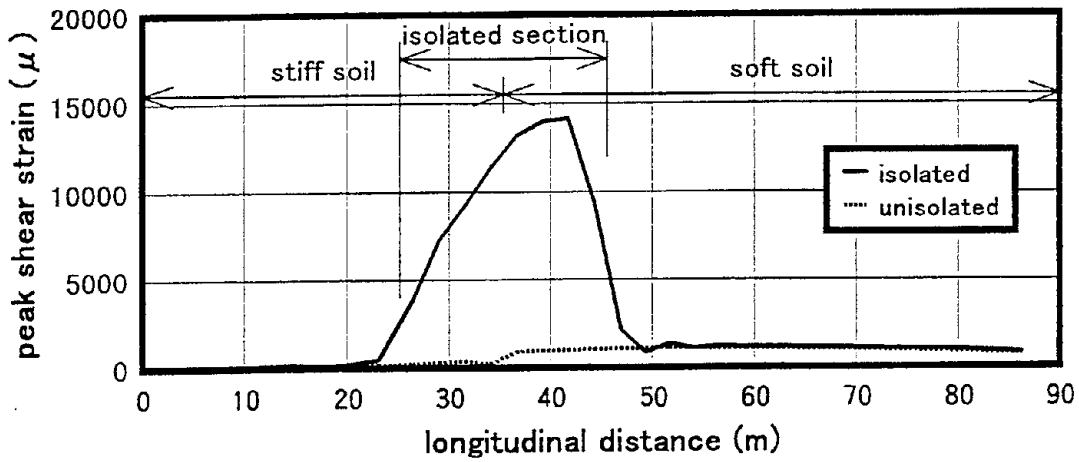


Fig.11 Distribution of Shear Strain at Element of Isolation layer Position

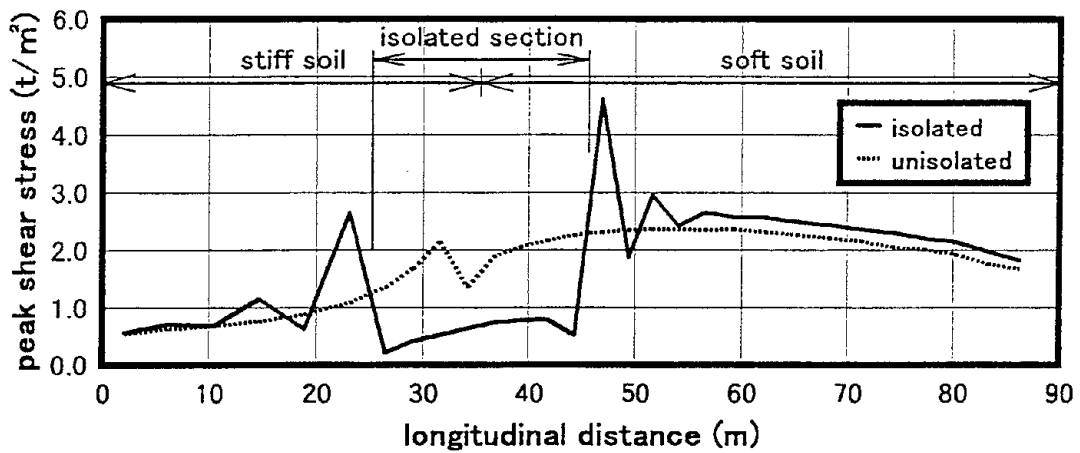


Fig.12 Distribution of Shear Strain at Element of Isolation layer Position

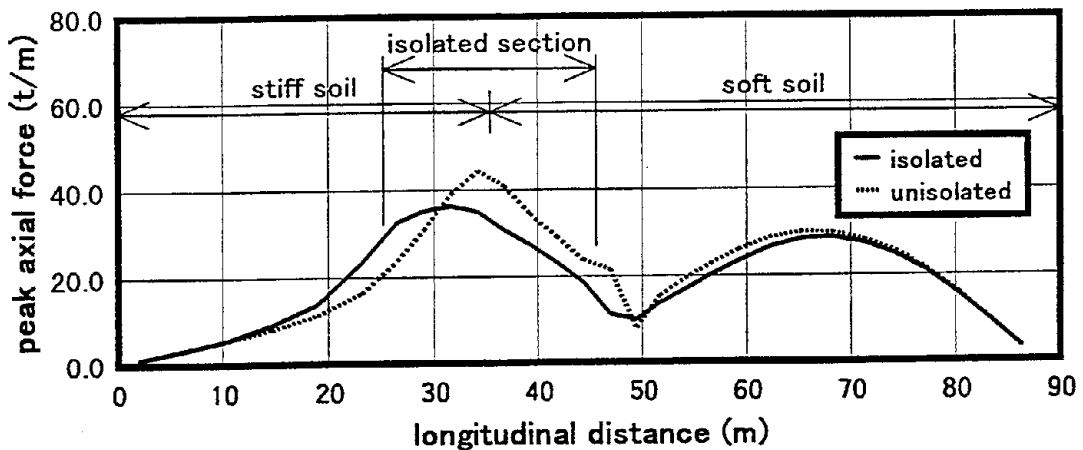


Fig.13 Distribution of Axial Force at Element of Tunnel Body

caused by the bending response is reduced by the isolation. Therefore, the isolation layer works efficiently for reducing the seismic effect in the transversal excitation as well as the longitudinal excitation.

Fig. 14 shows the axial force in the radial direction developed at the element of the isolation layer position. In the transversal excitation for the unisolated tunnel, the sharp axial force in the radial direction was developed at the section corresponding to the geological transition. On the other hand, it should be remarkable that such axial force was efficiently reduced at sections of the isolation. The reduction of the axial force would be derived from deformation of the isolation layer in radial direction, because the poisson's ratio of the isolation layer is 0.3, so that the volumetric strain is developed during the excitation.

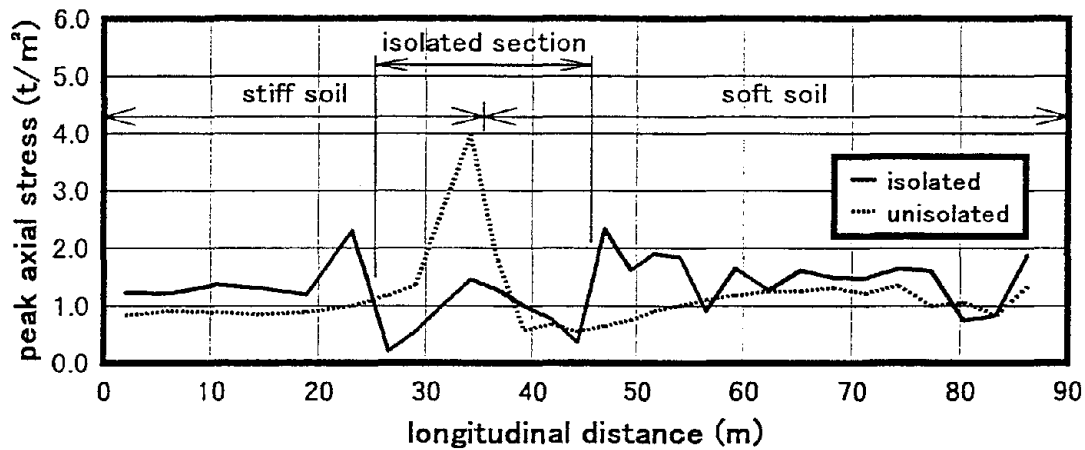


Fig.14 Distribution of Axial Force in Radial Direction at Element of Isolation layer Position

CONCLUDING REMARKS

This paper introduces the joint research program on the development of seismic isolation system for underground structures with the Public Works Research Center and 17 firms. The outline of the joint research program and the system of the seismic isolation are described. Furthermore, the mechanism of the seismic isolation is studied through the 3-dimensional finite element analysis. Following conclusions may be deduced from the studies presented herein:

(1) Appropriate materials to the seismic isolation system for underground structures were proposed; asphalt-based, urethane-based, silicone-based, liquid rubber and precast rubber panel. Construction methods for injecting these isolation materials were developed, and the feasibility of the construction was verified by the model tests.

(2) It was found out from the 3-dimensional analysis that the isolation layer would reduce the seismic force derived to the tunnel body in both longitudinal excitation and transversal one.

(3) The mechanism of the seismic isolation would be as follows: the interaction between soil and tunnel would be mitigated due to large shear deformation of the isolation layer, and seismic deformation of the subsurface soil is not transmitted to the tunnel in the isolated section, so that seismic force would be reduced.

ACKNOWLEDGMENTS

The research presented in this paper was one of products of the joint research program on development of seismic isolation system for underground structures. This program has been conducted by the Public Works Research Institute, the Public Works Research Center and following 17 firms; Asahi Denka Kogyo K.K., Japan Engineering Consultants Co., Ltd., Kawasaki Heavy Industries, Ltd., Komatsu Ltd., Konoike Construction Co., Ltd., Kumagai Gumi Co., Ltd., Maeda Co., Ltd., Nippon Civic Consultants Engineering, Nippon Koei Co., Ltd., Okumura Corporation, Oriental Consultants Co., Ltd., Sato Kogyo Co., Ltd., Shin-Etsu Chemical Co., Ltd., Sumitomo Rubber Industries, Ltd., Toa Doro Kogyo Co., Ltd., Tobishima Corporation, Tokai Rubber Industries, Ltd. The authors wish to appreciate all participants to the joint research program for their work.

REFERENCES

- 1) H. Otsuka, J. Hoshikuma and K. Nagaya: A Fundamental Study on innovative Menshin System for Underground Structures, 6th U.S.-Japan Workshop on Earthquake Disaster Prevention for Lifeline Systems, Osaka, Japan, July 1995
- 2) T. Suzuki and T. Tanaka: Research and Development of the Seismic Isolation System Applied to Urban Tunnels (Part-1: Development of Seismic Isolation Materials and Construction Methods), 7th U.S.-Japan Workshop on Earthquake Disaster Prevention for Lifeline Systems, Seattle, U.S.A., Nov. 1997
- 3) T. Tanaka and T. Suzuki: Research and Development of the Seismic Isolation System Applied to Urban Tunnels (Part-2: Effects of Seismic Isolation and Design Procedure), 7th U.S.-Japan Workshop on Earthquake Disaster Prevention for Lifeline Systems, Seattle, U.S.A., Nov. 1997

PERSONAL CAREER

NAME : Jun-ichi HOSHIKUMA

POSITION : Researcher
Earthquake Engineering Division
Earthquake Disaster Prevention Research Center
Public Works Research Institute
Ministry of Construction



ADDRESS : 1, Asahi, Tsukuba-shi
Ibaraki-ken
305 Japan
Tel. 0298-64-4966
Fax. 0298-64-4424

DATE OF BIRTH : March 12, 1968

EDUCATION : Bachelor of Engineering (1990, Kyushu University)
Master of Engineering (1992, Kyushu University)

MAJOR SUBJECT : Earthquake Engineering

MAJOR AREAS OF EXPERIENCE :

1992- Researcher, Earthquake Engineering Division

TRAVEL ABROAD :

U.S.A, Mexico, Italy

MAJOR PUBLICATIONS :

Stress-Strain Model for Confined Reinforced Concrete in Bridge Piers : Journal of Structural Engineering, Proceeding of ASCE, May 1997

Damage Analysis of R/C Bridge Piers by Kushiro-oki Earthquake Jan. 1993, and Hokkaido Nansei-oki Earthquake 1993 : 2nd Workshop on Seismic Retrofitting of Bridges

A seismic Retrofitting Method for Reinforced Concrete Bridge Piers and Their Analysis : 28th Joint Meeting of UJNR Panel

SEISMIC DESIGN OF LIQUID STORAGE TANKS

by

David P. Hu
City of San Diego

Bill Hendrickson
DYK Incorporated

ABSTRACT

This paper presents the approach of current seismic design and an innovative construction technique for circular prestressed concrete tanks. Seismic resistant design of liquid storage tanks has experienced significant changes over the past three decades. Earthquake damage to liquid storage tanks has been reported since the 1906 San Francisco earthquake. Older steel tanks that were not seismically designed suffered buckling at the bottom of the tank, in the shell, and in the roof from past earthquakes. Extensive storage tank damage has been observed in major earthquakes including the 1964 Alaska, the 1971 San Fernando, the 1989 Loma Prieta, the 1994 Northridge, and the 1995 Kobe earthquakes.

Liquid storage tanks seismically designed and constructed under the current American Water Works Association (AWWA) standards, such as AWWA D-100 for Welded Steel Tanks and AWWA D-110 for Wire-Wound Circular Prestressed Concrete Water Tanks, have performed very well during recent strong motion earthquakes. Failure to adopt seismic design standards for older water and wastewater storage tanks left many water and wastewater systems vulnerable to damage and/or failure during the previously mentioned earthquakes.

The significant effects of strong motion earthquakes in the last three decades or so, i.e. from 1964 to 1995, further confirmed extensive damage and disruption to the water and wastewater systems throughout California and abroad. The need for seismic retrofitting of older tanks, which were not seismically designed and constructed in the past, is anticipated by the engineering community. Beginning with the 1971 San Fernando earthquake and continuing with the 1989 Loma Prieta earthquake, the seismic design code

has undergone extensive modification and expansion. The current seismic design provisions are based on the AWWA D-100 and D-110 and the American Concrete Institute proposed ACI 350 codes. Adoption of current seismic design approaches would ensure that the structural integrity of important components within the water supply and wastewater system provides a reliable and consistent performance level with minimum damage.

Research and seismic design provisions may need additional investigation and improvement that reflect lessons learned from recent major destructive earthquakes in providing a safe and reliable lifeline system with adequate strength in order to avoid catastrophic damage and economic loss in the future.

INTRODUCTION

Potable water and wastewater tanks are essential lifeline facilities in any community. Circular prestressed concrete tanks, with their inherent structural efficiency, versatility and durability are an important means of liquid storage. The seismic design of these structures has evolved as our understanding of earthquakes and the structural response to them grows. This paper presents practical information on the development and use of current code design, requirements and preferred detailing and construction methods. Following state-of-the-art design and construction techniques, extended service life with minimal or no maintenance and that avoid the problems in the past can be expected.

Construction has been completed to upgrade the Alvarado Water Filtration Plant, which is the City of San Diego's oldest and largest drinking water treatment facility. Major renovation and rehabilitations will ensure that the plant will be able to meet the City's future water quality and capacity requirements, and operational needs. Two 21 MG regulatory reservoirs having 39 foot wall heights and flat roofs were innovatively designed and constructed by using machine-wrapped prestressed concrete walls. The City's Metropolitan Sewage upgrade serves the biosolid management needs of the existing Point Loma Wastewater Treatment Plant and the new North City Water Reclamation Plant which is currently complete and in operation, As an integral part of this upgrade, the Metropolitan Wastewater Department (MWW) designed and constructed two 140' diameter flow equalization basins which have 30' wall heights, hopper bottoms, flat roofs, machine-wrapped prestressed concrete walls and PVC-lined interior surfaces in the upper half of the

tanks. Furthermore, the two 10' diameter storage tanks, three 105' diameter digesters and two 45' diameter holding tanks for MWW's biosolids center jobsite are seismically designed and constructed to withstand the forces induced by a strong motion earthquake in Seismic Zone 4 in accordance with the Uniform Building Code (UBC). In California, the earthquake-resistant design approach has been significantly revised to reflect structural damage as occurred in past earthquakes. The seismic design of structures in the San Diego area has been upgraded to comply with Seismic Zone 4 requirements of the UBC. In order to ensure that all liquid storage tanks within the MWW's wastewater system perform well with structural integrity in the future, the City selected the proven technology, innovative design, and construction techniques of circular wire-wound prestressed concrete tanks. The seismic performance of circular prestressed concrete tanks has demonstrated their ability to resist the forces generated by earthquake ground motions and therefore the wastewater system will suffer insignificant damage and service disruption in the event of major earthquakes.

PRESTRESSED CONCRETE TANK DESIGN PHILOSOPHY

Under both static and seismic loading, water tanks are subjected to extremely large loads. Using the proper design and detailing, a prestressed concrete tank can carry these loads in a most efficient manner. The concrete core wall is placed in pure axial compression by wrapping high strength steel in pure axial tension around it. Therefore, both the concrete and steel are 100 percent utilized and in their most efficient states of stress. By comparison, when concrete is used in flexure to resist loads, only a small fraction of the concrete is effectively used to carry the load with the majority of the concrete simply used to space the steel away from the small compression zone. By utilizing construction equipment that applies the prestressing steel fully tensioned to the wall there is no friction losses and no variation in stress around the wall thereby allowing a more efficient wall. To improve the durability of the tank, galvanized prestressing strand is used for corrosion resistance. Current state-of-the-art technology includes the use of automated construction equipment that can apply the prestressing steel fully tensioned to within a tolerance of 1.5 percent at a rate of approximately 200 feet per minute (60 meters per minute). The prestressing steel is encased in a high cement content, high pH shotcrete applied with automated equipment holding the nozzle at the proper angle, distance and speed while building the shotcrete up in numerous, thin layers.

During a seismic event, the hoop stresses from the contained liquid increase and large translational forces and overturning moments develop. A typical water tank may be comparable in size to an industrial warehouse or large store, but due to the mass of the contained liquid, the seismic forces developed may be an order of magnitude larger.

HYDRODYNAMIC DESIGN PHILOSOPHY

Some of the earliest analysis of hydrodynamic loads was done by Jacobsen.¹² In the United States and elsewhere, the basic analysis of the hydrodynamic loads on liquid storage tanks follows the work of Housner.^{3,4} Later work by Haroun and Housner and Veletsos and Yang⁶ expanded on this work by including the influence of structural amplification and ductility. This theoretical work became the basis of the practical design requirements contained in the seismic portions of the tank design code AWWA D110-95 and the proposed ACI 350 code. A portion of the liquid is assumed to act impulsively with the tank structure and the remainder of the liquid is assumed to slosh back and forth producing convective forces. The relative size of the impulsive and convective portions of the liquid is a function of the tank height to diameter ratio. The impulsive and convective loads are linearly related to the seismic zone factor Z and the importance factor I . The impulsive and convective loads are also linearly related to impulsive and convective structure coefficients (C_i and C_c) and inversely related to impulsive and convective ductility factors (R_i and R_c).

STRUCTURAL ACCELERATION

The seismic zone factor Z , represents the maximum effective peak acceleration (EPA) corresponding to a site dependent ground motion having a 10 percent probability of exceedance in 50 years or a 475 year return period. Some Owners or Engineers may select a more restrictive criteria. The importance factor I is typically selected as unity or 1.25. The importance factor may also be thought of as a probability factor with a value of 1.25 effectively cutting a 10 percent probability of exceedance in 50 years to 5 percent.

STRUCTURAL FLEXIBILITY

Veletsos and Yang⁶ established that the impulsive forces developed during an earthquake would be amplified due to the shell flexibility and this amplification could be approximated

using the site response spectra. The impulsive structure coefficient (C_I) follows the form common to conventional building design with an assumed 5 percent damping. The convective structure coefficient (C_C) does not have such an analogy to building design but instead is a function of the structural geometry. The equations used to derive C_C are derived from Housner's work.

STRUCTURAL DUCTILITY

The impulsive ductility factor was determined based on consideration of not only ductility but redundancy, load path, energy absorption capacity and historical performance of structures. Over the evolution of the design of prestressed concrete tanks, various wall to footing connections generally classified in broad terms as fixed, pinned or free have been utilized. The earliest tanks typically used some form of rigid connection (fixed or pinned) partially to reduce prestressing requirements and partially to ease construction. Although this generally proved adequate for smaller tanks, problems began to develop as tank capacities grew. With larger tanks, the restraint to radial motion caused by a rigid base connection produced vertical bending in the wall that could lead to horizontal cracking and leakage. The vertical bending would be present under static loads and would be exacerbated under seismic loading.

BASE SHEAR RESTRAINT

To mitigate the problem of vertical bending, walls are supported on neoprene bearing pads that allow free radial movement with minimum vertical bending in the wall. To resist the tank sliding off the wall under horizontal acceleration, high strength flexible cables pass from the wall to the footing with the cables surrounded by a soft neoprene sleeve at the joint. This detail is very similar in construction to the base isolation systems now in vogue for building design. However, where a building base isolation system is often used to lengthen the structure period thereby lowering the structure response (lowering C_I), this is typically only of secondary importance for tank seismic cables. The primary purpose of the cables is to resist the lateral forces at the base of the wall in the plane of the wall, not normal to the wall. By directing the forces to where the wall is the strongest, vertical bending will be reduced and the restraint linkage will not damage the wall as it is engaged. This last point is described in the following quote from Park and Pauley⁷:

“The conventional approach to seismic-resistance design - namely, relying on ductile behavior of the structural members for energy dissipation - has the obvious disadvantage that the structure will be damaged during a major earthquake and will need to be repaired. The damage may even be so serious that the structure must be demolished. An alternative approach is to separate the load-carrying function of the structure from the energy-dissipating function. This can be achieved by incorporating into the structure special devices for dissipating the energy generated in the structure by the earthquake motions. These devices would protect the structures from damage.”

The performance of this various tank base configurations is reflected with AWWA D110-95 assigning the highest R_f value to the free base, seismic cable detail and a caution against a rigid base connection in high seismic zones. As structural ductility has little impact on the relatively smaller convective load, the R_c value is set at 1.0 for all base types.

WALL HOOP STRESSES

With the impulsive and convective base shear determined, the shear values can be distributed over the wall height using Housner's distributions or a linear approximation of his distributions. The seismic hoop stresses vary around the tank from a maximum suction to zero, to a maximum outward pressure. The prestressing is designed assuming the maximum outward pressure acts all around the tank. This distributed force is used to determine the increase in hoop force up the wall. In addition to the impulsive and convective pressures, the vertical acceleration adds to the hoop force. Data from recent earthquakes showing vertical accelerations with values at a significant fraction of the horizontal acceleration in the near field region highlight the importance of including the vertical component in the design. Due to the difference in periods of the three components, it is assumed the maximum value from each of the components will not occur concurrently and they are therefore added using the root mean square method. Under the increased seismic load, the wall is designed as partially prestressed for the short term seismic load. Again, the prestressed wall proves to be extremely efficient in handling large loads. Typically, no additional prestressing is required for tanks designed for ground accelerations up to 0.3 g.

OTHER DESIGN CONSIDERATIONS

Under seismic loading, in addition to the stresses imposed on the wall described above, the tank will be subjected to buckling and overturning. These are rarely a factor in design as they are in steel tank design as the thickness of the prestressed concrete wall resists buckling and the structural self-weight of the structure resists overturning. In unusual circumstances such as tall structures or very high seismic accelerations, overturning may become a concern but the problem can be mitigated by adding mass to the tank base.

HISTORICAL PERFORMANCE

The appropriateness of the design procedure has been demonstrated by the successful performance of existing structures. We are unaware of any significant structural damage to occur to any prestressed tank subject to earthquake ground motion. This includes dozens of tanks located near the epicenters of the San Fernando, Whittier Narrows, Loma Prieta and Northridge earthquakes. Brown, Davis, Rugar and Rulla⁸ reported no significant damage to any of the prestressed tanks the Los Angeles Department of Water and Power owns that experienced the Northridge earthquake. The Earthquake Engineering Research Institute⁹ reported similar successful results for prestressed concrete tanks. Demonstrating the reserve capacity of prestressed tanks, it is interesting to note that even with both recorded horizontal and vertical accelerations exceeding 1.0 g, there was no damage even to 40 year old tanks that never considered seismic loading in their initial design. Older steel tanks subjected to this large, but not the "Big One" seismic event did not fare as well.

A partial list of prestressed concrete tanks located near the epicenter of the Northridge earthquakes follows. We are unaware of any significant damage to any prestressed concrete tank during a seismic event.

TANK	CAPACITY	YEAR BUILT	REMARKS
Roscomare	1.0 mg (3.8 ml)	1956	No damage
Firenze	1.0 mg (3.8 ml)	1958	No damage
Simi Valley	0.5 mg (1.9 ml)	1962	No damage
Monterey Park	1.5 mg (5.7 ml)	1966	No damage

TANK	CAPACITY	YEAR BUILT	REMARKS
Westlake Village	5.0 mg (18.9 ml)	1970	No damage
Lower Franklin	1.0 mg (3.8 ml)	1976	No damage
Westlake Village	2 at 4.0 mg (15.1 ml)	1977	No damage
Westlake Village	1.2 mg (4.5 ml)	1983	No damage
Pacific Palisades	1.0 mg (3.8 ml)	1984	No damage
Ascot	10.0 mg (37.9 ml)	1989	No damage
Thousand Oaks	1.5 mg (5.7 ml)	1989	No damage
(Zone II)			
Pacific Palisades	1.0 mg (3.8 ml)	1989	No damage
Susana	10.0 mg (37.9 ml)	1989	1.0g (H), 0.5g(V), 40' above ground No damage
Glendale	6.0 mg (22.7 ml)	1989	No damage
Thousand Oaks	1.5 mg (5.7 ml)	1989	No damage
(Lake Sherwood)			
Maclay	2 at 10.0 mg (37.9 ml)	1991	0.6g (H), 0.4g (V), minor architectural movement - no damage
Thousand Oaks	6.0 mg (22.7 ml)	1992	No damage
(Potrero)			
Tujunga	4.0 mg (15.1 ml)	1992	No damage
Thousand Oaks	5.3 mg (20.1 ml)	1993	No damage
(Shopping Center)			

Even with the successful performance of prestressed tanks, as new geotechnical information raises the design level earthquakes, consideration is given to upgrading of existing tanks. This is similar to Caltrans upgrading bridges built prior to current seismic design standards. The East Bay Municipal Utility District located in Oakland, California, which has a large inventory of older tanks, has undertaken a major program to upgrade not only tanks but pumps and pipelines as well¹⁰.

DESIGN EXAMPLES

The City of San Diego has recently constructed several new tanks for potable water and wastewater storage. What follows are some design results demonstrating the calculation of seismic forces on some of these tanks. The design procedure follows the guidelines of AWWA D110-95. The base shear is calculated using equations similar to the standard UBC base shear equation except the two components (impulsive and convective) must be accounted for.

DESIGN EXAMPLE - BASE SHEAR

$$V_I = \frac{Z \cdot I \cdot C_I (W_S + W_R + W_D)}{R_I} \quad (\text{Eq 4-1})$$

where;

V_I = impulsive base shear

Z = zone factor (from zone map)

R_I = structure impulsive ductility coefficient
= 2.0 for unanchored and uncontained base
= 2.75 for reinforced nonsliding base
= 4.5 for anchored flexible base

C_I = impulsive structure coefficient (function of impulsive period but typically at 2.75 maximum)

I = importance factor
= 1.0 for tanks that must remain usable but suffer repairable damage
= 1.25 for tanks that must remain usable with slight damage

W_S = weight of tank shell

W_R = weight of tank roof

W_I = impulsive weight = $W_T \cdot (W_I/W_T)$

W_T = total weight of water

W_I/W_T = impulsive weight ratio (function of tank geometry, see AWWA D110 figure 7)

$$V_c = \frac{Z \cdot I \cdot C_c \cdot W_c}{R_c} \quad (\text{Eq 4-2})$$

where;

V_c = convective base shear

Z = zone factor (from zone map)

I = importance factor

= 1.0 for tanks that must remain usable but suffer repairable damage

= 1.25 for tanks that must remain usable with slight damage

C_c = convective structure coefficient = $4S/T_c^2$

S = soil profile coefficient

= 1.0 for rock or dense soil less than 200 feet (61 m) in depth

= 1.2 for dense soil more than 200 feet (61 m) in depth

= 1.5 for a soil profile 70 feet (21 m) or more in depth and containing more than 20 feet (6 m) of soft to medium-stiff clay but not more than 40 feet (12 m) of soft clay

= 2.0 for soil containing more than 40 feet (12 m) of soft clay

T_c = convective period (see AWWA D110 figure 6)

R_c = structure convective ductility coefficient

= 1.0 (for all base types)

W_c = convective weight = $W_T \cdot (W_c/W_T)$

W_T = total weight of water

W_c/W_T = convective weight ratio (function of tank geometry, see AWWA D110 figure 8)

$$V_T = ((V_I)^2 + (V_C)^2)^{1/2} \quad (\text{Eq 4-3})$$

where;

V_T = total base shear

V_I = impulsive base shear

V_C = convective base shear

	Point Loma <u>Water Storage</u>	<u>Digester 8</u>	105' Ø Digester <u>FIRP</u>	<u>Alvarado</u>
Capacity	650,000 gal (2.5 ml)	4.3 mg (16.3 ml)	3.3 mg (12.5 ml)	2 at 21.0 mg (79.5 ml)
Inside Diameter	61.00 ft (18.6 m)	125.0 ft (38.1 m)	105.0 ft (32.0 m)	155.5 ft (47.4 m)
Sidewater Depth	30.25 ft (9.2 m)	42.0 ft (12.8 m)	48.0 ft (14.6 m)	38.0 ft (11.6 m)
Corewall Thickness	12 in (305 mm)	16 in (400 mm)	12" (305 mm)	28" to 10" (710 mm to 250 mm)
Roof Load	2.0 ft soil plus 100 psf LL (0.6 m soil plus 4.8 kpa LL)	fixed steel	30 inch water column up (760 mm water column up)	2.5 ft soil plus 100 psf LL (0.76 m soil plus 4.8 kpa LL)
W _T	5662 k	3.608e+04 k	3.061e+04 k	1.804e+05 k
W _C	2439 k	2.185e+04 k	1.462e+04 k	1.428e+05 k
W _I	3110 k	1.174e+04 k	1.610e+04 k	2.545e+04 k
W _R	1760 k	232.0 k	4679 k	5.311e+04 k
W _S	1117 k	4363 k	3004 k	1.099e+04 k
R _C	1.0	1.0	1.0	1.0
R _I	4.5	4.5	4.5	4.5
T _C	4.618 sec	7.030 sec	6.095 sec	15.69 sec
C _C	0.2251	0.09710	0.1077	0.01950
C _I	2.75	2.75	2.75	2.75
I	1.25	1.25	1.25	1.25
Z	0.50	0.42	0.50	0.40
V _I	2286 k	5241 k	9265 k	2.736e+04 k
V _C	343.1 k	1114 k	984.1 k	1392 k
V _T	2311 k	5358 k	9318 k	2.739e+04 k

DESIGN EXAMPLE - HOOP STRESS

To determine the hoop loads in the tank shell, the equations below, similar in form to the base shear equations, are used to find the maximum hoop loads, summed over the full wall height. In addition to the impulsive and convective components, the vertical acceleration must be accounted for. The vertical acceleration is assumed to act uniformly all around the tank and thereafter will not contribute to base shear but will add to the hoop loads. The summed hoop loads can be distributed using Housner's distribution. Alternatively, the total force can be distributed using a trapezoidal distribution with the same centroid as Housner's distribution. AWWA D110-95 contains graphs showing the centroid for various height to radius ratios.

$$N_I = \frac{ZIC_1}{R_I} \frac{(W_S + W_R + W_I)}{2} \frac{1}{\pi} \quad (\text{Eq 4-24})$$

where;

N_I = maximum impulsive hoop load, summed over the full wall height

Z = zone factor (from zone map)

I = importance factor

= 1.0 for tanks that must remain usable but suffer repairable damage

= 1.25 for tanks that must remain usable with slight damage

C_1 = impulsive structure coefficient (function of impulsive period but typically at 2.75 maximum)

R_I = structure impulsive ductility coefficient

= 2.0 for unanchored and uncontained base

= 2.75 for reinforced nonsliding base

= 4.5 for anchored flexible base

W_S = weight of tank shell

W_R = weight of tank roof

W_I = impulsive weight = $W_T(W_I/W_T)$

W_T = total weight of water

W_I/W_T = impulsive weight ratio (function of tank geometry, see figure 7)

$$N_C = \frac{Z \cdot I \cdot C_C \cdot W_C}{R_C} \cdot \frac{8}{9\pi} \quad (\text{Eq 4-25})$$

where;

N_C = maximum convective hoop load, summed over the full wall height

Z = zone factor (from zone map)

I = importance factor

= 1.0 for tanks that must remain usable but suffer repairable damage

= 1.25 for tanks that must remain usable with slight damage

C_C = convective structure coefficient = $4S/T_C^2$

S = soil profile coefficient

T_C = convective period (see figure 6)

R_C = structure convective ductility coefficient 1.0 (for all base types)

W_C = convective weight = $W_T \cdot (W_C/W_T)$

W_T = total weight of water

W_C/W_T = convective weight ratio (function of tank geometry, see figure 8)

$$N_V = \frac{\mu_V \cdot \gamma \cdot H^2 \cdot R}{2} \quad (\text{Eq 4-26})$$

where;

N_V = maximum vertical hoop load, summed over the full wall height

μ_V = design vertical acceleration = $\frac{Z \cdot I \cdot C_V}{R_V} \cdot B$

γ = density of contained liquid

Z = zone factor (from zone map)

C_V = vertical structure coefficient

R_V = structure vertical ductility coefficient

B = vertical acceleration ratio = 0.25 for $Z = 1, 2A$ and $2B$

0.50 for $Z = 3$

0.60 for $Z = 4$

H = water depth

R = inside tank radius

$$N_T = ((N_D)^2 + (N_C)^2 + (N_V)^2)^{1/2} \quad (\text{Eq 4-27})$$

CONCLUSION

Water and wastewater tanks are critical facilities in all communities. Replacement or major rehabilitation of facilities damaged in an earthquake would leave the community without these lifeline facilities for a lengthy period of time creating hardship and health concerns. The design and construction of prestressed concrete tanks has matured and been proven over time such that when proper techniques are employed, a low maintenance, long-lived structure will result. Some key elements to include in a quality design include:

- Free base of wall to footing and top of wall to roof joints with flexible connections that allow free radial motion but resist translational forces
- Galvanized for durability and seven wire strand for bond and redundancy of all circumferential prestressing and seismic restraint systems
- Accurate stressing with continuous monitoring and correction of all prestressing that ensures efficient design and prevents overstressing
- High cement content, high pH shotcrete applied with fully automated equipment to protect the steel
- High strength vertical threadbars to resist tensile stresses from vertical bending
- Seismic design following the procedures of AWWA D110-95

With proper design and construction, prestressed concrete tanks are especially well suited for the large loads present under both static and seismic conditions.

REFERENCES

1. Jacobsen, L.S., "Impulsive Hydrodynamics of Fluid Inside a Cylindrical Tank and of Fluid Surrounding a Cylindrical Pier," BSSA, Vol. 39, No. 3, July 1949, pp. 189-204.
2. Jacobsen, L.S., and Ayre, R.S., "Hydrodynamic Experiments with Rigid Cylindrical Tanks Subjected to Transient Motions," BSSA, Vol. 41, 1951.
3. Housner, G.W., "Dynamic Pressures on Accelerated Fluid Containers," BSSA, Vol. 47, Jan. 1957, pp. 15-35.
4. Housner, G.W., "Dynamic Pressure on Fluid Containers," Technical Information (TID) Document 7024, Chapter 6, and Appendix F, U.S. Atomic Energy Commission, 1963.
5. Haroun, M.A. and Housner, G.W., "Seismic Design of Liquid Storage Tanks," Journal of the Technical Councils of ASCE, Vol. 107, No. TCI April 1981, pp. 191-207.
6. Veletsos, A.S., & Yang, Y., "Dynamics of Vertically Excited Liquid Storage Tanks," ASCE Journal of Structural Engineering, Vol. 110, No. 4, April 1984, pp. 706-714.
7. Park, R., and Paulay, T., Reinforced Concrete Structures, John Wiley and Sons, Inc., New York, 1975, 769 pp.
8. Brown, K.J., Rugar, P.J., Davis, C.A. and Rulla, T.A., "Seismic Performance of Los Angeles Water Tanks," Lifeline Earthquake Engineering, ASCE, 1995, pp. 668-675.
9. Earthquake Engineering Research Institute, "Supplement C to Volume 11, Northridge Earthquake Reconnaissance Report, Volume I.," EERI, 1995, pp. 162-168.
10. East Bay Municipal Utility District, "1996 Annual Progress Report, Seismic Improvement Program," EBMUD, 1996.

David P. Hu

Date of Birth: September 27, 1939
Birth place: Kwangshi, China
Education: Degrees
National Taiwan University, B.S.
Civil Engineering, 1961
Colorado State University, M.S.
Structural Engineering, 1965
University of Wisconsin, Ph.D.,
Engineering Mechanics, 1972
Position: Chief Structural Engineer and Senior Project Manager
Metropolitan Wastewater Department (MWWD)
City of San Diego, CA



Dr. Hu is responsible for the planning, technical support, project management of the Clean Water Program, MWWD, in the area of structural engineering, earthquake and geotechnical engineering, computer aided design and drafting, QA/QC, and GIS applications.

Dr. Hu has extensive engineering management experience in the private industry prior to joining MWWD, City of San Diego in 1991. His consulting experiences include technical consultation in design, engineering and management as president of Pacific Versatech, Inc. and DDH Enterprise, Inc., 1987 to 1989; Structural Engineering Department Manager, M&E, Inc., 1989 to 1991; Project Manager, Jaykim Engineering 1987 to 1989; Engineering Supervisor in Structural and Earthquake Engineering, SDG&E, 1976 to 1987; Senior Structural Engineer, United Engineers and Constructors, 1973 to 191976; Senior Engineer, Bechtel Power Corporation 1972 to 1973; Research Fellow, Department of Engineering Mechanics, University of Wisconsin, Madison, 1968 to 1972; Civil Engineer, BES Engineering Corporation, 1962 to 1964.

Dr. Hu has extensive knowledge of domestic and international markets in engineering and design and has provided effective consultation services in transportation, energy related projects, environmental engineering and earthquake engineering. He developed and conducted seminars on earthquake engineering, land-use management, wastewater facilities design for the private companies and other agencies both domestic and abroad. He has published technical papers involved in structural and earthquake engineering. Selected papers are listed as follows:

* "A Higher Order Theory for Circular Cylindrical Shells", The Fourth Canadian Congress of Applied Mechanics, Montreal, 1973; * "Repair of Deteriorated Power Plant Circulating Water Structures", ACI Fall Convention, 1982, Detroit, Michigan; * "Retrofit of Turning Vanes in the Combined Units Chimney System", ASCE, Fall Convention, 1982; * "Computer Modeling of Width Formation for Alluvial Rivers", ASCE, Special Conference, 1985; * "Seismic Risk Assessment of LNG Storage Tanks", Eighth World Conference on Earthquake Engineering, 1984; * "Cylindrical Shells Subjected to Tangential Surface Loads", The Southeastern Conference on Theoretical and Applied Mechanics, 1984; * "Seismic Risk Analysis of LNG Tanks", ASCE Spring Convention, 1986; * "Dynamic Tests of LNG Storage Tanks for Earthquake Analysis of Liquid-Tank-Pile-Soil Interaction", The Third ASCE Engineering Mechanics Specialty Conference, UCLA, March 1986; * "Seismic Design and Retrofit of Tunnels and Highway Bridges", Joint Conference on Transportation, NACTPA 1994; * "Earthquake Vulnerability and Seismic Resistant Design of Highway Bridges", The First Asian Pacific Transportation Development Conference, 1995; * "Seismic Resistant Design of Highway Bridges", Transportation Development and Technology Transfer Conference, 1997.

Dr. Hu is a member of ACI, ASCE, EERI, PMI, TCLEE/ASCE and is registered as Civil Engineer and Professional Engineer in the States of California and Wisconsin, and Adjunct Faculty Member, San Diego State University.

RESEARCH AND DEVELOPMENT ON THE SEISMIC ISOLATION SYSTEM APPLIED TO URBAN TUNNELS (PART-1: DEVELOPMENT OF SEISMIC ISOLATION MATERIALS AND CONSTRUCTION METHODS)

Takeyasu SUZUKI¹⁾ and Tsutomu TANAKA²⁾

1) Manager, Earthquake Engineering Research Group, Technical Research and Development Institute, Kumagai Gumi Co., Ltd.

2) Director, Central Research and Development Department, Oriental Consultants Co., Ltd.

ABSTRACT

Techniques for improving seismic safety of urban tunnels have hitherto been limited to those for increasing the flexibility of tunnel structures by applying flexible joints and segments. However, since such techniques are insufficient for ensuring seismic safety of underground lifelines in urban areas when strong earthquakes occur, there has been a demand for developing a new, highly reliable technique, especially for protecting tunnel sections where seismic strain is concentrated locally. Given this situation, an innovative joint research project between the Public Works Research Institute and private companies was commenced to develop a seismic isolation system to be applied to urban tunnels. This paper describes the tunnel sections where seismic isolation can be applied effectively, seismic isolation materials developed by the joint research, and validation experiments conducted to confirm the feasibility of the methods for applying these materials.

INTRODUCTION

Several researchers have been investigating the application of a seismic isolation system to underground structures since around 1988, and the effectiveness of seismic isolation has been confirmed by numerical analyses and laboratory experiments¹⁾⁻⁵⁾. As shown in Fig. 1, the fundamental principle of the seismic isolation system for underground structures is to cut off the transmission of ground strain by isolating a tunnel body from the peripheral soil by forming a thin, soft layer around the tunnel.

In the case of axial or bending deformation of a tunnel that occurs in the longitudinal direction due to earthquakes, tunnel sectional forces can be effectively reduced when a seismic isolation

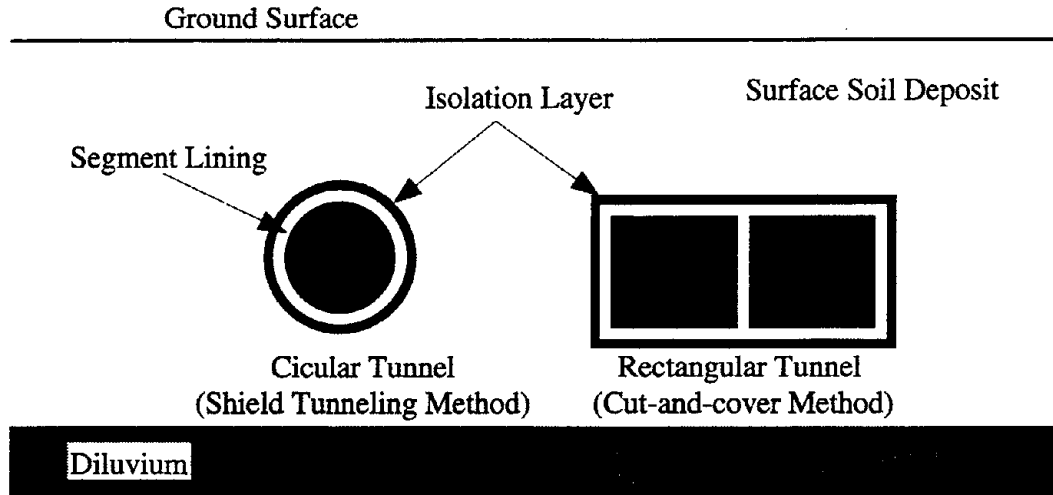


Fig.1 Schematic diagram to demonstrate the seismic isolation system for urban tunnels

layer is applied to a tunnel section where ground strain is concentrated locally. This is not only because the ground strain transmission to the tunnel body is cut off, but because the tunnel strain in the isolated section is dispersed.

In a similar vein, when cross-sectional deformation of a tunnel occurs, the results of numerical analyses have shown that the seismic isolation system helps to reduce the sectional forces concentrated at the corner portions in a tunnel with a rectangular cross-section constructed by the cut-and-cover method, thus contributing greatly to the reduction of sectional forces at the upper and lower slabs and side walls of such a tunnel^{6),7)}.

Meanwhile, earthquake response analyses were conducted to examine the effectiveness of the application of seismic isolation system to a subway tunnel that was severely damaged by the Hyogoken-nanbu earthquake of 1995⁶⁾. In the case of tunnels with a circular cross-section such as shield-driven tunnels, however, there was a report that the application of seismic isolation was not so effective in reducing sectional forces during cross-sectional deformation due to earthquakes⁸⁾.

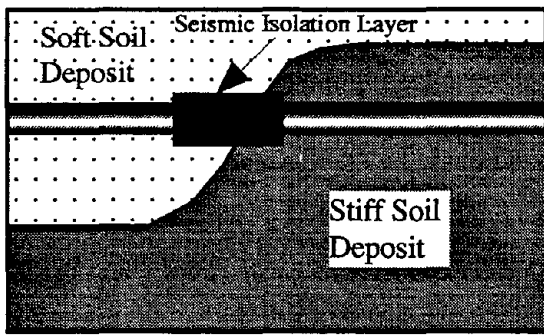
Since there has been no systematic research on the seismic isolation system, with which a thin seismic isolation layer is formed covering a tunnel body, studies on this system as described above, development of materials for the seismic isolation layer, and validation tests for developing construction methods have been conducted separately by various institutions^{8),9)}. Thus, a comprehensive three-year project for clarifying the seismic isolation mechanism, and for developing seismic isolation materials, application methods, and seismic design, was started in July 1995 as a joint research project between the Public Works Research Institute of the Ministry of Construction and 17 private-sector companies in Japan. This paper will examine the results of this joint research, focusing on the tunnel sections where the application of the seismic isolation is effective, as well as the development of seismic isolation materials and validation tests conducted for confirming the feasibility of application methods.

TUNNEL SECTIONS AND THE MECHANISM OF THE SEISMIC ISOLATION SYSTEM

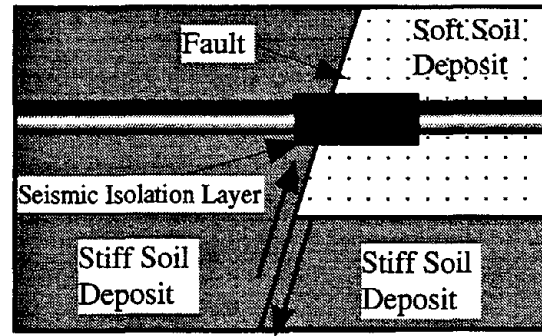
The tunnel sections where seismic isolation is considered to be effective are (1) sections where geological conditions change abruptly and (2) junctions with different structures, such as vertical shafts, and sections with sharp structural variations. The sections where geological conditions change abruptly can be further classified into several categories: (a) boundaries between soft and stiff soil deposits; (b) sections near fault or fracture zones; (c) sections where the thickness of subsurface layers changes abruptly due to irregular boundaries with bedrock; and (d) sections where the predominant frequency of the surface ground changes abruptly due to artificial filling and construction of structures as shown in Fig. 2.

Fig. 3 illustrates the distribution of longitudinal ground strain of the surface ground composed of two types of soil deposits with different soil impedances bounded by a vertical geological boundary, which is from a study on the boundary between soft and stiff soil deposits where abrupt change in geological conditions is commonly observed. As shown in Fig. 3, the more conspicuous the impedance contrast of the left and right soil deposits becomes, the more intense the local concentration of longitudinal strain on the soil boundary becomes. This means, in turn, that tunnels constructed in such places become subject to excessive ground strain transmitted through the tunnel structure during earthquakes. Fig. 4 is a schematic diagram that illustrates the effect of the seismic isolation applied to a section where the ground strain is concentrated. As shown in the figure, the seismic isolation layer can isolate the tunnel section from the surrounding ground, where ground strain is concentrated over a certain area. Idealistically, the values of the strain within the isolated section, which are determined by the tunnel stiffness and the displacement responses of the ground on both left and right sides of the isolated section, should be constant. In actuality, however, peak values of tunnel strain appear at the sections where strain is concentrated because small-scale ground strain is transmitted from the surrounding ground to the tunnel due to the slight stiffness of the seismic isolation layer. Thus, the tunnel sections where seismic isolation is applied and the shear modulus of seismic isolation materials should be determined according to the tunnel strain distribution.

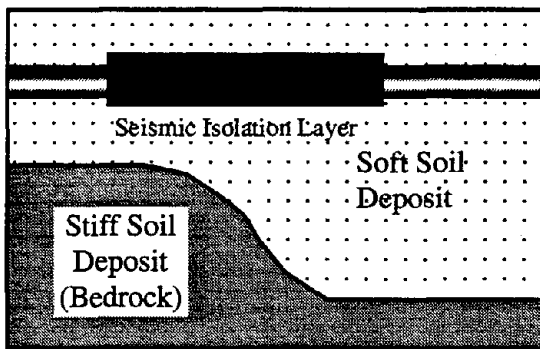
In addition to the concentration of ground strain, a tunnel section located close to a shaft which is connected to the tunnel becomes subject to the concentration of tunnel strain during earthquakes, since such a junction is a structural boundary between the tunnel and the shaft whose natural vibration characteristics are different from those of the tunnel body. Accordingly, such a section requires a seismic isolation layer for isolating the tunnel from both the peripheral soil and the shaft body. Fig. 5 is a schematic diagram showing the effect of seismic isolation applied to a tunnel-shaft junction of a shield-driven tunnel, along with a case in which a flexible segment is installed at a junction for comparison. Although the flexible segment provides high displacement absorption as shown in the figure, the distance in which the tunnel sectional force reduction takes effect is short in the case of non-isolation, since tunnel strain cannot be concentrated to the flexible segment due to the shear resistance from the peripheral soil around the segment neighboring the flexible segment. On the other hand, with the seismic isolation system, the sectional forces can be reduced effectively in accordance with the areas covered by the seismic isolation layer, which is more reliable than the flexible segment because there is no mechanical uncertainty.



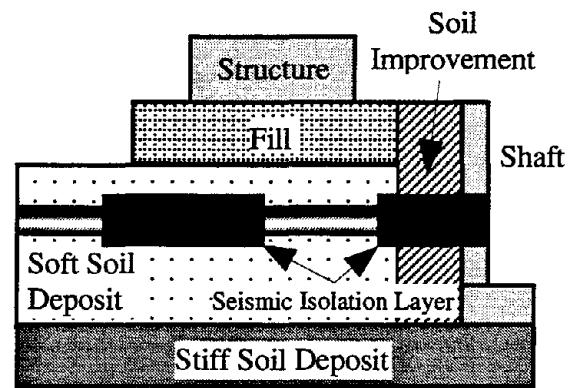
(a) Boundary between soft and stiff soil deposits formed in a sedimentary process



(b) Section near fault or fracture zones



(c) Section where the thickness of sub-surface layers changes abruptly due to irregular boundaries with bedrock



(d) Junction with a vertical shaft
(e) Transition of natural periods of sub-surface ground due to filling and construction of a structure

Fig.2 Sections where the application of seismic isolation is effective

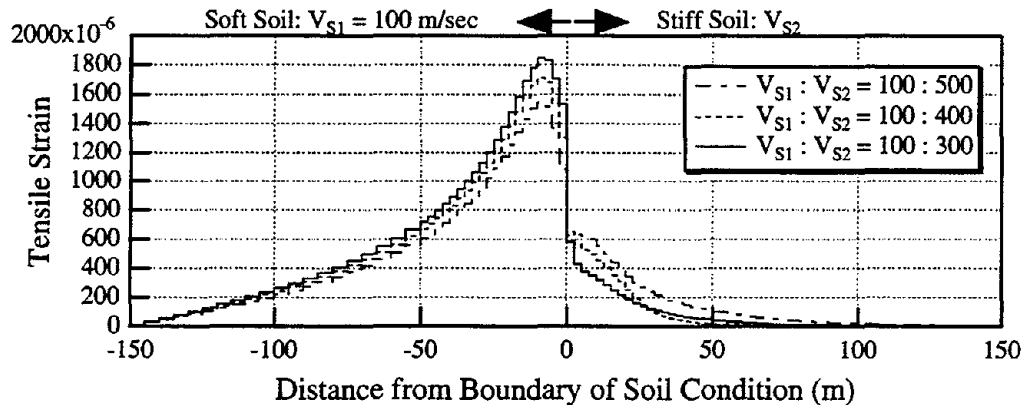


Fig.3 Longitudinal ground strain of the surface ground composed of two types of soil deposits with different soil impedances bounded by a vertical geological boundary

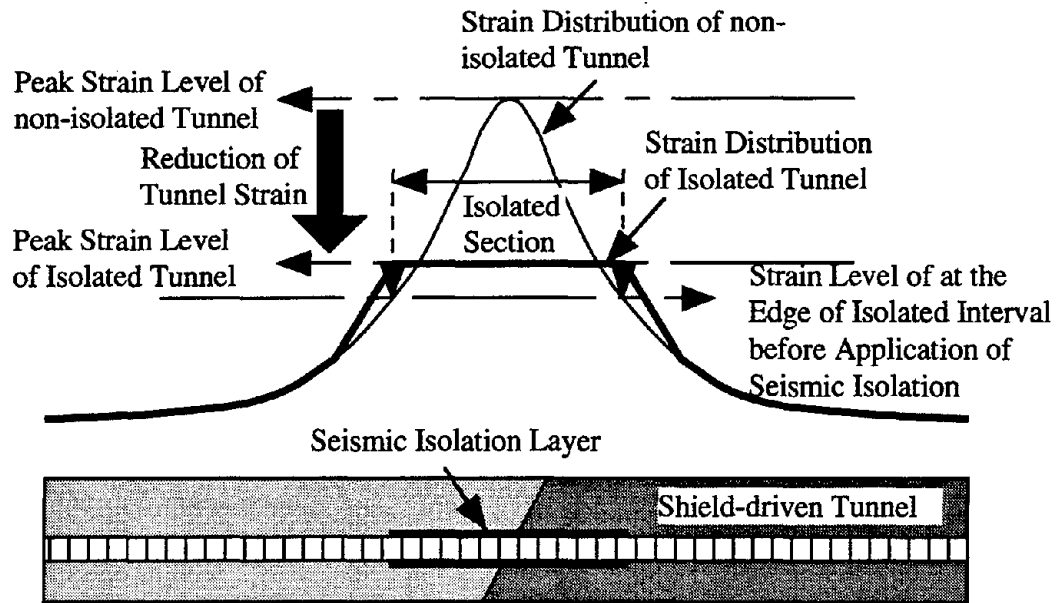


Fig.4 Schematic diagram to demonstrate the application of seismic isolation to the boundary between soft and stiff soil deposits

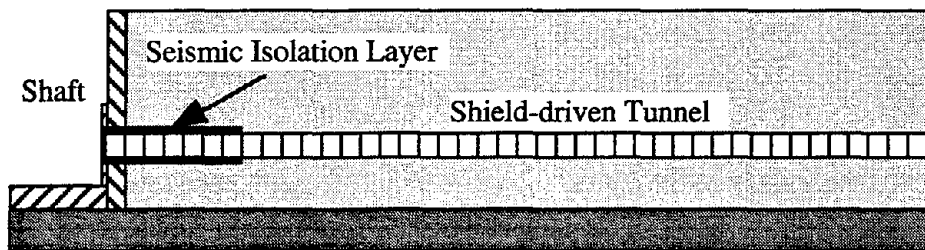
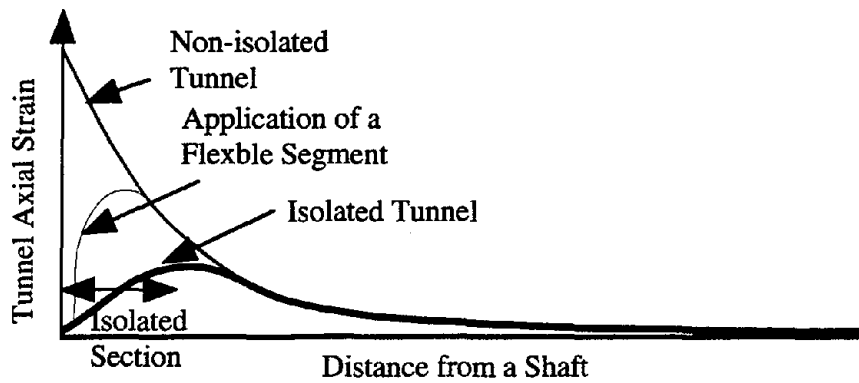


Fig.5 Schematic diagram to demonstrate the application of seismic isolation to a junction with a shaft

DEVELOPMENT OF SEISMIC ISOLATION MATERIALS

A total of five different seismic isolation materials were developed, three for shield-driven tunnels and two for tunnels by the cut-and-cover method. They provide highly effective seismic isolation, meet the criteria of properties that are considered indispensable in the ordinary static design of these tunnels (such as watertightness and ground settlement prevention), and have the performance that is required for constructing these tunnels.

Despite slight differences due to the type of tunnel (shield-driven tunnels and tunnels constructed by the cut-and-cover method), the main properties required for seismic isolation materials can be summarized as follows¹⁰⁾:

- (1) Low shear modulus
- (2) High shear deformability
- (3) High durability and long-term stability
- (4) Watertightness
- (5) Extremely small volumetric changes at injection, vulcanization, and thereafter
- (6) Transportability by pumping in a liquid state without any material separation
- (7) High filling-up performance
- (8) No dilution by groundwater
- (9) No contaminants

Seismic Isolation Materials for shield-driven tunnels

A seismic isolation layer for shield-driven tunnels is formed by injecting and filling up an isolation material to the tail void generated during shield driving work. The properties (4) through (9) listed above are also required of the materials for filling the tail void in ordinary shield driving. The seismic isolation materials developed in the joint research are outlined below:

Asphalt-based Material (Toa Doro Kogyo K. K.)

The base material of the asphalt-based material is a mixture of asphalt emulsion and high-early-strength portland cement. When mixed with a high water-absorbing polymer, it gels in 10 to 30 seconds, gradually hardens due to the hydration of the cement, then finally becomes a solid mass about one month after injection.

Urethane-based Material (Asahi Denka Kogyo K.K.)

The base material of the urethane-based material is isocyanate. When a mixture of fly ash and polyor is added as a hardener and mixed, it starts to vulcanize in several hours, and becomes urethane elastomer with low elastic modulus and high deformability one day after curing. The addition of a special polyor when mixing with the hardener can increase its viscosity up to 100 poise in one minute after injection, which stabilizes the excavated soil face of the tail void.

Silicone-based Material (Shin-Etsu Chemical Co., Ltd.)

The base material of the silicone-based material is composed mainly of silicone oil and fly ash. When a hardener is mixed in, it vulcanizes in about three hours after injection, and becomes a rubber-like solid in one day. Reacting to silica contained in the base material, polyether contained in the hardener increases the viscosity up to 200 poise in about 10 seconds, and stabilizes the excavated soil face of the tail void.

Seismic Isolation Materials for Tunnels by the Cut-and-Cover Method

In the case of tunnels constructed by the cut-and-cover method, seismic isolation materials are not injected into the earth, unlike the case with shield-driven tunnels. Since the space is narrow, where the seismic isolation system work is conducted, the materials must be well contrived. The seismic isolation materials developed in the joint research are outlined below:

Liquid Rubber (Tokai Rubber Industries, Ltd.)

The base material of the liquid rubber is a mixture of polybutadiene-type liquid rubber and asphalt. When polyisocyanate is mixed in as a hardener, this liquid rubber becomes a rubber-like solid in one day. Even when the job site is not spacious enough, such as when applied to the side walls of tunnels constructed by the cut-and-cover method, this uniform rubber-like solid can be formed by using molds.

Precast Rubber Panel (Sumitomo Rubber Industries, Ltd.)

The precast rubber panel is made by solidifying rubber tips made of shredded tires using urethane prepolymer resin. Coated by urethane resin, the panel surface is waterproof. This is a precast product produced in a factory, that is shaped into panels of a certain size to facilitate handling. Adhered to tunnel walls at job sites, the panels form a seismic isolation layer.

Hollow Cylindrical Cyclic Shear Tests

The seismic isolation layer is formed between a structure and its peripheral soil at a depth anywhere from a few meters to tens of meters below the ground level. In addition to a static constrained pressure generated underground, the layer becomes subject to compulsory shear deformation during earthquakes in both the axial and cross-sectional directions of the tunnel. Therefore, dynamic properties of the seismic isolation materials should be measured by giving cyclic shear loading under the same constrained conditions as underground. In consideration of the frequency dependency in the material properties, the loading frequency should be similar to the predominant frequency of the surface soil deposit. Thus, it was decided to measure the dynamic properties of seismic isolation materials by conducting hollow cylindrical dynamic shear tests (Photo 1), which are commonly conducted for testing dynamic shear properties of soil materials.

The frequency of cyclic loading used in the tests is 1 Hz which corresponds to the average frequency of the surface deposits. Starting with a small level, the shear amplitude was increased gradually until it reached 20% in the final stage. The rotational displacement measurement method using a laser displacement gauge was adopted, since the cyclic shearing was to be measured with such large shear amplitudes and at 1 Hz. To verify the dependency of the constrained pressure of material properties, similar cyclic loading tests were conducted using three different constrained pressures, i.e., 0.5, 1.5, and 3.5 kgf/cm². Using 11 sine waves, loading was applied cyclically to the respective shear strain amplitudes, and the shear modulus and the damping factor were calculated based on the hysteresis loop of the stress-strain relationship at the 10th cycle and thereafter. The dynamic properties of the silicone-based material, which is one of the most commonly used materials, are described below:

Figs. 6 and 7 show the strain-dependent curves of shear modulus G and damping factor h , respectively. These figures indicate that the material provides a constant property regardless of the depth where tunnels are constructed, since neither G nor h presents any constrained pressure dependency, despite the fact that the constrained pressure given in the tests had a considerably large range of 0.5 to 3.5 kgf/cm². Since the values of shear modulus G of the material are

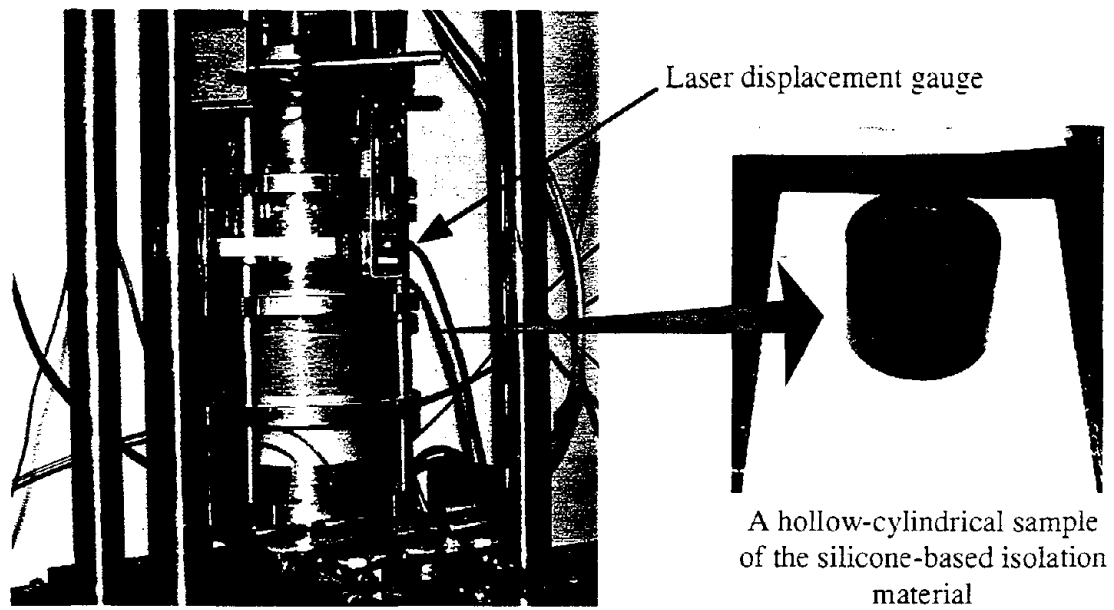


Photo.1 Dynamic shear test using a hollow-cylindrical cyclic shear apparatus

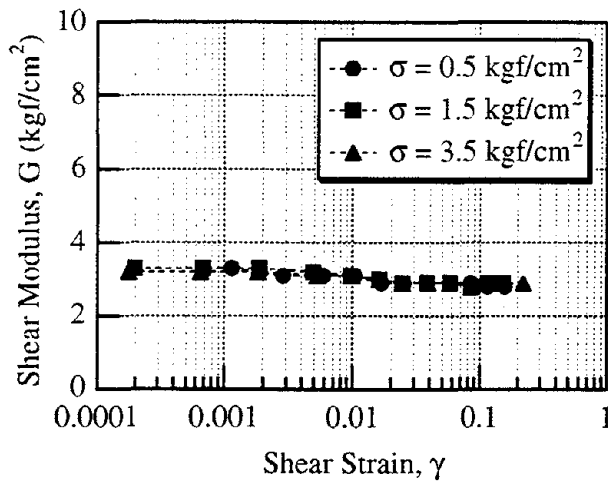


Fig.6 Strain-dependent characteristics of shear modulus for the silicone-based material

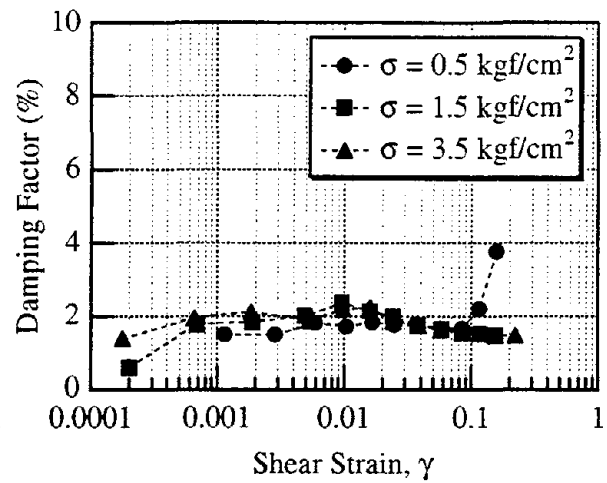


Fig.7 Strain-dependent characteristics of damping factor for the silicone-based material

constantly around 3 kgf/cm² without any strain amplitude dependency (unlike the case with soil materials), G measured during micro strain may be used when the seismic isolation effect is evaluated in the phase of design.

In addition, the values of damping factor h were around 2 % without any strain dependency. When the seismic isolation system is applied to underground structures, no hysteresis damping of the material is likely to occur. Thus, the seismic isolation materials developed in the joint research were proven stable even during the cyclic shear loading with large amplitudes.

DEVELOPMENT OF SEISMIC ISOLATION METHODS¹¹⁾

In the case of shield-driven tunnels, a seismic isolation layer should be formed securely around a tunnel by injecting and filling a liquid isolation material into the tail void which is generated during shield driving work, in the same manner as with the filling work conducted during shield driving. It is thus necessary to produce prototypes of the equipment for the mixing and pumping systems for each seismic isolation material to conduct experiments for confirming the feasibility of the respective methods. In the joint research, two feasibility tests were conducted to verify the methods for applying the seismic isolation materials, i. e., injection into a model ground chamber and a trial injection at actual tunneling sites.

Fig. 8 shows the time-dependent variations of the viscosity of the silicone-based material after injection. As shown in the figure, this material attains high viscosity immediately after injection, fills up the tail void, and sustains the earth pressure. If an additional injection is applied, this material becomes thixotropic and provides a plastic flow that expedites the filling. As shown in Photo 2, a prototype injection facility was produced, and injection tests using a model soil chamber were conducted to verify the feasibility and practicality of this experimental facility. The chamber used for the injection tests is also used for testing the backfilling materials for shield tunneling work; thus, the test results showed that silicone-based material injection was as practical as using backfilling materials. In addition, a similar test was also conducted for the urethane-based material using the same chamber.

Photo 3 shows a trial injection of the silicone-based material into the tail void at an actual shield tunneling site. The material was injected into the tail void of actual earth with groundwater, and sampling cores from grout holes that had been drilled in segment pieces beforehand confirmed that a seismic isolation layer with the target properties and thickness was formed. The same trial injection was conducted for the asphalt-based material, which was also confirmed to be highly feasible.

In the case of the liquid rubber applied to tunnels by the cut-and-cover method, it is necessary to confirm its mixing and vulcanization characteristics. This material was placed between a concrete sheet pile and a wooden form using a prototype injection facility. As a result, it was confirmed that a seismic isolation layer with a uniform property was formed on the concrete wall as shown in Photo 4. Another prototype was produced to test the precast rubber panel, and it was confirmed that a seismic isolation layer was formed satisfactorily as shown in Photo 5, as the panel adhered to a concrete sheet pile with sufficient strength.

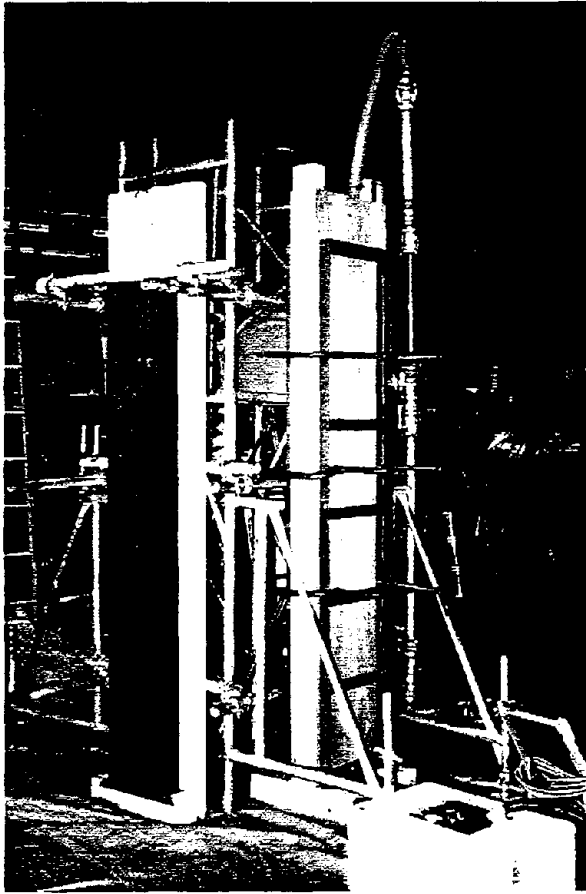
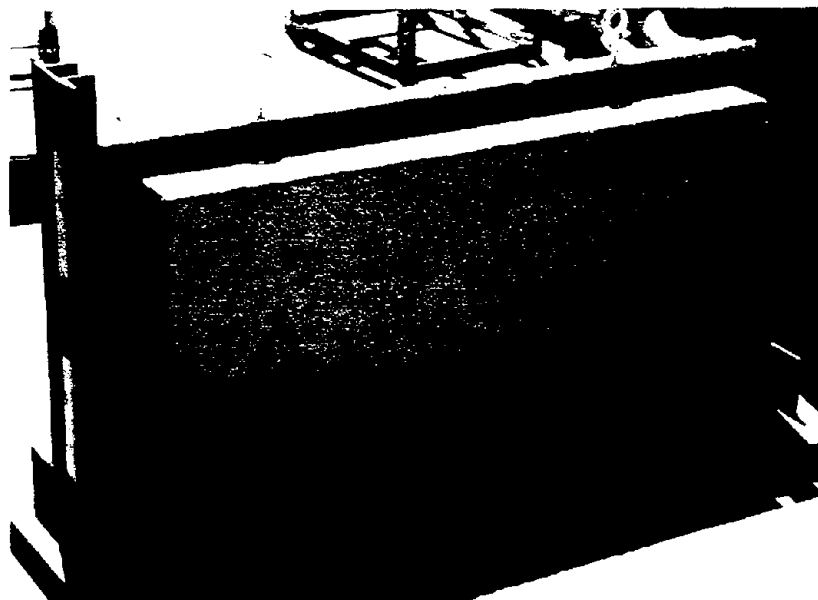


Photo.4 Injection test for the liquid rubber
A black panel stuck to a concrete sheet panel in the left hand side is the seismic isolation layer made of the liquid rubber.
The liquid rubber is being injected into a form in the right hand side.

Photo.5 Tests for the precast rubber panel
The precast rubber panel is adhered to the concrete sheet panel covered by a rubber sheet for water-proofing.



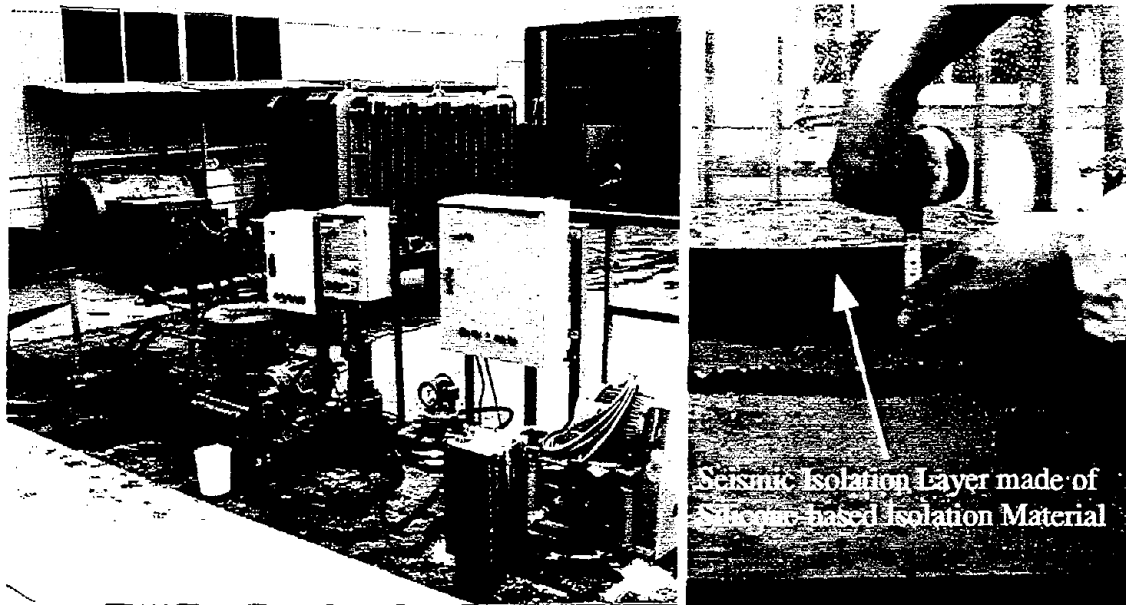


Photo.2 A Prototype injection facility and injection test using a model soil chamber (left) and the formation of an isolation layer after the injection test (right)

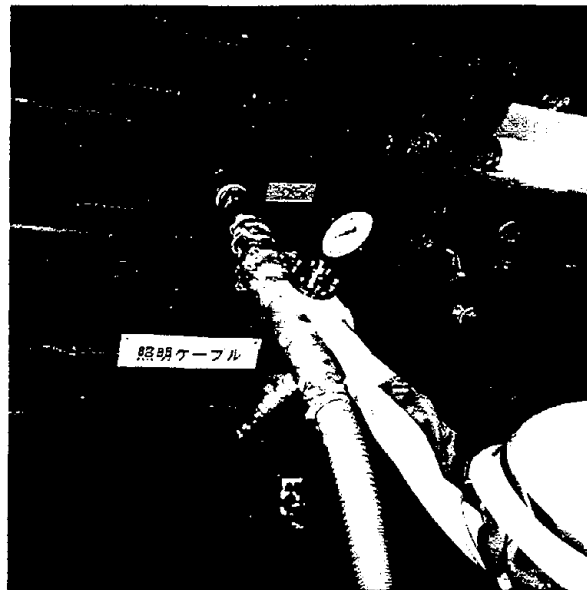


Photo.3 Trial Injection of the silicone-based material into a tail void at an actual shield tunneling site

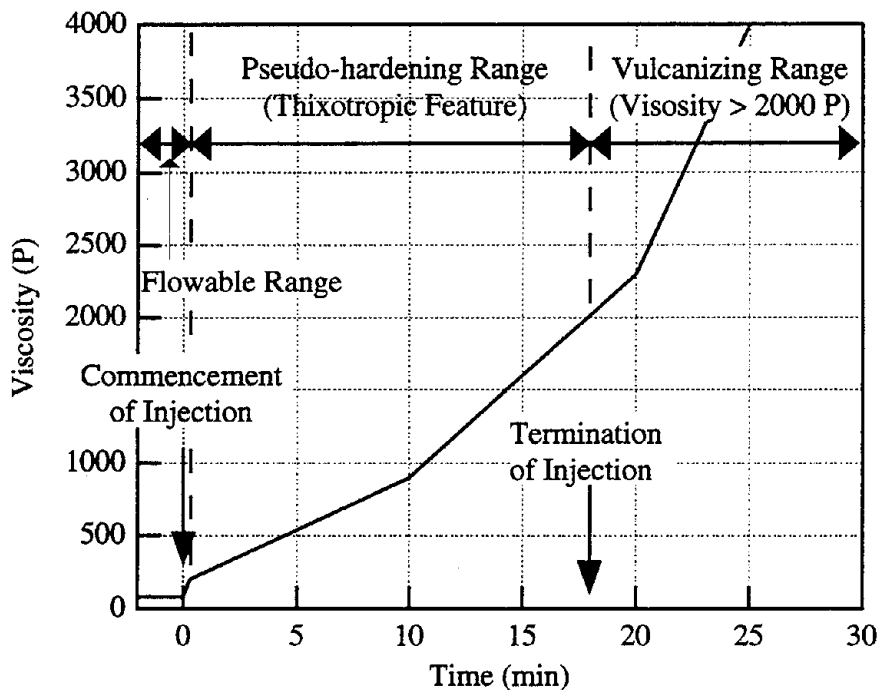


Fig.8 Representative time-dependent variations of the viscosity of the silicone-based material

CONCLUDING REMARKS

This paper has briefly described the seismic isolation system for underground structures focusing on the tunnel sections where the application of the seismic isolation takes effect, the development of seismic isolation materials, and validation experiments conducted for confirming the feasibility of the application methods. Five different seismic isolation materials applicable to shield-driven tunnels and tunnels by the cut-and-cover methods were developed, which have been proven promising for practical use as a result of material and validation tests. Now the authors intend to apply the developed technology to practical construction works to help prevent earthquake-related damage to lifelines.

ACKNOWLEDGMENTS

This study was conducted as part of the joint research between the Public Works Research Institute of the Ministry of Construction, the Public Works Research Center, and 17 private companies, under the title of "The Development of the Seismic Isolation System for Underground Structures." The authors would like to express their deep gratitude to the members of the joint research program for their warm cooperation and helpful suggestions and discussions.

REFERENCES

- 1) Suzuki, T.: Model Vibration Tests on the Seismic Isolation Structure for a Shield-driven Tunnel, Proc. 20th Earthquake Engineering Symposium, JSCE, pp.565-568, 1989. (in Japanese)
- 2) Unami, K. and Suzuki, T.: A Study on the Seismic Isolation Structure for a Shield-driven Tunnel (Confirmation of Isolation Effects by FEM), Proc. 44th Annual Meeting of JSCE, Vol.1, pp.1204-1205, 1990. (in Japanese)
- 3) Suzuki, T. and Unami, K.: A Study on the Seismic Isolation Structure for a Shield-driven Tunnel (Application to Earthquake Response Analyses), Proc. 44th Annual Meeting of JSCE, Vol.1, pp.1206-1207, 1990. (in Japanese)
- 4) Kawashima et al.: The Development of Seismic Design for Underground Structures, Joint Research Report No.29, PWRI, pp.208-235, 1989. (in Japanese)
- 5) Takeuchi M. et al.: Experimental Study on the Sectional Force Reduction in Cross-sectional Deformation of Shield-driven Tunnels due to Earthquakes, Proc. JSCE, No.483/I-26, 1994. (in Japanese)
- 6) Suzuki, T.: Damages of Urban Tunnels due to the Southern Hyogo Earthquake of January 17, 1995 and the Evaluation of Seismic Isolation Effect, CD-ROM of the Eleventh World Conference on Earthquake Engineering, Acapulco, Mexico, 1996.
- 7) Otsuka H., Hoshikuma, J. and K. Nagaya: A Fundamental Study on Innovative Menshin System for Underground Structures, Proc. 6th U.S.-Japan Workshop on Earthq. Dis. Prevent. for Lifeline Systems, Osaka, pp.427-436, 1995.
- 8) Suzuki, T. and Tamura C.: Proposal of a Seismic Isolation Structure for Shield-driven Tunnels and the Method to Evaluate Its Isolation Effect, Proc. JSCE, No.525/I-33, pp.275-285, 1995. (in Japanese)
- 9) Suzuki, T. et al.: Experimental Study on the Silicone-based Material for Seismic Isolation System for Urban Tunnels, Proc. JSCE, No.534/VI-30, pp.69-76, 1996. (in Japanese)
- 10) PWRI: Joint Research Report on the Development of the Seismic Isolation System for Underground Structures (PART-1), 1996.
- 11) PWRI: Joint Research Report on the Development of the Seismic Isolation System for Underground Structures (PART-2), 1997.

PERSONAL CAREER

NAME: Takeyasu Suzuki

POSITION: Manager
Earthquake Engineering Research Group
Tech. Resear. & Develop. Inst.
Kumagai Gumi Co., Ltd.

ADDRESS: 1043, Onigakubo, Tsukuba-shi,
300-26 IBARAKI, JAPAN
Tel. 81-298-47-7508
Fax.81-298-47-7480



DATE OF BIRTH: May 16, 1956

EDUCATION: Bachelor of Engineering, Saitama University (1980)
Master (1982) and Doctor (1991) Degrees of Engineering, University of Tokyo

MAJOR SUBJECT: Earthquake Engineering

MAJOR AREA OF EXPERIENCE:

- 1982-1983 Research Engineer, Institute of Construction Technology, Kumagai Gumi
- 1983-1984 Visiting Research Personell, Department of Civil Engineering, University of Tokyo
- 1984-1985 Research Engineer, Institute of Construction Technology, Kumagai Gumi
- 1986-1989 Visiting Research Personell, Institute of Industrial Science, University of Tokyo
- 1989-1991 Research Engineer, Technical Reserch and Development Institute (TRDI),
Kumagai Gumi
- 1991-1995 Assistant Manager, Civil Engineering Research Department, TRDI, Kumagai Gumi
- 1995- Manager, Earthquake Engineering Research Group, TRDI, Kumagai Gumi

TRAVEL ABROAD: USA, Mexico, England, Switzerland, France, Phillipine

MAJOR PUBLICATIONS:

- "The Extended Quasi-three-dimensional Ground Model for Irregularly Bounded Surface Ground", Structural Engineering/Earthquake Engineering, Vol.9, No.1, pp.21s-32s, 1992.
- "Application of Microtremor Measurement to the Estimation of Earthquake Ground Motions in Kushiro City during the Kushiro-oki Earthquake of 15 January 1993", Earthquake Engineering and Structural Dynamics, Vol.24, pp.595-613, 1995.
- "Proposal of a Seismic Isolation Structure for Urban Tunnels and the Method to Evaluate Its Isolation Effect" (in Japanese), Jour. JSCE, No.525/I-33, pp.275-285, 1995.
- "Experimental Study on the Silicone-based Material for Seismic Isolation System for Urban Tunnels (in Japanese)", Proc. JSCE, No.534/VI-30, pp.69-76, 1996.
- "Damages of Urban Tunnels due to the Southern Hyogo Earthquake of January 17, 1995 and the Evaluation of Seismic Isolation Effect", CD-ROM of the Eleventh World Conerence on Earthquake Engineering, Acapulco, Mexico, 1996.

**RESEARCH AND DEVELOPMENT ON THE SEISMIC ISOLATION SYSTEM
APPLIED TO URBAN TUNNELS
(PART-2: EFFECTS OF SEISMIC ISOLATION AND SEISMIC DESIGN)**

Tsutomu TANAKA¹⁾ and Takeyasu SUZUKI²⁾

- 1) Director, Central Research and Development Department, Oriental Consultants Co., Ltd.
2) Manager, Earthquake Engineering Research Group, Technical Research and Development Institute, Kumagai Gumi Co., Ltd.

ABSTRACT

Techniques for improving seismic safety of urban tunnels have hitherto been limited to those for increasing the flexibility of tunnel structures by applying flexible joints and segments. However, since such techniques are insufficient for ensuring seismic safety of underground lifelines in urban areas when strong earthquakes occur, there has been a demand for developing a new, highly reliable technique, especially for protecting tunnel sections where seismic strain is concentrated locally. Given this situation, an innovative joint research project between the Public Works Research Institute and private companies was commenced to develop a seismic isolation system to be applied to urban tunnels. This paper will describe the results of analyses and experiments conducted for validating the effectiveness of seismic isolation, as well as the development of design methods.

INTRODUCTION

Several researchers have been investigating the application of a seismic isolation system to underground structures since around 1988, and the effectiveness of seismic isolation has been confirmed by numerical analyses and laboratory experiments¹⁾⁻⁵⁾. As shown in Fig. 1, the fundamental principle of the seismic isolation system for underground structures is to cut off the transmission of ground strain by isolating a tunnel body from the peripheral soil by forming a thin, soft layer around the tunnel.

In the case of axial or bending deformation of a tunnel that occurs in the longitudinal direction due to earthquakes, tunnel sectional forces can be effectively reduced when a seismic isolation

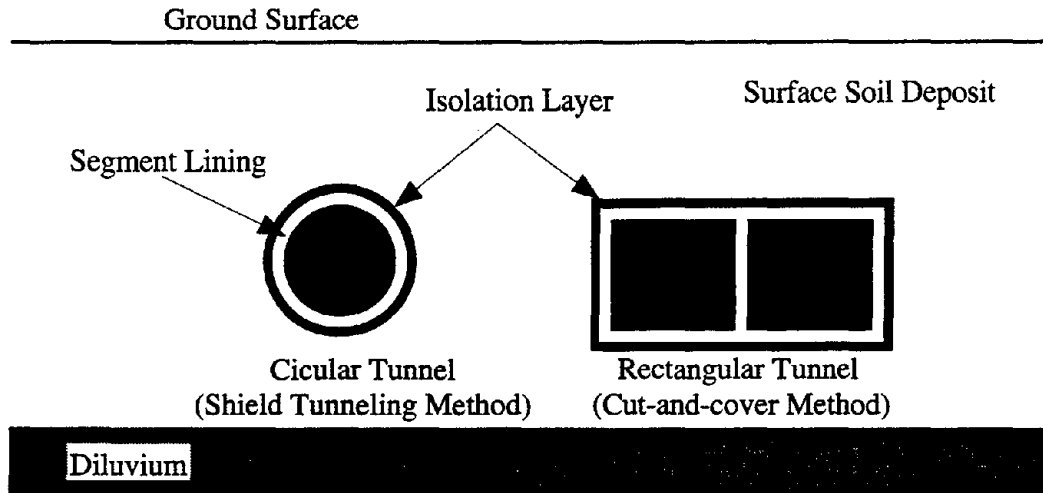


Fig.1 Schematic diagram to demonstrate the seismic isolation system for urban tunnels

layer is applied to a tunnel section where ground strain is concentrated locally. This is not only because the ground strain transmission to the tunnel body is cut off, but because the tunnel strain in the isolated section is dispersed.

In a similar vein, when cross-sectional deformation of a tunnel occurs, the results of numerical analyses have shown that the seismic isolation system helps to reduce the sectional forces concentrated at the corner portions in a tunnel with a rectangular cross-section constructed by the cut-and-cover method, thus contributing greatly to the reduction of sectional forces at the upper and lower slabs and side walls of such a tunnel^{6),7)}.

Meanwhile, earthquake response analyses were conducted to examine the effectiveness of the application of seismic isolation system to a subway tunnel that was severely damaged by the Hyogoken-nanbu earthquake of 1995⁶⁾. In the case of tunnels with a circular cross-section such as shield-driven tunnels, however, there was a report that the application of seismic isolation was not so effective in reducing sectional forces during cross-sectional deformation due to earthquakes⁸⁾.

Since there has been no systematic research on the seismic isolation system, with which a thin seismic isolation layer is formed covering a tunnel body, studies on this system as described above, development of materials for the seismic isolation layer, and validation tests for developing construction methods have been conducted separately by various institutions^{8),9)}. Thus, a comprehensive three-year project for clarifying the seismic isolation mechanism, and for developing seismic isolation materials, application methods, and seismic design, was started in July 1995 as a joint research project between the Public Works Research Institute of the Ministry of Construction and 17 private-sector companies in Japan. This paper will examine the results of this joint research, focusing on the results obtained by analyses and experiments conducted for validating the effectiveness of seismic isolation, describe the results of a study on the development of design methods for seismic isolation tunnels, and presents the flow of the design methods.

EFFECTS OF SEISMIC ISOLATION

Longitudinal tunnel deformation during earthquakes

This chapter will examine the results of numerical analyses conducted for identifying the effect of reducing tunnel sectional forces by applying seismic isolation to shield-driven tunnels. The sectional forces acting on a tunnel in the longitudinal direction can be reduced by applying a seismic isolation layer to a section that becomes subject to the concentration of the maximum local ground strain. Such a layer is formed by injecting and filling the seismic isolation materials developed by the joint research, which are soft with a shear modulus of around 3 kgf/cm², into the tail void that is created during shield driving, and which is usually 5 to 10 cm thick. In this chapter, the reduction of sectional forces and the behavior of the isolated tunnel section are described in detail for seismic isolation that is applied to a shield-driven tunnel section located underneath a caisson-type quay.

The longitudinal tunnel section and the surrounding ground structure selected for the earthquake response analyses are illustrated at the top of Fig. 2. The numerical models used in the analyses are analogous to those proposed by Tamura et al.¹⁰⁾, in which a mass-spring system and a beam-spring system are used for the ground and the tunnel, respectively. The ground model was made in consideration of the fundamental to the third shear vibration modes, using an extended quasi-two-dimensional model¹¹⁾ which is capable of handling the fundamental to the N-th shear vibration modes. The quay was considered a ground element with concrete properties. The soil was considered a linear material, whose stiffness had been reduced in reference to the initial value obtained beforehand by a one-dimensional equivalent linear analysis based on multiple reflection theory. Assuming that flexible segments absorb the displacement, extremely weak springs were used at a junction connecting the tunnel and shafts.

Two shield-driven tunnels composed of reinforced concrete segments of 5.4 m in outer diameter and 22.5 cm in thickness were used, one with and the other without seismic isolation. They are considered a non-linear element with stiffness that changes according to either tensile or compressive deformation.

The results of the analyses are summarized in (a) through (e) in Fig. 2. As shown in Fig. 2 (a), the maximum values of tunnel displacement are almost constant for the two tunnels regardless of seismic isolation; however, the gradient of the displacement distribution of the tunnel section located underneath the quay in the case of isolation is more gentle than in the case of non-isolation. The maximum axial force distributions in Fig. 2 (b) and (c) show that the seismic isolation layer reduced the axial force markedly to 1/10 for the compressive deformation and 1/5 for the tensile deformation. In addition, both the bending moment and the shear force decreased remarkably as shown in Fig. 2 (d) and (e). Thus, these analyses showed that the application of seismic isolation to a tunnel section where ground strain is concentrated is highly effective. Fig. 3 shows the time-dependent response of axial strain at a tunnel section where the tunnel sectional force hits the maximum for the two tunnels, one with and one without seismic isolation.

Seismic isolation at a junction with a shaft

When there is a junction with a shaft, seismic isolation takes effect when a seismic isolation layer is formed, covering a tunnel section measuring around 10 m from the shaft, for isolating the

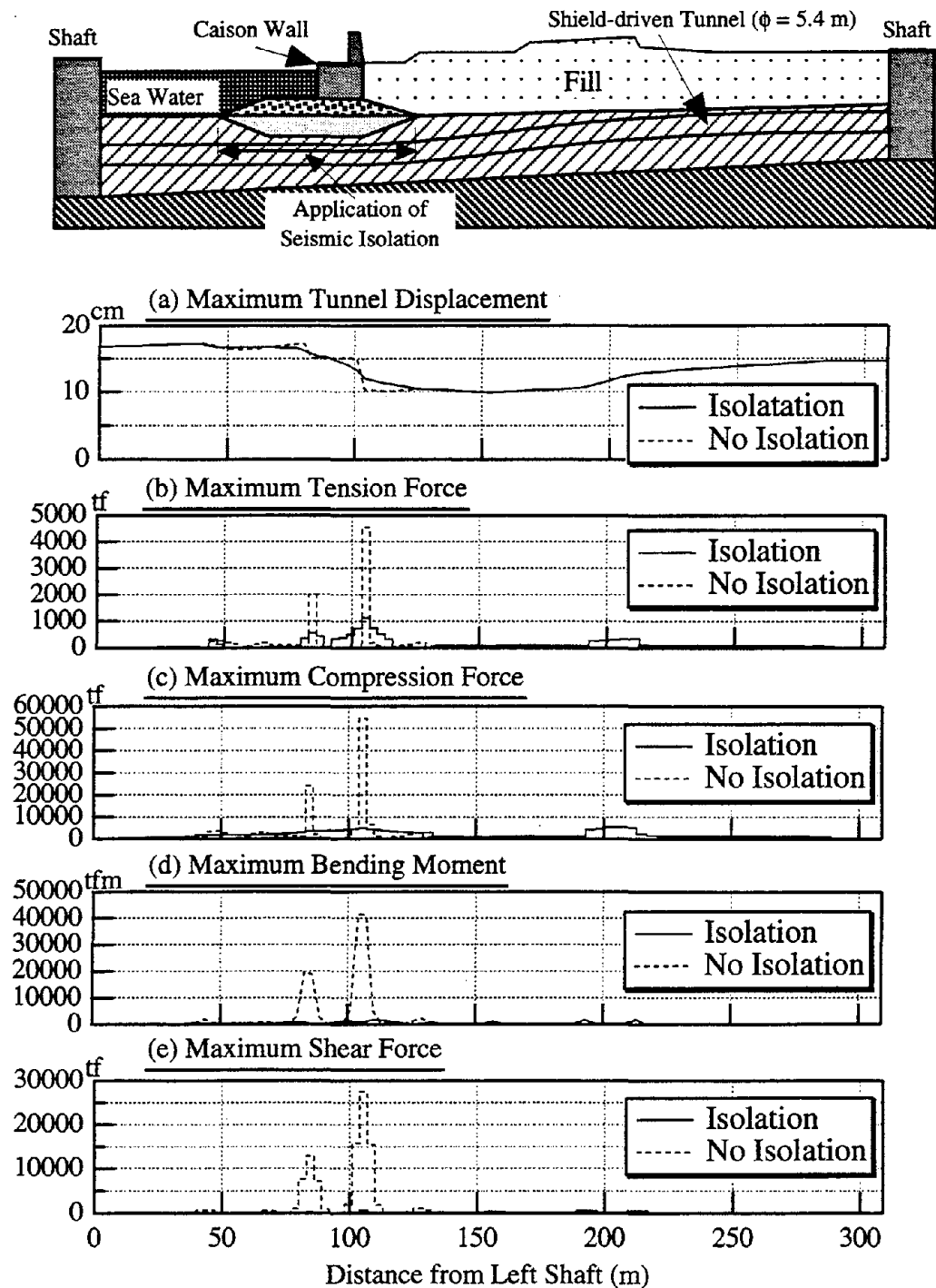


Fig.2 Comparison on tunnel displacement and internal forces between isolated and non-isolated tunnels, obtained by earthquake response analyses for a shield-driven tunnel underneath a caisson-type quay

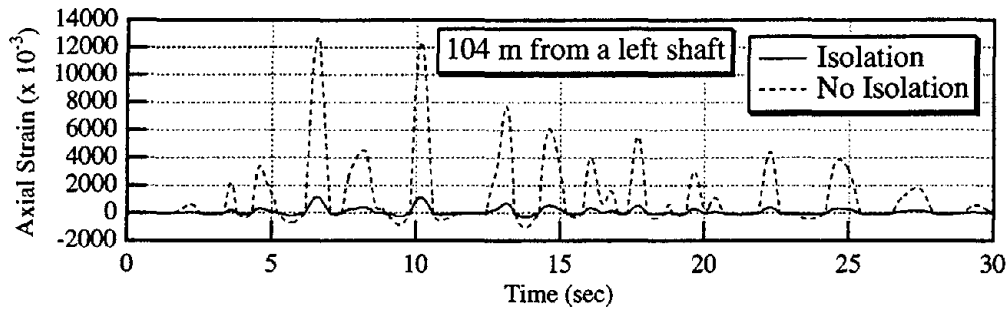


Fig.3 Comparison on time-dependent response of tunnel axial strain between non-isolated and isolated tunnels

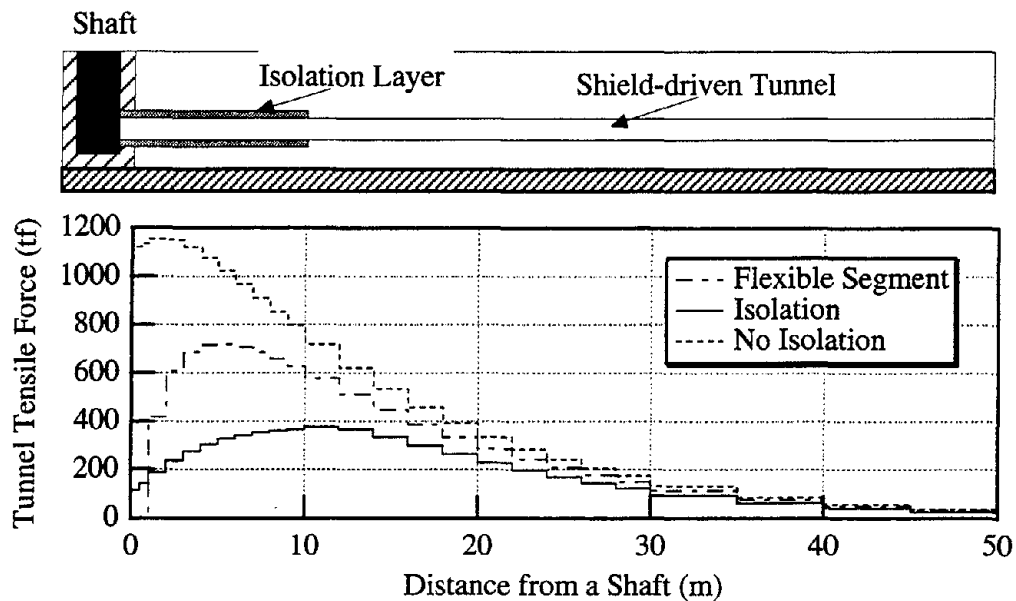


Fig.4 Comparison on tunnel axial forces at a junction with a shaft among three different cases

tunnel section from both its peripheral soil and the shaft body. Numerical analyses were conducted, using a shield-driven tunnel composed of reinforced concrete segments, 5.05 m in outer diameter and 25 cm in thickness, to examine the effect of the seismic isolation layer in reducing the sectional forces at such a junction. The model used was an axisymmetric finite element model (EASIT) developed in this joint research^{12),13)}. Statistically loading the entire model with inertial forces corresponding to 0.3 G of uniform horizontal earthquake acceleration, three cases were analyzed: (1) seismic isolation was applied to a ten-meter-long section around the shaft; (2) no seismic isolation was applied; (3) a flexible segment was installed on the first ring from the shaft. Fig. 4 compares the tunnel axial force distributions of these three cases. Despite the ability of the flexible segment to absorb large displacement, the effect of tunnel sectional force reduction reached only to the vicinity of the flexible segment. This is because the flexible segment failed to gather the tunnel strain completely due to the shear resistance of the peripheral soil acting on the outer surface of other tunnel segments nearby. When a seismic isolation layer was applied,

however, the tunnel maximum axial force decreased up to 1/3, since the tunnel strain could be dispersed toward the shaft effectively. In addition, unlike the technique which uses a flexible segment, the seismic isolation system is highly reliable because there is no mechanical uncertainty.

Cross-sectional deformation of tunnels by the cut-and-cover method

In the case of cross-sectional deformation of a tunnel with a rectangular cross-section, which is usually constructed by the cut-and-cover method, great sectional forces are concentrated at the corner portions and the upper and lower edges of slabs and side walls during earthquakes. Therefore, model vibration tests were conducted to verify that such sectional forces can be reduced by covering the tunnel body with a seismic isolation layer that isolates the tunnel from its peripheral soil.

Photo 1 shows a view of installing model tunnels made of acrylic resins in a soil chamber. A tunnel model covered with a silicone rubber isolation layer and another tunnel model without any seismic isolation device were placed end to end on a vibration table, and oscillation was applied in a direction perpendicular to the tunnel axis. Then, the tunnel strain, as well as the shear stress and the normal stress acting on the outer surface of the tunnel bodies, were measured. Photo 2 shows a general view of this vibration test.

Fig. 5 illustrates one of the test results, comparing the bending moment distribution of tunnels with and without seismic isolation. As shown in the figure, the seismic isolation layer decreased the bending moment up to 1/3, which is concentrated to the corner portions of the tunnel. The shear stress acting on the outer surface of the tunnel was decreased to 1/10 or less by the seismic isolation layer, which was proven to be the most important factor reducing the tunnel sectional forces. Fig. 6 illustrates a shear stress distribution of the ground surrounding the tunnel obtained by the earthquake response analyses⁶⁾. This is rather similar to the ground strain around a cavity without lining, since the seismic isolation layer that isolates the tunnel body from the peripheral soil changed the shear stress distribution around the tunnel greatly.

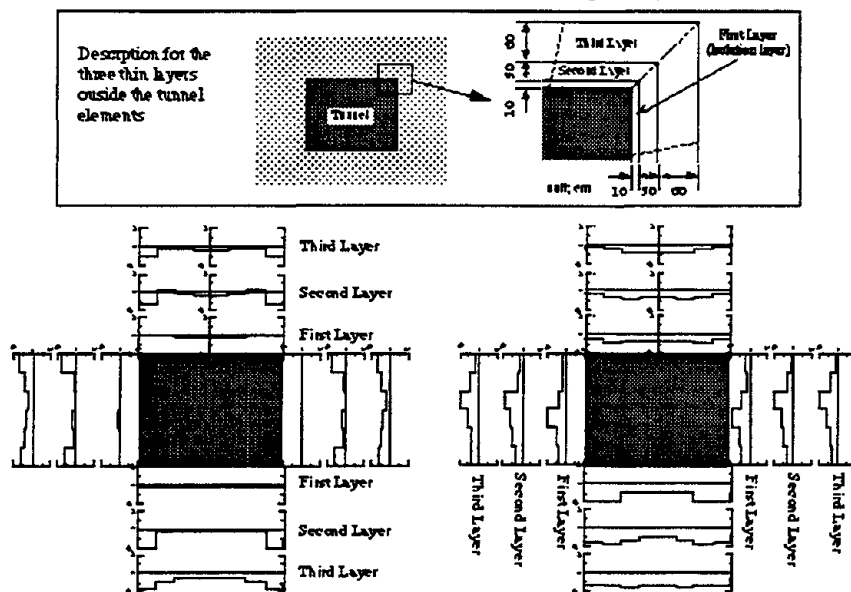


Fig.6 Shear stress distributions of thin layers around tunnel (left: isolated, right: non-isolated)⁶⁾

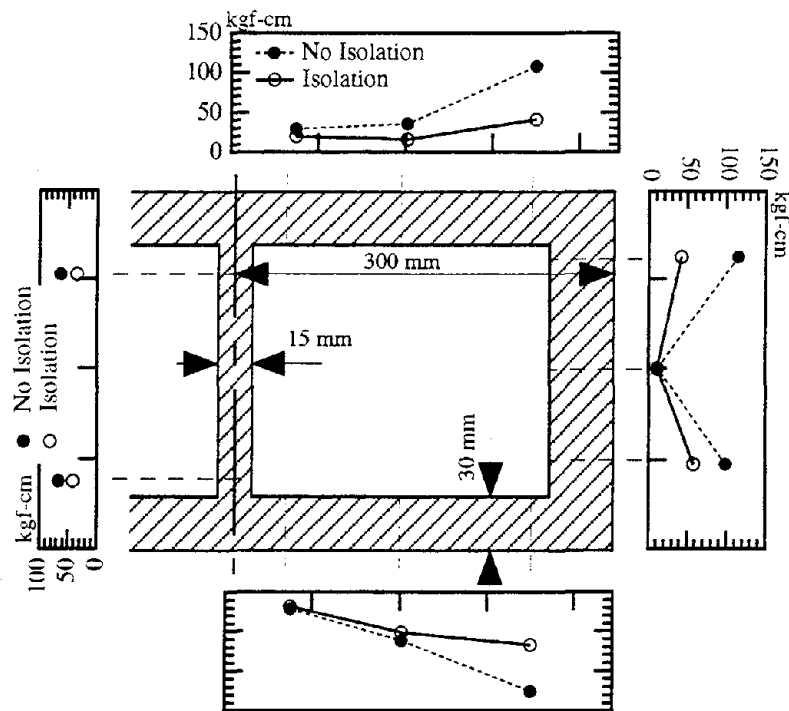


Fig.5 Maximum bending moment distribution obtained from model vibration tests

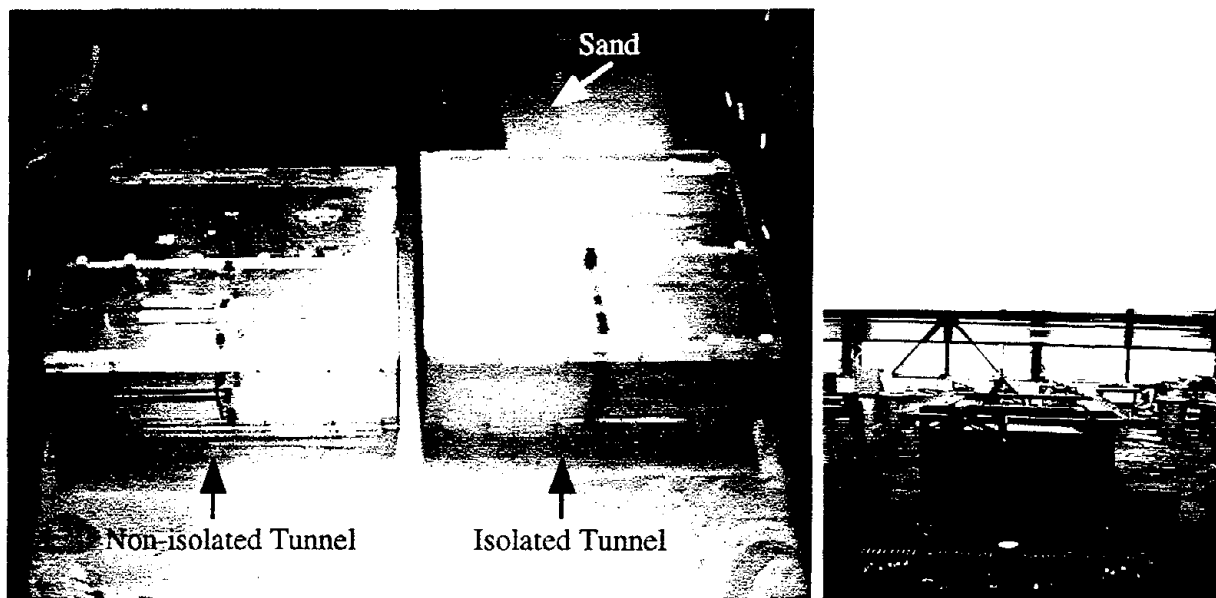


Photo.1 Arrangement of tunnel models (left) and a general view of the vibration test (right)

DEVELOPMENT OF SEISMIC DESIGN FOR ISOLATED TUNNELS

Factors affecting the seismic isolation effects

(a) Stiffness of a seismic isolation layer

As discussed in the previous chapter, seismic isolation takes effect when a seismic isolation layer is formed using materials with shear modulus of around 3 kgf/cm^2 .

To identify the range of shear modulus, in which seismic isolation takes effect in the cross-sectional deformation during earthquakes, numerical analyses were conducted based on the seismic deformation method using a finite element model (will be described later). Fig. 8 shows a model of a large box culvert (illustrated in Fig. 7) and a subsurface ground. Fig. 9 summarizes the maximum sectional force ratios obtained at a side wall of two tunnels, one with and the other without seismic isolation, in which M/M_0 denotes the ratio of the bending moment; Q/Q_0 , of the shear force; S/S_0 , of the axial force; and the horizontal axis G_m/G_g , the shear modulus ratio of an isolation material to a subsurface deposit¹²). As shown in Fig. 9, the tunnel sectional forces decrease, the smaller the shear modulus of the materials becomes, and the effect of sectional force reduction is considerable when the ratio becomes $1/100$.

Meanwhile, a shield-driven tunnel constructed in the subsurface ground composed of two soil deposits with different soil impedances bounded by a vertical geological boundary, was analyzed using an axisymmetric finite element model to identify the seismic isolation effect in the case of longitudinal deformation. Fig. 10 summarizes the results of the analysis in which the shear modulus of an isolation layer was used as a parameter¹³). As shown in the figure, the seismic isolation material reduced the tunnel sectional forces considerably, when the shear modulus was as low as 3 kgf/cm^2 , which is equivalent to around $1/50$ the peripheral ground.

When the shear modulus ratio of an isolation material is as low as $1/1000$, the natural period of tunnel resonance vibration shifts to a low frequency range, and the sectional force distribution becomes different from that usually observed under static conditions. Thus, the shear modulus of an isolation material should be around $1/100$ that of the peripheral ground.

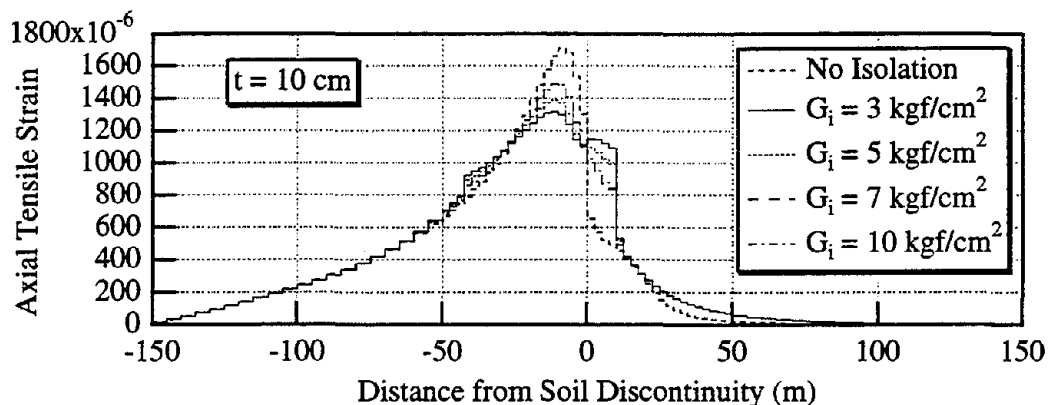


Fig.10 Effect of shear modulus of an isolation layer on the seismic isolation effect

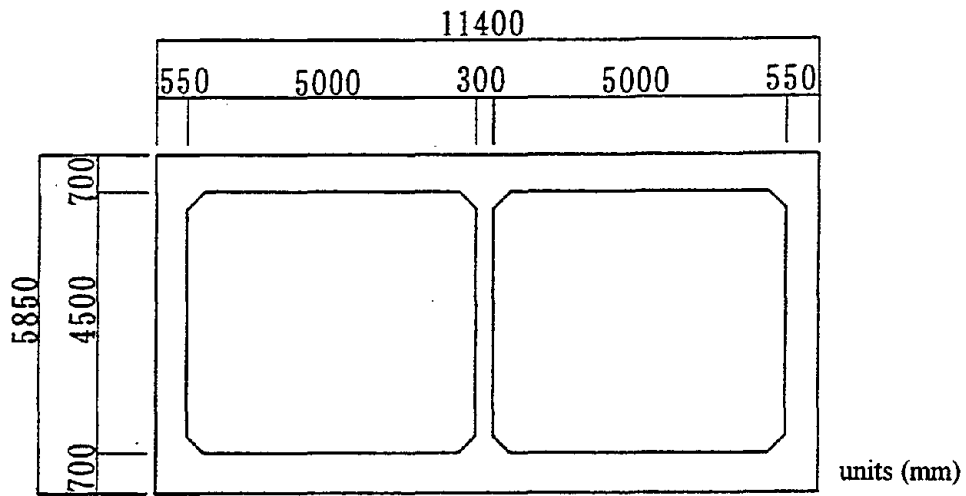


Fig. 7 Cross-section of a box culvert used for analyses

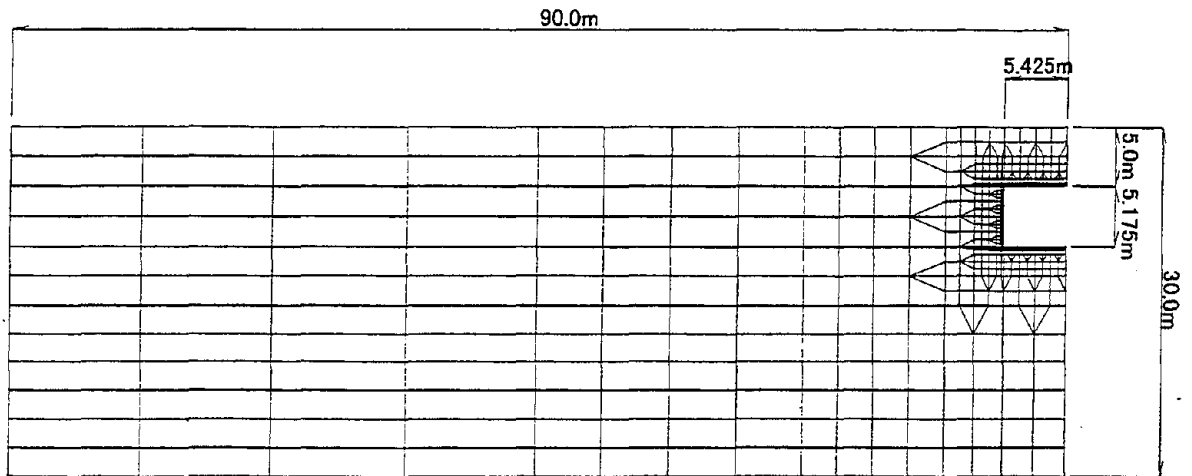


Fig. 8 Discretization of finite element mesh

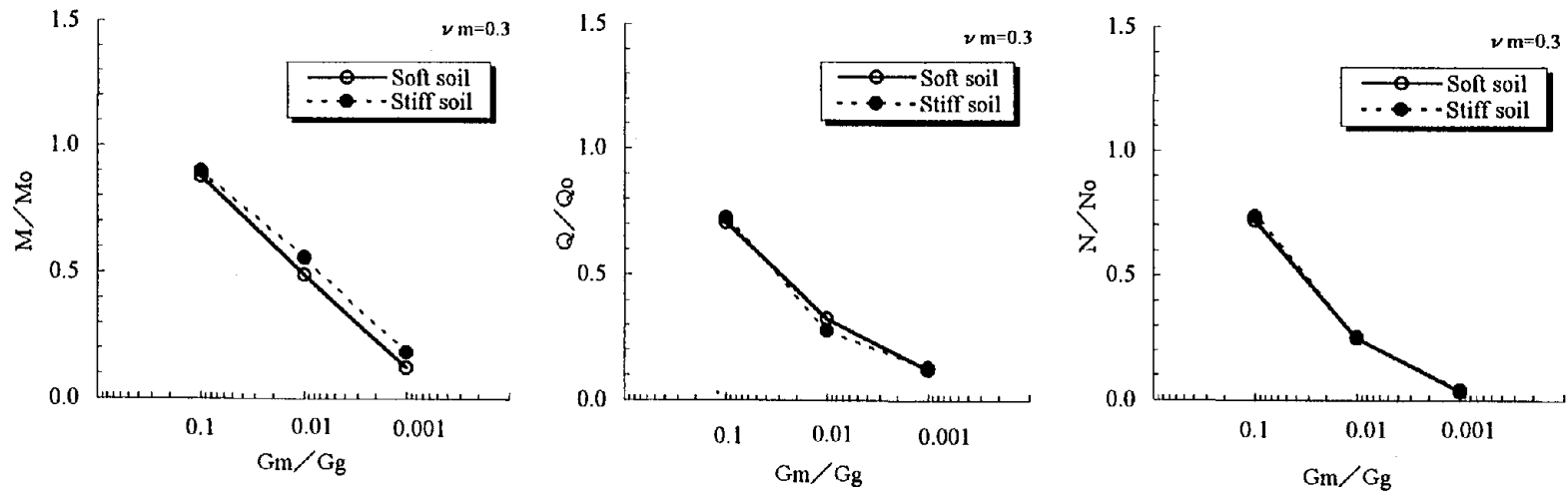


Fig. 9 The effect of the shear modulus ratio, G_m/G_g on sectional force reduction

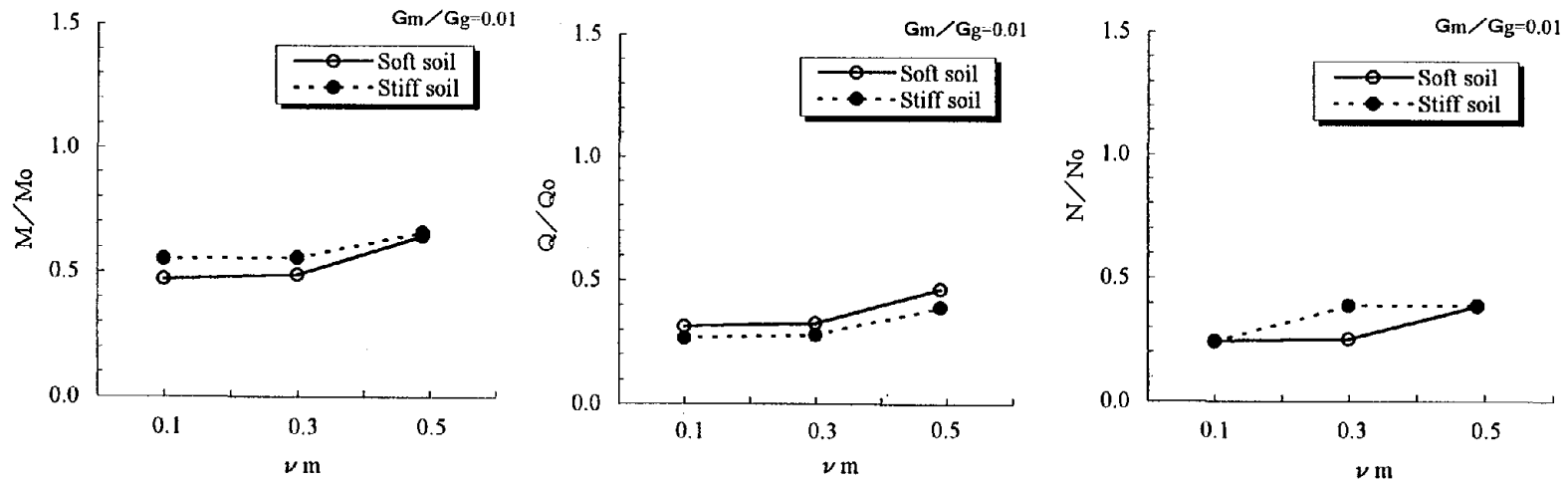


Fig.11 The effect of Poisson's ratio on sectional force reduction

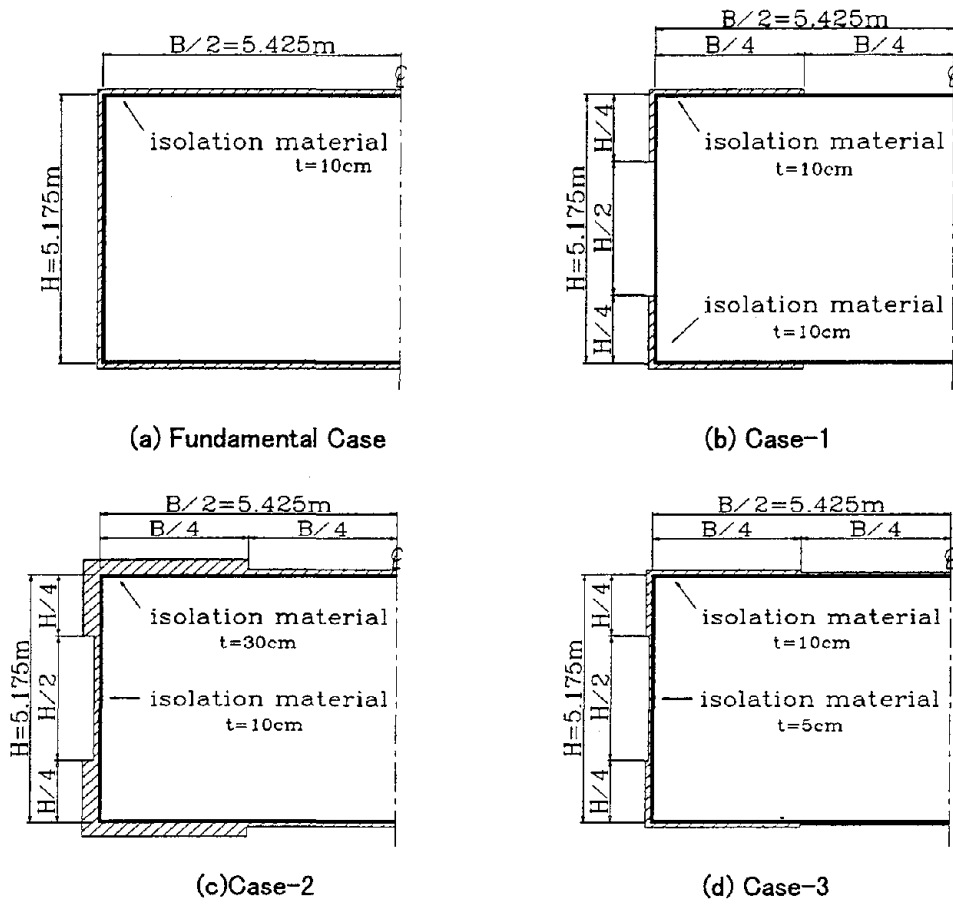


Fig. 12 Cases examined on the arrangement of seismic isolation layers

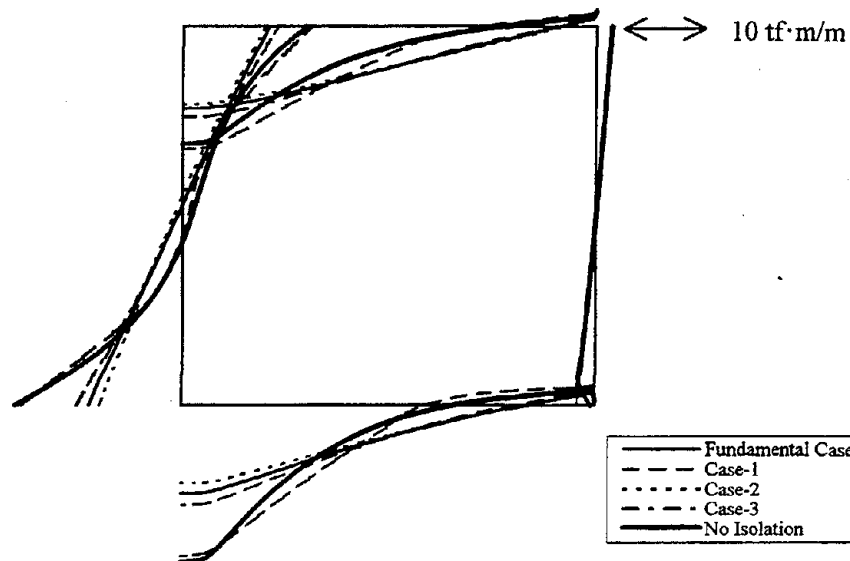


Fig. 13 Comparison of bending moment distributions among four cases

(2) Poisson's ratio of an isolation layer

Assuming that Poisson's ratio of an isolation layer may be affecting the effect of seismic isolation, since a seismic isolation layer is deformed greatly when the tunnel body is deformed in the cross-sectional direction, the authors conducted analyses based on the deformation method using the same model shown in Fig. 8, using Poisson's ratio as a parameter. Fig. 11 shows the result of analyses on sectional forces at a side wall. It was confirmed, however, Poisson's ratio of an isolation layer did not affect the seismic isolation effect.

(3) Arrangement and thickness of an isolation layer

The effect of the arrangement and the thickness of an isolation layer on seismic isolation was examined, focusing on the cross-sectional deformation of a tunnel with a rectangular cross-section. Four cases of arrangement (Fig. 12) were analyzed using a tunnel model shown in Fig. 8¹³⁾. The fundamental case is a tunnel covered by an isolation layer with a thickness of 10 cm. Comparing the bending moment distributions of the four cases in Fig. 13, one can notice that the thickness of an isolation layer scarcely affects the tunnel sectional forces within the range of thickness used in the analyses, and that the seismic isolation layer does not manifest its maximum effect unless it is installed covering the entire outer surface of the tunnel.

The same effect in the case of longitudinal deformation of a shield-driven tunnel constructed in the subsurface ground described above was also analyzed using an axisymmetric finite element model. Fig. 14 illustrates a summary of the analyses in which the thickness of an isolation layer is used as a parameter¹³⁾. The figure indicates that the effect of the thickness of an isolation layer on seismic isolation is negligible.

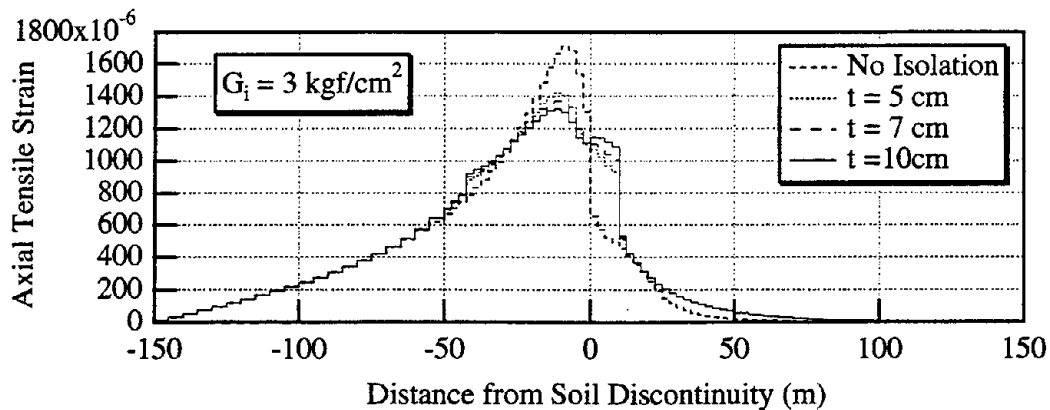


Fig.14 Effect of the thickness of an isolation layer on the seismic isolation effect

Procedures and the flow of design

(1) Static design

The static design for isolated tunnels is conducted in the same manner as that for non-isolated tunnels.

(2) Seismic design of the cross-sectional tunnel deformation

A finite element model as shown in Fig. 8 is used in the seismic design, so that the soil-structure interaction can be taken into consideration accurately. Although it is desired to conduct

dynamic analysis using such a model for a precise output, a static method was used for simplifying the design methods on the assumption that the fundamental tunnel structure is designed without sufficient geological data.

Since the deformation of underground structures is governed by the ground deformation, it is necessary to generate the ground deformation, when a tunnel sectional force reaches its maximum value, by a static method. It is supposed that the ground vibration can be represented only by a fundamental mode of shear vibration, which is appropriate in many cases. In the case of a resonant vibration, the time that the ground displacement reaches its maximum value is coincident with the time that the ground acceleration reaches its maximum value. Therefore, the maximum vertical distribution of horizontal ground displacement can be obtained by loading the force of inertia, which corresponds to the acceleration distribution for fundamental shear vibration, to the finite element model. The force of inertia can be given by equation (1).

$$F(z) = \frac{\gamma_t(z)}{g} A(z)$$

$$A(z) = \phi(z) \beta S_A \quad (1)$$

where, z: depth

F(z): force of inertia at depth z

$\gamma_t(z)$: weight per unit volume of soil at depth z

g: gravitational acceleration

A(z): absolute acceleration at depth z

$\phi(z)$: modal vector at depth z

β : participation factor of the fundamental shear vibration mode

S_A : absolute acceleration response vector at a natural period of fundamental mode of ground vibration

The authors named this method the "deformation method based on ground force of inertia."¹²⁾

(3) Seismic design on the longitudinal tunnel deformation

Seismic isolation in the longitudinal direction is conducted by applying a seismic isolation layer to a section where the tunnel strain is concentrated locally, such as a junction with a shaft and an area with abrupt transition of geological conditions. Thus, when conducting a seismic design, earthquake response analyses on the subsurface ground of a tunnel, using such numerical models as a mass-spring system and a 2-D finite element model, are conducted in the first place, followed by a determination of the section where seismic isolation should be applied based on the tunnel sectional forces obtained by the analyses.

As shown in Fig. 15, tunnel strain in an isolated region is dispersed and becomes uniform due to the redistribution of tunnel strain. The divergence of tunnel strain becomes remarkable, the smaller the shear modulus of an isolation layer becomes, and the larger the tunnel stiffness becomes. Such a tunnel strain redistribution is confirmed by static analyses using an axisymmetric finite element model, a simplified three-dimensional finite element model, or a three-dimensional finite element model.

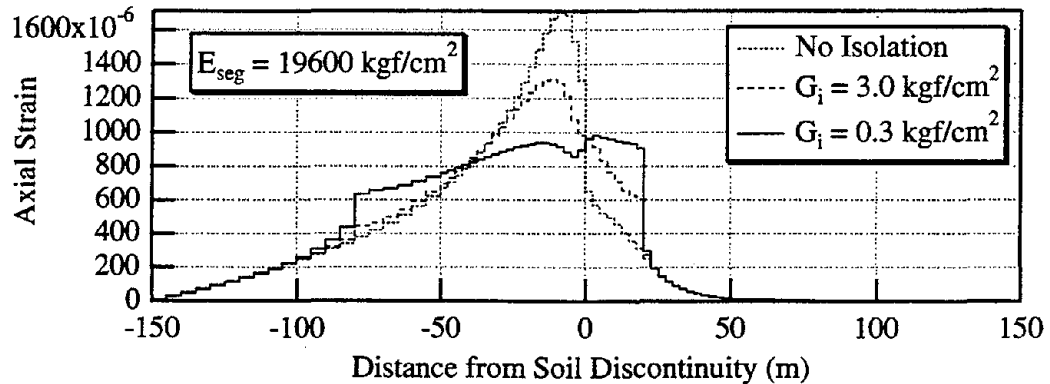


Fig.15 An example of the dispersion of tunnel strain due to the seismic isolation effect

CONCLUDING REMARKS

This paper has briefly described the results of numerical analyses and model vibration tests for identifying the effectiveness of seismic isolation applied to tunnels, as well as the study on the seismic design of tunnels. It was proved that adequate application of a seismic isolation layer provides reduction of tunnel sectional forces at a section where the ground conditions change abruptly, and that the sectional force reduction at a joint section with shafts by the seismic isolation system is far greater than that by the technique to use flexible segments, both of which have been proven promising for practical use. Given that the basic flow of the seismic design of tunnels has been consolidated, the authors intend to publish the results into a manual of design methods, apply the developed technology to practical construction works of seismic isolation tunnels to help prevent earthquake-related damage to lifelines.

ACKNOWLEDGMENTS

This study was conducted as part of the joint research between the Public Works Research Institute of the Ministry of Construction, the Public Works Research Center, and 17 private companies, under the title of "The Development of Seismic Isolation System for Underground Structures." The authors would like to express their deep gratitude to the members of the joint research program for their warm cooperation and helpful suggestions and discussions.

REFERENCES

- 1) Suzuki, T.: Model Vibration Tests on the Seismic Isolation Structure for a Shield-driven Tunnel, Proc. 20th Earthquake Engineering Symposium, JSCE, pp.565-568, 1989. (in Japanese)

- 2) Unami, K. and Suzuki, T.: A Study on the Seismic Isolation Structure for a Shield-driven Tunnel (Confirmation of Isolation Effects by FEM), Proc. 44th Annual Meeting of JSCE, Vol.1, pp.1204-1205, 1990. (in Japanese)
- 3) Suzuki, T. and Unami, K.: A Study on the Seismic Isolation Structure for a Shield-driven Tunnel (Application to Earthquake Response Analyses), Proc. 44th Annual Meeting of JSCE, Vol.1, pp.1206-1207, 1990. (in Japanese)
- 4) Kawashima et al.: The Development of Seismic Design for Underground Structures, Joint Research Report No.29, PWRI, pp.208-235, 1989. (in Japanese)
- 5) Takeuchi M. et al.: Experimental Study on the Sectional Force Reduction in Cross-sectional Deformation of Shield-driven Tunnels due to Earthquakes, Proc. JSCE, No.483/I-26, 1994. (in Japanese)
- 6) Suzuki, T.: Damages of Urban Tunnels due to the Southern Hyogo Earthquake of January 17, 1995 and the Evaluation of Seismic Isolation Effect, CD-ROM of the Eleventh World Conference on Earthquake Engineering, Acapulco, Mexico, 1996.
- 7) Otsuka H., Hoshikuma, J. and K. Nagaya: A Fundamental Study on Innovative Menshin System for Underground Structures, Proc. 6th U.S.-Japan Workshop on Earthq. Dis. Prevent. for Lifeline Systems, Osaka, pp.427-436, 1995.
- 8) Suzuki, T. and Tamura C.: Proposal of a Seismic Isolation Structure for Shield-driven Tunnels and the Method to Evaluate Its Isolation Effect, Proc. JSCE, No.525/I-33, pp.275-285, 1995. (in Japanese)
- 9) Suzuki, T. et al.: Experimental Study on the Silicone-based Material for Seismic Isolation System for Urban Tunnels, Proc. JSCE, No.534/VI-30, pp.69-76, 1996. (in Japanese)
- 10) Tamura C., S. Okamoto and M. Hamada: Dynamic Behavior of a Submerged Tunnel during Earthquakes, Report of Institute of Industrial Science, University of Tokyo, Vol.24, No.5, 1975.
- 11) Suzuki, T.: The Extended Quasi-three-dimensional Ground Model for Irregularly Bounded Surface Ground, Structural Engineering/Earthquake Engineering, Vol.9, No.1, pp.21s-32s, 1992.
- 12) PWRI: Joint Research Report on the Development of Seismic Isolation System for Underground Structures (PART-1), 1996.
- 13) PWRI: Joint Research Report on the Development of Seismic Isolation System for Underground Structures (PART-2), 1997.

PERSONAL CAREER

NAME: Tsutom Tanaka

POSITION: Director,
Central
Research and Development Department,
Oriental Consultants CO.,Ltd.

ADDRESS: Shibuya Chikatetsu Bldg.
1-16-14, Shibuya, Shibuya-ku.
Tokyo, 150, Japan
Tel.+81-3-3409-7555
Fax.+81-3-3409-7565



DATE OF BIRTH: January 7,1953

EDUCATION: Bachelor(1976) and Master Degree (1978) of Engineering,
Tokyo Metropolitan University

MAJOR SUBJECT: Eearthquake Engineering

MAJOR AREA OF EXPERIENCE:

- 1978-1994 Consulting Engineer, Infrastructure Engineering Department,
Tokyo Branch Office, Oriental Consultants CO.,Ltd.
- 1994-1997 Division Director, Seismic and Disaster Prevention Division,
Tokyo Branch Office, Oriental Consultants CO.,Ltd.
- 1997- Director, Central Research and Development Department,
Oriental Consultants Co.,Ltd.

TRAVEL ABROAD: USA

MAJOR PUBLICATIONS: non

**TRANSLATING EARTHQUAKE DAMAGE DATA INTO NEW
PERFORMANCE REQUIREMENTS FOR EARTHQUAKE ACTUATED
AUTOMATIC GAS SHUTOFF DEVICES IN THE UNITED STATES**

Douglas G. Honegger

Consultant

ABSTRACT

In 1992, a standards committee was formed within the American Society of Civil Engineers (ASCE) to revise the 1981 version of the national standard governing earthquake actuated automatic gas shutoff devices (shutoff valves). The 1994 Northridge earthquake provided an opportunity to collect and interpret data specifically applicable to the standard revision. Also, it was clear at the time that shake table tests of existing shutoff valves were necessary to understand the actuation characteristics of the various devices being marketed. This two-prong research activity received financial support from the Federal Emergency Management Agency (FEMA), natural gas utilities, and shutoff valve manufacturers.

The earthquake research effort focused on the 1994 Northridge earthquake and included a review of ground motions, building damage, fire ignitions, appliance damage and actuation data from existing shutoff valves. Gas-related fire locations and review of ground motion response spectra from the Northridge earthquake are the primary bases for actuation requirements in the new national standard. The new standard is specifically intended to be used for shutoff valves installed at grade on low-rise (less than three aboveground floors) residential buildings. The new standard is an example of how recent advances in the collection and graphical presentation of data can be used to translate information into performance requirements.

INTRODUCTION

Since the 1906 San Francisco earthquake, the threat of earthquake fire ignitions growing to large conflagrations has been recognized as a possible hazard scenario. Potential fire damage following an earthquake is dependent upon many factors. Some of the most important include the number and dispersion of fire ignitions, the amount and nature of combustible material available for the spread of fire, response capacity of the local fire departments, and weather conditions at the time of the fire. However, since 1906, fire damage has not been a significant factor in any US earthquake.

Post Earthquake Fires in the United States

Since the prevention of fires related to natural gas leakage is the goal for earthquake actuated automatic gas shutoff devices, examination of data regarding fires in the Northridge earthquake is especially important. Table 1 provides a summary of reported fire incidents and the number of fires with gas as a contributing factor for modern United States (US) earthquakes compiled from Honegger and Elliott (1990), Manning (1987), Mohammadi et al. (1992), Russel and Taylor (1987), Scawthorn (1985), and data from the Northridge earthquake.

For the Northridge earthquake, most of the data on building fire incidents on January 17, 1994 was available from the Office of the California State Fire Marshal. This information is provided as part of the California Fire Incident Reporting System (CFIRS). Compilation of fire statistics from summary reports such as the CFIRS involves some judgment in interpreting the standard categories used to define fire incidents. The data available as of February, 1997 was reviewed to limit consideration to structural fires and excluded other incidents related to vehicle, rubbish and brush fires. The data in Table 1 indicate that gas is a factor in 15% to 50% of all earthquake related fires in the US.

While there is considerable information on post-earthquake fire from outside the US (particularly Japan), this data is not applicable for studies of gas-related fire risk in the US. The reasons for this include significant differences in the age, maintenance, and operation of gas systems, building construction quality, building density, and typical residential gas appliance operation.

United States Requirements for Earthquake Actuated Gas Shutoff Devices

Justification exists for arguments for and against widespread use of earthquake activated shutoff valves. Some emergency planners advocate shutoff valves as a means to reduce fire loss in densely populated areas with large inventories of combustible structures. Industrial users of natural gas turn to automatic gas shutoff valves as a means to protect key structures and equipment. At the same time, industrial users are concerned with economic loss resulting from unnecessary tripping of earthquake valves which may have an economic risk as great as that posed by a potential fire. Gas utilities are concerned by oversensitive gas shutoff valves and the impact of a high number of such valves on recovery efforts. Gas relight service is by far the

greatest effort gas utilities face after an earthquake. The costs of relight efforts are eventually passed on to customers in the form of higher gas prices.

The first standard for earthquake actuated automatic gas shutoff systems was ANSI Z21.70 (1981). This standard was produced under secretariat of the American Gas Association (AGA) in 1981. After issuance of the Z21.70 specification, alternate secretariat sponsorship was sought. In 1981, the secretariat for the specification was transferred to the B31 committee of the American Society of Mechanical Engineers (ASME). Interest in the specification could not be generated by ASME and the subcommittee responsible for the specification was dissolved in the late 1980's. ASME sought to return secretariat for the specification to AGA in the fall of 1990. In 1992, ASCE accepted the secretariat of the standard. The Z21.70 standard was technically defunct in 1986 since ANSI standards must be reviewed every 5 years. However, the requirements of ANSI Z21.70 were incorporated into California state legislation and remain the governing requirements for devices marketed in California.

The crux of the Z21.70 specification is the seismic activation requirements. Actuation in Z21.70 is required between an acceleration of 0.08 g and 0.3 g for a sinusoidal motion at a frequency of 2.5 Hz. Actuation is not permitted for acceleration of 0.08g and frequencies of 1 and 10 Hz or at 0.4g for a sinusoidal motion at a frequency of 10 Hz. In testing for these conditions, a 5 second time interval is allowed for actuation or non-actuation.

Following the 1994 Northridge earthquake, an effort to mandate the installation of shutoff valves on structures under the jurisdiction of the City of Los Angeles was led by a member of the Los Angeles City Council. During ad-hoc meetings with the fire department and the department of building safety, it became evident that the current California requirements were inconsistent with the experiences of the Northridge earthquake as well as past earthquakes in California. The ad-hoc committee recommended postponement of the ordinance until the ASCE standards committee could complete its work. It is expected that California legislation will be changed to reflect the new ASCE standard once the standard is published. Against the recommendation by the ad-hoc committee, the Los Angeles City Council decided to proceed with an ordinance and directed the ad-hoc committee to work with the Department of Building and Safety to develop interim shutoff valve requirements to address concerns regarding the existing California state requirements. Preliminary findings from research that was underway for the ASCE standard committee were used by the ad-hoc committee to develop these interim requirements. The ordinance eventually adopted by the City of Los Angeles increased the non-actuation requirements of ANSI Z21.70 to 0.20 g at 1 Hz and 2.5 Hz.

OBSERVATIONS FROM THE 1994 NORTHRIDGE EARTHQUAKE

The exhaustive data collection effort undertaken by the California Office of Emergency Services (OES) under FEMA sponsorship following the Northridge earthquake provided a unique opportunity to investigate the necessary performance requirements for shutoff valves. Much of this information has since been disseminated by OES (EQE/OES, 1995, 1997). Another

important information source from the Northridge earthquake are the data contained in the California Fire Incident Reporting System (CFIRS) for the day of the earthquake. This information was reviewed in detail as part of a research effort undertaken by the ASCE committee revising the national shutoff valve standard (Diehl, 1995, Honegger, 1995). A summary of the findings of this research is provided below.

Summary of Northridge Earthquake Gas-Related Fire Incidents

The observations of gas-related fires following the Northridge earthquake summarized below are taken from the research report prepared for the ASCE standard committee (Honegger, 1995) and a recent (1997) review of CFIRS data for the region (including Los Angeles) impacted by the Northridge earthquake.

- The day of the earthquake, the region impacted by the Northridge earthquake experienced a total of 590 fire incidents
- Of the 590 incidents, about 345 involved buildings
- Of the 345 building fire incidents, 107 (31%) were identified as being related to the earthquake
- Of the 107 earthquake related building fire incidents, 95 involved residential buildings
- Of the 95 earthquake related residential building fire incidents, less than 50 were related to natural gas
- All of the gas-related fires in the Northridge earthquake occurred in regions experiencing spectral accelerations greater than 0.4g at a frequency range of 2 Hz to 5 Hz
- There were fewer than 40 gas-related fire incidents in areas experiencing levels of ground shaking of MMI VIII or greater
- The largest contributor to gas-related residential fire ignitions in the City of Los Angeles was unanchored gas appliances (82%) and water heater damage was the most common cause (59% of the ignitions related to gas appliances)
- The number of wood frame structures exposed to ground shaking of MMI VIII or greater was over 225,000
- Conservatively assuming that only 60% of the wood frame structures had gas appliances, the risk of gas-related residential fires experienced in the Northridge earthquake was 0.030% or 1 in 3,375
- The risk of 65% or greater structural damage in areas of MMI VIII or greater in the Northridge earthquake was approximately 15 times as high (0.45%) as the conservative estimate of gas-related fire risk

Building Damage

The region impacted by strong ground motion in the Northridge earthquake encompassed a wide variety of building types and building vintages. Residential buildings which account for approximately 93% of the building stock in Los Angeles County (OES, 1995). The regional distribution of building age was mapped as part of the FEMA data collection effort. Within the epicentral area, the majority of construction pre-dated 1960. There was clear correlation between the location of pre-1920 structures and the high concentration of structural damage. Therefore, the age of structures impacted by the Northridge earthquake is considered representative of a majority of the building stock both in California and the US.

Post-earthquake inspections of structures were mobilized by local building departments. These inspections were generally carried out at the request of the building owner. For this reason, nearly all inspections were for structures in which some damage had occurred or was otherwise suspected. Evaluation of structures was subjective and relied upon guidance contained in ATC 20, *Procedures for Postearthquake Safety Evaluation of Buildings* (ATC, 1989). Inspection of buildings resulted in the inspection team affixing a green, yellow or red tag on the structure with yellow or red tags denoting serious structural damage.

Considering only the yellow and red tagged structures, a map of the concentration of significant building damage in terms of occurrences per unit area was possible. Some caution was warranted because areas where the damage rate may have been relatively low could show as high damage areas in areas with a high concentration of structures. Still, the information was useful as a conservative means to represent the extent of significant structural damage in the Northridge earthquake.

Existing Shutoff Valve Data

Following the Northridge earthquake, several valve manufacturer's were asked to collect information on the performance of devices they had sold in the affected area. Another set of data on actuated shutoff-devices was collected by Southern California Gas Company during their service restoration efforts. This information consisted of address location of actuated devices. The manufacturer's data collection effort was spearheaded by Mr. Carl Strand as part of an ASCE post-earthquake investigation committee activity (Strand, 1995, 1997).

Information sought included the make and model of the device, the address location of the device, the size in terms of nominal pipe dimension, whether or not the valve actuated during the main shock, aftershocks or previous earthquakes, and whether or not a gas leak was found following the earthquake.

Unfortunately, the information collected is of only anecdotal interest. Much of the data collected was the result of Mr. Strand's review of his own files since he was a distributor for Pacific Seismic Products. Therefore the data is heavily skewed toward only one device. There is also no information on the total population of devices. This prohibits drawing conclusions

regarding the rate at which shutoff valves were actuated in areas where actuation was desirable as well as areas where actuation was unnecessary. Nonetheless, locations of actuated and non-actuated valves were mapped for comparison with observations of ground motion, building damage and gas-related fires.

If it is assumed that the mapped distribution of earthquake shutoff valves is representative of the true regional distribution, the following conclusions can be drawn:

1. There is a slight trend for greater actuation rates to the west of the earthquake epicenter than to the southeast. This is consistent with the ground motion contours.
2. The ability of existing shutoff valves to respond under strong ground motion is confirmed by the lack of a significant number of non-actuation locations within MMI VII.
3. Existing actuation characteristics appear to be too conservative as evidenced by the high proportion of actuation in the MMI VI contour west of the epicenter where little structural damage occurred.
4. The potential area encompassing the extent of shutoff valve actuation was approximately 950 square miles while the extent of significant structural damage was less than 500 square miles.

To draw definitive conclusions on the performance of shutoff valves in the Northridge earthquake or any future earthquake, an ongoing effort is needed to quantify the existing population of shutoff valves. Because of the serious problems with the quality of the automatic gas shutoff valve data, recommendations for earthquake actuation requirements in the Northridge earthquake did not consider any shutoff device performance data.

Boundary Estimates of Spectral Ground Motion

Specific strong motion recording station records were reviewed in order to obtain information on spectral accelerations at frequencies between 1 and 18.2 Hz. Two types of locations were examined to represent locations where onset of actuation would have been desirable and locations where there was no significant damage and actuation should not have occurred. The information reviewed consisted of maps of ground motion contours (peak ground acceleration (PGA), 1 Hz, 18 Hz, and 33 Hz accelerations) presented with building damage concentration and gas-related fire locations.

The governing location for onset of actuation in the Northridge earthquake was just south of downtown Los Angeles and north of Bell (see Figure 1). The governing location is defined by the area in the vicinity of a gas-related fire that experienced the lowest level of ground motion. This finding is believed to be directly attributable to the greater concentration of pre-1920 structures in this area. The bounding 33 Hz spectral acceleration in this area was estimated to be 0.43 g. This contour encompasses all but one of the identified gas-related fire locations in the ASCE study (Honegger, 1995).

To provide information on other spectral acceleration values in the frequency range of interest, computed response spectra for three California Division of Mines and Geology (CDMG) strong motion recording stations in governing location for onset of actuation were examined. Only three stations were selected because of the absence of processed records for other stations at the time of the research. The three stations examined are identified as 14368, 14403, and 24157 (Figure 1). Spectral accelerations for these three stations are summarized in Table 2. In the table, H1 and H2 refer to the two orthogonal horizontal components of ground motion recorded at the station.

A similar point-based evaluation was performed for processed data from stations located near Malibu, Port Hueneme, and just north of Oxnard (see Figure 1). These locations were selected because they lie outside the region that experienced significant damage and actuation of automatic gas shutoff devices would not have been desirable in the Northridge earthquake. The results, summarized in Table 3.

Residential Gas Fire Exposure

FEMA claims for damaged appliances exceeded 700,000 following the Northridge earthquake. Over 400,000 of the FEMA claims were for water heater damage. Note that the 400,000 claims for water heater damage indicates considerably more buildings were impacted by the Northridge earthquake than the number used to estimate the risk of gas-related fire in the Northridge earthquake. The number of FEMA claims paid would seem to support the viewpoint that considerable damage to gas connections to appliances could have occurred in the Northridge earthquake and hence more gas-related fires might have been expected. There are several explanations for why this wasn't the case in the Northridge earthquake and has not been observed in past US earthquakes. One possible explanation related to the quantity of gas leakage required to pose an imminent threat is presented below.

Ignition of leaking gas requires that the gas concentration in the potentially ignitable mixture to be above about 5% (AGA, 1965). Explosive gas mixtures require gas concentrations on the order of two to three times as great. Since natural gas is lighter than air and tends to disperse, the rate of gas leakage with potential for producing a gas explosion is related to the air exchange rate in the area where leakage is occurring. The degree of correlation between these two flow rates is dependent upon whether or not poor air mixing can cause pockets of gas to accumulate.

An estimate of the gas leakage rate requirement can be based on information regarding building ventilation requirements. Assuming a typical minimum ventilation requirement of 0.33 cfm (cubic feet per minute) per square foot of floor area and a floor area of 135 square feet leads to a ventilation rate of 45 cfm. Other guidelines for probable ventilation can be used if rooms are considered to be represented by poorly constructed residences. Note that many water heaters and gas clothes dryers in the US are often located in garages with much higher minimum air exchange rates.

The relative severity of gas leakage for an ignitable mixture can be estimated by comparing the estimated rate of gas leakage with standard gas capacity design charts developed to represent gas supply capacity as a function of pipe diameter and length of pipe from the meter to the appliance. For a 45 cfm air exchange rate, gas must be supplied at a rate of at least 2.3 cfm or 135 cfh (cubic feet per hour) to build to an ignitable mixture. For an allowable pressure drop of 0.5 inches of water column, gas specific gravity of 0.6, and supply pressure of 0.25 psig, this supply rate exceeds the maximum capacity for 1/2-inch pipe lengths greater than about 30 feet and 3/4-inch pipe lengths less than about 65 feet (AGA, 1965). Based on the assumed ventilation conditions, it is concluded that near open flow conditions need to exist in order to have a significant risk of gas-related fire unless significant pipe damage occurs near the meter. The limited amount of data available from the 1987 Whittier earthquake suggests that such large volumes of gas leakage are rare (Honegger and Elliott, 1990)

The above discussion implies that the risk of explosion from leakage at gas appliances sustaining moderate damage in an earthquake is very low. This is supported by the relative rarity of gas explosions and the low number of gas fires in past earthquakes, including the Northridge event. A very approximate assessment of the risk of residential gas-related fire given that the earthquake has damaged the gas appliance is less than 0.007% (50 in 700,000).

NEW ASCE NATIONAL STANDARD REQUIREMENTS

Efforts to create a new national standard for shutoff valves began in 1992 through ASCE in accordance with requirements set forth by the American National Standards Institute. In accordance with ANSI requirements for developing a consensus standard, the committee was formed with representation balanced between individuals from regulatory agencies, engineering consultants, academia, gas utilities, and shutoff valve manufacturers. The rules governing standard committee function and standard approval processes required compromise to address the diversity of technical, economic, and political viewpoints represented by committee members. At this time (November, 1997) the proposed standard has completed the committee and public ballot process and is expected to be published in early 1998.

Key changes in the proposed ASCE standard include the specification of an actuation range over a range of frequencies from 1 Hz to 10 Hz, more stringent mounting requirements, and the addition of a commentary. Other potential issues considered but left unchanged from the ANSI Z21.70 standard include providing external valve seating force, providing a means to lock the shutoff valve in closed position once actuation occurs, and supplemental testing requirements for valves in their actuated condition. The format of the standard was also greatly improved to focus on the seismic requirements. This was done by adopting existing valve standard requirements for automatic gas shutoff valves wherever possible.

New Actuation Requirements

There are numerous underlying assumptions that played a role in decisions regarding appropriate actuation limits:

1. The identified limits are based on encompassing more than 95% of all gas-related fires in the Northridge earthquake.
2. The typical structural configuration is considered to be a wood frame single or multi-family structure with a water heater on the first floor. Water heaters installed above the first floor are expected to see greater earthquake motions than the free field as a result of the dynamic response of the structure.
3. The structure and the gas appliance configurations are consistent with an assumed damping ratio of 5%.
4. It is assumed that no structural damage occurs to cause leaks in the gas appliances themselves or interior gas lines. This condition is generally satisfied as long as partial structural collapse does not occur.

The recommended actuation limits proposed in the new ASCE standard are presented in Figure 2. Also shown on Figure 2 are the average spectral acceleration values previously presented in Table 2 and Table 3. Based on the Northridge earthquake, it appears that the range of actuation proposed in the ASCE standard could be increased by 30% to 50% for frequencies between 2.5 Hz and 5 Hz.

Above 5 Hz, there is a significant difference in the proposed ASCE requirements and the spectral acceleration data. This difference is related to two considerations of the committee. First, high-frequency ground motions occur with very small displacements and are known to have limited damage potential. Second, the data plotted in Figure 2 are for a specific earthquake. A smaller earthquake is expected to have a much more localized damage area that is enveloped by high-frequency spectral accelerations of greater amplitude than were observed in the Northridge earthquake.

Proposed Changes Not Related to Earthquake Actuation

In addition to the changes in actuation levels and test requirements, the proposed ASCE standard incorporates several improvements related to assuring consistency in shutoff valve installation and response to earthquake motions.

Mounting Shutoff valves shall be mounted in a manner so as to have a fundamental resonance period less than 0.06 seconds (17 Hz). This requirement limits unnecessary amplification of dynamic motions sensed by the shutoff valve. This requirement essentially limits application of the standard to shutoff valves located near the ground surface.

- Seating Shutoff valves are required to maintain a seal in their actuated condition when subjected to rotations of up to 45° with respect to vertical at any azimuth. This requirement is intended to provide reasonable assurance that the valve will not unexpectedly open under subsequent aftershock activity.
- Warranty Manufacturers are required to warrant the performance of their devices for a period that is at the discretion of the manufacturer. Although the committee felt that a 20-year warranty should be a minimum requirement, stipulating this is not generally appropriate in a standard. Rather than eliminate the requirement altogether, it was felt that requiring some warranty would provide the end user with a basis for comparing the quality as well as the price of various shutoff valves.
- Impact ANSI Z21.70 included a provision for minimum impact energy absorption requirements. These requirements were minimal and are easily met by any material suitable for gas service at the temperature requirements specified. More stringent requirements were considered to account for impact from falling debris. However, the necessary minimum impact requirements are nearly impossible to quantify based on the highly variable nature of hypothetical debris impact scenarios. The impact requirement has been dropped from the proposed new standard in lieu of a general requirement for the use of “suitable” materials for shutoff valve construction.
- Applicability The proposed standard has been limited to single-family or multi-family structures with three aboveground stories or less. This limitation is related to the data used to develop standard actuation requirements.

CONSIDERATIONS FOR MANDATED SHUTOFF VALVE USAGE

After every earthquake in California, there renewed interest on the part of public officials to limit the risks from future earthquakes. Despite consistent evidence to the contrary, public perception is that natural gas is a key contributor to the earthquake related fire hazard and mandated installation of shutoff valves is one alternative that is often considered as a politically acceptable means to address public fears.

The primary impetus for owners installing devices to shutoff gas service in the event of strong ground shaking is to limiting potential collateral damage that might arise from leaking gas within their structure. The relative importance of reducing the occurrence of a low-risk phenomenon is largely a matter of personal perception.

Public officials, on the other hand, have a responsibility to focus their attention on the much more serious consequences from large conflagrations. Fires ignited directly as a cause of earthquake ground shaking have the potential to grow quickly and cause significant property damage given the right combination of flammable building stock, lack of fire-fighting resources, wind and humidity conditions, . It is obvious that the risk of conflagration is very low given the

recurrence intervals of large earthquakes and the requirement for a suite of environmental conditions be in place at the time of the earthquake. Although the risk of such an event is very low, the potential for long term adverse socio-economic impact in certain urban settings can warrant action to address this risk.

Earthquake actuated automatic gas shutoff devices is a means to limit the role of natural gas in post-earthquake conflagrations provided their use is implemented in a logical fashion. The first step in such implementation should be the identification of high risk areas based on factors that include the amount of flammable material in either the building stock or natural environment, location of fire fighting resources, access restrictions, water supply, and prevalent local wind conditions. This is often politically difficult in the US because of the potentially adverse impact on property values. Mandated installation of automatic gas shutoff devices in all structures located in high risk areas minimizes the chances that natural gas will be the source of an ignition leading to spread of fire in a high risk area. However, automatic isolation of electrical service should also be considered in high risk areas as historical evidence shows electrical fire ignitions are more often the source of post-earthquake fires.

Another consideration when assessing the impact of automatic gas shutoff devices is the performance of the structures with gas service. It is recommended that automatic gas shutoff devices be viewed as a means to reduce the potential for gas-related fires in structures not expected to be significantly damaged in an earthquake. This is the philosophy that has been adopted in formulating proposed actuation requirements in the new ASCE standard. There are three primary reasons for this. First, significant structural damage increases the likelihood of damage to external components of the gas delivery system upstream of the shutoff device (e.g., meter set assemblies, exposed piping) where gas can readily dissipate. Second, especially vulnerable structures may exhibit damage at levels of ground motion far below what has been used to develop shutoff valve standards. Third, it is logical from the viewpoint of the individual building owner to discount the risk of gas-related fire for structures that pose a far greater collapse hazard to their inhabitants than the risks attributable to natural gas.

In deciding to mandate installation of automatic gas shutoff devices, public officials need to be fully cognizant of the impact of such mandates on the time required to restore gas service. Prolonged restoration times can pose severe hardships by removing what may be the only source of heat as well as fuel for cooking and boiling water. This is especially true for elderly individuals that may not have the means to readily reach shelters providing emergency services following an earthquake.

Finally, there is a question regarding the cost-effectiveness of earthquake actuated automatic gas shutoff devices. The experience of the LAFD in the Northridge earthquake, with respect to the high number of fires related to gas appliances, is not unique. Simple, yet robust, restraint for major home gas appliances can be installed by homeowners at a fraction of the cost of shutoff devices. The mandated installation of appliance restraints could reduce the risk of a gas-related fire in an earthquake by more than 80%.

REFERENCES

1. American Gas Association (1965). Gas Engineers Handbook, C.G. Segeler, Editor, Industrial Press, Inc.
2. Applied Technology Council (1989). "Procedures for Post-Earthquake Safety Evaluation of Buildings," ATC-20, Redwood City, California.
3. Diehl, J.G. (1995). "Vibration Testing of Fifteen Earthquake Actuated Automatic Gas Shutoff Sytems: An Engineering Evaluation," prepared by Agbabian Associates for the ASCE Prestandards Committee for Earthquake Actuated Automatic Gas Shutoff Systems.
4. Hall, J.F. (ed.) (1995). "Northridge Earthquake of January 17, 1994 Reconnaissance Report," Earthquake Spectra, Supplement C to Volume II, Earthquake Engineering Research Institute.
5. Honegger, D.G. (1995). "Automatic Gas Shutoff Device Actuation Requirements Based on Damage in the January 17, 1994 Northridge Earthquake," EQE Report 52316, prepared for the American Society of Civil Engineers.
6. Honegger, D.G. and K.E. Elliott (1990). "Observations on the Distribution of Repairs Recorded by Southern California Gas Company Following the October 1987 Whittier Narrows Earthquake," EQE report to Southern California Gas Company.
7. Jennings, B.H. (1970). Environmental Engineering: Analysis and Practice, Harper and Row.
8. Manning, D.O. (1987). "A Report by the Los Angeles City Fire Department on the Whittier Narrows Earthquake of October 17, 1987"
9. Mohammadi, J., S. Alyasin, and D.N. Bak (1992). "Investigation of Cause and Effects of Fires Following the Loma Prieta Earthquake," Report IIT-CE-92-01, Illinois Institute of Technology, Chicago, IL.
10. OES/EQE (1995). "The Northridge Earthquake of January 17, 1994: Preliminary Report on Data Collection and Analysis," Part A: Damage and Inventory Data, prepared by EQE International and the Geographic Information Systems Group of the Governor's Office of Emergency Services.
11. Russell, A.E. and J.W. Taylor (1987). Southern California Gas Company's Preliminary Results and Findings on the Whittier Earthquake of October 1, 1987," presentation to California State Fireman's Association, Santa Rosa, California.
12. Scawthorn, C.G. (1985). "Post-Earthquake Fire", Proceedings of the US-Japan Workshop on Urban Earthquake Hazard Reduction, Publication No. 85-03, EERI, Berdeley, CA, pgs. 237-243.
13. Strand, C.L (1997) "Performance of Seismic Gas Shutoff Valves and the Occurrence of Gas-Related Fires and Gas Leaks During the 1994 Northridge Earthquake, with an Update on Legislation and Standards Development," CUREe Northridge Earthquake Research Conference, Los Angeles, August 20-22.

Table 1: Summary of Fire Incident Information for Recent US Earthquakes^{1,2}

EVENT	YEAR	MAGNITUDE	EARTHQUAKE FIRES	GAS RELATED FIRES ²
Anchorage	1964	8.4	4 to 7	0
Puget Sound	1965	5.6	1	Not Available
San Fernando	1971	6.6	109	15
Coalinga	1983	6.7	1 to 4	1
Morgan Hill	1984	6.2	3 to 6	1
Palm Springs	1986	5.9	3	0
Whittier Narrows	1987	5.9	6	3 ³
Loma Prieta	1989	6.9	67	16 ⁴
Northridge	1994	6.6	107	49 ⁵

¹ Data from Mohammadi et al. (1992) unless otherwise noted

² Data on gas related fires from Honegger and Elliott (1990) unless otherwise noted

³ From Manning (1987)

⁴ From Mohammadi et al. (1992)

⁵ From Honegger (1995) and updated CFIRS data

Table 2: Point Spectral Values Representing Governing Onset of Actuation Limits

STATION	10 Hz		5 Hz		2.5 Hz		1 Hz	
	H1, g	H2, g	H1, g	H2, g	H1, g	H2, g	H1, g	H2, g
14368	0.33	0.31	0.64	0.44	0.48	0.55	0.15	0.14
14403	0.32	0.24	0.43	0.37	0.49	0.38	0.15	0.12
24157	0.39	0.42	0.44	0.42	0.49	0.41	0.16	0.16
Average	0.34		0.46		0.77		0.15	

Table 3: Point Spectral Values Representing Non-Actuation Limits

STATION	10 Hz		5 Hz		2.5 Hz		1 Hz	
	H1, g	H2, g	H1, g	H2, g	H1, g	H2, g	H1, g	H2, g
24396	0.17	0.15	0.26	0.20	0.29	0.21	0.09	0.10
25282	0.17	0.17	0.24	0.26	0.34	0.29	0.17	0.19
25340	0.06	0.08	0.11	0.16	0.16	0.16	0.12	0.20
Average	0.13		0.21		.24		0.15	

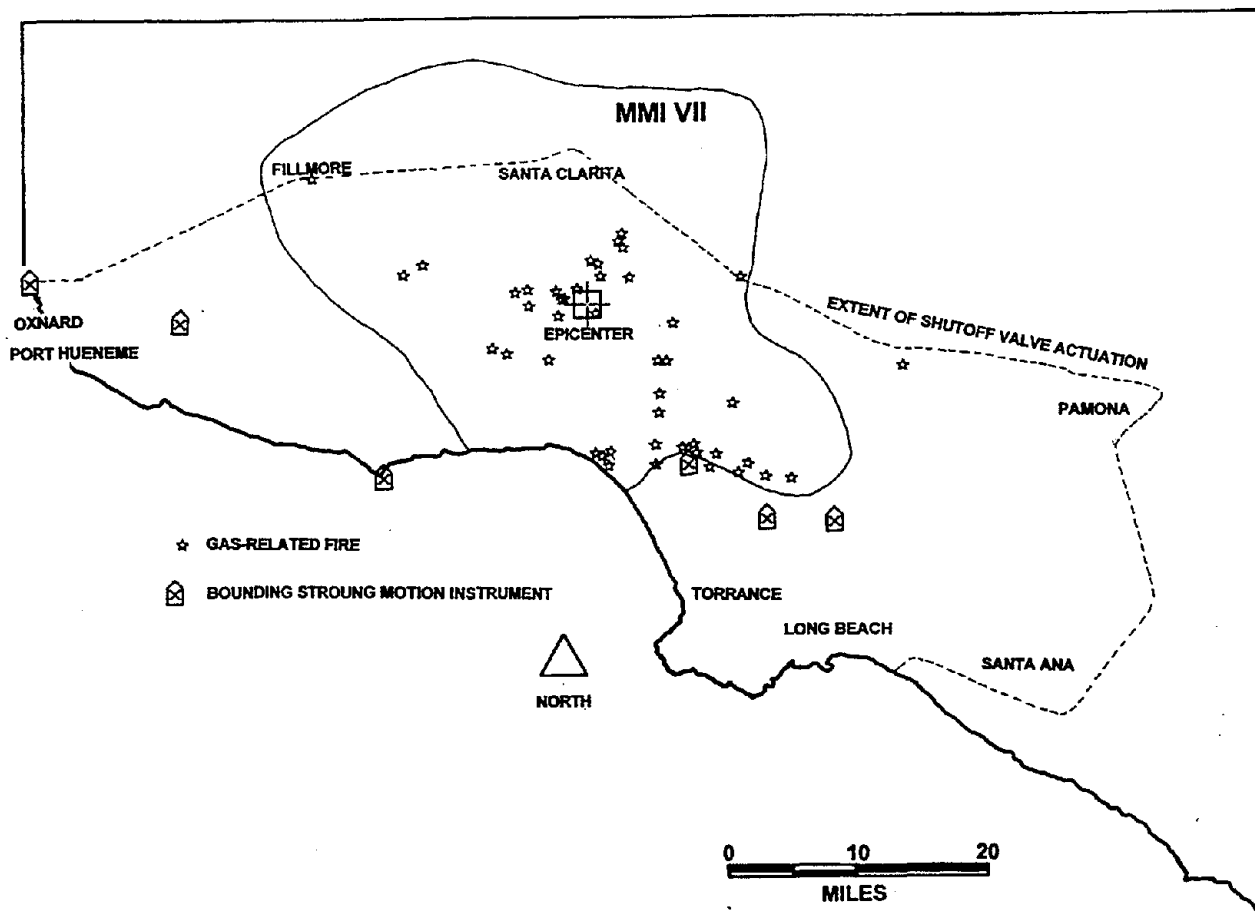
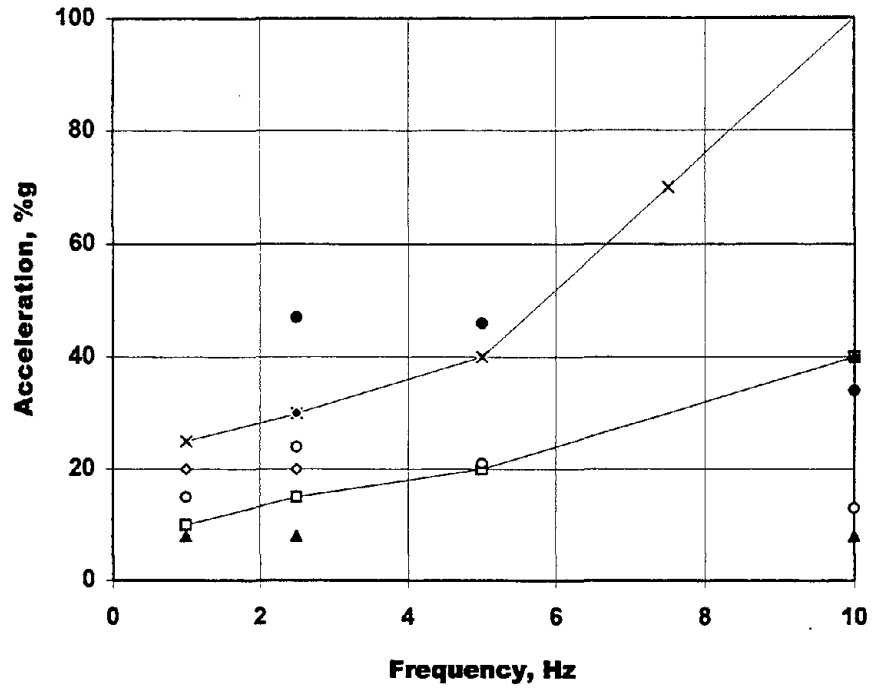


Figure 1: Map Showing Location of Gas-Related Earthquake Fires, Ground Shaking Intensity, and Extent of Shutoff Valve Actuation in the 1994 Northridge Earthquake



- x- Recommended Must Actuate Test Points (symbols represent test points)
- Recommended Non-Actuation Test Points (symbols represent test points)
- 1981 ANSI Z21.70 Must Actuate Test Point
- ▲ 1981 ANSI Z21.70 Non-Actuate Points
- ◇ Non-Actuation Levels for City of Los Angeles 1995 Ordinance
- Average Northridge Spectral Acceleration Near the Bounding Location for Actuation
- Average Northridge Spectral Acceleration Where Actuation Should Not Occur

Figure 2: Comparison of Shutoff Valve Actuation Requirements and Average Spectral Values from the 1994 Northridge Earthquake

DOUGLAS G. HONEGGER

POSITION: Independent Consultant

ADDRESS: 1728 Date Avenue
Torrance, California 90503-7210
Phone & Fax (310) 320-9283
e-mail dghconsult@aol.com

BIRTH DATE: January 2, 1958

EDUCATION: *University of Illinois*, M.S. Civil Engineering, 1981
University of Illinois, B.S. Civil Engineering, 1980

PROFESSIONAL HISTORY:

Independent Consultant, 1995-present

EQE International, Irvine, California, Technical Manager and Associate, 1989-1995

National Technical Systems, Long Beach, California, Project Engineer, 1985-1989

Structural Mechanics Associates, Houston, Texas, Staff Engineer, 1982-1985

Sargent and Lundy Engineers, Chicago, Illinois, Staff Engineer, 1981



SUMMARY:

Mr. Honegger has over 16 years of experience in a broad range of engineering activities related to understanding the response of structures, structural components and equipment to extreme loading resulting from earthquakes, wind, blast and impact. Mr. Honegger's career has been a consultant to pipeline operators, Department of Energy (DOE), Department of Defense, and nuclear power industry. Mr. Honegger's experience has covered experimental investigations, detailed analytic evaluations and engineering design. He is experienced in providing defensible results under the high level of scrutiny often associated with critical facilities. He has been the principal author of over 20 professional papers and has been a contributing author to two books on the subject of seismic design of pipeline systems. Mr. Honegger has worked as an independent consultant since 1995.

Mr. Honegger's experience in the seismic response of pipeline systems dates back to 1982, he participated in the development of a book on the seismic design guidelines for oil and gas transmission pipeline facilities. Mr. Honegger has remained active in the oil and gas industry throughout his career and has translated this experience to other buried systems subjected to ground deformations resulting from earthquake and other hazards. He is a recognized expert in evaluating the impacts of large permanent ground deformation on buried systems and the impact of earthquakes on a wide variety of aboveground and buried pipeline and conduit systems. He has developed vulnerability relationships and performed seismic risk assessments for a variety of pipeline systems including oil, natural gas, municipal water and dedicated fire protection systems. Mr. Honegger has been a consultant on the performance of pipeline systems in earthquakes for clients in the US, Canada, Mexico, Japan, Thailand, and the Philippines.

Mr. Honegger led several projects for the Department of Defense in the mid 1980's. Much of his work dealt with the effects of blast loading, impact, and ground shock on aboveground and buried structures. These projects typically involved experimental research in which designing measurement and instrumentation schemes was a necessary component. He has participated as an experimenter in underground nuclear tests of buried lifelines and large-scale high explosive tests simulating conditions generated by near-field nuclear weapon detonation.

Throughout his career, Mr. Honegger has gained expertise in the seismic qualification or evaluation of critical safety equipment and piping systems at nuclear facilities and chemical plants. Mr. Honegger's experience has encompassed a broad range of seismic evaluation activities including analysis, personnel training and in-plant inspections. Much of his experience in this area has involved developing seismic evaluation criteria and application of experience from past earthquakes. He has applied this experience to the development of seismic design criteria at US Department of Energy facilities and the evaluation of critical equipment in the nuclear power and chemical process industries.

Mr. Honegger is active in several professional and organizations and volunteer activities. He is an active member of ASCE where he chairs the Earthquake Actuated Automatic Gas Shutoff Devices standards committee, the Lifelines Standards Council, the joint ASCE/ASME Working Group on Buried Piping Design Issues, and the Gas and Liquid Fuel Lifelines Committee.

RESOLUTIONS OF
THE SEVENTH U.S.-JAPAN WORKSHOP ON
EARTHQUAKE DISASTER PREVENTION FOR LIFELINE SYSTEMS

Task Committee F
UJNR Panel on Wind and Seismic Effects

Seattle, Washington U.S.A.
November 4-7, 1997

The Seventh U.S.-Japan Workshop on Earthquake Disaster Prevention for Lifeline Systems was held in Seattle, Washington U.S.A., during November 4-7, 1997 under the auspices of Task Committee F, Disaster Prevention Methods for Lifeline System, UJNR Panel on Wind and Seismic Effects. The workshop was co-sponsored by the National Institute of Standards and Technology and the National Science Foundation of the United States and the Public Works Research Institute of Japan. Forty-nine experts, representing government, academia, industry and private practice participated in the workshop. Thirty papers were presented. In particular, results of studies of the two most recent damaging earthquakes; the January 17, 1994 Northridge Earthquake and the January 17, 1995 Hyogo-ken Nanbu (Kobe) Earthquake, were presented and discussed.

The Workshop provided a most valuable forum to exchange information, experiences, and ideas on technical as well as socio-economic issues important to the lifeline earthquake engineering community of both countries. The following topics were addressed:

- Seismic damage of lifeline facilities
- Seismic behavior of lifeline facilities
- Socio-economic impacts of seismic damage to lifeline facilities
- Seismic damage estimation and prediction for lifeline facilities
- Research and development in earthquake disaster prevention technologies after the Northridge and Kobe Earthquakes
- Lifeline facilities and urban earthquake disaster prevention

The Workshop participants have adopted the following resolutions:

1. The participants identified, without priority order, the following topics relevant to lifeline systems for future cooperative research programs:
 - a. Exchange of information on seismic design and performance of lifeline facilities;
 - b. Investigation of earthquake damage;
 - c. Study of the effect of liquefaction on the performance of lifeline systems;
 - d. Development of cost effective countermeasures against liquefaction for lifeline systems;
 - e. Repair and retrofit procedures and post-event service restoration strategies;
 - f. Improvement of post-earthquake fire suppression strategies;

- g. System analysis and network management strategies for improving lifeline performance during and after major earthquakes;
 - h. Evaluation of socio-economic impacts resulting from disruption of lifeline services after major earthquakes;
 - i. Adoption of emerging/mature methodologies, such as GIS, GPS, real-time conditional simulation, from related field of expertise to lifeline earthquake engineering;
 - j. Enhancing communication between the private sector and government agencies in both countries.
 - k. Research and development of pipeline systems with built in capability (e.g., smart pipe) to monitor structural, system, and contents parameters that would allow better post-earthquake operation, as well as operations under other normal or stress event situations
 - l. Development of system risk/reliability evaluation methodologies to address multiple hazards including earthquakes, floods, winds, and other disasters associated with the built environment.
2. The participants recognize the importance of continued exchange of personnel, technical information, research data and use of available research facilities in both countries, and the value of integrated multidisciplinary research. The participants further recognize the benefit of identifying and executing specific activities comparing the results of different design, analysis and experimental methods, and disaster mitigation strategies in both countries.
 3. Recognizing the need for the integrated nature of lifeline systems, the participants encourage the interaction of this Task Committee with other UJNR Task Committees and Panels to develop better methodologies for quantifying the vulnerability and implementing mitigation measures for lifeline systems against earthquake losses.
 4. The participants recognize the relevance of this task committee's missions with respect to the three thrusts identified at the conclusion of the Second Earthquake Policy Symposium held in Kobe, Japan, September 1997, under the auspices of the U.S.-Japan Common Agenda. These thrusts are real time seismic information, loss estimation models, and post-earthquake response and recovery. The participants recommend that future task committee activities be designed to support these thrusts of the Common Agenda.
 5. Considering the importance of continued cooperative research programs on seismic effects and earthquake disaster prevention methods for lifeline systems, the participants recommend to hold the next workshop in Japan in 1999. Location and time of the workshop will be determined through correspondence between the co-chairs of Task Committee F of the UJNR Panel on Wind and Seismic Effects.

Agenda

7th US-Japan Workshop on Earthquake Disaster Prevention for Lifeline Systems

TUESDAY, NOV. 4

7:30a.m. - 8:00a.m. Continental Breakfast

8:00a.m - 8:30a.m. Introduction

**8:30a.m. - 9:00a.m. Special Presentation – Past Liquefaction /Tsunami Ocurances at the Metro West Point Wastewater Treatment Plant.
Presented by Brian Atwater**

9:00a.m. - 10:20a.m. Technical Session I - Seismic Damage of Lifeline Facilities

Economical Damage at Kushiro Port due to the Kushiro-oki Earthquake and Cost-Benefit Analysis on Economical Rationality of countermeasures against Liquefaction. Atsushi Nozu and Tatsuo Uwabe

Liquefaction Induced Lateral Spread Estimation Techniques. Matthew Mabey

Earthquake Damage to Buried Pipes and their Renovation. Hose Lining, Tadanobu Sato, Isaburo Yagi, Tom Driver and Hiroyuki Sakuragi

Factors Impacting LADWP Pipeline Performance in the Northridge Earthquake. Seljick Toprak

10:20a.m. - 10:40a.m. Break

10:40a.m. - 12:00a.m. Technical Session II – Seismic Behavior of Lifeline Facilities

Liquefaction Assessment in the Pacific Northwest. Paul Grant

Liquefaction Assessment Issues. Steven Kramer

Floating Characteristics of a Sewer due to Liquefaction. Keiichi Tamura, Masahiro Kaneko and Hiroshi Kobayashi

Mechanism of Menshin Tunnel. Jun-ichi Hoshikuma

12:00p.m. - 1:00p.m. Lunch

Agenda Cont'd

1:00p.m. - 3:00p.m. Technical Session III – Socio-Economic Impacts of Seismic Damage to Lifeline Facilities

Measuring Lifeline System Performance. Stephanie Chang

System to Assess Socio-Economic Effects of Earthquake Disaster. Tomofumi Nozaki and Hideki Sugita

Multihazard Vulnerability Assessment of Water Systems. William Elliott

Evaluation of Bridge Damage Data from Recent California Earthquakes. Nesrin Basoz

Influence of the Seismic Restoration of Hanshin Expressway Kobe Route upon the Surrounding Area. Nobuhiko Hamada and Toru Yonekura

Reliability and Restoration of Water Supply Systems for Fire Suppression and Drinking Following Earthquakes. Donald Ballantyne

3:00p.m. - 3:20p.m. Break

3:20p.m. - 5:00p.m. Technical Session IV – Seismic Damage Estimation and Prediction for Lifeline Facilities

Pipeline Loss Estimation Modeling Approach Used in HAZUS. Michael O'Rourke

Real Time Earthquake Damage Estimation System for Civil Infrastructures. Hideki Sugita and Tadashi Hamada

Issues in Earthquake Hazard Mapping. Mei Mei Wang

Application of Real Time Ground Motion Monitoring Using the CUBE System. ?

Real Time Monitoring of Earthquake Losses. Ronald Eguchi

A g e n d a C o n t ' d

WEDNESDAY, NOV. 5

- 7:30a.m. – 8:00a.m. Continental Breakfast**
- 8:00a.m. - 8:20a.m. Special Presentation – Seismicity in the Pacific Northwest.
Presented by Dr. Craig Weaver**
- 8:20a.m – 10:00a.m. Technical Session V – Research and Development in Earthquake
Disaster Prevention Technology after the
Northridge and Kobe Earthquakes**

Progress of Earthquake Disaster Prevention of Electric Facilities. Jun'ichi Tohma

Current Development of Seismic Design Criteria and Mitigation of Electric Power
Transmission Systems. Leon Kempner

The 1996 Seismic Design Specifications for Highway Bridges. Koichi Yokoyama, Keiichi
Tamura, Shigeki Unjoh, Toru Terayama and Jun-ichi Hoshikuma

New Earthquake-proof Measure of Underground Telecommunication Facilities after the 1995
Hyogo-ken Nanbu Earthquake. Masaru Okutsu, Ken-ichi Honda, Yuzo Yamaguchi and
Akira Sawaguchi

Comparison on Emergency Response of Water Supply Systems between the Kobe and
Northridge Earthquakes. Shiro Takada and Ryuzo Ozaki

- 10:00a.m. - 10:20a.m. Break**
- 10:20a.m. - 12:00a.m. Break-out Session I**
- 12:00p.m. - 1:00p.m. Lunch**

Agenda Cont'd

**1:00p.m. - 3:00p.m. Technical Session VI – Lifeline Facilities and Urban Earthquake
Disaster Prevention**

Water System Reliability. *Presented by* Charles Scawthorn

Seismic Vulnerability Assessment of the City of San Diego Wastewater System. David Hu

Research and Development of the Seismic Isolation System Applied to Urban Tunnels (Part-1: Development of Seismic Isolation Materials and Construction Methods). Takeyasu Suzuki, and Tsutomu Tanaka

Research and Development of the Seismic Isolation System Applied to Urban Tunnels (Part-2: Effects of Seismic Isolation and Design Procedure). Tsutomu Tanaka and Takeyasu Suzuki

Seismic Vulnerability of Port and Harbor Facilities. Steve Dickenson

Standard Development of Automatic Gas Shutoff Valves. Douglas Honegger

3:00p.m. - 3:20p.m. Break

3:20p.m. - 5:00p.m. Break-out Session II

**7th US-Japan Workshop on Earthquake Disaster Prevention for Lifeline Systems
Participant List**

JAPAN

Dr. Koichi Yokoyama
Director, Earthquake Disaster Prevention Research
Center
Public Works Research Institute
Ministry of Construction
1, Asahi, Tsukuba-shi, Ibaraki-ken 305 Japan
Tel: 0298-64-2829
Fax: 0298-64-0598
E-mail: yokoyama@pwri.go.jp

Dr. Hideki Sugita
Head, Earthquake Disaster Prevention Technology
Division
Earthquake Disaster Prevention Research Center
Public Works Research Institute
Ministry of Construction
1, Asahi, Tsukuba-shi, Ibaraki-ken 305 Japan
Tel: 0298-64-3244
Fax: 0298-64-0598
E-mail: sugita@pwri.go.jp

Mr. Tomofumi Nozaki
Senior Research Engineer, Earthquake Disaster
Prevention Technology Division
Earthquake Disaster Prevention Research Center
Public Works Research Institute
Ministry of Construction
1, Asahi, Tsukuba-shi, Ibaraki-ken 305 Japan
Tel: 0298-64-3244
Fax: 0298-64-0598
E-mail: nozaki@pwri.go.jp

Dr. Keiichi Tamura
Head, Ground Vibration Division
Earthquake Disaster Prevention Research Center
Public Works Research Institute
Ministry of Construction
1, Asahi, Tsukuba-shi, Ibaraki-ken 305 Japan
Tel: 0298-64-2926
Fax: 0298-64-0598
E-mail: tamura@pwri.go.jp

Mr. Toru Terayama
Senior Research Engineer, Earthquake Engineering
Division
Earthquake Disaster Prevention Research Center
Public Works Research Institute
Ministry of Construction
1, Asahi, Tsukuba-shi, Ibaraki-ken 305 Japan
Tel: 0298-64-2932
Fax: 0298-64-4424
E-mail: terayama@pwri.go.jp

Mr. Jun-ichi Hoshikuma
Research Engineer, Earthquake Engineering
Division
Earthquake Disaster Prevention Research Center
Public Works Research Institute
Ministry of Construction
1, Asahi, Tsukuba-shi, Ibaraki-ken 305 Japan
Tel: 0298-64-2932
Fax: 0298-64-4424
E-mail: hosikuma@pwri.go.jp

Mr. Atsushi Nozu
Research Engineer, Earthquake Disaster Prevention
Laboratory
Structural Engineering Division
Port and Harbour Research Institute
Ministry of Transport
3-1-1, Nagase, Yokosuka-shi, Kanagawa-ken 239
Japan
Tel: 0468-44-5030
Fax: 0468-44-0839
E-mail: nozu@ipc.phri.go.jp

Mr. Nobuhiko Hamada
Assistant Manager, Research Division
Planning Department
Hanshin Expressway Public Corporation
4-1-3, Kyutaro-machi, Chuo-ku, Osaka-shi, Osaka-
fu 541 Japan
Tel: 06-252-8121
Fax: 06-252-7414
E-mail: BXG00162@niftyserve.or.jp

Mr. Masahiro Kaneko
Senior Research Engineer, Ground Vibration
Division
Earthquake Disaster Prevention Research Center
Public Works Research Institute
Ministry of Construction
1, Asahi, Tsukuba-shi, Ibaraki-ken 305 Jpn
Tel: 0298-64-4963
Fax: 0298-64-0598
E-mail: kaneko@pwri.go.jp

Mr. Masaru Okutsu
Civil Engineering Project
NTT Access Network Systems Laboratories
Nippon Telegraph and Telephone Corporation
1-7-1, Hanabatake, Tsukuba-shi, Ibaraki-ken 305
Japan
Tel: 0298-52-2543
Fax: 0298-52-2676
E-mail: okutsu@tsukuba.tecl.ntt.co.jp

Prof. Tadanobu Sato
Professor, Disaster Prevention Research Institute
Kyoto University
Gokanosyo, Uji-shi, Kyoto-fu 611 Japan
Tel: 0774-38-4065
Fax: 0774-38-4070
E-mail: sato@catfish.dpri.kyoto-u.ac.jp

Mr. Isaburo Yagi
General Manager, R&D Department
Ashimori Engineering Co., Ltd.
11-7, 7-chome, Senrioka, Settsu-shi
Osaka-fu 566 Japan
Tel: 06-337-6271
Fax: 06-388-7511

Dr. Jun'ichi Tohma
Research Fellow
Geotechnical & Earthquake Engineering Department
Abiko Research Laboratory
Central Research Institute of Electric Power
Industry
1646, Abiko, Abiko-shi, Chiba-ken 270-11 Japan
Tel: 0471-82-1181
Fax: 0471-84-2941
E-mail: tohma@criepi.denken.or.jp

Dr. Takeyasu Suzuki
Group Manager, Earthquake Engineering Research
Group
Technical Research & Development Institute
Kumagai Gumi Co., Ltd.
1043, Onigakubo, Tsukuba-shi, Ibaraki-ken 300-22
Japan
Tel: 0298-47-7508
Fax: 0298-47-7480
E-mail: tsuzuki@ku.kumagaigumi.co.jp

Mr. Tsutomu Tanaka
Director, Central Research and Development
Department
Oriental Consultants Co., Ltd.
1-16-14, Shibuya, Shibuya-ku, Tokyo 150 Japan
Tel: 03-3409-7555
Fax: 03-3409-7565
E-mail: tanaka-tt@oriconsul.co.jp

Mr. Junichi Ueno
Chief Engineer, Civil Engineering Division
Konoike Construction Co., Ltd.
3-6-1, Kitakyuhoji-machi, Chuo-ku, Osaka-shi
Osaka-fu 541 Japan
Tel: 06-244-3670
Fax: 06-244-3676
Email: ueno-ji@konoike.co.jp

UNITED STATES

Mr. Donald Ballantyne
Senior Consultant
EQE International, Inc.
1411 4th Avenue, #500
Seattle, WA 98101
Tel: 206-623-7232
Fax: 206-624-8268
E-mail: dbballan@eqe.com

Mr. Nesrin Basoz
Senior Staff Engineer
K2 Technologies Inc.
4000 Moorpark Ave., Suite 215
San Jose, CA 95117
Tel: 408-249-8800
Fax: 408-249-9020
E-mail: nesrinb@k2inc.com

Mehmet Celebi
US Geological Survey
345 Middlefield Road, MS 977
Menlo Park, CA 94025
Tel: 650-329-5623
Fax: 650-329-5163

Dr. Stephanie Chang
Engineering Economist
EQE International, Inc.
1411 4th Avenue, #500
Seattle, WA 98101
Tel: 206-623-7232
Fax: 206-624-8268
E-mail: sec@eqe.com

Dr. Riley Chung
Building and Fire Research Laboratory
National Institute of Standards and Technology
Bldg. 226, Rm. B158
Gaithersburg, MD 20899
Tel: 301-975-6062
Fax: 301-869-6275
E-mail: riley.Chung@nist.gov

Mr. Tom Driver
Divisional Vice President
Paltem-Gas
Insituform Technologies, Inc.
17988 Edison Avenue
Chesterfield, MO 63005-3700
Tel: 314-530-8000
Fax: 3214-537-1214

Mr. Ronald T. Eguchi
Vice President
EQE International, Inc.
18101 Von Karman Ave., Suite 400
Irvine, CA 92715
Tel: 714-833-3303
Fax: 714-442-9485
E-mail: rte@eqe.com

Mr. William Elliott
Senior Engineer
Portland Water Bureau
1120 SW Fifth Ave., 6th Floor
Portland, OR 97204-1926
Tel: 503-823-7486
Fax: 503-823-4500
E-mail: belliott@water.ci.portland.or.us

Mr. W. Paul Grant
Principal
Kleinfelder Associates
3380 167th Pl. SE, Suite 110
Bellevue, WA 98007-6472
Tel: 425-562-4200
Fax: 425-562-4201

Mr. Douglas Honegger
Consultant
1728 Date Avenue
Torrance, CA 90503-7210
Tel: 310-320-9283
Fax: 310-320-9283
E-mail: dghconsult@aol.com

Dr. Steve Dickenson
Oregon State University
Civil Engineering Department
Apperson Hall #202
Covallis, OR 97331-2302
Tel: 541-737-3111
Fax: 541-737-3052
E-mail: sed@engineer.orst.edu

Dr. Steven Kramer
University of Washington
Civil Engineering Department
265 Wilcox Hall, Box 352700
Seattle, WA 98195-2700
Tel: 206-685-2642
Fax: 206-685-3836
E-mail: kramer@u.washington.edu

Dr. Matthew Mabey
Brigham Young University
Department of Geology
P.O. Box 25111
Provo, UT 84602
Tel: 801-378-3918
Fax: 801-378-8143
E-mail: matthew_mabey@byu.edu

Dr. Bijan Mohraz
Building and Fire Research Laboratory
National Institute of Standards and Technology
Bldg. 226, Rm. B158
Gaithersburg, MD 20899
Fax: 301-869-6275

Dr. Michael O'Rourke
Rensselaer Polytechnic Institute
Civil Engineering Department
Troy, NY 12180-3590
Tel: 518-276-6933
Fax: 518-276-4833
E-mail: orourm@rpi.edu

Dr. David Hu
City of San Diego
600 B Street, Suite 500
MS-905
San Diego, CA 92101
Fax: 619-533-4267

Dr. Leon Kempner, Jr.
Structural Engineer
Bonneville Power Administration
Lines and Facilities, TNF-3
905 NE 11th Avenue (97232), PO Box 3621
Portland, OR 97208-3621
Tel: 503-230-5563
Fax: 503-230-3984
E-mail: lkempnerjr@bpa.gov

Mr. Craig Weaver
U.S. Geological Survey
Box 351650, Geophysics Program
University of Washington
Seattle, WA 98195
Tel: 206-685-2812
E-mail: craig@usgs.gov

Ms. Mei Mei Wang
Oregon Department of Geology
800 NE Oregon St., Suite 965
Portland, OR 97232
Tel: 503-731-4100x226
Fax: 503-731-4066
E-mail: meimei.wang@state.or.us

Mr. Richard Miller
City of Seattle
Seattle Transportation Department
Roadway Structures Division
600 4th Avenue, Room 510
Seattle, WA 98104

Dr. Charles Scawthorn
Senior Vice President
EQE International, Inc.
1111 Broadway, 10th Floor
Oakland, CA 94607
Tel: 510-817-3100
Fax: 510-663-1050
E-mail: crs@eqe.com

Mr. Mark Pierepiekarz
Associate & Project Manager
EQE International, Inc.
1411 4th Avenue, #500
Seattle, WA 98101
Tel: 206-624-8687
Fax: 206-624-8268
E-mail: mrp@eqe.com

Dr. Selcuk Toprak
Cornell University
Hollister Hall
Ithaca, NY 14850
Tel: 607-255-3438

Ms. Joyce Lem
HDR
500 10th Avenue NE, Suite 1200
Bellevue, WA 98004-5538
Tel: 425-453-1523
Fax: 425-453-7107

Dr. Brian Atwater
U.S. Geological Survey
Box 351650, Geophysics Program
University of Washington
Seattle, WA 98195
Tel: 206-553-2927

Mr. Robert Shulock
Sverdrup
600 108th NE Avenue, Suite 700
Bellevue, WA 98004
Tel: 425-452-8000

Mr. David McCormick
Washington State Department of Transportation
Northwest Region
15700 Dayton Avenue North
P.O. Box 330310
Seattle, WA 98133

Mr. Allen Alston
King County
Department of Natural Resources
Wastewater Treatment Division
821 Second Avenue, MS 83
Seattle, WA 98104

Mr. Aziz Alfi
City of Seattle
Engineering Services
6th Floor Dexter Horton Bldg.
710 Second Avenue
Seattle, WA 98104
Tel: 206-386-1834

Mr. Ron Borowski
City of Seattle
Department of Transportation
600 4th Avenue, Room 420
Seattle, WA 98104

Mr. Jack Harold
Seattle Public Utilities
710 2nd Avenue, 11th Floor
Seattle, WA 98104
Tel: 206-684-5911

Mr. Andy Taylor
KPF
1201 3rd Avenue, #900
Seattle, WA 98101
Tel: 206-622-5822

Dr. Masanobu Shinozuka
University of Southern California
Civil & Environmental Engineering
Los Angeles, CA 98009-2531
Tel: 213-740-9528



Photo 1

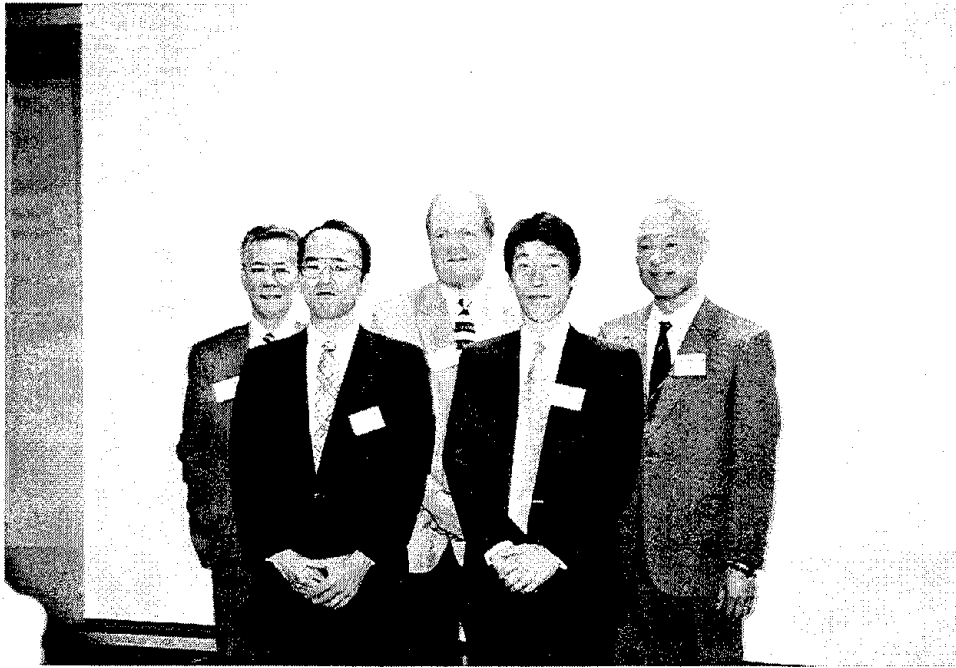


Photo 2

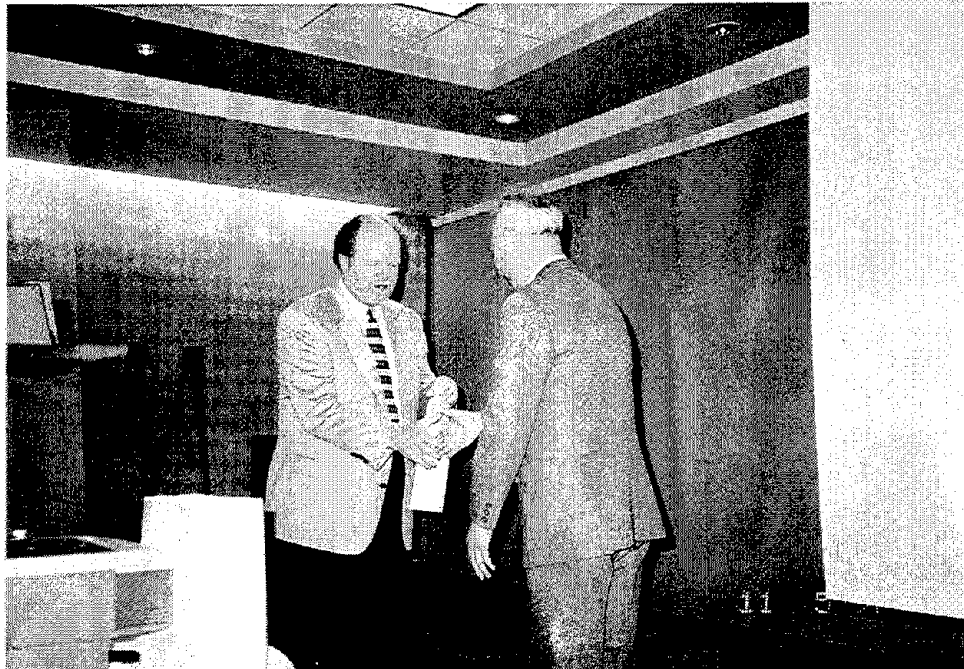


Photo 3



Photo 4



Photo 5



Photo 6



Photo 7



Photo 8: Seattle Public Utilities
Magnolia Elevated Tank Seismic Upgrade

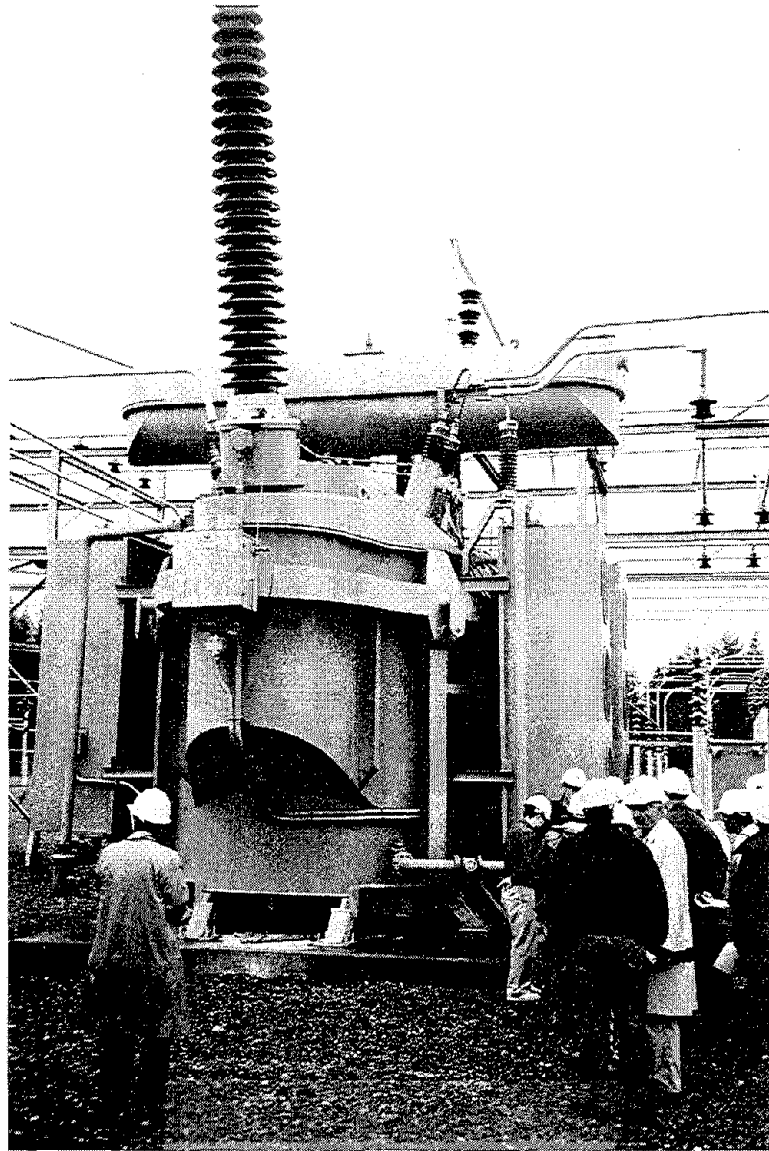


Photo 9: BPA Monroe Substation

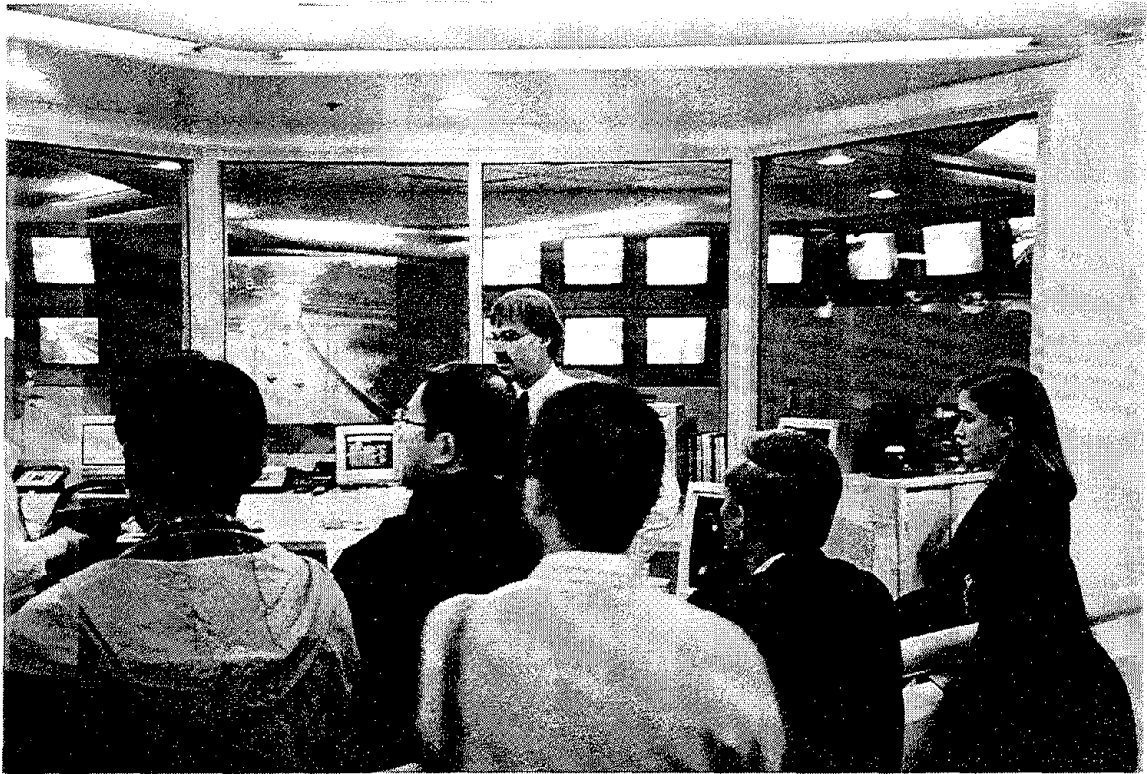


Photo 10: Washington State
Department of Transportation
Traffic Control Center

